frontiers | Research Topics

Rare immune-mediated diseases- novel insights into underlying mechanisms and therapeutic approaches

Edited by
Yuval Tal, Oded Shamriz and Irit Adini

Published in
Frontiers in Immunology

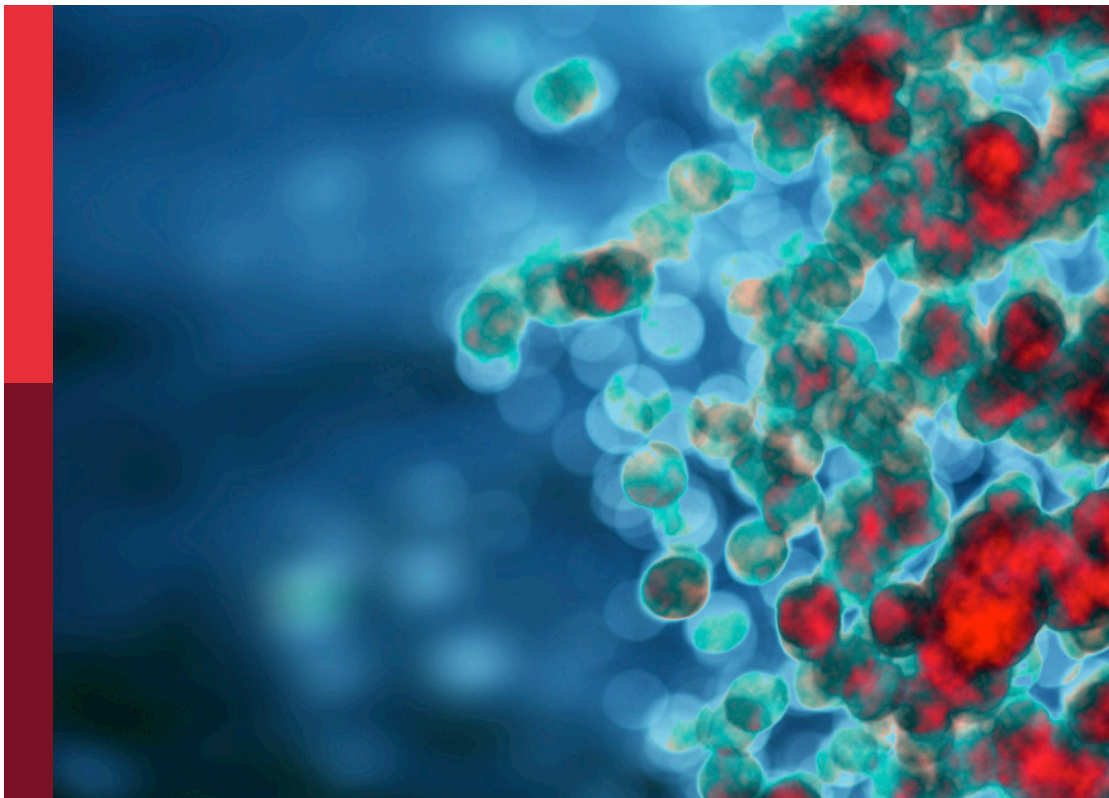

ISSN 1664-8714
ISBN 978-2-8325-3358-1
DOI 10.3389/978-2-8325-3358-1

About Frontiers

Frontiers is more than just an open access publisher of scholarly articles: it is a pioneering approach to the world of academia, radically improving the way scholarly research is managed. The grand vision of Frontiers is a world where all people have an equal opportunity to seek, share and generate knowledge. Frontiers provides immediate and permanent online open access to all its publications, but this alone is not enough to realize our grand goals.

Frontiers journal series

The Frontiers journal series is a multi-tier and interdisciplinary set of open-access, online journals, promising a paradigm shift from the current review, selection and dissemination processes in academic publishing. All Frontiers journals are driven by researchers for researchers; therefore, they constitute a service to the scholarly community. At the same time, the *Frontiers journal series* operates on a revolutionary invention, the tiered publishing system, initially addressing specific communities of scholars, and gradually climbing up to broader public understanding, thus serving the interests of the lay society, too.

Dedication to quality

Each Frontiers article is a landmark of the highest quality, thanks to genuinely collaborative interactions between authors and review editors, who include some of the world's best academicians. Research must be certified by peers before entering a stream of knowledge that may eventually reach the public - and shape society; therefore, Frontiers only applies the most rigorous and unbiased reviews. Frontiers revolutionizes research publishing by freely delivering the most outstanding research, evaluated with no bias from both the academic and social point of view. By applying the most advanced information technologies, Frontiers is catapulting scholarly publishing into a new generation.

What are Frontiers Research Topics?

Frontiers Research Topics are very popular trademarks of the *Frontiers journals series*: they are collections of at least ten articles, all centered on a particular subject. With their unique mix of varied contributions from Original Research to Review Articles, Frontiers Research Topics unify the most influential researchers, the latest key findings and historical advances in a hot research area.

Find out more on how to host your own Frontiers Research Topic or contribute to one as an author by contacting the Frontiers editorial office: frontiersin.org/about/contact

Rare immune-mediated diseases- novel insights into underlying mechanisms and therapeutic approaches

Topic editors

Yuval Tal — Hadassah Medical Center, Israel

Oded Shamriz — Hadassah Medical Center, Israel

Irit Adini — Massachusetts General Hospital, Harvard Medical School, United States

Citation

Tal, Y., Shamriz, O., Adini, I., eds. (2023). *Rare immune-mediated diseases- novel insights into underlying mechanisms and therapeutic approaches*.

Lausanne: Frontiers Media SA. doi: 10.3389/978-2-8325-3358-1

Table of contents

frontiers | Frontiers in Immunology

TYPE Editorial
PUBLISHED 14 August 2023
DOI 10.3389/fimmu.2023.1273062

OPEN ACCESS

EDITED AND REVIEWED BY
Betty Diamond,
Feinstein Institute for Medical Research,
United States

*CORRESPONDENCE
Oded Shamriz
oded.shamriz@mail.huji.ac.il
Yuval Tal
Yuvalt@hadassah.org.il

RECEIVED 05 August 2023
ACCEPTED 07 August 2023
PUBLISHED 14 August 2023

CITATION
Shamriz O, Adini I and Tal Y (2023) Editorial: Rare immune-mediated diseases- novel insights into underlying mechanisms and therapeutic approaches.
Front. Immunol. 14:1273062.
doi: 10.3389/fimmu.2023.1273062

Editorial: Rare immune-mediated diseases- novel insights into underlying mechanisms and therapeutic approaches

Oded Shamriz[1,2]*, Irit Adini[3] and Yuval Tal[1]*

[1]Allergy and Clinical Immunology Unit, Department of Medicine, Hadassah Medical Organization, Faculty of Medicine, Hebrew University of Jerusalem, Jerusalem, Israel, [2]The Lautenberg Center for Immunology and Cancer Research, Institute of Medical Research Israel-Canada, Faculty of Medicine, Hebrew University of Jerusalem, Jerusalem, Israel, [3]Department of Surgery, Center for Engineering in Medicine & Surgery, Massachusetts General Hospital, Harvard Medical School, Boston, MA, United States

KEYWORDS

pathway, personalized, mechanism, novel, pathophysiology, target

Editorial on the Research Topic
Rare immune-mediated diseases- novel insights into underlying mechanisms and therapeutic approaches

Our understanding of the underlying mechanisms of the immune system has vastly improved over the years. Description of new inborn errors of immunity (IEI) (1), as well as the introduction of novel biological treatments, which target specific pathways in the immune system, have revolutionized the field of clinical immunology.

As a result, treatment of patients with immune-mediated disorders has been increasingly altered from gross immune suppression by corticosteroids and cytotoxic agents to patient-tailored and pathway-specific treatments. For example, patients with lipopolysaccharide (LPS)-responsive and beige-like anchor protein (LRBA) deficiency, who present with immune dysregulation and decrease in CTLA4, are routinely being treated with abatacept, even as a bridge before hematopoietic stem cell transplantation (2). In addition, atopic dermatitis in the context of IEI, such as Wisckot Aldrich syndrome (WAS), and as a manifestation of increased T helper (Th)2-mediated immunity is now considered more manageable with dupilumab, a monoclonal antibody against interleukin (IL)-4/IL-13 receptor α subunit (3, 4). Finally, even the treatment of asthma has been revised. Understanding the different asthma endotypes, whether it is allergic or eosinophilic, will help physicians to offer a personalized treatment by using dupilumab or omalizumab for allergic asthma or anti-IL-5 agents, such as mepolizumab and benralizumab, for the eosinophilic endotype with good clinical outcome (5). This approach allows asthmatic patients to have decreased number of exacerbations without the need of long-period systemic corticosteroids.

Indeed, the treating immunologist must have an in-depth understanding of the underlying immune mechanism of the patient's disease, to accurately adjust the treatment and to avoid adverse reactions from unnecessary deep immune suppression.

This Research Topic of *Frontiers in Immunology* focuses on novel insights into the mechanisms and innovative treatments of rare immune-mediated diseases. Different

immune mechanisms are presented in various studies in this Research Topic. Li et al. analyze type 1 interferon signature in peripheral blood mononuclear cells of patients with idiopathic inflammatory myopathies (IIM). Exploring Th2 immune response, Does et al. depicts in detail the pathophysiology of itch and hypersensitivity reactions of mosquito bites including involvement of mast cells. In addition, Dolitzky et al. describes another important Th2 key player by revealing the regulation of eosinophil activation by apoptotic cells. Lastly, Bader et al. displays a comprehensive analysis of the adaptive immunity against the BNT162b2 mRNA vaccine in adolescents with various immune deficiencies.

There are several studies in this Research Topic that explore the emergence of novel treatments from comprehensive understating of the immune system. Defining eosinophils as key players in drug reaction with eosinophilia and systemic symptoms syndrome (DRESS), Rubin et al. report the use of anti-IL-5 agents as potential treatment with remarkable clinical outcome. Zhao et al. suggest that mesenchymal stem cell-derived extracellular vesicles can be used in multiple sclerosis (MS). Zhen et al. presents an extensive meta-analysis analyzing the use of rituximab in IIM. In addition, Yin et al. reports on the use of transicptome to identify drug repositioning for MS. The authors identify different PI3K-Akt and chemokine signaling pathways as potential novel targets for MS. Another interesting study by Adini et al. presents PR1P, a Vascular Endothelial Growth Factor (VEGF)-stabilizing peptide, as a possible therapeutic target in the inflammatory response of ulcerative colitis.

Finally, Pan et al. reviews the targeting of immune checkpoint inhibitors in anti-neutrophil cytoplasmic antibodies (ANCA)-associated vasculitis (AAV). Different co-inhibitory molecules, such as T cell immunoglobulin (Ig) and mucin domain-containing protein 3 (TIM-3), are suggested by the authors as potential targets for novel biological treatments for AAV.

In conclusion, the accumulating data regarding pathophysiology and novel treatments for immune-mediated disorders are the foundations for the practice of clinical immunologists. Further exploring immune pathways will help develop novel biologics, thus keeping the march towards a personalized and pathway-specific immune treatments.

Author contributions

OS: Conceptualization, Investigation, Supervision, Writing – original draft. IA: Writing – review & editing. YT: Supervision, Writing – review & editing.

Conflict of interest

The authors declare that the research was conducted in the absence of any commercial or financial relationships that could be construed as a potential conflict of interest.

Publisher's note

References

1. Bousfiha A, Moundir A, Tangye SG, Picard C, Jeddane L, Al-Herz W, et al. The 2022 update of IUIS phenotypical classification for human inborn errors of immunity. *J Clin Immunol* (2022) 42(7):1508–20. doi: 10.1007/s10875-022-01352-z0.1007/s10875-022-01352-z

2. Lo B, Zhang K, Lu W, Zheng L, Zhang Q, Kanellopoulou C, et al. AUTOIMMUNE DISEASE. Patients with LRBA deficiency show CTLA4 loss and immune dysregulation responsive to abatacept therapy. *Science* (2015) 349(6246):436–40. doi: 10.1126/science.aaa1663349/6246/436

3. Alzahrani F, Miller HK, Sacco K, Dupuy E. Severe eczema in Wiskott-Aldrich syndrome-related disorder successfully treated with dupilumab. *Pediatr Dermatol* (2023). doi: 10.1111/pde.15397

4. Guttman-Yassky E, Bissonnette R, Ungar B, Suarez-Farinas M, Ardeleanu M, Esaki H, et al. Dupilumab progressively improves systemic and cutaneous abnorMalities in patients with atopic dermatitis. *J Allergy Clin Immunol* (2019) 143(1):155–72. doi: 10.1016/j.jaci.2018.08.022

5. Kaur R, Chupp G. Phenotypes and endotypes of adult asthma: Moving toward precision medicine. *J Allergy Clin Immunol* (2019) 144(1):1–12. doi: 10.1016/j.jaci.2019.05.031

frontiers | Frontiers in Immunology

TYPE Review
PUBLISHED 21 September 2022
DOI 10.3389/fimmu.2022.1024559

OPEN ACCESS

EDITED BY
Yuval Tal,
Hadassah Medical Center, Israel

REVIEWED BY
Assi Levi,
Sackler Faculty of Medicine, Tel Aviv University, Israel
Alon Hershko,
Hadassah Medical Center, Israel

*CORRESPONDENCE
Gil Yosipovitch
gyosipovitch@med.miami.edu

SPECIALTY SECTION
This article was submitted to Autoimmune and Autoinflammatory Disorders: Autoimmune Disorders, a section of the journal Frontiers in Immunology

RECEIVED 21 August 2022
ACCEPTED 07 September 2022
PUBLISHED 21 September 2022

CITATION
Vander Does A, Labib A and Yosipovitch G (2022) Update on mosquito bite reaction: Itch and hypersensitivity, pathophysiology, prevention, and treatment. *Front. Immunol.* 13:1024559. doi: 10.3389/fimmu.2022.1024559

Update on mosquito bite reaction: Itch and hypersensitivity, pathophysiology, prevention, and treatment

Ashley Vander Does, Angelina Labib and Gil Yosipovitch*

Miami Itch Center, Dr Phillip Frost Department of Dermatology, University of Miami, Miami, FL, United States

Mosquito bites are endured by most populations worldwide. Reactions to mosquito bites range from localized wheals and papules with associated pruritus to rare systemic reactions and anaphylaxis in certain populations. The mechanism of itch is due to introduction of mosquito saliva components into the cutaneous tissue, although the exact pathophysiology is unclear. Histamine is thought to be a key player through mosquito saliva itself or through activation of mast cells by IgE or through an IgE-independent pathway. However, other salivary proteins such as tryptase and leukotrienes may induce non-histaminergic itch. Some individuals have a genetic predisposition for mosquito bites, and people with hematologic cancers, HIV, and other conditions are susceptible to robust reactions. Prevention of mosquito bites is key with physical barriers or chemical repellents. Treatment consists of second-generation antihistamines and topical corticosteroids. Further research on topical treatments that target neural-mediated itch is needed.

KEYWORDS

hypersensitivity, insect bite, repellant, itch, mosquito, mosquito allergy, genetic predisposition

Introduction

Mosquitos are ubiquitous and are responsible for most insect bites worldwide (1). Their bite causes a local cutaneous reaction leading to acute pruritus and the subsequent consequences of scratching: scarring, hyperpigmentation, and superinfection. In some individuals, this local cutaneous reaction is exaggerated and debilitating, worsening the clinical course and decreasing quality of life, especially if mosquito bites are a common occurrence.

Epidemiology

Mosquitos are found in all continents except Antarctica (1). While the incidence of mosquito bites is unknown due to lack of reporting, the largest populations of mosquitos reside in humid tropical regions such as Thailand, Brazil, Indonesia, and the Philippines. Due to global warming, the incidence of mosquito bites is expected to increase as more extensive growth occurs.

There are over 3,500 species and subspecies of mosquito in 42 genera, three genera of which cause human bites: *Anopheles*, *Culex*, and *Aedes* (1, 2). Feeding behavior varies with genus: for instance, *Culex* mosquitos are active mostly at night, whereas the *Aedes* genus is active during the day. Only female mosquitos bite humans, as blood provides the nutrients required to produce eggs (1). Mosquitos find their human or animal host *via* visual color cues, such as dark-colored objects (1, 3). As they draw nearer to the host, they increasingly rely on thermal and olfactory stimuli. Research has shown that mosquitos are particularly drawn to moist heat sources, exhaled carbon dioxide, and certain body odors (4).

The diseases transmitted by mosquitos include malaria (*Anopheles*); West Nile virus and western/eastern equine encephalitis (*Culex*); and Chikungunya, yellow fever, dengue, and the Zika virus (*Aedes*). The burden of mosquito-borne diseases is significant: 700 million infections leading to one million deaths every year (5).

Clinical features

Mosquito bite responses occur in phases: the immediate reaction and delayed reaction, along with large local reactions in some individuals. Immediately after a mosquito bite, a round wheal 2-10 mm in diameter forms with surrounding erythema peaking in 20-30 minutes (6–8). The delayed reaction consists of pruritic papules of the same size which peak in 24-36 hours. These gradually disappear over the course of several days.

Mosquito bites in human skin progress through a series of stages determined by cumulative number of mosquito bites accrued during a lifetime (6, 9). The first mosquito bite in an individual results in a small, red spot (stage I). Subsequent bites lead to first a delayed reaction only (stage II), then an immediate and delayed reaction (stage III), then an immediate reaction only (stage IV), and finally neither an immediate nor delayed reaction (stage V). Thus, it's understood that natural desensitization to mosquito saliva may occur with long-term exposure (10), though a subsequent observational study noted marked individual variability in course of the stage progression with 6 of 10 patients remaining in stage III over a 30-year period (11).

For some individuals, a large local reaction (wheal > 5 mm) occurs within minutes to hours (12). These individuals may be diagnosed with a mosquito allergy. In general, mosquito bite size is correlated to self-reported itch intensity (13). Secondary skin lesions due to scratching include excoriations which may obstruct primary skin findings, along with scarring and hyperpigmentation.

Finally, the diseases transmitted by mosquitos and their treatments may also induce pruritus. For instance, the Zika, West Nile, Chikungunya, and dengue viruses cause a generalized maculopapular rash that is often itchy (14–17). Additionally, the anti-malarial drug chloroquine is well-known for causing pruritus (18).

Predisposition to mosquito bites: Genetics and the skin microbiome

Numerous studies suggest a human susceptibility to mosquito bites and associated itch (19). Khan et al. reported that individuals attracted mosquitos with varying rates and demonstrated differing mosquito bite responses (20). Twin studies of monozygotic and dizygotic twins suggested a strong genetic association to bite susceptibility, possibly due to body odors derived from shared genetics between identical twins that are subsequently detected by mosquito olfaction (19, 21–23). Additionally, self-reported size of the mosquito bite, intensity of the related itch, and perceived attractiveness to mosquitos seemed to have a hereditary component and were greater in females compared to males (13). The sex difference is thought to be due to a specific locus of genes in the human leukocyte antigen (HLA) region that yields a more intense itch response in females to a 3-fold effect (13, 24).

Human body odor results in part from volatile organic compounds emitted by the skin's commensal bacteria (25). Many studies have shown a relationship between skin bacteria composition and mosquito attractiveness, including direct attractiveness of mosquitos to odors produced by these bacteria (24, 26–28). For example, low diversity of the skin microbiome is correlated with higher attraction rates and *Pseudomonas* spp. is associated with decreased attraction rates (24, 28). Future clinical opportunities may involve manipulating the composition of skin bacteria through application of a topical probiotic, a technique already emerging for management in other disease entities (i.e., psoriasis, eczema). Before microbiome alteration becomes an option, extensive research must answer remaining questions regarding its feasibility, including the duration of treatment effect (25).

Abbreviations: CNS, central nervous system; DEET, N,N-diethyl-3-methyl-benzamide (formerly N,N-diethyl-meta-toluamide); EBAAP, ethyl butylacetylaminopropionate; EBV, Epstein-Barr virus; HIV, human immunodeficiency virus; HLA, human leukocyte antigen; IL, interleukin; HEN, hypersensitivity to mosquito bites-Epstein-Barr virus-natural killer; HMB, hypersensitivity to mosquito bites; NK, natural killer; PAR-2, proteinase-activated receptor-2; TH, thiamine hydrochloride; TRP, transient receptor potential.

10.3389/fimmu.2022.1024559

Mosquito itch pathophysiology

While the mechanism of mosquito bite reaction isn't well-understood, a few hypotheses elucidate the responses occurring from cutaneous introduction of mosquito saliva components: a reaction to histamine found directly in mosquito saliva, an IgE-mediated (type I) hypersensitivity reaction, and an IgE-independent inflammatory response (Figure 1) (29).

A histaminergic response is a well-supported mechanism of reaction. Similar to other pruritic pathways like urticaria and mastocytosis, histamine found in mosquito saliva causes itch by binding to histamine-specific receptors on nerve endings (30). Histamine also instigates local vasodilation and edema, causing wheal formation. The amount of histamine found in mosquito saliva appears to be sufficient to induce an itch response. This mechanism is supported by reduction of wheal size and pruritus when patients are treated with anti-histaminergic medications.

Additionally, endogenous histamine is released through IgE activation of mast cells within the dermis in response to other mosquito saliva components (type 1 hypersensitivity). These mosquito saliva components include salivary odorant-binding proteins (Aed a 2, Aed al 2, Ano d 2, Cul q, Cul q 3) and other various proteins (Aed a 1, Aed a 3, Aed a 4, Aed al 3) (31). The D7 proteins, which are a subtype of odorant-binding proteins and abundant in mosquito saliva, were found to be the major allergenic proteins across mosquito species (31). They have been shown to bind to biogenic amine and leukotriene, effectively neutralizing their activity to inhibit host immune defenses and temporarily prevent scratching, which would interrupt feeding (32). Activation of mast cells by IgE primed against these allergens leads to the release of various inflammatory mediators, such as histamine (discussed earlier), cytokines, tryptase, and eicosanoids (such as leukotrienes). Kuraishi et al. studied the effects of various medications on scratching behavior in mice injected with mosquito salivary gland extract (33). They found that drugs which inhibit 5-lipoxygenase (like zileuton) inhibited theincreased activity of the cutaneous nerve branch induced by the extract and decreased scratching, while drugs modifying leukotriene B(4) and cysteinyl leukotrienes (LTC4, LTD4, and LTE4) had no such effect. Therefore, they deduced that 5-lipoxygenase metabolite(s) other than leukotriene B(4) and cysteinyl leukotrienes are involved in mosquito-associated itching. In addition to IgE, mosquito-saliva-specific IgG levels are also elevated during immediate and delayed reactions.

Another proposed mechanism for mosquito itch includes the IgE-independent inflammatory response, implicated in delayed reactions. This occurs through either direct stimulation of mast cells by saliva components resulting in degranulation and/or through a Th2 inflammatory cascade. Indeed, a murine model study by Demeure et al. showed that mosquito saliva can activate mast cells independent of IgE or IgG antibodies directed against salivary components (34). Future research should elicit which mosquito saliva component(s) or mast cell receptor(s) are responsible (34).

Studies have shown that SAAG-4 and sialokinin, proteins/peptides found in mosquito saliva, can induce interleukin (IL)-4 expression and decrease IFN-γ expression, driving the host

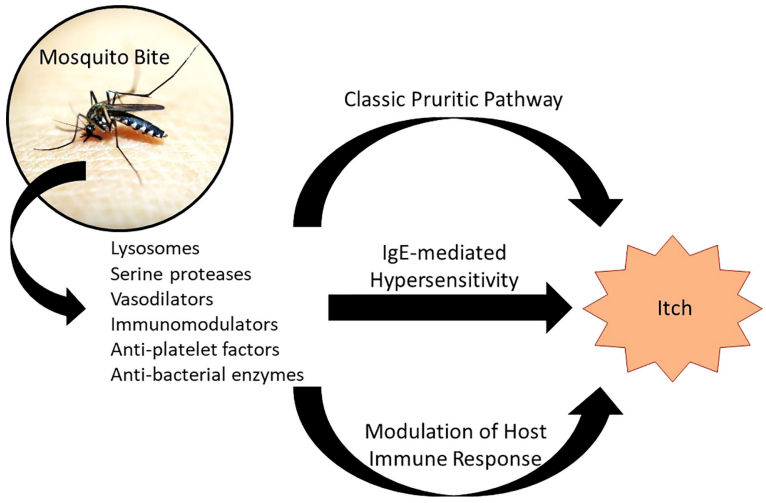

FIGURE 1
Pathophysiology of Mosquito Bite Itch. Introduction of mosquito saliva components results in a number of local responses, three of which are proposed to cause itch: (1) the classic pruritic pathway involving histamine found in mosquito saliva binding to histamine receptors on sensory nerve endings; (2) an IgE-mediated hypersensitivity, in which IgE primed against mosquito saliva components crosslinks with mast cells, causing degranulation; and (3) modulation of the host immune response through IgE-independent and non-histaminergic pathways. Adapted from: Fostini et al. (29).

immune response from a Th1 to a Th2-mediated response (35–37). The release of IL-4 and other cytokines of Th2-mediated responses such as IL-5, IL-13, and IL-31 are known players in itch responses, associated with other pruritic conditions like atopic dermatitis and urticaria (38–41).

Amplified mosquito bite reactions

Certain populations exhibit an increased reaction to mosquito bites beyond typical mast cell degranulation including children, outdoor workers with a high degree of exposure, and those with no previous exposure to indigenous mosquitoes (42). These rare, exaggerated responses also occur in several conditions, especially immune disorders. In general, a diagnosis of mosquito hypersensitivity is based on patient history; commercially available skin prick testing for whole body mosquito allergen extract is available only in select countries and does not have a significant role in patient evaluation.

Children

Children are at increased risk of developing mosquito allergy presenting as urticaria (irregular groups of pruritic papules) and Skeeter syndrome, a type of large local inflammatory reaction (43).

FIGURE 2
Skeeter Syndrome. The right flank of a middle-aged, male patient exhibiting Skeeter syndrome following a mosquito bite. This local area of redness and warmth was accompanied by fever. With previous episodes, he was given oral antibiotics from his primary care providers due to suspected cellulitis. This current episode responded well to topical corticosteroids and antihistamines.

Skeeter syndrome involves localized redness, warmth, swelling, and pruritus following mosquito bites that can be accompanied by fever and occasionally lymphadenopathy (Figure 2) (44). Skeeter syndrome mimics cellulitis, but the difference is in the duration of symptoms: Skeeter syndrome occurs within hours of a mosquito bite and cellulitis has a more protracted time course. Skeeter syndrome resolves in 3-10 days and is mediated by IgE and IgG primed against mosquito saliva; it also tends to occur in immunocompromised individuals and immigrants bitten by indigenous mosquitoes without previous exposure.

Atopic children are particularly susceptible to amplified reactions. In a case-control study of 180 children, large local or unusual reactions to mosquito bites were associated with atopy (35% of cases versus 12% of controls, $P < 0.001$) (45). In the children with bite reactions, 32% had an accompanying atopic disease such as asthma, allergic rhinitis, or atopic dermatitis.

Allergens involved in cross-reactivity with other arthropods

IgE-mediated allergic reactions to mosquito saliva components range from immediate or delayed large local reactions (wheals and flares) to very rare life-threatening anaphylaxis (presyncope, hypotension, and syncope) (46, 47). Less than thirty anaphylactic reactions to mosquitos have been reported worldwide, but they dramatically affect quality of life in those individuals affected (48). Of note, cross-reactivity of mosquito with other arthropods has been demonstrated; in particular, individuals with hypersensitivity to wasp venom, bees, dust mites, cockroaches, and shrimp may be susceptible to similar exaggerated reactions after *Aedes aegypti* exposure (49–51). This is due to salivary and non-salivary homologues including tropomyosin, odorant binding protein, mitochondrial cytochrome C, peptidyl-prolyl cis-trans isomerase, and protein with hypothetical magnesium ion binding function (48, 51). For patients exhibiting mosquito allergy, allergologic workup can include IgE against these potential cross-reactive allergens, although no evidence currently exists to support this testing.

Epstein-barr virus

A triad of hypersensitivity to mosquito bites (HMB), infection with EBV, and natural killer (NK) cell proliferative disorder [coined HMB-EBV-NK (HEN) disease when coexisting in a single patient] presents with an exaggerated, local response to mosquito bites manifesting as bulla, ulceration, or necrosis. This response is initiated by CD4 T cells and amplified reaction of NK cells to mosquito saliva (52). Infection with EBV has also been implicated in the development of novel EBV-infected NK-cell line and T cell lymphoma following mosquito bite (52–54) and in hemophagocytic lymphoma when coexisting with HMB (55).

Wells disease

Wells Disease is an eosinophilic-driven cellulitis that causes red, violaceous, blistering lesions that are pruritic. Although the etiology of Wells Disease is unknown, previous studies have suggested that mosquito bites may cause or propagate the course of the disease as patients develop extreme reactions to mosquito bites. As CD4 T cells play a large role in response to mosquito saliva antigen exposure, CD4 T cells may contribute to the proliferation of eosinophils in the case of Wells Disease (52, 56).

Hematologic cancer

Patients diagnosed with hematologic cancers such as chronic lymphocytic leukemia and mantle cell lymphoma have also demonstrated an exaggerated response to mosquito bites (52, 57). The response is typically characterized by pruritic erythematous papules and plaques. The leading hypothesis to this immune response similarly credits CD4 T cell proliferation in response to a mosquito bite and subsequent IL-4 production (52). There are also some reports of the development of primary cutaneous diffuse large B cell lymphomas that may be associated with mosquito bites (58).

Human immunodeficiency virus

Patients with HIV may also be more susceptible to intense mosquito bite reactions. One skin disorder that HIV patients may experience is pruritic papular eruption, although the underlying etiology is unknown. Studies examining the levels of IgE, CD4 cell counts, and eosinophilia following insect antigen exposure showed HIV patients exhibiting a positive skin response and hypersensitivity (59, 60). Therefore, it has been proposed that pruritic papular eruption in HIV patients may be in part due to mosquito bites.

Mosquito bite prevention and recent developments

The first-line control of mosquito bites is preventing mosquitos from successfully biting their hosts. One effective method involves reducing the mosquito population, such as by limiting the amount of standing water accessible for them to complete their life cycle. In addition, using insecticide, mosquito

traps, and introducing fish into ponds to consume mosquito larvae are helpful methods (61).

Other keys to prevention include utilizing physical barriers to prevent insect access to the skin, such as by staying indoors (particularly when mosquitos are most active), using mosquito netting, and wearing protective clothing. Insect repellents can be chemical or organic agents applied to clothing or to skin (62, 63). N,N-diethyl-3-methyl-benzamide (DEET) is effective at reducing the number of insect bites when applied to skin; though generally safe, exposure to concentrated formulations, excessive inhalation, or ingestion can cause neurotoxicity and systemic toxicity, urticaria syndrome, dermatitis, and bullous eruptions (Table 1) (67–69).

Permethrin is a broadly used, long-lasting pyrethroid insecticide coated on fabrics and mosquito nets, particularly in malaria-endemic countries enforcing control programs to curtail disease transmission. Permethrin also has some toxicity concerns, including a reduction in male fertility parameters and reduced testosterone demonstrated in rodent studies (65) as well as hepatotoxicity (66). The widespread use of pyrethroid insecticides has gained exponential traction over the past few years as mosquitos have developed pyrethroid resistance. In a 2019 study of *Anopheles gambiae* in eight farming communities in Nigeria, resistance to permethrin occurred in up to 46% of mosquitos (70). Resistance mechanisms identified in *Aedes aegypti* includes mutations in the voltage sensitive sodium channel gene (Vssc gene) and metabolic-mediated insecticide resistance (71). Due to the developing nature of resistance, more effective vector control strategies are warranted. One method involves combining a mixture of two insecticides or an insecticide and a synergist to create novel long lasting insecticide nets (LLIN; NCT03554616).

A few mosquito repellants, including several botanicals and essential oils, are gaining exposure due to decreased toxicity, increased pleasantness of the repellant smell, and improved environmental safety. Picaridin is an effective, less toxic alternative to chemical repellants (72) and thiamine hydrochloride (TH; vitamin B1) is a newer repellant currently being investigated. A 2020 pilot study of TH demonstrating an effective dose 50 of 4.57 mg (73) was followed by an *in-vivo*, ex-vivo study in 2021 which showed that TH-loaded hydrogel is comparable to DEET in terms of action duration (74).

Graphene, consisting of a single layer of carbon atoms, has recently been studied as a lightweight, wearable technology used for chemical, mechanical, and radiative protection (75). A new study examined whether graphene-based materials may also provide protection against mosquitos (75). In the dry state, graphene was highly effective at suppressing mosquito biting behavior by interfering with host chemosensing (trapping skin-associated molecular attracts beneath) and by mechanical bite prevention.

TABLE 1 Mosquito bite repellants and their safety profile.

Repellant	Average duration	Reported adverse reactions and toxicity	Special considerations
DEET	5 hours	Rare: CNS involvement (lethargy, headache, seizures, disorientation, ataxia, tremors, acute encephalopathy with psychosis), allergic or cutaneous manifestations, cardiovascular effects (orthostatic hypotension, bradycardia).[a] (62, 64)	Not recommended for children under 2 years of age. Maximum concentration of 33% in children (62) Contraindicated in individuals with urea cycle disorders (62) Pregnancy Category N[b]. Increased risk of toxicity when used in conjunction with retinoids or sunscreen
Picaridin	8-10 hours	Rare: skin irritation (62)	Not recommended in children under 2 years of age (62) Pregnancy Category N[b]. Odorless
Permethrin	6 weeks or 6 washings	Rare: conjunctivitis, numbness/tingling sensation, dermatitis, air conduction passageway irritation, headache, dizziness, fatigue, excessive salivation, muscle weakness, nausea, vomiting, and neurotoxicity (ataxia, hyperactivity, hyperthermia, seizures, paralysis). May affect male fertility or cause hepatoxicity (62, 65, 66).	Pregnancy Category B[c]
EBAAP	2-3 hours	Eye irritation	Odorless
Thiamine hydrochloride	Under investigation	None reported for topical application (further research needed)	
Oil of lemon eucalyptus	6 hours	Rare: skin irritation in atopic individuals (62)	Not recommended for children under 3 years of age (62) Pregnancy Category N[b]
Citronella	2 hours	Rare: eye irritation, skin irritation, and allergic symptoms (62)	Pregnancy Category N[b]

CNS, central nervous system; DEET, N,N-diethyl-3-methyl-benzamide (formerly N,N-diethyl-meta-toluamide); EBAAP, ethyl butylacetylaminopropionate.
[a]Between 1956 and 2008, there were 43 confirmed case reports of DEET toxicity: 25 with CNS involvement, 17 with allergic or dermatologic manifestations, and one with cardiovascular effects. Cutaneous manifestations include urticarial reactions and hemorrhagic vesicobullous erosions after topical exposure of 50% and stronger concentrations (50).
[b]This drug's pregnancy category has not yet been classified by the FDA.
[c]No adverse effects demonstrated in animals.

10.3389/fimmu.2022.1024559

TABLE 2 Second-line mosquito bite therapies.

Topical Treatments
• Calamine lotion
• Menthol-Camphor
• Local anesthetic (pramoxine, lidocaine, benzocaine, lidocaine/prilocaine)
• Antihistamines
• Corticosteroids
• Cold compresses
• Homeopathic after-bite gel
• Other home remedies, such as sodium bicarbonate
Oral Treatments
• Antihistamines[a]
• Glucocorticoids
• Leukotriene receptor antagonists
Other Treatments
• Intralesional corticosteroids
• Epinephrine (anaphylaxis)
• Immunotherapy
• Omalizumab (off-label)
• Suction tools
• Electronic heat device

[a]Supported efficacy for mosquito bite reactions through double-blind, placebo-controlled trials.

Therapies

When mosquito bites are inevitable, prophylaxis with second generation antihistamines can be given to reduce local skin reactions (Table 2). One study has suggested that this is especially true for individuals with hypersensitivity (wheals > 5 mm) (76). Oral daily dosing regimens with levocetirizine 5 mg, cetirizine 10 mg, and rupatadine 10 mg have been proven through placebo-controlled trials to decrease both size of whealing and skin pruritus in adults (77–79). Loratadine (0.3 mg/kg) in children likewise significantly decreased wheal size by 45% ($P < 0.001$, 25 children) and pruritus by 78% ($P = 0.011$, 12 children) (80). These medications can relieve both immediate and delayed allergic symptoms measured 12 and/or 24 hours afterwards. In a trial comparing cetirizine, ebastine, and loratadine 10 mg, Karppinen et al. showed cetirizine and ebastine were effective in decreasing wheal size by 30-40% and pruritus by 70–80% compared to placebo, with cetirizine improving itch to the greatest extent; however, cetirizine also induced the highest frequency of sedation (81). Of note, ebastine and rupatadine are not approved for use in the United States.

When mosquito bites do occur, treatment is aimed at alleviating pruritus through topical applications of medications and medication alternatives as well as oral antihistamines as described above. Topical therapies' target of action involves inhibiting the pruritic pathways or providing local anesthetic. For example, clinical studies have demonstrated decreased itch after repeated noxious heat, which is thought to activate transient receptor potential cation channel subfamily V member 1 (TRPV1), influencing proteinase-activated receptor-2 (PAR-2) carrying C-fibers and decreasing pruritus (82–84). A medical device utilizing local electrical discharges to generate skin warmth showed a statistically significant improvement in pruritus compared to placebo (19 of 27 patients reported at least a 40% improvement in itch) lasting up to 24 hours (85). Conversely, cooling is also shown to reduce itch through TRPM8, an ion channel expressed in peripheral afferent nerve endings (86). When menthol or cold activates the TRPM8 receptor, inhibition of both histaminergic and non-histaminergic itch pathways occurs.

Other options with a paucity of supporting evidence for specific alleviation of mosquito bite symptoms include topical therapy with glucocorticoids, calamine lotion, pramoxine or lidocaine, and other homeopathic remedies such as plant extracts (Echinacea angustifolia mother tincture, Ledum palustre D1 mother tincture, and Urtica Urens mother tincture) (87) and sodium bicarbonate. Interestingly, topical glucocorticoids, which broadly target the inflammatory pathways of itch and in the authors' opinion are effective, have not been subjected to controlled clinical trials for mosquito-related itch. Oral leukotriene receptor antagonists should also be explored further in clinical trials (1). Suction tools are designed to remove mosquito saliva, though no randomized, blinded clinical trials have evaluated their effectiveness. In the rare instances of severe local or systemic mosquito bite reactions, oral glucocorticoids may be indicated, as they are for other urticarias (1).

Finally, several trials studying immunotherapy with whole-body mosquito extract have revealed promising results, but insufficient evidence. A double blind, randomized, placebo-controlled trial demonstrated significant improvement in 40 patients receiving immunotherapy for one year compared to baseline and to the placebo group (88). Improvement was observed for skin reactions, symptom scores for rhinitis and asthma, and forced expiratory volume in one second, showing that mosquito immunotherapy is beneficial for both allergic rhinitis and bronchial asthma. Within the treatment group, serologic analysis showed a nonsignificant decrease in IgE ($P = 0.02$), significant elevation in IgG4 levels ($P = .001$), and a significant decrease in the IgE/IgG4 ratio ($P = .001$). In another study of two patients exhibiting anaphylactic episodes, immunotherapy resolved symptoms in one and decreased reactions in the other (89). Desensitization with immunotherapy may be considered for future patients with anaphylactic reactions, but it is not currently available and further studies with randomization, a control group, and blinding are needed to fully assess the effects of this intervention (12, 90–93). Additionally, future studies are needed utilizing salivary extracts in leu of whole-body mosquito extracts, as several mosquito saliva proteins have been identified as allergenic (31).

An available off-label alternative to anaphylaxis prevention may be found in omalizumab, an anti-IgE monoclonal antibody. One case report of a patient with systemic anaphylaxis to

mosquito manifesting as urticaria, presyncope, and hypotension reported neither anaphylaxis nor mild local reactions following mosquito bites after receiving 300 mg of omalizumab subcutaneously every 4 weeks for 3 months (48).

Interestingly, several studies have demonstrated that the local microenvironment induced by mosquito saliva facilitates the transmission of mosquito-borne diseases, providing an opportunity for therapeutic intervention. A few mechanisms have been identified. Mosquito saliva components reduce the host's antiviral Th1 immune response, permitting easier entry and replication of viruses in the host (94–96). Anti-saliva peptide antibodies provoked through vaccination could enable a more robust Th1 response and interferon release with dampened leukocyte influx to the inoculation site and subsequent decrease in cell trafficking to draining lymph nodes, thus lessening the ease with which the pathogen spreads systemically (97). Vaccines against mosquito saliva peptides are undergoing clinical assessment to determine whether they will be safe and useful for the prevention of pathogen transmission (98).

Conclusions

Mosquito bite-induced pruritus is caused by local reactions to mosquito saliva components. While the exact pathophysiology isn't well-understood, the reaction is thought to be mediated in the majority of cases by histamine release either from the saliva and/or IgE-mediated hypersensitivity reactions. IgE-independent pathways are associated with delayed reactions. However, other non-histaminergic itch mediators such as leukotrienes, proteases, and type 2 cytokines may have a role. Because mosquitos are ubiquitous with a significant induction of worldwide disease burden, it is critical for healthcare providers to recognize how to prevent and treat these mosquito bites. Treatment consists of second-generation antihistamines and topical steroids, and further research on topical pharmaceuticals is needed. Failure to treat the pruritus can result in secondary pigment changes, scarring, and infections.

Author contributions

AV and AL drafted the article. GY critically revised the article. All authors contributed to the article and approved the submitted version.

Conflict of interest

GY conducted clinical trials or received honoraria for serving as a member of the Scientific Advisory Board and consultant of Pfizer, TREVI, Regeneron, Sanofi, Galderma, Novartis, Bellus, Kiniksa, and Eli Lilly and received research funds from Pfizer, Leo, Sanofi, Regeneron, Eli Lilly, and Novartis.

The remaining authors declare that the research was conducted in the absence of any commercial or financial relationships that could be construed as a potential conflict of interest.

Publisher's note

References

1. Seda J, Horrall S. Mosquito bites. In: *StatPearls*. Treasure Island (FL): StatPearls Publishing (2021).

2. Rueda LM. Global diversity of mosquitoes (Insecta: Diptera: Culicidae) in freshwater. *Hydrobiologia* (2008) 595:477–87. doi: 10.1007/s10750-007-9037-x

3. Jung SH, Kim D, Jung KS, Lee DK. Color preference for host-seeking activity of aedes albopictus and culex pipiens (Diptera: Culicidae). *J Med Entomol* (2021) 58 (6):2446–52. doi: 10.1093/jme/tjab100

4. Zhou YH, Zhang ZW, Fu YF, Zhang GC, Yuan S. Carbon dioxide, odorants, heat and visible cues affect wild mosquito landing in open spaces. *Front Behav Neurosci* (2018) 12:86. doi: 10.3389/fnbeh.2018.00086

5. Caraballo H, King K. Emergency department management of mosquito-borne illness: malaria, dengue, and West Nile virus. *Emerg Med Pract* (2014) 16(5):1–24.

6. Mellanby K. Man's reaction to mosquito bites. *Nature* (1946) 158:554. doi: 10.1038/158554c0

7. Reunala T, Brummer-Korvenkontio H, Lappalainen P, Räsänen L, Palosuo T. Immunology and treatment of mosquito bites. *Clin Exp Allergy* (1990) 20(Suppl 4):19–24. doi: 10.1111/j.1365-2222.1990.tb02472.x

8. Peng Z, Yang M, Simons FE. Immunologic mechanisms in mosquito allergy: correlation of skin reactions with specific IgE and IgG antibodies and lymphocyte proliferation response to mosquito antigens. *Ann Allergy Asthma Immunol* (1996) 77(3):238–44. doi: 10.1016/S1081-1206(10)63262-0

9. Heilesen B. Studies on mosquito bites. *Acta Allergol* (1949) 2(3):245–67. doi: 10.1111/j.1398-9995.1949.tb03310.x

10. Peng Z, Simons FE. Mosquito allergy: immune mechanisms and recombinant salivary allergens. *Int Arch Allergy Immunol* (2004) 133(2):198–209. doi: 10.1159/000076787

11. Oka K, Ohtaki N, Igawa K, Yokozeki H. Study on the correlation between age and changes in mosquito bite response. *J Dermatol* (2018) 45(12):1471–4. doi: 10.1111/1346-8138.14688

12. Ariano R, Panzani RC. Efficacy and safety of specific immunotherapy to mosquito bites. *Eur Ann Allergy Clin Immunol* (2004) 36(4):131–8.

13. Jones AV, Tilley M, Gutteridge A, Hyde C, Nagle M, Ziemek D, et al. GWAS of self-reported mosquito bite size, itch intensity and attractiveness to mosquitoes implicates immune-related predisposition loci. *Hum Mol Genet* (2017) 26:1391–406. doi: 10.1093/hmg/ddx036

14. He A, Brasil P, Siqueira AM, Calvet GA, Kwatra SG. The emerging zika virus threat: A guide for dermatologists. *Am J Clin Dermatol* (2017) 18(2):231–6. doi: 10.1007/s40257-016-0243-z

15. Ferguson DD, Gershman K, LeBailly A, Petersen LR. Characteristics of the rash associated with West Nile virus fever. *Clin Infect Dis* (2005) 41(8):1204–7. doi: 10.1086/444506

16. Cunha BA, Leonichev VB, Raza M. Chikungunya fever presenting with protracted severe pruritus. *IDCases* (2016) 6:29–30. doi: 10.1016/j.idcr.2016.09.003

17. Huang HW, Tseng HC, Lee CH, Chuang HY, Lin SH. Clinical significance of skin rash in dengue fever: A focus on discomfort, complications, and disease outcome. *Asian Pac J Trop Med* (2016) 9(7):713–8. doi: 10.1016/j.apjtm.2016.05.013

18. Aghahowa SE, Obianwu HO, Isah AO, Arhewoh IM. Chloroquine-induced pruritus. *Indian J Pharm Sci* (2010) 72(3):283–9. doi: 10.4103/0250-474X.70471

19. McBride CS. Genes and odors underlying the recent evolution of mosquito preference for humans. *Curr Biol* (2016) 26(1):R41–6. doi: 10.1016/j.cub.2015.11.032

20. Khan AA, Maibach HI, Strauss WG. A quantitative study of variation in mosquito response and host attractiveness. *J Med Entomol* (1971) 8(1):41–3. doi: 10.1093/jmedent/8.1.41

21. Kirk KM, Eaves LJ, Meyer JM, Saul A, Martin NG. Twin study of adolescent genetic susceptibility to mosquito bites using ordinal and comparative rating data. *Genet Epidemiol* (2000) 19(2):178–90. doi: 10.1002/1098-2272(200009)19:2<178::AID-GEPI5>3.0.CO;2-3

22. Qiu YT, Smallegange RC, Van Loon JJ, Ter Braak CJ, Takken W. Interindividual variation in the attractiveness of human odours to the malaria mosquito anopheles gambiae s. s. *Med Vet Entomol* (2006) 20(3):280–7. doi: 10.1111/j.1365-2915.2006.00627.x

23. Fernández-Grandon GM, Gezan SA, Armour JA, Pickett JA, Logan JG. Heritability of attractiveness to mosquitoes. *PloS One* (2015) 10(4):e0122716. doi: 10.1371/journal.pone.0122716

24. Verhulst NO, Beijleveld H, Qiu YT, Maliepaard C, Verduyn W, Haasnoot GW, et al. Relation between HLA genes, human skin volatiles and attractiveness of humans to malaria mosquitoes. *Infect Genet Evol* (2013) 18:87–93. doi: 10.1016/j.meegid.2013.05.009

25. Lucas-Barbosa D, DeGennaro M, Mathis A, Verhulst NO. Skin bacterial volatiles: propelling the future of vector control. *Trends Parasitol* (2022) 38(1):15–22. doi: 10.1016/j.pt.2021.08.010

26. Michalet S, Minard G, Chevalier W, Meiffren G, Saucereau Y, Tran Van V, et al. Identification of human skin bacteria attractive to the Asian tiger mosquito. *Environ Microbiol* (2019) 21(12):4662–74. doi: 10.1111/1462-2920.14793

27. Zhang X, Crippen TL, Coates CJ, Wood TK, Tomberlin JK. Effect of quorum sensing by staphylococcus epidermidis on the attraction response of female adult yellow fever mosquitoes, aedes aegypti aegypti (Linnaeus) (Diptera: Culicidae), to a blood-feeding source. *PloS One* (2015) 10(12):e0143950. doi: 10.1371/journal.pone.0143950

28. Verhulst NO, Qiu YT, Beijleveld H, Maliepaard C, Knights D, Schulz S, et al. Composition of human skin microbiota affects attractiveness to malaria mosquitoes. *PloS One* (2011) 6(12):e28991. doi: 10.1371/journal.pone.0028991

29. Fostini AC, Golpanian RS, Rosen JD, Xue RD, Yosipovitch G. Beat the bite: pathophysiology and management of itch in mosquito bites. *Itch* (2019) 4(1):19. doi: 10.1097/itx.0000000000000019

30. Hassan I, Haji MLI. Understanding itch: an update on mediators and mechanisms of pruritus. *Indian J Dermatol Venereol Leprol* (2014) 80:106–14. doi: 10.4103/0378-6323.129377

31. Opasawatchai A, Yolwong W, Thuncharoen W, Inrueangsri N, Itsaradisaikul S, Sasisakulporn C, et al. Novel salivary gland allergens from tropical mosquito species and IgE reactivity in allergic patients. *World Allergy Organ J* (2020) 13(2):100099. doi: 10.1016/j.waojou.2020.100099

32. Calvo E, Mans BJ, Ribeiro JM, Andersen JF. Multifunctionality and mechanism of ligand binding in a mosquito antiinflammatory protein. *Proc Natl Acad Sci USA* (2009) 106(10):3728–33. doi: 10.1073/pnas.0813190106

33. Kuraishi Y, Ohtsuka E, Nakano T, Kawai S, Andoh T, Nojima H, et al. Possible involvement of 5-lipoxygenase metabolite in itch-associated response of mosquito allergy in mice. *J Pharmacol Sci* (2007) 105:41–7. doi: 10.1254/jphs.FP0070404

34. Demeure CE, Brahimi K, Hacini F, Marchand F, Péronet R, Huerre M, et al. Anopheles mosquito bites activate cutaneous mast cells leading to a local inflammatory response and lymph node hyperplasia. *J Immunol* (2005) 174(7):3932–40. doi: 10.4049/jimmunol.174.7.3932

35. Boppana VD, Thangamani S, Adler AJ, Wikel SK. SAAG-4 is a novel mosquito salivary protein that programmes host CD4+ T cells to express IL-4. *Parasit Immunol* (2009) 31:287–95. doi: 10.1111/j.1365-3024.2009.01096.x

36. Zeidner NS, Dolan MC, Massung R, Piesman J, Fish D. Coinfection with borrelia burgdorferi and the agent of human granulocytic ehrlichiosis suppresses IL-2 and IFNγ production and promotes an IL-4 response in C3H/HeJ mice. *Parasit Immunol* (2000) 22:581–8. doi: 10.1046/j.1365-3024.2000.00339.x

37. Storan ER, O'Gorman SM, McDonald ID, Steinhoff M. Role of cytokines and chemokines in itch. *Handb Exp Pharmacol* (2015) 226:163–76. doi: 10.1007/978-3-662-44605-8_9

38. Namkung JH, Lee JE, Kim E, Cho HJ, Kim S, Shin ES, et al. IL-5 and IL-5 receptor alpha polymorphisms are associated with atopic dermatitis in koreans. *Allergy* (2007) 62:934–42. doi: 10.1111/j.1398-9995.2007.01445.x

39. Kimura M, Tsuruta S, Yoshida T. Correlation of house dust mite–specific lymphocyte proliferation with IL-5 production, eosinophilia, and the severity of symptoms in infants with atopic dermatitis. *J Allergy Clin Immunol* (1998) 101:84–9. doi: 10.1016/S0091-6749(98)70197-6

40. Gandhi NA, Pirozzi G, Graham NM. Commonality of the IL-4/IL-13 pathway in atopic diseases. *Expert Rev Clin Immunol* (2017) 13:425–37. doi: 10.1080/1744666X.2017.1298443

41. Peng Z, Simons F, Estelle R. Advances in mosquito allergy. *Curr Opin Allergy Clin Immunol* (2007) 7(4):350–4. doi: 10.1097/ACI.0b013e328259c313

42. Steen CJ, Carbonaro PA, Schwartz RA. Arthropods in dermatology. *J Am Acad Dermatol* (2004) 50(6):819–42. doi: 10.1016/j.jaad.2003.12.019

43. Simons FE, Peng Z. Skeeter syndrome. *J Allergy Clin Immunol* (1999) 104(3 Pt 1):705–7. doi: 10.1016/s0091-6749(99)70348-9

44. Tatsuno K, Fujiyama T, Matsuoka H, Shimauchi T, Ito T, Tokura Y. Clinical categories of exaggerated skin reactions to mosquito bites and their pathophysiology. *J Dermatol Sci* (2016) 82(3):145–52. doi: 10.1016/j.jdermsci.2016.04.010

45. Yavuz ST, Akin O, Koc O, Güngör A, Bolat A, Gülec M. Mosquito hypersensitivity may be associated with atopic background in children. *Allergol Immunopathol (Madr)* (2021) 49(6):67–72. doi: 10.15586/aei.v49i6.448

46. Peng Z, Beckett AN, Engler RJ, Hoffman DR, Ott NL, Simons FER. Immune responses to mosquito saliva in 14 individuals with acute systemic allergic reactions to mosquito bites. *J Allergy Clin Immunol* (2004) 114(5):1189–94. doi: 10.1016/j.jaci.2004.08.014

47. Mohd Adnan K. A review on respiratory allergy caused by insects. *Bioinformation* (2018) 14(9):540–53. doi: 10.6026/97320630014540

48. Meucci E, Radice A, Fassio F, Iorno MLC, Macchia D. Omalizumab for prevention of anaphylactic episodes in a patient with severe mosquito allergy. *Clin Case Rep* (2021) 9(10):e04935. doi: 10.1002/ccr3.4935

49. Scala E, Pirrotta L, Uasuf CG, Mistrello G, Amato S, Guerra EC, et al. Aedes communis reactivity is associated with bee venom hypersensitivity: an *in vitro* and *in vivo* study. *Int Arch Allergy Immunol* (2018) 176(2):101–5. doi: 10.1159/000488866

50. Cantillo JF, Puerta L, Lafosse-Marin S, Subiza JL, Caraballo L, Fernandez-Caldas E. Allergens involved in the cross-reactivity of aedes aegypti with other arthropods. *Ann Allergy Asthma Immunol* (2017) 118(6):710–8. doi: 10.1016/j.anai.2017.03.011

51. Cantillo JF, Puerta L, Fernandez-Caldas E, Subiza JL, Soria I, Wöhrl S, et al. Tropomyosins in mosquito and house dust mite cross-react at the humoral and cellular level. *Clin Exp Allergy* (2018) 48(10):1354–63. doi: 10.1111/cea.13229

52. Kanno H, Onodera H, Endo M, Maeda F, Chida S, Akasaka T, et al. Vascular lesion in a patient of chronic active Epstein-Barr virus infection with hypersensitivity to mosquito bites: vasculitis induced by mosquito bite with the infiltration of nonneoplastic Epstein-Barr virus-positive cells and subsequent development of natural killer/T-cell lymphoma with angiodestruction. *Hum Pathol* (2005) 36(2):212–8. doi: 10.1016/j.humpath.2004.11.005

53. Washio K, Oka T, Abdalkader L, Muraoka M, Shimada A, Oda M, et al. Gene expression analysis of hypersensitivity to mosquito bite, chronic active EBV infection and NK/T-lymphoma/leukemia. *Leuk Lymphoma* (2017) 58(11):2683–94. doi: 10.1080/10428194.2017.1304762

54. Suzuki D, Tsuji K, Yamamoto T, Fujii K, Iwatsuki K. Production of proinflammatory cytokines without invocation of cytotoxic effects by an Epstein-Barr virus-infected natural killer cell line established from a patient with hypersensitivity to mosquito bites. *Exp Hematol* (2010) 38(10):933–44. doi: 10.1016/j.exphem.2010.06.005

55. Lee WI, Lin JJ, Hsieh MY, Lin SJ, Jaing TH, Chen SH, et al. Immunologic difference between hypersensitivity to mosquito bite and hemophagocytic lymphohistiocytosis associated with Epstein-Barr virus infection. *PloS One* (2013) 8(10):e76711. doi: 10.1371/journal.pone.0076711

56. Koga C, Sugita K, Kabashima K, Matsuoka H, Nakamura M, Tokura Y. High responses of peripheral lymphocytes to mosquito salivary gland extracts in patients with wells syndrome. *J Am Acad Dermatol* (2010) 63(1):160–1. doi: 10.1016/j.jaad.2009.08.041

57. Barzilai A, Shpiro D, Goldberg I, Yacob-Hirsch Y, Diaz-Cascajo C, Meytes D, et al. Insect bite-like reaction in patients with hematologic malignant neoplasms. *Arch Dermatol* (1999) 135(12):1503–7. doi: 10.1001/archderm.135.12.1503

58. Wang T, Jia L, Liao W, Chen L, Chen X, Xiong Y, et al. Primary cutaneous diffuse large b-cell lymphoma, leg type: A study of clinicopathology, immunophenotype and gene rearrangement. *Zhonghua Bing Li Xue Za Zhi* (2015) 44(2):100–5.

59. Jiamton S, Kaewarpai T, Ekapo P, Kulthanan K, Hunnangkul S, Boitano JJ, et al. Total IgE, mosquito saliva specific IgE and CD4+ count in HIV-infected patients with and without pruritic papular eruptions. *Asian Pac J Allergy Immunol* (2014) 32(1):53–9. doi: 10.12932/AP0317.32.1.2014

60. Rosatelli JB, Roselino AM. Hyper-IgE, eosinophilia, and immediate cutaneous hypersensitivity to insect antigens in the pruritic papular eruption of human immunodeficiency virus. *Arch Dermatol* (2001) 137(5):672–3.

61. Crisp HC, Johnson KS. Mosquito allergy. *Ann Allergy Asthma Immunol* (2013) 110(2):65–9. doi: 10.1016/j.anai.2012.07.023

62. Diaz JH. Chemical and plant-based insect repellents: Efficacy, safety, and toxicity. *Wilderness Environ Med* (2016) 27(1):153–63. doi: 10.1016/j.wem.2015.11.007

63. Nguyen QD, Vu MN, Hebert AA. Insect repellents: An updated review for the clinician. *J Am Acad Dermatol* (2018) S0190-9622(18):32824–X. doi: 10.1016/j.jaad.2018.10.053

64. Centers for Disease Control and Prevention. *N,N-Diethyl-meta-Toluamide (DEET) - ToxFAQs™. U.S. department of health and human services* (2015). Available at: https://www.atsdr.cdc.gov/toxfaqs/tfacts185.pdf.

65. Zhang X, Zhang T, Ren X, Chen X, Wang S, Qin C. Pyrethroids toxicity to Male reproductive system and offspring as a function of oxidative stress induction: Rodent studies. *Front Endocrinol (Lausanne)* (2021) 12:656106. doi: 10.3389/fendo.2021.656106

66. Hołyńska-Iwan I, Szewczyk-Golec K. Pyrethroids: How they affect human and animal health? *Med (Kaunas)* (2020) 56(11):582. doi: 10.3390/medicina56110582

67. Drago B, Shah NS, Shah SH. Acute permethrin neurotoxicity: Variable presentations, high index of suspicion. *Toxicol Rep* (2014) 1:1026–8. doi: 10.1016/j.toxrep.2014.09.007

68. Antwi FB, Shama LM, Peterson RKD. Risk assessments for the insect repellents DEET and picaridin. *Regul Toxicol Pharmacol* (2008) 51:31–6. doi: 10.1016/j.yrtph.2008.03.002

69. Swale DR, Bloomquist JR. Is DEET a dangerous neurotoxicant? *Pest Manag Sci* (2019) 75(8):2068–70. doi: 10.1002/ps.5476

70. Olatunbosun-Oduola A, Abba E, Adelaja O, Taiwo-Ande A, Poloma-Yoriyo K, Samson-Awolola T. Widespread report of multiple insecticide resistance in anopheles gambiae s.l. mosquitoes in eight communities in southern gombe, north-Eastern Nigeria. *J Arthropod Borne Dis* (2019) 13(1):50–61.

71. Amelia-Yap ZH, Chen CD, Sofian-Azirun M, Low VL. Pyrethroid resistance in the dengue vector aedes aegypti in southeast Asia: present situation and prospects for management. *Parasit Vectors* (2018) 11(1):332. doi: 10.1186/s13071-018-2899-0

72. Scheinfeld N. Picaridin: A new insect repellent. *J Drugs Dermatol* (2004) 3(1):59–60.

73. Badawi A, El Halawany M, Latif R. A pilot clinical study on thiamine hydrochloride as a new mosquito repellent: Determination of the minimum effective dose on human skin. *Biol Pharm Bull* (2020) 43(2):284–8. doi: 10.1248/bpb.b19-00538

74. Halawany ME, Latif R, Badawi A. The potential of a site-specific delivery of thiamine hydrochloride as a novel insect repellent exerting long-term protection on human skin: *In-vitro, ex-vivo* study and clinical assessment. *J Pharm Sci* (2021) 110(11):3659–69. doi: 10.1016/j.xphs.2021.07.017

75. Castilho CJ, Li D, Liu M, Liu Y, Gao H, Hurt RH. Mosquito bite prevention through graphene barrier layers. *Proc Natl Acad Sci U S A* (2019) 116(37):18304–9. doi: 10.1073/pnas.1906612116

76. Conway MJ. Type I hypersensitivity promotes aedes aegypti blood feeding. *Sci Rep* (2021) 11(1):14891. doi: 10.1038/s41598-021-94416-w

77. Karppinen A, Brummer-Korvenkontio H, Reunala T, Izquierdo I. Rupatadine 10 mg in the treatment of immediate mosquito-bite allergy. *J Eur Acad Dermatol Venereol* (2012) 26(7):919–22. doi: 10.1111/j.1468-3083.2012.04543.x

78. Karppinen A, Brummer-Korvenkontio H, Petman L, Kautiainen H, Hervé JP, Reunala T. Levocetirizine for treatment of immediate and delayed mosquito bite reactions. *Acta Derm Venereol* (2006) 86(4):329–31. doi: 10.2340/00015555-0085

79. Reunala T, Brummer-Korvenkontio H, Karppinen A, Coulie P, Palosuo T. Treatment of mosquito bites with cetirizine. *Clin Exp Allergy* (1993) 23(1):72–5. doi: 10.1111/j.1365-2222.1993.tb02487.x

80. Karppinen A, Kautiainen H, Reunala T, Petman L, Reunala T, Brummer-Korvenkontio H. Loratadine in the treatment of mosquito-bite-sensitive children. *Allergy* (2000) 55(7):668–71. doi: 10.1034/j.1398-9995.2000.00609.x

81. Karppinen A, Kautiainen H, Petman L, Burri P, Reunala T. Comparison of cetirizine, ebastine and loratadine in the treatment of immediate mosquito-bite allergy. *Allergy* (2002) 57(6):534–7. doi: 10.1034/j.1398-9995.2002.13201.x

82. Yosipovitch G, Duque MI, Fast K, Dawn AG, Coghill RC. Scratching and noxious heat stimuli inhibit itch in humans: a psychophysical study. *Br J Dermatol* (2007) 156(4):629–34. doi: 10.1111/j.1365-2133.2006.07711.x

83. Yosipovitch G, Fast K, Bernhard JD. Noxious heat and scratching decrease histamine-induced itch and skin blood flow. *J Invest Dermatol* (2005) 125(6):1268–72. doi: 10.1111/j.0022-202X.2005.23942.x

84. Müller C, Großjohann B, Fischer L. The use of concentrated heat after insect bites/stings as an alternative to reduce swelling, pain, and pruritus: an open cohort-study at German beaches and bathing-lakes. *Clin Cosmet Investig Dermatol* (2011) 4:191–6. doi: 10.2147/CCID.S27825

85. *Evaluation of automatic class III designation (de novo) for zap-it!* . Available at: https://www.accessdata.fda.gov/cdrh_docs/reviews/DEN100024.pdf (Accessed January 29, 2022).

86. Palkar R, Ongun S, Catich E, Li N, Borad N, Sarkisian A, et al. Cooling relief of acute and chronic itch requires TRPM8 channels and neurons. *J Invest Dermatol* (2018) 138(6):1391–9. doi: 10.1016/j.jid.2017.12.025

87. Hill N, Stam C, Tuinder S, van Haselen RA. A placebo controlled clinical trial investigating the efficacy of a homeopathic after-bite gel in reducing mosquito bite induced erythema. *Eur J Clin Pharmacol* (1995) 49:103–8. doi: 10.1007/BF00192367

88. Srivastava D, Singh BP, Sudha VT, Arora N, Gaur SN. Immunotherapy with mosquito (Culex quinquefasciatus) extract: a double-blind, placebo-controlled study. *Ann Allergy Asthma Immunol* (2007) 99(3):273–80. doi: 10.1016/S1081-1206(10)60664-3

89. McCormack DR, Salata KF, Hershey JN, Carpenter GB, Engler RJ. Mosquito bite anaphylaxis: immunotherapy with whole body extracts. *Ann Allergy Asthma Immunol* (1995) 74(1):39–44.

90. Tager A, Lass N, Gold D, Lengy J. Studies on *Culex pipiens molestus* in Israel. *Int Arch Allergy Immunol* (1969) 36:408–14. doi: 10.1159/000230761

91. Benaim-Pinto C, Fassrainer A. Intradermal immunotherapy in children with severe skin inflammatory reactions to aedes aegypti and culex quinquefasciatus mosquito bites. *Int J Dermatol* (1990) 29(8):600–1. doi: 10.1111/j.1365-4362.1990.tb03479.x

92. Manrique MA, González-Díaz S, Arias-Cruz A, Hernandez M, Gallego C, Garcia-Calderin D, et al. Efficacy of immunotherapy with allergenic extract of aedes aegypti in the treatment of Large local reaction to mosquito bites in children. *World Allergy Organ J* (2012) 5(2):164. doi: 10.1097/01.WOX.0000411578.60734.e0

93. Ridolo E, Montagni M, Incorvaia C, Senna G, Passalacqua G. Orphan immunotherapies for allergic diseases. *Ann Allergy Asthma Immunol* (2016) 116(3):194–8. doi: 10.1016/j.anai.2015.12.031

94. McCracken MK, Christofferson RC, Grasperge BJ, Calvo E, Chisenhall DM, Mores CN. Aedes aegypti salivary protein "aegyptin" co-inoculation modulates dengue virus infection in the vertebrate host. *Virology* (2014) 468-470:133–9. doi: 10.1016/j.virol.2014.07.019

95. Schneider BS, Soong L, Coffey LL, Stevenson HL, McGee CE, Higgs S. Aedes aegypti saliva alters leukocyte recruitment and cytokine signaling by antigen-presenting cells during West Nile virus infection. *PloS One* (2010) 5:e11704. doi: 10.1371/journal.pone.0011704

96. Manning JE, Morens DM, Kamhawi S, Valenzuela JG, Memoli M. Mosquito saliva: The hope for a universal arbovirus vaccine? *J Infect Dis* (2018) 218(1):7–15. doi: 10.1093/infdis/jiy179

97. Pingen M, Bryden SR, Pondeville E, Schnettler E, Kohl A, Merits A, et al. Host inflammatory response to mosquito bites enhances the severity of arbovirus infection. *Immunity* (2016) 44:1455–69. doi: 10.1016/j.immuni.2016.06.002

98. Manning JE, Oliveira F, Coutinho-Abreu IV, Herbert S, Meneses C, Kamhawi S, et al. Safety and immunogenicity of a mosquito saliva peptide-based vaccine: a randomised, placebo-controlled, double-blind, phase 1 trial. *Lancet* (2020) 395(10242):1998–2007. doi: 10.1016/S0140-6736(20)31048-5

frontiers | Frontiers in Immunology

TYPE Original Research
PUBLISHED 20 October 2022
DOI 10.3389/fimmu.2022.1020721

OPEN ACCESS

EDITED BY
Oded Shamriz,
Hadassah Medical Center, Israel

REVIEWED BY
Esraah Alharris,
University of Al-Qadisiyah, Iraq
Xiaoxiang Chen,
Shanghai Jiao Tong University, China

*CORRESPONDENCE
Jin Fu
fujin@hrbmu.edu.cn
Chaohan Xu
chaohanxu@hrbmu.edu.cn

SPECIALTY SECTION
This article was submitted to Autoimmune and Autoinflammatory Disorders : Autoimmune Disorders, a section of the journal Frontiers in Immunology

RECEIVED 16 August 2022
ACCEPTED 03 October 2022
PUBLISHED 20 October 2022

CITATION
Yin X, Rang X, Hong X, Zhou Y, Xu C and Fu J (2022) Immune cells transcriptome-based drug repositioning for multiple sclerosis. *Front. Immunol.* 13:1020721. doi: 10.3389/fimmu.2022.1020721

Immune cells transcriptome-based drug repositioning for multiple sclerosis

Xinyue Yin[1], Xinming Rang[1], Xiangxiang Hong[1], Yinglian Zhou[1], Chaohan Xu[2*] and Jin Fu[1*]

[1]Department of Neurology, the Second Affiliated Hospital of Harbin Medical University, Harbin, China, [2]College of Bioinformatics Science and Technology, Harbin Medical University, Harbin, China

Objective: Finding target genes and target pathways of existing drugs for drug repositioning in multiple sclerosis (MS) based on transcriptomic changes in MS immune cells.

Materials and Methods: Based on transcriptome data from Gene Expression Omnibus (GEO) database, differentially expressed genes (DEGs) in MS patients without treatment were identified by bioinformatics analysis according to the type of immune cells, as well as DEGs in MS patients before and after drug administration. Hub target genes of the drug for MS were analyzed by constructing the protein-protein interaction network, and candidate drugs targeting 2 or more hub target genes were obtained through the connectivity map (CMap) database and Drugbank database. Then, the enriched pathways of MS patients without treatment and the enriched pathways of MS patients before and after drug administration were intersected to obtain the target pathways of the drug for MS, and the candidate drugs targeting 2 or more target pathways were obtained through Kyoto Encyclopedia of Genes and Genomes (KEGG) database.

Results: We obtained 50 hub target genes for $CD4^+$ T cells in Fingolimod for MS, 15 hub target genes for Plasmacytoid dendritic cells (pDCs) and 7 hub target genes for Peripheral blood mononuclear cells (PBMC) in interferon-β (IFN-β) for MS. 6 candidate drugs targeting two or more hub targets (Fostamatinib, Copper, Artenimol, Phenethyl isothiocyanate, Aspirin and Zinc) were obtained. In addition, we obtained 4 target pathways for $CD19^+$ B cells and 15 target pathways for $CD4^+$ T cells in Fingolimod for MS, 7 target pathways for pDCs and 6 target pathways for PBMC in IFN-β for MS, most of which belong to the immune system and viral infectious disease pathways. We obtained 69 candidate drugs targeting two target pathways.

Conclusion: We found that applying candidate drugs that target both the "PI3K-Akt signaling pathway" and "Chemokine signaling pathway" (e.g., Nemiralisib and Umbralisib) or applying tyrosine kinase inhibitors (e.g., Fostamatinib) may be potential therapies for the treatment of MS.

KEYWORDS

multiple sclerosis, transcriptome, drug repositioning, differentially expressed gene, candidate drug

Introduction

Multiple sclerosis (MS) is one of the most common idiopathic inflammatory demyelinating diseases, involving the white matter of the central nervous system (CNS), with widely distributed lesions, high recurrence rate, and disability rate (1). The number of MS patients worldwide has increased to 2.8 million in 2020, the global prevalence rate was 35.9 per 100,000 people [95%CI: 35.87, 35.95], and the incidence rate was 2.1 per 100,000 persons/year [95%CI: 2.09, 2.12] (2). However, the treatment effect of MS patients is not ideal. Its effective prevention and treatment are urgent problems that need to be solved clinically.

For patients with poor prognosis and recurrent MS, the use of disease-modifying therapies (DMTs) should be considered early (3). There are currently more than a dozen DMTs approved for the treatment of MS, such as subcutaneous injection of Interferon-β (IFN-β), Fingolimod, Teriflunomide, Ocrelizumab, Natalizumab, etc. However, the medicines for the treatment of MS are expensive, have different degrees of side effects, and the control of the recurrence rate of MS is not ideal (4). Therefore, it is very important to find effective MS drugs.

Abbreviations: MS multiple sclerosis; GEO Gene Expression Omnibus; DEGs differentially expressed genes; CMap connectivity map; KEGG Kyoto Encyclopedia of Genes and Genomes; pDCs plasmacytoid dendritic cells; PBMC peripheral blood mononuclear cells; IFN-β interferon-β; CNS central nervous system; DMTs disease-modifying therapies; BBB blood-brain barrier BCR B-cell receptor; S1P sphingosine-1 phosphate; ARR annualized relapse rate; RRMS relapsing-remitting multiple sclerosis; FC fold-change; PPI protein-protein interaction; PRIDE; Proteomics Identifications database; EAE experimental allergic encephalomyelitis; Glut1 glucose transporter type 1; OPCs oligodendrocyte precursor cells; OLs oligodendrocytes; PIP3 phosphatidylinositol-3,4,5- trisphosphate; GPCR G protein-coupled receptors; TLR9 toll-like receptor 9; LCFAs long-chain fatty acids; SCFAs short-chain fatty acids; SYK spleen tyrosine kinase; TKI tyrosine kinase inhibitor; ECTRIMS European Committee for Treatment and Research in Multiple Sclerosis; BTKi Bruton's tyrosine kinase inhibitor; SEL slowly expanding lesion; ITP idiopathic thrombocytopenic purpura.

Traditional drug development has the characteristics of high cost, low success rate, lengthy development cycles, and heavy financial burden on patients. Drug repositioning is inspired by Sildenafil and Azidothymidine, which refers to the discovery of new indications of existing drugs in addition to the original indications. It is an increasingly attractive treatment discovery model, which not only saves time and money, but also has the advantage of already having been tested for safety, dosage, and toxicity (5, 6). There are no previous reports in the literature regarding the application of bioinformatic analysis to MS drug repositioning. Therefore, we aim to apply this method to determine candidate drugs for the treatment of MS.

The etiology and pathogenesis of MS are not fully understood, but scholars generally believe that MS is an autoimmune disease mediated by myelin-specific $CD4^+$ T cell attacks on CNS myelin sheaths triggered by environmental and infectious factors based on genetic susceptibility (7). $CD4^+$ T cells can be divided into 4 subpopulations, namely Th1, Th2, Th17 and Treg, according to their different functions. Th1 cells trigger neuroinflammatory responses in MS pathogenesis, while Th2 cells may have a protective role in suppressing neuroinflammation in MS pathogenesis. Th17 cells promote blood-brain barrier (BBB) injury and enter the CNS to trigger neuroinflammation, while Treg cells have immunosuppressive functions that downregulate the immune response. The tilt of the Th1/Th2 axis toward Th1 and the tilt of the Th17/Treg axis toward Th17 are both strongly associated with the development of MS (8). In recent years, the effective application of anti-CD20 therapy has also revealed an important role of B cells in the pathogenesis of MS (9). B cells play an important role in MS pathogenesis through antibody-dependent and antibody-independent mechanisms (10). Antibody-dependent mechanisms promote MS pathogenesis by producing autoantibodies against specific CNS tissues, while antibody-independent mechanisms promote MS pathogenesis by inducing B-cell receptor (BCR) internalization of autoantigens and presentation to specific CNS pathogenic T cells to promote T-cell activation, by producing cytokines and by forming ectopic lymphoid tissue (11). In addition, plasmacytoid dendritic cells (pDCs) in MS patients may also be involved in MS pathogenesis

due to their pro-inflammatory state, their migratory phenotype, and the influence of genetic risk factors (12). Therefore, our study analyzed the transcriptomic data of the above-mentioned immune cells from MS patients. In terms of treatment, DMTs are mainly used for MS remission, including IFN-β, Glatiramer acetate, Teriflunomide, Dimethyl fumarate, Fingolimod, Ocrelizumab, Alemtuzumab, Natalizumab, and Mitoxantrone, etc. Among them, IFN-β and Fingolimod are widely used in early clinical practice with significant efficacy. IFN-β has antiviral and immunomodulatory effects and inhibits T cell migration by disrupting the balance of anti-inflammatory Th2 cells and by blocking metalloproteinases and adhesion molecules (13). Fingolimod is an inhibitor of the sphingosine-1 phosphate (S1P) receptor and inhibits S1P-mediated T-lymphocyte migration, thus favoring the retention of T-lymphocytes in lymph nodes and triggering a "homing response" of peripheral lymphocytes and thus immunosuppression (14). Patients with MS treated with Fingolimod or IFN-β have a significantly lower annualized relapse rate (ARR) (15, 16), so our analysis is reliable using the currently reported transcriptomic dataset of MS patients treated with these two drugs. We obtained the original data from Gene Expression Omnibus (GEO) database, analyzed the target genes and pathways in drug treatment of MS, and obtained potential MS candidate drugs targeting these target genes/pathways based on the connectivity map (CMap) database, Drugbank database and Kyoto Encyclopedia of Genes and Genomes (KEGG) database. Our study may help provide clues to potential MS therapeutic strategies.

Materials and methods

Identification of MS transcriptome data

A total of 295 sets of MS transcriptomic data were obtained in the GEO database (https://www.ncbi.nlm.nih.gov/geo/), and transcriptomic datasets of MS patients without treatment, as well as transcriptomic datasets of MS patients before and after treatment, were screened according to the following criteria (17). Inclusion criteria: ① The study samples were immune cells of patients with relapsing-remitting multiple sclerosis (RRMS); ② The number of samples in the experimental group and the control group should not be less than 3 (First, the transcriptome datasets of MS patients without treatment were screened, in which MS patients were the experimental group and healthy people were the control group; second, the transcriptome datasets of MS patients before and after medication were screened, in which the experimental group was the MS patients after the treatment, and the control group was the MS patients before the treatment); MS patients without treatment and MS patients before the treatment have not received DMTs or have not received DMTs for at least one month before the start of the experiment; There is an additional inclusion criteria for the transcriptome datasets of MS patients before and after medication: ④ The drugs used for MS patients before and after the treatment were widely used clinically and have significant effects.

Transcriptome data preprocessing

The mRNA raw data (CEL files) and the annotation file of the sequencing platform were downloaded from the GEO database and processed using the R language. Due to the large difference between the data, the data were log2 *t*ransformed and normalized using quantile normalization.

Identification of the differentially expressed genes

The R package "Limma" was used for linear fitting and difference analysis on each group of data to calculate the difference in gene expression between MS patients without treatment and the difference in gene expression of MS patients before and after medication (18). Differentially expressed genes (DEGs) were screened by $P < 0.05$ and fold-change (FC) > 1.2 or $0 < FC < 1/1.2$. When FC > 1.2, they were regarded as up-regulated DEGs and when $0 < FC < 1/1.2$, they were regarded as down-regulated DEGs.

Identification of target genes for drug treatment of MS

According to the type of immune cells, the up-regulated DEGs of MS patients without treatment and the down-regulated DEGs of MS patients before and after medication were intersected to obtain the up-regulated target genes for MS drug therapy, the down-regulated DEGs of MS patients without treatment and the up-regulated DEGs of MS patients before and after medication were intersected to obtain the down-regulated target genes for MS drug therapy.

Construction of protein-protein interaction network and identification of hub target genes for drug treatment of MS

According to the type of immune cells, the protein-protein interaction (PPI) network of target genes was constructed using the STRING database (https://cn.string-db.org/, version 11.5) (combined confidence score > 0.400), visualized by Cytoscape (https://cytoscape.org/, version 3.9.1) and the degree of nodes was calculated (19). Using the CytoHubba plugin in Cytoscape, the top 10% of nodes with the highest degree of PPI network connectivity were identified as hub target genes.

Identification of candidate drugs through CMap database and Drugbank database

Candidate drugs targeting hub target genes were identified through the CMap database (https://clue.io/) and Drugbank database (https://go.drugbank.com/) according to the different types of immune cells (Inclusion criteria: Approved/Investigational drugs) (20, 21). The drug-hub target gene network diagram was visualized through Cytoscape.

Pathway enrichment analysis of DEGs

The pathway enrichment analysis for the DEGs of MS patients without treatment and the DEGs of MS patients before and after the medication was performed using Rstudio (Ver.3.6.1) according to the different types of immune cells (22), and only the pathways with $P < 0.05$ were included. Then, the pathways of MS patients without treatment and the pathways of MS patients before and after medication were intersected to obtain the target pathways of MS treatment. According to the type of immune cells, calculate the types of DEGs of MS patients without treatment included in each target pathway, the types of DEGs of MS patients before and after medication included in each target pathway, and the types of common DEGs included in each target pathway, and identify the target pathways that were mainly targeted when these drugs were used to treat MS.

Identification of candidate drugs through the KEGG database

According to the type of immune cells, the candidate drugs targeting target pathways were obtained through the KEGG database (www.genome.jp/kegg/pathway.html) and drug-pathway interaction networks were conducted by Cytoscape (23).

Proteomic data validation

We extensively screened proteomic data of MS patients without treatment and MS patients before and after drug administration that applying liquid chromatography-tandem mass spectrometry (LC-MS/MS) for further validation through the Proteomics Identification Database (PRIDE, http://www.ebi.ac.uk/pride) (24), the GEO database and Google Scholar (https://scholar.google.com) (25). We only found PXD011785 and PXD028702 data from the PRIDE that could be used to validate the transcriptomic data of MS patients without treatment, both of which were protein-level data on $CD4^+$ T cells in MS patients without treatment (26, 27). Unfortunately, we did not find the proteomic dataset of MS patients before and after drug administration, so only the transcriptomic data of MS patients without treatment on $CD4^+$ T cells were validated in this article.

The workflow of the study was shown in Figure 1.

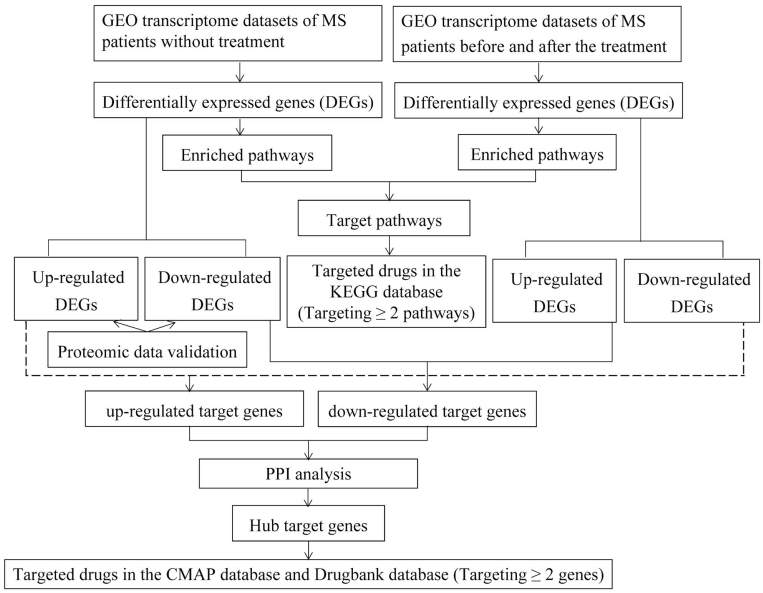

FIGURE 1
The workflow of the study.

Results

Identification of DEGs of MS patients without treatment and DEGs before and after IFN-β or Fingolimod treatment

4 sets of transcriptome datasets of $CD19^+$ B cells, $CD4^+$ T cells, pDCs, and Peripheral blood mononuclear cells (PBMC) from MS patients without treatment were obtained (GSE117935 (28), GSE172009 (29), GSE37750 (30), GSE41890 (31). Then, according to the type of $CD19^+$ B cells, $CD4^+$ T cells, pDCs and PBMC, 5142 DEGs of MS patients without treatment were obtained according to the standards of $P < 0.05$ and FC > 1.2 or 0 < FC < 1/1.2 ($CD19^+$ B cells: 293 DEGs; $CD4^+$ T cells: 2032 DEGs; pDCs: 1712 DEGs; PBMC: 1561 DEGs) (Table 1; Supplementary Table S1). Furthermore, we could only obtain the transcriptome datasets of MS patients before and after the application of IFN-β or Fingolimod. There were 2 sets of transcriptome datasets of $CD19^+$ B cells and $CD4^+$ T cells from MS patients before and after the application of Fingolimod and 2 sets of transcriptome datasets of pDCs and PBMC from MS patients before and after the application of IFN-β (GSE81604 (32, 33), GSE73079 (32–34), GSE37750 (30), GSE33464 (35, 36)). According to the type of $CD19^+$ B cells, $CD4^+$ T cells, pDCs and PBMC, 14300 DEGs in MS patients before and after the application of Fingolimod and IFN-β were obtained according to the standards of $P < 0.05$ and FC > 1.2 or 0 < FC < 1/1.2 ($CD19^+$ B cells: 1164 DEGs; $CD4^+$ T cells: 13201 DEGs; pDCs: 668 DEGs; PBMC: 593 DEGs) (Table 2, Supplementary Table S2).

Identification of hub target genes in MS patients before and after the application of Fingolimod or IFN-β

According to the type of $CD19^+$ B cells, $CD4^+$ T cells, pDCs, and PBMC, a total of 164 up-regulated target genes and 649 down-regulated target genes were obtained (Figure 2; Supplementary Table S3). The types of target genes targeting $CD4^+$ T cells were the most and mainly focused on down-regulated target genes. A PPI network of 560 nodes and 2386 edges was constructed using target genes of $CD4^+$ T cells from MS patients after the application of Fingolimod, and 50 hub target genes (top 10%: degree ≥ 21) were identified by PPI analysis and visualization with Cytoscape. In addition, a PPI network with 138 nodes and 115 edges was constructed using target genes targeting pDCs from MS patients after the application of IFN-β, and 15 hub target genes were identified (top 10%: degree ≥ 6). A PPI network with 73 nodes and 40 edges was constructed using target genes targeting PBMC from MS patients after the application of IFN-β, and 7 hub target genes (top 10%: degree ≥ 3) were identified (Figure 3).

Identification of potential candidate drugs for the treatment of MS through the CMap database and Drugbank database

A total of 193 candidate drugs ($CD4^+$ T cells: 51; pDCs: 13; PBMC: 134) targeting hub target genes were obtained through

TABLE 1 Transcriptome datasets of MS patients without treatment.

ID	Disease	Platform ID	Case/control	Sample	Publish time	DEG	
						Up-regulated DEG	Down-regulated DEG
GSE117935	RRMS	GPL5175	10/10	$CD19^+$ B cells	2018	216	77
GSE172009	RRMS	GPL20301 GPL24676	4/4	$CD4^+$ T cells	2021	163	1869
GSE37750	RRMS	GPL570	9/8	pDCs	2015	792	920
GSE41890	RRMS	GPL6244	8/4	Peripheral blood leukocytes	2013	883	678

TABLE 2 Transcriptome datasets of MS patients before and after medication.

ID	Disease	Platform ID	Drug	Case/control	Sample	Publish time	DEG	
							Up-regulated DEG	Down-regulated DEG
GSE81604	RRMS	GPL17586	Fingolimod	5/5	$CD19^+$ B cells	2016	723	441
GSE73079	RRMS	GPL17586	Fingolimod	5/5	$CD4^+$ T cells	2015	4162	9039
GSE37750	RRMS	GPL570	IFN-β	9/9	pDCs	2015	263	405
GSE33464	RRMS	GPL14837	IFN-β	12/12	PBMC	2011	296	297

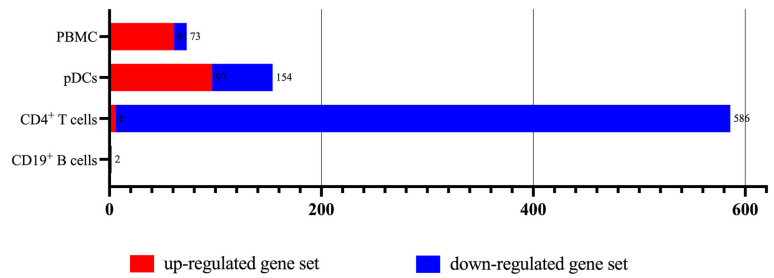

FIGURE 2
The types of up-regulated and down-regulated target genes for $CD19^+$ B cells, $CD4^+$ T cells, pDCs, and PBMC in MS patients treated with Fingolimod or IFN-β.

the CMap database and Drugbank database according to the types of $CD4^+$ T cells, pDCs, and PBMC (Figure 4), most of which belonged to antineoplastic drugs and 6 candidates targeted more than 2 hub target genes (Table 3).

Identification of target pathways for Fingolimod and IFN-β in the treatment of MS

According to the type of $CD19^+$ B cells, $CD4^+$ T cells, pDCs, and PBMC, a total of 139 pathways were enriched at $P < 0.05$ for DEGs in MS patients without treatment (Supplementary Table S4), and a total of 112 pathways were enriched at $P < 0.05$ for DEGs in MS patients before and after Fingolimod or IFN-β application (Supplementary Table S5). The 28 target pathways of Fingolimod and IFN-β for MS treatment were obtained by taking the intersection processing (Tables 4, 5). The target pathways were classified according to the classification of pathways in the KEGG database into immune system pathways (22%), nervous system pathways (11%), endocrine system pathways (7%), excretory system pathways (4%), viral infectious disease pathways (22%), bacterial infectious disease pathways (7%), parasitic infectious disease pathways (4%), specific types of cancer pathways (4%), metabolism pathways (7%), cellular process pathway (4%), genetic information processing pathway (4%) and environmental information processing pathway (4%) (Figure 5). Among them, the immune system pathways and viral infectious disease pathways accounted for the largest proportion. The main target pathways of Fingolimod and IFN-β for MS treatment were identified according to the type of $CD19^+$ B cells, $CD4^+$ T cells, pDCs, and PBMC (Figure 6), where the main target pathway of Fingolimod for MS treatment against $CD19^+$ B cells was "Yersinia infection", the main target pathways for $CD4^+$ T cells in Fingolimod therapy for MS were "Endocytosis", "PI3K-Akt signaling pathway", "Chemokine signaling pathway" and "Neurotrophin signaling pathway", the main target pathways for pDCs in MS treatment with IFN-β were "Influenza A", "Epstein-Barr virus infection" and "NOD-like receptor signaling pathway", the main target pathways for PBMC in MS treatment with IFN-β were "Fatty acid metabolism" and "Hepatitis C".

Identification of potential candidate drugs for the treatment of MS based on the KEGG database

Our approach is based on two biological assumptions: first, proteins always have cascading effects in pathways, not just acting alone; second, drugs exert therapeutic effects by modulating pathways involved in disease pathology, rather than directly targeting disease-related proteins (37), so we considered drug candidates that target pathways as potential therapeutic agents for MS. A total of 1062 candidate drugs targeting target pathways were obtained through the KEGG database ($CD19^+$ B cells: 33; $CD4^+$ T cells: 495; pDCs: 26; PBMC: 304) (Supplementary Table S6), most of which were antineoplastic and immunosuppressive drugs. There were 58 candidate drugs targeting 2 target pathways (Supplementary Table S7).

Proteomic data validation

From a biological point of view, the transcriptome represents the intermediate state of gene expression, while proteins are the direct functional performers of the organism, and therefore the study of protein expression levels has an irreplaceable advantage. In the PXD011785 data, a total of 228 proteins were differentially expressed between MS patients and healthy individuals ($P < 0.05$), of which 24 proteins encoded genes consistent with the DEGs we obtained (Supplementary Table S8). Among them, 12 were regulated with the same trend at transcriptome level and protein level (TES, GABPA, ARF6, VCL, TYMP, LIMS1, YWHAG, ATP6V1A, PDIA3, ATP2A2, TPM4, CLTC). Among these 24 overlapping coding genes, YWHAG was involved in the "PI3K-Akt signaling pathway". A total of 10

10.3389/fimmu.2022.1020721

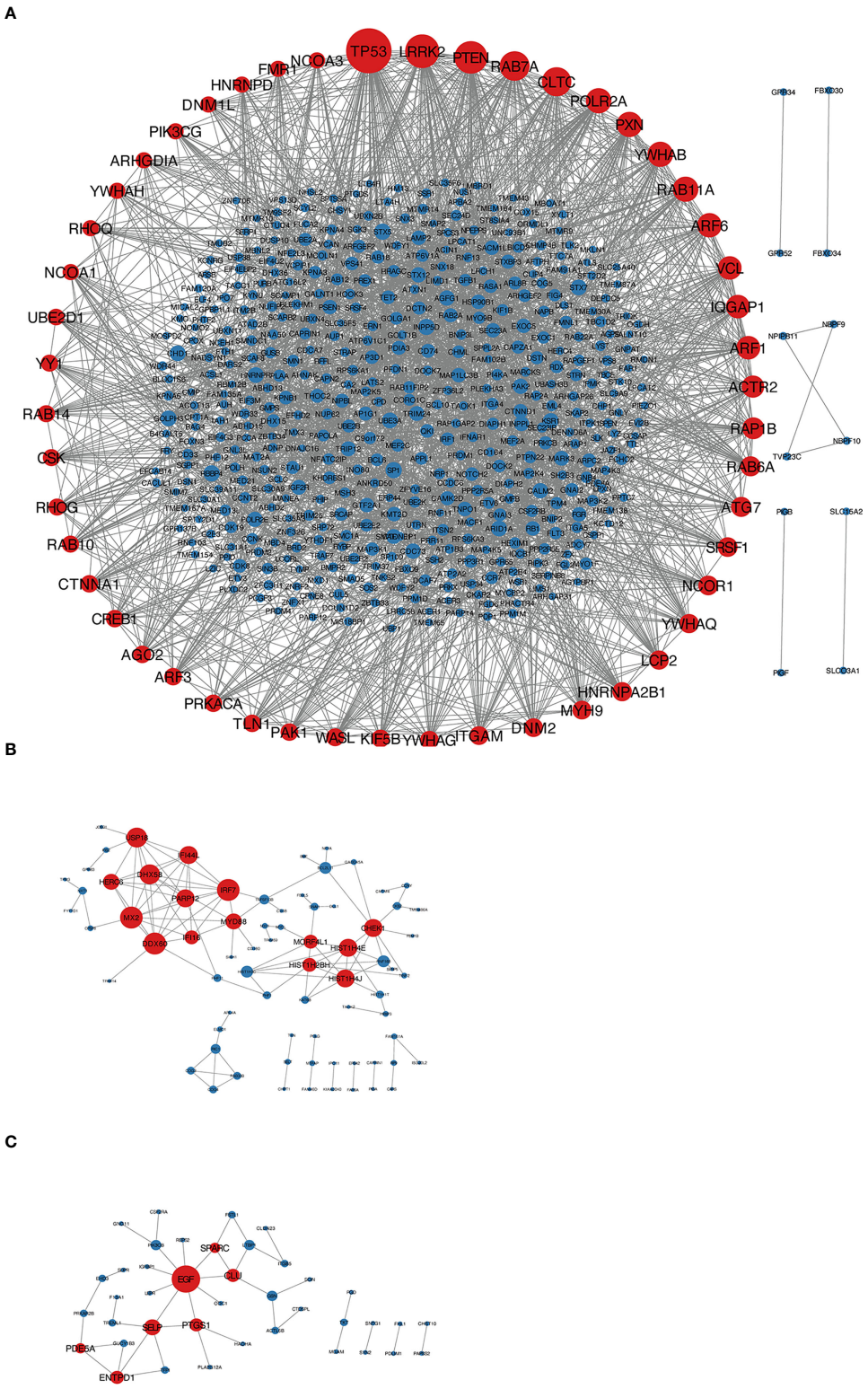

FIGURE 3
(A) Target genes of CD4$^+$ T cells in MS patients treated with Fingolimod, red nodes were hub target genes; **(B)** target genes of pDCs in MS patients treated with IFN-β, red nodes were hub target genes; **(C)** target genes of PBMC in MS patients treated with IFN-β, red nodes were hub target genes.

10.3389/fimmu.2022.1020721

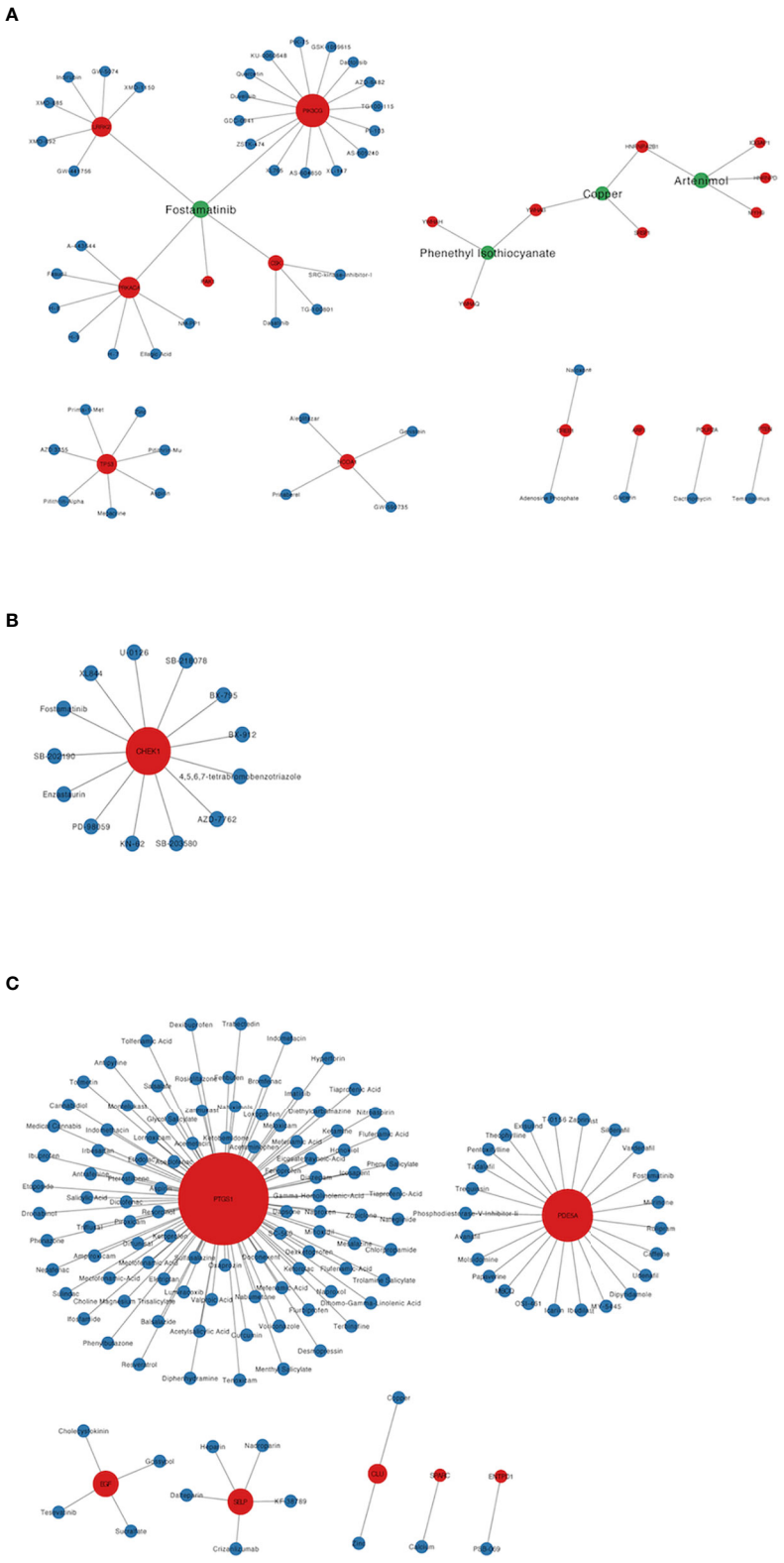

FIGURE 4
Candidate drugs targeting hub target genes were identified based on the CMap database and Drugbank database. Red nodes represent hub target genes, blue nodes represent candidate drugs targeting hub target genes, and green nodes represent candidate drugs targeting 2 or more than 2 hub target genes. **(A)** The candidate drugs targeting hub target genes of CD4+ T cells in MS patients treated with Fingolimod. **(B)** The candidate drugs targeting hub target genes of pDCs in MS patients treated with IFN-β. **(C)** The candidate drugs targeting hub target genes of PBMC in MS patients treated with IFN-β.

TABLE 3 The candidate drugs that target 2 or more than 2 hub target genes.

Drug	Target Gene	Effect	Sample
Fostamatinib	LRRK2, PAK1, PRKACA, CSK, PIK3CG, CHEK1, PDE5A	Antineoplastic, Immunomodulator, Spleen tyrosine kinase inhibitor	CD4+ T cells, pDCs, PBMC
Copper	YWHAB, SRSF1, HNRNPA2B1, CLU	Supplement	CD4+ T cells, PBMC
Artenimol	IQGAP1, HNRNPA2B1, MYH9, HNRNPD	Antimalarial	CD4+ T cells
Phenethyl Isothiocyanate	YWHAB, YWHAQ, YWHAH	Antineoplastic	CD4+ T cells
Aspirin	TP53, PTGS1	Analgesic, Anti-inflammatory, Antipyretic, Antirheumatic, Antiplatelet, Cyclooxygenase inhibitor	CD4+ T cells, PBMC
Zinc	TP53, CLU	Supplement	CD4+ T cells, PBMC

pathways were enriched for the 24 overlapping coding genes at $P < 0.05$ (Supplementary Table S9), in which the "Endocytosis" pathway was enriched in both transcriptome and proteome, further validating the confidence of the transcriptome data. In the PXD028702 data, a total of 18 proteins were differentially expressed (adjusted $p \leq 0.05$) between MS patients and healthy individuals (DPH6, GNPDA2, ACAD8, CORO2A, PHF20L1, SRA1, EPC1, PTPN13, DENND10, LAMTOR5, NRDE2, PSMD5, GOPC, ASPH, TCEA3, RHOC, TYK2, BORCS6). With a more stringent threshold, we still obtained 2 protein-coding genes (SRA1 and DENND1) that were consistent with the DEGs we obtained.

Discussion

MS is considered to be a chronic inflammatory and demyelinating disease of the CNS, and various immune cells play a crucial role in the development of MS (38). In this study, we obtained the target genes and target pathways of Fingolimod and IFN-β for MS treatment based on immune cell transcriptomic datasets of MS patients without treatment and immune cell transcriptomic datasets of MS patients before and after application of Fingolimod or IFN-β, and identified MS candidate drugs targeting hub target genes and target pathways.

Target genes and target pathways for $CD4^+$ T cells in the treatment of MS with Fingolimod

15 target pathways and 586 target genes (6 up-regulated target genes and 580 down-regulated target genes) were obtained by the analysis of $CD4^+$ T cell transcriptomic data from MS patients without treatment and $CD4^+$ T cell transcriptomic data before and after Fingolimod treatment, suggesting that Fingolimod treatment for MS mainly targeted $CD4^+$ T cells, which was consistent with the mechanism that Fingolimod inhibited the migration of T lymphocytes to the CNS and thus relieved MS. Recent clinical trial data suggested that increased Th1/Th17 cells ($CD4^+$ T cell subpopulation) in CNS tissue, cerebrospinal fluid, and blood predominate in the pathogenesis of MS (8), so we focused on target genes and target pathways that target $CD4^+$ T cells.

TABLE 4 The number of enriched pathways of DEGs in MS patients without treatment, the number of enriched pathways of DEGs before and after application of Fingolimod or IFN-β, and the number of target pathways.

ID	Sample	Drug	Pathway	Target pathway
GSE117935	$CD19^+$ B cells	/	50	4
GSE81604		Fingolimod	24	
GSE172009	$CD4^+$ T cells	/	40	15
GSE73079		Fingolimod	75	
GSE37750	pDCs	/	54	7
GSE37750		IFN-β	20	
GSE41890	PBMC	/	58	6
GSE33464		IFN-β	19	

10.3389/fimmu.2022.1020721

TABLE 5 Target pathways of Fingolimod and IFN-β for MS.

Sample	Pathway ID	Pathway Name	Pathway Class
$CD19^+$ B cells	hsa04062	Chemokine signaling pathway	Organismal Systems (Immune system)
	hsa05135	Yersinia infection	Human Diseases (Infectious disease: bacterial)
	hsa05163	Human cytomegalovirus infection	Human Diseases (Infectious disease: viral)
	hsa04120	Ubiquitin mediated proteolysis	Genetic Information Processing (Folding, sorting and degradation)
$CD4^+$ T Cells	hsa04670	Leukocyte transendothelial migration	Organismal Systems (Immune system)
	hsa04611	Platelet activation	Organismal Systems (Immune system)
	hsa04062	Chemokine signaling pathway	Organismal Systems (Immune system)
	hsa04722	Neurotrophin signaling pathway	Organismal Systems (Nervous system)
	hsa04720	Long-term potentiation	Organismal Systems (Nervous system)
	hsa04728	Dopaminergic synapse	Organismal Systems (Nervous system)
	hsa04927	Cortisol synthesis and secretion	Organismal Systems (Endocrine system)
	hsa04935	Growth hormone synthesis, secretion and action	Organismal Systems (Endocrine system)
	hsa04962	Vasopressin-regulated water reabsorption	Organismal Systems (Excretory system)
	hsa05161	Hepatitis B	Human Diseases (Infectious disease: viral)
	hsa05135	Yersinia infection	Human Diseases (Infectious disease: bacterial)
	hsa05120	Epithelial cell signaling in Helicobacter pylori infection	Human Diseases (Infectious disease: bacterial)
	hsa04120	Ubiquitin mediated proteolysis	Genetic Information Processing (Folding, sorting and degradation)
	hsa04144	Endocytosis	Cellular Processes (catabolism)
	hsa04151	PI3K-Akt signaling pathway	Environmental Information Processing (Signal transduction)
pDCs	hsa04621	NOD-like receptor signaling pathway	Organismal Systems (Immune system)
	hsa04962	Vasopressin-regulated water reabsorption	Organismal Systems (Excretory system)
	hsa05164	Influenza A	Human Diseases (Infectious disease: viral)
	hsa05162	Measles	Human Diseases (Infectious disease: viral)
	hsa05169	Epstein-Barr virus infection	Human Diseases (Infectious disease: viral)
	hsa05142	Chagas disease	Human Diseases (Infectious disease: parasitic)
	hsa05216	Thyroid cancer	Human Diseases (Cancer: specific types)
PBMC	hsa04610	Complement and coagulation cascades	Organismal Systems (Immune system)
	hsa04640	Hematopoietic cell lineage	Organismal Systems (Immune system)
	hsa05160	Hepatitis C	Human Diseases (Infectious disease: viral)
	hsa00590	Arachidonic acid metabolism	Metabolism (Lipid metabolism)
	hsa00480	Glutathione metabolism	Metabolism (Metabolism of other amino acids)
	hsa01212	Fatty acid metabolism	

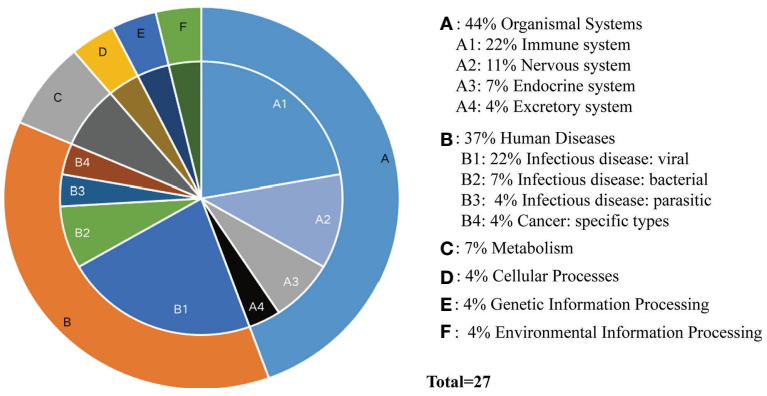

FIGURE 5
Classification of target pathways in MS patients treated with Fingolimod or IFN-β. **(A)** Organismal Systems; **(B)** Human Diseases; **(C)** Metabolism; **(D)** Cellular Processes; **(E)** Genetic Information Processing; **(F)** Environmental Information Processing. "Fatty acid metabolism" is not classified yet.

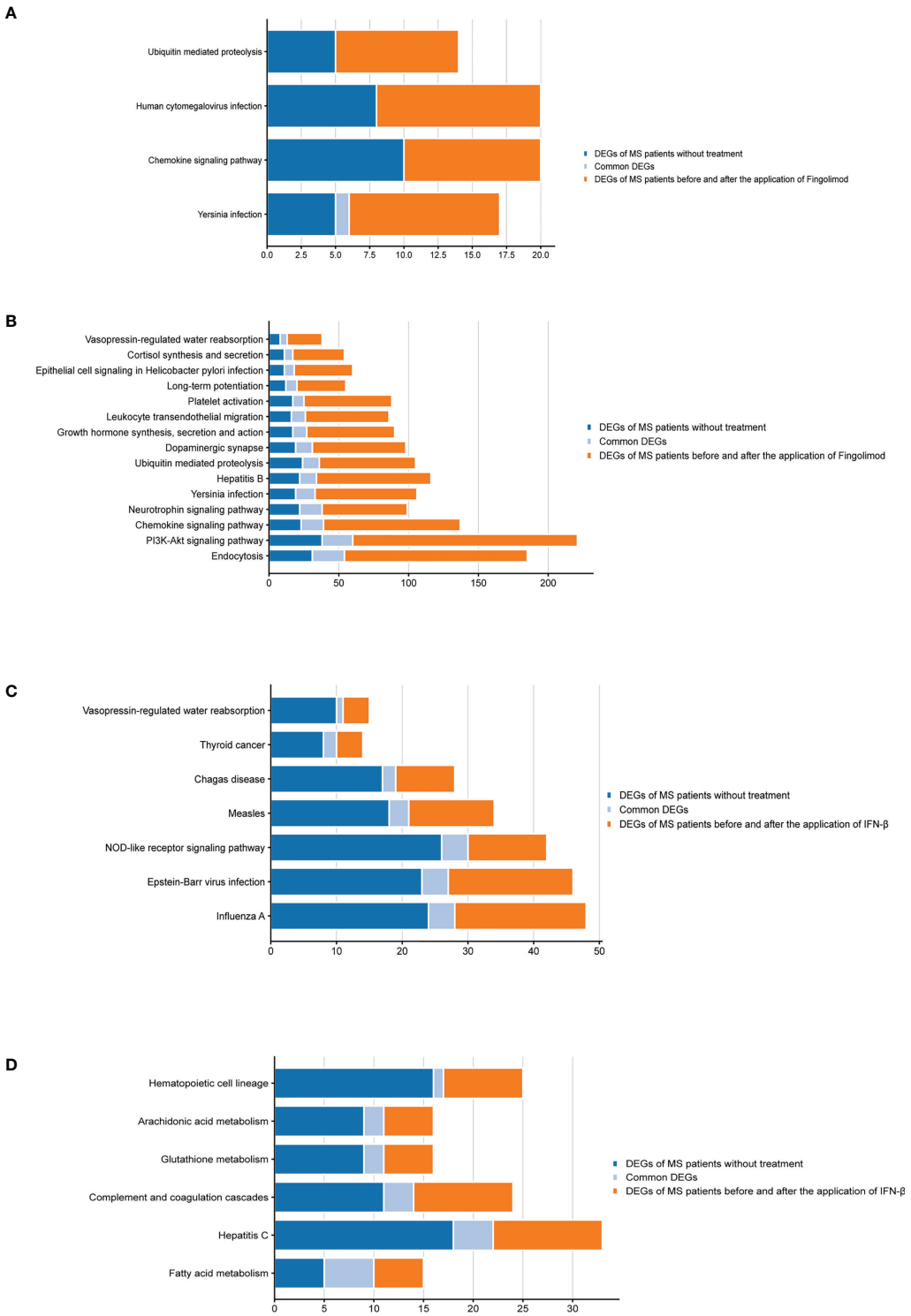

FIGURE 6
Bar graphs of the target pathways in MS patients treated with Fingolimod or IFN-β. **(A)** DEGs contained in the target pathways of CD19+ B cells in MS patients treated with Fingolimod; **(B)** DEGs contained in the target pathways of CD4+ T cells in MS patients treated with Fingolimod; **(C)** DEGs contained in the target pathways of pDCs in MS patients treated with IFN-β; **(D)** DEGs contained in the target pathways of PBMC in MS patients treated with IFN-β.

Among these 15 target pathways, "Endocytosis", "PI3K-Akt signaling pathway", "Chemokine signaling pathway" and "Neurotrophin signaling pathway" are more important. Many studies have shown that the "PI3K-Akt signaling pathway" is associated with autoimmune diseases, inflammation and hematological malignancies and plays an important role in the activation and migration of leukocytes (39). PI3K can be classified into type I, II and III according to the structure and substrate. And according to its type I catalytic subunit, type I PI3K can be further subdivided into 4 subtypes (α, β, γ, δ). The distribution of PI3K expression differs among different catalytic subunits, with PI3Kα and PI3Kβ being expressed in a variety of cells, while PI3Kδ and PI3Kγ are only expressed in the immune system. Among them, PI3Kδ is highly expressed in all leukocyte types, conferring it an important position in immunotherapy. PI3Kδ protects $CD4^+$ T cells from apoptosis during autoimmune responses (40). In PI3Kδ-inactivated mice, T cell activation and function were significantly reduced in experimental allergic encephalomyelitis (EAE) and fewer T cells were observed in CNS (40). AKT is a serine/threonine kinase, also known as protein kinase B. Inhibition of Akt phosphorylation in the CNS of EAE reduced the worsening of clinical symptoms (41). Regarding the effect of the PI3K-AKT pathway on MS patients, PI3K is a key signaling mediator of CD28. CD28 can promote the increase of c-myc and Glucose transporter type 1 (Glut1) in $CD4^+$ T cells of MS patients by activating the PI3K-AKT pathway, upregulating glycolysis and increasing Th17 cell-associated inflammatory cytokine expression (42). Therefore, inhibition of PI3K-Akt activity plays an important role in the treatment of MS. In addition, the "Chemokine signaling pathway" is an important immune system-related pathway also associated with leukocyte migration (43), and changes in chemokine expression and distribution are closely associated with the pathological process of MS demyelination (44). There is evidence that CCR2 on human Th17 cells (CCR2 (+) CCR5(-) memory $CD4^+$ T cells) may serve as a therapeutic target for MS (45). Blockade of the "Chemokine signaling pathway" is expected to be a new therapeutic approach (45). The "Neurotrophin signaling pathway" is a neurologically relevant pathway. Oligodendrocyte precursor cells (OPCs) are differentiated into myelin-forming oligodendrocytes (OLs) under the influence of various factors (including trophic factors, growth factors, and inhibitory factors in the microenvironment), and on this basis, OLs cross-link with each other to form myelin sheaths outside the axons of the central nervous system, a process called myelin regeneration (46). Therefore, regulation of neurotrophic factors is crucial for myelin regeneration in MS patients. Although no studies clearly show the relevance of "Endocytosis" to the treatment of MS, based on our analysis, we believe that relevant studies are necessary.

The top 3 node degrees among the 50 hub target genes obtained by constructing PPI networks were TP53 (down-regulated in MS), LRRK2 (down-regulated in MS), and PTEN (down-regulated in MS). TP53 and PTEN are both tumor suppressor genes associated with PI3K-Akt signaling. Among them, TP53 is one of the most frequently inactivated tumor suppressor genes in human cancer (47). It is a downstream target of the PI3K-Akt signaling pathway, and activation of PI3K-Akt signaling decreases TP53 expression (48). Production of IL-6, granulocyte-macrophage colony-stimulating factor and IL-10 is significantly higher in TP53-deficient EAE mice than in wild-type EAE mice and CNS-infiltrating cells are less apoptotic, suggesting that TP53 may be involved in the regulatory process of EAE by controlling cytokine production and/or inhibiting apoptosis of inflammatory cells (49). PTEN is a phosphatidylinositol-3,4,5- trisphosphate (PIP3)-phosphatase that is required to antagonize PI3K-AKT signaling by dephosphorylating PIP3 on the cell membrane to generate PIP2, which in turn antagonizes PI3K-mediated cell growth, metabolism, proliferation and survival signaling (50). PTEN also dephosphorylates Akt and reduces Akt activation while blocking all downstream signaling events regulated by Akt (50). Reduced PTEN expression indirectly stimulates PI3K-AKT activity. In the last two decades, our understanding of PI3K has evolved from recognition of growth factors, G protein-coupled receptors (GPCR) and enzymatic activities associated with certain oncogene products to targets in cancer and inflammatory diseases (50). Among these, PTEN plays a key role in Th17 cell differentiation by blocking IL-2 expression, and PTEN deficiency increases IL-2, promotes phosphorylation of STAT5 and inhibits phosphorylation of STAT3, thereby inhibiting Th17 cell differentiation (51). LRRK2 is a protein kinase, a gene highly associated with Parkinson's disease (52), and has not been studied in MS and EAE.

Target genes and target pathways for $CD19^+$ B cells in the treatment of MS with Fingolimod

4 target pathways were obtained by analyzing $CD19^+$ B cell transcriptome data from MS patients without treatment and $CD19^+$ B cell transcriptome data before and after Fingolimod treatment, and no target genes were obtained, suggesting that Fingolimod treatment in MS has less effect on B cells. Most of these 4 target pathways are associated with immune and infectious diseases, with "Yersinia infection" being the main target pathway. Yersinia is an intestinal bacterium and intestinal bacteria have an important regulatory role in CNS disorders. The concept of the "brain-gut axis" has been proposed early (53). The gut is rich in nerve cells and immune cells, which reach the brain *via* the vagus system or the immune system, thus affecting

brain function (54). Intestinal microorganisms can be in direct contact with intestinal cells, and the metabolic by-products of intestinal microorganisms can also activate the intestinal nervous system, interfere with the intestinal neurometabolic secretion system, and regulate the intestinal immune system, and this mode of action is called the "intestinal microbial-gut-brain axis" (55). Intestinal bacteria have been shown to regulate the differentiation, maturation and activation of B cells (56). Yersinia infection can induce polyclonal B-cell activation leading to increased autoantibodies resulting in autoimmune rheumatic diseases such as reactive arthritis and Lyme disease (57), and the relationship between Yersinia infection and MS has not been confirmed.

Target genes and target pathways for pDCs in the treatment of MS with IFN- β

7 target pathways and 154 target genes (97 up-regulated target genes and 57 down-regulated target genes) were obtained by analyzing the transcriptomic data of pDCs from MS patients without treatment and before and after the application of IFN-β treatment. Most of these 7 target pathways are associated with viral infectious diseases. We know that pDCs sense and process viral DNA through Toll-like receptor 9 (TLR9) and that IFN-β treatment of MS leads to a reduction in the activation of pDCs by viral pathogens and a decrease in the frequency of MS progression by inhibiting TLR9 processing (58). Therefore, it can explain the results obtained from our analysis that the hub target genes with the top 3 node degrees and most of the target pathways were associated with viral infectious diseases. Among them, "Epstein-Barr virus infection" is more important. EBV, one of the most studied viruses regarding MS, is a persistent and frequently reactivated virus with close to 100% epidemiological relevance to MS, triggering local inflammation near or within the CNS and thought to play a dominant role in MS pathogenesis (59).

By constructing a PPI network, 15 hub target genes were obtained, and the top 3 node degrees were MX2 (down-regulated in MS), DDX60 (down-regulated in MS) and IRF7 (down-regulated in MS), all of which were associated with the viral infection. IRF7 (Interferon regulatory factor 7) is a key regulator of the host antiviral defense response and is one of the most important members of the interferon regulatory factor family, playing an essential role in the induction of type I interferon synthesis and in the cellular innate immune response (60). IRF7-deficient mice have a higher degree of CNS leukocyte infiltration, and IRF7 is essential for regulating the inflammatory response in the CNS of MS patients (61). MX2 and DDX60 have not been studied about MS and EAE.

Target genes and target pathways for PBMC in the treatment of MS with IFN- β

6 target pathways and 73 target genes (61 up-regulated target genes and 12 down-regulated target genes) were obtained by analyzing PBMC transcriptomic data from MS patients without treatment and before and after the application of IFN-β treatment. "Fatty acid metabolism" is more important, as fatty acids are key regulators in the gut, altering the balance between Th1 and Th17 and Treg cells in autoimmune neuroinflammation (62). Long-chain fatty acids (LCFAs) exacerbate EAE by increasing pathogenic Th1 and Th17 cell populations, and short-chain fatty acids (SCFAs) improve EAE and reduce axonal damage by promoting differentiation and proliferation of Treg cells (62), suggesting that regulation of fatty acid metabolism may have an impact on the autoimmune response of MS patients by regulating the intestinal immune microenvironment.

By constructing the PPI network, 7 hub target genes were obtained. Among them, the highest node degree target gene is EGF (upregulated in MS), which is an epidermal growth factor that binds to receptors on the cell membrane and activates the PI3K-Akt signaling pathway (63), and as mentioned earlier, inhibition of the "PI3K-Akt signaling pathway" is essential for MS treatment.

Potential candidate drugs for MS treatment

Among the 6 candidates obtained for 2 or more hub target genes, Fostamatinib is particularly important, targeting 7 hub target genes (LRRK2, PAK1, PRKACA, CSK, PIK3CG, CHEK1, PDE5A), which are targets of $CD4^+$ T cells in Fingolimod for MS and targets of pDCs and PBMCs in IFN-β for MS. Fostamatinib is a spleen tyrosine kinase (SYK) inhibitor. A phase 2 clinical trial of a tyrosine kinase inhibitor (TKI) (Evobrutinib) has been completed in MS with promising results (64), and data from a *post-hoc* analysis of a phase 2 trial of Evobrutinib were presented at the 37th Congress of the European Committee for Treatment and Research in Multiple Sclerosis (ECTRIMS) in 2021, confirming that oral Bruton's tyrosine kinase inhibitor (BTKi) Evobrutinib affects brain injury associated with chronic inflammation in the CNS, making it the first BTKi shown to significantly reduce slowly expanding lesion (SEL) (65). Among these, SELs are chronic, active, demyelinating MS lesions that are considered to be early indicators of MS disease progression. Fostamatinib is currently used to treat chronic adult idiopathic thrombocytopenic purpura (ITP), which has been poorly treated with previous therapy, by

blocking platelet destruction and is the only approved SYK inhibitor on the market (66). Clinical trials have also been conducted on Fostamatinib for the treatment of RA, but the results have not been satisfactory (67). Whether it is effective in treating MS remains unclear.

Based on the target pathways of $CD19^+$ B cells and $CD4^+$ T cells in Fingolimod for MS and pDCs and PBMCs in IFN-β for MS, we can know that the "PI3K-Akt signaling pathway" and the "Chemokine signaling pathway" are more important, so we focus on drugs that target these pathways simultaneously. Among the 58 candidate drugs obtained that target 2 target pathways, Nemiralisib and Umbralisib target both the "PI3K-Akt signaling pathway" and the "Chemokine signaling pathway". Nemiralisib, a PI3Kδ inhibitor, is an anti-asthmatic and anti-inflammatory agent (68), while Umbralisib, a dual PI3Kδ/CK1ϵ inhibitor, is an anti-tumor agent currently used in the treatment of lymphoma (69). Neither of them has been studied in MS, and they deserve focused attention.

Our study has the following limitations. First, we could only obtain the transcriptomic dataset of MS patients treated with IFN-β and Fingolimod in the GEO database. If the transcriptome datasets of MS patients treated with other effective drugs are reported in the future, this method can continue to be used to find potential candidate drugs for MS. Second, in our study, the critical values of DEG were relatively low ($P < 0.05$, FC > 1.2 or 0 < FC < 1/1.2). When we increased the FC used for common cases to 2 and performed subsequent analyses, the DEGs for MS patients without treatment were shown in Supplementary Table S10, and the DEGs for MS patients before and after the application of IFN-β or Fingolimod were shown in Supplementary Table S11. Target genes for $CD19^+$ B cells and PBMC were reduced to 0. The upregulated target genes for $CD4^+$ T cells were reduced to 0 and the downregulated target genes were reduced to 55. The upregulated target genes of pDCs were reduced to 0 and the downregulated target genes were reduced to 2. In terms of pathway enrichment, $CD19^+$ B cells and PBMC did not obtain target pathways, $CD4^+$ T cells obtained 7 target pathways, and pDCs obtained 11 target pathways (Supplementary Table S12). Although the cutoff for DEGs was relatively low, the results based on transcriptome data were meaningful to a certain extent. Third, limited by the lack of compliant proteomic datasets, we were only able to validate a small portion of our transcriptomic data – the transcriptomic data on $CD4^+$ T cells from MS patients without treatment, and protein validation may continue in the future. Fourth, no basic trials or clinical trials have been conducted with Nermiralisib, Umbralisib or Fostamatinib. More work needs to be done in this area to fully realize the practical value of this study.

Conclusion

In this study, we applied bioinformatics analysis of MS transcriptome data to reposition drugs that may treat MS, which can help identify target genes and target pathways for the treatment of MS, redirect the use of approved drugs, and find new effective drugs that may treat MS. According to our analysis, MS treatment is a complex process involving multiple systemic pathways, including immunity, infection, and signal transduction, etc. We should focus on candidate drugs that target both the "PI3K-Akt signaling pathway" and the "Chemokine signaling pathway" (e.g., Nemiralisib and Umbralisib) and TKI (e.g., Fostamatinib).

Data availability statement

The datasets presented in this study can be found in online repositories. The names of the repository/repositories and accession number(s) can be found in the article/Supplementary Material.

Author contributions

XY, XR, XH, CX, and JF: conceptualization. XY, XR, and JF: data curation. XY, XH, YZ, CX, and JF: formal analysis. XY, XR, YZ, and JF: funding acquisition. XY: writing—original draft. XY, XR, CX, and JF: writing—review and editing. All authors contributed to the article and approved the submitted version.

Funding

This work was supported by the project of Nature Scientific Foundation of Heilongjiang Province (ZD2020H004).

Conflict of interest

The authors declare that the research was conducted in the absence of any commercial or financial relationships that could be construed as a potential conflict of interest.

Publisher's note

All claims expressed in this article are solely those of the authors and do not necessarily represent those of their affiliated organizations, or those of the publisher, the editors and the reviewers. Any product that may be evaluated in this article, or

claim that may be made by its manufacturer, is not guaranteed or endorsed by the publisher.

Supplementary material

The Supplementary Material for this article can be found online at: https://www.frontiersin.org/articles/10.3389/fimmu.2022.1020721/full#supplementary-material

SUPPLEMENTARY TABLE 1
Detailed DEGs obtained from MS patients without treatment according to the type of $CD19^+$ B cells, $CD4^+$ T cells, pDCs and PBMC.

SUPPLEMENTARY TABLE 2
Detailed DEGs obtained from MS patients before and after the application of Fingolimod and IFN-β according to the type of $CD19^+$ B cells, $CD4^+$ T cells, pDCs and PBMC.

SUPPLEMENTARY TABLE 3
Detailed target genes obtained from MS patients after the application of Fingolimod or IFN-β according to the type of $CD19^+$ B cells, $CD4^+$ T cells, pDCs and PBMC.

SUPPLEMENTARY TABLE 4
Detailed pathways obtained from MS patients without treatment according to the type of $CD19^+$ B cells, $CD4^+$ T cells, pDCs and PBMC.

SUPPLEMENTARY TABLE 5
Detailed pathways obtained from MS patients before and after the application of Fingolimod and IFN-β according to the type of $CD19^+$ B cells, $CD4^+$ T cells, pDCs and PBMC.

SUPPLEMENTARY TABLE 6
Detailed candidate drugs for targeting target pathways obtained from the KEGG database according to the types of $CD19^+$ B cells, $CD4^+$ T cells, pDCs and PBMC.

SUPPLEMENTARY TABLE 7
Detailed candidate drugs for targeting 2 target pathways obtained from the KEGG database according to the types of $CD19^+$ B cells, $CD4^+$ T cells, pDCs and PBMC.

SUPPLEMENTARY TABLE 8
The genes differentially expressed in $CD4^+$ T cells of MS patients without treatment at both mRNA and protein levels.

SUPPLEMENTARY TABLE 9
\The pathways that were enriched by genes differentially expressed in $CD4^+$ T cells of MS patients without treatment at both mRNA and protein levels.

SUPPLEMENTARY TABLE 10
The DEGs of MS patients and healthy individuals (FC > 2).

SUPPLEMENTARY TABLE 11
The DEGs of MS patients before and after the application of IFN-β or Fingolimod (FC > 2).

SUPPLEMENTARY TABLE 12
The target pathways of Fingolimod and IFN-β for MS treatment (FC > 2).

References

1. Yamasaki R, Kira J. Multiple sclerosis. *Adv Exp Med Biol* (2019) 1190:217–47. doi: 10.1007/978-981-32-9636-7_14

2. Walton C, King R, Rechtman L, Kaye W, Leray E, Marrie RA, et al. Rising prevalence of multiple sclerosis worldwide: Insights from the atlas of MS, third edition. *Mult Scler* (2020) 26:1816–21. doi: 10.1177/1352458520970841

3. Polman CH. Regular review: Drug treatment of multiple sclerosis. *BMJ* (2000) 321:490–4. doi: 10.1136/bmj.321.7259.490

4. Taskapilioglu O. Recent advances in the treatment for multiple sclerosis; current new drugs specific for multiple sclerosis. *Arch Neuropsychiatry* (2018) 55 (Suppl 1):S15–S20. doi: 10.29399/npa.23402

5. Jahchan NS, Dudley JT, Mazur PK, Flores N, Yang D, Palmerton A, et al. A drug repositioning approach identifies tricyclic antidepressants as inhibitors of small cell lung cancer and other neuroendocrine tumors. *Cancer Discov* (2013) 3:1364–77. doi: 10.1158/2159-8290.CD-13-0183

6. Nosengo N. Can you teach old drugs new tricks? *Nature* (2016) 534:314–6. doi: 10.1038/534314a

7. Stinissen P, Raus J, Zhang J. Autoimmune pathogenesis of multiple sclerosis: Role of autoreactive T lymphocytes and new immunotherapeutic strategies. *Crit Rev Immunol* (1997) 17:33–75. doi: 10.1615/CritRevImmunol.v17.i1.20

8. Kaskow BJ, Baecher-Allan C. Effector T cells in multiple sclerosis. *Cold Spring Harb Perspect Med* (2018) 8:a029025. doi: 10.1101/cshperspect.a029025

9. Hauser SL, Waubant E, Arnold DL, Vollmer T, Antel J, Fox RJ, et al. B-cell depletion with rituximab in relapsing-remitting multiple sclerosis. *N Engl J Med* (2008) 358:676–88. doi: 10.1056/NEJMoa0706383

10. Wilson HL. B cells contribute to MS pathogenesis through antibody-dependent and antibody-independent mechanisms. *Biologics* (2012) 6:117–23. doi: 10.2147/BTT.S24734

11. Wanleenuwat P, Iwanowski P. Role of b cells and antibodies in multiple sclerosis. *Multiple Sclerosis Related Disord* (2019) 36:101416. doi: 10.1016/j.msard.2019.101416

12. Thewissen K, Nuyts AH, Deckx N, Wijmeersch BV, Nagels G, D'hooghe M, et al. Circulating dendritic cells of multiple sclerosis patients are proinflammatory and their frequency is correlated with MS-associated genetic risk factors. *Mult Scler* (2014) 20:548–57. doi: 10.1177/1352458513505352

13. Jakimovski D, Kolb C, Ramanathan M, Zivadinov R, Weinstock-Guttman B. Interferon β for multiple sclerosis. *Cold Spring Harb Perspect Med* (2018) 8: a032003. doi: 10.1101/cshperspect.a032003

14. Brinkmann V, Davis MD, Heise CE, Albert R, Cottens S, Hof R, et al. The immune modulator FTY720 targets sphingosine 1-phosphate receptors. *J Biol Chem* (2002) 277:21453–7. doi: 10.1074/jbc.C200176200

15. Freedman MS, Brod S, Singer BA, Cohen BA, Hayward B, Dangond F, et al. Clinical and MRI efficacy of Sc IFN β-1a tiw in patients with relapsing MS appearing to transition to secondary progressive MS: *Post hoc* analyses of PRISMS and SPECTRIMS. *J Neurol* (2020) 267:64–75. doi: 10.1007/s00415-019-09532-5

16. Fox E, Vieira MC, Johnson K, Peeples M, Bensimon AG, Signorovitch J, et al. Real-world durability of relapse rate reduction in patients with multiple sclerosis receiving fingolimod for up to 3 years: A retrospective US claims database analysis. *J Neurological Sci* (2019) 398:163–70. doi: 10.1016/j.jns.2019.01.036

17. Barrett T, Wilhite SE, Ledoux P, Evangelista C, Kim IF, Tomashevsky M, et al. NCBI GEO: Archive for functional genomics data sets–update. *Nucleic Acids Res* (2012) 41:D991–5. doi: 10.1093/nar/gks1193

18. Ritchie ME, Phipson B, Wu D, Hu Y, Law CW, Shi W. Et al. limma powers differential expression analyses for RNA-sequencing and microarray studies. *Nucleic Acids Res* (2015) 43:e47–7. doi: 10.1093/nar/gkv007

19. Shannon P, Markiel A, Ozier O, Baliga NS, Wang JT, Ramage D, et al. Cytoscape: A software environment for integrated models of biomolecular interaction networks. *Genome Res* (2003) 13:2498–504. doi: 10.1101/gr.1239303

20. Lamb J, Crawford ED, Peck D, Modell JW, Blat IC, Wrobel MJ, et al. The connectivity map: Using gene-expression signatures to connect small molecules, genes, and disease. *Science* (2006) 313:1929–35. doi: 10.1126/science.1132939

21. Wishart DS. DrugBank: A comprehensive resource for in silico drug discovery and exploration. *Nucleic Acids Res* (2006) 34:D668–72. doi: 10.1093/nar/gkj067

22. Yu G, Wang L-G, Han Y, He Q-Y. ClusterProfiler: An r package for comparing biological themes among gene clusters. *OMICS: A J Integr Biol* (2012) 16:284–7. doi: 10.1089/omi.2011.0118

23. Kanehisa M, Goto S, Furumichi M, Tanabe M, Hirakawa M. KEGG for representation and analysis of molecular networks involving diseases and drugs. *Nucleic Acids Res* (2010) 38:D355–60. doi: 10.1093/nar/gkp896

24. Martens L, Hermjakob H, Jones P, Adamski M, Taylor C, States D, et al. PRIDE: The proteomics identifications database. *Proteomics* (2005) 5:3537–45. doi: 10.1002/pmic.200401303

25. Henderson J. Google Scholar: A source for clinicians? *CMAJ* (2005) 172:1549–50. doi: 10.1503/cmaj.050404

26. Berge T, Eriksson A, Brorson IS, Høgestøl EA, Berg-Hansen P, Døskeland A, et al. Quantitative proteomic analyses of CD4+ and CD8+ T cells reveal differentially expressed proteins in multiple sclerosis patients and healthy controls. *Clin Proteomics* (2019) 16:19. doi: 10.1186/s12014-019-9241-5

27. Cappelletti C, Eriksson A, Brorson IS, Leikfoss IS, Kråbøl O, Høgestøl EA, et al. Quantitative proteomics reveals protein dysregulation during T cell activation in multiple sclerosis patients compared to healthy controls. *Clin Proteomics* (2022) 19:23. doi: 10.1186/s12014-022-09361-1

28. Annibali V, Umeton R, Palermo A, Severa M, Etna MP, Giglio S, et al. Analysis of coding and non-coding transcriptome of peripheral b cells reveals an altered interferon response factor (IRF)-1 pathway in multiple sclerosis patients. *J Neuroimmunology* (2018) 324:165–71. doi: 10.1016/j.jneuroim.2018.09.005

29. Salehi Z, Talebi S, Maleknia S, Palizban F, Naser Moghadasi A, Kavousi K, et al. RNA Sequencing of CD4+ T cells in relapsing–remitting multiple sclerosis patients at relapse: Deciphering the involvement of novel genes and pathways. *J Mol Neurosci* (2021) 71:2628–45. doi: 10.1007/s12031-021-01878-8

30. Aung LL, Brooks A, Greenberg SA, Rosenberg ML, Dhib-Jalbut S, Balashov KE. Multiple sclerosis-linked and interferon-Beta-Regulated gene expression in plasmacytoid dendritic cells. *J Neuroimmunology* (2012) 250:99–105. doi: 10.1016/j.jneuroim.2012.05.013

31. Irizar H, Muñoz-Culla M, Sepúlveda L, Sáenz-Cuesta M, Prada Á., Castillo-Triviño T, et al. Transcriptomic profile reveals gender-specific molecular mechanisms driving multiple sclerosis progression. *PloS One* (2014) 9:e90482. doi: 10.1371/journal.pone.0090482

32. Angerer IC, Hecker M, Koczan D, Roch L, Friess J, Rüge A, et al. Transcriptome profiling of peripheral blood immune cell populations in multiple sclerosis patients before and during treatment with a sphingosine-1-Phosphate receptor modulator. *CNS Neurosci Ther* (2018) 24:193–201. doi: 10.1111/cns.12793

33. Koczan D, Fitzner B, Zettl UK, Hecker M. Microarray data of transcriptome shifts in blood cell subsets during S1P receptor modulator therapy. *Sci Data* (2018) 5:180145. doi: 10.1038/sdata.2018.145

34. Friess J, Hecker M, Roch L, Koczan D, Fitzner B, Angerer IC, et al. Fingolimod alters the transcriptome profile of circulating CD4+ cells in multiple sclerosis. *Sci Rep* (2017) 7:42087. doi: 10.1038/srep42087

35. Hecker M, Hartmann C, Kandulski O, Paap BK, Koczan D, Thiesen H-J, et al. Interferon-beta therapy in multiple sclerosis: The short-term and long-term effects on the patients' individual gene expression in peripheral blood. *Mol Neurobiol* (2013) 48:737–56. doi: 10.1007/s12035-013-8463-1

36. Hundeshagen A, Hecker M, Paap BK, Angerstein C, Kandulski O, Fatum C, et al. Elevated type I interferon-like activity in a subset of multiple sclerosis patients: Molecular basis and clinical relevance. *J Neuroinflamm* (2012) 9:574. doi: 10.1186/1742-2094-9-140

37. Ye H, Yang L, Cao Z, Tang K, Li YA. Pathway profile-based method for drug repositioning. *Chin Sci Bull* (2012) 57:2106–12. doi: 10.1007/s11434-012-4982-9

38. Constantinescu CS, Gran B. Multiple sclerosis: Autoimmune associations in multiple sclerosis. *Nat Rev Neurol* (2010) 6:591–2. doi: 10.1038/nrneurol.2010.147

39. Puri KD, Doggett TA, Douangpanya J, Hou Y, Tino WT, Wilson T, et al. Mechanisms and implications of phosphoinositide 3-kinase δ in promoting neutrophil trafficking into inflamed tissue. *Blood* (2004) 103:3448–56. doi: 10.1182/blood-2003-05-1667

40. Haylock-Jacobs S, Comerford I, Bunting M, Kara E, Townley S, Klingler-Hoffmann M, et al. PI3Kδ drives the pathogenesis of experimental autoimmune encephalomyelitis by inhibiting effector T cell apoptosis and promoting Th17 differentiation. *J Autoimmun* (2011) 36:278–87. doi: 10.1016/j.jaut.2011.02.006

41. da Silva LC, Lima IVdeA, da Silva MCM, Corrêa TA, de Souza VP, de Almeida MV, et al. A new lipophilic amino alcohol, chemically similar to compound FTY720, attenuates the pathogenesis of experimental autoimmune encephalomyelitis by PI3K/Akt pathway inhibition. *Int Immunopharmacol* (2020) 88:106919. doi: 10.1016/j.intimp.2020.106919

42. Kunkl M, Sambucci M, Ruggieri S, Amormino C, Tortorella C, Gasperini C, et al. CD28 autonomous signaling up-regulates c-myc expression and promotes glycolysis enabling inflammatory T cell responses in multiple sclerosis. *Cells* (2019) 8:E575. doi: 10.3390/cells8060575

43. Laudanna C, Alon R. Right on the spot. chemokine triggering of integrin-mediated arrest of rolling leukocytes. *Thromb Haemost* (2006) 95:5–11. doi: 10.1160/TH05-07-0482

44. Chu T, Shields LBE, Zhang YP, Feng S-Q, Shields CB, Cai J. CXCL12/CXCR4/CXCR7 chemokine axis in the central nervous system: Therapeutic targets for remyelination in demyelinating diseases. *Neuroscientist* (2017) 23:627–48. doi: 10.1177/1073858416685690

45. Aranami T, Yamamura T. Th17 cells and autoimmune encephalomyelitis (EAE/MS). *Allergology Int* (2008) 57:115–20. doi: 10.2332/allergolint.R-07-159

46. Sun J, Zhou H, Bai F, Zhang Z, Ren Q. Remyelination: A potential therapeutic strategy for alzheimer's disease? *JAD* (2017) 58:597–612. doi: 10.3233/JAD-170036

47. Martinez LA. Mutant P53 and ETS2, a tale of reciprocity. *Front Oncol* (2016) 6:35. doi: 10.3389/fonc.2016.00035

48. Schaefer T, Steiner R, Lengerke C. SOX2 and P53 expression control converges in PI3K/AKT signaling with versatile implications for stemness and cancer. *IJMS* (2020) 21:4902. doi: 10.3390/ijms21144902

49. Okuda Y, Okuda M, Bernard CCA. Regulatory role of P53 in experimental autoimmune encephalomyelitis. *J Neuroimmunology* (2003) 135:29–37. doi: 10.1016/S0165-5728(02)00428-9

50. Vanhaesebroeck B, Stephens L, Hawkins P. PI3K signalling: The path to discovery and understanding. *Nat Rev Mol Cell Biol* (2012) 13:195–203. doi: 10.1038/nrm3290

51. Kim HS, Jang SW, Lee W, Kim K, Sohn H, Hwang SS, et al. PTEN drives Th17 cell differentiation by preventing IL-2 production. *J Exp Med* (2017) 214:3381–98. doi: 10.1084/jem.20170523

52. Bandres-Ciga S, Diez-Fairen M, Kim JJ, Singleton AB. Genetics of parkinson's disease: An introspection of its journey towards precision medicine. *Neurobiol Dis* (2020) 137:104782. doi: 10.1016/j.nbd.2020.104782

53. Walsh JH. The brain-gut axis: A new frontier. Proceedings of an international symposium held in Florence Italy, June 29-July 1, 1981. *Peptides* (1981) 2 Suppl 2:1–299. doi: 10.1016/0196-9781(82)90151-6

54. Shen X, Sun Z. Microbe-gut-brain axis and neurological disorders: A review. *Sheng Wu Gong Cheng Xue Bao* (2021) 37:3781–8. doi: 10.13345/j.cjb.200773

55. Montiel-Castro AJ, González-Cervantes RM, Bravo-Ruiseco G, Pacheco-López G. The microbiota-Gut-Brain axis: Neurobehavioral correlates, health and sociality. *Front Integr Neurosci* (2013) 7:70. doi: 10.3389/fnint.2013.00070

56. Lundell A-C, Björnsson V, Ljung A, Ceder M, Johansen S, Lindhagen G, et al. Infant b cell memory differentiation and early gut bacterial colonization. *J.I.* (2012) 188:4315–22. doi: 10.4049/jimmunol.1103223

57. Crespo A. De M.C.; falcão, D.P.; Ferreira de araújo, P.M.; machado de medeiros, B.M. effects of yersinia enterocolitica O:3 derivatives on b lymphocyte activation in vivo. *Microbiol Immunol* (2002) 46:95–100. doi: 10.1111/j.1348-0421.2002.tb02664.x

58. Balashov KE, Aung LL, Vaknin-Dembinsky A, Dhib-Jalbut S, Weiner HL. Interferon-β inhibits toll-like receptor 9 processing in multiple sclerosis. *Ann Neurol* (2010) 68:899–906. doi: 10.1002/ana.22136

59. Meier U-C, Cipian RC, Karimi A, Ramasamy R, Middeldorp JM. Cumulative roles for Epstein-Barr virus, human endogenous retroviruses, and human herpes virus-6 in driving an inflammatory cascade underlying MS pathogenesis. *Front Immunol* (2021) 12:757302. doi: 10.3389/fimmu.2021.757302

60. Sgarbanti M, Marsili G, Remoli AL, Orsatti R, Battistini A. IRF-7: New role in the regulation of genes involved in adaptive immunity. *Ann N Y Acad Sci* (2007) 1095:325–33. doi: 10.1196/annals.1397.036

61. Salem M, Mony JT, Løbner M, Khorooshi R, Owens T. Interferon regulatory factor-7 modulates experimental autoimmune encephalomyelitis in mice. *J Neuroinflamm* (2011) 8:181. doi: 10.1186/1742-2094-8-181

62. Haghikia A, Jörg S, Duscha A, Berg J, Manzel A, Waschbisch A, et al. Dietary fatty acids directly impact central nervous system autoimmunity. *via Small Intestine. Immun* (2015) 43:817–29. doi: 10.1016/j.immuni.2015.09.007

63. Díaz ME, González L, Miquet JG, Martínez CS, Sotelo AI, Bartke A, et al. Growth hormone modulation of EGF-induced PI3K-akt pathway in mice liver. *Cell Signal* (2012) 24:514–23. doi: 10.1016/j.cellsig.2011.10.001

64. Montalban X, Arnold DL, Weber MS, Staikov I, Piasecka-Stryczynska K, Willmer J, et al. Placebo-controlled trial of an oral BTK inhibitor in multiple sclerosis. *N Engl J Med* (2019) 380:2406–17. doi: 10.1056/NEJMoa1901981

65. Pochon S. 37th congress of the European committee for treatment and research in multiple sclerosis (ECTRIMS 2021): 13–15 October, 2021. *Pharm Med* (2021) 35:367–70. doi: 10.1007/s40290-021-00411-x

66. Markham A. Fostamatinib: First global approval. *Drugs* (2018) 78:959–63. doi: 10.1007/s40265-018-0927-1

67. Scott IC, Scott DL. Spleen tyrosine kinase inhibitors for rheumatoid arthritis: Where are we now? *Drugs* (2014) 74:415–22. doi: 10.1007/s40265-014-0193-9

68. Khindri S, Cahn A, Begg M, Montembault M, Leemereise C, Cui Y, et al. A multicentre, randomized, double-blind, placebo-controlled, crossover study to investigate the efficacy, safety, tolerability, and pharmacokinetics of repeat doses of inhaled nemiralisib in adults with persistent, uncontrolled asthma. *J Pharmacol Exp Ther* (2018) 367:405–13. doi: 10.1124/jpet.118.249516

69. Dhillon S, Keam SJ. Umbralisib: First approval. *Drugs* (2021) 81:857–66. doi: 10.1007/s40265-021-01504-2

frontiers | Frontiers in Immunology

TYPE Original Research
PUBLISHED 31 October 2022
DOI 10.3389/fimmu.2022.1041660

OPEN ACCESS

EDITED BY
Yuval Tal,
Hadassah Medical Center, Israel

REVIEWED BY
Amali E. Samarasinghe,
University of Tennessee Health Science Center (UTHSC), United States
Leo Koenderman,
Utrecht University, Netherlands

*CORRESPONDENCE
Ariel Munitz
arielm@post.tau.ac.il

SPECIALTY SECTION
This article was submitted to Autoimmune and Autoinflammatory Disorders : Autoimmune Disorders, a section of the journal Frontiers in Immunology

RECEIVED 11 September 2022
ACCEPTED 07 October 2022
PUBLISHED 31 October 2022

CITATION
Dolitzky A, Hazut I, Avlas S, Grisaru-Tal S, Itan M, Zaffran I, Levi-Schaffer F, Gerlic M and Munitz A (2022) Differential regulation of Type 1 and Type 2 mouse eosinophil activation by apoptotic cells. *Front. Immunol.* 13:1041660. doi: 10.3389/fimmu.2022.1041660

Differential regulation of Type 1 and Type 2 mouse eosinophil activation by apoptotic cells

Avishay Dolitzky[1], Inbal Hazut[1], Shmulik Avlas[1], Sharon Grisaru-Tal[1], Michal Itan[1], Ilan Zaffran[2], Francesca Levi-Schaffer[2], Motti Gerlic[1] and Ariel Munitz[1]*

[1]Department of Clinical Microbiology and Immunology, Faculty of Medicine, Tel Aviv University, Tel Aviv, Israel, [2]Institute for Drug Research, School of Pharmacy, Faculty of Medicine, The Hebrew University of Jerusalem, Jerusalem, Israel

Eosinophils are multifunctional, evolutionary conserved leukocytes that are involved in a plethora of responses ranging from regulation of tissue homeostasis, host defense and cancer. Although eosinophils have been studied mostly in the context of Type 2 inflammatory responses, it is now evident that they participate in Type 1 inflammatory responses and can respond to Type 1 cytokines such as IFN-γ. Notably, both Type 1- and Type 2 inflammatory environments are characterized by tissue damage and cell death. Collectively, this raises the possibility that eosinophils can interact with apoptotic cells, which can alter eosinophil activation in the inflammatory milieu. Herein, we demonstrate that eosinophils can bind and engulf apoptotic cells. We further show that exposure of eosinophils to apoptotic cells induces marked transcriptional changes in eosinophils, which polarize eosinophils towards an anti-inflammatory phenotype that is associated with wound healing and cell migration. Using an unbiased RNA sequencing approach, we demonstrate that apoptotic cells suppress the inflammatory responses of eosinophils that were activated with IFN-γ + *E. coli* (e.g., Type 1 eosinophils) and augment IL-4-induced eosinophil activation (e.g., Type 2 eosinophils). These data contribute to the growing understanding regarding the heterogeneity of eosinophil activation patterns and highlight apoptotic cells as potential regulators of eosinophil polarization.

KEYWORDS

eosinophils, allergy, inflammation, IL-4, IFN-gamma, apoptotic cells

Introduction

Eosinophils are bone marrow-derived granulocytes, that are mainly present in mucosal surfaces such as the gastrointestinal and respiratory tract (1). Eosinophils can produce a plethora of immunoregulatory cytokines and are actively involved in the regulation of multiple immune responses (2). In response to diverse stimuli, eosinophils

are recruited from the circulation into the inflammatory site, where they modulate immune responses through an array of mechanisms. For example, they can promote tissue damage or, conversely, encourage repair, which may eventually lead to tissue remodeling and fibrosis (3). Triggering of eosinophils by engagement of receptors for cytokines, immunoglobulins, and complement can lead to the generation of a wide range of inflammatory cytokines, lipid-derived mediators, and neuromediators (3). Thus, eosinophils can display direct or indirect effector functions by modulating multiple aspects of the immune response (1–3). Due to their ability to respond to, and secrete a multitude of mediators, eosinophils have pleotropic activities in numerous homeostatic processes (especially in mice) and display key roles in inflammatory responses that range from allergic diseases, host-defense and even cancer (4).

Eosinophils are considered terminally differentiated cells. Nonetheless, recent data demonstrate that exposure of eosinophils to distinct inflammatory microenvironments can induce differential transcriptional profiles in these cells (5–8). This could explain, at least in part their pleotropic activities in different disease contexts. For instance, exposure of eosinophils to cytokines such as IL-4, which is present in allergic diseases induces a unique transcriptome signature that is markedly different than the transcriptome signature that is induced by exposure of eosinophils to IFN-γ and/or innate immune stimulation (i.e., *E.* coli) (6). Based on these differential responses, we recently characterized the transcriptional profile of eosinophils and termed them Type-1 eosinophils (in response to IFN-γ with or without *E. coli* stimulation) and Type-2 eosinophils (in response to IL-4) (6). The presence of factors that are capable of modulating Type 1 and Type 2 eosinophil responses are largely unknown.

Cell death is a common feature of infected and damaged tissues in inflammatory sites (9). Engulfment of apoptotic cells by phagocytes (i.e., efferocytosis) (10) is a critical event in the resolution of inflammatory responses. The importance of efferocytosis in homeostasis is demonstrated by the finding that mice, which lack components that enable sensing, recognition and/or engulfment of dead cells, develop autoimmune diseases and/or chronic inflammation (11, 12). Indeed, efferocytosis can inhibit inflammatory signaling in macrophages and is associated with induction of tissue repair and wound healing. In agreement with this, the inflammatory response induced by lipopolysaccharide (LPS)-activated macrophages, is attenuated by their incubation with apoptotic cells (13). Conversely, optimal activation of macrophages with IL-4, which induces an anti-inflammatory phenotype in macrophages (e.g., M2 macrophages), requires the presence of apoptotic cells (14). Furthermore, apoptotic cells can induce the activation of STAT6, a key transcription factor in the IL-4/IL-13 signaling pathway (15).

Increased infiltration of eosinophils is observed in multiple diseases that are characterized by the presence of apoptotic cells. We have recently shown that eosinophils reside in the proximity of Caspase 3^+ cells in the colons of mice with colorectal cancer (16). Furthermore, we have shown that eosinophils express various receptors mainly of the CD300 family (17–22), that may bind phosphatidylserine (PtdSer) (23), the most common 'eat-me' signal, which promotes the engulfment of apoptotic cells (24). Thus, eosinophils are potentially capable of detecting and responding to apoptotic cells. Whether apoptotic cells regulate transcriptional programs in eosinophils is largely unknown.

Herein, we demonstrate that eosinophils can bind and engulf to some extent apoptotic cells. We show that exposure of eosinophils to apoptotic cells induces marked transcriptional changes in eosinophils that are associated with wound healing and cell migration. Furthermore, using an unbiased RNA sequencing approach, we show that apoptotic cells suppress the inflammatory responses of Type 1 eosinophils and augment Type 2 eosinophil activation. These data contribute to the growing understanding regarding the heterogeneity of eosinophil activation patterns and highlight apoptotic cells as potential regulators of eosinophil polarization.

Materials and methods

Mice

Wild type (WT) C57BL/6 and BALB/c mice were obtained from Envigo, Israel. BALB/c *Cd300a*$^{-/-}$, C57BL/6 *Cd300b*$^{-/-}$, C57BL/6 *Cd300f*$^{-/-}$ were recently descried (19–22). NJ.1638 *Il5*^{Tg} mice (kindly provided by Dr. James L. Lee, Mayo Clinic, Phoenix, USA), were used for all studies using primary mouse cells. The mice were housed under specific pathogen-free conditions. All experiments were reviewed and approved by the Animal Health Care Committee of Tel Aviv University and were performed in accordance with the regulations and guidelines regarding the care and use of animals for experimental procedures.

Eosinophil isolation

Mouse eosinophils were isolated from the peritoneal cavity of *Il5*^{Tg} mice under sterile conditions (22). Peritoneal cavity was washed with 10mL of PBS. Thereafter, negative selection of eosinophils was performed using anti-Thy1.2 (11443D, Invitrogen) and anti-B220 (11331D, Invitrogen) Dynabead-conjugated antibodies according to the manufacturer's instructions. Eosinophil purity was validated using flow

cytometry; CD45-APC 07512-80-05 biogems; Siglec-F-PE Rat IgG2aκ, 552126/552128 BD Biosciences. Eosinophils were used when purity >97% and viability > 97%.

Generation of bone marrow-derived eosinophils

Bone marrow-derived eosinophils (BMDEs) were generated as described (25). Briefly, bone marrow cells were collected from the femur and tibia bones by crushing and red blood cells will be lysed with ACK lysis buffer (Sigma). Low-density bone marrow progenitors were separated by gradient centrifugation (Histopaque 1083, Sigma) of 1700 RPM for 30 minutes. Low density bone marrow cells were seeded at 5 X 10^5 cells/mL in 24 wells plate (BD Falcon) in media containing IMDM (Gibco) with 10% fetal bovine serum (HyClone), 1% penicillin-streptomycin (Biological industries), 2 mM glutamine (Gibco),50 μM β-mercaptoethanol (Sigma) and supplemented with 100 ng/mL stem-cell factor (SCF; PeproTech) and 100 ng/mL FLT3-Ligand (FLT3-L; PeproTech) from day 0 to day 4. On day 4, the media containing SCF, and FLT3-L replaced with media containing 10 ng/ml recombinant mouse interleukin-5 (rmIL-5; Peprotech) alone. Medium refreshing was done every 3 days from day 4 to 14 until eosinophil purity reached >85%. Purity was assessed by flow cytometry using CCR3 (R&D) and Siglec-F (BD Bioscience) as eosinophils markers.

Generation of apoptotic cells

Wild-type mice (4- to 6-week-old) were euthanized and the thymus was collected, homogenized and thymocytes were incubated in an RPMI-1640 culture medium containing 0.1mM dexamethasone (Sigma). Following 6 hours of incubation, the cells were washed 3 times in the cell's media by centrifugation.

Annexin DAPI staining

After induction of apoptosis, thymocytes were washed once in PBS and suspended in Annexin binding buffer. Thereafter, the cells were stained with PE.Cy7-conjugated Annexin V (eBioscience) and DAPI as per the manufacturer's instructions. After staining, cells were washed with Annexin binding buffer and suspended with PBS. Apoptotic cells were evaluated by flow cytometry and considered as AnnexinV^+/$DAPI^-$ cells.

Efferocytosis and co culture assays

Eosinophils were labeled using CFSE - Cell Labeling Kit (Invitrogen, Carlsbad, CA) according to the manufacturer's instructions. Apoptotic thymocytes were labeled using DiD (Invitrogen, Carlsbad, CA). Eosinophils and apoptotic cells were co-cultured (1:5 ratio, eosinophils:apoptotic cells) for 18 hours. Engulfment was determined by image-stream flow cytometry which captures single-cell images showing either single cells or engulfment. Live imaging was performed by snapping pictures every 5 min using IncuCyte®. All our stimulating conditions (including those of eosinophils without apoptotic cells) were conducted on eosinophil samples that were purified after the co culture by positive selection using anti-Siglec-F magnetic beads, and immediately resuspend in TRIzol™ Reagent (Invitrogen, Thermo Fisher). This procedure was conducted to ensure that apoptotic cells are not sequenced as well. Eosinophils from all the samples were then assessed by flow cytometry for their viability, which was >90% and purity >95%.

In other experiments, thymocytes were treated for 6 hours with Dexamethasone for the induction of apoptosis. Thereafter, the cells were washed and resuspended in PBS at a concentration of 10^6/ml and labeled with 20nM pHrodo™ Red succinimidyl ester (SE) (Invitrogen, Thermo Fisher) by incubating them for 1 hour at 37^0 C. The labeled cells were co-cultured with peritoneal eosinophils that were obtained from *Il5*^{Tg} mice for 18 hours. Uptake was assessed by flow cytometry assessing cells that were positive for Siglec-F (as an eosinophils marker) and pHrodo™ Red, SE.

Quantitative PCR analysis

RNA extracted using TRIzol Reagent (Invitrogen Life Technologies) and cDNA synthesis performed using the iScript™ cDNA Kit (Bio-Rad) according to the manufacturers' instructions. PCR reactions were done using qPCR GreenMaster with ROX (Larova, Ornat). All primers are murine and were synthesized by Sigma-Aldrich Israel using the following primers: *Tim4:* Fwd (5' 3')- ATTCTCCCATCCACTTCACAG, Rev (3'-5')- CACCATTAGCACAAATCCCAC (band size: 147bp); *Tim3*: Fwd-ACCCTGGCACTTATCATTGG, Rev-TTTTCCTCAGAGCGAATCCTG (band size: 149bp); *Cd300a: Fwd*-CAGGACCAACACTAGAGACAC, Rev-CAGGAGAGCTAACACAGACAAC (band size: 146bp); *Cd300b: Fwd*- AATGACACGGACACTTACTGG, Rev-CATGTCTGTACTGCCGTCC (band size: 150bp); *Cd300c: Fwd*-AAGGTTGAGGTGTTCGTGG, Rev-

CTTTCTGGTCACGCTGGG (band size: 150bp); *Cd300d: Fwd*-CAGTTCTCTGCTCTACTCCTATTC, Rev-CTTGTAACCCTTCCAGTATGAGG (band size: 144bp); *Cd300e: Fwd*-GTCTGCTCCTTCTCTGCTTC, Rev-GTCCTCGGCACCAGTATTTC (band size: 141bp); *Cd300f: Fwd*-ACCACAGTAAAAGAGACCAGC, Rev-GAGATCCAGAAACCCATCACC (band size: 120bp); *Cd300g: Fwd*-TCATTGTCTTTCCAGGGAGC, Rev-GGACAAGAGTATCAGGACTGG (band size: 149bp); *MerTk: Fwd*-CCTGAGCCCGTCAATATCTTC, Rev-CGTCAGTCCTTTGTCATTGTG (band size: 144bp); *Axl: Fwd*-TGGGAGAAGGAGAATTTGGC, Rev-AGACAGCTTCACTCAGGAAATC (band size: 138bp). All qPCR reactions were conducted on a Bio-Rad CFX96 real-time PCR machine. Quantitation and normalization were relative to the housekeeping gene hypoxanthine-guanine phosphoribosyltransferase (*Hprt*).

Flow cytometry

Flow cytometry was performed using a Gallios flow cytometer (Beckman-Coulter) to validate the expression level of selected surface markers on isolated eosinophils (3 X 105 cells in 200 µl). Staining was performed on ice for 30 minutes in HBSS supplemented with 1% BSA, 0.1% sodium azide. Data were analyzed using Kaluza analysis software on 10,000-50,000 acquired events. Surface molecule expression was calculated by defining the delta mean fluorescent intensity between the specific antibody stain and the isotype-matched control antibody.

The following antibodies were used to stain for PtdSer-recognizing cell surface receptors: Anti-mouse LMIR5/CD300b/CLM-7, Rat monoclonal clone 339003, MAB2580; Anti-mouse CD300c/d Rat IgG2bκ 148002, (Biolegend); Anti-mouse CD300LF/CLM-1 Goat polyclonal IgG Santa Cruz sc-161464; Anti-mouse TIM-4-PE Rat/IgG2a, kappa 12-5866 (eBioscience); Anti-mouse TIM-1 Rat/IgG2b, kappa 14-5861 (eBioscience).

RNAseq

RNA was extracted using TRIzol™ Reagent (Invitrogen, Thermo Fisher) according to the manufacturer's instructions. The RNA integrity number (RIN) was analyzed using Typestation (Agilent) and only samples of RIN>8 were used. RNA samples were prepared using the CEL-Seq2 protocol (26) with minor changes: instead of single-cells as input, 2 ng of purified RNA (obtained from 10^6 eosinophils), was used for library preparation. The CEL-Seq library was run on an Illumina NextSeq 550 apparatus according to manufacturer's recommendation. The number of reads ranged from 3,093,819 to 10,621,072 per sample. The reads were mapped to the Mus musculus, GRCm38 genome (fasta:ftp://ftp.ensembl.org/pub/release97/fasta/mus_musculus/pep/Mus_musculus.GRCm38.pep.abinitio.fa.gzgtfftp:// ftp.ensembl.org/

pub/release97/gtf/mus_musculus/Mus_musculus.GRCm38.97.chr_patch_hapl_scaff.gtf.gz) using Tophat2 version 2.1.0 (27) with up to 2 mismatches allowed per read, the minimum and maximum intron sizes were set to 50 and 100,000, respectively, and an annotation file was provided to the mapper. The percentage of uniquely mapped reads ranged from 2,599,806 to 8,909,751 per sample. Only uniquely mapped reads were counted to genes, using 'HTSeq-count' package version 0.6.1 with 'union' mode (28). Normalization and differential expression analyses were conducted using DESeq2 R package version 1.10.0 (29). Sample preparation, sequencing, quality control, and normalization were conducted by the Technion Genome Center, Life Science and Engineering Interdisciplinary Research Center, Technion, Haifa, Israel.

Bioinformatics analysis

RNA-Seq data from the experiment was trimmed using fastp 0.20.1 (30) and aligned using STAR 2.7.2a (31). Normalization and differential expression analyses were conducted using DESeq2 R package version 1.32.0. Genes were regarded as statistically significant and differentially expressed if they presented false discovery rate (FDR) lower than 0.05 and changed their expression by a factor of 1.5 or more (6). P values were adjusted with FDR multiple comparison correction. Gene ontology annotations were obtained from Ensembl and pathway graphs were obtained from KEGG. In several analyses, datasets were retrieved from public domains and therefore not all genes were identified. In such cases NA represents non-applicable. All datasets presented in this study are available online in accession accession numbers: GSE189213 and GSE216110.

Enzyme-linked immunosorbent assay

Cytokines were measured by enzyme-linked immunosorbent assay (ELISA) according to the manufacturer's instructions kit: IL-6, TNF-α, and CCL17 (R&D Systems, Minneapolis, MN).

Statistical analysis

P values of data sets were adjusted with false discovery rate (FDR) using multiple comparison correction (32). FDR lower than 0.05 and fold-change by a factor of 1.5 or more were analyzed. In *in vitro* experiments, one-way analysis of variance (ANOVA), unpaired two-tailed Student's *t* test with 95%

confidence interval were used. All statistical tests were performed with GraphPad Prism V8 software. Experiments are from n=3 biological replicates. Data are shown as mean ± SEM. *-$p < 0.05$; **-$p < 0.01$; ***-$p < 0.001$.

Results

Eosinophils bind and engulf apoptotic cells

Extracellularly exposed PtdSer is recognized by multiple cell surface receptors and bridging molecules, such as CD300-family members, T-cell immunoglobulin mucin (Tim) receptors, brain-specific angiogenesis inhibitor 1 (BAI1), and or Tryo3-Axl-Mer (TAM) receptors (23, 33–35). Thus, we were first interested to determine the expression pattern of PtdSer-recognizing receptors in eosinophils. To this end, RNA was extracted from peritoneal eosinophils and mRNA expression of CD300-family members, TIM-3, TIM-4, AXL and MerTK were assessed by quantitative PCR. Eosinophils expressed mRNA for multiple PtdSer-recognizing receptors including *Cd300a*, *Cd300b*, *Cd300d*, *Cd300f*, *Cd300g*, *Tim4*, and to and to lesser extent *Cd300c* and *Mertk* (Figure 1A). Next, we aimed to confirm protein expression of the aforementioned receptors. Flow cytometric analysis revealed that eosinophils express detectable levels of CD300a, CD300b, CD300f but do not express TIM-4 and TIM-1(Figures 1B, C).

Expression of PtdSer-binding receptors on eosinophils suggest that they may interact with apoptotic cells. Thus, we determined whether eosinophils bind and/or engulf apoptotic cells. Peritoneal eosinophils were isolated from $Il5^{Tg}$ mice and labeled with CFSE. Subsequently, the eosinophils (marked in green color) were co-cultured with DiD-labeled apoptotic cells (marked in red) and eosinophil-apoptotic cell interactions was measured by image stream (Figure 1D), which enables to capture single-cell images of interacting cells. This analysis revealed eosinophils in three different states. Namely, eosinophils that have no interaction with apoptotic cells (Figure 1D- upper panel), Eosinophils that are attached to apoptotic cells (Figure 1D- middle panel) and eosinophils that engulfed apoptotic cells (Figure 1D- lower panel). Quantitative analysis showed that approximately 20% of the eosinophils were either attached to apoptotic cells (2.25%) or engulfed apoptotic cells (17.25%) (Figure 1E). The ability of eosinophils to bind and engulf apoptotic cells was further established using real-time, live-cell imaging analysis where upon introduction of DiD-labeled apoptotic cells (Figure 1F, time 0:00), eosinophils were capable of binding them (Figure 1F, time 0:09) and rapidly engulfing them (Figure 1F, time 0:17 and 0:25).

To further confirm the ability of eosinophils to uptake dead cells, the uptake of pHrodo-labeled *thymocytes* was measured *in vitro* by flow cytometry. This method uses a unique pHrodo dye that fluoresces in response to an acidic environment that is found in the phagosome (36). Indeed, ~13% of the eosinophils, which were co-cultured with apoptotic cells were postive for pHrodod (Figure 1G).

Apoptotic cells induce transcriptional changes in eosinophils

Following the observation that eosinophils can interact with apoptotic cells, we were interested to determine whether interaction of eosinophils with apoptotic cells will alter their transcriptional profile. To this end, mouse eosinophils were incubated with apoptotic cells and subjected to RNA sequencing. Pairwise comparison analysis revealed that eosinophils that were co cultured with apoptotic cells upregulated 1,795 transcripts and downregulated 1,678 transcripts, (adjusted p-value < 0.05 and fold change of >< ± 1.5, Figure 2A and Table S1). The list of up- and down-regulated transcripts were further analyzed using gene ontology (GO) based on biological processes. This analysis identified that upon interaction with apoptotic cells, eosinophil upregulate pathways that are related to global "leukocyte activation" including "response to wound healing" and "cell migration" (Figure 2B). In contrast, GO analysis of the biological processes that were dictated by the downregulated transcripts indicated that following interaction with apoptotic cells, eosinophils downregulated pathways related to "defense response", "response to IFN-γ", and "inflammatory response" (Figure 2B). These data are consistent with the anti-inflammatory effects of apoptotic cells on additional myeloid cell types (10, 13). To further characterize the transcriptional changes induced in eosinophils by apoptotic cells we analyzed the expression of cell surface receptors (Figures 2C, D, Supplementary Tables 2–3), Secreted factors (Figures 2E, F, Supplementary Tables 4–5), and transcription factors (Figures 2G, H, Supplementary Tables 6–7).

Cell surface receptors

Following incubation with apoptotic cells eosinophils upregulated the expression of *Cd34*, which we previously identified as a Type-2 activated eosinophil marker (6) (Figure 2C). In addition, the expression of several cytokine and chemokine receptors including *Il2ra, Il7r Il18rap, Il1rl2, Il13ra1, Tgfbr2* and *Cxcr4*, was increased. Apoptotic cells also increased the expression of adhesion molecules such as *Selp* (P-selectin), *Itgb3*, and *Icam2*, (Figure 2C). Interestingly, apoptotic cells markedly downregulated the expression of CD300 family members including *Cd300a, Cd300lb* and *Cd300ld* (Figure 2D). Furthermore, multiple SLAM-family receptors such as *Slamf7, Slamf8 and Slamf9* were decreased (Figure 2D). *Ccr3*, the main receptor for eotaxin chemokines (37), which have key roles in eosinophil biology was downregulated as well (38). Finally, and

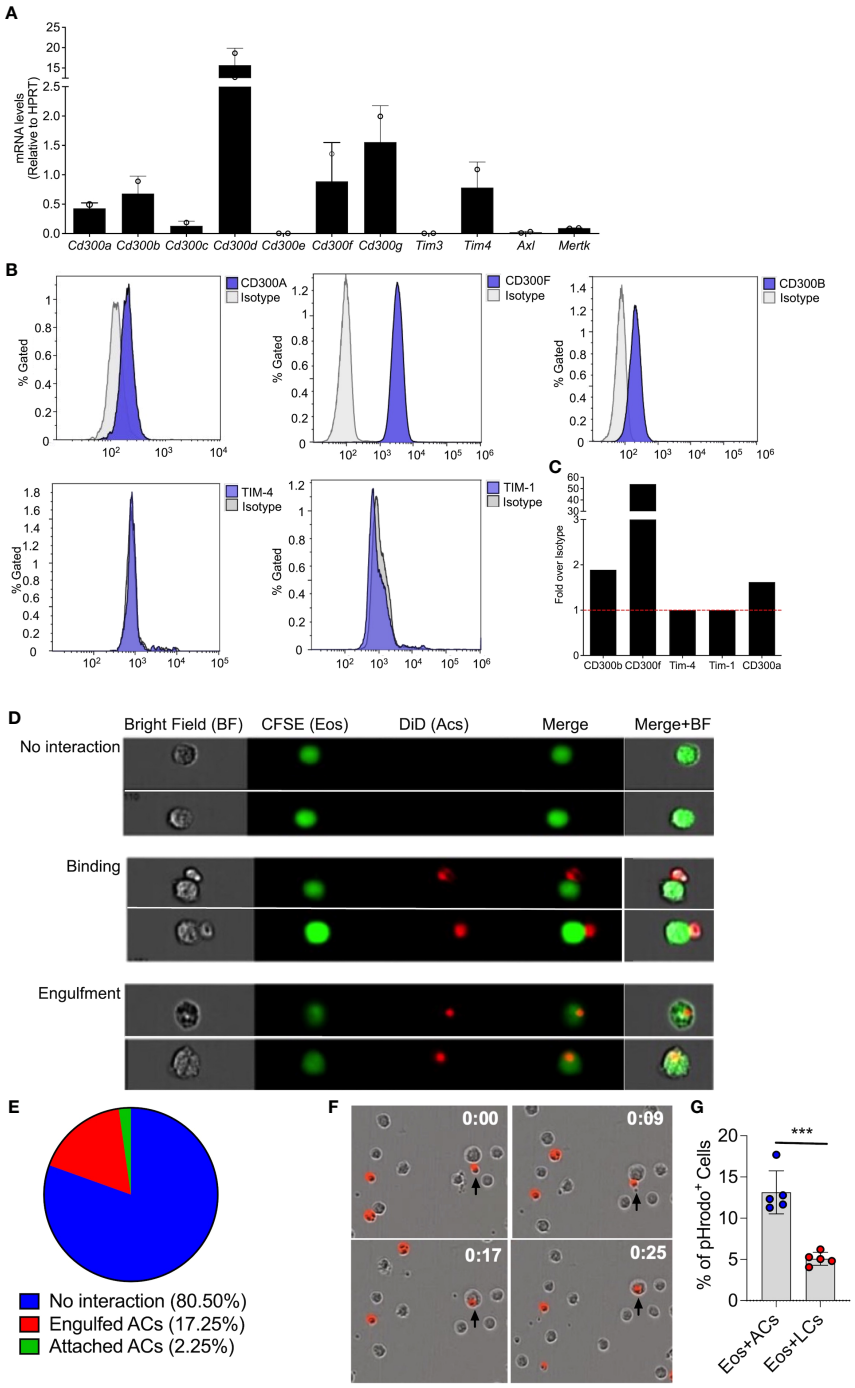

FIGURE 1
Eosinophils bind and engulf apoptotic cells. mRNA expression of various phosphatidylserine binding receptors was determined in eosinophils by quantitative PCR analysis and normalized to the expression of the house keeping gene hypoxanthine-guanine phosphoribosyltransferase (*Hprt*) **(A)** Protein expression of CD300a, CD300b, CD300f, TIM-1 and TIM-4 was determined by flow cytometry **(B)** and presented as fold expression over isotype control **(C)** Representative photomicrographs **(D)** obtained from ImageStream analysis of CFSE-labeled eosinophils (Eos, green) interacting with DiD-labeled apoptotic cells (red) **(D)**. Quantitative analysis of eosinophil-apoptotic cell interactions is presented **(E)** Snap-shot images from time lapse microscopic analysis of eosinophils (unstained) engulfing DiD-labeled apoptotic cells (red; time-0, 9, 17 and 25 min) **(F)** apoptotic cells (ACs) and live cells (LCs) were labeled with pHrodo™ SE Red and co cultured with eosinophils. The percentage of pHrodo™ SE Red positive cells is shown **(G)** Data are from n=3 **(A, E)** or representative images from n=3 independent experiments. In **(G)**, n=5.
***- p< 0.001.

10.3389/fimmu.2022.1041660

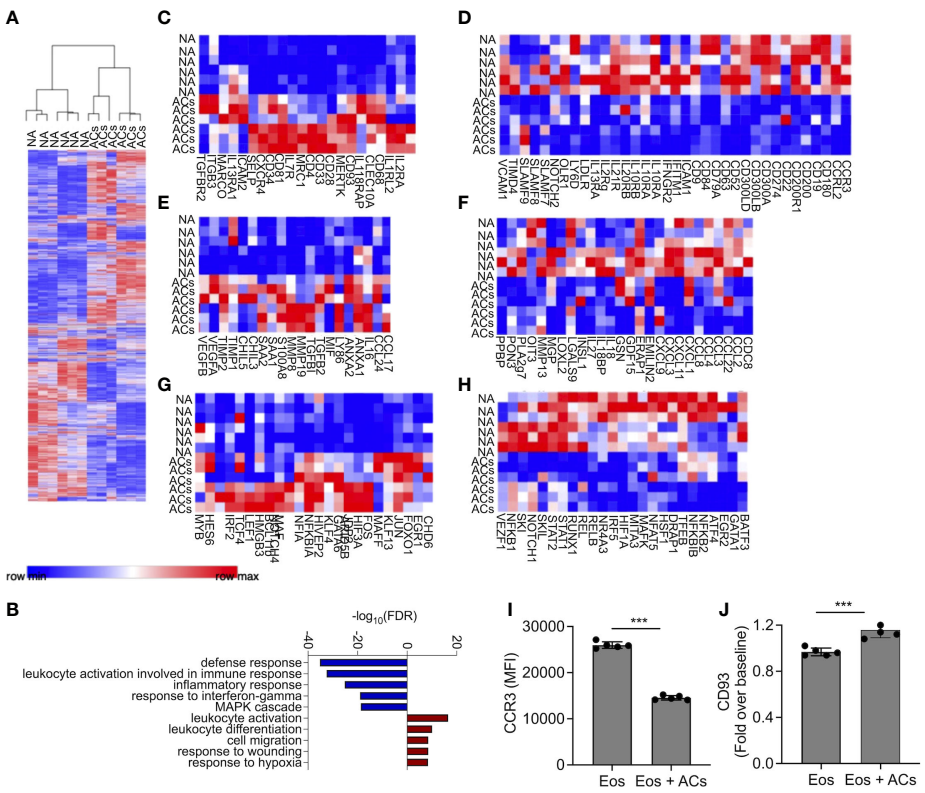

FIGURE 2
Apoptotic cells induce transcriptional changes in eosinophils. Heat-plot analysis of statistically significant (≥≤ +/-1.5-fold, adj. p value ≤ 0.05) differentially expressed transcripts of eosinophils that were co-cultured with apoptotic cells (ACs) in comparison to non activated eosinophils (NA) **(A)** In **(B)**, Gene ontology (GO) analysis based on biological processes (BP) using the statistically significant differently express transcripts that were induced by apoptotic cells is shown. Heat plot analysis of apoptotic cell-induced up and downregulated cell surface receptors **(C, D)**, secreted factors **(E, F)**, and transcription factors **(G, H)** of eosinophils following incubation with apoptotic cells. Expression of CCR3 **(I)** and CD93 **(J)** was determined by flow cytometry on the surface of eosinophils, which were incubated in the presence of apoptotic cells. Each lane indicates eosinophils that were obtained from a different mouse. ***- p< 0.001.

consistent with the overall anti-inflammatory effects that are associated with the interactions of immune cells with apoptotic cells, the expression of multiple IFN-γ-related transcripts including *Ifitm1*, *Ifngr2*, and the recently described Type1-activated eosinophil marker *Cd274* (PD-L1) were decreased.

Secreted factors

Incubation of eosinophils with apoptotic cells induced the expression of soluble factors that are associated with Type-2 immune responses and tissue repair. For example, the IL-4/IL-13-associated factors *Ccl17*, *Ccl24*, *Chil3*, and *Chil5* (39) were upregulated (Figure 2E, Table S4). *S100a8*, which was previously shown to be highly upregulated by eosinophils during colonic repair (8), was also upregulated. In addition, the pro-fibrotic factors/anti-inflammatory factors *Tgfbi*, and *Tgfb2* (40), were also increased following interaction with apoptotic cells. Interestingly, vascular endothelial growth factor (*Vegf*)a/b, which induces angiogenesis (41), and *Anxa1/2*, a regulator of innate immune responses, were also increased (42). Apoptotic cells decreased the expression of numerous pro-inflammatory secreted factors (Figure 2F, Table S5). These include multiple chemokines (e.g., *Cxcl1, Cxcl3 Cxcl9, Cxcl11, Ccl2, Ccl3, Ccl4 Ccl8, and Ccl22*) and cytokines (e.g., *Il18* and *Il27*) (Figure 2F).

Transcription factors

Transcription factor analysis revealed that apoptotic cells increased the expression of *Gata6* and *Maf* (43, 44), which are associated with Th2 activation. The expression of *Klf4*, which is associated with M2 macrophage polarization was increased as well, and several wnt- and *Notch*-family associated transcription factors such as *Lef1* and *Notch4* were increased (Figure 2G). Consistently, apoptotic cells downregulated the expression of several pro-inflammatory transcription factors (Figure 2H). These include the signal transducer and activator of

transcription (STAT) family members, *Stat1* and *Stat2*. Furthermore, *Nfkb1* and *Nfkb2* were also downregulated (Table S7).

To confirm our RNA sequencing data, we chose to examine protein expression of CD93 and CCR3 which were suggested to be up- and downregulated by apoptotic cells, respectively (Table S2–3). Incubation of eosinophils with apoptotic cells decreased cell surface expression of CCR3 and increased CD93 expression (Figures 2I, J). Collectively, these data suggest that apoptotic cells suppress pro-inflammatory genes activation on eosinophils and may augment their responses in settings of tissue repair and remodeling.

Apoptotic cells suppress proinflammatory responses in Type 1-activated eosinophils

Next, we aimed to determine whether apoptotic cells could suppress proinflammatory responses in eosinophils following stimulation with IFN-γ and/or *E. coli*. To this end, eosinophils were stimulated with IFN-γ, *E. coli*, and IFN-γ followed by *E.* coli to elicit Type 1-polarized eosinophils (6). We specifically classify Type 1 eosinophils as cells that are exposed to IFN-γ in the presence of bacterial/innate stimuli since this condition has been widely used to characterize M1 macrophages (45). Thereafter, the cells were subjected to RNA sequencing. Principal component analysis (PCA) analysis, which represents the relationship between biological replicates, revealed that the major factor, which was responsible for the differences between the samples was the presence of apoptotic cells (Figure 3A). This is demonstrated by the PC1 axis that segregated between the samples according to the presence or absence of apoptotic cells and represents 50% of the variance between all groups (Figure 3A). Using Venn plot analysis, we compared the effects of apoptotic cells on transcripts that were upregulated in eosinophils following activation with IFN-γ with or without *E. coli*. (Figures 3B–D). Apoptotic cells suppressed the expression of 515 transcripts, which were upregulated by eosinophils that were stimulated with *E. coli* and IFN-γ (Figure 3B, Table S8). Apoptotic cells inhibited the expression of several surface markers that are associated with an inflammatory phenotype of eosinophils (Table S8). For instance, *Cd274*, a key Type-1 activated eosinophil marker (6, 32), was decreased by ~2.4-fold following interaction with apoptotic cells. Moreover, the expression levels of *Cd83* and *Cd86* were downregulated by ~3.8 and ~1.5 respectively. In addition, the expression of the antiviral transmembrane proteins *Ifitm1* and *Ifitm2* were also decreased by apoptotic cells, (~2.7 and ~1.5-fold, respectively). Notably, apoptotic cells inhibited the expression of proinflammatory soluble mediators including *Il1a*, *Il1b*, *Il6*, *Il12b*, *Cxcl1*, *Cxcl2*, and *Tnfa*. Furthermore, apoptotic cells downregulated the expression levels of several hallmark inflammatory transcription factors such as *Nfkb2*, *Mapk*, *Mapkapk2*, *Ppard*, and Lipopolysaccharide-Induced TNF-α (*Litaf*) (Table S8). The anti-inflammatory effects of apoptotic cells on eosinophils were also observed towards stimulation of eosinophils with IFN-γ or *E. coli* as single activation agents. Out of 1,073 transcripts that were upregulated by IFN-γ, apoptotic cells downregulated the expression of 345 (32%, Figure 3C, Table S8) and out of 857 transcripts that were upregulated by *E. coli*, apoptotic cells decreased the expression of 384 (45%) of total (Figure 3D, Table S8). Down regulated transcripts in response to IFN-γ stimulation included surface markers (e.g., *Cd36*, *Ldlr*, *Olr1*, *Ly6g*, and *Tlr6*), proinflammatory chemokines/cytokines (e.g., *Cxcl2*, *Cxcl3*, *Il1a*, *Il1b*, *Mif*, and *Il6*), and transcription factors (e.g., *Mapk7*, *Nfkb2*, *Stat1*, *Stat5b*, I*rf1*, and *Nlrc5*). Similarly, down regulated transcripts in response to *E. coli* stimulation included surface markers such as *Cd274* and *Pdcd1lg2* (PD-L2), the pro-inflammatory receptors *Cd80* and *Ldlr* and the LPS receptor *Tlr4* were also downregulated. Interestingly, *Csf2rb* (The common beta chain for IL-3, IL-5 and GM-CSF), was also decreased by 1.69-fold. Moreover, proinflammatory secreted factors (e.g., *Ccl2*, *Ccl3*, *Cxcl1*, *Cxcl2*, *Cxcl3*, I*l1a*, *Il6*, and *Tnfa*), were downregulated.

To further characterize the effects of apoptotic cells on the suppression inflammatory pathways in Type-1 activated eosinophils, a bioinformatics gene ontology pathway analysis was conducted. The pathways, which were suppressed by apoptotic cells were associated with "response to IFN-γ", "Inflammatory response", "response to LPS", and "defense response" (Figures 3E–G). To functionally validate the ability of apoptotic cells to inhibit Type 1 eosinophil responses, eosinophils were stimulated with IFN-γ, *E. coli* and IFN-γ with *E. coli*. Stimulation of eosinophils with IFN-γ, *E. coli*, and *E. coli* + IFN-γ resulted in increased the secretion of TNF-α and IL-6, Incubation of eosinophils with apoptotic cells markedly suppressed IFN-γ-, *E. coli*- and IFN-γ+*E.coli*-induced secretion of TNF-α and IL-6 (Figures 3H, I).

Apoptotic cells augment Type 2 eosinophil activation

Recently, apoptotic cells were shown to enhance macrophage responses towards IL-4. Thus, we were interested to determine whether apoptotic cells will increase IL-4-induced responses in eosinophils as well. To this end, eosinophils were stimulated with IL-4 in the presence or absence of apoptotic cells. Thereafter, RNA was extracted and subjected to RNA sequencing. PCA plot of the top 500 variable genes, revealed that the factor, which was accounted for the major variance between the samples (62.7%), was explained by the presence of apoptotic cells (Figure 4A). PC2 that represents the differences induced by IL-4, accounted for only 18% of the variance

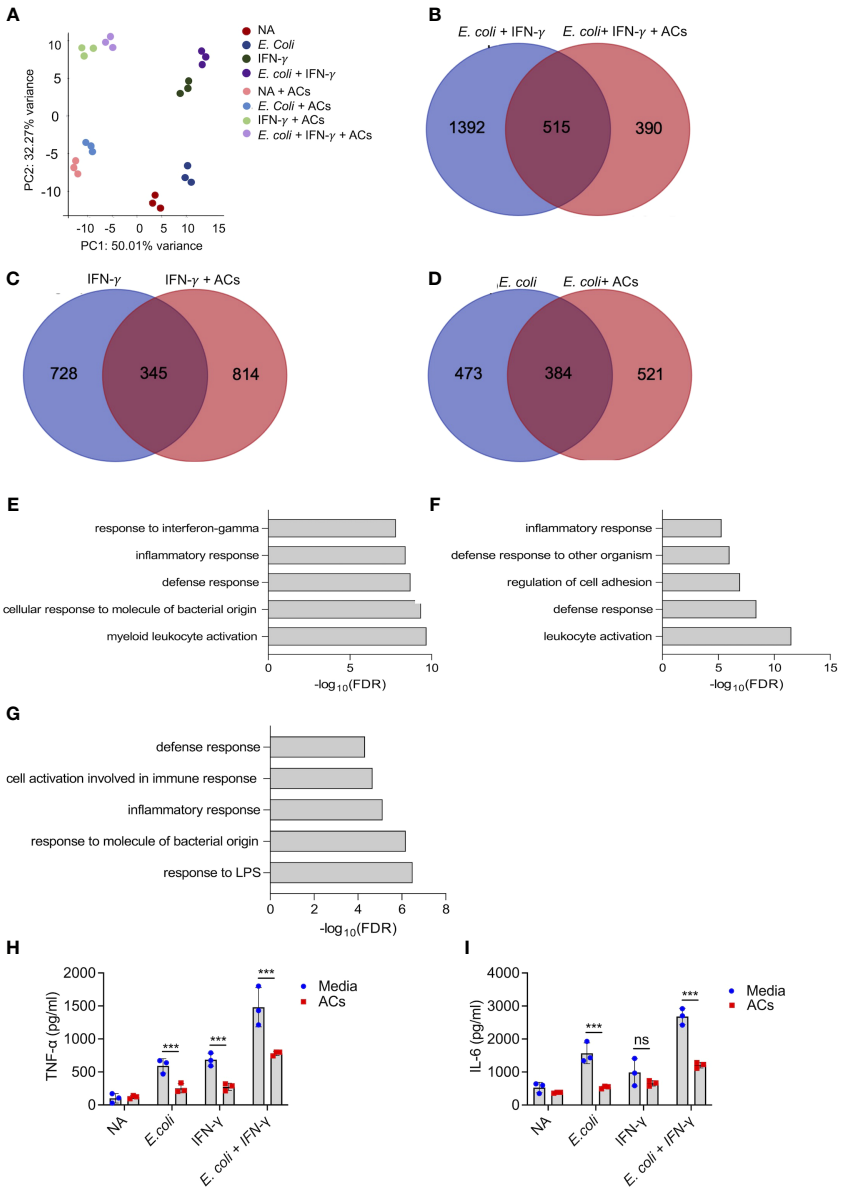

FIGURE 3
Apoptotic cells suppress proinflammatory responses in Type 1-activated eosinophils. Principal components analysis (PCA) of differentially expressed transcripts following incubation of non activated eosinophils (NA) or eosinophils with *E coli*, IFN-γ, *E coli*+ IFN-γ, in the presence or absence of apoptotic cells (ACs, A). Venn-plot representation compering the transcriptome signatures of transcripts that were upregulated in eosinophils by *E coli* + IFN-γ, *E coli*, or IFN-γ, with the transcripts that downregulated when *E coli* + IFN-γ, *E coli*, or IFN-γ stimulated eosinophils in the presence of apoptotic cells **(B-D)**. Gene ontology (GO) analysis based on biological processes (BP) using the statistically significant transcripts inhibited by apoptotic cells following activation with *E coli* + IFN-γ, *E coli*, or IFN-γ **(E-G)**. Purified eosinophils were stimulated with *E coli* + IFN-γ, *E coli*, or IFN-γ in the presence or absence of apoptotic cells (ACs). Subsequently, the secretion of TNF-α **(H)** and IL-6 **(I)** were determined by ELISA. In **(A)**, each dot represents a different sample (n=3). In **(H, I)** data are representative of n=3 different experiments conducted in triplicates; ns- nonsignificant, ***p<0.001.

(Figure 4A). The PCA plot further demonstrated that the groups, which displayed the largest difference were unstimulated eosinophils and eosinophils stimulated with IL-4 in the presence of apoptotic cells (Figure 4A). Our analyses revealed that 62 transcripts were significantly upregulated by the combination of IL-4 and apoptotic cells compared to IL-4 or apoptotic cells alone (Figure 4B, Table S9). Among these transcripts, several were associated with tissue remodeling and repair. For example, IL-4 increased the expression of *Chil3* by 1.7-fold compared to unstimulated cells. The presence of

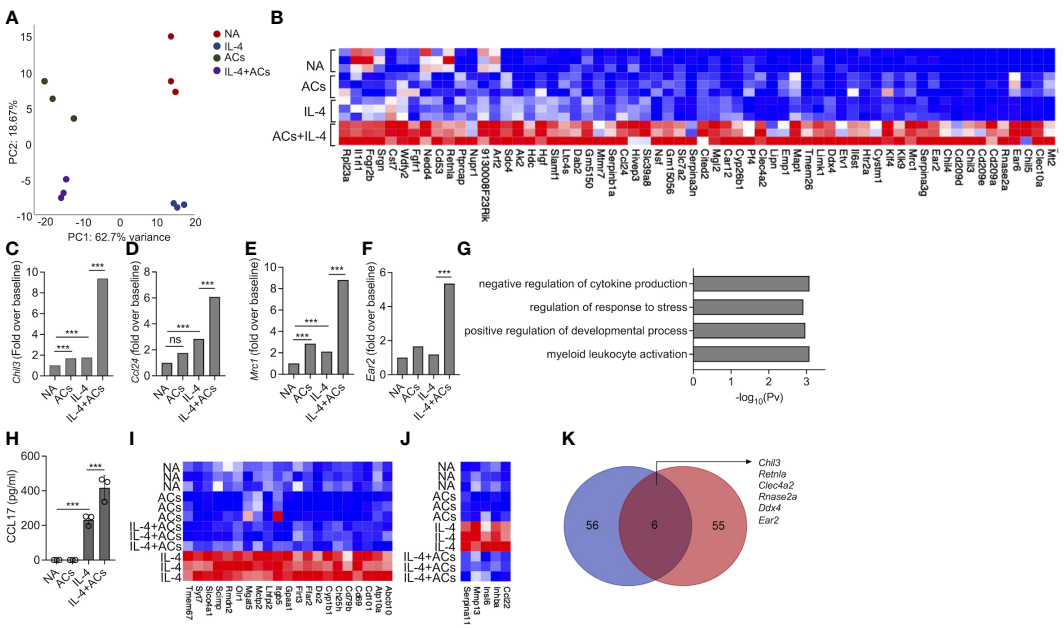

FIGURE 4
Apoptotic cells augment Type 2 eosinophil activation. Principal components analysis (PCA) of differentially expressed transcripts following incubation of non activated eosinophils (NA) or eosinophils stimulated with IL-4, apoptotic cells (ACs) or IL-4 in the presence of apoptotic cells **(A)**. Heat-map representation of the set of transcripts (62 transcripts) that were augmented by ACs following stimulation with IL-4 compared with apoptotic cells alone and IL-4 alone **(B)**. mRNA levels, of Type-2 eosinophil-associated transcripts, as identified by RNAseq **(C-F)**. Gene ontology (GO) analysis based on biological processes (BP) using the statistically significant differently expressed transcripts following which were increased in eosinophils following their incubation with IL-4 and ACs in in comparison with IL-4 **(G)**. Purified eosinophils were either not activated (NA) or stimulated with IL-4, ACs or the combination of IL-4 + ACs. Thereafter, the secretion of CCL17 was determined by ELISA **(H)**. Heat-map representation of the set of transcripts that were decreased by ACs following stimulation with IL-4 compared with IL-4 alone **(I, J)**. Venn-plot representation comparing the set of transcripts, which were augmented by ACs in the presence of IL-4 in eosinophils (Eos) and macrophages (Mac) **(K)**. In **(A)**, each dot represents a different sample (n=3). In **(H)** data are representative of n=3 different experiments conducted in triplicates; ns- nonsignificant, ***p<0.001.

apoptotic cells induced *Chil3* expression to 9.3-fold (Figure 4C, Table S9). Similarly, the expression of *Chil4* and *Chil5* were also augmented from a fold increase of 4.1 and 1.4 with IL-4 alone to ~20.5 and ~17.5 with IL-4 in the presence of apoptotic cells. Combination of apoptotic cells and IL-4 also increased the expression of hallmark eosinophil-associated transcripts (e.g., *Ccl24* and *Ear2*) and several markers of alternatively activated macrophages such as *Cd209*, *Retnla*, *Klf4, Serpina3, Car12* and *Mrc1 (*46, 47)(Figures 4D–F). Gene ontology (GO) analysis based on biological process demonstrated that stimulation of eosinophils with apoptotic cells and IL-4 enriched pathways that are associated with "negative regulation of cytokine production", "regulation of response to stress" and "regulation of developmental process" (Figure 4G). To functionally validate our RNA sequencing data, secretion of CCL17, an IL-4-induced chemokine, was determined following stimulation of eosinophils with IL-4 or IL-4 and apoptotic cells. As expected, IL-4 induced the secretion of CCL17 (Figure 4H). Addition of apoptotic cells to IL-4 enhanced CCL17 secretion (Figure 4H).

Stimulation of eosinophils with IL-4 in the presence of apoptotic cells resulted also in decreased expression of 69 transcripts (Figure 4I, Table S10). Among these, the expression of *Cd69*, an eosinophil activation marker and expression of *Cd101*, a recently described Type 2 eosinophil marker and *Ccl22*, an IL-4-induced chemokine were decreased (Figures 4I, J). GO analysis of the downregulated transcript signature resulted in no enrichment of a specific biological pathway (data not shown).

Next, we examined whether the 62 transcripts, which were amplified in eosinophils by stimulation by IL-4 in the presence of apoptotic cells were similar to that, which was previously shown for macrophages (14). IL-4 stimulation in the presence of apoptotic cells induced a minor overlap in transcript identity between eosinophils and macrophages (Figure 4K). Nonetheless, the shared transcripts (i.e., *Chil3*, *Retnla*, *Clec4a2*, *Rnase2a*, *Ddx4*, and *Ear2*) (Figure 4K, Table S10) were previously associated with tissue repair and remodeling activities tissue repair-related genes. Taken together, these findings suggest that

apoptotic cells enhance eosinophil activities in Type-2 inflammatory settings.

Eosinophil recognition of apoptotic cells is independent of CD300b and CD300f

Eosinophils express various CD300 receptor family members that could potentially interact with apoptotic cells *via* recognition of PtdSer with specifically high levels of CD300f [Figures 1B, C and (18–22, 48)]. Hence, we examined whether apoptotic cells suppress Type 1 eosinophil activation or augment Type 2 eosinophil activation *via* these CD300-family receptors. Our RNA sequencing data suggested that apoptotic cells decreased the expression of CD300-family members. Interestingly, exposure of eosinophils to apoptotic cells markedly increased cell surface expression of CD300b but decreased CD300f expression (Figures 5A–F).

Given the relative high expression level of CD300f in eosinophils and the finding that CD300b expression was increased following interaction with apoptotic cells, we hypothesized that CD300b and CD300f will mediate apoptotic cell recognition in eosinophils. Despite high mRNA expression of CD300d in eosinophils we did not functionally examine its involvement in eosinophil-apoptotic cell interactions since it was previously shown to be retained intracellularly, and we could not detect any surface expression of CD300d in eosinophils (data not shown). To examine this, eosinophils from WT, *Cd300b*$^{-/-}$ and *Cd300f*$^{-/-}$ mice were obtained and stimulated with *E. coli* or IL-4. Apoptotic cells were capable of suppressing *E. coli*-induced secretion of IL-6 and TNF-α in *CD300b*$^{-/-}$ and *Cd300f*$^{-/-}$ eosinophils to a similar extent as in WT BMDEs (Figures 5G–J). Simulation of *Cd300b*$^{-/-}$ BMDEs with IL-4 in the presence of apoptotic cells induced similar levels of CCL17 secretion as in WT BMDEs stimulated with IL-4 and apoptotic cells (Figure 5K). Consistent with our previous data, *Cd300f*$^{-/-}$ BMDEs did not respond to IL-4 stimulation (20). Nonetheless, the presence of apoptotic cells restored the responses of *Cd300f*$^{-/-}$ BMDEs to IL-4 to a similar extent as WT eosinophils (Figure 5L). These data demonstrate that CD300b and CD300f do not mediate apoptotic cell-driven responses in eosinophils.

Surprisingly, *Cd300a*$^{-/-}$ BMDEs did not respond to *E. coli*-induced stimulation, and we could not detect TNF-α or IL-6 in the culture supernatants (Figures 5M, N). Similarly, although IL-4-stimulated *Cd300a*$^{-/-}$ BMDEs displayed slightly reduced levels of CCL17 secretion in comparison with IL-4-stimulated WT BMDEs, addition of apoptotic cells augmented CCL17 secretion in *Cd300a*$^{-/-}$ and WT BMDEs to a similar extent (Figure 5O).

Discussion

Eosinophils are white blood cells that are traditionally associated with allergic and parasitic diseases. Nonetheless, accumulating data suggest key roles for eosinophils in homeostasis and host defense. Since eosinophils are considered terminally differentiated cells, much knowledge has been gained regarding the signals which mediate eosinophil survival and prevent apoptosis. Much less is known regarding the ability of eosinophils to interact with apoptotic cells in the microenvironment and how these interactions can shape eosinophil activities. This is of specific interest since clearance of apoptotic cells and engulfment of apoptotic cells by phagocytes is a key event in the resolution of inflammatory responses (10, 13). The importance of efferocytosis in homeostasis is further demonstrated by the finding that mice, which lack components that enable sensing, recognition and/or engulfment of dead cells, develop autoimmune diseases and/or chronic inflammation (49). Like additional immune cells, eosinophils are constantly exposed to apoptotic cells that are present in their microenvironment (1). Thus, we aimed to characterize the effects of apoptotic cells on eosinophil activities. We demonstrate that eosinophils can physically bind and engulf apoptotic cells. Furthermore, using an unbiased global RNA sequencing approach we show that interaction of eosinophils with apoptotic cells renders them anti-inflammatory. Stimulation of eosinophils with Type 1 polarizing agents (i.e., IFN-γ, *E. coli* and combinations of thereof) (6) in the presence of apoptotic cells markedly suppressed their proinflammatory transcriptome signature and ability to secrete inflammatory cytokines. Furthermore, apoptotic cells augment eosinophil responses towards IL-4, which induces a transcriptome signature that is associated with tissue repair and remodeling. Taken together our data demonstrate that apoptotic cells shape the transcriptome landscape of eosinophils by polarizing eosinophils into an anti-inflammatory phenotype.

Using high resolution and live-imaging techniques, we show that eosinophils can bind and engulf to some extent apoptotic cells. The interaction of eosinophils with apoptotic cells induced marked transcriptional changes in eosinophils that were associated with induction of an anti-inflammatory, immunosuppressive phenotype. These data are consistent with the overall understanding that engulfment of apoptotic cells induces potent immunosuppressive activities in immune cells. For example, the immunosuppressive activities of apoptotic cells upon their interaction with immune cells results in induction of various suppressive mechanisms including the secretion of

10.3389/fimmu.2022.1041660

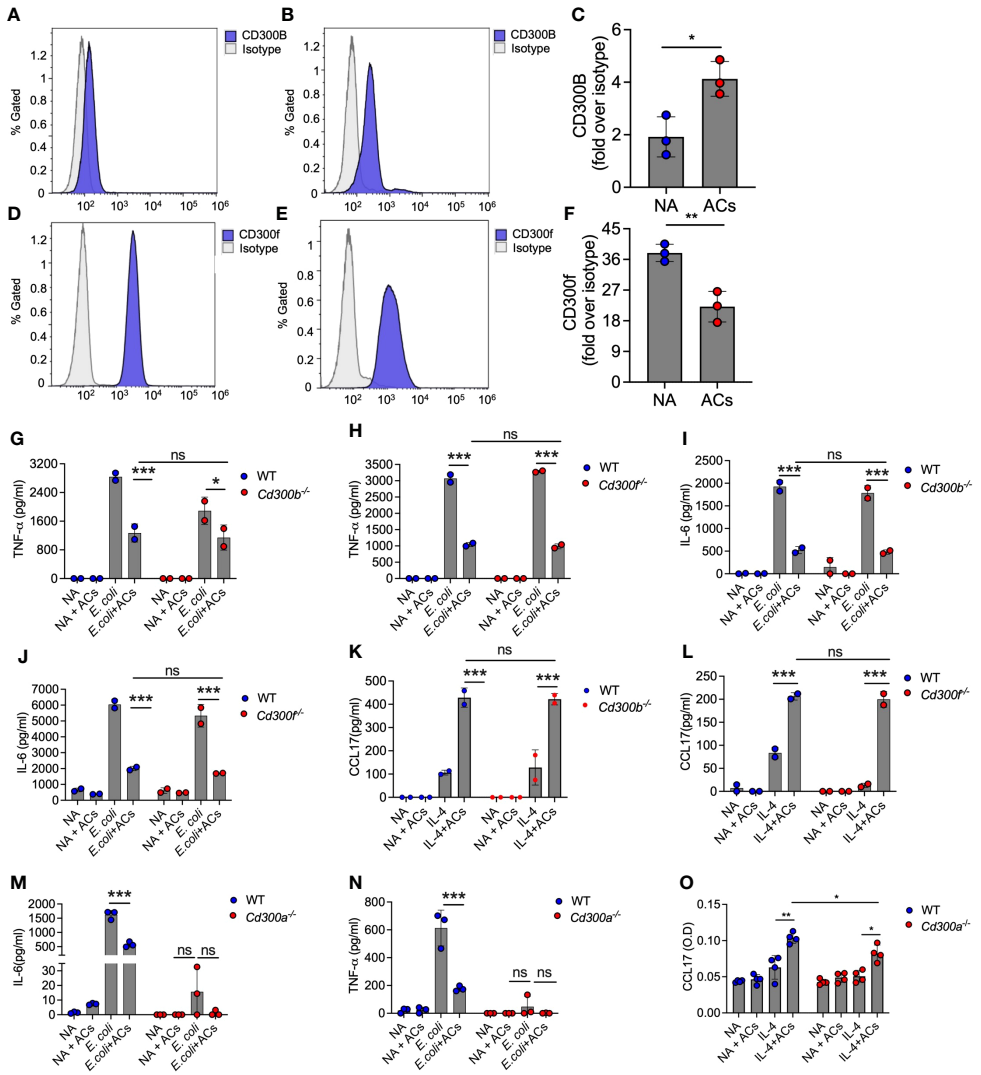

FIGURE 5
Eosinophil recognition of apoptotic cells is independent of CD300b and CD300f. Surface expression and quantitative analysis of CD300b **(A–C)** and CD300f **(D–F)** following incubation of eosinophils with apoptotic cells (ACs) was determined by flow cytometry. Purified eosinophils from wild type (WT), *Cd300b*$^{-/-}$ **(G, I, K)**, *Cd300f*$^{-/-}$ **(H, J, L)**, or *Cd300a*$^{-/-}$ **(M–O)** were obtained and stimulated with *E. coli* **(G-J, M, N)** or IL-4 **(K, L, O)** in the presence or absence of apoptotic cells (ACs). Thereafter, the secretion of TNF-α **(G, H, N)**, IL-6 **(I, J, M)** and CCL17 **(K, L, O)** were determined by ELISA. In **(A)**, each dot represents a different sample (n=3). In **(A, B, D, E)** data are representative of n=3 different experiments, which are summarized in **(C–F)**. In all other experiments, data are representative of n=3 different experiments conducted in triplicates; ns-nonsignificant, *p<0.05, **p<0.01, ***p<0.001.

potent anti-inflammatory cytokines [e.g., TGF-β and interleukin-10 (IL-10)] (50, 51). Similarly, apoptotic cells induced the expression of *Tgfb2* in eosinophils and decreased the expression of numerous pro-inflammatory chemokines/cytokines including *Cxcl1, Cxcl3 Cxcl9, Cxcl11, Ccl2, Ccl3, Ccl4 Ccl8, and Ccl22*, *Il18* and *Il27*. In contrast, chemokines/cytokines that are associated with anti-inflammatory responses including *Ccl17*, *Ccl24*, *Chil3*, and *Vegf* were increased. Furthermore, while the expression of several key proinflammatory transcription factors was decreased (e.g., *Stat1, Stat2, Nfkb1* and *Nfkb2*), the expression of inhibitory transcription factors [e.g., NFκB inhibitor alpha (*Nfkbia*)] and factors associated with tissue repair and wound healing were increased. It was previously shown that apoptotic cells upregulated the expression of *Nr4a1* in macrophages (52), which in turn inhibited the activation of NF-κB and Egr1 (52), which suppress pro-inflammatory gene expression. Notably, apoptotic cells upregulated the expression of *Nr4a1* and *Egr1* in eosinophils as well. Collectively, these data suggest that apoptotic cells do not induce a global "shut down" of eosinophil transcriptional activity but rather actively

reprogram transcriptional activity that results in an anti-inflammatory immunosuppressive eosinophil phenotype.

Although the major cells that are responsible for efferocytosis and clearance of apoptotic cells are macrophages (10), eosinophils are posed in various anatomical locations such as the gastrointestinal tract and are present in multiple inflammatory conditions that are characterized by tissue damage and cell death including colitis, cancer, parasite infections and asthma (1, 2). We have recently shown that like macrophages, exposure of eosinophils to Type 1-associated cytokines (e.g., IFN-γ in the presence of bacterial stimuli) polarized them to display a pro-inflammatory phenotype (termed Type 1 eosinophils). In contrast, exposure to Type 2-associated cytokines (e.g., IL-4) drove them towards immunomodulatory activities (termed Type 2 eosinophils) (6). Whether apoptotic cells could further augment eosinophil polarization is unclear. Herein, we show that apoptotic cells markedly suppressed IFN-γ, *E. coli* and combination of IFN-γ+*E. coli*-induced inflammatory responses and secretion of inflammatory cytokines in eosinophils. In contrast, interaction of eosinophils with apoptotic cells augments their Type 2-associated signature, which is associated with tissue repair and wound healing. Our data are consistent with earlier studies using monocytes, which showed that co-culture of LPS-stimulated monocytes with apoptotic cells resulted in inhibition of TNF-α secretion and induction of IL-10 release (53). Furthermore, they are also in line with the recent finding that IL-4 or IL-13 alone were insufficient to induce an optimal tissue repair transcriptional program in macrophages. Rather, IL-4/IL-13 required the presence of apoptotic cells (14). Interestingly, exposure of eosinophils to IL-4 in the presence of apoptotic cells resulted in transcriptional profile that was different than the one observed for macrophages, which were stimulated with IL-4 in the presence of apoptotic cells and resulted in an overlap of only 6 transcripts (*Chil3*, *Retnla*, *Clec4a2*, *Rnase2a*, *Ddx4*, and *Ear2*). This was unexpected since the transcriptional profile of Type 2 polarized eosinophils was shown to display marked overlap and similarity with that of M2-polarized macrophages (6). The different transcriptional phenotype of eosinophils and macrophages in response to IL-4 and apoptotic cells likely results from the fact that macrophages express a large and different repertoire of receptors and intracellular molecules that can bind, engulf and digest apoptotic cells (54).

In addition to the 6 transcripts, which were shared with macrophages, additional transcripts that are associated with M2 macrophage activities were identified in our analysis. DAB adaptor protein 2 (*Dab2*) which has been shown to display immunosuppressive activities in macrophages and is involved in TGF-β signaling (55), was upregulated in eosinophils following activation of IL-4 in the presence of apoptotic cells. The expression of *Hivep3*, a transcription factor that negatively regulates gene expression and is suggested as a suppressor of pro-inflammatory gene expression in M2 macrophages (56), was augmented in response to IL-4 and apoptotic cells. Furthermore, expression of *Klf4*, a transcription factor that is associated with the suppression of M1 macrophage polarization and the promotion of M2 polarization (57), was upregulated in IL-4-activated eosinophils in the presence of apoptotic cells. Finally, several IL-4-induced surface molecules were augmented by apoptotic cells in eosinophils. Among these, we identified *Cd209* and *Car12*, which were previously shown to be expressed by M2 macrophages (58), and the alternative (IL-4)-activated macrophages marker, *Mrc1* (CD206) (58). Together, these findings indicate that IL-4 and apoptotic cells induce a distinct transcript signature in eosinophils that augments IL-4 induced responses and polarizes eosinophils into a cell that is associated with Type 2 immune responses such as tissue repair and remodeling.

Our study bears several limitations. First, we could not identify the cell surface receptor in eosinophils, which interacts with apoptotic cells. Nonetheless, we demonstrate that CD300b and CD300f are not involved in suppression of Type 1 eosinophil responses and augmentation of Type 2 eosinophil responses by apoptotic cells. One of our study limitations is that we cannot exclude possible involvement for CD300a especially since *Cd300a*$^{-/-}$ eosinophils did not response to *E. coli* stimulation. We did not use neutralizing antibodies to overcome this limitation since we are unaware of neutralizing antibodies capable of locking CD300a (or other CD300 family members). While the inability of CD300a to response to *E. coli* stimulation was unanticipated it was not surprising since we have previously shown that CD300 family members are required for eosinophil activation by IL-4 and IL-33 (20, 59). An addition limitation is that our efferocytosis assays were conducted for long time periods (~18 hrs). This time frame was specifically chosen to assess global transcriptome changes in eosinophils. Nonetheless, it may introduce the activation of various pathways in eosinophils that may be triggered by danger-associated molecular patterns (DAMPs) that in turn can activate a plethora of innate immune receptors. Finally, our study was conducted on murine eosinophils that have been obtained from the peritoneal cavity of *Il5Tg* mice or generated *in vitro* from BM progenitor cells. Thus, the relevance of these findings to human eosinophils remains to be determined. It will be of specific interest to determine whether eosinophils can engulf apoptotic cells in colon cancer where eosinophils have been suggested to directly kill tumor cells (16). Despite these limitations, our global sequencing approach, microscopy studies and efferocytosis assays demonstrate that eosinophils can bind, engulf, and functionally respond to apoptotic cells. Future studies should comprehensively characterize the molecular mechanisms, which enable the interaction of eosinophils with apoptotic cells.

Taken together, in this study we extend our knowledge regarding the transcriptional plasticity of eosinophils. We provide important insights into the regulation of eosinophil gene expression in distinct inflammatory environments and

demonstrate the key regulatory effects of apoptotic cells on eosinophil activation especially in Type-1 and Type-2-associated immune settings.

Data availability statement

The data presented in the study are deposited in the NCBI repository, accession numbers GSE189213 and GSE216110.

Ethics statement

The animal study was reviewed and approved by Animal Health Care Committee of the Tel Aviv University and were performed in accordance with the regulations and guidelines regarding the care and use of animals for experimental procedures.

Author contributions

DA and AM- conception and/or design of the work. AD, IH, SA, MI- Data Collection. AD, IH, SA, MI, AM- Data analysis and interpretation. AZ, FL-S- Critical reagents for the study. AD, AM- Drafting the article. AD, FL-S, AM - Revision of the article. AM- Final approval of the version to be published.

Funding

This work was supported by grants and fellowships to MA from the US-Israel Bi-national Science Foundation (grant no. 2015163), Israel Science Foundation (grants no. 886/15 and 542/20), Israel Cancer Research Fund, Richard Eimert Research Fund on Solid Tumors, Israel Cancer Association, Dotan Hemato Oncology Fund, Cancer Biology Research Center, Tel Aviv University, The Tel Aviv University Faculty of Medicine Recanati Fund, and Azrieli Foundation Canada-Israel, and in part by grants to Francesca Levi-Schaffer from the US-Israel Bi-national Science Foundation (grant no 2015045.) and Aimwell Charitable Trust (UK).

Conflict of interest

AM is a consultant for Glaxo Smith Kline, Astra Zeneca, Sanofi, Oravax, Sartorious and is an inventor of three patents owned by the Tel Aviv University.

The remaining authors declare that the research was conducted in the absence of any commercial or financial relationships that could be construed as a potential conflict of interest.

The handling editor YT declared a shared parent affiliation with the authors IZ and F-LS at the time of review.

Publisher's note

Supplementary material

The Supplementary Material for this article can be found online at: https://www.frontiersin.org/articles/10.3389/fimmu.2022.1041660/full#supplementary-material

References

1. Lee JJ, Jacobsen EA, McGarry MP, Schleimer RP, Lee NA. Eosinophils in health and disease: the LIAR hypothesis. *Clin Exp Allergy* (2010) 40(4):563–75. doi: 10.1111/j.1365-2222.2010.03484.x

2. Rosenberg HF, Dyer KD, Foster PS. Eosinophils: changing perspectives in health and disease. *Nat Rev Immunol* (2013) 13(1):9–22. doi: 10.1038/nri3341

3. Wechsler ME, Munitz A, Ackerman SJ, Drake MG, Jackson DJ, Wardlaw AJ, et al. Eosinophils in health and disease: A state-of-the-Art review. *Mayo Clin Proc* (2021) 96(10):2694–707. doi: 10.1016/j.mayocp.2021.04.025

4. Grisaru-Tal S, Itan M, Klion AD, Munitz A. A new dawn for eosinophils in the tumour microenvironment. *Nat Rev Cancer* (2020) 20(10):594–607. doi: 10.1038/s41568-020-0283-9

5. Grisaru-Tal S, Dulberg S, Beck L, Zhang C, Itan I, Hediyeh-Zadeh S, et al. Metastasis-entrained eosinophils enhance lymphocyte-mediated anti-tumor immunity. *Cancer Res* (2021) 81(21):5555–71. doi: 10.1158/0008-5472.CAN-21-0839

6. Dolitzky A, Shapira G, Grisaru-Tal S, Hazut I, Avlas S, Gordon Y, et al. Transcriptional profiling of mouse eosinophils identifies distinct gene signatures following cellular activation. *Front Immunol* (2021) 12:802839. doi: 10.3389/fimmu.2021.802839

7. Gadkari M, Makiya MA, Legrand F, Stokes K, Brown T, Howe K, et al. Transcript- and protein-level analyses of the response of human eosinophils to glucocorticoids. *Sci Data* (2018) 5:180275. doi: 10.1038/sdata.2018.275

8. Reichman H, Moshkovits I, Itan M, Pasmanik-Chor M, Vogl T, Roth J, et al. Transcriptome profiling of mouse colonic eosinophils reveals a key role for eosinophils in the induction of s100a8 and s100a9 in mucosal healing. *Sci Rep* (2017) 7(1):7117. doi: 10.1038/s41598-017-07738-z

9. Nagata S, Tanaka M. Programmed cell death and the immune system. *Nat Rev Immunol* (2017) 17(5):333–40. doi: 10.1038/nri.2016.153

10. Doran AC, Yurdagul A Jr., Tabas I. Efferocytosis in health and disease. *Nat Rev Immunol* (2020) 20(4):254–67. doi: 10.1038/s41577-019-0240-6

11. Tian L, Choi SC, Murakami Y, Allen J, Morse HC, Qi CF, et al. p85alpha recruitment by the CD300f phosphatidylserine receptor mediates apoptotic cell clearance required for autoimmunity suppression. *Nat Commun* (2014) 5:3146. doi: 10.1038/ncomms4146

12. Nagata S, Hanayama R, Kawane K. Autoimmunity and the clearance of dead cells. *Cell* (2010) 140(5):619–30. doi: 10.1016/j.cell.2010.02.014

13. Korns D, Frasch SC, Fernandez-Boyanapalli R, Henson PM, Bratton DL. Modulation of macrophage efferocytosis in inflammation. *Front Immunol* (2011) 2:57. doi: 10.3389/fimmu.2011.00057

14. Bosurgi L, Cao YG, Cabeza-Cabrerizo M, Tucci A, Hughes LD, Kong Y, et al. Macrophage function in tissue repair and remodeling requires IL-4 or IL-13 with apoptotic cells. *Science* (2017) 356(6342):1072–6. doi: 10.1126/science.aai8132

15. Kim MJ, Lee YJ, Yoon YS, Kim M, Choi JH, Kim HS, et al. Apoptotic cells trigger the ABCA1/STAT6 pathway leading to PPAR-gamma expression and activation in macrophages. *J Leukoc Biol* (2018) 103(5):885–95. doi: 10.1002/JLB.2A0817-341RR

16. Reichman H, Itan M, Rozenberg P, Yarmolovski T, Brazowski E, Varol C, et al. Activated eosinophils exert antitumorigenic activities in colorectal cancer. *Cancer Immunol Res* (2019) 7(3):388–400. doi: 10.1158/2326-6066.CIR-18-0494

17. Bachelet I, Munitz A, Moretta A, Moretta L, Levi-Schaffer F. The inhibitory receptor IRp60 (CD300a) is expressed and functional on human mast cells. *J Immunol* (2005) 175(12):7989–95. doi: 10.4049/jimmunol.175.12.7989

18. Munitz A, Bachelet I, Eliashar R, Moretta A, Moretta L, Levi-Schaffer F. The inhibitory receptor IRp60 (CD300a) suppresses the effects of IL-5, GM-CSF, and eotaxin on human peripheral blood eosinophils. *Blood* (2006) 107(5):1996–2003. doi: 10.1182/blood-2005-07-2926

19. Moshkovits I, Shik D, Itan M, Atar D, Bernshtein B, Hershko AY, et al. CMRF35-like molecule 1 (CLM-1) regulates eosinophil homeostasis by suppressing cellular chemotaxis. *Mucosal Immunol* (2013). doi: 10.1038/mi.2013.47

20. Moshkovits I, Karo-Atar D, Itan M, Reichman H, Rozenberg P, Morgenstern-Ben-Baruch N, et al. CD300f associates with IL-4 receptor alpha and amplifies IL-4-induced immune cell responses. *Proc Natl Acad Sci USA* (2015) 112(28):8708–13. doi: 10.1073/pnas.1507625112

21. Moshkovits I, Reichman H, Karo-Atar D, Rozenberg P, Zigmond E, Haberman Y, et al. A key requirement for CD300f in innate immune responses of eosinophils in colitis. *Mucosal Immunol* (2017) 10(1):172–83. doi: 10.1038/mi.2016.37

22. Rozenberg P, Reichman H, Zab-Bar I, Itan M, Pasmanik-Chor M, Bouffi C, et al. CD300f:IL-5 cross-talk inhibits adipose tissue eosinophil homing and subsequent IL-4 production. *Sci Rep* (2017) 7(1):5922. doi: 10.1038/s41598-017-06397-4

23. Borrego F. The CD300 molecules: an emerging family of regulators of the immune system. *Blood* (2013) 121(11):1951–60. doi: 10.1182/blood-2012-09-435057

24. Ravichandran KS. Find-me and eat-me signals in apoptotic cell clearance: progress and conundrums. *J Exp Med* (2010) 207(9):1807–17. doi: 10.1084/jem.20101157

25. Dyer KD, Moser JM, Czapiga M, Siegel SJ, Percopo CM, Rosenberg HF. Functionally competent eosinophils differentiated ex vivo in high purity from normal mouse bone marrow. *J Immunol* (2008) 181(6):4004–9. doi: 10.4049/jimmunol.181.6.4004

26. Hashimshony T, Senderovich N, Avital G, Klochendler A, de Leeuw Y, Anavy L, et al. CEL-Seq2: Sensitive highly-multiplexed single-cell RNA-seq. *Genome Biol* (2016) 17:77. doi: 10.1186/s13059-016-0938-8

27. Trapnell C, Pachter L, Salzberg SL. TopHat: discovering splice junctions with RNA-seq. *Bioinformatics* (2009) 25(9):1105–11. doi: 10.1093/bioinformatics/btp120

28. Anders S, Pyl PT, Huber W. HTSeq–a Python framework to work with high-throughput sequencing data. *Bioinformatics* (2015) 31(2):166–9. doi: 10.1093/bioinformatics/btu638

29. Love MI, Huber W, Anders S. Moderated estimation of fold change and dispersion for RNA-seq data with DESeq2. *Genome Biol* (2014) 15(12):550. doi: 10.1186/s13059-014-0550-8

30. Chen S, Zhou Y, Chen Y, Gu J. Fastp: an ultra-fast all-in-one FASTQ preprocessor. *Bioinformatics* (2018) 34(17):i884–90. doi: 10.1093/bioinformatics/bty560

31. Dobin A, Davis CA, Schlesinger F, Schlesinger F, Drenkow J, Zaleski C, Jha S, et al. STAR: ultrafast universal RNA-seq aligner. *Bioinformatics* (2013) 29(1):15–21. doi: 10.1093/bioinformatics/bts635

32. Onyema OO, Guo Y, Wang Q, Stoler MH, Lau C, Li K, et al. Eosinophils promote inducible NOS-mediated lung allograft acceptance. *JCI Insight* (2017) 2(24):e96455. doi: 10.1172/jci.insight.96455

33. Rothlin CV, Ghosh S, Zuniga EI, Oldstone MB, Lemke G. TAM receptors are pleiotropic inhibitors of the innate immune response. *Cell* (2007) 131(6):1124–36. doi: 10.1016/j.cell.2007.10.034

34. Freeman GJ, Casasnovas JM, Umetsu DT, DeKruyff RH. TIM genes: a family of cell surface phosphatidylserine receptors that regulate innate and adaptive immunity. *Immunol Rev* (2010) 235(1):172–89. doi: 10.1111/j.0105-2896.2010.00903.x

35. Simhadri VR, Andersen JF, Calvo E, Choi SC, Coligan JE, Borrego F. Human CD300a binds to phosphatidylethanolamine and phosphatidylserine, and modulates the phagocytosis of dead cells. *Blood* (2012) 119(12):2799–809. doi: 10.1182/blood-2011-08-372425

36. Lenzo JC, O'Brien-Simpson NM, Cecil J, Holden JA, Reynolds EC. Determination of active phagocytosis of unopsonized porphyromonas gingivalis by macrophages and neutrophils using the pH-sensitive fluorescent dye pHrodo. *Infect Immun* (2016) 84(6):1753–60. doi: 10.1128/IAI.01482-15

37. Foster PS, Mould AW, Yang M, Mackenzie J, Mattes J, Hogan SP, et al. Elemental signals regulating eosinophil accumulation in the lung. *Immunol Rev* (2001) 179:173–81. doi: 10.1034/j.1600-065X.2001.790117.x

38. Rothenberg ME, Hogan SP. The eosinophil. *Annu Rev Immunol* (2006) 24:147–74. doi: 10.1146/annurev.immunol.24.021605.090720

39. Munitz A, Brandt EB, Mingler M, Finkelman FD, Rothenberg ME. Distinct roles for IL-13 and IL-4 *via* IL-13 receptor alpha1 and the type II IL-4 receptor in asthma pathogenesis. *Proc Natl Acad Sci U S A.* (2008) 105(20):7240–5. doi: 10.1073/pnas.0802465105

40. Meng XM, Nikolic-Paterson DJ, Lan HY. TGF-beta: the master regulator of fibrosis. *Nat Rev Nephrol* (2016) 12(6):325–38. doi: 10.1038/nrneph.2016.48

41. Apte RS, Chen DS, Ferrara N. VEGF in signaling and disease: Beyond discovery and development. *Cell* (2019) 176(6):1248–64. doi: 10.1016/j.cell.2019.01.021

42. D'Acquisto F, Perretti M, Flower RJ. Annexin-A1: a pivotal regulator of the innate and adaptive immune systems. *Br J Pharmacol* (2008) 155(2):152–69. doi: 10.1038/bjp.2008.252

43. Ranganath S, Murphy KM. Structure and specificity of GATA proteins in Th2 development. *Mol Cell Biol* (2001) 21(8):2716–25. doi: 10.1128/MCB.21.8.2716-2725.2001

44. Ho IC, Lo D, Glimcher LH. C-maf promotes T helper cell type 2 (Th2) and attenuates Th1 differentiation by both interleukin 4-dependent and -independent mechanisms. *J Exp Med* (1998) 188(10):1859–66. doi: 10.1084/jem.188.10.1859

45. Orecchioni M, Ghosheh Y, Pramod AB, Ley K. Macrophage polarization: Different gene signatures in M1(LPS+) vs. classically and M2(LPS-) vs. alternatively activated macrophages. *Front Immunol* (2019) 10:1084. doi: 10.3389/fimmu.2019.01084

46. He L, Jhong JH, Chen Q, Huang KY, Strittmatter K, Kreuzer J, et al. Global characterization of macrophage polarization mechanisms and identification of M2-type polarization inhibitors. *Cell Rep* (2021) 37(5):109955. doi: 10.1016/j.celrep.2021.109955

47. Gundra UM, Girgis NM, Ruckerl D, Jenkins S, Ward LN, Kurtz ZD, et al. Alternatively activated macrophages derived from monocytes and tissue macrophages are phenotypically and functionally distinct. *Blood* (2014) 123(20):e110–122. doi: 10.1182/blood-2013-08-520619

48. Rozenberg P, Reichman H, Moshkovits I, Munitz A. CD300 family receptors regulate eosinophil survival, chemotaxis, and effector functions. *J Leukoc Biol* (2018) 104(1):21–9. doi: 10.1002/JLB.2MR1117-433R

49. Rothlin CV, Lemke G. TAM receptor signaling and autoimmune disease. *Curr Opin Immunol* (2010) 22(6):740–6. doi: 10.1016/j.coi.2010.10.001

50. Chung EY, Liu J, Homma Y, Zhang Y, Brendolan A, Saggese M, et al. Interleukin-10 expression in macrophages during phagocytosis of apoptotic cells is mediated by homeodomain proteins Pbx1 and prep-1. *Immunity* (2007) 27(6):952–64. doi: 10.1016/j.immuni.2007.11.014

51. Xiong W, Frasch SC, Thomas SM, Bratton DL, Henson PM. Induction of TGF-beta1 synthesis by macrophages in response to apoptotic cells requires activation of the scavenger receptor CD36. *PloS One* (2013) 8(8):e72772. doi: 10.1371/journal.pone.0072772

52. Ipseiz N, Uderhardt S, Scholtysek C, Steffen M, Schabbauer G, Bozec A, et al. The nuclear receptor Nr4a1 mediates anti-inflammatory effects of apoptotic cells. *J Immunol* (2014) 192(10):4852–8. doi: 10.4049/jimmunol.1303377

53. Byrne A, Reen DJ. Lipopolysaccharide induces rapid production of IL-10 by monocytes in the presence of apoptotic neutrophils. *J Immunol* (2002) 168(4):1968–77. doi: 10.4049/jimmunol.168.4.1968

54. Mehrotra P, Ravichandran KS. Drugging the efferocytosis process: concepts and opportunities. *Nat Rev Drug Discovery* (2022) 21(8):601–20. doi: 10.1038/s41573-022-00470-y

55. Figliuolo da Paz V, Ghishan FK, Kiela PR. Emerging roles of disabled homolog 2 (DAB2) in immune regulation. *Front Immunol* (2020) 11:580302. doi: 10.3389/fimmu.2020.580302

56. Nilsson R, Bajic VB, Suzuki H, di Bernardo D, Björkegren J, Katayama S, et al. Transcriptional network dynamics in macrophage activation. *Genomics* (2006) 88(2):133–42. doi: 10.1016/j.ygeno.2006.03.022

57. Liao X, Sharma N, Kapadia F, Zhou G, Lu Y, Hong H, et al. Kruppel-like factor 4 regulates macrophage polarization. *J Clin Invest* (2011) 121(7):2736–49. doi: 10.1172/JCI45444

58. Das A, Yang CS, Arifuzzaman S, Kim S, Kim SY, Jung KH, et al. High-resolution mapping and dynamics of the transcriptome, transcription factors, and transcription Co-factor networks in classically and alternatively activated macrophages. *Front Immunol* (2018) 9:22. doi: 10.3389/fimmu.2018.00022

59. Shik D, Moshkovits I, Karo-Atar D, Reichman H, Munitz A. Interleukin-33 requires CMRF35-like molecule-1 expression for induction of myeloid cell activation. *Allergy* (2014) 69(6):719–29. doi: 10.1111/all.12388

frontiers | Frontiers in Immunology

TYPE Systematic Review
PUBLISHED 12 December 2022
DOI 10.3389/fimmu.2022.1051609

OPEN ACCESS

EDITED BY
Oded Shamriz,
Hadassah Medical Center, Israel

REVIEWED BY
Devis Benfaremo,
Marche Polytechnic University, Italy
Eleni Tiniakou,
Johns Hopkins University,
United States
Linlu Tian,
Medical College of Wisconsin,
United States

*CORRESPONDENCE
Tingjun Dai
tingjundai@sdu.edu.cn
Chuanzhu Yan
czyan@sdu.edu.cn

†These authors have contributed equally to this work

SPECIALTY SECTION
This article was submitted to Autoimmune and Autoinflammatory Disorders : Autoimmune Disorders, a section of the journal Frontiers in Immunology

RECEIVED 23 September 2022
ACCEPTED 16 November 2022
PUBLISHED 12 December 2022

CITATION
Zhen C, Hou Y, Zhao B, Ma X, Dai T and Yan C (2022) Efficacy and safety of rituximab treatment in patients with idiopathic inflammatory myopathies: A systematic review and meta-analysis. *Front. Immunol.* 13:1051609. doi: 10.3389/fimmu.2022.1051609

Efficacy and safety of rituximab treatment in patients with idiopathic inflammatory myopathies: A systematic review and meta-analysis

Chao Zhen[1,2], Ying Hou[1], Bing Zhao[3], Xiaotian Ma[4], Tingjun Dai[1*†] and Chuanzhu Yan[1,5,6*†]

[1]Research Institute of Neuromuscular and Neurodegenerative Diseases and Department of Neurology, Qilu Hospital, Cheeloo College of Medicine, Shandong University, Jinan, China, [2]Department of Neurology, Qingdao Municipal Hospital, School of Medicine, Qingdao University, Qingdao, China, [3]Department of Neurology, Qilu Hospital (Qingdao), Cheeloo College of Medicine, Shandong University, Qingdao, China, [4]Department of Medicine Experimental Center, Qilu Hospital (Qingdao), Cheeloo College of Medicine, Shandong University, Qingdao, China, [5]Department of Central Laboratory and Mitochondrial Medicine Laboratory, Qilu Hospital (Qingdao), Cheeloo College of Medicine, Shandong University, Qingdao, China, [6]Brain Science Research Institute, Shandong University, Jinan, China

Objective: Idiopathic inflammatory myopathies (IIMs) are a heterogeneous group of autoimmune diseases with various subtypes, myositis-specific antibodies, and affect multiple systems. The treatment of IIMs remains challenging, especially for refractory myositis. In addition to steroids and traditional immunosuppressants, rituximab (RTX), a B cell-depleting monoclonal antibody, is emerging as an alternative treatment for refractory myositis. However, the therapeutic response to RTX remains controversial. This meta-analysis aimed to systematically evaluate the efficacy and safety of RTX in patients with IIMs, excluding sporadic inclusion body myositis.

Methods: PubMed, Embase, Cochrane Library, China National Knowledge Infrastructure, and WanFang Data were searched for relevant studies. The overall effective rate, complete response rate, and partial response rate were calculated to assess the efficacy of RTX. The incidences of adverse events, infection, severe adverse events, severe infection, and infusion reactions were collected to evaluate the safety of RTX. Subgroup analyses were performed using IIM subtypes, affected organs, continents, and countries. We also performed a sensitivity analysis to identify the sources of heterogeneity.

Results: A total of 26 studies were included in the quantitative analysis, which showed that 65% (95% confidence interval [CI]: 54%, 75%) of patients with IIMs responded to RTX, 45% (95% CI: 22%, 70%) of patients achieved a complete response, and 39% (95% CI: 26%, 53%) achieved a partial response. Subgroup analyses indicated that the overall efficacy rates in patients with refractory IIMs, dermatomyositis and polymyositis, as well as anti-synthetase syndrome were 62%, 68%, and 62%, respectively. The overall efficacy rates for muscle, lungs,

10.3389/fimmu.2022.1051609

and skin involvement were 59%, 65%, and 81%, respectively. In addition, studies conducted in Germany and the United States showed that patients with IIMs had an excellent response to RTX, with an effective rate of 90% and 77%, respectively. The incidence of severe adverse events and infections was 8% and 2%, respectively.

Conclusion: RTX may be an effective and relatively safe treatment choice in patients with IIMs, especially for refractory cases. However, further verification *via* randomized controlled trials is warranted.

KEYWORDS

rituximab, idiopathic inflammatory myopathies, meta-analysis, efficacy, safety

1 Introduction

Idiopathic inflammatory myopathies (IIMs), collectively known as myositis, are a heterogeneous group of acquired autoimmune-mediated myopathies that may be classified into the following subtypes: dermatomyositis (DM), polymyositis (PM), sporadic inclusion body myositis (sIBM), anti-synthetase syndrome (ASS), immune-mediated necrotizing myopathy (IMNM), and overlap myositis (1–3). IIMs are a group of multisystem diseases that may affect multiple organs other than muscles, including the skin, lungs, joints, or even the heart. The annual incidence rate ranges from 11 to 660 per 1,000,000 person-years (1). Treatment mainly involves the use of glucocorticoids, in combination with other immunosuppressive agents. Owing to the wide phenotypic heterogeneity, the therapeutic effect varies. The treatment of IIMs, especially refractory myositis, remains a challenge.

Rituximab (RTX) is a human/chimeric, monoclonal antibody with a specific affinity for CD20, a B-lymphocyte transmembrane protein, and usually leads to the depletion of peripheral B lymphocytes, lasting 6–9 months in patients with lymphoma (4). RTX depletes CD20+ B cells *via* at least four mechanisms: antibody-dependent cell-mediated cytotoxicity, complement-mediated cytotoxicity (CDC), antibody-dependent phagocytosis and direct apoptosis (5). RTX has been approved by the Food and Drug Administration (FDA) for rheumatoid arthritis and antineutrophil cytoplasmic antibody (ANCA)-associated vasculitis (AAV) (6, 7). Moreover, increasing evidence for the efficacy of RTX in various other rheumatic inflammatory diseases has been reported over the past two decades. Based on the European League Against Rheumatism (EULAR) recommendations for the management of SLE, RTX may be considered to treat organ-threatening, refractory SLE manifestations, such as nephritis and neuropsychiatric diseases (8, 9). Two randomized placebo-controlled phase 2 trials demonstrated the benefits of RTX in patients with relapsing-remitting MS (RRMS) and primary progressive MS (PPMS), respectively (10, 11). The efficacy and safety of RTX in MS were also validated in a large multicenter cohort study in Sweden (12).

Increasing evidence suggests that B cells may also be involved in IIM pathogenesis. In juvenile DM (JDM), immature transitional B cells expand significantly and are correlated with the type 1 interferon (IFN) signature, which plays a crucial role in innate and adaptive immunity, and is involved in DM. Thus, B cells may play a role in JDM development (13). Moreover, the expression of the TNF family member B cell activating factor (BAFF) is increased in both the serum and muscle fibers of IIM (14, 15). Therefore, B cell depletion may have a favorable effect on IIM. The Rituximab in Myositis (RIM) trial was a large, randomized placebo-controlled clinical trial conducted in 200 refractory adult patients with PM and adult and juvenile DM. Patients were randomized into the RTX early group or RTX late group. Although there was no difference in the time to achieve the definition of improvement (DOI) between groups (the primary end point), up to 83% of patients achieved DOI by the end of the trial (16). In a Colombian cohort, 62% of patients with refractory myositis achieved remission (17). While in an open-label, phase II trial conducted by Allenbach et al., only 20% of patients with ASS achieved the primary endpoint (an improvement of at least two points in at least two different muscle groups) (18). A number of case series and small open-label trials that have reported the efficacy of RTX for refractory myositis. Considering the large outcome differences in outcomes reported in previous studies, we aimed to resolve the limitations of individual trials and systematically assess the efficacy and safety of RTX in patients with IIM in this meta-analysis.

2 Methods

2.1 Search strategy

Two independent investigators (CZ and YH) conducted a systematic literature search using PubMed, Embase, the Cochrane Library, China National Knowledge Infrastructure, and WanFangData, from their commencement to June 2021. The following search terms were used: "Myositis" OR "Idiopathic Inflammatory Myopathies" OR "Inflammatory Myopathies" OR "Dermatomyositis" OR "Polymyositis" OR "immune-mediated necrotizing myopathy" AND "Rituximab" OR "Mabthera" OR "anti-CD20" OR "Rituxan" (the complete search strategy is provided in the Supplemental Information).

2.2 Selection criteria

The eligibility criteria were as follows. 1. IIM was diagnosed according to Bohan and Peter's criteria (19), the 119th European Neuro Muscular Center criteria (20), or the 2017 EULAR/ACR classification for IIM (3). 2. Patients received RTX therapy in any dosage, with or without combination therapy, and part of a study with a sample size of not less than five. 3. The study evaluated the efficacy and/or safety of RTX for the treatment of IIM, and included patients who received RTX and the number of responders and/or the number of patients who experienced adverse effects, or sufficient raw data to allow the calculation of the aforementioned numbers. 4. The study was published in English or Chinese.

The exclusion criteria were as follows. 1. Reviews, meeting abstracts, case reports, and animal experiments. 2. Trials without extractible data. 3. The study included patients with sIBM.

2.3 Data extraction and quality assessment

Two investigators independently extracted the following data from the included studies: authors, year of publication, type of study, country, number of cases, IIM subtype of enrolled patients, age, disease duration, RTX regimen, outcome measurements, outcome evaluation time, and follow-up time. Since most of the included articles were single-arm tests, the methodological index for non-randomized studies (MINORS) criteria were used to evaluate the methodological quality of the included studies. For studies without a control group, the MINORS scale was used and consisted of the following items: clear aims, the inclusion of consecutive patients, prospective collection of data, appropriate endpoints to the aim of the study, unbiased evaluation of endpoints, follow-up period appropriate to the major endpoint, loss to follow-up of <5%, and prospective calculation of the sample size, was used. For studies with a control group, the following items were considered: a control group with standard intervention, contemporary groups, comparable baseline equivalence of groups, and statistical analysis adapted to the study design (21), were considered. Each item was scored as 0 (not reported), 1 (reported but inadequate), or 2 (reported and adequate). The optimal total score was 16 or 24.

2.4 Statistical analysis

STATA 16.0 was used for the single-group rate meta-analysis. The original data were normalized using the double arcsine method, and the final results were restored using the formula $P=(\sin(tpda/2))^2$. We used the I^2 test to evaluate statistical heterogeneity among studies. We used the fixed effects model if I^2 was <50%, and the random effects model if I^2 was >50%. We conducted a series of pooled analyses of eligible studies to assess the effective rate of RTX (overall effective rate, complete response rate, and partial response rate) and the safety of RTX (incidence rate of adverse events, infection, severe adverse events, severe infection, and infusion reaction). Subgroup analyses were performed according to the IIM subtypes (ASS, refractory IIM, DM, and PM), affected organs (muscle, lung, and skin), continent (Europe and America), and country (USA, France, UK, and Germany). We also conducted a sensitivity analysis to identify the sources of heterogeneity. A graphical examination of funnel plots and Begg's test were performed to assess publication bias. A two-tailed *p*-value <0.10 was considered statistically significant in the assessment of heterogeneity.

3 Results

3.1 Study selection and characteristics of the eligible studies

A flow diagram of the search process is shown in Figure 1. A total of 1547 potentially related articles were identified using the search strategy (216 articles from PubMed, 827 from Embase, 14 from the Cochrane Library, 364 from the China National Knowledge Infrastructure, and 126 from Wanfang). After excluding 481 duplicates, the titles and abstracts of the remaining 1066 articles were screened, and 78 articles were reviewed for full-text screening. Subsequently, 27 articles were included in the qualitative analysis, and one article was excluded because of a low MINORS score (less than 10 points). Ultimately, 26 articles were deemed eligible and were included in the quantitative analysis (16–18, 22–44). Detailed characteristics and the MINORS quality assessments of the eligible studies are presented in Table 1. Of the included studies, 18 were conducted in patients with refractory IIM (16–18, 22–25, 28–30, 35–37, 39, 40, 42–44), and 8 included patients with ASS (17, 23, 28, 30, 39, 40, 43). Among the 23

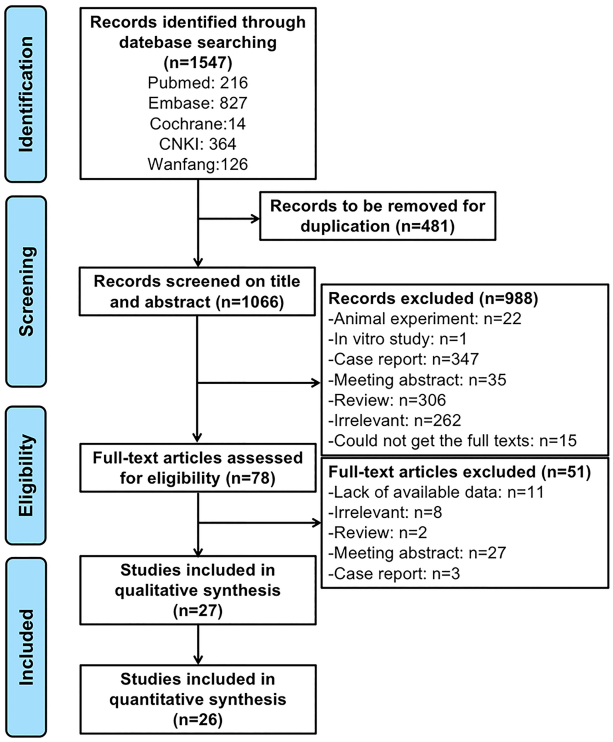

FIGURE 1
Flow diagram of the study identification and selection process.

single-arm trials, the quality score of two articles were 14 points, 13 articles were 12 points, one article was 11 points, and seven articles were 10 points.

3.2 Efficacy of RTX treatment

3.2.1 Complete response rate

The complete response rate was determined from seven trials (n = 121), and the pooled estimate of effectiveness was 45% (95% CI: 23%, 70%) (Figure 2A and Table 2). Significant heterogeneity was found (I^2 = 86.5%, P = 0.000). After we conducted the sensitivity analysis, one study was omitted because the study population included patients with Jo-1-associated ASS and the patients received an average of 4.6 cycles of RTX, which may lead to a high response rate (22). Following the omission, the heterogeneity was resolved (I^2 = 0, P = 0.425) and the complete response rate became 35% (95% CI: 26%, 44%). Notably, although most included studies defined complete response and partial response based on clinical status, the daily dose of corticosteroid, CK level, and/or physician opinion, the details of the criteria differed. Since most of included studies only provided the numbers of patients who achieved complete or partial responses, and specific values of the above index for every patient were not available, we could not set a unified standard to recalculate the numbers. Therefore, for this meta-analysis, we could only directly extract the number of complete and partial responses from the original studies, which may contribute to heterogeneity.

3.2.2 Partial response rate

The partial response rate was calculated from three trials (n = 44), and the pooled estimate of effectiveness was 39% (95% CI: 26%, 53%) (Figure 2B and Table 2). No heterogeneity was observed (I^2 = 0, P = 0.487).

3.2.3 Overall effective rate

The overall efficacy rate was determined from 18 trials (n = 480). The pooled effectiveness estimate was 65% (95% CI: 54%, 75%) (Figure 2C and Table 2). The calculation method for the total effective number is as follows. If the studies provided both the number of complete responders and partial responders, the total effective number was taken as the sum of the two. For studies that only provided the number of improved cases, without a specific classification of whether they were complete or partial responders, the total effective number was taken as the former. There was high heterogeneity (I^2 = 78.8%, P = 0.000), therefore, we conducted a sensitivity analysis, but studies leading to heterogeneity were not found.

TABLE 1 Baseline characteristics of included studies.

Author, Year	Type of study	Region	Enrolled patients	Number	Age (years) (mean ± SD)	Disease Duration	RTX regime	Outcome measurements	Evaluation time	Follow-up	MINORS score
Shahin et al, 2021	single center, prospective	Egypt	14DM 8PM	14DM 8PM	Total: 34.9 ± 14.9 (16.0–62.0) years CYC: 35.7 ± 14.8 (16.0–62.0) years RTX: 32.2 ± 16.6 (17.0–59.0) years	NA	4 patients received 3 doses, 1 g each with 6 months apart, 1 patient received only one dose	MRC-SS CK	18 months (after end of RTX)	Total: 7.7 ± 4.3 (0.7–19.0) years CYC:8.5 ± 4.4(0.7–19.0) years RTX:5.0 ± 2.7(1.0–8.0) years	20
Ahn et al, 2020	retrospective multicenter study	Korea	refractory IIM, 10DM 6PM	Total 16	51.8 (42.5–59.0) years	88.4 (24.3–162.8) months	6 patients received 2 doses of 1g RTX 2 weeks apart, 4 received 2 doses of 0.5 g RTX 2 weeks apart, 3 received a single dose of 1g, 1patient received 0.5g weekly for a total of 4 doses, 1 patient received 0.6g RTX 2 weeks apart, and 1 received a single dose of 0.2g RTX	CPK level daily dose of corticosteroid, physician's global assessment(PRA).CR PR	12 and 24 weeks after RTX treatment	median 24 weeks, range 24–68 weeks	12
Aggarwal et al, 2016	prospective, randomized, double-blind trial	U.S.A	refractory myositis	72 adult DM, 48 JDM	36.1 ± 19.7 years	5.3 ± 6.9 years	rituximab early (drug at weeks 0/1, placebo at weeks 8/9) or rituximab late arms (placebo at weeks 0/1, drug at weeks 8/9), Rituximab dosing was based on the patient's body surface area; children with a body surface area 41.5 m^2 received 575 mg/m^2 at each infusion, and adults and children with a body surface area >1.5 m^2 received 750 mg/m2 up to 1 g/infusion	10 cm visual analog scale (VAS)	week 36	36weeks	12
Oddis et al, 2013	Randomized, double-blind, Placebo-Phase Trial	U.S.A	refractory myositis PM,DM, JDM	Total 195	NA	NA	Patients in the rituximab early arm received the drug at weeks 0 and 1, and placebo infusions were given at weeks 8 and 9. Patients in the rituximab late arm received placebo infusions at weeks 0 and 1,and rituximab was given at weeks 8 and 9	improvement prednisone dosage AEs and SAEs	week 44	44weeks	12
Levine et al, 2005	Open-Label uncontrolled Pilot Study	U.S.A	adult DM	6	21–64 years	0.3-15 years	4 intravenous infusions of rituximab given at weekly intervals on days 1, 8, 15, and 22. 3 patients received rituximab at a dose of 100 mg/m^2/infusion. 3 patients received rituximab at a dose of 375 mg/m^2/infusion.	muscle strength CPK level FVC Safety	weeks 4, 12, 24,36,and 52	52weeks	10

(Continued)

10.3389/fimmu.2022.1051609

TABLE 1 Continued

Author, Year	Type of study	Region	Enrolled patients	Number	Age (years) (mean ± SD)	Disease Duration	RTX regime	Outcome measurements	Evaluation time	Follow-up	MINORS score
Ramos-Casals et al, 2010	multicentre study	Spain	refractory IIM : DM PM ASS	Total 20 DM 11 PM 4 ASS 5	49.20 ± 2.98 years (23-77) years	NA	18 patients 375 mg/m^2/week (x4) 2 patients 1g/15 days (x2)	Overall response Overall response by disease Organ-specific response Adverse events Relapses Deaths	NA	19.00 ± 2.65 (1-52) months	12
Sultan et al, 2008	open-label study	UK	refractory Adult IIM, PM DM	Total 8 2PM 5DM 1JDM	31-63years	14.9 years (range 4-40 years)	1g intravenous infusions on day 0 and day 14.	MMT CPK level	6 months	6 months	12
Bader-Meunier et al, 2011	multicenter prospective cohort study	France	Severe JDM	9	6.2-16 years	3.4 years (range 1 month to 8.4 yrs)	5 patients 4 × 375 mg/m^2 1 patient 2 × 375 mg/m^2 3 patients 2 × 500 mg/m^2	MMT CPK level complete clinical response severe infection	NA	1.3 to 3 years	10
de Souza et al, 2018	retrospective single-center cohort study	Brazil	refractory IIM : ASS DM PM	Total 38 13ASS 15DM 10PM	42.6 ± 10.9 years	3.0 (2.0–6.5) years	two infusions (1 g each, 2 weeks apart) and this same scheme was repeated 6 months after the first dose for patients showing no response or stable disease	clinical and laboratory improvements MMT-8, physician' and patient' VAS, HAQ and serum levels of muscle enzymes	6 months and 12 months	one-year	12
Chung et al, 2007	open-label, single-arm trial	U.S.A	refractory DM	8	38-76 years	3.5 years (range, 1-24 years)	2 doses of 1 g of rituximab 2 weeks apart	partial remission Muscle Strength: MMT Muscle Enzymes : CPK Skin Disease : DSSI B-Cell Levels Safety	24 weeks	48 weeks	10
Korsten et al, 2020	retrospective observational study	Italy	ASS with ILD	Total 12 RTX 7	NA	NA	2 doses of 1 g of rituximab, 1patient received a 2nd cycle	the alteration of lung parenchyma on HRCT as well as PFTs	NA	31 (6–156) months	18
Sem et al, 2009	a retrospective case series	Norway	ASS patients with severe ILD	11	52 years	1.5-156 months	8 patients two infusions of 1000 mg rituximab, at Days 0 and 14,1 patient received two doses of 700 mg. 2 patients received four weekly infusions of 375 mg/m^2 body surface.	Pulmonary function tests (PFTs) Safety and adverse effects	6month	≥6 months	12
Mahler et al, 2011	single center, prospective	Netherlands	refractory DM or PM	13	44.4 ± 12.1years	4.0 years (IQR 2.5-6.5 years)	1000 mg i.v., twice, with a 2-week interval, the median number of rituximab courses was 2.0 (IQR 1.5 - 3.5).	CPK LDH levels MMT general health, disease activity and pain, CS dose, functional ability,	24month	27 months	12

(Continued)

10.3389/fimmu.2022.1051609

TABLE 1 Continued

Author, Year	Type of study	Region	Enrolled patients	Number	Age (years) (mean ± SD)	Disease Duration	RTX regime	Outcome measurements	Evaluation time	Follow-up	MINORS score
								health-related quality of life and safety			
Couderc et al, 2011	multicenter, prospective	France	refractory IIMs	Total 30 12PM 6DM 12ASS	52.5 ± 14.7years (26 - 76 years)	6.1 ± 4.3 years (range 1-18 years)	5 patients 4 × 375 mg 25 patients 2 × 1000 mg	CPK level daily dose of CSs and the opinion of the physician Safety of RTX adverse event infection	NA	17.2 ± 11.3 months (range 1-50 months)	12
Unger et al, 2014	retrospective	Germany	severe, refractory DM or PM	Total 18 13 PM 5 DM	57 ± 18 years	5.4 years (range 0.1-15)	13 patients 2×1000 mg RTX infusions. 1 patient 4 × 375 mg/m^2 + 600mg. 2 Patients were switched from 4 × 375 mg/m^2 to 2×1 g after the first cycle. 1 patient received a single 600 mg RTX infusion.1 patient was treated with a normal 2 × 1000 mg course first and with a reduced dose of 1 × 1000 mg in further courses.	glucocorticoid dose, creatine phosphokinase (CPK) and lung function tests, serious adverse events	50week	2.5 ± 1.6 years (range 0.5-5.4)	10
Marie et al, 2012	retrospective	France	ASS-associated interstitial lung disease	7	57 years (47-59 years)	12 months (8-60 months)	2 infusions of 1 g at days 0 and 14; and a third infusion of 1 g at 6-month follow-up.	PFT CK safety prednisone dose	12 month	12 months	12
Meyer et al, 2015	retrospective case–control study	France	ASS	8	50.4 ± 7.4 years	NA	NA	joint lung musle improvement	NA	93.19 ± 61.31months	11
Leclair et al, 2018	prospective	Canada	IIM	Total 43 27 ARS-ab positive IIM 16 ARS-ab negative IIM	ARS-ab+ 57 ± 10 years ARS-ab- 57 ± 19 years	(months) median (IQR) ARS-ab+ 15 (4-52) ARS-ab-69 (9-166)	500 mg to 1000 mg given 2 weeks apart or 750 mg/m^2 weekly for two doses or 375 mg/m^2 weekly for four doses (induction); or any following administration separated from the previous cycle by more than three months (maintenance)	MMT-8 HAQ VAS EQ-5D ACR/EULAR improvement glucocorticoid doses respectively adverse events	at 5-10 months after the first and last RTX cycles	5-10 months	20
Allenbachet al, 2015	open-label, prospective, multicenter	France	Refractory ASS	10	51 years (range, 18–57 years)	0.5-8years	patients received two 1 g infusions of rituximab separated by 2 weeks, followed by 1g infusion 6 months after the day 15 injection was performed.	muscle strength improvement in ILD Adverse events	12month	12months	10
Santos et al, 2021	retrospective	Colombia	Refractory myositis	Total 18 15DM 2PM 1JDM	40.5 years (IQR, 31–49 years)	21 months (IQR, 6.5–40.5 months)	1 g at day 0 and day 15 5 patients 1 circle, 8 patients 2 circles, 2 patients 5 circles, 2 patients 9 circles, 1 patient 11 circles	Clinical, Serological	NA	11 months (IQR, 4–57 months)	12

(Continued)

10.3389/fimmu.2022.1051609

TABLE 1 Continued

Author, Year	Type of study	Region	Enrolled patients	Number	Age (years) (mean ± SD)	Disease Duration	RTX regime	Outcome measurements	Evaluation time	Follow-up	MINORS score
Muñoz-Beamud et al, 2013	retrospective	UK	DM and PM	16	51.1 years (range 30–62 yrs)	9.75 years (range 2–44 yrs)	2 doses of 1 gram RTX infusions two weeks apart.	Clinical outcomes were measured using the MITAX	6month	NA	12
Bauhammeret al, 2016	retrospective cohort study	Germany	Jo1 Antibody–associated ASS	the RTX group 18	median (range) RTX group 50.9 (26–78)	NA	patients received on average 4.6 cycles of RTX (range 1–13) in a mean interval of 6.4 months	Clinical, CK, Prednisolone-equivalent doses	NA	35 months	10
Landon-Cardinal et al, 2018	retrospective case series	France	anti-HMGCR IMNM	9	43 years	0.75-23years	most patients were administered 2 doses of 1 gram RTX infusions two weeks apart. One patient received a dose of 375 mg/m^2/body surface area once weekly for 4 weeks. Patients were subsequently re-perfused with RTX 1 g every 6 months at the discretion of the treating physician.	muscle strength CK level	NA	NA	12
Ge et al, 2020	retrospective	China	anti-MDA5 DM	11	39 years (24–59 years)	NA	Seven patients received intravenous RTX (375 mg/m^2) at 0 and 14 days. Three patients were administered with intravenous RTX (100 mg) at 0, 7, 14, and 21 days. One patient was treated with RTX (100 mg) at 0 and 7 days	Skin ILD infection	NA	≥12 months	14
Andersson et al, 2015	retrospective	Norway	ASS-associated severe interstitial lung disease	24	28-78 years	11-440months	The mean number of Rtx cycles was 2.7 (range 1-11). The first cycle of Rtx treatment was given as one infusion of 1000 mg on each of days 0 and 14, except for three patients (#1, #7 and #11). Patients #7 and #11 were treated according to standard lymphoma protocol (4 × 375 mg/m^2), while patient #1 was treated with a reduced dose because of perceived infection risk.	ILD MMT8 CK Serious adverse events and mortality	NA	median 52 months	10
Behrens Pinto et al, 2020	prospective	Brazil	ASS	16	43.1 ± 10.1 years	1.5 (0.0–5.8) years	Rituximab treatment consisted of two infusions (1 g each, 2 weeks apart), and this same scheme was repeated every 6 months for 2 years in patients showing clinical response.	MMT-8 HAQ VAS glucocorticoid doses lung computed tomography pulmonary function testing	6 and 12 months	12 months	14

DM, dermatomyositis; PM, polymyositis; CYC, cyclophosphamide; RTX, rituximab; NA, not available; MRC-SS, Medical Research Council sum score; CK, creatine kinase; IIM,idiopathic inflammatory myopathy; CPK, creatine phosphokinase; CR, complete response; PR, partial response; JDM, juvenile dermatomyositis; AE, adverse event; SAE, severe adverse event; FVC, forced vital capacity; ASS, antisynthetase syndrome; MMT, manual muscle testing; VAS, visual analogue scale; HAQ, health assessment questionnaire; DSSI, dermatomyositis skin severity index; ILD, interstitial lung disease; HRCT, high-resolution chest computed tomography; PFT, pulmonary function tests; LDH, lactate dehydrogenase; CS, corticosteroids; ARS-ab, anti-tRNA synthetase autoantibodies; ED-5Q, EuroQol five Dimensions; IQR, interquartile range; HMGCR, Anti-3-hydroxy-3-methylglutaryl-coenzyme A reductase; IMNM, immune-mediated necrotizing myopathy; MDA-5, melanoma differentiation-associated gene 5.

10.3389/fimmu.2022.1051609

3.3 Safety of RTX treatment

3.3.1 Incidence of adverse events and severe adverse events

Seven trials reported adverse events (n = 135). The pooled incidence estimate was 18% (95% CI: 7%, 33%) (Figure 3A, and Table 2). Significant heterogeneity was detected (I^2 = 74.1%, P = 0.001). After the sensitivity analysis, two studies were excluded (30, 41). Consequently, the heterogeneity was resolved (I^2 = 0, P = 0.45) and the incidence of adverse events decreased to 10% (95% CI: 5%, 16%). Regarding the two excluded studies, one focused on patients with ASS with severe interstitial lung disease (ILD), who had poor basic health conditions and six patients had unexplained fever and increased CRP levels (41). In the other study, 16.7% of patients had a history of cancer, and 30% had a systemic disease. These patients have a high incidence of adverse events because of their poor overall health status (30).

Severe adverse events were defined as events that required hospitalization. The incidence of severe adverse events was determined from seven trials (n = 248). The pooled incidence estimate was 8% (95% CI: 2%, 17%) (Figure 3B and Table 2). Heterogeneity was significant (I^2 = 74.8%, P = 0.001). A sensitivity analysis was conducted. After excluding two studies (16, 26), the heterogeneity was resolved (I^2 = 0, P = 0.715), and the incidence of severe adverse events decreased to 3% (95% CI: 1%, 8%). Regarding the two excluded studies, one was a large randomized, placebo-controlled clinical trial (16), while the other was not a randomized controlled trial (RCT) (26). This difference may have led to the heterogeneity. The latter study (26) focused on patients with ASS and severe ILD, who were prone to severe adverse events, which may have further contributed to heterogeneity.

3.3.2 Incidence of infections and severe infections

Fifteen trials reported the incidence of infections (n = 386). The pooled incidence estimate was 26% (95% CI: 17%, 35%) (Figure 3C and Table 2). Moderate heterogeneity was detected (I^2 = 52.1%, P = 0.022). After conducting sensitivity analyses, one study was excluded (41), and the heterogeneity decreased (I^2 = 33.3%, P = 0.142). The incidence of infections also decreased to 23% (95% CI: 16%, 31%). In the above-mentioned paper, seven patients developed an infection including one patient with *Pneumocystis jirovecii* infection, while the other six patients showed fever and increased CRP without definite infection foci. These differences may have contributed to the heterogeneity.

Severe infection was defined as one that required hospitalization and/or intravenous antibiotic therapy. The incidence of severe infections was determined from 5 trials (n = 81). The pooled incidence estimate was 2% (95% CI: 0, 6%) (Figure 3D and Table 2). No heterogeneity was observed (I^2 = 0, P = 0.578).

3.3.3 Incidence of infusion reactions

The incidence of infusion reactions was determined in seven trials (n = 245). The pooled incidence estimate was 12% (95% CI: 6%, 20%) (Figure 3E and Table 2). No heterogeneity was observed (I^2 = 25.4%, P = 0.244).

3.4 Subgroup analyses

3.4.1 Effectiveness of RTX treatment in patients with different IIM subtypes

Refractory IIM was defined as a failure to respond to or tolerate glucocorticoids, combined with at least one of the other standard immunosuppressive or immunomodulatory agents (e.g., azathioprine, methotrexate, mycophenolate mofetil, cyclosporine, tacrolimus, or intravenous immunoglobulin [IVIg]). The overall efficacy rate of RTX in patients with refractory IIMs was determined from 15 trials (n = 412). The pooled effectiveness estimate was 62% (95% CI: 50%, 73%) (Figure 4A and Table 2). Significant heterogeneity was detected (I^2 = 77.2%, P = 0.000). Hence, we conducted a sensitivity analysis but studies that contributed to heterogeneity, were not found.

Among the included studies, several regarded patients with DM and PM together. Therefore, we evaluated the effectiveness of RTX in these populations. The overall efficacy rate was determined from seven trials (n = 284). The pooled effectiveness estimate was 68% (95% CI: 54%, 80%) (Figure 4A and Table 2). Significant heterogeneity was detected (I^2 = 69.6%, P = 0.003). After conducting sensitivity analyses, two studies were excluded (39, 43). The heterogeneity was resolved (I^2 = 0, P = 0.528), and the effective rate increased to 80% (95% CI: 75%, 85%). The mean disease duration of the two excluded articles was longer than that in other studies. One was 9.75 years (39) and the other was 14.9 years (43). This may have contributed to a poor response to RTX treatment and to heterogeneity.

The overall efficacy rate of RTX in ASS was determined from eight trials (n = 80), and the pooled effectiveness estimate was 62% (95% CI: 41%, 81%) (Figure 4A and Table 2). Significant heterogeneity was detected (I^2 = 74.3%, P = 0.000). After conducting sensitivity analyses, two studies were excluded (22, 36), and the heterogeneity decreased (I^2 = 18.1%, P = 0.296). The effective rate became 47% (95% CI: 33%, 61%). Regarding the two excluded studies, one focused on Jo-1 antibody–associated ASS and the other focused on anticitrullinated peptide/protein antibody (ACPA)-associated ASS. The remaining six studies targeted patients with ASS without mentioning specific antibodies. The original data suggested that patients with ASS patients who were Jo-1-positive or ACPA-positive responded well to the treatment effect of RTX. These differences may have contributed to the heterogeneity.

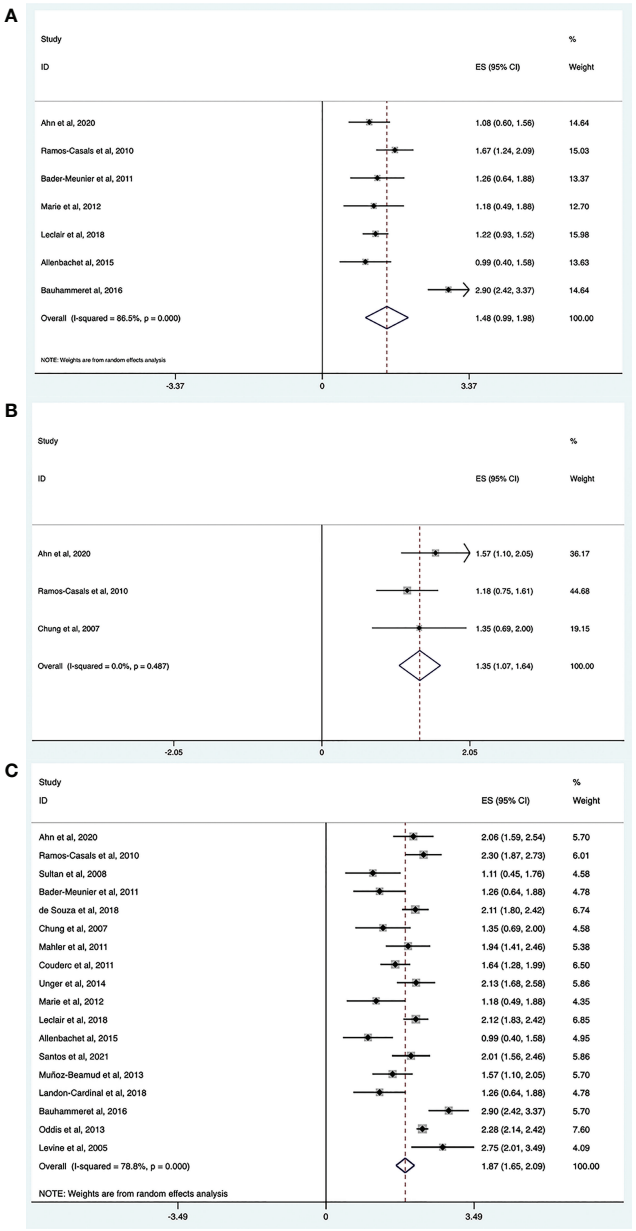

FIGURE 2
Meta-analysis results of efficacy for RTX in IIMs. Complete response rate **(A)**, partial response rate **(B)** and overall effective rate **(C)**.

3.4.2 Effectiveness of RTX treatment in patients with IIM: The organ-specific responses

Among the included studies, there were several evaluated organ-specific responses. Muscle strength with manual muscle testing (MMT) and/or CK levels were recorded to assess muscle improvement. Six articles (n = 61) assessed the rate of muscle improvement in patients with myositis after RTX treatment, and the pooled estimate of the muscle improvement rate was 59% (95% CI: 25%, 89%; $I^2 = 88\%$, $P = 0.000$). ILD was defined as ground-glass changes and/or fibrosis on high-resolution chest computed tomography (HRCT). Regarding the efficacy of RTX for patients with IIM and ILD, pulmonary function tests and/or radiographic changes on HRCT were performed before and after RTX treatment in the included studies. Nine studies (n = 88) assessed the rate of lung improvement after RTX treatment, and the pooled estimate of the improvement rate was 65% (95% CI: 48%, 80%; $I^2 = 61.8\%$, $P = 0.007$). Three studies (n = 22) assessed the rate of skin improvement, and the pooled estimate was 81% (95% CI: 63%–94%; $I^2 = 3.8\%$, $P = 0.354$) (Figure 4B and Table 2).

10.3389/fimmu.2022.1051609

TABLE 2 A pooled results summary of response rate, safety analysis, and subgroup analyses for RTX in IIMs.

Outcome			Number of included references	Number of cases	Overall effects	Transformed overall effects	I^2 (%)	p value
Response rates	overall effective rate		18	480	1.87 (1.65, 2.09)	0.65 (0.54,0.75)	78.8	0.000
	complete response rate		7	121	1.48 (0.99, 1.98)	0.45 (0.23, 0.70)	86.5	0.000
	partial response rate		3	44	1.35 (1.07, 1.64)	0.39 (0.26, 0.53)	0	0.487
Safety	Incidence of adverse events		7	135	0.88 (0.55, 1.22)	0.18(0.07, 0.33)	74.1	0.001
	Incidence of infection		15	386	1.07 (0.86, 1.27)	0.26 (0.17, 0.35)	52.1	0.022
	Incidence of severe adverse events		7	248	0.57 (0.28, 0.85)	0.08 (0.02, 0.17)	74.8	0.001
	Incidence of severe infection		5	81	0.29 (0.08, 0.5)	0.02 (0.00, 0.06)	0	0.578
	Incidence of infusion reaction		7	245	0.71 (0.48, 0.93)	0.12 (0.06, 0.20)	25.4	0.244
Subgroup analysis (overall response rate)	patients	refractory IIMs	15	412	1.81 (1.58, 2.05)	0.62 (0.50, 0.73)	77.2	0.000
		DM and PM	7	284	1.93 (1.65, 2.21)	0.68 (0.54, 0.80)	69.6	0.003
		ASS	8	80	1.81 (1.39, 2.23)	0.62 (0.41, 0.81)	74.3	0.000
	affected organs	muscle	6	61	1.75 (1.05, 2.46)	0.59 (0.25, 0.89)	88	0.000
		lung-ILD	9	88	1.87 (1.54, 2.21)	0.65 (0.48, 0.80)	61.8	0.007
		skin	3	22	2.23 (1.83, 2.63)	0.81 (0.63, 0.94)	3.8	0.354
	continent	Europe	11	156	1.69 (1.35, 2.04)	0.56 (0.39, 0.73)	80	0.000
		America	6	308	2.13 (1.91, 2.34)	0.77 (0.67, 0.85)	80	0.000
	country	U.S.A	3	209	2.13 (1.49, 2.76)	0.77 (0.46, 0.96)	78.4	0.01
		France	5	65	1.36 (1.12, 1.61)	0.40 (0.28, 0.52)	6.4	0.37
		UK	2	24	1.39 (0.95, 1.84)	0.41 (0.21, 0.63)	21.2	0.26
		Germany	2	34	2.51 (1.75, 3.26)	0.90 (0.59, 1.00)	81.2	0.021

ASS, antisynthetase syndrome; ILD, interstitial lung disease.

3.4.3 Effectiveness of RTX treatment in patients with IIM from different continents and countries

The included studies did not provide the ethnicity of the patients. Most of the included studies were conducted in Europe and America. Therefore, we performed a subgroup analysis according to the region where the study was conducted rather than race. Among the included studies, 11 trials were conducted in Europe (n = 156), and the pooled estimate of the overall efficacy rate was 56% (95% CI: 39%, 73%). Of these, five studies were performed in France (n = 65) and the overall effective rate was 40% (95% CI: 28%, 52%). Two studies were done in the UK (n = 24) and the overall effective rate of 41% (95% CI: 21%, 63%). Two other studies were from Germany (n = 34) and the overall effective rate of 90% (95% CI: 59%, 100%). Six trials were from America, and the pooled estimate of the overall effective rate was 77% (95% CI: 67%, 85%). Among these, three studies were performed in the United States (n = 209), and the overall efficacy rate was 77% (95% CI: 46%, 96%) (Figure 4C and Table 2).

3.5 Evaluation for publication bias and meta-regression

Funnel plot analyses and Begg's test for publication bias were performed, and the results are presented in Figure 5. Egger's test showed no apparent publication bias in the complete response rate group (p = 0.930, Figure 5A), adverse event group (p = 0.627, Figure 5C), infection group (p = 0.973, Figure 5D), and the ASS group (p = 0.770, Figure 5G). Conversely, there was a publication bias in the overall effective rate group (p = 0.013, Figure 5B), refractory IIM group (p = 0.006, Figure 5E), and DM and PM groups (p = 0.021, Figure 5F). To explore potential sources of heterogeneity, random-effects meta-regression analyses were conducted for the three groups with bias. The independent variables included sample size, study quality, and publication year. None of these variables significantly contributed to the heterogeneity in the overall effective rate group and refractory IIM group ($p > 0.05$). The sample size may be responsible for the heterogeneity in the DM and PM groups (p = 0.027).

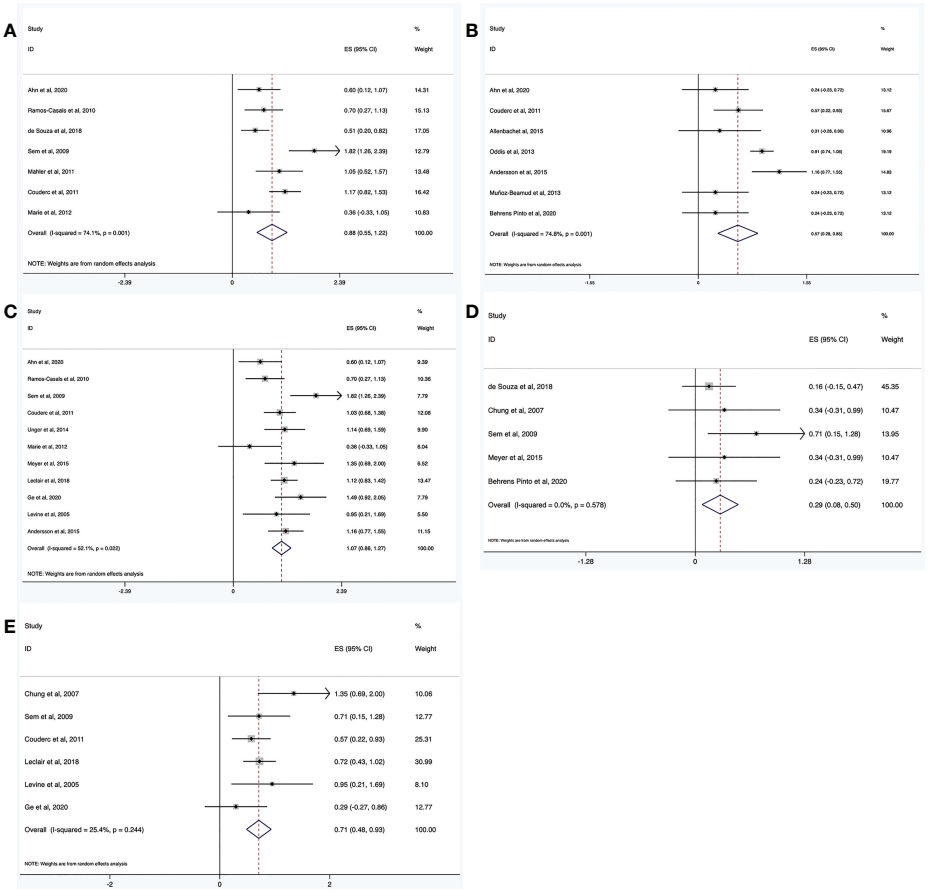

FIGURE 3
Meta-analysis results of safety for RTX in IIMs. The incidence of adverse events **(A)**, severe adverse events **(B)**, infection **(C)**, severe infection **(D)**, and infusion reaction **(E)**.

4 Discussion

IIMs are heterogeneous autoimmune disorders with multiple subtypes, including DM, PM, sIBM, IMNM, and ASS. The condition's low incidence makes it difficult to perform large-scale RCTs. Currently, glucocorticoids are the first-line treatment (45), and classic immunosuppressants, such as methotrexate or azathioprine, are usually used in combination with glucocorticoids as the initial therapy (1). Mycophenolate is a second-line treatment, but for patients with moderate-to-severe myositis associated with ILD, it may be used as the first-line treatment (46, 47). Cyclosporine and tacrolimus are used as second-line treatments for refractory myositis (48, 49). Previously, IVIg was used as a second- or third-line treatment (1). However, based on the positive results reported by the recent ProDERM (Progress in DERMatomyositis) study, the FDA, and European Medicines Agency have approved IVIg administration in adult DM (1). The ProDERM study was a double-blind, randomized, placebo-controlled, multicenter phase III study that assessed the efficacy, safety, and tolerability of IVIg in the management of DM; the percentage of patients who achieved at least minimal improvement at week 16 was significantly greater in the IVIg group than in the placebo group (50). IVIg is now increasingly used as a first-line treatment for IMNM (51, 52). In a cohort study, half of the patients with IMNM used IVIg as a first-line therapy and 92% at the end of the follow-up period for anti-SRP patients. Patients with anti-SRP receiving IVIg showed an obviously higher remission rate than those without IVIg (52). Among the biological agents used as third-line therapies, RTX is the most common. Evidence supporting the current treatment options come from retrospective cohort studies. Thus, robust clinical evidence is lacking and the management of IIM remains challenging.

The pathogenesis of IIM is still unclear. B cells are involved in many autoimmune responses, including the production of autoantibodies, cytokines secretion, antigen presentation, and

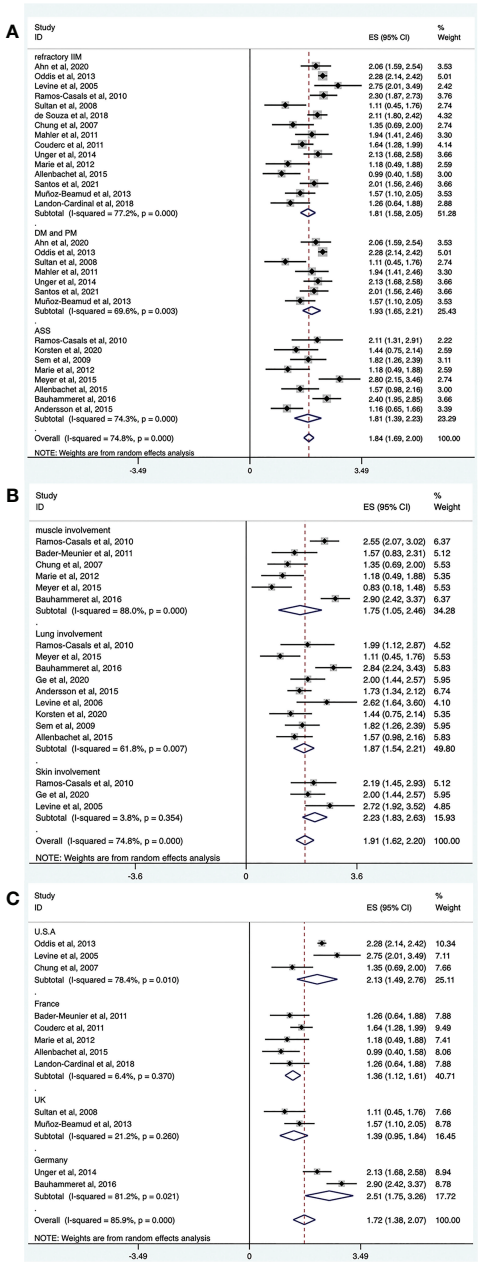

FIGURE 4
Forest plots of subgroup analysis results. RTX efficacy in patients with different IIM subtypes **(A)**, organ-specific response of RTX in IIMs **(B)**, efficacy of RTX in IIMs from different continents **(C)**.

modulation of T cells functions. Currently, there is increasing evidence suggesting that B lymphocytes may play an important role in the pathogenesis of IIM, which is summarized as follows.

First, B cells are observed in the perivascular infiltrates of the DM muscle tissues (53). BAFF is important for B cell maturation and survival, and is thought to be involved in the production of autoantibodies as well as the activation and differentiation of T cells. Krystufkova et al. showed that the serum BAFF level was significantly higher in patients with IIMs than in healthy individuals (14). The high serum BAFF level was especially demonstrated in patients with DM, anti-Jo-1 autoantibodies, and ILD (14). Moreover, the level of BAFF expression was significantly increased in DM muscles. BAFF was also expressed in the perifascicular muscle fibers, but not in the

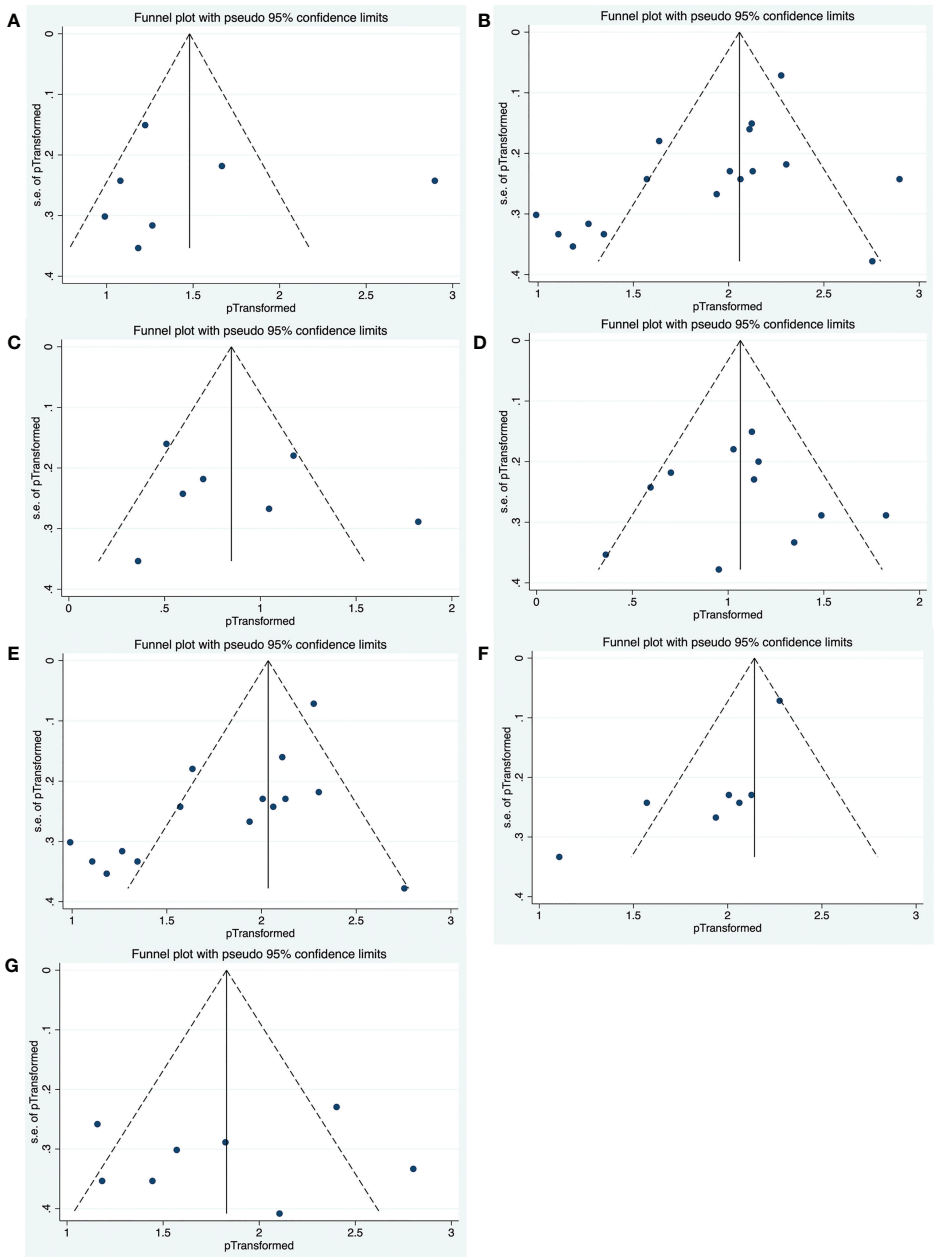

FIGURE 5
Funnel plots of publication bias in complete response rate group **(A)**, overall effective rate group **(B)**, adverse events group **(C)**, infection group **(D)**, refractory IIM group **(E)**, DM and PM group **(F)**, as well as ASS group **(G)**.

blood vessels (15). In addition, a study suggested that the BAFF/BAFF-receptor pathway is involved in T and B cell responses in DM (15).

Second, a previous study identified CD138+ plasma cells in IBM and PM muscles. These plasma cells are terminally differentiated B cells (54). Furthermore, several studies have reported that 60%-80% of patients with IIM are positive for autoantibodies (55, 56), including myositis-specific antibodies (MSAs) and myositis-associated autoantibodies (MAAs). Up to 40% of patients with PM and DM test positive for MSAs (57). MSAs are critical for the diagnosis of IIM and correlate with a unique clinicopathological phenotype. The frequent presence of MSAs and MAAs in IIM suggests that B cells play a role in their pathogenesis. The above evidence supports the feasibility of depleting B-cell using RTX as therapy for patients with IIMs.

Treatment efficacy was the main focus of our meta-analysis. In our study, the overall effective rate of rituximab in IIM was 65%, with higher effective rates of 90% and 77% in studies conducted in Germany and the U.S., respectively. The complete response rate of RTX in patients with IIM was 45% and the partial response rate was 39%. Most patients received RTX because of refractory disease or ILD. This meta-analysis demonstrated that RTX was effective in 62% of patients with refractory IIMs and 68% of patients with DM and PM. However, the lack of head-to-head studies and the presence of heterogeneity make it difficult to draw definitive conclusions.

ASS, a more common subtype of IIM, is characterized by myositis, ILD, fever, Raynaud phenomenon, arthritis, and/or mechanic hands. ILD is the most frequent manifestation of the disease. Arthritis, myositis, and ILD are the classical clinical triads of ASS. In our meta-analysis, the overall efficacy rate of RTX in patients with ASS was 62% (95% CI: 41%, 81%).

IIMs are multi-systemic inflammatory disorders involving not only the muscles but also other organs, such as the skin, lungs, heart, joints, and the gastrointestinal tract. Symmetric proximal muscle weakness and myalgia were the most common symptoms. Skin rashes, ILD, and arthritis were also common and may even be the predominant manifestations. Subgroup analysis showed that the organ-specific response to RTX in the muscle was 59%. Moreover, 65% of the patients with ILD responded to treatment. Furthermore, the therapeutic response was excellent for patients with skin involvement (81%).

How to identify which populations with IIM would be the most likely to benefit from receiving treatment with RTX? Are there any clinical and laboratory factors that predict clinical prognosis? First, the presence of MSAs or MAAs may be associated with the clinical response. In Nalotto's study, five out of six refractory IIM patients achieved significant clinical improvement 6 months after RTX. All five patients were positive for MSAs or MAAs, whereas those without improvement were negative for autoantibodies (58). Aggarwal et al. conducted a *post hoc* analysis of the RIM trial, revealing that the presence of anti-synthetase autoantibodies (predominantly anti-Jo-1) and anti-Mi-2 autoantibodies strongly predicted clinical improvement in refractory myositis patients, whereas the absence of myositis autoantibodies was associated with a worse outcome (59). In a Korean trial, all six ANA-positive patients responded to RTX (four achieved complete response, two achieved partial response), whereas among the four ANA-negative patients, two achieved partial response and the remainder had no response to RTX. All three anti-Jo-1 antibody positive patients achieved a complete response (25). As mentioned above, the frequent presence of MSAs and MAAs in IIM suggests an important role of B cells in the disease; RTX could effectively deplete B cells to make these populations to achieve a better outcome. Second, the JDM subset may have a better response to RTX, which was not attributable to a shorter disease duration, or these populations may have had lower myositis-related damage (59). Third, lower disease damage predicts better outcomes in patients with refractory myositis (59). Patients with dysphagia, a known serious problem in patients with IIM, showed worse outcomes than those treated with RTX (23).

In Nalotto's study (58), although five patients with positive autoantibodies responded well to RTX, only one exhibited decreased antibody levels after B cell depletion, suggesting that autoantibody levels may not correlate with clinical response. However, Aggarwal et al. showed that the autoantibody levels correlated with the clinical response to RTX in the RIM trial, demonstrating that the four autoantibodies (anti-Jo-1, -SRP, -TIF1-γ, -Mi-2) levels decreased after B cell depletion; the first three correlated with changes in disease activity (60). These contradictory results require verification in additional RCTs.

The safety of rituximab in patients with IIM was another essential component of our meta-analysis and must be considered in clinical practice. We found that the incidence of adverse events was 18% (95% CI: 7%, 33%), and the incidence of infection was 26% (95% CI: 17%, 35%). In addition, the incidences of severe adverse events and infections, were 8% and 2%, respectively. The infusion reaction was thought to be a joint adverse event of RTX. Our meta-analysis showed that the incidence of infusion reactions was 12%. In brief, RTX was considered relatively safe and well-tolerated in patients with IIM.

This meta-analysis had several notable strengths. To the best of our knowledge, this is the first systematic meta-analysis to evaluate the effectiveness and safety of RTX in patients with IIM. Second, we evaluated the overall efficacy rate, complete response rate, partial response rate, and organ-specific response rate to fully assess the efficacy of RTX. Third, we conducted a comprehensive literature search across five databases using a standardized methodology. Finally, strict inclusion and exclusion criteria were used and case reports and case series with fewer than five participants were excluded, to ensure the quality of the included studies.

Our meta-analysis also has several limitations. First, the included studies failed to provide the mean ± standard deviation (SD) of corticosteroid dosage and CK levels before and after RTX treatment. Therefore, the effects of RTX on corticosteroid tapering and the influence of CK levels could not be evaluated. Second, the RTX regime varied among the included studies, which contributed to the heterogeneity. Third,

the included studies had inconsistent definitions of complete and partial responses. This may have been another source of heterogeneity. Fourth, most of the included studies were single-arm tests without control groups, and no RCT data could be summarized, which is difficult to circumvent owing to the rarity of IIMs. Therefore, the conclusions of this study should be verified in clinical practice.

5 Conclusion

In summary, this meta-analysis suggests that RTX is a feasible treatment option for patients with IIMs. It is effective and relatively safe in this patient population. Future RCTs are required to further evaluate the efficacy and safety of RTX treatment for patients with IIMs.

Data availability statement

The original contributions presented in the study are included in the article/Supplementary Material. Further inquiries can be directed to the corresponding authors.

Author contributions

CZ had the conception, collected and analyzed the data, and wrote the manuscript. YH collected and analyzed the data. BZ revised the manuscript. XM analyzed the data. CZ and TD had the conception, help the methods and revised the manuscript. All authors contributed to the article and approved the submitted version.

Funding

This study was supported by the National Natural Science Foundation of China (Grant No. 82171395), Natural Science Foundation of Shandong Province (Grant No. ZR2021QH120), Key Research and Development Project of Shandong Province (2019GXRC050), and Qingdao Technology Program for Health and Welfare (20-3-3-42-nsh).

Conflict of interest

The authors declare that the research was conducted in the absence of any commercial or financial relationships that could be construed as a potential conflict of interest.

Publisher's note

All claims expressed in this article are solely those of the authors and do not necessarily represent those of their affiliated organizations, or those of the publisher, the editors and the reviewers. Any product that may be evaluated in this article, or claim that may be made by its manufacturer, is not guaranteed or endorsed by the publisher.

Supplementary material

The Supplementary Material for this article can be found online at: https://www.frontiersin.org/articles/10.3389/fimmu.2022.1051609/full#supplementary-material

References

1. Lundberg I, Fujimoto M, Vencovsky J, Aggarwal R, Holmqvist M, Christopher-Stine L, et al. Idiopathic inflammatory myopathies. *Nat Rev Dis Primers* (2021) 7(1):86. doi: 10.1038/s41572-021-00321-x

2. Vencovský J, Alexanderson H, Lundberg I. Idiopathic inflammatory myopathies. *Rheumatic Dis Clinics North America* (2019) 45(4):569–81. doi: 10.1016/j.rdc.2019.07.006

3. Lundberg I, Tjärnlund A, Bottai M, Werth V, Pilkington C, Visser M, et al. 2017 European league against Rheumatism/American college of rheumatology classification criteria for adult and juvenile idiopathic inflammatory myopathies and their major subgroups. *Ann rheumatic Dis* (2017) 76(12):1955–64. doi: 10.1136/annrheumdis-2017-211468

4. Leandro MJ, Cambridge G, Ehrenstein MR, Edwards J. Reconstitution of peripheral blood b cells after depletion with rituximab in patients with rheumatoid arthritis. *Arthritis Rheumatism* (2006) 54(2):613–20. doi: 10.1002/art.21617

5. Boross P, Leusen JH. Mechanisms of action of Cd20 antibodies. *Am J Cancer Res* (2012) 2(6):676–90.

6. Buch MH, Smolen JS, Betteridge N, Breedveld FC, Burmester G, Dörner T, et al. Updated consensus statement on the use of rituximab in patients with rheumatoid arthritis. *Ann Rheum Dis* (2011) 70(6):909–20. doi: 10.1136/ard.2010.144998

7. Smith RM, Jones RB, Specks U, Bond S, Nodale M, Aljayyousi R, et al. Rituximab as therapy to induce remission after relapse in anca-associated vasculitis. *Ann Rheum Dis* (2020) 79(9):1243–9. doi: 10.1136/annrheumdis-2019-216863

8. Fanouriakis A, Tziolos N, Bertsias G, Boumpas DT. Update On the diagnosis and management of systemic lupus erythematosus. *Ann Rheum Dis* (2021) 80 (1):14–25. doi: 10.1136/annrheumdis-2020-218272

9. Fanouriakis A, Kostopoulou M, Alunno A, Aringer M, Bajema I, Boletis JN, et al. 2019 update of the eular recommendations for the management of systemic lupus erythematosus. *Ann Rheum Dis* (2019) 78(6):736–45. doi: 10.1136/annrheumdis-2019-215089

10. Hauser SL, Waubant E, Arnold DL, Vollmer T, Antel J, Fox RJ, et al. B-cell depletion with rituximab in relapsing-remitting multiple sclerosis. *N Engl J Med* (2008) 358(7):676–88. doi: 10.1056/NEJMoa0706383

11. Hawker K, O'Connor P, Freedman MS, Calabresi PA, Antel J, Simon J, et al. Rituximab in patients with primary progressive multiple sclerosis: Results of a randomized double-blind placebo-controlled multicenter trial. *Ann Neurol* (2009) 66(4):460–71. doi: 10.1002/ana.21867

12. Salzer J, Svenningsson R, Alping P, Novakova L, Björck A, Fink K, et al. Rituximab in multiple sclerosis: A retrospective observational study on safety and efficacy. *Neurology* (2016) 87(20):2074–81. doi: 10.1212/wnl.0000000000003331

13. Piper C, Wilkinson M, Deakin C, Otto G, Dowle S, Duurland C, et al. Cd19cd24cd38 b cells are expanded in juvenile dermatomyositis and exhibit a pro-inflammatory phenotype after activation through toll-like receptor 7 and interferon-A. *Front Immunol* (2018) 9:1372. doi: 10.3389/fimmu.2018.01372

14. Krystufková O, Vallerskog T, Helmers S, Mann H, Putová I, Belácek J, et al. Increased serum levels of b cell activating factor (Baff) in subsets of patients with idiopathic inflammatory myopathies. *Ann rheumatic Dis* (2009) 68(6):836–43. doi: 10.1136/ard.2008.091405

15. Baek A, Park H, Na S, Shim D, Moon J, Yang Y, et al. The expression of baff in the muscles of patients with dermatomyositis. *J neuroimmunology* (2012) 249:96–100. doi: 10.1016/j.jneuroim.2012.04.006

16. Oddis C, Reed A, Aggarwal R, Rider L, Ascherman D, Levesque M, et al. Rituximab in the treatment of refractory adult and juvenile dermatomyositis and adult polymyositis: A randomized, placebo-phase trial. *Arthritis rheumatism* (2013) 65(2):314–24. doi: 10.1002/art.37754

17. Santos V, Aragón C, Posso-Osorio I, Naranjo-Escobar J, Milisenda J, Obando M, et al. Rituximab for inflammatory myopathies in a Colombian cohort. *J Clin Rheumatol Pract Rep rheumatic musculoskeletal Dis* (2021) 27: S232–S5. doi: 10.1097/rhu.0000000000001620

18. Allenbach Y, Guiguet M, Rigolet A, Marie I, Hachulla E, Drouot L, et al. Efficacy of rituximab in refractory inflammatory myopathies associated with anti-synthetase auto-antibodies: An open-label, phase ii trial. *PloS One* (2015) 10(11): e0133702. doi: 10.1371/journal.pone.0133702

19. Bohan A, Peter J. Polymyositis and dermatomyositis (First of two parts). *New Engl J Med* (1975) 292(7):344–7. doi: 10.1056/nejm197502132920706

20. Hoogendijk J, Amato A, Lecky B, Choy E, Lundberg I, Rose M, et al. 119th enmc international workshop: Trial design in adult idiopathic inflammatory myopathies, with the exception of inclusion body myositis, 10-12 October 2003, naarden, the Netherlands. *Neuromuscular Disord* (2004) 14(5):337–45. doi: 10.1016/j.nmd.2004.02.006

21. Slim K, Nini E, Forestier D, Kwiatkowski F, Panis Y, Chipponi J. Methodological index for non-randomized studies (Minors): Development and validation of a new instrument. *ANZ J Surg* (2003) 73(9):712–6. doi: 10.1046/j.1445-2197.2003.02748.x

22. Bauhammer J, Blank N, Max R, Lorenz H, Wagner U, Krause D, et al. Rituximab in the treatment of Jo1 antibody-associated antisynthetase syndrome: Anti-Ro52 positivity as a marker for severity and treatment response. *J Rheumatol* (2016) 43(8):1566–74. doi: 10.3899/jrheum.150844

23. de Souza F, Miossi R, de Moraes J, Bonfá E, Shinjo S. Favorable rituximab response in patients with refractory idiopathic inflammatory myopathies. *Adv Rheumatol (London England)* (2018) 58(1):31. doi: 10.1186/s42358-018-0030-z

24. Aggarwal R, Loganathan P, Koontz D, Qi Z, Reed A, Oddis C. Cutaneous improvement in refractory adult and juvenile dermatomyositis after treatment with rituximab. *Rheumatol (Oxford England)* (2017) 56(2):247–54. doi: 10.1093/rheumatology/kew396

25. Ahn G, Suh C, Kim Y, Park Y, Shim S, Lee S, et al. Efficacy and safety of rituximab in Korean patients with refractory inflammatory myopathies. *J Korean Med Sci* (2020) 35(38):e335. doi: 10.3346/jkms.2020.35.e335

26. Andersson H, Sem M, Lund M, Aaløkken T, Günther A, Walle-Hansen R, et al. Long-term experience with rituximab in anti-synthetase syndrome-related interstitial lung disease. *Rheumatol (Oxford England)* (2015) 54(8):1420–8. doi: 10.1093/rheumatology/kev004

27. Bader-Meunier B, Decaluwe H, Barnerias C, Gherardi R, Quartier P, Faye A, et al. Safety and efficacy of rituximab in severe juvenile dermatomyositis: Results from 9 patients from the French autoimmunity and rituximab registry. *J Rheumatol* (2011) 38(7):1436–40. doi: 10.3899/jrheum.101321

28. Behrens Pinto G, Carboni R, de Souza F, Shinjo S. A prospective cross-sectional study of serum il-17a in antisynthetase syndrome. *Clin Rheumatol* (2020) 39(9):2763–71. doi: 10.1007/s10067-020-05013-7

29. Chung L, Genovese M, Fiorentino D. A pilot trial of rituximab in the treatment of patients with dermatomyositis. *Arch Dermatol* (2007) 143(6):763–7. doi: 10.1001/archderm.143.6.763

30. Couderc M, Gottenberg J, Mariette X, Hachulla E, Sibilia J, Fain O, et al. Efficacy and safety of rituximab in the treatment of refractory inflammatory myopathies in adults: Results from the air registry. *Rheumatol (Oxford England)* (2011) 50(12):2283–9. doi: 10.1093/rheumatology/ker305

31. Ge Y, Li S, Tian X, He L, Lu X, Wang G. Anti-melanoma differentiation-associated gene 5 (Mda5) antibody-positive dermatomyositis responds to rituximab therapy. *Clin Rheumatol* (2021) 40(6):2311–7. doi: 10.1007/s10067-020-05530-5

32. Korsten P, Rademacher J, Riedel L, Schnitzler E, Olgemöller U, Seitz C, et al. Antisynthetase syndrome-associated interstitial lung disease: Monitoring of immunosuppressive treatment effects by chest computed tomography. *Front Med* (2020) 7:609595. doi: 10.3389/fmed.2020.609595

33. Landon-Cardinal O, Allenbach Y, Soulages A, Rigolet A, Hervier B, Champtiaux N, et al. Rituximab in the treatment of refractory anti-hmgcr immune-mediated necrotizing myopathy. *J Rheumatol* (2019) 46(6):623–7. doi: 10.3899/jrheum.171495

34. Leclair V, Galindo-Feria A, Dastmalchi M, Holmqvist M, Lundberg I. Efficacy and safety of rituximab in anti-synthetase antibody positive and negative subjects with idiopathic inflammatory myopathy: A registry-based study. *Rheumatol (Oxford England)* (2019) 58(7):1214–20. doi: 10.1093/rheumatology/key450

35. Levine T. Rituximab in the treatment of dermatomyositis: An open-label pilot study. *Arthritis rheumatism* (2005) 52(2):601–7. doi: 10.1002/art.20849

36. Mahler E, Marlies B, Voermans NC, Van EBGM, Van RPLCM, Vonk MC. Rituximab treatment in patients with refractory inflammatory myopathies. *Rheumatology* (2011) 12):2206–13. doi: 10.1093/rheumatology/ker088

37. Marie I, Dominique S, Janvresse A, Levesque H, Menard J. Rituximab therapy for refractory interstitial lung disease related to antisynthetase syndrome. *Respir Med* (2012) 106(4):581–7. doi: 10.1016/j.rmed.2012.01.001

38. Meyer A, Lefevre G, Bierry G, Duval A, Ottaviani S, Meyer O, et al. In antisynthetase syndrome, acpa are associated with severe and erosive arthritis: An overlapping rheumatoid arthritis and antisynthetase syndrome. *Medicine* (2015) 94 (20):e523. doi: 10.1097/md.0000000000000523

39. Muñoz-Beamud F, Isenberg D. Rituximab as an effective alternative therapy in refractory idiopathic inflammatory myopathies. *Clin Exp Rheumatol* (2013) 31 (6):896–903.

40. Ramos-Casals M, García-Hernández F, de Ramón E, Callejas J, Martínez-Berriotxoa A, Pallarés L, et al. Off-label use of rituximab in 196 patients with severe, refractory systemic autoimmune diseases. *Clin Exp Rheumatol* (2010) 28 (4):468–76.

41. Sem M, Molberg O, Lund M, Gran J. Rituximab treatment of the anti-synthetase syndrome: A retrospective case series. *Rheumatol (Oxford England)* (2009) 48(8):968–71. doi: 10.1093/rheumatology/kep157

42. Shahin AA, Niazy MH, Haroon MM. Response to cyclophosphamide and rituximab therapy in idiopathic inflammatory myopathies: A single center experience. *Egyptian Rheumatologist* (2021) 43:247–51. doi: 10.1016/j.ejr.2021.03.005

43. Sultan S, Ng K, Edwards J, Isenberg D, Cambridge G. Clinical outcome following b cell depletion therapy in eight patients with refractory idiopathic inflammatory myopathy. *Clin Exp Rheumatol* (2008) 26(5):887–93.

44. Unger L, Kampf S, Lüthke K, Aringer M. Rituximab therapy in patients with refractory dermatomyositis or polymyositis: Differential effects in a real-life population. *Rheumatol (Oxford England)* (2014) 53(9):1630–8. doi: 10.1093/rheumatology/keu024

45. Chandra T, Aggarwal R. Clinical trials and novel therapeutics in dermatomyositis. *Expert Opin emerging Drugs* (2020) 25(3):213–28. doi: 10.1080/14728214.2020.1787985

46. Morganroth P, Kreider M, Werth V. Mycophenolate mofetil for interstitial lung disease in dermatomyositis. *Arthritis Care Res* (2010) 62(10):1496–501. doi: 10.1002/acr.20212

47. Saketkoo L, Espinoza L. Experience of mycophenolate mofetil in 10 patients with autoimmune-related interstitial lung disease demonstrates promising effects. *Am J Med Sci* (2009) 337(5):329–35. doi: 10.1097/MAJ.0b013e31818d094b

48. Oddis CV, Sciurba FC, Elmagd KA, Starzl TE. Tacrolimus in refractory polymyositis with interstitial lung disease. *Lancet* (1999) 353(9166):1762–3. doi: 10.1016/S0140-6736(99)01927-3

49. Labirua-Iturburu A, Selva-O'Callaghan A, Martínez-Gómez X, Trallero-Araguás E, Labrador-Horrillo M, Vilardell-Tarrés M. Calcineurin inhibitors in a cohort of patients with antisynthetase-associated interstitial lung disease. *Clin Exp Rheumatol* (2013) 31(3):436–9.

50. Aggarwal R, Charles-Schoeman C, Schessl J, Bata-Csörgő Z, Dimachkie MM, Griger Z, et al. Trial of intravenous immune globulin in dermatomyositis. *N Engl J Med* (2022) 387(14):1264–78. doi: 10.1056/NEJMoa2117912

51. Lim J, Eftimov F, Verhamme C, Brusse E, Hoogendijk JE, Saris CGJ, et al. Intravenous immunoglobulins as first-line treatment in idiopathic inflammatory myopathies: A pilot study. *Rheumatol (Oxford)* (2021) 60(4):1784–92. doi: 10.1093/rheumatology/keaa459

52. Allenbach Y, Mammen AL, Benveniste O, Stenzel W. 224th enmc international workshop:: Clinico-Sero-Pathological classification of immune-mediated necrotizing myopathies zandvoort, the Netherlands, 14-16 October 2016. *Neuromuscul Disord* (2018) 28(1):87–99. doi: 10.1016/j.nmd.2017.09.016

53. Arahata K, Engel A. Monoclonal antibody analysis of mononuclear cells in myopathies. I: Quantitation of subsets according to diagnosis and sites of accumulation and demonstration and counts of muscle fibers invaded by T cells. *Ann Neurol* (1984) 16(2):193–208. doi: 10.1002/ana.410160206

54. Greenberg S, Bradshaw E, Pinkus J, Pinkus G, Burleson T, Due B, et al. Plasma cells in muscle in inclusion body myositis and polymyositis. *Neurology* (2005) 65(11):1782–7. doi: 10.1212/01.wnl.0000187124.92826.20

55. Damoiseaux J, Vulsteke J, Tseng C, Platteel A, Piette Y, Shovman O, et al. Autoantibodies in idiopathic inflammatory myopathies: Clinical associations and laboratory evaluation by mono- and multispecific immunoassays. *Autoimmun Rev* (2019) 18(3):293–305. doi: 10.1016/j.autrev.2018.10.004

56. Gunawardena H, Betteridge Z, McHugh N. Myositis-specific autoantibodies: Their clinical and pathogenic significance in disease expression. *Rheumatol (Oxford England)* (2009) 48(6):607–12. doi: 10.1093/rheumatology/kep078

57. Brouwer R, Hengstman G, Vree Egberts W, Ehrfeld H, Bozic B, Ghirardello A, et al. Autoantibody profiles in the sera of European patients with myositis. *Ann rheumatic Dis* (2001) 60(2):116–23. doi: 10.1136/ard.60.2.116

58. Nalotto L, Iaccarino L, Zen M, Gatto M, Borella E, Domenighetti M, et al. Rituximab in refractory idiopathic inflammatory myopathies and antisynthetase syndrome: Personal experience and review of the literature. *Immunol Res* (2013) 56 (2-3):362–70. doi: 10.1007/s12026-013-8408-9

59. Aggarwal R, Bandos A, Reed AM, Ascherman DP, Barohn RJ, Feldman BM, et al. Predictors of clinical improvement in rituximab-treated refractory adult and juvenile dermatomyositis and adult polymyositis. *Arthritis Rheumatol* (2014) 66 (3):740–9. doi: 10.1002/art.38270

60. Aggarwal R, Oddis CV, Goudeau D, Koontz D, Qi Z, Reed AM, et al. Autoantibody levels in myositis patients correlate with clinical response during b cell depletion with rituximab. *Rheumatol (Oxford)* (2016) 55(6):991–9. doi: 10.1093/rheumatology/kev444

frontiers | Frontiers in Immunology

TYPE Original Research
PUBLISHED 20 December 2022
DOI 10.3389/fimmu.2022.1044933

OPEN ACCESS

EDITED BY
Roberto Paganelli,
Institute for Advanced Biologic Therapies, Italy

REVIEWED BY
Saul Oswaldo Lugo Reyes,
National Institute of Pediatrics (Mexico), Mexico
Capucine Picard,
Hôpital Necker-Enfants Malades, France

*CORRESPONDENCE
Oded Shamriz
oded.shamriz@mail.huji.ac.il

†These authors have contributed equally to this work and share first authorship

‡These authors have contributed equally to this work and share last authorship

SPECIALTY SECTION
This article was submitted to Autoimmune and Autoinflammatory Disorders : Autoimmune Disorders, a section of the journal Frontiers in Immunology

RECEIVED 15 September 2022
ACCEPTED 07 December 2022
PUBLISHED 20 December 2022

CITATION
Shamriz O, Rubin L, Simon AJ, Lev A, Barel O, Somech R, Korem M, Matza Porges M, Freund T, Hagin D, Garty BZ, Nahum A, Molho Pessach V and Tal Y (2022) Dominant-negative signal transducer and activator of transcription (STAT)3 variants in adult patients: A single center experience. *Front. Immunol.* 13:1044933. doi: 10.3389/fimmu.2022.1044933

Dominant-negative signal transducer and activator of transcription (STAT)3 variants in adult patients: A single center experience

Oded Shamriz[1,2*†], Limor Rubin[1†], Amos J. Simon[3,4], Atar Lev[4], Ortal Barel[5,6], Raz Somech[4], Maya Korem[7], Sigal Matza Porges[8,9], Tal Freund[10], David Hagin[10], Ben Zion Garty[11,12,13], Amit Nahum[14], Vered Molho Pessach[15‡] and Yuval Tal[1‡]

[1]Allergy and Clinical Immunology Unit, Department of Medicine, Hadassah Medical Organization, Faculty of Medicine, Hebrew University of Jerusalem, Jerusalem, Israel, [2]The Lautenberg Center for Immunology and Cancer Research, Institute of Medical Research Israel-Canada, Faculty of Medicine, Hebrew University of Jerusalem, Jerusalem, Israel, [3]Sheba Cancer Research Center and Institute of Hematology, Sheba Medical Center, Ramat Gan, Israel, [4]Pediatric Department A and the Immunology Service, Jeffrey Modell Foundation Center, Edmond and Lily Safra Children's Hospital, Tel-Hashomer Medical Center, Affiliated to the Sackler Faculty of Medicine, Tel Aviv University, Tel Aviv, Israel, [5]The Genomic Unit, Sheba Cancer Research Center, Sheba Medical Center, Ramat Gan, Israel, [6]Sheba Medical Center, Wohl Institute of Translational Medicine, Ramat Gan, Israel, [7]Department of Clinical Microbiology and Infectious Diseases, Hadassah Medical Center, Faculty of Medicine, Hebrew University of Jerusalem, Jerusalem, Israel, [8]Department of Human Genetics, Institute for Medical Research, the Hebrew University of Jerusalem, Jerusalem, Israel, [9]Department of Biotechnology, Hadassah Academic College, Jerusalem, Israel, [10]Allergy and Clinical Immunology Unit, Department of Medicine, Tel-Aviv Sourasky Medical Center and Sackler Faculty of Medicine, Tel Aviv University, Tel Aviv, Israel, [11]Sackler School of Medicine, Tel Aviv University, Tel-Aviv, Israel, [12]Felsenstein Medical Research Center, Rabin Medical Center, Petach-Tikva, Israel, [13]Allergy and Clinical Immunology Unit, Schneider Children's Medical Center, Petach-Tikva, Israel, [14]Pediatrics Department A, Soroka University Medical Center and Faculty of Health Sciences, Ben-Gurion University of the Negev, Beer Sheva, Israel, [15]Pediatric Dermatology Service, Department of Dermatology, Hadassah Medical Organization, Faculty of Medicine, Hebrew University of Jerusalem, Jerusalem, Israel

Background: Autosomal dominant hyper-IgE syndrome (AD-HIES) caused by dominant negative (DN) variants in the signal transducer and activator of transcription 3 gene (*STAT3*) is characterized by recurrent Staphylococcal abscesses, severe eczema, chronic mucocutaneous candidiasis (CMC), and non-immunological facial and skeletal features.

Objectives: To describe our experience with the diagnosis and treatment of adult patients with AD-HIES induced by DN-*STAT3* variants.

Methods: The medical records of adult patients (>18 years) treated at the Allergy and Clinical Immunology Clinic of Hadassah Medical Center, Jerusalem, Israel, were retrospectively analyzed. Immune and genetic workups were used to confirm diagnosis.

10.3389/fimmu.2022.1044933

Results: Three adult patients (2 males; age 29-41 years) were diagnosed with DN-*STAT3* variants. All patients had non-immunological features, including coarse faces and osteopenia. Serious bacterial infections were noted in all patients, including recurrent abscesses, recurrent pneumonia, and bronchiectasis. CMC and diffuse dermatophytosis were noted in two patients. Two patients had severe atopic dermatitis refractory to topical steroids and phototherapy. Immune workup revealed elevated IgE in three patients and eosinophilia in two patients. Whole exome sequencing revealed DN-*STAT3* variants (c.1166C>T; p.Thr389Ile in two patients and c.1268G>A; p.Arg423Gln in one patient). Variants were located in DNA-binding domain (DBD) and did not hamper STAT3 phosphorylation Treatment included antimicrobial prophylaxis with trimethoprim/sulfamethoxazole (n=2) and amoxycillin-clavulanic acid (n=1), and anti-fungal treatment with fluconazole (n=2) and voriconazole (n=1). Two patients who had severe atopic dermatitis, were treated with dupilumab with complete resolution of their rash. No adverse responses were noted in the dupilumab-treated patients.

Discussion: Dupilumab can be used safely as a biotherapy for atopic dermatitis in these patients as it can effectively alleviate eczema-related symptoms. Immunologists and dermatologists treating AD-HIES adult patients should be aware of demodicosis as a possible manifestation. DN-*STAT3* variants in DBD do not hamper STAT3 phosphorylation.

KEYWORDS

stat3, hyper IgE syndrome, adults, inborn errors of imunity, dupilumab

1 Introduction

Signal transducer and activator of transcription (STAT)3 is a key transcription factor involved in the function and development of T helper (Th)17 cells (1). Following stimulation with interleukin (IL)-6 and transforming growth factor (TGF)-β, STAT3 is phosphorylated and, together with RORγT, induces differentiation of $CD4^+$ T cells into functional Th17 cells. These cells secrete IL-17 and IL-22 and play a critical role in immune responses against fungal and bacterial infections (1).

Dominant negative (DN) heterozygous variants of *STAT3* induce autosomal dominant hyper immunoglobulin (Ig)E syndrome (AD-HIES) (2). This inborn error of immunity (IEI) is characterized by impaired counts and effector functions of Th17 cells and increased susceptibility to fungal and Staphylococcal infections (3). Immune features also include decreased plasma and memory B-cell counts, *via* impaired IL-21-mediated signaling (4) and a shift towards a Th2-mediated immune response, which manifests as atopic dermatitis and eosinophilia (5).

AD-HIES is also characterized by non-immunological features. Coarse faces are a known feature of AD-HIES (6). Furthermore, retained primary teeth can be seen in AD-HIEs patients, as evident in 72% of a previously reported 30-patient cohort (6). IL-4 and other cytokines-mediated bone resorption may induce osteopenia, osteoporosis and frequent bone fractures (6). Other skeletal characteristics of AD-HIES consist of joint hyperextensibility and craniosynostosis. Scoliosis is also seen in up to a third of the patients (6). Finally, rates of vascular anomalies, including brain and cardiac arterial ectasias and aneurysms, were reported in a cohort of 21 adult patients to be as high as 84% and 50%, respectively (7).

In recent years, advances in mechanism-targeted biological treatments have revolutionized the care of patients with IEI and other rare immune-mediated diseases. Different biologic treatments were used in patients with AD-HIES and demonstrated efficacy in relieving symptoms. For example, benralizumab, an anti-IL-5 receptor α chain, monoclonal antibody was used to treat AD-HIES with eosinophilic asthma (8). Omalizumab, an anti-IgE antibody, was also used to treat patients with AD-HIES and was shown to alleviate respiratory symptoms and pulmonary function tests (9). However, there is an increasing amount of reports of AD-HIES patients that were successfully treated with dupilumab, an anti-IL-4/IL-13 receptor α subunit monoclonal antibody (10–17).

Here, we present additional information regarding the clinical course, diagnosis, and treatment of adult patients with AD-HIES, as well as details on the successful treatment of these patients with dupilumab.

2 Methods

2.1 Study design and patients

This is a retrospective analysis of the medical records of adult patients (age >18 years) with AD-HIES who were treated at the Allergy and Clinical Immunology Unit of Hadassah Medical Center, Jerusalem, Israel. All patients underwent genetic diagnostic tests that confirmed DN-*STAT3* variants. Variant pathogenicity was confirmed by *in vitro* assays. The clinical severity of AD-HIES was evaluated using the National Institute of Health (NIH) score (10). The severity of atopic dermatitis in the AD-HIES patients was assessed by the Investigator's Global Assessment (IGA) scale (18) and Eczema Area and Severity Index (EASI) score (18).

2.2 Immune analysis

Lymphocyte subsets of peripheral blood mononuclear cells (PBMCs) were obtained using flow cytometry. T-cell proliferation capacity was evaluated using a thymidine-based DNA incorporation assay as described previously (19). T-cell stimuli consisted of 6 and 25 μg/mL phytohemagglutinin (PHA) and anti-CD3 antibody. In one patient (P2), data regarding the thymidine-based DNA incorporation assay was available from a previous analysis, which consisted of PHA, concanavalin A (CON A), and pokeweed mitogen (PWM) stimuli.

In addition, the humoral immune response was assessed in patients by testing their immunoglobulin levels and specific IgG antibody titers to past vaccines. Confirmation of AD-HIES was obtained by immunoblot analysis or flow cytometry assays of phosphorylated (p) STAT3 protein or measurements of Th17 counts using flow cytometry.

2.3 STAT3 immunoblotting and phosphorylation assays

PBMCs were isolated from patients and healthy controls using Ficoll-Hypaque and stimulated with IL-6 (20-50 ng/mL) for the indicated times at 37°C. Cells were lysed in RIPA buffer and lysates probed with anti-phospho-STAT3 (Y705) and STAT3 (Cell Signaling Technology, Danvers, MA) using standard Western blotting techniques.

For the flow cytometry-based STAT3 phosphorylation assay, PBMCs were stained with anti-CD4 (Pacific Blue clone RPA-T4; BioLegend Cat #300521) before being stimulated with either IL-10 (10n g/mL; Miltenyi Biotec) or IL-21 (100 ng/mL; Miltenyi Biotec) for 20 min at 37°C. Cells were then fixed with 4% paraformaldehyde for 10 min at 37°C and incubated in permeabilization buffer (True-Phos Perm Buffer, BioLegend Cat #425401) overnight at -20°C. The next day, cells were washed and stained with anti-phospho-STAT3 (pY705) (PE clone 13A3-1; BioLegend Cat #651004) for 4 hours at 4°C.

2.4 Intracellular IL-17 staining

Frozen PBMCs from patients and healthy controls were thawed and stimulated with phorbol myristate acetate (20 ng/mL) and ionomycin (1 μg/mL) overnight at 37°C in a 5% CO_2 atmosphere in the presence of Brefeldin A (1 μL/mL of 1000X; BioLegend Cat #420601). After 16 hours, cells were fixed, permeabilized, and stained for CD4 (Pacific Blue clone RPA-T4; BioLegend Cat #300521), IFNγ (AF647 clone 4S.B3; BioLegend Cat #502516), and IL-17 (FITC clone BL168; BioLegend Cat #512304). Cells were acquired using a BD FACSCanto II flow cytometer and data analysis performed using FlowJo software (V10.0, TreeStar). The aim was to evaluate intracellular cytokine staining within $CD4^+$ lymphocytes.

2.5 Genetic workup

Exome sequencing was performed using the Twist Human Core Exome Plus Kit (Twist Bioscience, San Francisco, CA, USA) on a NovaSeq 6000 sequencing machine (Illumina, San Diego, CA, USA). Paired end reads (2 × 100 bp) were obtained and processed for each sample. The Illumina Dragen Bio-IT Platform version 3.9 was used to align reads to the human reference genome (hg38) based on the Smith-Waterman algorithm (20) and to call variants based on GATK variant caller version 3.7 (21). Additional variants were called with Freebayes version 1.2.0 (22). Variant annotation was performed using KGG-Seq version 1.2 (23). Further annotation and filtration steps were performed by in-house scripts using various additional datasets.

2.6 Ethical review of the study

This study was approved by the institutional review board (IRB) of Hadassah Medical Center (IRB number: HMO-0473-22). A waiver for participant consent was gained by the IRB of Hadassah Medical Center.

10.3389/fimmu.2022.1044933

3 Results

3.1 Patient characteristics

Clinical characteristics of the patients are presented in Table 1. Three adult patients with AD-HIES due to DN-*STAT3* (two males and one female) were followed at our Allergy and Clinical Immunology Unit during the study period. Patient ages at symptom onset ranged from 2 months to 20 years. All patients were genetically diagnosed with DN-*STAT3* in adulthood (21-41 years).

Patient 1 (P1) and P2 were briefly reported on by Woellner et al. (24) and Scheuerman (25) et al.; they are siblings born to a non-consanguineous Ashkenazi Jewish family harboring three generations of AD-HIES patients. The mother died at 42 years old from pulmonary emboli. She had seven children, and one of them died from pneumonia at the age of 3 months without a definitive diagnosis of AD-HIES. P1 has two children with AD-HIES.

P3 was born to a consanguineous Arab family. He has two children with chronic facial rashes compatible with atopic dermatitis who have not yet been evaluated. The family pedigrees of the patients are presented in Figure 1. Although he had course facial features compatible with AD-HIES since childhood, there is no record of significant infections before the age of 20 years. At that age, he presented with severe pneumonia that had a prolonged course and required intravenous antibiotics. At the age of 35 years, he was diagnosed with a liver abscess with growth of *Staphylococcus aureus*, which has resolved with antibiotics. He then presented to our clinic at the age of 41 years, with recurrent pyomoyositis for further immune investigation.

NIH scores for clinical severity of AD-HIES were 55, 48, and 37 in P1, P2, and P3, respectively. All patients had typical infectious manifestations consisting of myositis (Figure 1C) and recurrent Staphylococcal abscesses of the skin, breast, and liver (Figure 1D). Serious bacterial infections also included recurrent sinopulmonary infections and bronchiectasis in all three patients. Pneumatocele was noted in the history of P2. Dermatological manifestations in P1 and P2 involved severe atopic dermatitis (Figure 1E). These patients also had papulopustular rosacea due to demodex, which was observed by dermoscopy. Chronic mucocutaneous candidiasis (CMC) was noted in P1 and P2 and manifested as persistent oral candidiasis, diffuse tinea corporis (Figure 1F), and onychomycosis. Severe viral infections occurred in P2, who had cytomegalovirus (CMV) and varicella zoster virus (VZV) pneumonias.

Non-immunological manifestations occurred in all patients. These consisted of coarse facial features in P1-P3, retained primary teeth in P1, and osteoporosis with recurrent skeletal fractures in P2. None of the patients had scoliosis.

3.2 Immune workup

Patients were evaluated as adults in our clinic. Their immune workup is presented in Table 2. Eosinophilia was noted in P1 and P3 (0.9 and 1 x10^9/L, respectively; normal: <0.6 x10^9/L). Lymphocyte subsets revealed inverted $CD4^+/CD8^+$ ratios in all patients. B-cell counts were within normal range in all patients. Lymphocyte proliferation studies were available for P1 and P2 but were normal in both.

All patients had non-diminished IgM, IgA, and IgG levels. IgE was markedly increased in all patients, ranging from 13,500 to 57,000 IU/mL (0-100 IU/mL). Specific IgG production to past vaccines was intact (Table 2) and positive IgG titers were noted for CMV and Epstein-Barr virus (EBV) in all patients.

3.3 Genetic diagnosis

All patients were found to harbor previously reported heterozygous missense variants in the DNA-binding domain (DBD) of *STAT3*; P1 and P2 had c.1166C>T, p.Thr38Ile (2, 5, 24, 25), and P3 had c.1268G>A p.Arg423Gln. The latter variant was previously associated with AD-HIES in 2 families (26), and its pathogenicity was validated in another study (27). The variants found in the three patients were predicted to be pathogenic. The combined annotation dependent depletion (CADD) scores for the variants in P1/P2 and P3 are 29 and 32, respectively, and the frequencies (SeenB4) of the variants are 0 and 1 out of 7934 cases, respectively. Variants' frequencies in GnomAD of P1/P2 and P3 were 0% and 0.000657% (1 out of 152210 alleles), respectively. Sanger sequencing of these *STAT3* variants is presented in Figure 2. The *STAT3* variants are found at evolutionarily preserved sites in all three patients, as seen in genetic analysis from humans to frogs (Figures 2C, D, respectively).

P3 had a late and relatively mild presentation of AD-HIES. Unfortunately, hair or nail samples from P3 were not available for Sanger sequencing. Thus, genetic diagnosis of the DN-*STAT3* variant was completed using peripheral blood and cannot rule out that this patient is a mosaic. Moreover, due to a lack of compliance, family segregation studies of P3, including Sanger sequencing of his two children with atopic dermatitis for the DN-*STAT3* variant, are currently not available.

3.4 Functional confirmation of variant pathogenicity

The pathogenicity of the identified variants was confirmed by functional studies and included either flow cytometry-based evaluation of $CD4^+$ $IL\text{-}17^+$ T cells (Th17 cells), or Western blot and staining using anti-Y705 phospho-STAT3 antibody. Flow cytometric analysis of PBMCs showed that, compared to a

10.3389/fimmu.2022.1044933

TABLE 1 Clinical characteristics of adult patients with dominant-negative (DN)-*STAT3* variants.

Pt	Age at onset/genetic diagnosis/current age(years)	Gender/ethnicity	Consanguinity/Family history	*STAT3 LOF Heterozygous* variant	NIH score	Clinical presentation					Antibiotic and antifungal treatment	Biological treatment (dose)	Duration of dupilumab treatment (months)	Outcome/follow-up period(years)
						Infectious			Dermatological	Non-immunologic				
						Bacterial	Fungal	Viral						
P1	3 months 24/37	M/J	No/Yes	c.1166C>T, p.Thr389Ile (missense)*	55	Recurrent Abscesses, Bronchiectasis, Recurrent pneumonia with *Haemophilus influenzae* in BAL	Tinea corporis, Onychomycosis, Candida esophagitis	None	Severe AD, Rosacea; demodicosis	Coarse face; Retained primary teeth	Trimethoprim/sulfamethoxazole, fluconazole itraconazole, terbinafine, voriconazole	Dupilumab/loading dose 600 mg followed by 300 mg every 2 weeks	17	Resolution of AD/37
P2	2 months 21/29	F/J	No/Yes	c.1166C>T, p.Thr389Ile (missense)*	48	Recurrent pneumonia and OM Recurrent MSSA breast abscesses, skin abscesses Bronchiectasis pneumatocele chronic sinusitis	Oral candidiasis Tinea corporis and tines pedis	Varicella pneumonia; CMV pneumonia	Seborrheic dermatitis, Severe AD, Rosacea; demodicosis	Coarse face. Osteoporosis and recurrent skeletal fractures, Fat embolism following fracture	Amoxicillin/Clavulanic acid, fluconazole	Dupilumab/loading dose 600 mg followed by 300 mg every 2 weeks	7	Resolution of AD/29
P3	20/41/41	M/A	Yes/No	c.1268G>A, p. Arg423Gln, (missense)**	37	Recurrent MSSA. abscesses (liver, prostate, pyomyositis, hidradenitis suppurativa), Recurrent otitis externa, Multifocal pneumonia, Bronchiectasis	None	None	None	Coarse face. Spondylosis, peripheral neuropathy	trimethoprim/sulfamethoxazole	None	None	Alive/1

Pt, Patient; F, Female; M, Male; A, Arab; J, Jew; AD, Atopic dermatitis; MSSA, Methicillin Sensitive Staphylococcus aureus; BAL, Bronchoalveolar lavage; OM, Otitis media; CMV, Cytomegalovirus; PUVA, psoralen and UVA therapy.
*Patients were previously reported by Woellner et al. (24) and Scheuerman et al. (25). Variants were also previously reported by Minegishi et al. (2) and Crosby et al. (5) **STAT3 Variant was previously reported by Holland et al. (26) and Asano et al. (27).

healthy control, Th17 cells were nearly absent in P3 (Figure 2E). Though there may have been decreased expression of pSTAT3 at baseline, patients' cells did show STAT3 phosphorylation (Figures 2F, G). This finding is in accordance with the location of the identified variants within the DBD, which would allow normal phosphorylation due to an intact SH2 domain but abnormal STAT3 signaling due to mutations in the DBD. The pathogenicity of the variant (c.1166C>T, p.Thr389Ile) identified in P1 and P2 was demonstrated previously (2, 4, 5, 13). The abnormal IL-17 expression confirms the pathogenicity of the variant (c.1268G>A p.Arg423Gln) identified in P3.

3.5 Treatment and outcome

Treatments are presented in Table 1. All patients are alive and were treated with prophylactic antibiotics, either trimethoprim/sulfamethoxazole (n=2) or amoxycillin-clavulanate (n=1). P1 and P2 received fluconazole treatment for CMC and severe dermatophyosis. P1 was also treated with itraconazole and terbinafine due to tinea corporis, but without improvement. He also received a course of voriconazole with partial but significant resolution of his tinea corporis.

P1 and P2 had severe atopic dermatitis. P2 had multiple erosive nodules on the face and extremities, consistent with lesions of prurigo nodularis, which are common in patients with severe atopic dermatitis. Both patients failed treatment with potent topical steroids. P1 was also treated with narrow band UVB phototherapy with no improvement of the rash and pruritus. Considering these patients' impaired immune systems, we were reluctant to treat them with systemic immunosuppressive agents. Thus, subcutaneous injections of dupilumab were initiated at a dose of 300 mg every 2 weeks after a loading dose of 600 mg.

Duration of dupilumab treatment in P1 and P2 was 17 and 7 months, respectively. Following treatment, complete resolution of the atopic dermatitis rash and pruritus was seen in both patients (Figures 3A–D). Atopic dermatitis scores available for the patients consisted of the IGA (P1 and P2) and EASI scores (P2). IGA for P1 before and after 1 year of dupilumab treatment was 3 and 0, respectively. P2 had baseline EASI and IGA scores of 20 and 4, respectively. Following 3 months of dupilumab treatment, both scores markedly decreased, to 1 and 0, respectively In addition, examination of serum IgE levels following dupilumab treatment was available in P1. A significant reduction was observed from baseline (13,500 to 953 U/mL; 3-100 U/mL) following 17 months of treatment. No adverse responses were noted in the dupilumab-treated patients.

4 Discussion

In this study, we describe three adult patients with AD-HIES induced by DN-*STAT3* variants. Regarding treatment,

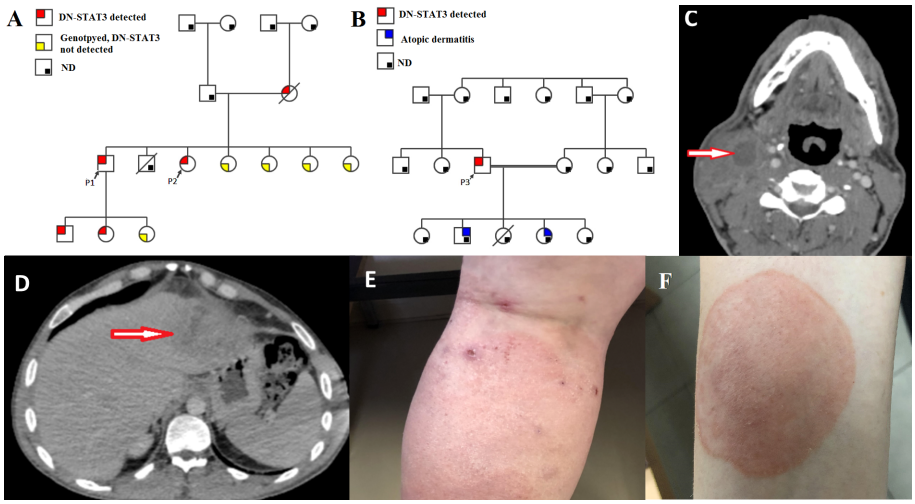

FIGURE 1
Clinical characteristics of the patients. **(A, B)** Family pedigrees of P1-P2 and P3, respectively, demonstrative of an autosomal dominant inheritance. In red, patients that were genotyped for *STAT3* and were found to harbor DN-*STAT3* variants; In yellow – Subjects that were genotyped and were not found to harbor the DN-*STAT3* variant; In grey – Subjects that were not genotyped and therefore presence of DN-*STAT3* variant cannot be determined or ruled out. ND- not determined. Note patients within 3 generations in the family of P1-P2. DN-STAT3-Dominant negative STAT3 variant. **(C)** Computed tomography (CT) scan of cervical spine of P3, axial view, demonstrating a collection with septations in the sternocleidomastoid muscle measuring 20*41*14 mm with reactive muscle and soft tissue edema. **(D)** Abdominal CT scan of P3, coronal view, demonstrating multiple hypodensities in the left liver lobe (segment 2 and 3) and a hepatic abscess measures 8.2*7.9 cm. **(E)** Atopic dermatitis, as seen in P2. **(F)** Tinea corporis, as seen in P2.

TABLE 2 Immune workup of adult patients with DN-*STAT3* variants.

Parameter			P1 (37 yo)	P2 (29 yo)	P3 (41 yo)	Normal Range
Absolute lymphocyte count (10^9/L)			2.6	2.7	3.5	1.1-3.5
Absolute eosinophil count (10^9/L)			**0.9**	0.49	**1**	0.0-0.6
Lymphocyte subpopulations (% of total lymphocytes)	T cells	$CD3^+$	74	84	84	60-85
		$CD4^+$	44	46	48	36-63
		$CD8^+$	22	36	33	15-40
		$CD4^+/CD8^+$ Ratio	*0.5*	*1.28*	*1.4*	1.5-3.3
	NK cells	$CD56^+$	7	7	19	6-30
	B cells	$CD20^+$	15	9	8	5-25
Lymphocyte proliferation study			Normal	Normal	NA	–
Serum immunoglobulins		IgG (mg/dL)	**1562**	**1666**	1185	639-1349
		IgA (mg/dL)	172	151	214	70-312
		IgM (mg/dL)	130	155	57.6	56-352
		IgE (U/mL)	**13500**	**50700**	**25000**	3-100
Specific IgG antibodies		Measles (AU/mL)	**6.20**	**1.1**	**>300**	≥1.1
		VZV (AI)	NA	**2.7**	NA	≥1.1
		Rubella (IU/mL)	**>100**	*19*	**253**	>30

(Continued)

TABLE 2 Continued

Parameter		P1 (37 yo)	P2 (29 yo)	P3 (41 yo)	Normal Range
	Mumps (AI)	**2.30**	*0.7*	**19**	>1.1
	HBV surface (mU/mL)	**0.07**	Neg	**62.1**	>0.05
	HAV	**Pos**	Neg	**Pos**	0
	Diphtheria (IU/mL)	NA	*0.03*	NA	≥0.1
	Tetanus (IU/mL)	NA	**0.39**	NA	>0.1
	EBV EBNA (S/CO)	*0.12*	**Pos**	14.82	0-20
	EBV VCA (S/CO)	**28.15**	NA	**16.73**	≥1
	CMV (AU/mL)	**>250**	**>250**	**>250**	>20

NA, Data is not available; Pos, Positive; Neg, Negative; NK, Natural killer; CPM, Counts per minute; PHA, Phytohemagglutinin; PHA6, PHA 6 μg/mL; PHA25, PHA 25 μg/mL; Ig, Immunoglobulins; HBV, Hepatitis B virus; HAV, Hepatitis A virus; CMV, Cytomegalovirus; VZV, Varicella Zoster Virus EBV, Epstein-Barr virus; EBNA, Epstein-Barr nuclear antigen; VCA, Viral capsid antigen. In bold- values above normal range; Italics – below normal range.

dupilumab was shown in our adult-patient cohort to be a novel treatment for atopic dermatitis in AD-HIES, which was both effective and safe.

Our patients were genetically diagnosed in adulthood. P1 and P2 had delayed genetic diagnosis, though clinical onset of symptoms was at infancy. However, P3 presented with disease manifestation at 20 years of age. A recently published review did not mention variants in DN-*STAT3* as possible triggers of monogenic adult-onset IEI, unlike STAT3 gain-of-function (GOF) mutations, which have been reported to induce immune dysregulation and

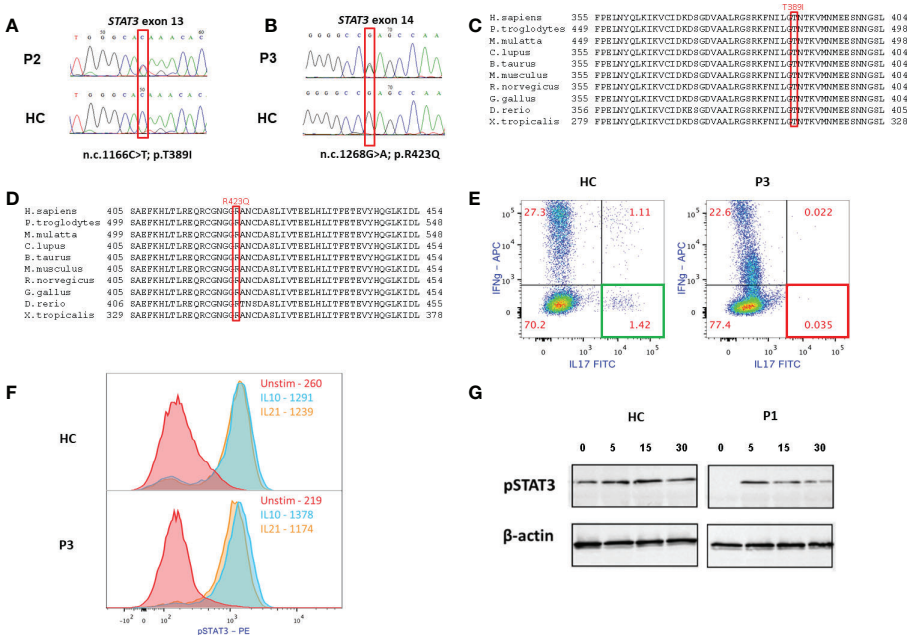

FIGURE 2
Immune and genetic analyses of the patients. **(A, B)** Sanger sequencings of the *STAT3* variants of P2 and P3, respectively (HC- healthy control). **(C, D)** *STAT3* variants in P1-P2 and P3, respectively, are in evolutionary preserved sites. **(E)** Overnight stimulation of PBMC of P3 with phorbol myristate acetate (PMA) and Ionomycin shows normal production of interleukin (IL)-17 in HC $CD4^+$ T cells (left) and near absent IL-17 production in the patient's $CD4^+$ T cells. **(F)** P3's cells were stimulated with either IL-10 (10ng/mL) or IL-21 (100ng/mL) for 20 minutes. Cells were then fixed, permeabilized and stained for phosphorylated (p) STAT3 Y705. Both HC's and P3's $CD4^+$ T cells showed normal STAT3 phosphorylation, as can be expected in cases of variant located at the DNA binding domain (DBD). **(G)** Immunoblotting of P1, demonstrating levels of pSTAT3 in T=0,5,15, and 30 minutes following IL-6 stimulation. While there might be decreased expression of pSTAT3 at baseline, P1's cells did show STAT3 phosphorylation following stimulation, which is compatible with location of the *STAT3* variant in the DBD.

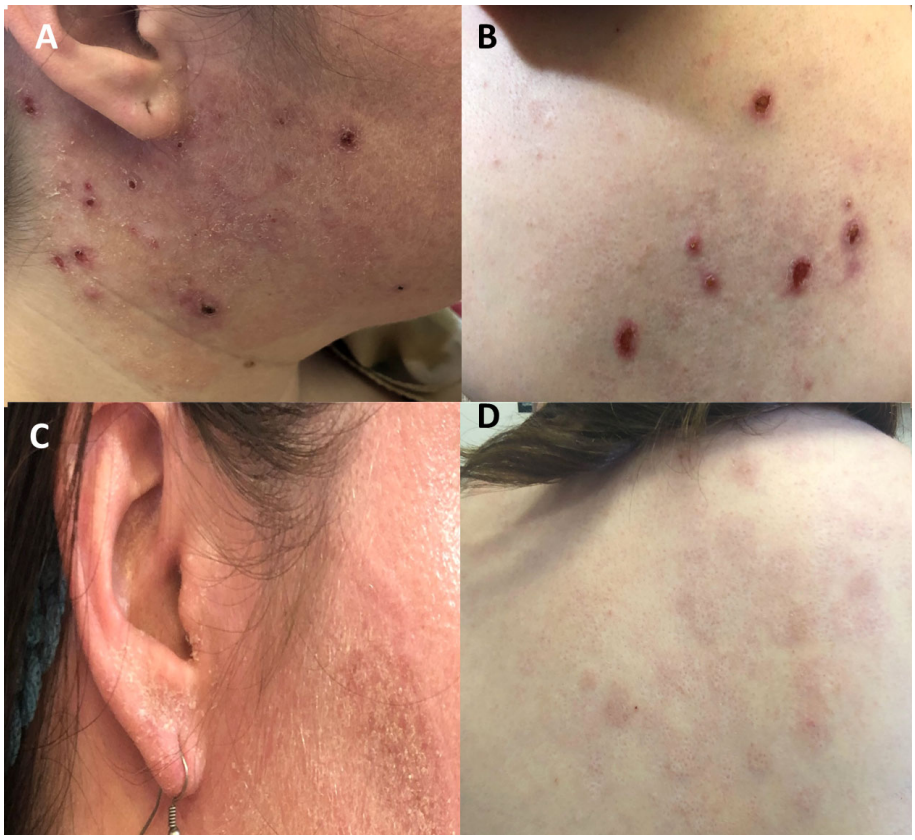

FIGURE 3
Response to treatment with dupilumab in patients with DN-*STAT3* variants. **(A, B)** Baseline status of atopic dermatitis in P2 with multiple erosive nodules, consistent with prurigo nodularis **(C, D)** Following 3 months of dupilumab treatment, atopic dermatitis eczema has completely resolved.

predispose adults to cancer (23). Thus, our report further emphasizes the need for awareness and a high index of suspicion towards IEI by physicians treating adult patients. "Red flags" for IEI, either in the history or findings on physical examination, even if the treated patients are undiagnosed adults, should trigger prompt immune and genetic workups. This will allow early diagnosis, better patient care, and genetic counseling for family members.

Supportive therapy of AD-HIES consists of antibiotics and anti-fungal treatments, either as prophylaxis or upon signs of infections. Other therapies consist of immunoglobulin replacement treatments, by intravenous (IVIG) or subcutaneous (SCIG) routes (28). Use of hematopoietic stem cell transplantations (HSCT) in AD-HIES patients is currently increasing. A recent review of 14 AD-HIES patients demonstrated high rates of long-term survival, as well as resolution of respiratory, dermatologic, and immune features of the disease (29). Osteoporosis and recurrent fractures in AD-HIES, as seen in P2 from our cohort, can be treated with bisphosphonates. It is a result of increased osteoclast quantities and bone resorption due to abnormal IL-6–mediated differentiation (29). Regarding treatment of our patients, none had humoral defects. Apart from the accepted antimicrobial prophylaxis, two patients were successfully treated with dupilumab. One patient with recalcitrant tinea corporis responded well to voriconazole, a second-generation triazole approved for systemic mycoses that has been reported to be effective against dermatophytes *in vitro*, and its use is considered a last resort in unresponsive patients with tinea infections (30).

Previously published cohorts of adult patients with DN-*STAT3* variants are scarce. Some adults with AD-HIES are characterized by normalized IgE levels and degenerative joint diseases (29). Rates of delayed diagnosis are not available in the literature. Interestingly, P3 had a delayed diagnosis of 21 years, since he first presented with severe pneumonia at the age of 20 years, until genetic diagnosis was made. However, delay in diagnosis is expected to decrease in current days, with increasing awareness to disease presentation and wide use of next generation sequencing and molecular diagnosis. Previous life expectancy reports are estimated by a median of 20.5 years and a maximal expectancy of 40 years (29). Major cause of death of adults with AD-HIES is attributed to pulmonary infections and their complications (29). Our patients' current ages range between 29 and 41 years. All patients in our cohort had recurrent pneumonias and currently they all have

bronchiectasis, as seen in CT scans. One patient (P2) also had pneumatocele. Hopefully with improved supportive care and monitoring, survival rates of these patients will increase, as previously suggested by others (29).

The clinical manifestations of our patients are consistent with AD-HIES. Susceptibility to Staphylococcal and fungal infections, high incidence of abscesses, recurrent sinopulmonary infections, bronchiectasis, and CMC are known features of AD-HIES (31). Non-immunological features, such as retained primary teeth, coarse faces, and osteoporosis, were also previously reported (31). Other non-immunologic features, such as scoliosis, are not found in our patients.

All the patients had non-diminished levels of pSTAT3, as demonstrated by immunoblotting or flow cytometry. This is compatible with the location of the variants in the DBD, suggesting decreased function of STAT3 without hampering its phosphorylation. A reduced Th17 subpopulation in P3, despite normal levels of pSTAT3 in flow cytometry, supports this notion and confirms the variant's pathogenicity. This observation was previously demonstrated in other studies (26).

P3 is notable in our cohort, as he was diagnosed in adulthood and had no reported CMC or recurrent infections during childhood. Indeed, we have not ruled out somatic mosaicism in P3. Intermediate phenotype of 2 patients with DN-*STAT3* variants was previously reported. These patients had non-reduced levels of Th17and a milder clinical presentation, although CMC was noted (32). Suspicion of DN-*STAT3* in P3 was raised due to recurrent abscesses in his liver and striated muscles, as well as coarse facial features. Interestingly, two of his children are currently being evaluated due to atopic dermatitis. However, due to lack of compliance, Sanger sequencings of the children for the relevant DN-*STAT3* variant is currently not available. Thus, the diagnosis of AD-HIES in P3 should be considered even with a lack of classical childhood infections.

A unique feature in two of our patients (P1 and P2) is papulopustular rosacea due to demodicosis. To the best of our knowledge, our study is the first report of chronic demodicosis in DN-*STAT3*. Demodicosis was not originally reported by the international study group of STAT1 GOF (33). Recently, our group described chronic demodicosis in patients from two families with *STAT1* GOF variants (19). Chronic demodicosis has also been reported in other patients with *STAT1* GOF (34–36).

The underlying immune pathogenesis in chronic demodicosis is not well defined. It probably consists of an impaired innate immune response *via* Toll-like receptor (TLR)-2 and decreased counts and effector function of Th17, among other immune pathways (12). In *STAT1* GOF, overexpressed cytokines, such as interferon (IFN)-γ and IL-27, inhibit the function of Th17 *via* suppression of IL-17 and RORγT (37). This mechanistic pathway of impaired Th17-mediated immunity is common to both *STAT1* GOF and *STAT3* loss-of-function and may account for the chronic demodicosis diagnosed in our patients.

STAT3 has a role in regulating Th2 inflammation. This is seen in over-activation of STAT3, which inhibits GATA3, impairing the differentiation of inflammatory T helper cells into Th2 cells and reducing their activities (38). The eosinophilia and atopic dermatitis in our patients are suggestive of increased Th2 function *via* elevated production of IL-5 and IL-4, respectively. Therefore, dupilumab has enabled successful treatment of the patients' atopic dermatitis by manipulating the underlying immune mechanism without the need for systemic immunosuppressive or cytotoxic drugs. The dose of dupilumab was decided according to current indications for atopic dermatitis in non-HIES patients, with adverse events noted in none of the patients.

It is plausible to suspect that decreasing the Th2-mediated pathway will result in enhanced function of Th1, reducing susceptibility to severe infections. Severe viral infections were noted in P2, suggesting decreased Th1 activity. However, the effect of dupilumab on the Th1-mediated response and secreted cytokines was not evaluated in our study. Nevertheless, Th1 enhancement following dupilumab treatment has been demonstrated in AD-HIES (14).

We further reviewed the literature on reported AD-HIES patients with DN-*STAT3* variants who were treated with dupilumab (Table 3). Our search yielded 22 patients (11 males, age 9-42 years) with a mean duration of dupilumab treatment of 11.5 (2–15) months. All of the patients were reported to clinically improve following dupilumab treatment, independent of their *STAT3* variant or age and with no severe adverse reactions. As in our patient, dupilumab doses ranged from 200 to 300 mg per injection every 2 or 4 weeks.

IgE levels of P1 decreased following dupilumab treatment. Reduced IgE levels were previously shown in dupilumab-treated patients, as demonstrated in a meta-analysis of seven studies (39). Published reports of DN-*STAT3* patients treated with dupilumab with subsequent IgE reduction further support that notion (15, 17).

Previous studies also support dupilumab treatment of atopic dermatitis in non-*STAT3*-related-IEI, such as DOCK8 deficiency (40), CARD11-associated atopy with dominant interference of NF-kB signaling (CADINS) (41), Wiskott-Aldrich Syndrome (42), common variable immune deficiency (CVID) (43), TTC7A-associated combined immunodeficiency (44), and X-linked agammaglobulinemia (45–47). Thus, indications for dupilumab use in IEI are rapidly expanding, and it should be considered a main therapeutic modality in adult patients with AD-HIES along with standard topical care.

Our study has several limitations, mainly its small number of patients and retrospective design. Nevertheless, we hope this cohort of adult AD-HIES patients will shed further light on the diagnosis and treatment of these patients.

In conclusion, immunologists and dermatologists treating AD-HIES patients should be aware of demodicosis as a possible clinical manifestation. Chronic and recalcitrant dermatophytosis may respond, at least partially, to voriconazole. Treatment with

TABLE 3 Previously published dupilumab-treated patients with AD-HIES due to DN-*STAT3* variants.

Number of Reported Patients	Age at dupilumab initiation (years)	Gender	Clinical Manifestations (Baseline SCORAD score)	*STAT3 LOF Heterozygous* variant	Dupilumab Therapeutic regimen (mg)	Outcome (SCORAD following dupilumab)	Duration of dupilumab treatment (months)	Ref.
2	29 and 37	M, F	Recurrent skin and pulmonary infections (NA)	c.1166C>T, p.Thr389Ile	Loading dose 600 mg followed by 200 mg every 2 weeks	Resolution of AD (NA)	7 and 17	Current report
1	2.5	F	Recurrent skin and pulmonary infections (NA)	1144 C>T, p.Arg382Trp	300 mg every 4 weeks	Resolution of AD (NA)	6	(10)
1	17	M	Severe AD, recurrent staph infections, allergy to inhalants (45)	c.1150T>C. p.F384L	300 mg every 2 weeks	Resolution of AD (28/103)	12	(14)
1	9	M	Generalized pruritic erythematous papules and Xerosis; eczema, oral candidiasis, furuncles, pneumatoceles, recurrent pneumonia, abscess in liver and gingiva, knee and finger joint deformities since birth (73)	c.1145G>A, p.R382Q	Loading dose of 200 mg followed by 100 mg every 2 weeks.	Resolution of AD (0)	10.5	(12)
3	9	3-M	PJP, chronic OM(58-78)	c.21323C>G	Loading dose 300 mg every 2 weeks, followed by injections every 28 days	Mild dermatitis in all patients after 4 months (5-15).	4	(13)
			Pneumonia (NA)	p.V343L				
			Neonatal pneumonia, chronic OM (NA)	p.R32Q				
1	21	M	AD, recurrent skin and respiratory tract infections, refractory diarrhea and recurrent colon perforations (NA)	Int10(-2)A>G	300 mg every 3 weeks	Resolution of skin and GI manifestations (NA)	6	(11)
1	33	F	Pruritic eczema, dermatitis (67.45)	1907C > T, p.S636F	loading dose of 600 mg followed by 300 mg every 2 weeks	Resolution of AD (< 10)	10	(17)
1	14	M	Severe AD and EoE (NA)	c. 1294 G>A. p.V432S	Loading dose of 600 mg followed by 300 mg every 2 weeks	Resolution of AD (10)	2	(15)
13	10-42	9-F 4-M	ABPA, AD, Asthma (53.85, 80.3)	c.1144 C > T, p. R382W	200 or 300 mg every two weeks	Resolution of AD (0)	15	(16)
				c.1003 C > T, p.R335W				
				c.2137 G > T, p.V713L				
				c.1979 T > C, p.N660T				

(Continued)

10.3389/fimmu.2022.1044933

TABLE 3 Continued

Number of Reported Patients	Age at dupilumab initiation (years)	Gender	Clinical Manifestations (Baseline SCORAD score)	*STAT3 LOF Heterozygous* variant	Dupilumab Therapeutic regimen (mg)	Outcome (SCORAD following dupilumab)	Duration of dupilumab treatment (months)	Ref.
				c.1110(-2) A-G				
				c.1864 A > G, p.T622A				
				c.1388 T > A, p.V463E				
				c.1962_1964delATC, p.I654del				
				c.1144 C > T, p.R382W				
				c.1861 T > G, p.F621V				
				c.1909 G > A, p.V637M				
				c.1003C > T, p.R335W				
				c.1110(-3) C > A, p.V637M				

M, Male; F, Female; AD, Atopic dermatitis; Eo, Eosinophilic esophagitis; GI, Gastrointestinal; OM, Otitis media; ABPA, Allergic bronchopulmonary aspergillosis; PJP, Pneumocystis Jirovecii Pneumonia; NA, Data is not available.

10.3389/fimmu.2022.1044933

dupilumab appears to be safe and effective without need for systemic immunosuppressive agents and should be offered to these patients to alleviate their atopic dermatitis.

Data availability statement

The original contributions presented in the study are included in the article/supplementary materials, further inquiries can be directed to the corresponding author.

Ethics statement

The studies involving human participants were reviewed and approved by Hadassah Medical Center IRB. Written informed consent for participation was not required for this study in accordance with the national legislation and the institutional requirements.

Author contributions

OS- Treatment of patients, study design and writing of the manuscript. LR- treatment of patients and manuscript revisions. AS- genetic and immune workup. AL – immune workup. OB-genetic workup. RS- immune workup. TF- immune workup, DH- immune workup and manuscript revisions. BG-manuscript revisions and treatment of patients. AN- immune workup,VP – dermatologic consultation, treatment of patients and study supervision, YT – study conceptualization and supervision. All authors contributed to the article and approved the submitted version.

Conflict of interest

The authors declare that the research was conducted in the absence of any commercial or financial relationships that could be construed as a potential conflict of interest.

Publisher's note

References

1. Abbass AK, Lichtman, Andrew H. *Pillai shiv chapter 10- differntiation and functions of CD4+ effector T cells, cellular and molecular immunology*. 239. *Ninth ed*. Elsevier (2018).

2. Minegishi Y, Saito M, Tsuchiya S, Tsuge I, Takada H, Hara T, et al. Dominant-negative mutations in the DNA-binding domain of STAT3 cause hyper-IgE syndrome. *Nature* (2007) 448(7157):1058–62. doi: 10.1038/nature06096

3. Hsu AP, Davis J, Puck JM, Holland SM, Freeman AF. STAT3 hyper IgE syndrome. In: GeneReviews® [Internet]. Seattle (WA): University of Washington, Seattle. 1–19. (1993).

4. Avery DT, Deenick EK, Ma CS, Suryani S, Simpson N, Chew GY, et al. B cell-intrinsic signaling through IL-21 receptor and STAT3 is required for establishing long-lived antibody responses in humans. *J Exp Med* (2010) 207(1):155–71. doi: 10.1084/jem.20091706

5. Crosby K, Swender D, Chernin L, Hafez-Khayyata S, Ochs H, Tcheurekdjian H, et al. Signal transducer and activator of transcription 3 mutation with invasive eosinophilic disease. *Allergy Rhinol (Providence).* (2012) 3(2):e94–7. doi: 10.2500/ar.2012.3.0035

6. Grimbacher B, Holland SM, Gallin JI, Greenberg F, Hill SC, Malech HL, et al. Hyper-IgE syndrome with recurrent infections–an autosomal dominant multisystem disorder. *N Engl J Med* (1999) 340(9):692–702. doi: 10.1056/NEJM199903043400904

7. Chandesris MO, Azarine A, Ong KT, Taleb S, Boutouyrie P, Mousseaux E, et al. Frequent and widespread vascular abnormalities in human signal transducer and activator of transcription 3 deficiency. *Circ Cardiovasc Genet* (2012) 5(1):25–34. doi: 10.1161/CIRCGENETICS.111.961235

8. Adatia A, Allen CJ, Wald J, Richards CD, Waserman S, Nair P. Benralizumab for prednisone-dependent eosinophilic asthma associated with novel STAT3 loss of function mutation. *Chest* (2021) 159(4):e181–e4. doi: 10.1016/j.chest.2020.11.042

9. Lan J, Zhang Y, Song M, Cai S, Luo H, OuYang R, et al. Omalizumab for STAT3 hyper-IgE syndromes in adulthood: A case report and literature review. *Front Med (Lausanne).* (2022) 9:835257. doi: 10.3389/fmed.2022.835257

10. Nihal A, Comstock JR, Holland KE, Singh AM, Seroogy CM, Arkin LM. Clearance of atypical cutaneous manifestations of hyper-IgE syndrome with dupilumab. *Pediatr Dermatol* (2022) 39(6):940–42. doi: 10.1111/pde.15072

11. Lu CW, Lee WI, Chung WH. Dupilumab for STAT3-Hyper-IgE syndrome with refractory intestinal complication. *Pediatrics* (2021) 148(3):e2021050351. doi: 10.1542/peds.2021-050351

12. Wang HJ, Yang TT, Lan CE. Dupilumab treatment of eczema in a child with STAT3 hyper-immunoglobulin e syndrome. *J Eur Acad Dermatol Venereol.* (2022) 36(5):e367–e9. doi: 10.1111/jdv.17889

13. Staudacher O, Kruger R, Kolsch U, Thee S, Gratopp A, Wahn V, et al. Relieving job: Dupilumab in autosomal dominant STAT3 hyper-IgE syndrome. *J Allergy Clin Immunol Pract* (2022) 10(1):349–51 e1. doi: 10.1016/j.jaip.2021.08.042

14. Matucci-Cerinic C, Viglizzo G, Pastorino C, Corcione A, Prigione I, Bocca P, et al. Remission of eczema and recovery of Th1 polarization following treatment with dupilumab in STAT3 hyper IgE syndrome. *Pediatr Allergy Immunol* (2022) 33 (4):e13770. doi: 10.1111/pai.13770

15. Dixit C, Thatayatikom A, Pappa H, Knutsen AP. Treatment of severe atopic dermatitis and eosinophilic esophagitis with dupilumab in a 14-year-old boy with autosomal dominant hyper-IgE syndrome. *J Allergy Clin Immunol Pract* (2021) 9 (11):4167–9. doi: 10.1016/j.jaip.2021.06.049

16. James AE, West L, Schloss K, Nataraj P, Urban A, Hirsch A, et al. Treatment of STAT3-deficient hyper-immunoglobulin e syndrome with monoclonal antibodies targeting allergic inflammation. *J Allergy Clin Immunol Pract* (2022) 10(5):1367–70 e1. doi: 10.1016/j.jaip.2022.01.011

17. Sogkas G, Hirsch S, Jablonka A, Witte T, Schmidt RE, Atschekzei F. Dupilumab to treat severe atopic dermatitis in autosomal dominant hyper-IgE syndrome. *Clin Immunol* (2020) 215:108452. doi: 10.1016/j.clim.2020.108452

18. Health CAfDaTi. *Clinical review report: Dupilumab (Dupixent): (Sanofi-aventis Canada inc.): Indication: Moderate-to-severe atopic dermatitis (AD).* (Ottawa (ON): Canadian Agency for Drugs and Technologies in Health). (2018).

19. Shamriz O, Lev A, Simon AJ, Barel O, Javasky E, Matza-Porges S, et al. Chronic demodicosis in patients with immune dysregulation: An unexpected infectious manifestation of signal transducer and activator of transcription (STAT)1 gain-of-function. *Clin Exp Immunol* (2021) 206(1):56–67. doi: 10.1111/cei.13636

20. Smith TF, Waterman MS. Identification of common molecular subsequences. *J Mol Biol* (1981) 147(1):195–7. doi: 10.1016/0022-2836(81)90087-5

21. Poplin R, Ruano-Rubio V, DePristo M, Fennell TJ, Carneiro MO, van der Auwera GA, et al. Scaling accurate genetic variant discovery to tens of thousands of samples. *bioRxiv* (2017). doi: 10.1101/201178

22. MGG E. Haplotype-based variant detection from short-read sequencing. *arXiv* (2012). doi: 10.48550/arXiv.1207.3907

23. Li M, Li J, Li MJ, Pan Z, Hsu JS, Liu DJ, et al. Robust and rapid algorithms facilitate large-scale whole genome sequencing downstream analysis in an integrative framework. *Nucleic Acids Res* (2017) 45(9):e75. doi: 10.1093/nar/gkx019

24. Woellner C, Gertz EM, Schaffer AA, Lagos M, Perro M, Glocker EO, et al. Mutations in STAT3 and diagnostic guidelines for hyper-IgE syndrome. *J Allergy Clin Immunol* (2010) 125(2):424–32 e8. doi: 10.1016/j.jaci.2009.10.059

25. Scheuerman O, Hoffer V, Cohen AH, Woellner C, Grimbacher B, Garty BZ. Reduced bone density in patients with autosomal dominant hyper-IgE syndrome. *J Clin Immunol* (2013) 33(5):903–8. doi: 10.1007/s10875-013-9895-0

26. Holland SM, DeLeo FR, Elloumi HZ, Hsu AP, Uzel G, Brodsky N, et al. STAT3 mutations in the hyper-IgE syndrome. *N Engl J Med* (2007) 357(16):1608–19. doi: 10.1056/NEJMoa073687

27. Asano T, Khourieh J, Zhang P, Rapaport F, Spaan AN, Li J, et al. Human STAT3 variants underlie autosomal dominant hyper-IgE syndrome by negative dominance. *J Exp Med* (2021) 218(8):e20202592. doi: 10.1084/jem.20202592

28. Gharehzadehshirazi A, Amini A, Rezaei N. Hyper IgE syndromes: A clinical approach. *Clin Immunol* (2022) 237:108988. doi: 10.1016/j.clim.2022.108988

29. Tsilifis C, Freeman AF, Gennery AR. STAT3 hyper-IgE syndrome-an update and unanswered questions. *J Clin Immunol* (2021) 41(5):864–80. doi: 10.1007/s10875-021-01051-1

30. Khurana A, Agarwal A, Agrawal D, Sardana K, Singh A, Chowdhary A. Multidrug resistant tinea corporis/cruris: Response to voriconazole. *J Mycol Med* (2022) 32(4):101306. doi: 10.1016/j.mycmed.2022.101306

31. Shamriz O, Chandrakasan S. Update on advances in hematopoietic cell transplantation for primary immunodeficiency disorders. *Immunol Allergy Clin North Am* (2019) 39(1):113–28. doi: 10.1016/j.iac.2018.08.003

32. Hsu AP, Sowerwine KJ, Lawrence MG, Davis J, Henderson CJ, Zarember KA, et al. Intermediate phenotypes in patients with autosomal dominant hyper-IgE syndrome caused by somatic mosaicism. *J Allergy Clin Immunol* (2013) 131 (6):1586–93. doi: 10.1016/j.jaci.2013.02.038

33. Toubiana J, Okada S, Hiller J, Oleastro M, Lagos Gomez M, Aldave Becerra JC, et al. Heterozygous STAT1 gain-of-function mutations underlie an unexpectedly broad clinical phenotype. *Blood* (2016) 127(25):3154–64. doi: 10.1182/blood-2015-11-679902

34. Martinot M, Korganow AS, Wald M, Second J, Birckel E, Mahe A, et al. Case report: A new gain-of-Function mutation of STAT1 identified in a patient with chronic mucocutaneous candidiasis and rosacea-like demodicosis: An emerging association. *Front Immunol* (2021) 12:760019. doi: 10.3389/fimmu.2021.760019

35. Baghad B, El Fatoiki FZ, Benhsaien I, Bousfiha AA, Puel A, Migaud M, et al. Pediatric demodicosis associated with gain-of-Function variant in STAT1 presenting as rosacea-type rash. *J Clin Immunol* (2021) 41(3):698–700. doi: 10.1007/s10875-020-00942-z

36. Molho-Pessach V, Meltser A, Kamshov A, Ramot Y, Zlotogorski A. STAT1 gain-of-function and chronic demodicosis. *Pediatr Dermatol* (2020) 37(1):153–5. doi: 10.1111/pde.14011

37. Villarino AV, Gallo E, Abbas AK. STAT1-activating cytokines limit Th17 responses through both T-bet-dependent and -independent mechanisms. *J Immunol* (2010) 185(11):6461–71. doi: 10.4049/jimmunol.1001343

38. Yang XO, Panopoulos AD, Nurieva R, Chang SH, Wang D, Watowich SS, et al. STAT3 regulates cytokine-mediated generation of inflammatory helper T cells. *J Biol Chem* (2007) 282(13):9358–63. doi: 10.1074/jbc.C600321200

39. Zhou B, Dong J, Liang S, Shang S, Li L. The changes of IgE levels in type 2 inflammatory diseases after treatment of dupilumab: a systematic review and meta-analysis. *Expert Rev Clin Pharmacol* (2022), 15(10):1233–42. doi: 10.1080/17512433.2022.2120469

40. Ollech A, Mashiah J, Lev A, Simon AJ, Somech R, Adam E, et al. Treatment options for DOCK8 deficiency-related severe dermatitis. *J Dermatol* (2021) 48 (9):1386–93. doi: 10.1111/1346-8138.15955

41. Pietzsch L, Korholz J, Boschann F, Sergon M, Dorjbal B, Yee D, et al. Hyper-IgE and carcinoma in CADINS disease. *Front Immunol* (2022) 13:878989. doi: 10.3389/fimmu.2022.878989

42. Consiglieri G, Ferrua F, Aiuti A, Cicalese MP. A case of two adult brothers with wiskott-Aldrich syndrome, one treated with gene therapy and one with HLA-identical hematopoietic stem cell transplantation. *J Clin Immunol* (2022) 42 (2):421–5. doi: 10.1007/s10875-021-01157-6

43. Votquenne N, Dupire G, Michel O, Ben Said B. Dupilumab for severe generalized eczematous eruption complicating common variable immunodeficiency. *Eur J Dermatol* (2021) 31(1):93–4. doi: 10.1684/ejd.2020.3954

44. Alipour Tehrany Y, Marois L, Colmant C, Marchand V, Kokta V, Coulombe J, et al. Refractory pruritus responds to dupilumab in a patient with TTC7A mutation. *JAAD Case Rep* (2021) 8:9–12. doi: 10.1016/j.jdcr.2020.12.004

45. Fan YH, Lin TL, Sun HL, Pan HH, Ku MS, Lue KH. Successful treatment of atopic dermatitis with dupilumab in the setting of X-linked agammaglobulinemia. *J Allergy Clin Immunol Pract* (2022) 10(11):3032–034.e1. doi: 10.1016/j.jaip.2022.07.026

46. Atwal S, Ong PY. Successful use of dupilumab to treat eczema in a child with X-linked agammaglobulinemia. *Ann Allergy Asthma Immunol* (2022) 129(3):384–6. doi: 10.1016/j.anai.2022.06.020

47. Fujishima C, Munemoto S, Hioki C, Sasaki H, Yoshida H, Yamamoto T, et al. Successful dupilumab therapy for atopic dermatitis in a patient with X-linked agammaglobulinaemia. *Eur J Dermatol* (2022) 32(3):416–7. doi: 10.1684/ejd.2022.4288

frontiers | Frontiers in Immunology

TYPE Original Research
PUBLISHED 27 March 2023
DOI 10.3389/fimmu.2023.1131965

OPEN ACCESS

EDITED BY
Yuval Tal,
Hadassah Medical Center, Israel

REVIEWED BY
Valter R. Fonseca,
University of Lisbon, Portugal
Miriam A. Shelef,
University of Wisconsin-Madison,
United States

*CORRESPONDENCE
Ariel Munitz
arielm@tauex.tau.ac.il
Nufar Marcus Mandelblit
Nofarmk@clalit.org.il
Motti Gerlic
mgerlic@tauex.tau.ac.il

†These authors have contributed equally to this work and share first authorship

‡These authors have contributed equally to this work and share senior authorship

SPECIALTY SECTION
This article was submitted to Autoimmune and Autoinflammatory Disorders : Autoimmune Disorders, a section of the journal Frontiers in Immunology

RECEIVED 26 December 2022
ACCEPTED 13 March 2023
PUBLISHED 27 March 2023

CITATION
Bader G, Itan M, Edry-Botzer L, Cohen H, Haskin O, Mozer-Glassberg Y, Harel L, Munitz A, Mandelblit NM and Gerlic M (2023) Adaptive immune response to BNT162b2 mRNA vaccine in immunocompromised adolescent patients. *Front. Immunol.* 14:1131965. doi: 10.3389/fimmu.2023.1131965

Adaptive immune response to BNT162b2 mRNA vaccine in immunocompromised adolescent patients

Guy Bader[1†], Michal Itan[1†], Liat Edry-Botzer[1], Hadar Cohen[1], Orly Haskin[2,3], Yael Mozer-Glassberg[2,4], Liora Harel[2,5], Ariel Munitz[1*‡], Nufar Marcus Mandelblit[2,6*‡] and Motti Gerlic[1*‡]

[1]Department of Clinical Microbiology and Immunology, Sackler School of Medicine Tel Aviv University, Tel Aviv, Israel, [2]Sackler School, Medicine Tel Aviv University, Tel Aviv, Israel, [3]Nephrology Unit, Schneider Children's Medical Center of Israel, Petach Tikva, Israel, [4]Gastroenterology Unit, Schneider Children's Medical Center of Israel, Petach Tikva, Israel, [5]Rheumatology Unit, Schneider Children's Medical Center of Israel, Petach Tikva, Israel, [6]Kipper Institute of Immunology, Schneider Children's Medical Center of Israel, Petach Tikva, Israel

Protective immunity against COVID-19 is orchestrated by an intricate network of innate and adaptive anti-viral immune responses. Several vaccines have been rapidly developed to combat the destructive effects of COVID-19, which initiate an immunological cascade that results in the generation of neutralizing antibodies and effector T cells towards the SARS-CoV-2 spike protein. Developing optimal vaccine-induced anti-SARS- CoV-2 protective immunity depends on a fully competent immune response. Some evidence was gathered on the effects of vaccination outcomes in immunocompromised adult individuals. Nonetheless, protective immunity elicited by the Pfizer Biontech BNT162b2 vaccine in immunocompromised adolescents received less attention and was mainly focused on the antibody response and their neutralization potential. The overall immune response, including T-cell activities, was largely understudied. In this study, we characterized the immune response of vaccinated immunocompromised adolescents. We found that immunocompromised adolescents, which may fail to elicit a humoral response and develop antibodies, may still develop cellular T-cell immunity towards SARS-CoV-2 infections. Furthermore, most immunocompromised adolescents due to genetic disorders or drugs (Kidney and liver transplantation) still develop either humoral, cellular or both arms of immunity towards SARS-CoV-2 infections. We also demonstrate that most patients could mount a cellular or humoral response even after six months post 2nd vaccination. The findings that adolescents immunocompromised patients respond to some extent to vaccination are promising. Finally, they question the necessity for additional vaccination boosting regimens for this population who are not at high risk for severe disease, without further testing of their post-vaccination immune status.

KEYWORDS

transplantation, immunodeficiency - primary, vaccination, COVID-19, adaptive immunity

Introduction

The severe acute respiratory syndrome coronavirus 2 (SARS-CoV-2) was identified in late 2019 and described as causing a pneumonia outbreak, known as coronavirus-induced disease-19 (COVID-19) (1). COVID-19 has affected and still affects millions of people worldwide, resulting in mortality and morbidity rates as well as high healthcare costs, difficulties in treatment (2), and overwhelming economic burden that resulted in the loss of numerous additional lives and extensive long-term damage (3).

Protective immunity against COVID-19 is orchestrated by an intricate network of innate and adaptive anti-viral immune responses (4). Initially, SARS-CoV-2 infection triggers a local inflammatory response that recruits neutrophils and monocytes to the lungs and is accompanied by the release of multiple cytokines including IL-1β, IL-6, TNF-α, IL-12 and interferons (α, β and γ) (5, 6). Subsequently, activation of antigen presentation processes primes an adaptive T and B cell response that generates neutralizing antibodies and effector T cells that can recognize and kill virally infected cells (4). In most cases this process can resolve the infection. However, in some cases, a dysfunctional immune response can cause severe lung and even systemic pathology (7). If a protective inflammatory response does not occur, a cytokine storm could develop, resulting in multiple organ failure (8). Patients with various co-morbidities aged over 60 years are more likely to develop such a dysfunctional immune response that causes pathology and fails to successfully eradicate the pathogen (9).

To combat the destructive effects of COVID-19, several vaccines have been rapidly developed, including the Pfizer-Biontech BNT162b2 mRNA vaccine (10, 11). In this vaccine, mRNA encoding the SARS-CoV-2 spike (S) protein was encapsulated in lipid nanoparticle vectors encoding the viral S protein (12). Injection of the encapsulated mRNA results in the production of high levels of S protein. Following vaccination, S protein-specific memory T cells and B cells develop and circulate along with high-affinity SARS-CoV-2 antibodies, which jointly act to prevent SARS-CoV-2 infection and disease (13). Thus, developing optimal vaccine-induced anti-SARS-CoV-2 protective immunity depends on a fully competent immune response.

The decision to vaccinate immunocompromised patients is not trivial, especially in adolescent patients, which are not at high risk of developing severe disease (14, 15). On the one hand, recent reports (primarily in adult patients) have suggested that immunocompromised patients might display an increased risk of developing severe COVID-19 (16, 17). Thus, these patients should be prioritized for vaccination. In contrast, their underlying immune deficiency or immunosuppressive treatment might impair their ability to respond to the vaccine and develop protective immunity, characterized by generating anti-SARS-CoV-2 antibodies and cellular immune responses (5, 13). Some evidence exists regarding the effects of vaccination outcomes in adult immunocompromised individuals (18), while the protective immunity elicited by vaccines in immunocompromised children was mainly focused on the humoral response (19, 20). In one study, it was shown that adolescents who are immunocompromised (post-transplantation, cancer, or due to immunosuppressive drugs) displayed impaired *in vitro* neutralization capacity as measured by competition with ACE2, and total IgG against RBD, in comparison to adolescents who have chronic diseases, such as HIV. Another study, which focused on adolescents with inflammatory bowel disease (IBD), found no difference in antibody neutralization capacity as measured by competition with ACE2 (neutralization *in-vitro*) between IBD patients and healthy adolescents. However, combination therapy (anti-tumor necrosis factor-α + immunomodulators) showed significantly reduced neutralization capacity relative to those in other therapies and controls. Nevertheless, and most importantly, the breakthrough infection was similar between all groups without statistical differences. These results emphasize the need to characterize not only the humoral immune response, but also the cellular immune response of adolescent patients following SARS-CoV-2 vaccination since this will enhance our understanding of the potential degree of protection that these patients have. Furthermore, it will enable the design of an optimal immunization regimen for this patient population. This is especially important for future vaccination regimens utilizing relevant sequences of viral S proteins.

Results

Herein, we hypothesize that immunocompromised adolescent patients, which fail to elicit a humoral response and develop antibodies, will still develop cellular T-cell immunity toward SARS-CoV-2 infections. A cohort of 17 kidney transplant patients (two of which were not immunosuppressed at the time of vaccination), five liver transplant patients, two B-cell deficient patients, and four inflammatory disease patients that received two doses of the BNT162b2 mRNA vaccine were recruited (Table 1). Their humoral immune responses were determined using a flow cytometry ELISA capable of recognizing anti-spike IgG, IgM, and IgA simultaneously (Supplemental Figure 1), similar to our recent study on Covid-19 patients (6). Their cellular immune response was determined by an IFN-γ ELISPOT of isolated mononuclear cells stimulated with N- and S SARS-CoV-2 peptides. Even though the patients displaying B-cell deficiencies were unable to generate antibodies in response to BNT162b2 mRNA vaccination, they all generated a cellular response (Figure 1 and Supplemental Figure 2A and Supplemental Figure 3). Thus, they may still benefit from vaccination since it triggers the cellular arm, which is most important in eliciting protective immunity against SARS-CoV-2 infections (21). Assessment of humoral and cellular immunity in a cohort of immunocompromised adolescent patients, which were under a medication regimen that generally suppressed innate immune responses or suppressed their T cell or B cell responses (Table 1), revealed that vaccination with BNT162b2 could induce either a humoral or cellular immune response. It should be noted that out of the 26 immunocompromised adolescent patients (two with B cell

TABLE 1 immunocompromised adolescent patients recruited in this study.

P#	Clinical dignosis	Age at 2nd vaccination	Date of 2nd vaccination	Date of blood collection	Time from 2nd dose in days	Medications (mode of action)										
						Suppresses innate immune responses			B-cell inhibition	T-cell inhibition	B & T-cell inhibition		Imuunoglobulin	Anti bacterial	Anti viral	mTOR blocker
						Steroids	anti TNFα	Prednisolone	Rituximab	Tacrolimus	Mycophenolate	Methotrexate	IVIG	Azithromycin	Zidovudine	Everolimus
1	Received the vaccination while being in a kidney failure before transplantation. Immunosuppressive treatment started five weeks post 2nd vaccination	16.9	05/03/2021	20/06/2021	107.00	+				+	+					
2	Kidney ANCA vasculitis - After kidney transplantation	17	07/03/2021	20/06/2021	105.00			+	+	+	+					
3	After kidney transplantation	19.5	26/01/2021	04/07/2021	159.00	+				+	+					
4	After kidney transplantation	16.9	05/03/2021	04/07/2021	121.00	+				+	+					
5	Joubert syndrome - After 2nd kidney transplantation	18.5	21/02/2021	11/07/2021	140.00	+				+	+					
6	Chronic kidney disease (CKD) - After kidney transplantation	15	05/04/2021	25/07/2021	111.00											
7	Lymphoma - After kidney transplantation	18.5	02/04/2021	25/07/2021	114.00	+				+	+					
8	Gorlin syndrome - After kidney transplantation	15.5	03/05/2021	25/07/2021	83.00	+				+						+
9	Cerebral palsy (CP) - After kidney transplantation	16.5	23/01/2021	25/07/2021	183.00	+				+	+					
10	Gorlin syndrome - After kidney transplantation	15.5	03/05/2021	01/08/2021	90.00	+				+						+
11	Posterior urethral valves (PUV) - After kidney transplantation	13	21/03/2021	01/08/2021	133.00	+				+	+					
12	Genetic nephrotic syndrome - After kidney transplantation	12	23/07/2021	01/08/2021	9.00	+				+	+					
13	Genetic nephrotic syndrome - After kidney transplantation	20	22/01/2021	01/08/2021	191.00	+				+	+					
14	Posterior urethral valves (PUV) - After kidney transplantation	16.3	25/03/2021	16/08/2021	144.00	+				+	+					
15	Genetic nephrotic syndrome - After kidney transplantation	20	16/02/2021	16/08/2021	181.00	+				+	+					
16	After kidney transplantation	13	15/01/2021	09/02/2021	25	+				+	+					
17	After kidney transplantation	14	02/07/2020	09/02/2021	222	+				+	+					
18	After liver transplantation	15.11	27/04/2021	20/06/2021	54.00					+						
19	After liver transplantation	17.7	- לא חוסן חלה	20/06/2021	156.00					+						
20	After liver transplantation	18.1	31/01/2021	28/06/2021	148.00					+	+					
21	After liver transplantation	17.5	07/02/2021	04/07/2021	147.00					+						
22	After liver transplantation	19		09/08/2021	183.00					+	+					
23	CVID disease	14	11/04/2021	20/06/2021	70.00				+				+		+	
24	X-Linked Agammaglobulinemia disease	16	07/04/2021	27/06/2021	81.00								+	+		

(Continued)

10.3389/fimmu.2023.1131965

10.3389/fimmu.2023.1131965

TABLE 1 Continued

P#	Clinical dignosis	Age at 2nd vaccination	Date of 2nd vaccination	Date of blood collection	Time from 2nd dose in days	Medications (mode of action)											
						Suppresses innate immune responses			B-cell inhibition	T-cell inhibition	B & T-cell inhibition		Imuunoglobulin	Anti bacterial	Anti viral	mTOR blocker
						Steroids	anti TNFα	Prednisolone	Rituximab	Tacrolimus	Mycophenolate	Methotrexate	IVIG	Azithromycin	Zidovudine	Everolimus
25	Immunodeficiency-WAS	12	03/07/2021	09/08/2021	37.00											
26	Bone marrow transplantation	14.2	08/04/2021	16/08/2021	130.00											
27	Crohn's disease	13.4	20/03/2021	16/08/2021	149.00		+									
28	Juvenile idiopathic arthritis (JIA) associated uveitis	17	02/01/2021	20/06/2021	169.00		+					+				
29	Healthy control	12.5	08/04/2021	16/08/2021	130.00											
30	Healthy control	16.8	13/02/2021	16/08/2021	184.00											
31	Healthy control	13.11	13/07/2021	16/08/2021	34.00											
32	Healthy control	13.11	25/07/2021	16/08/2021	22.00											

deficiency diseases), 18 subjects generated a partial antibody response, from whom only 9 subjects generated IgG. On the other hand, out of the 23 immunocompromised adolescent patients that were tested for T cell response, 17 subjects generated a positive response. In fact, out of the 23 immunocompromised adolescent patients, which we assessed for both B and T cell mediated response, only one did not develop a humoral or cellular immune response. This patient (patient number 15) was already six months after his 2nd vaccination dose. Thus, his antibody levels may have naturally declined, as we have shown for patients in the past (6) and as suggested by plotting the patient data on a timeline (Supplemental Figure 2B). It should be noted that the decline that is shown by the semilog scale in Supplemental Figure 2B is not statistically significant. This is likely due to the fact that the majority of samples were taken 12 weeks or more after the 2nd vaccination, where antibody response was already shown to decline by others (22, 23). Nevertheless, these patients may still have a memory response (22, 23).

Discussion

Our study bears several limitations. Our relatively low sample size limits the ability of appropriate statistical analysis, especially when stratifying each subgroup of patients according to their medication, immunopathology, and affected organs. Second, our patient's recruitment post-vaccination was done randomly, the time post their 2nd vaccination may be too long, which may lead to a false negative conclusion, especially regarding their humoral immune response. Furthermore, as we have shown for patients who developed a mild disease following SARS-CoV-2 infection (6), a general statistical cutoff for determining whether a patient developed antibodies following infection using ROC analysis can be misleading. This is due to the fact that each patient has a different antibody titer baseline, and therefore, patients with a mild response, who may develop low antibody titers, may still develop antibodies that are above their personal baseline levels but not above the positivity threshold that was set by ROC analysis. Similarly, immunocompromised patients may develop mild antibody titers that would not be considered positive by ROC analysis-based methods. We suggest that, when possible, antibody titer (and maybe even T cell responses) should be determined prior to vaccination to set the individual background for each immunocompromised patient. These limitations can also explain the diversity and unpredicted response in all the immunocompromised adolescents, except for the B-cell deficiency. Despite these limitations, our data demonstrate that most patients could mount cellular or humoral responses. Collectively, these data are promising and question the necessity for additional vaccination boosts for adolescents who are not at high risk for severe disease (14, 15). Further studies that will focus on *in-vivo* neutralization assays, functionality of T-cell responses (e.g., CD4 vs CD8 responses) as well as monitoring the risk of these patients to infection and/or severe disease are required. This will

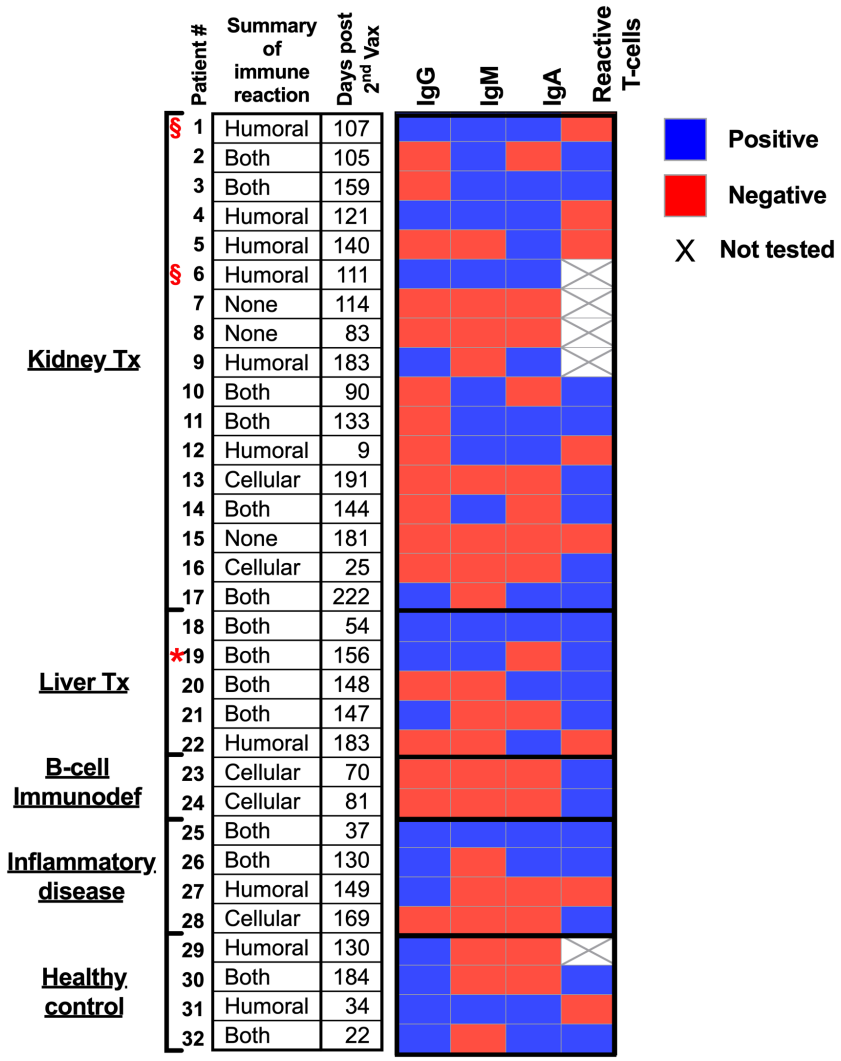

FIGURE 1
Humoral and cellular responses to BNT162b2 mRNA vaccine in immunocompromised adolescent patients.

enable comprehensive understanding of the immune responses generated upon vaccination especially in these patient populations.

Peripheral blood from immunocompromised adolescent patients was collected and separated into PBMCs and plasma. SARS-Cov2 RBD IgG/IgA/IgM antibodies were analyzed using iQue® SARS-CoV-2 (IgG, IgM and IgA) Kit (Sartorius). Reactive T-cells were analyzed using T-SPOT® Discovery SARS-CoV-2 (Oxford Immunotec).

Red star – Patient 19 was positive for infection with covid19. § symbol – not immunocompromised at time of vaccination (see Table 1).

Material and methods

Patients and their sample collection

Peripheral blood was obtained (~ 5 ml) from each patient during a routine check-up in the clinic at Schneider children's medical center of Israel. All experiments were reviewed and approved by the Ethics committee of the Schneider children's medical center (IRB#0209-21-RMC) and were performed according to their regulations and guidelines. Written informed consent to participate in this study was provided by all subjects or by the participants' legal guardian/next of kin.

Plasma and PBMCs preparation

Whole blood was centrifuged in EDTA (500×g, 5 min) in secure buckets. The supernatant was transferred into a clean 1.7/2 ml Eppendorf tube. The samples (plasma) were apportioned into 50 µl aliquots and stored at – 20°C or – 80°C for later use in iQue® SARS-CoV-2 (IgG, IgM and IgA) Kit. The pellet was resuspended in RPMI (Biological Industries, Beit-Haemek, Israel), and PBMCs were isolated by density-gradient centrifugation using Histopaque-1077 (Sigma-Aldrich, 10771), as previously reported (24).

Anti SARS-CoV-2 serological testing

Quantifications of IgG, IgM and IgA against SARS-CoV-2 RBD antigen were measured in subjects' plasma (diluted 1:100) according to the protocol of iQue® SARS-CoV-2 (IgG, IgM, and IgA) Kit (Sartorius).

Measurement of T-cell response to SARS-CoV-2 peptides

Isolated PBMCs from subjects were used for reactive T-cell assays according to the T-SPOT® Discovery SARS-CoV-2 protocol (Oxford Immunotec).

Data analysis

Data were calculated using GraphPad Prism 9, and details can be found in the figure legends.

Data availability statement

The original contributions presented in the study are included in the article/Supplementary Material. Further inquiries can be directed to the corresponding authors.

Ethics statement

All experiments were reviewed and approved by the Ethics committee of the Schneider children's medical center (IRB#0209-21-RMC) and were performed according to their regulations and guidelines. Written informed consent to participate in this study was provided by all subjects or by the participants' legal guardian/next of kin.

Author contributions

GB, MI, L-EB, and HC, performed experiments; GB, MI, AM, NM, and MG designed the experiments; HO, YM-G, LH, and NM, drew blood and provided patient characteristics; GB, AM, NM, and MG analyzed the data; AM, and MG, wrote and edited the manuscript; AM, and MG, supervised the work. All authors contributed to the article and approved the submitted version.

Funding

AM acknowledges funding from the US-BSF grant #2011244, ISF grant #886/15, ICRF, and the Cancer Biology Research Center, Tel Aviv University. MG acknowledges funding from Alpha-1 foundation grant #615533 and US-BSF grant #2017176, ISF grant #818/18, Israel Cancer Association Grant # 20220099, the Recanati Foundation, and the Varda and Boaz Dotan Research Center in Hemato-Oncology.

Conflict of interest

AM and MG received funding as part of the development team of the iQue® SARS-CoV-2 IgG, IgM and IgA Kit by Sartorius that is used in this study and have a royalty's agreement on this matter as part of Tel Aviv University.

The remaining authors declare that the research was conducted in the absence of any commercial or financial relationships that could be construed as a potential conflict of interest.

Publisher's note

Supplementary material

The Supplementary Material for this article can be found online at: https://www.frontiersin.org/articles/10.3389/fimmu.2023.1131965/full#supplementary-material

SUPPLEMENTARY FIGURE 1
Determining the cutoff for positivity and negativity values using the iQue® SARS-CoV-2 (IgG, IgM and IgA) Kit. **(A-C)** Peripheral blood was collected from hospitalized COVID-19 patients (at least 14 days post symptoms (DPS)) and anonymous recovered patients (IgG n=103, IgM n=56, IgA n=54). Negative samples were obtained from true SARS-CoV-2 negative patients (i.e., prior to the SARS-CoV-2 pandemic) (IgG n=128, IgM n=128, IgA n=128). Plasma was obtained, diluted 1:100, and prepared according to the protocol of the iQue® SARS-CoV-2 Kit. Data were calculated using GraphPad Prism 9; the dotted line represents the calculated cutoff value discriminating between positive and negative samples (specificity and sensitivity are shown for each antibody). An unpaired t-test with Welch's correction was performed. P values are shown. Data were calculated using GraphPad Prism 9; the dotted line represents the calculated cutoff value discriminating between positive and negative samples.

SUPPLEMENTARY FIGURE 2
Immunocompromised adolescents' individual anti-SARS-CoV-2-RBD antibodies response. **(A)** Immunocompromised adolescents' individual anti-SARS-CoV-2-RBD antibodies. Individual IgG (blue), IgM (red), and IgA (green) levels of each of the immunocompromised adolescents were plotted. **(B)** Individual IgG (blue), IgM (red), and IgA (green) levels of each of the immunocompromised adolescents were plotted according to the time post 2nd vaccination. Data were calculated using GraphPad Prism 9; the dotted line represents the calculated cutoff value discriminating between positive and negative samples. Solid lines - antibody kinetics was evaluated by calculating the nonlinear regression (fitting method - least square regression). Line's slopes and R squares were S=-0.005 and R^2 = 0.155 for IgG, S=-0.001 and R^2 = 0.016 for IgM, and -S=0.007 and R^2 = 0.39 for IgA.

SUPPLEMENTARY FIGURE 3

Immunocompromised adolescents' individual T-cell response to SARS-CoV-2 peptides. Isolated PBMCs from Immunocompromised adolescents' individual were used for reactive T-cell assays according to the T-SPOT® Discovery SARS-CoV-2 protocol. Spots were counted for positive control, negative control, and either Covid-19 spike peptides or nucleocapsid and plotted using GraphPad Prism 9. Representative wells and spots of four different patients are shown.

References

1. Zhou P, Yang XL, Wang XG, Hu B, Zhang L, Zhang W, et al. A pneumonia outbreak associated with a new coronavirus of probable bat origin. *Nature* (2020) 579:270–3. doi: 10.1038/s41586-020-2012-7

2. World Health Organization. *Novel coronavirus (COVID-19) situation*. (2020) WHO. Available at: https://apps.who.int/iris/handle/10665/330760.

3. McKibbin WJ, Fernando R. *The global macroeconomic impacts of COVID-19: Seven scenarios*. (2020). CAMA Working Paper No. 19/2020. doi: 10.2139/ssrn.3547729

4. Tay MZ, Poh CM, Rénia L, MacAry PA, Ng LFP. The trinity of COVID-19: immunity, inflammation and intervention. *Nat Rev Immunol* (2020) 20(6):363–74. doi: 10.1038/s41577-020-0311-8

5. Park A, Iwasaki A. Type I and type III interferons – induction, signaling, evasion, and application to combat COVID-19. *Cell Host Microbe* (2020) 27(6):870–8. doi: 10.1016/j.chom.2020.05.008

6. Munitz A, Edry-Botzer L, Itan M, Tur-Kaspa R, Dicker D, Marcoviciu D, et al. Rapid seroconversion and persistent functional IgG antibodies in severe COVID-19 patients correlates with an IL-12p70 and IL-33 signature. *Sci Rep* (2021) 11(1). doi: 10.1038/s41598-021-83019-0

7. Wang C, Wang Z, Wang G, Lau JYN, Zhang K, Li W. COVID-19 in early 2021: current status and looking forward. *Signal Transduct Target Ther* (2021) 6:114. doi: 10.1038/s41392-021-00527-1

8. Mokhtari T, Hassani F, Ghaffari N, Ebrahimi B, Yarahmadi A, Hassanzadeh G. COVID-19 and multiorgan failure: A narrative review on potential mechanisms. *J Mol Histol* (2020) 51(6):613–28. doi: 10.1007/s10735-020-09915-3

9. Kim HJ, Hwang H, Hong H, Yim JJ, Lee J. A systematic review and meta-analysis of regional risk factors for critical outcomes of COVID-19 during early phase of the pandemic. *Sci Rep* (2021) 11:9784. doi: 10.1038/s41598-021-89182-8

10. Polack FP, Thomas SJ, Kitchin N, Absalon J, Gurtman A, Lockhart S, et al. Safety and efficacy of the BNT162b2 mRNA covid-19 vaccine. *New Engl J Med* (2020) 383 (27):2603–15. doi: 10.1056/nejmoa2034577

11. Tregoning JS, Flight KE, Higham SL, Wang Z, Pierce BF. Progress of the COVID-19 vaccine effort: viruses, vaccines and variants versus efficacy, effectiveness and escape. *Nat Rev Immunol* (2021) 21(10):626–36. doi: 10.1038/s41577-021-00592-1

12. Teo SP. Review of COVID-19 mRNA vaccines: BNT162b2 and mRNA-1273. *J Pharm Pract* (2021) 35(6):947–51. doi: 10.1177/08971900211009650

13. Teijaro JR, Farber DL. COVID-19 vaccines: modes of immune activation and future challenges. *Nat Rev Immunol* (2021) 21(4):195–7. doi: 10.1038/s41577-021-00526-x

14. Woodruff RC, Campbell AP, Taylor CA, Chai SJ, Kawasaki B, Meek J, et al. Risk factors for severe COVID-19 in children. *Pediatrics* (2022) 149(1):e2021053418. doi: 10.1542/peds.2021-053418

15. Nicastro E, Verdoni L, Bettini LR, Zuin G, Balduzzi A, Montini G, et al. COVID-19 in immunosuppressed children. *Front Pediatr* (2021) 9:629240/BIBTEX. doi: 10.3389/FPED.2021.629240/BIBTEX

16. Shields AM, Burns SO, Savic S, Richter AG, Anantharachagan A, Arumugakani G, et al. COVID-19 in patients with primary and secondary immunodeficiency: The united kingdom experience. *J Allergy Clin Immunol* (2021) 147(3):870–5.e1. doi: 10.1016/j.jaci.2020.12.620

17. Meyts I, Bucciol G, Quinti I, Neven B, Fischer A, Seoane E, et al. Coronavirus disease 2019 in patients with inborn errors of immunity: An international study. *J Allergy Clin Immunol* (2021) 147(2):520–31. doi: 10.1016/j.jaci.2020.09.010

18. Hagin D, Freund T, Navon M, Halperin T, Adir D, Marom R, et al. Immunogenicity of pfizer-BioNTech COVID-19 vaccine in patients with inborn errors of immunity. *J Allergy Clin Immunol* (2021) 148(3):739–49. doi: 10.1016/j.jaci.2021.05.029

19. Chantasrisawad N, Puthanakit T, Tangsathapornpong A, Techasaensiri C, Phongsamart W, Suwanpakdee D, et al. Immunogenicity and reactogenicity of mRNA BNT162b2 COVID-19 vaccine among Thai adolescents with chronic diseases. *Vaccines* (2022) 10(6):871. doi: 10.3390/VACCINES10060871

20. Lee KJ, Choi SY, Lee YM, Kim HW. Neutralizing antibody response, safety, and efficacy of mRNA COVID-19 vaccines in pediatric patients with inflammatory bowel disease: A prospective multicenter Case—Control study. *Vaccines* (2022) 10 (8):1265. doi: 10.3390/VACCINES10081265

21. Moss P. The T cell immune response against SARS-CoV-2. *Nat Immunol* (2022) 23:2. doi: 10.1038/s41590-021-01122-w

22. Terreri S, Mortari EP, Vinci MR, Russo C, Alteri C, Albano C, et al. Persistent b cell memory after SARS-CoV-2 vaccination is functional during breakthrough infections. *Cell Host Microbe* (2022) 30(3):400–408.e4. doi: 10.1016/J.CHOM.2022.01.003

23. Schaefer-Babajew D, Wang Z, Muecksch F, Cho A, Loewe M, Cipolla M, et al. Antibody feedback regulates immune memory after SARS-CoV-2 mRNA vaccination. *Nature* (2022) 613:7945. doi: 10.1038/s41586-022-05609-w

24. Cohen H, Baram N, Edry-Botzer L, Munitz A, Salomon D, Gerlic M. Vibrio pore-forming leukocidin activates pyroptotic cell death via the NLRP3 inflammasome. *Emerg Microbes Infect* (2020) 9:278–90. doi: 10.1080/22221751.2020.1720526

frontiers | Frontiers in Immunology

TYPE Review
PUBLISHED 06 April 2023
DOI 10.3389/fimmu.2023.1156212

OPEN ACCESS

EDITED BY
Yuval Tal,
Hadassah Medical Center, Israel

REVIEWED BY
Sung Soo Ahn,
Yonsei University Health System, Republic of Korea
Uma Sriram,
Temple University, United States

*CORRESPONDENCE
Zongwen Shuai
shuaizongwen@ahmu.edu.cn
Patrick S. C. Leung
psleung@ucdavis.edu

†These authors have contributed equally to this work and share first authorship

SPECIALTY SECTION
This article was submitted to Autoimmune and Autoinflammatory Disorders: Autoinflammatory Disorders, a section of the journal Frontiers in Immunology

RECEIVED 01 February 2023
ACCEPTED 27 March 2023
PUBLISHED 06 April 2023

CITATION
Pan M, Zhao H, Jin R, Leung PSC and Shuai Z (2023) Targeting immune checkpoints in anti-neutrophil cytoplasmic antibodies associated vasculitis: the potential therapeutic targets in the future. *Front. Immunol.* 14:1156212. doi: 10.3389/fimmu.2023.1156212

Targeting immune checkpoints in anti-neutrophil cytoplasmic antibodies associated vasculitis: the potential therapeutic targets in the future

Menglu Pan[1†], Huanhuan Zhao[1†], Ruimin Jin[1], Patrick S. C. Leung[2*] and Zongwen Shuai[1,3*]

[1]Department of Rheumatology and Immunology, First Affiliated Hospital of Anhui Medical University, Hefei, China, [2]Division of Rheumatology/Allergy and Clinical Immunology, University of California, Davis, Davis, CA, United States, [3]Inflammation and Immune Mediated Diseases Laboratory of Anhui Province, Hefei, China

Anti-neutrophil cytoplasmic autoantibodies (ANCA) associated vasculitis (AAV) is a necrotizing vasculitis mainly involving small blood vessels. It is demonstrated that T cells are important in the pathogenesis of AAV, including regulatory T cells (Treg) and helper T cells (Th), especially Th2, Th17, and follicular Th cells (Tfh). In addition, the exhaustion of T cells predicted the favorable prognosis of AAV. The immune checkpoints (ICs) consist of a group of co-stimulatory and co-inhibitory molecules expressed on the surface of T cells, which maintains a balance between the activation and exhaustion of T cells. CD28, inducible T-cell co-stimulator (ICOS), OX40, CD40L, glucocorticoid induced tumor necrosis factor receptor (GITR), and CD137 are the common co-stimulatory molecules, while the programmed cell death 1 (PD-1), cytotoxic T lymphocyte-associated molecule 4 (CTLA-4), T cell immunoglobulin (Ig) and mucin domain-containing protein 3 (TIM-3), B and T lymphocyte attenuator (BTLA), V-domain Ig suppressor of T cell activation (VISTA), T-cell Ig and ITIM domain (TIGIT), CD200, and lymphocyte activation gene 3 (LAG-3) belong to co-inhibitory molecules. If this balance was disrupted and the activation of T cells was increased, autoimmune diseases (AIDs) might be induced. Even in the treatment of malignant tumors, activation of T cells by immune checkpoint inhibitors (ICIs) may result in AIDs known as rheumatic immune-related adverse events (Rh-irAEs), suggesting the importance of ICs in AIDs. In this review, we summarized the features of AAV induced by immunotherapy using ICIs in patients with malignant tumors, and then reviewed the biological characteristics of different ICs. Our aim was to explore potential targets in ICs for future treatment of AAV.

KEYWORDS

antineutrophil cytoplasmic autoantibody associated vasculitis, immune checkpoint, co-stimulatory signal pathway, co-inhibitory signal pathway, T cells, immunotherapy

1 Introduction

Anti-neutrophil cytoplasmic antibody (ANCA) associated vasculitis (AAV) is a group of life-threatening diseases, characterized by necrotizing inflammation of small blood vessels, with pauci-immune complex depositions. According to different clinical manifestations, it was mainly divided into three types, including granulomatosis with polyangiitis (GPA), microscopic polyangiitis (MPA), and eosinophilic granulomatosis with polyangiitis (EGPA) (1–4). ANCA is composed of series of autoantibodies identifying their autoantigens in neutrophil plasma, including proteinase-3 (PR3) and myeloperoxidase (MPO) which may be expressed on activated neutrophils. GPA, mainly associated with PR3-ANCA, usually affects the sinuses, the lung, and the kidney with specific granulomatous inflammation. In contrast to GPA, MPA frequently damages the lung and the kidney with necrotizing vasculitis. In general, MPO-ANCA is predominantly detected in patients with MPA and EGPA. The clinical characteristics of EGPA include asthma, eosinophilia, and vasculitis (5, 6), but it is much less common than GPA and MPA. The distribution of AAV might be influenced by geographical and race. In east Asia, especially in China and Japan, MPA with MPO-ANCA is the predominant AAV, whereas in Europe, such as the UK and France, GPA with PR3-ANCA is the more common AAV (7, 8).

Although the exact etiopathogenesis of AAV remains unclear, studies have demonstrated that some factors, such as T and B cells, ANCA, the complement alternative pathway (cAP), and neutrophil extracellular traps (NETs), might play various important roles in the pathogenesis (Figure 1). On the genetic background, the interaction of infections, environmental and other factors might activate T cells, which could help B cells develop into plasma cells. Meanwhile, neutrophils could also be activated and express PR3 and MPO to combine with the ANCA secreted by plasma cells (9–11). The fragment a of fifth complement (C5a) produced by activating cAP could connect with the C5a receptor on neutrophils (12, 13). The combinations of these factors on neutrophils could activate the neutrophils further to promote their degranulation and NETs production, intensify respiratory burst, injury the vascular endothelium, accelerate the inflammatory response, and ultimately lead to clinical damages of AAV (11, 13–15).

T cells play essential and pivotal roles in autoimmunity. Studies have revealed that subgroups of T cells, including regulatory T cells (Treg) and helper T cells (Th), especially follicular Th cells (Tfh), Th2 and Th17, were involved in the pathogenesis of AAV (16–19). The exhaustion of T cells could predict the favorable prognosis of AAV (20). Notably, the activation of T cells requires two signals. The first signal is traditional T cell receptor (TCR) signaling triggered by the recognition between TCR and specific peptides from the major histocompatibility complex (MHC) on the surface of antigen-presenting cells (APC). Immune checkpoint (IC) molecules transmit the second signal. ICs are a class of surface proteins to provide co-stimulatory or co-inhibitory signals by combining with the corresponding receptors or ligands on the surface of APCs (21, 22). Currently, immune checkpoint inhibitors (ICIs) have been used in treating various malignant tumors (23–26). However, 3.5% of patients treated with ICIs occurred rheumatic disease (27), suggesting that targeting ICs might have potential values in the treatment of rheumatic diseases. In this review, we summarized the association between ICIs and AAV, focused on the characteristics of ICs, and explored the potential therapeutic prospect of targeting ICs in AAV.

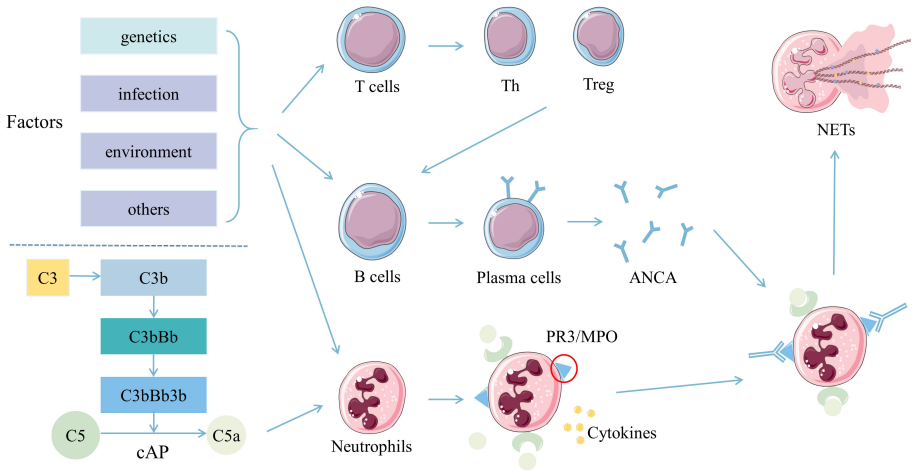

FIGURE 1
Pathogenesis of ANCA associated vasculitis. T cells, B cells, and neutrophils were activated by multiple stimulations in the background of genetic susceptibility. Th and Treg cells differentiated from T cells synergistically promote B cells to develop into plasma cells, and produce ANCA. ANCA then combined with PR3 or MPO expressed on neutrophils pre-activated by inflammatory cytokines. Also, C5a derived from activated cAP might combine with the C5a receptor on neutrophils. Neutrophils activated by ANCA, C5a and various cytokines might produce more NETs conducive for the inflammatory response and adaptive immunity, ultimately leading to clinical damages. Abbreviations: ANCA, anti-neutrophil cytoplasmic autoantibodies; C5a, fragment a of the fifth complement; cAP, complement alternative pathway; MPO, myeloperoxidase; NETs, neutrophil extracellular traps; PR3, proteinase-3; Th, helper T; Treg, regulatory T.

2 The association between ICIs and AAV

Currently, there are three types of ICIs in blocking co-inhibitory pathways, targeting programmed cell death 1 (PD-1) (nivolumab, pembrolizumab and cemiplimab), programmed death ligand 1 (PD-L1) (avelumab, atezolizumab and durvalumab), and cytotoxic T lymphocyte-associated molecule 4 (CTLA-4) (ipilimumab and tremelimumab). As the signal transductions of co-inhibitory were blocked, T cells could be activated, and then the tumor immunity could be enhanced (28, 29). Consequently, the inflammatory response might also be increased due to the activation of T cells, resulting in most patients developing immune-related adverse events (irAEs). The damages of irAEs could involve multiple organs, including but not limited to the skin, the gastrointestinal tract, the lung, and the kidney (29, 30). It is shown that CTLA-4 inhibitors may induce more irAEs than PD-1 inhibitors, and the combination of these two kinds of inhibitors can further increase the incidence of irAEs (31, 32).

Despite the rheumatic irAEs (Rh-irAEs) are not common in all irAEs, rheumatologists are still concerned about these Rh-irAEs. It was reported that the frequent Rh-irAEs were inflammatory arthritis and inflammatory myopathy. ICIs-induced vasculitis is less common than other rheumatic diseases and mainly affects the medium and large arteries (27, 29, 33). In Table 1, we summarized the cases of ICIs-induced AAV reported to date (23–25, 34–40). Interestingly, even with ICIs treatment, some AAV patients in remission did not relapse (41–43). Therefore, we speculated that the ICs molecules might be involved in the pathogenesis of AAV. What is more, different ICs might dominate in various stages.

3 Co- stimulatory signal pathways

The co-stimulatory molecules expressed on the surface of T cells contained CD28, inducible T-cell co-stimulator (ICOS), OX40, and others (Figure 2). They will be discussed in detail below.

3.1 CD28 signal pathway

CD28 is a member of the immunoglobulin (Ig) superfamily (IgSF) with typical Ig variable (IgV) domains. This transmembrane protein of 44 kDa is composed of a disulfide-linked homodimer. It was involved in the formation of immunologic synapses, the phosphorylation of proteins, and the remodeling of actin in T cells. Consequently, T cells were activated and produced cytokines (44–46). CD28 signal transduction is relied on two motifs in its

TABLE 1 Demographic characteristics and clinical data of patients with ICIs-induced AAV.

Case	Age/ Gender	ICIs	Target	irAEs	Clinical Features	Treatments	Outcome
Kato, et al. (34)	N	nivolumab	PD-1	AAV	–	–	–
Hung, et al. (35)	66/female	ipilimumab and nivolumab	CTLA-4 and PD-1	GPA	headache, polyarthralgia, proteinuria, and hemoptysis	glucocorticoid, rituximab and one dose of infliximab	chronic kidney disease
Uner, et al. (36)	65/male	pembrolizumab	PD-1	AAV	diarrhea, increased creatinine, microscopic hematuria, and proteinuria	glucocorticoid and rituximab	chronic kidney disease
Harada, et al. (37)	65/male	nivolumab	PD-1	EGPA	asthma, eosinophilia, dyspnea on exertion, arthritis.	glucocorticoid	remission
Mamlouk, et al. (38)	70/male	tremelimumab	CTLA-4	MPA	microscopic hematuria, pyuria, and proteinuria	glucocorticoid, plasmapheresis, and rituximab	chronic kidney disease
Roger, et al. (23)	34/female	nivolumab	PD-1	EGPA	asthma, eosinophilia, arthritis, and pansinusitis	glucocorticoid	–
Nabel, et al. (25)	56/male	pembrolizumab	PD-1	GPA	arthritis, cough, emesis, and diffuse expiratory wheezes in the right lung	glucocorticoid and rituximab	remission
Sibille, et al. (39)	64/male	pembrolizumab	PD-1	GPA	myositis, dyspnea, and arthritis	glucocorticoid	remission
Heo, et al. (24)	56/male	pembrolizumab	PD-1	GPA	rash, fever, arthralgia, myalgia, increased creatinine, microscopic hematuria, and proteinuria	glucocorticoid and hemodialysis	remission
van den Brom, et al. (40)	56/female	ipilimumab and pembrolizumab	CTLA-4	GPA	fever, arthritis, cutaneous vasculitis, and pulmonary nodules	glucocorticoid and cyclophosphamide	remission

AAV, anti-neutrophil cytoplasmic autoantibodies associated vasculitis; CTLA-4, cytotoxic T lymphocyte-associated molecule 4; EGPA, eosinophilic granulomatosis with polyangiitis; GPA, granulomatosis with polyangiitis; ICIs, immune checkpoint inhibitors; MPA, microscopic polyangiitis; PD-1, programmed cell death 1.

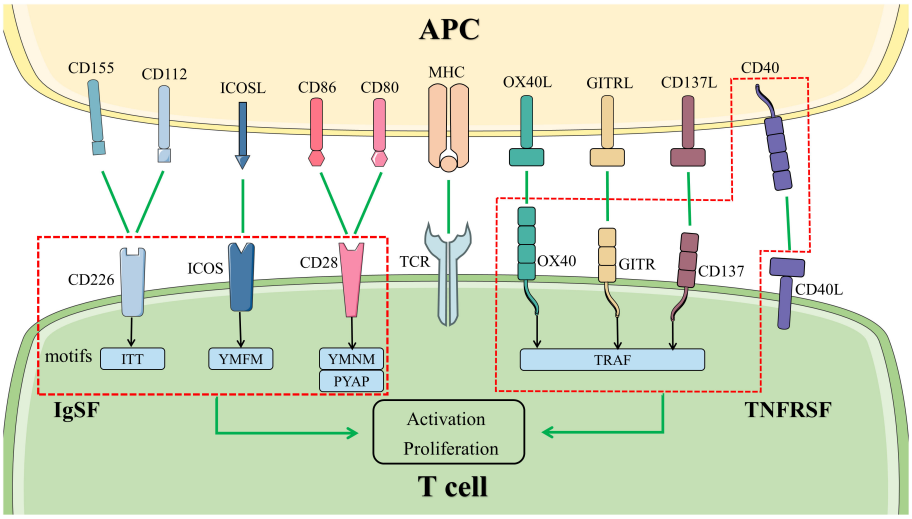

FIGURE 2
Co-stimulatory signal pathways in T cells. The activation and proliferation of T cells at least need two signals. The first signal is provided by the binding of TCR to MHC with antigenic polypeptide processed by APC. Co-stimulatory molecules bind to the ligand or receptor presented by APCs, transmitting the second signal. The molecules in the left box are members of IgSF, activating the signal pathways downstream by different motifs in the cytoplasmic tail. The members of TNFRSF are represented in the right box. They bind to TRAF to activate the signal pathways downstream. Abbreviations: APC, antigen-presenting cell; GITR, glucocorticoid induced tumor necrosis factor receptor; ICOS, inducible T-cell co-stimulator; IgSF, immunoglobulin superfamily; MHC, major histocompatibility complex; TCR, T cell receptor; TNFRSF, tumor necrosis factor receptor superfamily; TRAF, tumor necrosis factor receptor-associated factor.

cytoplasmic tail: YMNM and PYAP. The phosphorylated Src homology-2 (SH2) domain in the proximal YMNM motif binds the p85 subunit of phosphatidylinositol 3-kinase (PI3K), the growth factor receptor-bound protein 2 (GRB2), and the GRB2-related adapter protein 2. The distal PYAP motif combines with the lymphocyte cell-specific protein-tyrosine kinase (LCK) and GRB2. Their bindings could activate the downstream targets, including nuclear factor-κB (NF-κB), nuclear factor of activated T cells (NFAT), mammalian target of rapamycin (mTOR), and mitogen-activated protein kinase to affect cell cycle progression, apoptosis, and especially interleukin (IL)-2 transcription (47).

CD80 and CD86 are cognate ligands of CD28, which are mainly expressed on the surface of APCs, such as B cells, dendritic cells (DCs), and monocytes (17, 22, 48). However, there are some differences between their features and functions. CD80, which is existed as a dimer, is expressed rarely on resting B cells whereas the expression of CD86, which is in the form of a monomer, is higher than CD80. When B cells were activated, the density of CD86 on its surface increased early and even more compared with CD80 (49, 50). In animal experiments, it is demonstrated that in CD86-deficient mice, neither the antibody isotypes were switched nor germinal centers (GCs) were formed, whereas it is contrary in CD80-deficient mice (51). Furthermore, because CTLA-4, a co-stimulatory molecule with highly homologous to CD28, has a higher affinity for CD80 and CD86, it competitively inhibits the bindings of CD28 to CD80 and CD86, and actually restrains the cellular immune responses (52).

CD28 signal pathway plays a vital role in vasculitis. Zhang et al. constructed human artery-severe combined immunodeficiency mice chimeras with peripheral blood mononuclear cells from patients with giant cell arteritis (GCA) to induce vasculitis. Blocking the CD28 signal pathway significantly disrupted T-cell metabolic fitness and inhibited the remodeling of the vessel wall (53). In Takayasu's arteritis (TAK), another large vasculitis, the active patients had higher mRNA levels of CD28 than the inactive patients (54). In patients with active GPA, T cells had a higher proliferative response to the stimulation of CD2/CD28 than healthy controls (HCs) (55). In addition, the expressions of CD80 and CD86 were also significantly increased in $CD19^+$ B cells from patients with frequently relapsing EGPA (17). Besides ICs in cell membranes, soluble ICs have received attention gradually. Soluble ICs were produced by the proteolytic cleavage of extracellular regions, or by alternative splicing (56). Elevated soluble CD28 (sCD28) levels was observed in sera samples in patients with active AAV. Such increase in was significantly positively correlated with disease activity markers, such as the Birmingham Vasculitis Activity Score, C-reactive protein, and erythrocyte sedimentation rate (57). Noteworthy, sCD28 level decreased when AAV patients from the active state became inactive after treatment (57), suggesting that sCD28 might play a potential immunopathological role in AAV and could be a novel biomarker to evaluate disease activity. Therefore, targeting the CD28 signal pathway may be effective for AAV. Abatacept, a CTLA-4-Ig fusion protein composed of the ligand-binding domain of CTLA-4 and the modified Fc portion of IgG, can block CD28 signal transduction by bindings to CD80 and CD86 (58). An open-label trial reported that Abatacept had improved the disease condition in patients with non-severe relapsing GPA (59). We prefer to inhibit the CD28 signal transduction directly. FR104 is a pegylated antigen-binding fragment (Fab) antibody. In the non-human primate (NHP) graft-versus-host disease (GVHD) model, the survival of GVHD-free was improved by FR104/sirolimus. Still,

the overall survival was not improved because of the sepsis and a paralyzed interferon (IFN)-γ response in some patients without GVHD (60). In conclusion, it has clinical significance for targeting the CD28 signal pathway. Nevertheless, the challenge is to develop a more effective anti-CD28 antibody with fewer side effects.

3.2 ICOS signal pathway

Even though ICOS and CD28 belong to the same family, they still have several differences. Firstly, ICOS is expressed on the surface of activated T cells. The activation of T cells by TCR and CD28 signal is essential for the expression of ICOS. Then, ICOS can promote the activation of T cells further (61). Secondly, there is only one particular YMFM motif in the cytoplasmic tail of ICOS. YMFM binds to the p50α and p85 subunits of PI3K and tends to recruit the former. Subsequently, the AKT signal enhances markedly. The ICOS-PI3K-AKT pathway promotes the expression of cytokines as well as induces the formation of Tfh cells. Tfh cells migrate into the follicles, maintain in GCs, and promote the differentiation of B cells into plasma cells to secrete ANCA (21, 62–64). Thirdly, ICOS could combine with the ICOS ligand (ICOSL) instead of CD80 and CD86 (65).

ICOSL is expressed on the surface of B cells, macrophages, fibroblasts, muscle cells, podocytes, and other cells (65–68). Several factors regulated the expression of ICOSL on the surface of B cells. B cell receptor (BCR) signal reduced the expression of ICOSL on naïve B cells, which affected the formation of Tfh cells. The BCR signal was more substantial, and the reduction of ICOSL was more obvious. This inhibitory response could be reversed by the CD40 signal (69, 70). Similarly, in both NF-κB–inducing kinase (NIK) KO mice and B-cell activating factor belonging to tumor necrosis factor (TNF) receptor (TNFR) family receptor-deficient mice, Hu et al. revealed that the expression of ICOSL decreased significantly. They discovered the recombinant ICOSL-Fc fusion protein could increase the levels of Tfh cells in NIK KO mice, suggesting ICOSL is a target of the noncanonical NF-κB pathway (71).

Several studies focused on the differences of $ICOS^+$ Tfh cells in vasculitis (19, 72, 73). Circulating $CD4^+$ $CXCR5^+$ $ICOS^+$ Tfh cells were elevated and correlated with disease activity in patients with Henoch-Schönlein purpura (HSP) (72). The same results were observed in patients with active MPO-AAV (19) and Behcet's disease (73). In patients with active AAV, the serum concentration of soluble ICOS was also higher than HCs (57). In addition, the production of pro-inflammatory factors was decreased by blocking the ICOS signal (73). AMG 557 is a fully human IgG2 monoclonal antibody (mAb) with a higher affinity to ICOSL that prevents the binding of ICOS and ICOSL. The safety and tolerability of AMG 557 are acceptable in patients with mild, stable systemic lupus erythematosus (SLE) (74). In another phase Ib, randomized, double-blind, placebo-controlled study, the potential efficacy of AMG 557 was evaluated (75). Fewer patients receiving AMG 577 (3 of 10 patients) or placebo (1 of 10 patients) achieved the primary efficacy endpoints. On day 169, compared with the placebo group, more patients in the AMG 557 group showed a ≥4-point improvement in the SLE disease activity index (SLEDAI) (70.0% *vs.* 20.0%, p=0.07), indicating the potential efficacy of AMG 557 (75). As mentioned above, ANCA is thought to be the pathogenic antibody of AAV, and the secretion of ANCA by plasma cells is regulated by Tfh cells. Therefore, the investigations on mAb targeting ICOS molecules on the surface of Tfh cells will be one of research directions of AAV treatment in the future.

3.3 OX40 signal pathway

The costimulatory molecule OX40 belongs to the TNFR superfamily (TNFRSF), also known as TNFRSF4 or CD134. Similar to other members of TNFRSF, OX40 is a type I transmembrane glycoprotein with four cysteine-rich domains in the extracellular region (76). Different from ICOS, OX40 expressed on $CD4^+$ T cells was driven by the TCR signal. After the activation of T cells, the expression of OX40 is promoted by CD28 and CD40 signals (77). In the intracellular region, OX40 binds to TNF receptor-associated factor (TRAF) 2, TRAF3, TRAF 5, and TRAF6, which activates the NF-κB, PI3K-AKT, and NFAT signal pathways downstream. It promotes the survival of T cells and the secretion of cytokines (21, 78).

The only ligand of OX40 is OX40L (also known as TNFSF4, CD252), which is expressed on the surface of DCs, B cells, T cells, vascular endothelial cells (VECs), mast cells, Langerhans cells, and other types of cells (79–84). There is a conserved extracellular TNF homology domain on the OX40L for trimerization (76). OX40L trimer combines with three OX40 molecules to polarize T cells to Th cells, expand Treg cells, sustain the function of memory T cells, and promote the adhesion of activated T cells to VECs (77, 85).

The OX40 signal pathway is vital in rheumatic diseases. In patients with SLE or TAK, the expression of OX40L was enhanced on VECs (82, 86). Besides the expression of OX40, the soluble OX40L was increased in patients with HSP, and both of them were associated with disease activity (87). It was observed in patients with AAV that the expression of CD134 as well as the $CD134^+$ T cells were increased. The majority of $CD134^+$ T cells mainly secreted TNF-α (88, 89). The results were consistent with *in vitro* studies. So far, several mAbs against OX40 (KHK 4083 and GBR 830) and OX40L (KY 1005) have been developed. KHK 4083 demonstrated the safety and tolerability in patients with mild to moderate plaque psoriasis (90) and moderate to severe ulcerative colitis (UC) (91). In the phase II a study, GBR 830 showed the therapeutic potential for patients with moderate to severe atopic dermatitis (AD) (92). The pharmacological activity of KY 1005 in humans was evaluated. It is considered that targeting OX40L might be effective (93). These findings indicated that the OX40 signal pathway might be a potential therapeutic target in patients with AAV. The problem is that OX40 blockade might inhibit the function of Treg cells, which then leads to disease relapse. In the NHP GVAD model, Tkachev et al. reported that the combined administration with KY 1005 and sirolimus could control the activation of effector T cells while maintaining the reconstitution of Treg cells (94). It seems that combination treatments may be more promising.

3.4 Other co-stimulatory signal pathways

There are some other co-stimulatory molecules involving in the activation of T cells as well. We focused on the possibility of targeting CD40L, glucocorticoid induced TNF receptor (GITR), and CD137 for therapy in AAV.

CD40L (also known as TNFSF5 or CD154), mainly expressed in activated T cells and platelets, is the ligand of CD40 (95, 96). CD40, expressed in B cells, monocytes, DCs, and VECs, has similar structures to the other members of TNFRSF (96–99). The connection of CD40 and CD40L regulated Th cells differentiation, maintained GCs response, activated the $CD8^+$ cytotoxic T lymphocytes (CTL), and sustained memory CTLs (100). Although the gene polymorphisms of CD40 were not related to the susceptibility of AAV (101), the levels of CD40L and soluble CD40L were raised in AAV patients, which was correlated with disease activity (102). It was a pity that the anti-CD40 mAb BI 655064 and the polyethylene glycol conjugated anti-CD40L Fab' fragment dapirolizumab pegol (DZP) both did not achieve the expected clinical efficacy in the phase II studies (103, 104). Furthermore, blocking CD40L could lead to severe thromboembolic events. Because of the myocardial infarction and thromboembolic events occurring in patients, the study of BG9588 was terminated (105). In comparison, the CD40L binding protein VIB4920, which lacks an Fc domain, may have more therapeutic potential in AAV. By blocking the downstream CD40 signal, VIB4920 could inhibit the differentiation of plasma cells without platelet aggregation. The safety and efficacy of VIB4920 have been preliminarily demonstrated in patients with rheumatoid arthritis (RA) (106), and further exploration of the clinical efficacy is needed.

GITR (also known as TNFRSF18) and CD137 (also known as 4-1BB or TNFRSF9) are both members of TNFRSF (85). They are expressed in different types of activated T cells, that is, GITR is mainly expressed in Treg cells (107) while CD137 is primarily expressed in $CD8^+$ T cells (108). The stimulations of the GITR signal as well as the CD137 signal enhanced T cells proliferation, raised the secretion of cytokines, and eliminated the suppressive effect of Treg cells (109–111). Compared to HCs, the expression of GITR was increased in patients with GPA and significantly correlated with disease activity (88). Giscombe et al. reported that, similar to animal tests, the expanded $CD8^+$ T cells expressed more CD137 (89). The anti-GITR mAb exacerbated the disease severity in the murine model of collagen-induced arthritis (CIA) (112) and experimental autoimmune encephalomyelitis (EAE) (113). In contrast, the agonistic anti-CD137 mAb improved the CIA and EAE maybe by inducing expansion of $CD11c^+$ $CD8^+$ T cells (114, 115). Among the members of TNFRSF, CD137 was superior in increasing the secretion of cytokines by $CD8^+$ T cells (116, 117). So far, the effects of inhibiting or stimulating GITR and anti-CD137 in the treatment of AAV are unknown. There is no doubt that this is a tempting field worthy of further exploration for AAV treatment.

4 Co-inhibitory signal pathways

The exhaustion of T cells in AAV and other autoimmune diseases (AIDs) predicts advantageous clinical outcomes. The expressions of co-inhibitory molecules restrain the differentiation of non-exhausted T cells, indicating the importance of co-inhibitory molecules in the exhaustion of T cells (20). At present, the research on PD-1 and CTLA-4 signal pathways is reported widely, whose blockers have been used in the treatment of many malignant tumors. In the previous section, we summarized the association between AAV and inhibitors of PD-1, PD-L1, and CTLA-4. In this section, we described more details on the mechanisms and roles of PD-1 and CTLA-4 signal pathways in AAV. We assessed the therapeutic potential of other co-inhibitory molecules associated with the exhaustion of T cells as well (Figure 3).

4.1 PD-1 signal pathway

PD-1 is a co-inhibitory receptor expressed in many types of activated or exhausted immune cells (118). PD-1, a transmembrane protein with 288 amino acids, consists of an extracellular domain, a transmembrane domain, and an intracellular cytoplasmic tail. Although PD-1 belongs to the CD28 family, it has unique molecular characteristics. PD-1 has an IgV-like domain in the extracellular domain whereas an immunoreceptor tyrosine-based inhibition motif (ITIM) and an immunoreceptor tyrosine-based switch motif (ITSM) in the cytoplasmic tail (119). ITIM and ITSM mediated the inhibition signal of PD-1, while ITSM might be more important. It has been reported that only the mutation of ITSM affected the transduction of the PD-1 signal (120–122). With the bindings of PD-1 and its ligand, ITSM was phosphorylated, the SH2-containing protein tyrosine phosphatase 2 (SHP-2) was recruited, and the PI3K/AKT signal pathway was inhibited, which suppressed the activation of T cells and the production of pro-inflammatory cytokines (119, 123). RAS/MEK/ERK signal pathway, which is responsible for activating T cells, is another target of the PD-1 signal to suppress the activity of T cells and concurrent inflammation (119).

PD-L1 and PD-L2 are the ligands of PD-1. Both of them are members of B7 family, which are known as B7-H1 and B7-DC, respectively. The expression of PD-L1 is detected on many types of cells (T and B cells, DCs, VECs, placenta, eyes, and others) whereas PD-L2 is mainly limited to express on the surface of macrophages, DCs, and mast cells (119, 124). As PD-L1 and PD-L2 are close in the distance on the same chromosome, they are regulated similarly by inflammatory factors (IFN-1, IFN-2, TNF-α and ILs). In addition, PD-L1 is regulated with post-translational regulation and microRNAs, including but not limited to miR-513, miR-155, miR-34a, miR-142-5p, and miR-93 (118, 125, 126). PD-1 is not the only receptor for PD-L1 and PD-L2. PD-L1 can also bind to CD80 to inhibit the immune response of T cells (127), while PD-L2 may combine with repulsive guidance molecule B (RGMB) to impair respiratory tolerance (128). Therefore, targeting PD-L1 or

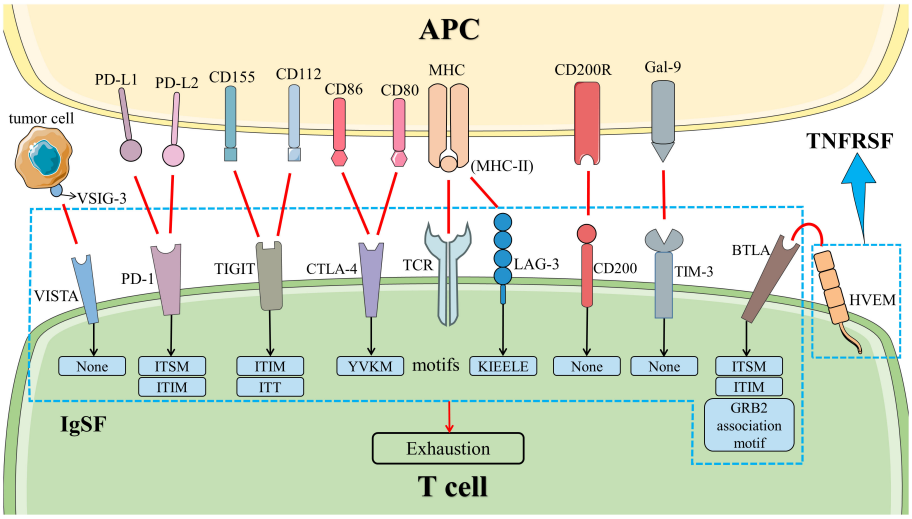

FIGURE 3
Co-inhibitory signal pathways in T cells. The co-inhibitory signal pathways induced the exhaustion of T cells. HVEM is a member of TNFRSF. Other molecules belong to IgSF. Except for LAG-3, VISTA, TIM-3, and CD200, all of them have inhibitory signal motifs in the cytoplasmic tail. LAG-3 has a unique KIEELE motif whose role is unclear, while VISTA, TIM-3, and CD200 do not have any motifs in the cytoplasmic tail. Abbreviation: APC, antigen-presenting cell; BTLA, B and T lymphocyte attenuator; CTLA-4, cytotoxic T lymphocyte-associated molecule 4; Gal-9, galactin-9; HVEM, herpesvirus entry mediator; IgSF, immunoglobulin superfamily; LAG-3, lymphocyte activation gene 3; MHC, major histocompatibility complex; PD-1, programmed cell death 1; PD-L1, programmed death ligand 1; TCR, T cell receptor; TIGIT, T-cell immunoglobulin and ITIM domain; TIM-3, T cell immunoglobulin and mucin domain-containing protein 3; TNFRSF, tumor necrosis factor receptor superfamily; VISTA, V-domain immunoglobulin suppressor of T cell activation; VSIG-3, V-set and immunoglobulin domain containing 3. .

PD-L2 is also important immunotherapy, and actually, PD-L1 inhibitors have been developed to treat malignant tumors.

Zhang et al. demonstrated that, in contrast to patients with GCA, PD-1$^+$ T cells were not enriched at renal lesions in patients with GPA, suggesting that PD-1 might play a different role in different diseases (129). Similarly, Zeisbrich et al. measured the expression of PD-L1 in monocytes and found that the frequency of PD-L1$^+$ monocytes was not related to renal involvement although these monocytes tended to decrease in active patients with AAV (130). A previous study revealed that the expression of PD-1 on Th cells was lower in patients with localized GPA than that in patients with systemic GPA (131). We then detected the expression of PD-1 in Tfh cells. Compared to HCs, the expression intensity of PD-1 in Tfh cells was higher in patients with MPO-AAV. We also found that the expression of ICOS/PD-1 instead of PD-1 was associated with the levels of MPO-ANCA (19), indicating that co-stimulatory and co-inhibitory molecules were involved in the activation of T cells together. Although the fusion proteins containing an anti-PD-1 single-chain variable fragment could improve symptoms of type 1 diabetes (TID) and EAE models (132), its effects in AAV have yet to be explored. Soluble ICs in PD-1 signaling pathway also play an important role in AAV. It was observed that although the serum concentration of soluble PD-L2 in active AAV was lower than that in HCs, its level was significantly increased after treatment (57). In addition, the levels of serum soluble PD-1 (sPD-1) was higher in MPO-AAV (133). Noting that sPD-1 could restrain the exhaustion of T cells by binding to PD-L1 in cell membranes (134), sPD-1 is therefore likely an effective therapeutic target in MPO-AAV. Significantly, Targeting the PD-1 signal pathway alone may be less effective because of the poorer inhibitory impact on PD-1 of T cells (131). This may explain why PD-1 inhibitors induce fewer irAEs than CTLA-4 inhibitors. Compared to PD-1, PD-L1 may be a better target. The frequency of PD-L1$^+$ monocytes is negatively correlated with the level of ANCA (130), so increasing the expression of PD-L1 may reduce the level of ANCA and improve disease activity. In lupus nephritis mice models, the recombinant adenovirus containing the full-length PD-L1 gene improved the renal lesions (135). In the same experiment, the anti-ICOSL mAb was also added to reinforce this process (135). As the results we found, targeting both ICOS and PD-1 in patients with AAV may be more effective.

4.2 CTLA-4 signal pathway

CTLA-4 is transiently expressed in the activated T cells. Beforehand, it localized in intracellular compartments of naïve T cells (136, 137). The gene expressing CTLA-4 is located in the same chromosomal region (2q33-34) as the gene expressing CD28, so CTLA-4 and CD28 exhibit a significant homology (138). CTLA-4 and CD28 bind to the same ligand but transduce an opposite signal. CTLA-4 leads to co-inhibitory signaling whereas CD28 provides the co-stimulatory signal. As a member of IgSF, CTLA-4 is also a transmembrane protein that contains an IgV-like domain in the extracellular domain and a YVKM motif in the intracellular cytoplasmic tail (139, 140). The IgV-like domain is the site that binding to CD80 and CD86 for CTLA-4, and the YVKM motif is important for CTLA-4 signal transduction in T cells. The interaction of the phosphorylated YVKM motif with SHP2 and serine/threonine protein phosphatase 2A (PP2A) dephosphorylated

the TCR-CD3ζ complex so that the activated signal from TCR was suppressive (21). On the other hand, the phosphorylation of the YVKM motif inhibited the interaction with the clathrin-associated adaptor complex AP-2, resulting in the internalization of CTLA-4 (141). CTLA-4 expressed on the surface of activated T cells captured and degraded CD80 and CD86 by trans-endocytosis to inhibit the co-stimulatory signal from CD28 (142). Ultimately, CTLA-4 suppressed the activation of T cells.

In patients with GPA, the expression of CTLA-4 in T cells was found to be elevated, and to be related to disease severity. After stimulating with phytohaemagglutinin (PHA), the expression of CTLA-4 in T cells in patients with GPA did not increase, suggesting that the activation of T cells in patients with GPA was persistent (143). As mentioned above, Abatacept bind to CD80 and CD86 to inhibit the activation of T cells, and its efficacy in patients with GPA has been reported (59). Although agonistic CTLA-4 antibodies have not yet been successfully developed, directly targeting CTLA-4 may be less effective because of the CTLA-4 endocytosis. It is probably more effective to inhibit the bindings of CD28 to CD80 and CD86. In addition, polymorphisms of the CTLA-4 gene were associated with GPA (144–146), while they were not related to MPA in Japanese patients (147), indicating that there were race differences in CTLA-4 polymorphism. A meta-analysis showed that CTLA-4 $(AT)_{86}$ and CTLA-4 $(AT)_{106}$ were significantly associated with AAV in the Caucasian patients instead of the Asian patients (144). Therefore, when targeting CTLA-4, genetic variation should be considered to avoid invalid treatment.

4.3 Other co-inhibitory signal pathways

T cell Ig and mucin domain-containing protein 3 (TIM-3), as a co-inhibitory receptor for Th1, was reported in 2002 to be associated with the severity of EAE (148). After that, it was shown that TIM-3 was expressed in Treg cells, DCs, natural killer (NK) cells, and macrophages (149, 150). Similar to other members of IgSF, TIM-3 contains an IgV domain, a mucin domain, a transmembrane domain, and a cytoplasmic tail lacking inhibitory signaling motifs (151). TIM-3 binds to ligands through the IgV domain, and five conserved tyrosine residues at the cytoplasmic tails trigger the signaling downstream (152). Galactin-9 (Gal-9), phosphatidyl serine (PtdSer), high mobility group protein B1 (HMGB1), and carcinoembryonic antigen cell adhesion molecule 1 (CEACAM-1) are known ligands of TIM-3. Gal-9 is the earliest discovered as well as the most explored ligand. TIM-3-Gal-9 signal pathway induced intracellular calcium flux, apoptosis, and the suppression of Th1 (153). PtdSer and HMGB1 did not directly suppress the activation of T cells, but rather affected the immune responses of DCs (154, 155). CEACAM-1 promoted the exhaustion of T cells through cis- and trans-interactions with TIM-3 (156). In patients with AAV, the expression of TIM-3 was significantly reduced on DCs, and blocking TIM-3 enhanced the expression of DC cytokines. Also, there were no differences in the expression of TIM-3 on the surface of different T cell subtypes ($CD4^+$ T cells and $CD8^+$ T cells) between MPO-AAV and HCs (157). Further explorations might be needed to assess the expression of TIM-3 on Th and Treg cells. Studies have shown that the serum concentrations of soluble TIM-3 correlated with the diseases state of AAV (57, 133), i.e. it was increased in active AAV (57), and could predict the relapse in PR3-AAV with rituximab treatment (133). However, the specific mechanism of soluble TIM-3 in AAV remains to be further examined before considering as a therapeutic target. Yoon et al. demonstrated that the serum Gal-9 levels were independently related to disease activity in patients with AAV (158). In mice models of CIA and SLE, injection of Gal-9 improved symptoms (159, 160). Although targeting the TIM-3 signal pathway has a potential efficacy in AAV, the problem is the need to clarify in which immune cells the TIM-3 signal pathway is more dominant to confirm the effectiveness. Another problem is that TIM-3 is not the only receptor for its ligand, so targeting the ligands of TIM-3 may not completely enhance TIM-3 signaling.

B and T lymphocyte attenuator (BTLA, also known as CD272) is mainly expressed in B and T cells, especially in naïve B cells and Th1 (161). BTLA is a co-inhibitory molecule with similar structures to PD-1 and CTLA-4 (162). Similar to PD-1, ITSM and ITIM in the cytoplasmic tail of BTLA inhibit the activation of T cells. However, unlike PD-1, SHP-1 rather than SHP-2 is mainly recruited by BTLA (163, 164). The third signal motif in the cytoplasmic tail of BTLA is the GRB2 association motif, which binds to GRB2 and p85 subunits of PI3K and induces the activation of T cells (165). Accordingly, BTLA transmits bidirectional signaling. Herpesvirus entry mediator (HVEM, also known as TNFRSF14) is a ligand of BTLA. HVEM is a member of TNFRSF, which is expressed in T cells, B cells, NK cells, monocytes, and neutrophils (166). There are two types of interaction between HVEM and BTLA. When BTLA and HVEM interacted in the same T lymphocyte, a cis complex was formed, inhibiting HVEM-dependent NF-κB activation (167). When BTLA or HVEM was expressed in APCs, trans interaction provided a co-stimulatory signal (168). Therefore, the regulation of the BTLA-HVEM signal pathway in AIDs is complex. In patients with remission AAV, the expression of BTLA was decreased only on double negative T-cells ($CD3^+CD4^-CD8^-$). *In vitro* experiments, it has been shown that agonistic anti-BTLA antibody inhibit the activation and proliferation of T cells, especially Th17 (169), suggesting that targeting BTLA to inhibit the activation of T cells may be one of the future therapeutic directions of AAV.

V-domain Ig suppressor of T cell activation (VISTA), also known as PD-1 homolog (PD-1H), is a member of IgSF first discovered in 2011 (170). Different from other members of IgSF, VISTA has four additional invariant cysteines (170, 171). Subsequently, the same laboratory confirmed that VISTA in humans is a co-inhibitory molecule, which inhibits the proliferation of T cells and the production of cytokines (172). VISTA is mainly expressed in hematopoietic cells, especially in $CD11b^{hi}$ myeloid cells. Within the T cell compartment, the expression of VISTA was highest in naïve T cells and $FoxP3^+$ Treg cells (171, 172). It is certain that VISTA is a ligand for T cells (170, 172). Moreover, it may also be a receptor in T cells to transmit inhibitory signals (173). Wang et al. demonstrated that V-set and Ig domain containing 3 (VSIG-3) is a ligand of VISTA. The binding between VISTA and VSIG-3 induced the inhibitory effects (174). It is a pity that VSIG-3 is mainly expressed in tumor cells but not in normal immune cells (174). Currently, targeting

VISTA is explored in AIDs. It was reported that VISTA KO mice developed SLE (175) and EAE (176). In mice models with SLE, agonistic VISTA mAb improved symptoms (175). In patients with AAV, VISTA was expressed in mononuclear phagocytes, $CD4^+$ T cells, and $CD8^+$ T cells. Compared to patients with a lower expression of VISTA, patients with a higher expression of VISTA might have a higher risk of renal progression (177). Therefore, targeting VISTA may inhibit disease severity in patients with AAV, which needs more experiments to confirm.

T-cell Ig and ITIM domain (TIGIT), CD200, and lymphocyte activation gene 3 (LAG-3) are popular co-inhibitory molecules in recent studies. CD155 and CD112 are ligands of TIGIT, binding to CD226 as well (152). CD200 binds to CD200Rs, especially CD200R1 (178). Besides MHC-II, fibrinogen-like protein 1 (FGL-1) was also discovered to be a ligand for LAG-3 (179, 180). These signal pathways transmit inhibitory signals. As a result, their roles in AIDs are noted. TIGIT-Ig fusion protein has revealed the therapeutic effects in mice with SLE (181). In EAE mice models, agonistic TIGIT mAb as well as CD200-Fc fusion protein improved disease severity (182, 183). CD200-Fc fusion protein reduced the disease severity of CIA at the clinical and histologic levels (184). Remarkably, LAG-3-deficient mice do not induce AIDs. After exposure to mercury (Hg), it not only had increased susceptibility to AIDs but also did not respond to tolerance induction (185). In AAV, there are no relevant reports about the influences of TIGIT, CD200, and LAG-3, so it is unknown whether targeting these signal pathways will improve disease severity.

5 Conclusion

The pathogenesis of AAV involves multiple aspects of innate immunity and adaptive immunity in which the role of T cells is pivotal and complex. With the understanding of the IC molecules, its importance will be confirmed further in AAV. Firstly, some ICIs used for malignant tumors induced the attack or relapse of AAV. Secondly, inhibiting the co-stimulatory signal pathways or enhancing the co-inhibitory signal pathways inhibited the activation and proliferation of T cells so that AIDs could be improved. In AAV, although it is demonstrated that Abatacept is effective in clinical trials, the efficacy of targeting other ICs has not been demonstrated. Thirdly, since co-stimulatory and co-inhibitory molecules work together to regulate T cells, it may be more reasonable to target multiple ICs simultaneously in severe or refractory cases. The questions to be aware of are that targeting ICs may increase the risk of tumors and infections, and different ICs are dominant in different subsets of T cells, so it is required to precise dosing and localization. In conclusion, targeting ICs has therapeutic potential, and more preclinical research is needed to clarify their effectiveness and safety in AAV treatment.

Author contributions

PSCL originated the topic and revised the manuscript. ZS wrote the outline, organize and supervise the writing. MP and HZ wrote the original text and figures draft. RJ searched literatures and made the table. All authors contributed to the article and approved the submitted version.

Funding

This work was supported by National Natural Science Foundation of China, Grant/Award Number: 81871296.

Conflict of interest

The authors declare that the research was conducted in the absence of any commercial or financial relationships that could be construed as a potential conflict of interest.

Publisher's note

References

1. Jennette JC, Falk RJ, Bacon PA, Basu N, Cid MC, Ferrario F, et al. 2012 Revised international chapel hill consensus conference nomenclature of vasculitides. *Arthritis Rheum* (2013) 65(1):1–11. doi: 10.1002/art.37715

2. Grayson PC, Ponte C, Suppiah R, Robson JC, Craven A, Judge A, et al. 2022 American College of Rheumatology/European alliance of associations for rheumatology classification criteria for eosinophilic granulomatosis with polyangiitis. *Ann Rheum Dis* (2022) 81(3):309–14. doi: 10.1136/annrheumdis-2021-221794

3. Robson JC, Grayson PC, Ponte C, Suppiah R, Craven A, Judge A, et al. 2022 American College of Rheumatology/European alliance of associations for rheumatology classification criteria for granulomatosis with polyangiitis. *Ann Rheum Dis* (2022) 81(3):315–20. doi: 10.1136/annrheumdis-2021-221795

4. Suppiah R, Robson JC, Grayson PC, Ponte C, Craven A, Khalid S, et al. 2022 American College of Rheumatology/European alliance of associations for rheumatology classification criteria for microscopic polyangiitis. *Ann Rheum Dis* (2022) 81(3):321–6. doi: 10.1136/annrheumdis-2021-221796

5. Walker BS, Peterson LK, Koening C, White SK, Schmidt RL, Tebo AE. Performance of mpo-anca and Pr3-anca immunoassays for the stratification of specific anca-associated vasculitis: A systematic review and meta-analysis. *Autoimmun Rev* (2022) 21(6):103100. doi: 10.1016/j.autrev.2022.103100

6. Kitching AR, Anders HJ, Basu N, Brouwer E, Gordon J, Jayne DR, et al. Anca-associated vasculitis. *Nat Rev Dis Primers* (2020) 6(1):71. doi: 10.1038/s41572-020-0204-y

7. Pearce FA, Craven A, Merkel PA, Luqmani RA, Watts RA. Global ethnic and geographic differences in the clinical presentations of anti-neutrophil cytoplasm antibody-associated vasculitis. *Rheumatol (Oxford)* (2017) 56(11):1962–9. doi: 10.1093/rheumatology/kex293

8. Fujimoto S, Watts RA, Kobayashi S, Suzuki K, Jayne DR, Scott DG, et al. Comparison of the epidemiology of anti-neutrophil cytoplasmic antibody-associated vasculitis between Japan and the U.K. *Rheumatol (Oxford)* (2011) 50(10):1916–20. doi: 10.1093/rheumatology/ker205

9. Sharma RK, Lovstrom B, Gunnarsson I, Malmstrom V. Proteinase 3 autoreactivity in anti-neutrophil cytoplasmic antibody-associated vasculitis-immunological versus clinical features. *Scand J Immunol* (2020) 92(5):e12958. doi: 10.1111/sji.12958

10. London J, Dumoitier N, Lofek S, Dion J, Chaigne B, Mocek J, et al. Skewed peripheral b- and T-cell compartments in patients with anca-associated vasculitis. *Rheumatol (Oxford)* (2021) 60(5):2157–68. doi: 10.1093/rheumatology/keaa432

11. Falk RJ, Terrell RS, Charles LA, Jennette JC. Anti-neutrophil cytoplasmic autoantibodies induce neutrophils to degranulate and produce oxygen radicals in vitro. *Proc Natl Acad Sci U.S.A.* (1990) 87(11):4115–9. doi: 10.1073/pnas.87.11.4115

12. Mathern DR, Heeger PS. Molecules great and small: The complement system. *Clin J Am Soc Nephrol* (2015) 10(9):1636–50. doi: 10.2215/CJN.06230614

13. Brilland B, Garnier AS, Chevailler A, Jeannin P, Subra JF, Augusto JF. Complement alternative pathway in anca-associated vasculitis: Two decades from bench to bedside. *Autoimmun Rev* (2020) 19(1):102424. doi: 10.1016/j.autrev.2019.102424

14. Massicotte-Azarniouch D, Herrera CA, Jennette JC, Falk RJ, Free ME. Mechanisms of vascular damage in anca vasculitis. *Semin Immunopathol* (2022) 44 (3):325–45. doi: 10.1007/s00281-022-00920-0

15. Soderberg D, Segelmark M. Neutrophil extracellular traps in vasculitis, friend or foe? *Curr Opin Rheumatol* (2018) 30(1):16–23. doi: 10.1097/BOR.0000000000000450

16. Abdulahad WH, Stegeman CA, Limburg PC, Kallenberg CG. Skewed distribution of Th17 lymphocytes in patients with wegener's granulomatosis in remission. *Arthritis Rheum* (2008) 58(7):2196–205. doi: 10.1002/art.23557

17. Tsurikisawa N, Saito H, Oshikata C, Tsuburai T, Akiyama K. Decreases in the numbers of peripheral blood regulatory T cells, and increases in the levels of memory and activated b cells, in patients with active eosinophilic granulomatosis and polyangiitis. *J Clin Immunol* (2013) 33(5):965–76. doi: 10.1007/s10875-013-9898-x

18. Kerstein A, Schuler S, Cabral-Marques O, Fazio J, Hasler R, Muller A, et al. Environmental factor and inflammation-driven alteration of the total peripheral T-cell compartment in granulomatosis with polyangiitis. *J Autoimmun* (2017) 78:79–91. doi: 10.1016/j.jaut.2016.12.004

19. Xu J, Zhao H, Wang S, Zheng M, Shuai Z. Elevated level of serum interleukin-21 and its influence on disease activity in anti-neutrophil cytoplasmic antibodies against myeloperoxidase-associated vasculitis. *J Interferon Cytokine Res* (2022) 42(6):290–300. doi: 10.1089/jir.2022.0014

20. McKinney EF, Lee JC, Jayne DR, Lyons PA, Smith KG. T-Cell exhaustion, Co-stimulation and clinical outcome in autoimmunity and infection. *Nature* (2015) 523 (7562):612–6. doi: 10.1038/nature14468

21. Chen L, Flies DB. Molecular mechanisms of T cell Co-stimulation and Co-inhibition. *Nat Rev Immunol* (2013) 13(4):227–42. doi: 10.1038/nri3405

22. Hid Cadena R, Reitsema RD, Huitema MG, van Sleen Y, van der Geest KSM, Heeringa P, et al. Decreased expression of negative immune checkpoint vista by Cd4+ T cells facilitates T helper 1, T helper 17, and T follicular helper lineage differentiation in gca. *Front Immunol* (2019) 10:1638. doi: 10.3389/fimmu.2019.01638

23. Roger A, Groh M, Lorillon G, Le Pendu C, Maillet J, Arangalage D, et al. Eosinophilic granulomatosis with polyangiitis (Churg-Strauss) induced by immune checkpoint inhibitors. *Ann Rheum Dis* (2019) 78(8):e82. doi: 10.1136/annrheumdis-2018-213857

24. Heo MH, Kim HK, Lee H, Ahn MJ. Antineutrophil cytoplasmic antibody-associated rapid progressive glomerulonephritis after pembrolizumab treatment in thymic epithelial tumor: A case report. *J Thorac Oncol* (2017) 12(8):e103–e5. doi: 10.1016/j.jtho.2017.03.011

25. Nabel CS, Severgnini M, Hung YP, Cunningham-Bussel A, Gjini E, Kleinsteuber K, et al. Anti-Pd-1 immunotherapy-induced flare of a known underlying relapsing vasculitis mimicking recurrent cancer. *Oncologist* (2019) 24(8):1013–21. doi: 10.1634/theoncologist.2018-0633

26. Cano-Cruz LG, Barrera-Vargas A, Mateos-Soria A, Soto-Perez-de-Celis E, Merayo-Chalico J. Rheumatological adverse events of cancer therapy with immune checkpoint inhibitors. *Arch Med Res* (2022) 53(2):113–21. doi: 10.1016/j.arcmed.2021.09.004

27. Richter MD, Crowson C, Kottschade LA, Finnes HD, Markovic SN, Thanarajasingam U. Rheumatic syndromes associated with immune checkpoint inhibitors: A single-center cohort of sixty-one patients. *Arthritis Rheumatol* (2019) 71(3):468–75. doi: 10.1002/art.40745

28. Dulos J, Carven GJ, van Boxtel SJ, Evers S, Driessen-Engels LJ, Hobo W, et al. Pd-1 blockade augments Th1 and Th17 and suppresses Th2 responses in peripheral blood from patients with prostate and advanced melanoma cancer. *J Immunother* (2012) 35(2):169–78. doi: 10.1097/CJI.0b013e318247a4e7

29. Kostine M, Finckh A, Bingham CO, Visser K, Leipe J, Schulze-Koops H, et al. Eular points to consider for the diagnosis and management of rheumatic immune-related adverse events due to cancer immunotherapy with checkpoint inhibitors. *Ann Rheum Dis* (2021) 80(1):36–48. doi: 10.1136/annrheumdis-2020-217139

30. Crout TM, Lennep DS, Kishore S, Majithia V. Systemic vasculitis associated with immune check point inhibition: Analysis and review. *Curr Rheumatol Rep* (2019) 21 (6):28. doi: 10.1007/s11926-019-0828-7

31. Tocut M, Brenner R, Zandman-Goddard G. Autoimmune phenomena and disease in cancer patients treated with immune checkpoint inhibitors. *Autoimmun Rev* (2018) 17(6):610–6. doi: 10.1016/j.autrev.2018.01.010

32. Robert C, Schachter J, Long GV, Arance A, Grob JJ, Mortier L, et al. Pembrolizumab versus ipilimumab in advanced melanoma. *N Engl J Med* (2015) 372 (26):2521–32. doi: 10.1056/NEJMoa1503093

33. Shen P, Deng X, Hu Z, Chen Z, Huang Y, Wang K, et al. Rheumatic manifestations and diseases from immune checkpoint inhibitors in cancer immunotherapy. *Front Med (Lausanne)* (2021) 8:762247. doi: 10.3389/fmed.2021.762247

34. Kato K, Mizuno T, Koseki T, Ito Y, Takahashi K, Tsuboi N, et al. Frequency of immune checkpoint inhibitor-induced vasculitides: An observational study using data from the Japanese adverse drug event report database. *Front Pharmacol* (2022) 13:803706. doi: 10.3389/fphar.2022.803706

35. Hung W, Cusnir I, Habib S, Smylie M, Solez K, Yacyshyn E. Immune checkpoint inhibitor-induced granulomatosis with polyangiitis. *Rheumatol (Oxford)* (2021) 60(6): e190–e1. doi: 10.1093/rheumatology/keaa818

36. Uner M, Alhasson B, Obhrai J, Bagnasco SM. Anca-associated pauci-immune necrotizing glomerulonephritis during the treatment with pembrolizumab. *Virchows Arch* (2021) 478(4):801–4. doi: 10.1007/s00428-020-02882-w

37. Harada M, Naoi H, Yasuda K, Ito Y, Kagoo N, Kubota T, et al. Programmed cell death-1 blockade in kidney carcinoma may induce eosinophilic granulomatosis with polyangiitis: A case report. *BMC Pulm Med* (2021) 21(1):6. doi: 10.1186/s12890-020-01375-5

38. Mamlouk O, Lin JS, Abdelrahim M, Tchakarov AS, Glass WF, Selamet U, et al. Checkpoint inhibitor-related renal vasculitis and use of rituximab. *J Immunother Cancer* (2020) 8(2):e000750. doi: 10.1136/jitc-2020-000750

39. Sibille A, Alfieri R, Malaise O, Detrembleur N, Pirotte M, Louis R, et al. Granulomatosis with polyangiitis in a patient on programmed death-1 inhibitor for advanced non-Small-Cell lung cancer. *Front Oncol* (2019) 9:478. doi: 10.3389/fonc.2019.00478

40. van den Brom RR, Abdulahad WH, Rutgers A, Kroesen BJ, Roozendaal C, de Groot DJ, et al. Rapid granulomatosis with polyangiitis induced by immune checkpoint inhibition. *Rheumatol (Oxford)* (2016) 55(6):1143–5. doi: 10.1093/rheumatology/kew063

41. Wulfken LM, Becker JC, Hayajneh R, Wagner AD, Schaper-Gerhardt K, Flatt N, et al. Case report: Sustained remission due to pd-1-Inhibition in a metastatic melanoma patient with depleted b cells. *Front Immunol* (2021) 12:733961. doi: 10.3389/fimmu.2021.733961

42. Yamada T, Masuda T, Yamaguchi K, Sakamoto S, Horimasu Y, Miyamoto S, et al. Non-small cell lung cancer treated by an anti-programmed cell death-1 antibody without a flare-up of preexisting granulomatosis with polyangiitis. *Intern Med* (2019) 58(21):3129–32. doi: 10.2169/internalmedicine.3018-19

43. Maul LV, Weichenthal M, Kahler KC, Hauschild A. Successful anti-Pd-1 antibody treatment in a metastatic melanoma patient with known severe autoimmune disease. *J Immunother* (2016) 39(4):188–90. doi: 10.1097/CJI.0000000000000118

44. Esensten JH, Helou YA, Chopra G, Weiss A, Bluestone JA. Cd28 costimulation: From mechanism to therapy. *Immunity* (2016) 44(5):973–88. doi: 10.1016/j.immuni.2016.04.020

45. June CH, Ledbetter JA, Gillespie MM, Lindsten T, Thompson CB. T-Cell proliferation involving the Cd28 pathway is associated with cyclosporine-resistant interleukin 2 gene expression. *Mol Cell Biol* (1987) 7(12):4472–81. doi: 10.1128/mcb.7.12.4472-4481.1987

46. Martin PJ, Ledbetter JA, Morishita Y, June CH, Beatty PG, Hansen JA. A 44 kilodalton cell surface homodimer regulates interleukin 2 production by activated human T lymphocytes. *J Immunol* (1986) 136(9):3282–7.

47. Boomer JS, Green JM. An enigmatic tail of Cd28 signaling. *Cold Spring Harb Perspect Biol* (2010) 2(8):a002436. doi: 10.1101/cshperspect.a002436

48. Csernok E, Ai M, Gross WL, Wicklein D, Petersen A, Lindner B, et al. Wegener autoantigen induces maturation of dendritic cells and licenses them for Th1 priming *Via* the protease-activated receptor-2 pathway. *Blood* (2006) 107(11):4440–8. doi: 10.1182/blood-2005-05-1875

49. Bhatia S, Edidin M, Almo SC, Nathenson SG. Different cell surface oligomeric states of B7-1 and B7-2: Implications for signaling. *Proc Natl Acad Sci U.S.A.* (2005) 102 (43):15569–74. doi: 10.1073/pnas.0507257102

50. MacPhee IA, Turner DR, Yagita H, Oliveira DB. Cd80(B7.1) and Cd86(B7.2) do not have distinct roles in setting the Th1/Th2 balance in autoimmunity in rats. *Scand J Immunol* (2001) 54(5):486–94. doi: 10.1046/j.1365-3083.2001.00998.x

51. Borriello F, Sethna MP, Boyd SD, Schweitzer AN, Tivol EA, Jacoby D, et al. B7-1 and B7-2 have overlapping, critical roles in immunoglobulin class switching and germinal center formation. *Immunity* (1997) 6(3):303–13. doi: 10.1016/s1074-7613(00)80333-7

52. Levine SM, Stone JH. New approaches to treatment in systemic vasculitis: Biological therapies. *Best Pract Res Clin Rheumatol* (2001) 15(2):315–33. doi: 10.1053/berh.2000.0146

53. Zhang H, Watanabe R, Berry GJ, Nadler SG, Goronzy JJ, Weyand CM. Cd28 signaling controls metabolic fitness of pathogenic T cells in medium and Large vessel vasculitis. *J Am Coll Cardiol* (2019) 73(14):1811–23. doi: 10.1016/j.jacc.2019.01.049

54. Tian Y, Li J, Tian X, Zeng X. Using the Co-expression network of T cell-Activation-Related genes to assess the disease activity in takayasu's arteritis patients. *Arthritis Res Ther* (2021) 23(1):303. doi: 10.1186/s13075-021-02636-2

55. Ludviksson BR, Sneller MC, Chua KS, Talar-Williams C, Langford CA, Ehrhardt RO, et al. Active wegener's granulomatosis is associated with hla-dr+ Cd4+ T cells exhibiting an unbalanced Th1-type T cell cytokine pattern: Reversal with il-10. *J Immunol* (1998) 160(7):3602–9.

56. Khan M, Arooj S, Wang H. Soluble B7-Cd28 family inhibitory immune checkpoint proteins and anti-cancer immunotherapy. *Front Immunol* (2021) 12:651634. doi: 10.3389/fimmu.2021.651634

57. Pyo JY, Yoon T, Ahn SS, Song JJ, Park YB, Lee SW. Soluble immune checkpoint molecules in patients with antineutrophil cytoplasmic antibody-associated vasculitis. *Sci Rep* (2022) 12(1):21319. doi: 10.1038/s41598-022-25466-x

58. Edner NM, Carlesso G, Rush JS, Walker LSK. Targeting Co-stimulatory molecules in autoimmune disease. *Nat Rev Drug Discovery* (2020) 19(12):860–83. doi: 10.1038/s41573-020-0081-9

59. Langford CA, Monach PA, Specks U, Seo P, Cuthbertson D, McAlear CA, et al. An open-label trial of abatacept (Ctla4-ig) in non-severe relapsing granulomatosis with polyangiitis (Wegener's). *Ann Rheum Dis* (2014) 73(7):1376–9. doi: 10.1136/annrheumdis-2013-204164

60. Watkins BK, Tkachev V, Furlan SN, Hunt DJ, Betz K, Yu A, et al. Cd28 blockade controls T cell activation to prevent graft-Versus-Host disease in primates. *J Clin Invest* (2018) 128(9):3991–4007. doi: 10.1172/JCI98793

61. Huang C, Zhu HX, Yao Y, Bian ZH, Zheng YJ, Li L, et al. Immune checkpoint molecules. possible future therapeutic implications in autoimmune diseases. *J Autoimmun* (2019) 104:102333. doi: 10.1016/j.jaut.2019.102333

62. Choi YS, Kageyama R, Eto D, Escobar TC, Johnston RJ, Monticelli L, et al. Icos receptor instructs T follicular helper cell versus effector cell differentiation *Via* induction of the transcriptional repressor Bcl6. *Immunity* (2011) 34(6):932–46. doi: 10.1016/j.immuni.2011.03.023

63. Xu H, Li X, Liu D, Li J, Zhang X, Chen X, et al. Follicular T-helper cell recruitment governed by bystander b cells and icos-driven motility. *Nature* (2013) 496 (7446):523–7. doi: 10.1038/nature12058

64. Long Y, Feng J, Ma Y, Sun Y, Xu L, Song Y, et al. Altered follicular regulatory T (Tfr)- and helper T (Tfh)-cell subsets are associated with autoantibody levels in microscopic polyangiitis patients. *Eur J Immunol* (2021) 51(7):1809–23. doi: 10.1002/eji.202049093

65. Yoshinaga SK, Whoriskey JS, Khare SD, Sarmiento U, Guo J, Horan T, et al. T-Cell Co-stimulation through B7rp-1 and icos. *Nature* (1999) 402(6763):827–32. doi: 10.1038/45582

66. Koh KH, Cao Y, Mangos S, Tardi NJ, Dande RR, Lee HW, et al. Nonimmune cell-derived icos ligand functions as a renoprotective Alphavbeta3 integrin-selective antagonist. *J Clin Invest* (2019) 129(4):1713–26. doi: 10.1172/JCI123386

67. Wiendl H, Mitsdoerffer M, Schneider D, Melms A, Lochmuller H, Hohlfeld R, et al. Muscle fibres and cultured muscle cells express the B7.1/2-related inducible Co-stimulatory molecule, icosl: Implications for the pathogenesis of inflammatory myopathies. *Brain* (2003) 126(Pt 5):1026–35. doi: 10.1093/brain/awg114

68. Swallow MM, Wallin JJ, Sha WC. B7h, a novel costimulatory homolog of B7.1 and B7.2, is induced by tnfalpha. *Immunity* (1999) 11(4):423–32. doi: 10.1016/s1074-7613(00)80117-x

69. Liang L, Porter EM, Sha WC. Constitutive expression of the B7h ligand for inducible costimulator on naive b cells is extinguished after activation by distinct b cell receptor and interleukin 4 receptor-mediated pathways and can be rescued by Cd40 signaling. *J Exp Med* (2002) 196(1):97–108. doi: 10.1084/jem.20020298

70. Sacquin A, Gador M, Fazilleau N. The strength of bcr signaling shapes terminal development of follicular helper T cells in mice. *Eur J Immunol* (2017) 47(8):1295–304. doi: 10.1002/eji.201746952

71. Hu H, Wu X, Jin W, Chang M, Cheng X, Sun SC. Noncanonical nf-kappab regulates inducible costimulator (Icos) ligand expression and T follicular helper cell development. *Proc Natl Acad Sci U.S.A.* (2011) 108(31):12827–32. doi: 10.1073/pnas.1105774108

72. Zhang Z, Zhao S, Zhang L, Crew R, Zhang N, Sun X, et al. A higher frequency of Cd4(+)Cxcr5(+) T follicular helper cells in patients with newly diagnosed henoch-schonlein purpura nephritis. *Int Immunopharmacol* (2016) 32:8–15. doi: 10.1016/j.intimp.2015.12.037

73. Usui Y, Takeuchi M, Yamakawa N, Takeuchi A, Kezuka T, Ma J, et al. Expression and function of inducible costimulator on peripheral blood Cd4+ T cells in behcet's patients with uveitis: A new activity marker? *Invest Ophthalmol Vis Sci* (2010) 51(10):5099–104. doi: 10.1167/iovs.10-5286

74. Sullivan BA, Tsuji W, Kivitz A, Peng J, Arnold GE, Boedigheimer MJ, et al. Inducible T-cell Co-stimulator ligand (Icosl) blockade leads to selective inhibition of anti-klh igg responses in subjects with systemic lupus erythematosus. *Lupus Sci Med* (2016) 3(1):e000146. doi: 10.1136/lupus-2016-000146

75. Cheng LE, Amoura Z, Cheah B, Hiepe F, Sullivan BA, Zhou L, et al. Brief report: A randomized, double-blind, parallel-group, placebo-controlled, multiple-dose study to evaluate amg 557 in patients with systemic lupus erythematosus and active lupus arthritis. *Arthritis Rheumatol* (2018) 70(7):1071–6. doi: 10.1002/art.40479

76. Buchan SL, Rogel A, Al-Shamkhani A. The immunobiology of Cd27 and Ox40 and their potential as targets for cancer immunotherapy. *Blood* (2018) 131(1):39–48. doi: 10.1182/blood-2017-07-741025

77. Webb GJ, Hirschfield GM, Lane PJ. Ox40, Ox40l and autoimmunity: A comprehensive review. *Clin Rev Allergy Immunol* (2016) 50(3):312–32. doi: 10.1007/s12016-015-8498-3

78. Croft M. The role of tnf superfamily members in T-cell function and diseases. *Nat Rev Immunol* (2009) 9(4):271–85. doi: 10.1038/nri2526

79. Ohshima Y, Tanaka Y, Tozawa H, Takahashi Y, Maliszewski C, Delespesse G. Expression and function of Ox40 ligand on human dendritic cells. *J Immunol* (1997) 159(8):3838–48.

80. Stuber E, Neurath M, Calderhead D, Fell HP, Strober W. Cross-linking of Ox40 ligand, a member of the Tnf/Ngf cytokine family, induces proliferation and differentiation in murine splenic b cells. *Immunity* (1995) 2(5):507–21. doi: 10.1016/1074-7613(95)90031-4

81. Imura A, Hori T, Imada K, Ishikawa T, Tanaka Y, Maeda M, et al. The human Ox40/Gp34 system directly mediates adhesion of activated T cells to vascular endothelial cells. *J Exp Med* (1996) 183(5):2185–95. doi: 10.1084/jem.183.5.2185

82. Aten J, Roos A, Claessen N, Schilder-Tol EJM, Ten Berge IJM, Weening JJ. Strong and selective glomerular localization of Cd134 ligand and tnf receptor-1 in proliferative lupus nephritis. *J Am Soc Nephrol* (2000) 11(8):1426–38. doi: 10.1681/ASN.V1181426

83. Kashiwakura J, Yokoi H, Saito H, Okayama Y. T Cell proliferation by direct cross-talk between Ox40 ligand on human mast cells and Ox40 on human T cells: Comparison of gene expression profiles between human tonsillar and lung-cultured mast cells. *J Immunol* (2004) 173(8):5247–57. doi: 10.4049/jimmunol.173.8.5247

84. Sato T, Ishii N, Murata K, Kikuchi K, Nakagawa S, Ndhlovu LC, et al. Consequences of Ox40-Ox40 ligand interactions in langerhans cell function: Enhanced contact hypersensitivity responses in Ox40l-transgenic mice. *Eur J Immunol* (2002) 32 (11):3326–35. doi: 10.1002/1521-4141(200211)32:11<3326::AID-IMMU3326>3.0.CO;2-9

85. Croft M, Siegel RM. Beyond tnf: Tnf superfamily cytokines as targets for the treatment of rheumatic diseases. *Nat Rev Rheumatol* (2017) 13(4):217–33. doi: 10.1038/nrrheum.2017.22

86. Seko Y, Takahashi N, Tada Y, Yagita H, Okumura K, Nagai R. Restricted usage of T-cell receptor vgamma-vdelta genes and expression of costimulatory molecules in takayasu's arteritis. *Int J Cardiol* (2000) 75 Suppl 1:S77–83. doi: 10.1016/s0167-5273(00)00194-7

87. Qin W, Hongya W, Yongjing C, Fang X, Yue M, Xuekun Z, et al. Increased Ox40 and soluble Ox40 ligands in children with henoch-schonlein purpura: Association with renal involvement. *Pediatr Allergy Immunol* (2011) 22(1 Pt 1):54–9. doi: 10.1111/j.1399-3038.2010.01111.x

88. Wilde B, Dolff S, Cai X, Specker C, Becker J, Totsch M, et al. Cd4+Cd25+ T-cell populations expressing Cd134 and gitr are associated with disease activity in patients with wegener's granulomatosis. *Nephrol Dial Transplant* (2009) 24(1):161–71. doi: 10.1093/ndt/gfn461

89. Giscombe R, Wang XB, Kakoulidou M, Lefvert AK. Characterization of the expanded T-cell populations in patients with wegener's granulomatosis. *J Intern Med* (2006) 260(3):224–30. doi: 10.1111/j.1365-2796.2006.01688.x

90. Papp KA, Gooderham MJ, Girard G, Raman M, Strout V. Phase I randomized study of Khk4083, an anti-Ox40 monoclonal antibody, in patients with mild to moderate plaque psoriasis. *J Eur Acad Dermatol Venereol* (2017) 31(8):1324–32. doi: 10.1111/jdv.14313

91. Furihata K, Ishiguro Y, Yoshimura N, Ito H, Katsushima S, Kaneko E, et al. A phase 1 study of Khk4083: A single-blind, randomized, placebo-controlled single-Ascending-Dose study in healthy adults and an open-label multiple-dose study in patients with ulcerative colitis. *Clin Pharmacol Drug Dev* (2021) 10(8):870–83. doi: 10.1002/cpdd.918

92. Guttman-Yassky E, Pavel AB, Zhou L, Estrada YD, Zhang N, Xu H, et al. Gbr 830, an anti-Ox40, improves skin gene signatures and clinical scores in patients with atopic dermatitis. *J Allergy Clin Immunol* (2019) 144(2):482–93 e7. doi: 10.1016/j.jaci.2018.11.053

93. Saghari M, Gal P, Gilbert S, Yateman M, Porter-Brown B, Brennan N, et al. Ox40l inhibition suppresses klh-driven immune responses in healthy volunteers: A randomized controlled trial demonstrating proof-of-Pharmacology for Ky1005. *Clin Pharmacol Ther* (2022) 111(5):1121–32. doi: 10.1002/cpt.2539

94. Tkachev V, Furlan SN, Watkins B, Hunt DJ, Zheng HB, Panoskaltsis-Mortari A, et al. Combined Ox40l and mtor blockade controls effector T cell activation while preserving treg reconstitution after transplant. *Sci Transl Med* (2017) 9(408):eaan3085. doi: 10.1126/scitranslmed.aan3085

95. Armitage RJ, Fanslow WC, Strockbine L, Sato TA, Clifford KN, Macduff BM, et al. Molecular and biological characterization of a murine ligand for Cd40. *Nature* (1992) 357(6373):80–2. doi: 10.1038/357080a0

96. Henn V, Slupsky JR, Grafe M, Anagnostopoulos I, Forster R, Muller-Berghaus G, et al. Cd40 ligand on activated platelets triggers an inflammatory reaction of endothelial cells. *Nature* (1998) 391(6667):591–4. doi: 10.1038/35393

97. Clark EA, Ledbetter JA. Activation of human b cells mediated through two distinct cell surface differentiation antigens, Bp35 and Bp50. *Proc Natl Acad Sci U.S.A.* (1986) 83(12):4494–8. doi: 10.1073/pnas.83.12.4494

98. Kiener PA, Moran-Davis P, Rankin BM, Wahl AF, Aruffo A, Hollenbaugh D. Stimulation of Cd40 with purified soluble Gp39 induces proinflammatory responses in human monocytes. *J Immunol* (1995) 155(10):4917–25.

99. Caux C, Massacrier C, Vanbervliet B, Dubois B, Van Kooten C, Durand I, et al. Activation of human dendritic cells through Cd40 cross-linking. *J Exp Med* (1994) 180 (4):1263–72. doi: 10.1084/jem.180.4.1263

100. Tang T, Cheng X, Truong B, Sun L, Yang X, Wang H. Molecular basis and therapeutic implications of Cd40/Cd40l immune checkpoint. *Pharmacol Ther* (2021) 219:107709. doi: 10.1016/j.pharmthera.2020.107709

101. Wieczorek S, Holle JU, Muller S, Fricke H, Gross WL, Epplen JT. A functionally relevant Irf5 haplotype is associated with reduced risk to wegener's granulomatosis. *J Mol Med (Berl)* (2010) 88(4):413–21. doi: 10.1007/s00109-009-0580-y

102. Hoffmann JC, Patschan D, Dihazi H, Muller C, Schwarze K, Henze E, et al. Cytokine profiling in anti neutrophil cytoplasmic antibody-associated vasculitis: A cross-sectional cohort study. *Rheumatol Int* (2019) 39(11):1907–17. doi: 10.1007/s00296-019-04364-y

103. Visvanathan S, Daniluk S, Ptaszynski R, Muller-Ladner U, Ramanujam M, Rosenstock B, et al. Effects of bi 655064, an antagonistic anti-Cd40 antibody, on clinical and biomarker variables in patients with active rheumatoid arthritis: A randomised, double-blind, placebo-controlled, phase iia study. *Ann Rheum Dis* (2019) 78(6):754–60. doi: 10.1136/annrheumdis-2018-214729

104. Furie RA, Bruce IN, Dorner T, Leon MG, Leszczynski P, Urowitz M, et al. Phase 2, randomized, placebo-controlled trial of dapirolizumab pegol in patients with moderate-to-Severe active systemic lupus erythematosus. *Rheumatol (Oxford)* (2021) 60(11):5397–407. doi: 10.1093/rheumatology/keab381

105. Boumpas DT, Furie R, Manzi S, Illei GG, Wallace DJ, Balow JE, et al. A short course of Bg9588 (Anti-Cd40 ligand antibody) improves serologic activity and decreases hematuria in patients with proliferative lupus glomerulonephritis. *Arthritis Rheum* (2003) 48(3):719–27. doi: 10.1002/art.10856

106. Karnell JL, Albulescu M, Drabic S, Wang L, Moate R, Baca M, et al. A Cd40l-targeting protein reduces autoantibodies and improves disease activity in patients with autoimmunity. *Sci Transl Med* (2019) 11(489):eaar6584. doi: 10.1126/scitranslmed.aar6584

107. McHugh RS, Whitters MJ, Piccirillo CA, Young DA, Shevach EM, Collins M, et al. Cd4(+)Cd25(+) immunoregulatory T cells: Gene expression analysis reveals a functional role for the glucocorticoid-induced tnf receptor. *Immunity* (2002) 16 (2):311–23. doi: 10.1016/s1074-7613(02)00280-7

108. Dawicki W, Watts TH. Expression and function of 4-1bb during Cd4 versus Cd8 T cell responses in vivo. *Eur J Immunol* (2004) 34(3):743–51. doi: 10.1002/eji.200324278

109. Tian J, Zhang B, Rui K, Wang S. The role of Gitr/Gitrl interaction in autoimmune diseases. *Front Immunol* (2020) 11:588682. doi: 10.3389/fimmu.2020.588682

110. Takahashi C, Mittler RS, Vella AT. Cutting edge: 4-1bb is a bona fide Cd8 T cell survival signal. *J Immunol* (1999) 162(9):5037–40.

111. Choi BK, Bae JS, Choi EM, Kang WJ, Sakaguchi S, Vinay DS, et al. 4-1bb-Dependent inhibition of immunosuppression by activated Cd4+Cd25+ T cells. *J Leukoc Biol* (2004) 75(5):785–91. doi: 10.1189/jlb.1003491

112. Patel M, Xu D, Kewin P, Choo-Kang B, McSharry C, Thomson NC, et al. Glucocorticoid-induced tnfr family-related protein (Gitr) activation exacerbates murine asthma and collagen-induced arthritis. *Eur J Immunol* (2005) 35(12):3581–90. doi: 10.1002/eji.200535421

113. Kohm AP, Williams JS, Miller SD. Cutting edge: Ligation of the glucocorticoid-induced tnf receptor enhances autoreactive Cd4+ T cell activation and experimental autoimmune encephalomyelitis. *J Immunol* (2004) 172(8):4686–90. doi: 10.4049/jimmunol.172.8.4686

114. Seo SK, Choi JH, Kim YH, Kang WJ, Park HY, Suh JH, et al. 4-1bb-Mediated immunotherapy of rheumatoid arthritis. *Nat Med* (2004) 10(10):1088–94. doi: 10.1038/nm1107

115. Kim YH, Choi BK, Shin SM, Kim CH, Oh HS, Park SH, et al. 4-1bb triggering ameliorates experimental autoimmune encephalomyelitis by modulating the balance between Th17 and regulatory T cells. *J Immunol* (2011) 187(3):1120–8. doi: 10.4049/jimmunol.1002681

116. Oh HS, Choi BK, Kim YH, Lee DG, Hwang S, Lee MJ, et al. 4-1bb signaling enhances primary and secondary population expansion of Cd8+ T cells by maximizing autocrine il-2/Il-2 receptor signaling. *PloS One* (2015) 10(5):e0126765. doi: 10.1371/journal.pone.0126765

117. Nguyen J, Pettmann J, Kruger P, Dushek O. Quantitative contributions of tnf receptor superfamily members to Cd8(+) T-cell responses. *Mol Syst Biol* (2021) 17(11): e10560. doi: 10.15252/msb.202110560

118. Kuchroo JR, Hafler DA, Sharpe AH, Lucca LE. The double-edged sword: Harnessing pd-1 blockade in tumor and autoimmunity. *Sci Immunol* (2021) 6(65): eabf4034. doi: 10.1126/sciimmunol.abf4034

119. Boussiotis VA. Molecular and biochemical aspects of the pd-1 checkpoint pathway. *N Engl J Med* (2016) 375(18):1767–78. doi: 10.1056/NEJMra1514296

120. Chemnitz JM, Parry RV, Nichols KE, June CH, Riley JL. Shp-1 and shp-2 associate with immunoreceptor tyrosine-based switch motif of programmed death 1 upon primary human T cell stimulation, but only receptor ligation prevents T cell activation. *J Immunol* (2004) 173(2):945–54. doi: 10.4049/jimmunol.173.2.945

121. Parry RV, Chemnitz JM, Frauwirth KA, Lanfranco AR, Braunstein I, Kobayashi SV, et al. Ctla-4 and pd-1 receptors inhibit T-cell activation by distinct mechanisms. *Mol Cell Biol* (2005) 25(21):9543–53. doi: 10.1128/MCB.25.21.9543-9553.2005

122. Yokosuka T, Takamatsu M, Kobayashi-Imanishi W, Hashimoto-Tane A, Azuma M, Saito T. Programmed cell death 1 forms negative costimulatory microclusters that directly inhibit T cell receptor signaling by recruiting phosphatase Shp2. *J Exp Med* (2012) 209(6):1201–17. doi: 10.1084/jem.20112741

123. Kreileder M, Barrett I, Bendtsen C, Brennan D, Kolch W. Signaling dynamics regulating crosstalks between T-cell activation and immune checkpoints. *Trends Cell Biol* (2021) 31(3):224–35. doi: 10.1016/j.tcb.2020.12.001

124. Sharpe AH, Pauken KE. The diverse functions of the Pd1 inhibitory pathway. *Nat Rev Immunol* (2018) 18(3):153–67. doi: 10.1038/nri.2017.108

125. Sun C, Mezzadra R, Schumacher TN. Regulation and function of the pd-L1 checkpoint. *Immunity* (2018) 48(3):434–52. doi: 10.1016/j.immuni.2018.03.014

126. Ibanez-Vega J, Vilchez C, Jimenez K, Guevara C, Burgos PI, Naves R. Cellular and molecular regulation of the programmed death-1/Programmed death ligand system and its role in multiple sclerosis and other autoimmune diseases. *J Autoimmun* (2021) 123:102702. doi: 10.1016/j.jaut.2021.102702

127. Butte MJ, Keir ME, Phamduy TB, Sharpe AH, Freeman GJ. Programmed death-1 ligand 1 interacts specifically with the B7-1 costimulatory molecule to inhibit T cell responses. *Immunity* (2007) 27(1):111–22. doi: 10.1016/j.immuni.2007.05.016

128. Xiao Y, Yu S, Zhu B, Bedoret D, Bu X, Francisco LM, et al. Rgmb is a novel binding partner for pd-L2 and its engagement with pd-L2 promotes respiratory tolerance. *J Exp Med* (2014) 211(5):943–59. doi: 10.1084/jem.20130790

129. Zhang H, Watanabe R, Berry GJ, Vaglio A, Liao YJ, Warrington KJ, et al. Immunoinhibitory checkpoint deficiency in medium and Large vessel vasculitis. *Proc Natl Acad Sci U.S.A.* (2017) 114(6):E970–E9. doi: 10.1073/pnas.1616848114

130. Zeisbrich M, Chevalier N, Sehnert B, Rizzi M, Venhoff N, Thiel J, et al. Cmtm6-deficient monocytes in anca-associated vasculitis fail to present the immune checkpoint pd-L1. *Front Immunol* (2021) 12:673912. doi: 10.3389/fimmu.2021.673912

131. Wilde B, Hua F, Dolff S, Jun C, Cai X, Specker C, et al. Aberrant expression of the negative costimulator pd-1 on T cells in granulomatosis with polyangiitis. *Rheumatol (Oxford)* (2012) 51(7):1188–97. doi: 10.1093/rheumatology/kes034

132. Zhao P, Wang P, Dong S, Zhou Z, Cao Y, Yagita H, et al. Depletion of pd-1-Positive cells ameliorates autoimmune disease. *Nat BioMed Eng* (2019) 3(4):292–305. doi: 10.1038/s41551-019-0360-0

133. Gamerith G, Mildner F, Merkel PA, Harris K, Cooney L, Lim N, et al. Association of baseline soluble immune checkpoints with the risk of relapse in Pr3-anca vasculitis following induction of remission. *Ann Rheum Dis* (2023) 82(2):253–61. doi: 10.1136/ard-2022-222479

134. Soltani-Zangbar MS, Parhizkar F, Abdollahi M, Shomali N, Aghebati-Maleki L, Shahmohammadi Farid S, et al. Immune system-related soluble mediators and covid-19: Basic mechanisms and clinical perspectives. *Cell Commun Signal* (2022) 20(1):131. doi: 10.1186/s12964-022-00948-7

135. Ding H, Wu X, Wu J, Yagita H, He Y, Zhang J, et al. Delivering pd-1 inhibitory signal concomitant with blocking icos Co-stimulation suppresses lupus-like syndrome in autoimmune bxsb mice. *Clin Immunol* (2006) 118(2-3):258–67. doi: 10.1016/j.clim.2005.10.017

136. He X, Xu C. Immune checkpoint signaling and cancer immunotherapy. *Cell Res* (2020) 30(8):660–9. doi: 10.1038/s41422-020-0343-4

137. Nagai K. Co-Inhibitory receptor signaling in T-Cell-Mediated autoimmune glomerulonephritis. *Front Med (Lausanne)* (2020) 7:584382. doi: 10.3389/fmed.2020.584382

138. Linsley PS, Brady W, Urnes M, Grosmaire LS, Damle NK, Ledbetter JA. Ctla-4 is a second receptor for the b cell activation antigen B7. *J Exp Med* (1991) 174(3):561–9. doi: 10.1084/jem.174.3.561

139. Rowshanravan B, Halliday N, Sansom DM. Ctla-4: A moving target in immunotherapy. *Blood* (2018) 131(1):58–67. doi: 10.1182/blood-2017-06-741033

140. Kumar P, Bhattacharya P, Prabhakar BS. A comprehensive review on the role of Co-signaling receptors and treg homeostasis in autoimmunity and tumor immunity. *J Autoimmun* (2018) 95:77–99. doi: 10.1016/j.jaut.2018.08.007

141. Shiratori T, Miyatake S, Ohno H, Nakaseko C, Isono K, Bonifacino JS, et al. Tyrosine phosphorylation controls internalization of ctla-4 by regulating its interaction with clathrin-associated adaptor complex ap-2. *Immunity* (1997) 6(5):583–9. doi: 10.1016/s1074-7613(00)80346-5

142. Qureshi OS, Zheng Y, Nakamura K, Attridge K, Manzotti C, Schmidt EM, et al. Trans-endocytosis of Cd80 and Cd86: A molecular basis for the cell-extrinsic function of ctla-4. *Science* (2011) 332(6029):600–3. doi: 10.1126/science.1202947

143. Steiner K, Moosig F, Csernok E, Selleng K, Gross WL, Fleischer B, et al. Increased expression of ctla-4 (Cd152) by T and b lymphocytes in wegener's granulomatosis. *Clin Exp Immunol* (2001) 126(1):143–50. doi: 10.1046/j.1365-2249.2001.01575.x

144. Rahmattulla C, Mooyaart AL, van Hooven D, Schoones JW, Bruijn JA, Dekkers OM, et al. Genetic variants in anca-associated vasculitis: A meta-analysis. *Ann Rheum Dis* (2016) 75(9):1687–92. doi: 10.1136/annrheumdis-2015-207601

145. Chung SA, Xie G, Roshandel D, Sherva R, Edberg JC, Kravitz M, et al. Meta-analysis of genetic polymorphisms in granulomatosis with polyangiitis (Wegener's) reveals shared susceptibility loci with rheumatoid arthritis. *Arthritis Rheum* (2012) 64 (10):3463–71. doi: 10.1002/art.34496

146. Spriewald BM, Witzke O, Wassmuth R, Wenzel RR, Arnold ML, Philipp T, et al. Distinct tumour necrosis factor alpha, interferon gamma, interleukin 10, and cytotoxic T cell antigen 4 gene polymorphisms in disease occurrence and end stage renal disease in wegener's granulomatosis. *Ann Rheum Dis* (2005) 64(3):457–61. doi: 10.1136/ard.2004.025809

147. Tsuchiya N, Kobayashi S, Kawasaki A, Kyogoku C, Arimura Y, Yoshida M, et al. Genetic background of Japanese patients with antineutrophil cytoplasmic antibody-associated vasculitis: Association of hla-Drb1*0901 with microscopic polyangiitis. *J Rheumatol* (2003) 30(7):1534–40.

148. Monney L, Sabatos CA, Gaglia JL, Ryu A, Waldner H, Chernova T, et al. Th1-specific cell surface protein Tim-3 regulates macrophage activation and severity of an autoimmune disease. *Nature* (2002) 415(6871):536–41. doi: 10.1038/415536a

149. Gautron AS, Dominguez-Villar M, de Marcken M, Hafler DA. Enhanced suppressor function of Tim-3+ Foxp3+ regulatory T cells. *Eur J Immunol* (2014) 44 (9):2703–11. doi: 10.1002/eji.201344392

150. Andrews LP, Yano H, Vignali DAA. Inhibitory receptors and ligands beyond pd-1, pd-L1 and ctla-4: Breakthroughs or backups. *Nat Immunol* (2019) 20(11):1425–34. doi: 10.1038/s41590-019-0512-0

151. Wolf Y, Anderson AC, Kuchroo VK. Tim3 comes of age as an inhibitory receptor. *Nat Rev Immunol* (2020) 20(3):173–85. doi: 10.1038/s41577-019-0224-6

152. Anderson AC, Joller N, Kuchroo VK. Lag-3, Tim-3, and tigit: Co-inhibitory receptors with specialized functions in immune regulation. *Immunity* (2016) 44 (5):989–1004. doi: 10.1016/j.immuni.2016.05.001

153. Zhu C, Anderson AC, Schubart A, Xiong H, Imitola J, Khoury SJ, et al. The Tim-3 ligand galectin-9 negatively regulates T helper type 1 immunity. *Nat Immunol* (2005) 6(12):1245–52. doi: 10.1038/ni1271

154. Nakayama M, Akiba H, Takeda K, Kojima Y, Hashiguchi M, Azuma M, et al. Tim-3 mediates phagocytosis of apoptotic cells and cross-presentation. *Blood* (2009) 113(16):3821–30. doi: 10.1182/blood-2008-10-185884

155. Chiba S, Baghdadi M, Akiba H, Yoshiyama H, Kinoshita I, Dosaka-Akita H, et al. Tumor-infiltrating dcs suppress nucleic acid-mediated innate immune responses through interactions between the receptor Tim-3 and the alarmin Hmgb1. *Nat Immunol* (2012) 13(9):832–42. doi: 10.1038/ni.2376

156. Huang YH, Zhu C, Kondo Y, Anderson AC, Gandhi A, Russell A, et al. Ceacam1 regulates Tim-3-Mediated tolerance and exhaustion. *Nature* (2015) 517 (7534):386–90. doi: 10.1038/nature13848

157. Su B, Mao X, Yin B, Chen C, Zhang M, Cui T, et al. Tim-3 regulates the nets-mediated dendritic cell activation in myeloperoxidase-Anca-Associated vasculitis. *Clin Exp Rheumatol* (2021) 39 Suppl 129(2):13–20. doi: 10.55563/clinexprheumatol/6y0bjb

158. Yoon T, Ahn SS, Pyo JY, Lee LE, Song JJ, Park YB, et al. Serum galectin-9 could be a potential biomarker in assessing the disease activity of antineutrophil cytoplasmic antibody-associated vasculitis. *Clin Exp Rheumatol* (2022) 40(4):779–86. doi: 10.55563/clinexprheumatol/xfqnx6

159. Seki M, Oomizu S, Sakata KM, Sakata A, Arikawa T, Watanabe K, et al. Galectin-9 suppresses the generation of Th17, promotes the induction of regulatory T cells, and regulates experimental autoimmune arthritis. *Clin Immunol* (2008) 127 (1):78–88. doi: 10.1016/j.clim.2008.01.006

160. Moritoki M, Kadowaki T, Niki T, Nakano D, Soma G, Mori H, et al. Galectin-9 ameliorates clinical severity of Mrl/Lpr lupus-prone mice by inducing plasma cell apoptosis independently of Tim-3. *PloS One* (2013) 8(4):e60807. doi: 10.1371/journal.pone.0060807

161. Gaikwad S, Agrawal MY, Kaushik I, Ramachandran S, Srivastava SK. Immune checkpoint proteins: Signaling mechanisms and molecular interactions in cancer immunotherapy. *Semin Cancer Biol* (2022) 86(3):137–50. doi: 10.1016/j.semcancer.2022.03.014

162. Watanabe N, Gavrieli M, Sedy JR, Yang J, Fallarino F, Loftin SK, et al. Btla is a lymphocyte inhibitory receptor with similarities to ctla-4 and pd-1. *Nat Immunol* (2003) 4(7):670–9. doi: 10.1038/ni944

163. Gavrieli M, Watanabe N, Loftin SK, Murphy TL, Murphy KM. Characterization of phosphotyrosine binding motifs in the cytoplasmic domain of b and T lymphocyte attenuator required for association with protein tyrosine phosphatases shp-1 and shp-2. *Biochem Biophys Res Commun* (2003) 312(4):1236–43. doi: 10.1016/j.bbrc.2003.11.070

164. Celis-Gutierrez J, Blattmann P, Zhai Y, Jarmuzynski N, Ruminski K, Gregoire C, et al. Quantitative interactomics in primary T cells provides a rationale for concomitant pd-1 and btla coinhibitor blockade in cancer immunotherapy. *Cell Rep* (2019) 27(11):3315–30 e7. doi: 10.1016/j.celrep.2019.05.041

165. Gavrieli M, Murphy KM. Association of grb-2 and Pi3k P85 with phosphotyrosile peptides derived from btla. *Biochem Biophys Res Commun* (2006) 345(4):1440–5. doi: 10.1016/j.bbrc.2006.05.036

166. Wojciechowicz K, Spodzieja M, Lisowska KA, Wardowska A. The role of the btla-hvem complex in the pathogenesis of autoimmune diseases. *Cell Immunol* (2022) 376:104532. doi: 10.1016/j.cellimm.2022.104532

167. Cheung TC, Oborne LM, Steinberg MW, Macauley MG, Fukuyama S, Sanjo H, et al. T Cell intrinsic heterodimeric complexes between hvem and btla determine receptivity to the surrounding microenvironment. *J Immunol* (2009) 183(11):7286–96. doi: 10.4049/jimmunol.0902490

168. Cheung TC, Steinberg MW, Oborne LM, Macauley MG, Fukuyama S, Sanjo H, et al. Unconventional ligand activation of herpesvirus entry mediator signals cell survival. *Proc Natl Acad Sci U.S.A.* (2009) 106(15):6244–9. doi: 10.1073/pnas.0902115106

169. Werner K, Dolff S, Dai Y, Ma X, Brinkhoff A, Korth J, et al. The Co-inhibitor btla is functional in anca-associated vasculitis and suppresses Th17 cells. *Front Immunol* (2019) 10:2843. doi: 10.3389/fimmu.2019.02843

170. Wang L, Rubinstein R, Lines JL, Wasiuk A, Ahonen C, Guo Y, et al. Vista, a novel mouse ig superfamily ligand that negatively regulates T cell responses. *J Exp Med* (2011) 208(3):577–92. doi: 10.1084/jem.20100619

171. Nowak EC, Lines JL, Varn FS, Deng J, Sarde A, Mabaera R, et al. Immunoregulatory functions of vista. *Immunol Rev* (2017) 276(1):66–79. doi: 10.1111/imr.12525

172. Lines JL, Pantazi E, Mak J, Sempere LF, Wang L, O'Connell S, et al. Vista is an immune checkpoint molecule for human T cells. *Cancer Res* (2014) 74(7):1924–32. doi: 10.1158/0008-5472.CAN-13-1504

173. Flies DB, Han X, Higuchi T, Zheng L, Sun J, Ye JJ, et al. Coinhibitory receptor pd-1h preferentially suppresses Cd4(+) T cell-mediated immunity. *J Clin Invest* (2014) 124(5):1966–75. doi: 10.1172/JCI74589

174. Wang J, Wu G, Manick B, Hernandez V, Renelt M, Erickson C, et al. Vsig-3 as a ligand of vista inhibits human T-cell function. *Immunology* (2019) 156(1):74–85. doi: 10.1111/imm.13001

175. Han X, Vesely MD, Yang W, Sanmamed MF, Badri T, Alawa J, et al. Pd-1h (Vista)-mediated suppression of autoimmunity in systemic and cutaneous lupus erythematosus. *Sci Transl Med* (2019) 11(522):eaax1159. doi: 10.1126/scitranslmed.aax1159

176. Wang L, Le Mercier I, Putra J, Chen W, Liu J, Schenk AD, et al. Disruption of the immune-checkpoint vista gene imparts a proinflammatory phenotype with predisposition to the development of autoimmunity. *Proc Natl Acad Sci U.S.A.* (2014) 111(41):14846–51. doi: 10.1073/pnas.1407447111

177. Kim MG, Yun D, Kang CL, Hong M, Hwang J, Moon KC, et al. Kidney vista prevents ifn-Gamma/Il-9 axis-mediated tubulointerstitial fibrosis after acute glomerular injury. *J Clin Invest* (2022) 132(1):e151189. doi: 10.1172/JCI151189

178. Gorczynski R, Chen Z, Kai Y, Lee L, Wong S, Marsden PA. Cd200 is a ligand for all members of the Cd200r family of immunoregulatory molecules. *J Immunol* (2004) 172(12):7744–9. doi: 10.4049/jimmunol.172.12.7744

179. Baixeras E, Huard B, Miossec C, Jitsukawa S, Martin M, Hercend T, et al. Characterization of the lymphocyte activation gene 3-encoded protein. a new ligand for human leukocyte antigen class ii antigens. *J Exp Med* (1992) 176(2):327–37. doi: 10.1084/jem.176.2.327

180. Wang J, Sanmamed MF, Datar I, Su TT, Ji L, Sun J, et al. Fibrinogen-like protein 1 is a major immune inhibitory ligand of lag-3. *Cell* (2019) 176(1-2):334–47.e12. doi: 10.1016/j.cell.2018.11.010

181. Liu S, Sun L, Wang C, Cui Y, Ling Y, Li T, et al. Treatment of murine lupus with tigit-ig. *Clin Immunol* (2019) 203:72–80. doi: 10.1016/j.clim.2019.04.007

182. Dixon KO, Schorer M, Nevin J, Etminan Y, Amoozgar Z, Kondo T, et al. Functional anti-tigit antibodies regulate development of autoimmunity and antitumor immunity. *J Immunol* (2018) 200(8):3000–7. doi: 10.4049/jimmunol.1700407

183. Liu Y, Bando Y, Vargas-Lowy D, Elyaman W, Khoury SJ, Huang T, et al. Cd200r1 agonist attenuates mechanisms of chronic disease in a murine model of multiple sclerosis. *J Neurosci* (2010) 30(6):2025–38. doi: 10.1523/JNEUROSCI.4272-09.2010

184. Simelyte E, Criado G, Essex D, Uger RA, Feldmann M, Williams RO. Cd200-fc, a novel antiarthritic biologic agent that targets proinflammatory cytokine expression in the joints of mice with collagen-induced arthritis. *Arthritis Rheum* (2008) 58(4):1038–43. doi: 10.1002/art.23378

185. Jha V, Workman CJ, McGaha TL, Li L, Vas J, Vignali DA, et al. Lymphocyte activation gene-3 (Lag-3) negatively regulates environmentally-induced autoimmunity. *PloS One* (2014) 9(8):e104484. doi: 10.1371/journal.pone.0104484

10.3389/fimmu.2023.1156212

Glossary

AAV	ANCA associated vasculitis
AIDs	autoimmune diseases
ANCA	anti-neutrophil cytoplasmic antibody
APC	antigen-presenting cells
BCR	B cell receptor
BTLA	B and T lymphocyte attenuator
C5a	fragment a of fifth complement
cAP	complement alternative pathway
CEACAM-1	carcinoembryonic antigen cell adhesion molecule 1
CIA	collagen-induced arthritis
CTL	cytotoxic T lymphocytes
CTLA-4	cytotoxic T lymphocyte-associated molecule 4
DCs	dendritic cells
EAE	experimental autoimmune encephalomyelitis
EGPA	eosinophilic granulomatosis with polyangiitis
Gal-9	Galactin-9
GCA	giant cell arteritis
GCs	germinal centers
GITR	glucocorticoid induced TNF receptor
GPA	granulomatosis with polyangiitis
GRB2	growth factor receptor-bound protein 2
GVHD	graft-versus-host disease
HCs	healthy controls
HMGB1	high mobility group protein B1
HSP	Henoch-Schönlein purpura
HVEM	herpesvirus entry mediator
IC	immune checkpoint
ICIs	immune checkpoint inhibitors
ICOS	inducible T-cell co-stimulator
ICOSL	inducible T-cell co-stimulator (ICOS) ligand
IFN	interferon
Ig	immunoglobulin
IgSF	immunoglobulin superfamily
IgV	Ig variable
IL	interleukin
irAEs	immune-related adverse events
LAG-3	lymphocyte activation gene 3
LCK	lymphocyte cell-specific protein-tyrosine kinase
mAb	monoclonal antibody
MHC	major histocompatibility complex
MNPs	mononuclear phagocytes
MPA	microscopic polyangiitis
MPO	myeloperoxidase
mTOR	mammalian target of rapamycin
NETs	neutrophil extracellular traps
NFAT	nuclear factor of activated T cells
NF-κB	nuclear factor-κB
NHP	non-human primate
NIK	NF-κB–inducing kinase
NIKR	tumor necrosis factor receptor
NK	natural killer cell
OX40L	OX40 ligand
PD-1	programmed cell death 1
PD-L	programmed death ligand
PI3K	phosphatidylinositol 3-kinase
PR3	proteinase-3
PtdSer	phosphatidyl serine
Rh-irAEs	rheumatic immune-related adverse events
sCD28	soluble CD28
SH2	Src homology-2
SHP-2	SH2-containing protein tyrosine phosphatase 2
SLE	systemic lupus erythematosus
SLEDAI	SLE disease activity index
sPD-1	soluble PD-1
TAK	Takayasu's arteritis
TCR	T cell receptor
Teff	effector T
Tfh	follicular helper T cells
Th	helper T cells
THD	TNF homology domain
TIGIT	T-cell Ig and ITIM domain
TIM-3	T cell Ig and mucin domain-containing protein 3
TNF	tumor necrosis factor
TNFR	tumor necrosis factor receptor
TNFRSF	tumor necrosis factor receptor superfamily
TRAF	tumor necrosis factor receptor-associated factor
Treg	regulatory T cells
VECs	vascular endothelial cells
VISTA	V-domain Ig suppressor of T cell activation
VSIG-3	V-set and Ig domain containing 3

frontiers | Frontiers in Immunology

TYPE Original Research
PUBLISHED 28 April 2023
DOI 10.3389/fimmu.2023.1168676

OPEN ACCESS

EDITED BY
Oded Shamriz,
Hadassah Medical Center, Israel

REVIEWED BY
Seung-Hyo Lee,
Korea Advanced Institute of Science and Technology (KAIST), Republic of Korea
Mohammad-Ali Assarehzadegan,
Iran University of Medical Sciences, Iran

*CORRESPONDENCE
Avner Adini
avner.adini@childrens.harvard.edu

RECEIVED 17 February 2023
ACCEPTED 12 April 2023
PUBLISHED 28 April 2023

CITATION
Adini A, Ko VH, Puder M, Louie SM, Kim CF, Baron J and Matthews BD (2023) PR1P, a VEGF-stabilizing peptide, reduces injury and inflammation in acute lung injury and ulcerative colitis animal models.
Front. Immunol. 14:1168676.
doi: 10.3389/fimmu.2023.1168676

PR1P, a VEGF-stabilizing peptide, reduces injury and inflammation in acute lung injury and ulcerative colitis animal models

Avner Adini[1,2]*, Victoria H. Ko[3], Mark Puder[3], Sharon M. Louie[4], Carla F. Kim[4], Joseph Baron[5] and Benjamin D. Matthews[1,2]

[1]Vascular Biology Program, Children's Hospital Boston and Harvard Medical School, Boston, MA, United States, [2]Department of Medicine, Boston Children's Hospital, Boston, MA, United States, [3]Department of Surgery, Boston Children's Hospital, Boston, MA, United States, [4]Stem Cell Program and Divisions of Hematology/Oncology, Boston Children's Hospital, Boston, MA, United States, [5]Janus Biotherapeutics, Inc, Wellesley, MA, United States

Acute Respiratory Distress Syndrome (ARDS) and Ulcerative Colitis (UC) are each characterized by tissue damage and uncontrolled inflammation. Neutrophils and other inflammatory cells play a primary role in disease progression by acutely responding to direct and indirect insults to tissue injury and by promoting inflammation through secretion of inflammatory cytokines and proteases. Vascular Endothelial Growth Factor (VEGF) is a ubiquitous signaling molecule that plays a key role in maintaining and promoting cell and tissue health, and is dysregulated in both ARDS and UC. Recent evidence suggests a role for VEGF in mediating inflammation, however, the molecular mechanism by which this occurs is not well understood. We recently showed that PR1P, a 12-amino acid peptide that binds to and upregulates VEGF, stabilizes VEGF from degradation by inflammatory proteases such as elastase and plasmin thereby limiting the production of VEGF degradation products (fragmented VEGF (fVEGF)). Here we show that fVEGF is a neutrophil chemoattractant *in vitro* and that PR1P can be used to reduce neutrophil migration *in vitro* by preventing the production of fVEGF during VEGF proteolysis. In addition, inhaled PR1P reduced neutrophil migration into airways following injury in three separate murine acute lung injury models including from lipopolysaccharide (LPS), bleomycin and acid. Reduced presence of neutrophils in the airways was associated with decreased pro-inflammatory cytokines (including TNF-α, IL-1β, IL-6) and Myeloperoxidase (MPO) in broncho-alveolar lavage fluid (BALF). Finally, PR1P prevented weight loss and tissue injury and reduced plasma levels of key inflammatory cytokines IL-1β and IL-6 in a rat TNBS-induced colitis model. Taken together, our data demonstrate that VEGF and fVEGF may each play separate and pivotal roles in mediating inflammation in ARDS and UC, and that PR1P, by preventing proteolytic degradation of VEGF and the production of fVEGF may represent a novel therapeutic approach to preserve VEGF signaling and inhibit inflammation in acute and chronic inflammatory diseases.

KEYWORDS

PR1P, ARDS, Acute Lung Injury, (ALI), ulcerative colitis, inflammation, VEGF

Introduction

ARDS and UC are two common diseases characterized by tissue injury, VEGF dysregulation and severe inflammation. ARDS is an acute and fulminant form of respiratory failure characterized by lung inflammation, hypoxemia and multi-organ failure requiring mechanical ventilation and prolonged ICU hospitalization (1, 2). There are no medical therapies to prevent or cure ARDS and management of ARDS remains supportive (3). UC is similarly characterized by chronic inflammation within the gastro-intestinal tract, and is associated with weight loss, abdominal pain, recurrent diarrhea, and bleeding (4). Treatments for UC include immunomodulatory medicines that are often insufficient to control disease. Proctocolectomy surgery remains the only curative option and is utilized in 15% of all UC patients (5). Neutrophils are the most abundant white blood cells in humans and are the first circulating inflammatory cell to arrive at sites of tissue injury during acute inflammation such as seen in ARDS and UC (6). Upon neutrophil activation, neutrophil-derived proteases including elastase, plasmin, MMP-8, MMP-9, and pro-inflammatory cytokines, including tumor necrosis factor α (TNF-α), interleukin (IL)-1β, and IL-6, are released at the sites of inflammation leading to structural local tissue damage and amplification of the inflammatory response. Further recruitment of neutrophils and other inflammatory cells including lymphocytes and macrophages during ARDS (7, 8) and UC (9, 10) ensues, which in turn contributes to heightened inflammation, the production of reactive oxygen species (ROS) (11) with disruption of cell membranes and ongoing tissue damage. Curiously, neutrophils and other inflammatory cells are also required to prevent invasion of disrupted epithelial cell barriers by infectious pathogens, and so anti-inflammation strategies envisioned to cure or treat ARDS and/or UC must balance their effects on inflammatory cell function and numbers. Also, as noted above, VEGF dysregulation is often associated with tissue injury and inflammation, and a clear understanding of how VEGF might simultaneously mediate inflammation and restoration of tissue to health is not clear.

VEGFs are a family of endogenous growth factors with angiogenic, survival and anti-apoptotic properties (12, 13). VEGF-A is a highly conserved member of the VEGF family, and $VEGF_{165}$ (a 165-amino acid isoform of VEGF-A, henceforth referred to as VEGF) is an ubiquitous angiogenic and survival factor that binds VEGF receptor 1 (VEGFR1) and 2 (VEGFR2), as well as neuropilin-1 (NRP-1) (14). These receptors are on multiple cell types and tissues throughout the body including lung endothelial and epithelial cells, neutrophils and other inflammatory cells that are resident in, or which infiltrate the lungs and GI tract following injury (10, 15). VEGF signaling leads to a wide variety of biological and functional outcomes that are critical in maintenance of cell and tissue health and healing following tissue insults (16–19). Neutrophil derived proteases such as elastase and plasmin cleave VEGF (20–22) into a smaller VEGF isomer (fragmented VEGF (fVEGF)) with altered VEGF signaling (20), and so an important but underrecognized effect of increased neutrophil activity during acute and chronic inflammation such as seen in ARDS (23, 24) and UC (25) is VEGF dysregulation.

We recently developed a 12 amino-acid VEGF binding peptide (PR1P (26)) that protects VEGF from degradation by the proteases elastase and plasmin, and upregulates VEGF signaling (27). We and others have identified potential therapeutic efficacy for PR1P in multiple animal models all characterized by tissue injury with subsequent inflammation and VEGF dysregulation, including in emphysema (27), myocardial infarction (28), nerve degeneration (29), hind-limb and cerebral ischemia (26, 30), ligament regeneration (31), and chronic wounds (32). fVEGF, the by-product of VEGF degradation, was recently shown to be a chemoattractant to macrophages (20, 21). We therefore hypothesized that fVEGF is a chemoattractant to neutrophils, and that by preventing fVEGF production *via* VEGF stabilization, PR1P reduces neutrophil migration into sites of ongoing inflammation all the while upregulating VEGF signaling by preserving local VEGF levels and concentration gradients.

To test this hypothesis, we first designed an *in vitro* neutrophil migration assay to characterize the ability of PR1P to mediate fVEGF induced neutrophil chemoattraction, and then tested the potential of PR1P to mitigate inflammation in lung injury and ulcerative colitis animal models. Here we present data showing that fVEGF is chemoattractant to neutrophils *in vitro*, and that by blocking the production of fVEGF during VEGF proteolysis by elastase, PR1P can mediate VEGF dependent neutrophil chemoattraction. Subsequently, inhaled PR1P reduced neutrophil migration into the airways following injury in three separate murine acute lung injury models including from lipopolysaccharide (LPS), bleomycin and acid. Reduced presence of neutrophils in the airways was associated with decreased pro-inflammatory cytokines (including TNF-α, IL-1β, IL-6, and Myeloperoxiase (MPO)) in broncho-alveolar lavage fluid (BALF). Finally, PR1P prevented weight loss and tissue injury and reduced plasma levels of key inflammatory cytokines IL-1β and IL-6 in a TNBS-induced colitis model in the rat. Together these data demonstrate that fVEGF may play a key role in mediating inflammation in acute lung injury (ALI) and UC, and that PR1P may represent a novel therapeutic approach to stabilize VEGF and preserve VEGF signaling and inhibit inflammation to improve outcome in acute and chronic inflammatory diseases.

Materials and methods

Mice

6-week-old female C57BL/6J mice were purchased from Jackson Laboratory (Bar Harbor, ME) and were kept in a pathogen-controlled environment in standard cages and were fed ad libitum. Protocols for the *in vivo* studies were approved by the Institutional Animal Care and Use Committee (IACUC) at Boston Children's Hospital.

Rats

Experiments with rats were performed by the CRO Washington Biotechnology Inc. (Simpsonville, MD). Male Sprague-Dawley rats were purchased from Envigo (Dublin, VA). The rats were cared for per company protocol, were examined daily and found to be free of any clinical signs of disease or distress.

Peptides

The 12-mer peptides PR1P (DRVQRQTTTVVA), scrambled PR1P (VRQVVTARDTTQ) and fVEGF(ARQENPCGPCSE RRKHLVQDPQTCKCSCKNTDSRCKARQLELNERT CRCDKPRR) were all synthetized by Genscript (Piscataway, NJ).

Induction of ulcerative colitis in rats by tri-nitrobenzene sulfonic acid

The tri-nitrobenzene sulfonic acid (TNBS) model is the most commonly used model to investigate the pathogenesis of, and for developing new anti-inflammatory strategies for ulcerative colitis (UC) (33). Colonic damage is created by the intrarectal application of a barrier disrupting ethanol and hapten mixture and since ethanol splits the epithelial layer, it allows the lamina propria to be exposed to bacterial components (34, 35). The rat model was performed by the (CRO) Washington Biotechnology (Simpsonville, MD). Sprague-Dawley male rats (210-230 grams) were randomly divided into five experimental groups with eight rats in each group including: (1) vehicle control, (2) TNBS-treated, (3) TNBS+PR1P (0.5 mg/kg), (4) TNBS+PR1P (5mg/kg), and (5) TNBS+ prednisolone, (50 mg/kg). Rats were deprived of food for 24 hours, anesthetized with intraperitoneal ketamine (80 mg/kg) + xylazine (10 mg/kg) and a polyurethane nutritional cannula was inserted through the anus. To induce acute colitis, 48 mg/kg TNBS dissolved in 0.25 mL 50% ethanol was instilled into the colon through the cannula. Control animals were instilled with vehicle (50% ethanol in saline). To evaluate the potential effects of PR1P in TNBS-induced colitis, rats were treated daily for 7 days with either PR1P, prednisolone or saline as noted above. Body weight, stool consistency and quality (diarrhea, blood) were recorded daily. Rats were sacrificed on day 7, weighed, and blood collected and stored using pre-chilled EDTA-microtainer tubes (Becton-Dickinson),. Blood samples were processed for plasma and stored at -80°C. After a midline incision in the abdomen, the colon was scored for adhesions and stricture. The colon was then removed from the rectum to the ileo-caecal juncture and the colon length recorded. After a longitudinal incision of the colon, the fecal material was removed and the colon weight, colon wall thickness, ulcer length, and ulcer width were recorded. A Colonic Score (maximum = 12) was calculated as follows: Adhesion: (i) none = 0, ii) minimal = 1, iii) involving several bowel loops = 2, Stricture: i) none = 0, ii) minimal = 1, iii) mild = 2, iv) severe, proximal dilatation = 3, Ulcer: i) none = 0, ii) focal hyperemia, no ulcers = 1, iii) ulcer without significant inflammation (hyperemia and bowel wall thickening = 2, iv) ulceration of 1 - ¾ 3 cm = 3, v) ulceration > 3 - < 6 cm = 4, vi) ulceration ≥ 6 cm = 5, Wall thickness: i) less than 1 mm = 0, ii) 1 – 3 mm = 1, iii) > 3 mm = 2. A section of the colon was preserved in 20 volume 10% neutral buffered formalin (Richard-Allan Scientific). The carcasses were disposed of appropriately. The formalin-preserved colon samples were submitted for histopathological processing and evaluation. Each tissue was embedded longitudinally in its own block. One slide per block was sectioned at - 4µm and stained with hematoxylin and eosin (H&E). Slides were evaluated with light microscopy by an ACVP board-certified veterinary pathologist. Histologic findings were diagnosed and were given a severity score of 0- 5 (0 = not present/normal, 1 = minimal, 2 = mild, 3 = moderate, 4 = marked, 5 = severe). Features were scored according to extent as follows: Grade 0: Not present/within normal limits, Grade 1: Minimal; <10% of sample affected, Grade 2: Mild; 10-25% of sample affected, Grade 3: Moderate; 26-50% of sample affected, Grade 4: Marked; 51-75% of tissue affected, Grade 5: Severe; >75% of tissue affected.

Murine LPS model of acute lung injury

Mice (22 + 2 g) were placed in a whole-animal nebulization chamber (14x5x8cm) and allowed to spontaneously breathe nebulized lipopolysaccharide LPS (salmonella enterica) (Sigma-Aldrich, St. Louis, MO) (0.6mg/mice), followed by PR1P or scrambled peptide (SP) (300 µg/ml in 3 ml of 0.9% normal saline) for 20 minutes (Proneb Ultra II Nebulizer, Pari Respiratory Equipment). Animals were sacrificed 24h after inhalation experiments and lungs were harvested. The lung tissue was minced using surgical scissors and suspended in 3 ml of serum-free bronchial epithelial-cell growth basal medium containing Liberase (2 mg/ml; Sigma-Aldrich), Dispase (5 U/ml; Stemcell Technology), and DNase (50 U/ml; Sigma-Aldrich) for 30 minutes at 37 C. Digested tissue was filtered (70-mm mesh Thermo Fisher Scientific), and filtered cells were washed twice with FACS media (PBS containing 3% FCS) and centrifuged at 1,000 rotations/min for 5 minutes. Pelleted material was incubated for 90 seconds in erythrocyte–lysis buffer (Sigma-Aldrich), resuspended in FACS media, and prepared for FACS analysis.

Murine bleomycin model of ALI

Mice were anesthetized with ketamine/xylazine (ketamine (125 mg/kg; Sanofi Winthrop Pharmaceuticals, New York, NY), xylazine (12.5 mg/kg; Phoenix Scientific, St. Joseph, MO) and injected intratracheally using a 24-gauge angiocatheter with 100µl sterile PBS or bleomycin (Cayman Chemicals, Arbor, MI, 0.75 mg/kg dissolved in PBS). Four days later, animals were sacrificed and bronchoalveolar lavage fluid (BALF) was collected by instilling 1 mL chilled PBS into the lungs *via* a 24-gauge angiocatheter (Becton Dickinson) and collected. The procedure was repeated 5X each with fresh PBS. The BALF was then centrifuged for 5 min at 300 g. as analyzed for total cell count and leukocyte differential. Cells were

characterized morphologically and counted by adhering them to glass slides using the Cytospin system (Shandon, Southern Sewickley, PA) and then staining them by Kwik-Diff (Fisher Scientific, Boston MA). The adhered stained cells were air-dried and counted in a blinded manner under a light microscope.

Murine HCL model of ALI

Mice were anesthetized with ketamine/xylazine (ketamine (125 mg/kg; Sanofi Winthrop Pharmaceuticals, New York, NY), xylazine (12.5 mg/kg; Phoenix Scientific, St. Joseph, MO) and 50 µl of hydrochloric acid (0.1 N HCl, pH 1.5, endotoxin free; Sigma-Aldrich) was instilled selectively into the left mainstem bronchus of anesthetized mice *via* a 24-gauge angiocatheter inserted intratracheally. 24 hours after acid instillation, bronchoalveolar lavage (BAL) was performed as described above and the BALF analyzed for total cell count and leukocyte differential as described above.

FACS and cytospin analysis of neutrophils derived from bronchoalveolar lavage fluid following HCL or bleomycin treatment

Three days after bleomycin and 24h after HCL and LPS exposure, mice were anesthetized with an intraperitoneal injection of ketamine (125 mg/kg; Sanofi Winthrop Pharmaceuticals, New York, NY) and xylazine (12.5 mg/kg; Phoenix Scientific, St. Joseph, MO). The trachea was cannulated using a (24 gauge angiocatheter (Becton Dickinson), and BALF collected as described above. Filtered BALF and red blood cell–lysed blood cells were resuspended in FACS buffer (Mouse PBS, 2% fetal calf serum, 2 mM EDTA). Cells were stained with the two monoclonal specific monoclonal antibodies against neutrophils Anti-CD11B-PE and Ly6G-FITC (BD Bioscience, Woburn, MA) (20 min, 4 °C on ice). Cells were then washed and resuspended in 50 µl FACS buffer. All studies were performed on a FACS Calibur (Becton Dickinson, San Jose, CA), and data were analyzed with FlowJo software (Tree Star, Ashland, OR). To confirm the presence of neutrophils within the different flow cytometry samples, we separately characterized a sample from each group by adhering the cells to glass slides using the Cytospin system (Shandon, Southern Sewickley, PA) and then staining them by Kwik-Diff (Fisher Scientific, Boston MA). The adhered stained cells were air-dried and counted in a blinded manner under a light microscope.

Cytokine analysis

Murine BALF

The Broncho-Alveolar Lavage fluid (BALF) supernatant from mice was collected following centrifugation (4 min at 7000g) and stored at -80°C. Inflammatory cytokine levels (IL1-β, IL-6 and TNF-α) in the BALF were determined as per manufacturer instructions using Enzyme Linked Immunosorbent Assay (ELISA) kits obtained from Biolegend, Inc, (San Diego, CA).

Rat plasma

Rats were anesthetized and bled into pre-chilled EDTA-microtainer tubes (BectonDickinson). The blood samples were processed to plasma which was stored in labeled 1.5-ml Eppendorf tubes at -80°C. Plasma samples were thawed to room temperature and assayed by ELISA for IL-6, IL-β and TNF-α (R&D Systems).

Neutrophil migration assay

Neutrophil migration assays were performed using a modification of the Boyden chamber technique (20) using 24-well Transwell permeable supports (Corning, NY) with migration inserts (3.5µm pore size, 6.5 mm diameter). The bottom parts of the 24-well plate were pre-incubated for 60 minutes in serum-free DMEM containing 25 mM HEPES, pH 7.5 at 37°C (5% CO_2, humidified) with either fVEGF (50nM, Genscript (Piscataway, NJ)), elastase (100 µg/ml, Fitzgerald, UK) + VEGF (10 ng/ml, Peprotech, Israel), or elastase 1 ug/ml µg/ml + VEGF (10 νg/ml) + PR1P (100 ug/ml). At the end of the 60-minute (digestion period) human neutrophils (IQ Biosciences, Alameda, CA) were plated onto the upper Transwell inserts at a density of 100,000 cells/insert and allowed to migrate towards the bottom chamber for two hours (migration period). Upon conclusion of the migration period cells that had migrated through the membrane were scraped and collected and washed once in PBS without Ca^{2+} and Mg^{2+}, fixed with 100% pre-chilled methanol for 10 min, adhered to glass coverslips and then stained by H&E. Images of migrated cells were captured by light microscopy from six random regions of interest (10X magnification) and counted.

Results

PR1P mediates neutrophil migration *in vitro* by preventing VEGF degradation

fVEGF was recently shown to be chemoattractant to macrophages (21) and so we hypothesized that it similarly mediates neutrophil migration. Furthermore, we recently showed that PR1P protects VEGF from neutrophil-derived protease degradation by binding to the heparin binding domain (HBD) (27) on VEGF and preventing the formation of fVEGF. We therefore surmised that by binding to and stabilizing VEGF from proteolytic degradation into fVEGF, PR1P indirectly mediates neutrophil chemoattraction. To test this hypothesis, we modified an inflammatory cell migration assay (20) to test the effect of fVEGF and PR1P on neutrophil migration. As shown in Figure 1, both commercially synthesized fVEGF, as well as the product of VEGF pre-incubated with neutrophil derived elastase, induced migration of human neutrophils. In contrast, when PR1P was present during

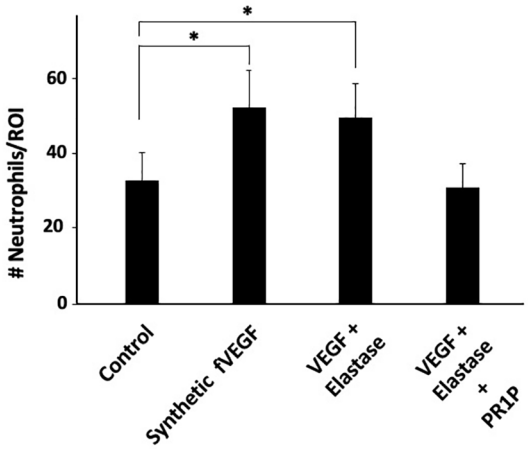

FIGURE 1
PR1P attenuates neutrophil migration *in vitro* by preventing VEGF degradation. Bar graph showing the quantification of neutrophils (# Neutrophils/Region of Interest (ROI)) during Transwell Plate Migration assay in which neutrophil migration (2h) was in response to indicated stimulants. 'fVEGF' was commercially synthesized based on a published amino acid sequence (20). 'VEGF + Elastase' and 'VEGF + Elastase + PR1P' were products of 30 min incubation of VEGF and elastase in presence or absence of PR1P, respectively. (n=6 repeated 3 times). Data are mean +/- SEM. *p<0.004.

elastase treatment of VEGF, the ensuing product failed to induce neutrophil migration, indicating that PR1P prevents the generation of fVEGF and subsequent induction of neutrophil migration. Thus, PR1P indirectly influences neutrophil migration through its ability to protect VEGF from proteolytic degradation.

PR1P limits neutrophil migration to sites of tissue injury in lung and gastro-intestinal injury models *in vivo*

Circulating neutrophils are often the first immune cells to arrive at sites of tissue injury and are thought to initiate the necessary inflammatory response required to restore tissue integrity (36). We therefore next sought to determine whether PR1P could be used to reduce neutrophil migration into injured lungs and/or GI tract following tissue injury in established animal models. Lung injury models were chosen to characterize the effect of PR1P on inflammation from diverse insults and injury mechanisms, and over different time courses. Specifically, lung injury was induced either by inhalation of lipopolysaccharide (LPS, a component of the bacterial cell wall and used as a potent trigger of acute lung inflammation whereby neutrophils migrate into the lungs within 4-24 hours (37)) or by intra-tracheal administration of bleomycin (38) (which induces acute inflammation and later fibrosis through a multi-factorial mechanism), or HCL (39) (also multifactorial in nature through damage to the alveolar-capillary membrane (40) resulting in immediate polymorphonuclear neutrophil (PMN) recruitment (41), pulmonary edema, and hypoxia (42)). In each of the lung injury models, tissue injury was followed by daily inhalation of PR1P or scrambled peptide (SP) until completion of each of the experiments according to the injury model (i.e. LPS and HCL for 24 hours, and bleomycin for 72 hours). FACS analyses of BALF following HCL- and bleomycin-induced lung injury revealed that inhaled PR1P significantly reduced toxin-induced neutrophil migration into the airways (i.e. BALF, HCl, Figure 2A, Bleomycin, Figure 2C). Representative Diff-Quik© stained cells used in the FACS analyses following acid injury are shown in Figure 2B. Similarly, FACS analyses of cells from whole lung digests from LPS injured lungs show that inhaled PR1P significantly reduced the presence of migrated neutrophils into the lungs 24h after exposure to LPS (Figures 2D-E).

To determine whether reduced neutrophil migration into lungs correlates with reduced inflammation, we measured the levels of pro-inflammatory cytokines in BALF following bleomycin injury and found that inhaled PR1P significantly reduced levels of TNF-α, IL-1β, and, IL-6 compared to scrambled peptide (see Figure 2F). Furthermore, inhaled PR1P reduced myeloperoxidase (MPO) activity in lung tissue following bleomycin injury (Figure 2F). Together these data suggest that inhaled PR1P effectively reduces neutrophil migration into the lungs, and in so doing PR1P attenuates lung inflammation as determined by reduced cytokine levels and MPO activity.

PR1P improves disease parameters in TNBS-induced colitis in

We next characterized the anti-inflammatory and potential therapeutic activity of PR1P in a TNBS-induced ulcerative colitis model (33). In this model, animals treated with TNBS develop acute colitis with bloody, mucus laden diarrhea and sustained weight loss that lasts UP TO three weeks (33). Induction of TNBS colitis (on Day 0) resulted in a decrease in body weight in all experimental groups (Figure 3A). Treatment with PR1P (low and high doses) and with prednisolone (which served as a positive control) significantly improved weights as early as Day 3 (PR1P, both doses) and Day 2 (Prednisolone) following injury as indicated. Upon study completion on Day 7, the colons of each animal were removed and measured for length and weight and examined macroscopically

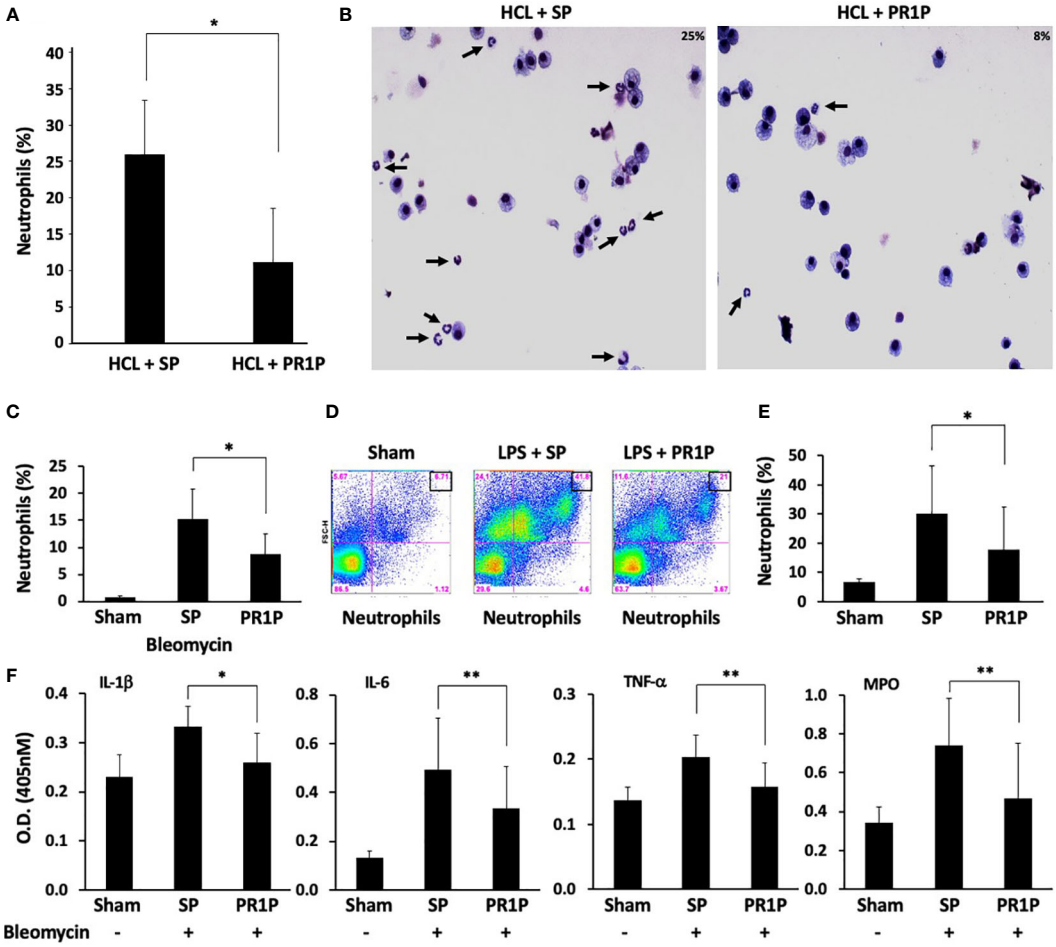

FIGURE 2
PR1P inhalation reduces neutrophil migration into lungs and lung inflammation following bleomycin, LPS and HCL injury in mice. **(A)** Bar graph showing percentage of neutrophils present (% of total cells in region of interest (ROI)) in BALF following IT administration of acid (HCl) and daily inhalation of PR1P or scrambled peptide (SP). n=8 repeated 3 times. *p<0.023 **(B)** Representative Diff-Quik stained cells from murine BALF described in **(A)** showing reduced neutrophils (black arrows) following PR1P treatment (25%) compared to SP (9%). **(C)** Bar graph showing percentage of neutrophils present (% of total cells in ROI) in BALF following IT administration of Bleomycin and daily inhalation of PR1P or scrambled peptide (SP). n=7 repeated 3 times *p<0.02. **(D)** Representative FACS analysis of cells from whole lung digests from mice treated with PR1P or SP after LPS injury showing reduced presence 24h after injury of neutrophils following PR1P inhalation. **(E)** Bar graph showing quantification of neutrophils (% of total cells) in whole lung cell digests from FACS experiments described in **(D)** n=8, repeated 3 times *p<0.02. **(F)** Bar graph showing quantification (Optical Density (OD) at 405 nm) of indicated cytokines or myeloperoxidase (MPO) activity in BALF following bleomycin injury in experiments described in **(A)** All data are mean + SEM. n=5. *p<0.004, **p<0.05.

for ulcers. Both PR1P (high dose) and Prednisolone significantly attenuated TNBS-induced gain in colon weight (Figure 3B) and both low and high dose PR1P, and Prednisolone attenuated TNBS-induced colon shortening and widening (Figure 3B). Also, high dose PR1P and prednisolone each significantly reduced the TNBS-induced drop in the Length/Weight index (Figure 3B). Macroscopic examination of the colons also revealed that high-dose PR1P and prednisolone significantly attenuated increases in TNBS-induced ulcer length and colon wall thickness (Figure 3C) (Note the grades of Ulcer Lengths and Colon Wall Thickness in the control groups (i.e.-TNBS) are not visible in the graphs because their values are 0). Further macroscopic analysis and grading of the colons revealed that both high-dose PR1P and prednisolone significantly reduced TNBS-induced effects on adhesions, strictures, ulcers, and colon wall thickness (Figure 3D, note that each condition is graded 0-2, see Methods). Importantly, both low- and high-dose PR1P, and prednisolone significantly reduced the overall Colonic Score (Sums of the above conditions, Maximum score of 12, see Methods). These results suggest that PR1P significantly reduces critical disease indices following exposure to TNBS in rats.

PR1P reduces inflammation in TNBS-induced rat colitis

To characterize the anti-inflammatory therapeutic potential of PR1P in TNBS-induced colitis, we quantified plasma levels of the pro-inflammatory mediators IL-1β, IL-6 and TNF-α on Day 7 following necropsy. As shown in Figures 4A-C, PR1P and prednisolone significantly reduced the TNBS-induced increases in plasma IL-1β and IL-6. Interestingly, high-dose PR1P treatment of

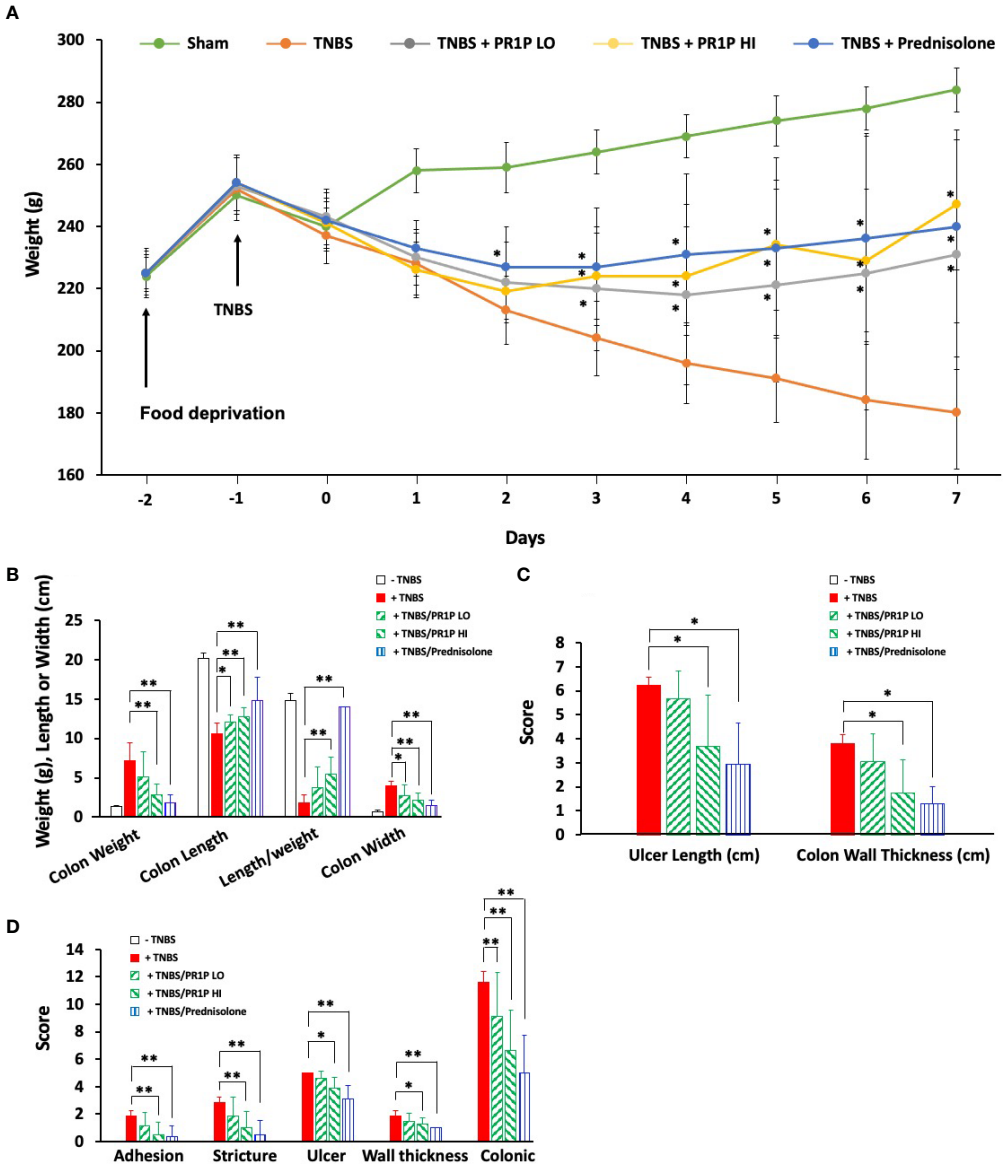

FIGURE 3
PR1P improves disease outcome parameters in TNBS-induced colitis in rats. **(A)** Line graph showing average daily weights of rats treated with daily low-dose PR1P (0.5 mg/kg IP, TNBS + PR1P LO) or high-dose PR1P (5 mg/kg IP, TNBS + PR1P HI) or prednisolone (10 mg/kg po, TNBS + Prednisolone) following induction of colitis from administration of intra-rectal TNBS. Sham animals received intra-rectal 50% ethanol (vehicle) to induce colitis and no treatments. TNBS group (+TNBS) received daily treatment with vehicles IP or po. *p<0.001 vs +TNBS group. **(B-D)** Bar graphs showing average colon weight, colon length, length/weight ratio and colon wall thickness **(B)**, *p<0.03, **p<0.004), ulcer length and colon wall thickness (**C**, *p<0.005) and average scores for adhesions, strictures, ulcer, wall thickness and colonic score using scoring system described in methods (**D**, *p<0.05, **p<0.009) from indicated treatment groups at the end of experiments described in **(A)**. Data in **(A-D)** are mean ± SEM. n=8 animals per group.

TNBS-exposed animals led to a significant increase in plasma TNF-α (see Discussion). Together these results suggest that PR1P mediates the serum levels of critical pro-inflammatory cytokines during disease progression in TNBS-induced colitis in rats.

Histopathologic findings in this study were consistent with the TNBS-induced rat colitis model (33), and administration of TNBS was associated with the highest mean histopathology scores for most features, including sub/mucosal inflammation, necrosis, erosion, hemorrhage, transmural inflammation, and serosal granulation tissue (Figure 5A). As shown in Figure 5A, both the low- and high dose PR1P, and prednisolone, significantly reduced the effects of TNBS in our model on many features scored including inflammation, gland loss/necrosis, erosion/ulceration, sub-mucosal hemorrhage, and granulation tissue. Representative images of H&E stained colon sections (Day 7) from naïve animals and those exposed to TNBS and indicated treatment protocols are shown in Figures 5B-E and illustrate the effect of PR1P on disease development. It is known that neutrophil migration into the colon begins immediately after injury, peaks at 24 hours, and drops to approximately 50% and 20% of maximum by days 3 and 10, respectively (43). Representative H&E stained images of colonic tissue sections from animals on Day 7 are shown in Figures 5B-E

and illustrate the changes reported in Figure 5A showing PR1P dose-associated reductions in histopathologic features that are similar to prednisolone treated animals.

Discussion

Here we show that VEGF degradation products generated *via* VEGF proteolysis by neutrophil elastase are chemoattractant to neutrophils. We subsequently characterized the ability of a novel VEGF binding and stabilizing peptide we developed to mediate endogenous VEGF signaling and inflammation in three murine models of acute lung injury and in a rat ulcerative colitis model in which tissue injuries were induced by diverse mechanisms. Importantly, by binding VEGF within the VEGF heparin-binding domain where proteases are known to bind VEGF (44, 45), PR1P prevents VEGF degradation (46). As we hypothesized, PR1P reduced neutrophil migration into injured tissue and reduced local inflammation following tissue injury. Our results underscore the importance of VEGF in mediating inflammation following tissue injury, and support its importance in maintaining and restoring tissue to health. Furthermore, these studies support a potential role for PR1P in treating diseases commonly caused by tissue injury and characterized by inflammation and VEGF dysregulation.

We chose ARDS and UC animal models to characterize the ability of PR1P to improve outcome because both these diseases are induced by tissue injury and are characterized by local inflammation and VEGF dysregulation (2, 15, 19). Despite widely disparate injury mechanisms, all four models we tested (LPS, acid, bleomycin and TNBS) are known to result in early neutrophil migration into injured tissue and acute inflammation (47–49). Neutrophils are central to innate immunity (50), and are implicated in the onset and progression of many inflammatory diseases, including ARDS (24) and UC (9, 51). Neutrophils are often the first immune cells to arrive at sites of tissue injury and mediate both the initiation and resolution of the inflammatory response that is crucial in returning injured tissue to health (36). Production and release of pro-inflammatory cytokines including tumor necrosis factor (TNF)-α, interleukin (IL)-1β and interleukin (IL)-6 (52), secreted by a variety of immune cells including neutrophils, macrophages, T- and B- cells, dendritic cells, and vascular endothelial cells (53) also follow tissue injury, and together with the appearance of neutrophils in both ARDS and IBD, are central to the initiation and maintenance of inflammation (53). VEGF dysregulation following tissue injury is due to the release by inflammatory cells, including neutrophils, of serine proteases including elastase and plasmin (54, 55) which degrade VEGF into smaller VEGF isomers (VEGF degradation products, fVEGF) with altered VEGF receptor binding and signaling properties (20, 21). Thus, it is not surprising that injury to most tissues, irrespective of mechanism, results in acute inflammation and VEGF dysregulation.

Although it is well documented that VEGF levels and VEGF signaling are dynamic during both ARDS and IBD: it is not clear how this important growth and angiogenic factor mediates disease outcome during illness (15, 18, 19). ARDS is an acute inflammatory disease resulting from diverse direct and indirect insults to the lungs (1) and is characterized by fulminant acute respiratory failure requiring mechanical ventilation and prolonged ICU admission (3). There are no medicines to cure ARDS, and mortality remains

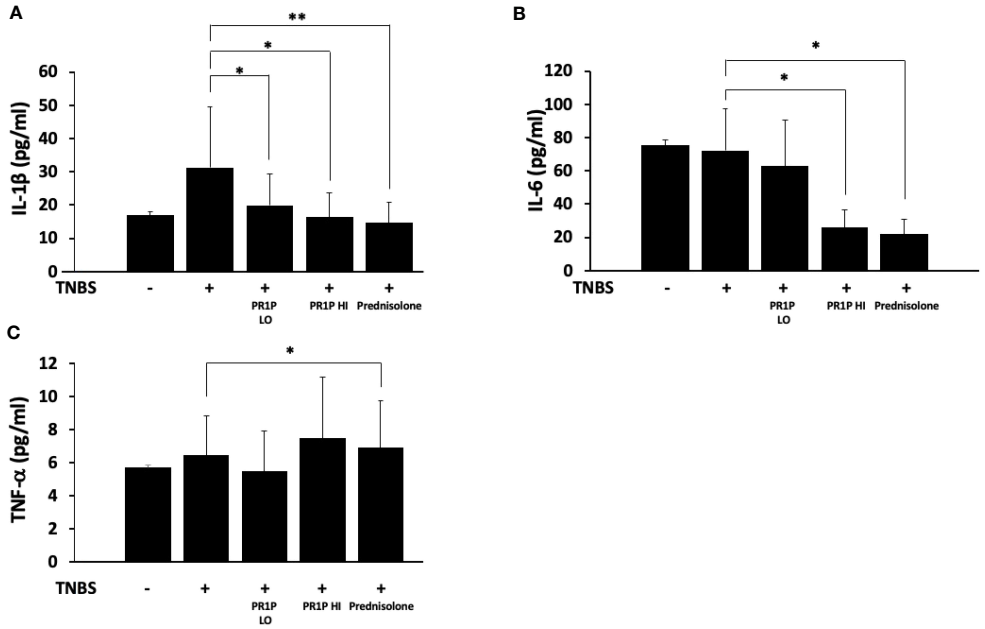

FIGURE 4
PR1P mediates inflammation in TNBS-induced colitis in rats. **(A-C)** Bar graphs showing quantification of IL-1β (**A,** *p<0.03, **p<0.003), IL-6 (**B,** *p<0.0001) and TNF-α (**C,** *p<0.04) in plasma on day 7 in rats treated with daily low-dose PR1P (0.5 mg/kg IP, PR1P-LO) or high-dose PR1P (5 mg/kg IP, PR1P-HI) or prednisolone (10 mg/kg) following induction of colitis from administration of intra-rectal TNBS. Control rats were treated with vehicle only. Data are mean ± SEM. n=8 animals per group.

10.3389/fimmu.2023.1168676

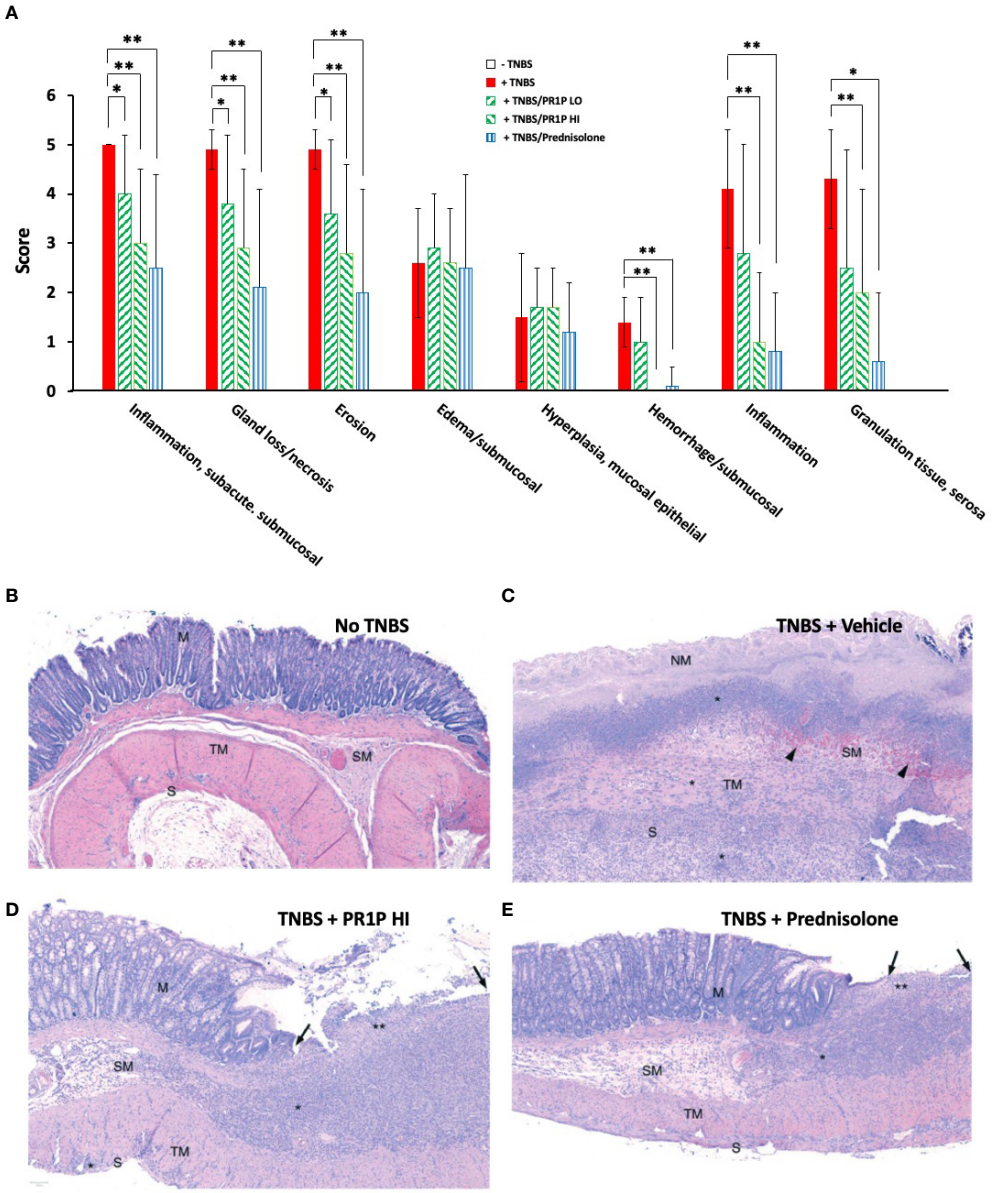

FIGURE 5
PR1P reduces disease and inflammation on histopathology in TNBS-induced colitis in rats. **(A)** Bar graphs showing Average Scores (Score) of indicated lesions from histology sections of the colon of rats 7 days after intra-rectal administration of TNBS (or carrier) and daily treatment of PR1P (0.5 or 5 mg/kg IP) or Prednisolone (10 mg/kg po) as indicated (See Methods), Data are mean + SEM. *p<0.04, **p<0.005. (n=8). **(B-E)** Representative images of H&E stained colon sections (100X) obtained from rats on day 7 following experiments described in **(A)**. **(B)** Representative image from Naïve animal. No histologic lesions observed in captured region. The mucosal glands (M) are within normal limits, as are the submucosa (SM), tunica muscularis externa (TM), and the serosa (S). **(C)** Representative image from animal with TNBS-induced colitis treated with vehicle (TNBS + Vehicle). No normal mucosa remains in captured region; all mucosa exhibits coagulative necrosis (NM: necrotic mucosa), with complete loss of the surface epithelium, consistent with erosion. A thick band of inflammatory cells (*) are visible at the mucosal-submucosal (SM) border. The submucosa is edema-expanded and contains abundant hemorrhage and erythrophagocytic macrophages (black arrowheads). Inflammatory cells (*) also extend transmurally through the tunica musuclaris (TM) and serosa (S) into the serosal granulation tissue visible at the bottom of the image. **(D)** Representative image from animal with TNBS-induced colitis treated with high dose PR1P (5 mg/kg, TNBS + PR1P HI). The right side of the image exhibits inflammatory cell infiltration and gland loss (**) with surface epithelial loss (erosion; black arrows). The adjacent mucosa (M) is hyperplastic, with elongated colonic glands observed. The submucosa (SM) is expanded by edema and inflammatory cell infiltration (*). Very mild extension of inflammation (*) is seen through the tunica muscularis (TM) and into the serosa (S). **(E)** Representative image from animal with TNBS-induced colitis treated with Prednisolone (TNBS + Prednisolone). Inflammatory cell infiltration with gland loss (**) and erosion (black arrows) are mild; the adjacent mucosa (M) exhibits reactive hyperplasia. There is expansion of the submucosa (SM) by edema (clear/pale pink area) and inflammatory cell infiltration (*). Inflammatory cells are generally limited to the mucosal and submucosa with minimal involvement of the tunica muscularis externa (TM) and serosa (S).

high (56). VEGF is widely thought to play a protective role during ARDS progression as VEGF has been shown to mediate the survival of lung airway epithelial cells, and the repair of damaged alveolar capillary membrane barriers thereby reducing pulmonary edema (17, 18). Decreased VEGF levels in the lungs as measured in broncho-alveolar lavage fluid and in exhaled breath condensate (57) of critically ill patients with ARDS are associated with poor prognosis (58, 59). The decline in VEGF levels in the lungs in patients with ARDS is thought to be due to degradation of VEGF by inflammatory cell derived proteases in the alveoli (20, 21). Interestingly, serum concentrations of VEGF increase early in ARDS and return to normal if patients recover (60, 61). This dynamic is thought to be due to release of VEGF from the lungs into the systemic circulation due to impaired epithelial and endothelial barriers (61).

IBD occurs in two forms, ulcerative colitis (UC) and Crohn's disease, which are generally, but not always, distinguished by the portion of the gastrointestinal tract affected by disease (62). IBD is thought to be a consequence of inappropriate and unrelenting activation of the mucosal immune system (63) whereby inflammatory cells including neutrophils, secrete proteases which impair mucosal repair through inhibition of epithelial cell proliferation and through degradation of adhesion and signaling molecules including adherens junction protein, E-cadherin, elastin, collagen, and MMP inhibitors that participate in the maintenance of the intestinal barrier (25, 64–68). In a similar fashion to ARDS, systemic levels of VEGF may elevate during disease due to the release of VEGF from the GI tract from vascular endothelial breakdown (69). Chronic inflammation in IBD is due in part to ongoing production of cytokines by inflammatory cells. There are several drugs available to treat IBD that each target the inflammatory process *via* different mechanisms and include amino-salicylates, corticosteroids, immunomodulators, and anti-TNF-α antibodies. Despite these multiple medical options, proctocolectomy to remove irreversibly diseased intestine is performed in 30% of patients with IBD (9, 70, 71). Thus, the lack of a medical therapy to treat ARDS, and the fact that one-third of patients with IBD do not respond to therapy (71) highlight the need for the development of an alternative therapeutic such as PR1P to treat these common and debilitating diseases that are characterized by inflammation and VEGF dysregulation.

The mechanism of action of PR1P is through its binding to VEGF within the VEGF Heparin Binding Domain (HBD) thereby impeding the binding of VEGF by proteolytic enzymes. In so doing, PR1P prevents degradation of VEGF into fVEGF, which we demonstrate is a neutrophil chemoattractant, and which therefore stimulates further inflammation. It is intriguing that PR1P had opposite effects on TNF-α levels in the lung and GI tract, respectively, at the different timepoints sampled in our models. Cytokines play an important role in dysregulated immune responses and an imbalance between pro- and anti-inflammatory cytokines can have deleterious effects on disease outcome. Patterns of pro- and anti-inflammatory cytokine levels are dynamic over the course of specific diseases and cytokine levels reflect animal- and organ- specific stages of illness. Also, TNF- α was recently shown to have anti-inflammatory properties in a dextran sodium sulfate (DSS)–induced colitis model (72). Regardless of mechanism, results of these studies support our own and point to a critical role for PR1P in mediating inflammation. VEGF therapy involves strategies to deliver VEGF (through direct delivery of VEGF or modified VEGF), or *via* gene therapy to increase local tissue VEGF concentrations (73). Although successful in animal models, VEGF therapy has proven unsuccessful in human studies for many reasons, including that the treatment of acute or chronically inflamed tissue with VEGF likely leads to rapid VEGF degradation and increased local concentrations of fVEGF due to elevated concentration of proteases. This therapeutic approach fails to upregulate VEGF signaling locally and instead likely stimulates further inflammation. Thus, PR1P is fundamentally different than conventional VEGF therapy as PR1P stabilizes endogenous VEGF within local tissue microenvironments, preserves endogenous VEGF signaling, and reduces the production of fVEGF.

As noted, PR1P binds VEGF within the VEGF HBD (46) thereby competing with proteases for binding to VEGF. The HBD is an important carboxy-terminal region on VEGF that plays a critical role in VEGF signaling and therefore may serve as an important target for drug development. Disparities in HBD expression between alternate splice forms of different VEGF isoforms result in subtle variations in downstream signaling (74, 75). For example, proteolytic degradation of the whole or parts of the carboxy-terminal region of the VEGF HBD significantly reduced VEGF-induced mitosis in human vascular endothelial cells (22, 76). Furthermore, Kurtagic et al. showed that neutrophil-derived elastase (NE) cleaved VEGF within internal regions of the N-terminus of VEGF in addition to regions at the C-terminus (20, 21). They subsequently showed that NE generated VEGF fragments (fVEGF) demonstrated higher binding affinity to VEGF Receptor 1 (VEGFR1) compared to VEGFR2 (20, 21) which is significant because VEGFR1 is expressed on neutrophils (77). Thus, in addition to attracting neutrophils into sites of tissue injury, fVEGF also likely upregulates neutrophil activity once present within the inflamed tissue. Collectively, these findings provide key evidence that the VEGF HBD may play a central role in mediating VEGF signaling during both health and in disease. Keyt et al. showed that chronic wounds are associated with a high concentration of proteases, elevated levels of fVEGF, and decreased VEGF activity (44). Treatment of chronic wounds with a mutant VEGF containing a modified HBD that prevents plasmin binding to VEGF resulted in increased VEGF stability within the wound that resulted in increased angiogenesis (in surrounding wound tissue) and improved wound healing (44). It is well known that VEGF signaling controls a wide variety of biological and functional outcomes (78, 79) that are important in maintenance of tissue health and healing (12, 80). Although the signaling and binding properties of fVEGF are not fully elucidated, our data and those of others suggest that fVEGF may serve as a point of convergence in VEGF signaling that may determine whether tissues begin to heal and remodel or remain inflamed.

In summary, we investigated the potential link between neutrophils, often the first immune cell to arrive at the site of tissue injury from multiple disparate direct and indirect insults, and VEGF, a ubiquitous signaling molecule implicated in mediating healing of injured tissues. We discovered that fVEGF, a product of VEGF

degradation by inflammatory cell derived proteases, is chemoattractant to neutrophils. Furthermore, we showed that PR1P, a VEGF binding and stabilizing peptide reduced neutrophil migration into injured tissue and inflammation in animal models of ARDS and UC. PR1P is a distinct alternative to conventional VEGF therapy. Our studies underscore the importance of VEGF in mediating tissue during both health and disease and also point to fVEGF serving as a point of convergence in VEGF signaling that may determine whether tissues begin to heal and remodel or remain inflamed. To date there has been little work done in developing pharmaceuticals for ARDS and UC that target VEGF. Our work suggests that drug development to support PR1P or other molecules targeting fVEGF biology may prove impactful in treating diseases like ARDS or UC that are characterized by VEGF dysregulation and inflammation.

Data availability statement

The raw data supporting the conclusions of this article will be made available by the authors, without undue reservation.

Ethics statement

The animal study was reviewed and approved by Boston Children's Hospital (BCH) Institutional Animal Care and Use Committee (IACUC) Protocol Title: PR1P therapy for murine emphysema 20-05-4174R.

Author contributions

AA and BM designed and performed the experiments, analyzed the data, and wrote the manuscript. VK MP, CK and SL assisted in performing lung's experiments. JB assisted in performing UC experiments. All authors contributed to the article and approved the submitted version.

Conflict of interest

JB was employed by Janus Biotherapeutics, Inc. BM declares that he is currently a medical consultant to Orpheus Inc. which now owns the IP to PR1P.

The remaining authors declare that the research was conducted in the absence of any commercial or financial relationships that could be construed as a potential conflict of interest.

Publisher's note

References

1. Matthay MA, Zemans RL, Zimmerman GA, Arabi YM, Beitler JR, Mercat A, et al. Acute respiratory distress syndrome. *Nat Rev Dis Primers* (2019) 5:18. doi: 10.1038/s41572-019-0069-0

2. Zdravkovic ND, Jovanovic IP, Radosavljevic GD, Arsenijevic AN, Zdravkovic ND, Mitrovic S, et al. Potential dual immunomodulatory role of VEGF in ulcerative colitis and colorectal carcinoma. *Int J Med Sci* (2014) 11:936–47. doi: 10.7150/ijms.8277

3. Banavasi H, Nguyen P, Osman H, Soubani AO. Management of ARDS - what works and what does not. *Am J Med Sci* (2021) 362:13–23. doi: 10.1016/j.amjms.2020.12.019

4. Lynch WD, Hsu R. *StatPearls*. Treasure Island, Florida, USA: StatPearls Publishing LLC (2022).

5. Ferretti F, Cannatelli R, Monico MC, Maconi G, Ardizzone S. An update on current pharmacotherapeutic options for the treatment of ulcerative colitis. *J Clin Med* (2022) 11. doi: 10.3390/jcm11092302

6. Liew PX, Kubes P. The neutrophil's role during health and disease. *Physiol Rev* (2019) 99:1223–48. doi: 10.1152/physrev.00012.2018

7. Beeh KM, Kornmann O, Buhl R, Culpitt SV, Giembycz MA, Barnes PJ, et al. Neutrophil chemotactic activity of sputum from patients with COPD: role of interleukin 8 and leukotriene B4. *Chest* (2003) 123:1240–7. doi: 10.1378/chest.123.4.1240

8. Moldoveanu B, Otmishi P, Jani P, Walker J, Sarmiento X, Guardiola J, et al. Inflammatory mechanisms in the lung. *J Inflammation Res* (2009) 2:1–11.

9. Podolsky DK. Inflammatory bowel disease. *N Engl J Med* (2002) 347:417–29. doi: 10.1056/NEJMra020831

10. Wera O, Lancellotti P, Oury C. The dual role of neutrophils in inflammatory bowel diseases. *J Clin Med* (2016) 5. doi: 10.3390/jcm5120118

11. Frigerio S, Lartey DA, D'Haens GR, Grootjans J. The role of the immune system in IBD-associated colorectal cancer: from pro to anti-tumorigenic mechanisms. *Int J Mol Sci* (2021) 22. doi: 10.3390/ijms222312739

12. Ferrara N. Vascular endothelial growth factor: basic science and clinical progress. *Endocr Rev* (2004) 25:581–611. doi: 10.1210/er.2003-0027

13. Apte RS, Chen DS, Ferrara N. VEGF in signaling and disease: beyond discovery and development. *Cell* (2019) 176:1248–64. doi: 10.1016/j.cell.2019.01.021

14. Ferrara N, Gerber HP, LeCouter J. The biology of VEGF and its receptors. *Nat Med* (2003) 9:669–76. doi: 10.1038/nm0603-669

15. Barratt S, Medford AR, Millar AB. Vascular endothelial growth factor in acute lung injury and acute respiratory distress syndrome. *Respiration* (2014) 87:329–42. doi: 10.1159/000356034

16. Holmes DI, Zachary I. The vascular endothelial growth factor (VEGF) family: angiogenic factors in health and disease. *Genome Biol* (2005) 6:209. doi: 10.1186/gb-2005-6-2-209

17. Medford AR, Millar AB. Vascular endothelial growth factor (VEGF) in acute lung injury (ALI) and acute respiratory distress syndrome (ARDS): paradox or paradigm? *Thorax* (2006) 61:621–6. doi: 10.1136/thx.2005.040204

18. Medford ARL, Godinho SIH, Keen LJ, Bidwell JL, Millar AB. Relationship between vascular endothelial growth factor + 936 genotype and plasma/epithelial lining fluid vascular endothelial growth factor protein levels in patients with and at risk for ARDS. *Chest* (2009) 136:457–64. doi: 10.1378/chest.09-0383

19. Mateescu RB, Bastian AE, Nichita L, Marinescu M, Rouhani F, Voiosu AM, et al. Vascular endothelial growth factor - key mediator of angiogenesis and promising therapeutical target in ulcerative colitis. *Rom J Morphol Embryol* (2017) 58:1339–45.

20. Kurtagic E, Jedrychowski MP, Nugent MA. Neutrophil elastase cleaves VEGF to generate a VEGF fragment with altered activity. *Am J Physiol Lung Cell Mol Physiol* (2009) 296:L534–546. doi: 10.1152/ajplung.90505.2008

21. Kurtagic E, Rich CB, Buczek-Thomas JA, Nugent MA. Neutrophil elastase-generated fragment of vascular endothelial growth factor-a stimulates macrophage and endothelial progenitor cell migration. *PloS One* (2015) 10:e0145115. doi: 10.1371/journal.pone.0145115

22. Lauer G, Sollberg S, Cole M, Flamme I, Sturzebecher J, Mann K, et al. Expression and proteolysis of vascular endothelial growth factor is increased in chronic wounds. *J Invest Dermatol* (2000) 115:12–8. doi: 10.1046/j.1523-1747.2000.00036.x

23. Kawabata K, Hagio T, Matsuoka S. The role of neutrophil elastase in acute lung injury. *Eur J Pharmacol* (2002) 451:1–10. doi: 10.1016/s0014-2999(02)02182-9

24. Grommes J, Soehnlein O. Contribution of neutrophils to acute lung injury. *Mol Med* (2011) 17:293–307. doi: 10.2119/molmed.2010.00138

25. Kuno Y, Ina K, Nishiwaki T, Tsuzuki T, Shimada M, Imada A, et al. Possible involvement of neutrophil elastase in impaired mucosal repair in patients with ulcerative colitis. *J Gastroenterol* (2002) 37 Suppl 14:22–32. doi: 10.1007/BF03326409

26. Adini A, Adini I, Chi ZL, Derda R, Birsner AE, Matthews BD, et al. A novel strategy to enhance angiogenesis *in vivo* using the small VEGF-binding peptide PR1P. *Angiogenesis* (2017) 20:399–408. doi: 10.1007/s10456-017-9556-7

27. Adini A, Wu H, Dao DT, Ko VH, Yu LJ, Pan A, et al. PR1P stabilizes VEGF and upregulates its signaling to reduce elastase induced murine emphysema. *Am J Respir Cell Mol Biol* (2020) 63:452–63. doi: 10.1165/rcmb.2019-0434OC

28. Adini A, Adini I, Grad E, Tal Y, Danenberg HD, Kang PM, et al. The prominin-1-Derived peptide improves cardiac function following ischemia. *Int J Mol Sci* (2021) 22. doi: 10.3390/ijms22105169

29. Chi ZL, Adini A, Birsner AE, Bazinet L, Akula JD, D'Amato RJ, et al. PR1P ameliorates neurodegeneration through activation of VEGF signaling pathway and remodeling of the extracellular environment. *Neuropharmacology* (2019) 148:96–106. doi: 10.1016/j.neuropharm.2018.12.029

30. Yin J, Shi C, He W, Yan W, Deng J, Zhang B, et al. Specific bio-functional CBD-PR1P peptide binding VEGF to collagen hydrogels promotes the recovery of cerebral ischemia in rats. *J BioMed Mater Res A* (2022) 110:1579–89. doi: 10.1002/jbm.a.37409

31. Yuan Z, Sheng D, Jiang L, Shafiq M, Khan AUR, Hashim R, et al. Vascular endothelial growth factor-capturing aligned electrospun Polycaprolactone/Gelatin nanofibers promote patellar ligament regeneration. *Acta Biomater* (2022) 140:233–46. doi: 10.1016/j.actbio.2021.11.040

32. Chen Y, Yuan Z, Sun W, Shafiq M, Zhu J, Chen J, et al. Vascular endothelial growth factor-recruiting nanofiber bandages promote multifunctional skin regeneration *via* improved angiogenesis and immunomodulation. *Advanced Fiber Materials* (2023) 5:327–48. doi: 10.1007/s42765-022-00226-8

33. Antoniou E, Margonis GA, Angelou A, Pikouli A, Argiri P, Karavokyros I, et al. The TNBS-induced colitis animal model: an overview. *Ann Med Surg (Lond)* (2016) 11:9–15. doi: 10.1016/j.amsu.2016.07.019

34. Kawada M, Arihiro A, Mizoguchi E. Insights from advances in research of chemically induced experimental models of human inflammatory bowel disease. *World J Gastroenterol* (2007) 13:5581–93. doi: 10.3748/wjg.v13.i42.5581

35. Morris GP, Beck PL, Herridge MS, Depew WT, Szewczuk MR, Wallace JL, et al. Hapten-induced model of chronic inflammation and ulceration in the rat colon. *Gastroenterology* (1989) 96:795–803. doi: 10.1016/S0016-5085(89)80079-4

36. Selders GS, Fetz AE, Radic MZ, Bowlin GL. An overview of the role of neutrophils in innate immunity, inflammation and host-biomaterial integration. *Regener Biomater* (2017) 4:55–68. doi: 10.1093/rb/rbw041

37. Chen H, Bai C, Wang X. The value of the lipopolysaccharide-induced acute lung injury model in respiratory medicine. *Expert Rev Respir Med* (2010) 4:773–83. doi: 10.1586/ers.10.71

38. Ge V, Banakh I, Tiruvoipati R, Haji K. Bleomycin-induced pulmonary toxicity and treatment with infliximab: a case report. *Clin Case Rep* (2018) 6:2011–4. doi: 10.1002/ccr3.1790

39. Zarbock A, Singbartl K, Ley K. Complete reversal of acid-induced acute lung injury by blocking of platelet-neutrophil aggregation. *J Clin Invest* (2006) 116:3211–9. doi: 10.1172/JCI29499

40. Eijking EP, Gommers D, So KL, Vergeer M, Lachmann B. Surfactant treatment of respiratory failure induced by hydrochloric acid aspiration in rats. *Anesthesiology* (1993) 78:1145–51. doi: 10.1097/00000542-199306000-00019

41. Goldman G, Welbourn R, Kobzik L, Valeri CR, Shepro D, Hechtman HB, et al. Reactive oxygen species and elastase mediate lung permeability after acid aspiration. *J Appl Physiol (1985)* (1992) 73:571–5. doi: 10.1152/jappl.1992.73.2.571

42. Nagase T, Uozumi N, Ishii S, Kume K, Izumi T, Ouchi Y, et al. Acute lung injury by sepsis and acid aspiration: a key role for cytosolic phospholipase A2. *Nat Immunol* (2000) 1:42–6. doi: 10.1038/76897

43. van Lierop PP, de Haar C, Lindenbergh-Kortleve DJ, Simons-Oosterhuis Y, van Rijt LS, Lambrecht BN, et al. T-Cell regulation of neutrophil infiltrate at the early stages of a murine colitis model. *Inflammation Bowel Dis* (2010) 16:442–51. doi: 10.1002/ibd.21073

44. Keyt BA, Berleau LT, Nguyen HV, Chen H, Heinsohn H, Vandlen R, et al. The carboxyl-terminal domain (111-165) of vascular endothelial growth factor is critical for its mitogenic potency. *J Biol Chem* (1996) 271:7788–95. doi: 10.1074/jbc.271.13.7788

45. Roth D, Piekarek M, Paulsson M, Christ H, Bloch W, Krieg T, et al. Plasmin modulates vascular endothelial growth factor-a-mediated angiogenesis during wound repair. *Am J Pathol* (2006) 168:670–84. doi: 10.2353/ajpath.2006.050372

46. Adini A, Wu H, Dao DT, Ko VH, Yu LJ, Pan A, et al. PR1P stabilizes VEGF and upregulates its signaling to reduce elastase-induced murine emphysema. *Am J Respir Cell Mol Biol* (2020) 63:452–63. doi: 10.1165/rcmb.2019-0434OC

47. Wilson MS, Wynn TA. Pulmonary fibrosis: pathogenesis, etiology and regulation. *Mucosal Immunol* (2009) 2:103–21. doi: 10.1038/mi.2008.85

48. Fournier BM, Parkos CA. The role of neutrophils during intestinal inflammation. *Mucosal Immunol* (2012) 5:354–66. doi: 10.1038/mi.2012.24

49. Van de Louw A, Jean D, Frisdal E, Cerf C, d'Ortho MP, Baker AH, et al. Neutrophil proteinases in hydrochloric acid- and endotoxin-induced acute lung injury: evaluation of interstitial protease activity by *in situ* zymography. *Lab Invest* (2002) 82:133–45. doi: 10.1038/labinvest.3780406

50. Kraus RF, Gruber MA. Neutrophils-from bone marrow to first-line defense of the innate immune system. *Front Immunol* (2021) 12:767175. doi: 10.3389/fimmu.2021.767175

51. Camba-Gomez M, Arosa L, Gualillo O, Conde-Aranda J. Chemokines and chemokine receptors in inflammatory bowel disease: recent findings and future perspectives. *Drug Discovery Today* (2022) 27:1167–75. doi: 10.1016/j.drudis.2021.12.004

52. Donnelly SC, MacGregor I, Zamani A, Gordon MW, Robertson CE, Steedman DJ, et al. Plasma elastase levels and the development of the adult respiratory distress syndrome. *Am J Respir Crit Care Med* (1995) 151:1428–33. doi: 10.1164/ajrccm.151.5.7735596

53. Kany S, Vollrath JT, Relja B. Cytokines in inflammatory disease. *Int J Mol Sci* (2019) 20. doi: 10.3390/ijms20236008

54. Bank U, Ansorge S. More than destructive: neutrophil-derived serine proteases in cytokine bioactivity control. *J Leukoc Biol* (2001) 69:197–206. doi: 10.1189/jlb.69.2.197

55. Lee KH, Lee CH, Jeong J, Jang AH, Yoo CG. Neutrophil elastase differentially regulates interleukin 8 (IL-8) and vascular endothelial growth factor (VEGF) production by cigarette smoke extract. *J Biol Chem* (2015) 290:28438–45. doi: 10.1074/jbc.M115.663567

56. Nanchal RS, Truwit JD. Recent advances in understanding and treating acute respiratory distress syndrome. *F1000Res* (2018) 7. doi: 10.12688/f1000research.15493.1

57. Chen J, Lv X, He H, Qi F, Chen J. Significance of vascular endothelium growth factor testing in exhaled breath condensate of patients with acute respiratory distress syndrome. *Technol Health Care* (2020) 28:347–54. doi: 10.3233/THC-209035

58. Abadie Y, Bregeon F, Papazian L, Lange F, Chailley-Heu B, Thomas P, et al. Decreased VEGF concentration in lung tissue and vascular injury during ARDS. *Eur Respir J* (2005) 25:139–46. doi: 10.1183/09031936.04.00065504

59. Maitre B, Boussat S, Jean D, Gouge M, Brochard L, Housset B, et al. Vascular endothelial growth factor synthesis in the acute phase of experimental and clinical lung injury. *Eur Respir J* (2001) 18:100–6. doi: 10.1183/09031936.01.00074701

60. Tomita K, Saito Y, Suzuki T, Imbaby S, Hattori K, Matsuda N, et al. Vascular endothelial growth factor contributes to lung vascular hyperpermeability in sepsis-associated acute lung injury. *Naunyn Schmiedebergs Arch Pharmacol* (2020) 393:2365–74. doi: 10.1007/s00210-020-01947-6

61. Thickett DR, Armstrong L, Christie SJ, Millar AB. Vascular endothelial growth factor may contribute to increased vascular permeability in acute respiratory distress syndrome. *Am J Respir Crit Care Med* (2001) 164:1601–5. doi: 10.1164/ajrccm.164.9.2011071

62. McDowell C, Farooq U, Haseeb M. *StatPearls*. Treasure Island, Florida, USA: StatPearls Publishing LLC (2022).

63. Keighley MR, Stockbrugger RW. Inflammatory bowel disease. *Aliment Pharmacol Ther* (2003) 18 Suppl 3:66–70. doi: 10.1046/j.0953-0673.2003.01727.x

64. Ginzberg HH, Cherapanov V, Dong Q, Cantin A, McCulloch CA, Shannon PT, et al. Neutrophil-mediated epithelial injury during transmigration: role of elastase. *Am J Physiol Gastrointest Liver Physiol* (2001) 281:G705–717. doi: 10.1152/ajpgi.2001.281.3.G705

65. Ginzberg HH, Shannon PT, Suzuki T, Hong O, Vachon E, Moraes T, et al. Leukocyte elastase induces epithelial apoptosis: role of mitochondial permeability changes and akt. *Am J Physiol Gastrointest Liver Physiol* (2004) 287:G286–298. doi: 10.1152/ajpgi.00350.2003

66. Morohoshi Y, Matsuoka K, Chinen H, Kamada N, Sato T, Hisamatsu T, et al. Inhibition of neutrophil elastase prevents the development of murine dextran sulfate sodium-induced colitis. *J Gastroenterol* (2006) 41:318–24. doi: 10.1007/s00535-005-1768-8

67. Geraghty P, Rogan MP, Greene CM, Boxio RM, Poiriert T, O'Mahony M, et al. Neutrophil elastase up-regulates cathepsin b and matrix metalloprotease-2 expression. *J Immunol* (2007) 178:5871–8. doi: 10.4049/jimmunol.178.9.5871

68. Gordon MH, Chauvin A, Boisvert FM, MacNaughton WK. Proteolytic processing of the epithelial adherens junction molecule e-cadherin by neutrophil elastase generates short peptides with novel wound-healing bioactivity. *Cell Mol Gastroenterol Hepatol* (2019) 7:483–486 e488. doi: 10.1016/j.jcmgh.2018.10.012

69. Staels W, Heremans Y, Heimberg H, De Leu N. VEGF-a and blood vessels: a beta cell perspective. *Diabetologia* (2019) 62:1961–8. doi: 10.1007/s00125-019-4969-z

70. McLean MH, Neurath MF, Durum SK. Targeting interleukins for the treatment of inflammatory bowel disease-what lies beyond anti-TNF therapy? *Inflammation Bowel Dis* (2014) 20:389–97. doi: 10.1097/01.MIB.0000437616.37000.41

71. Bernstein CN. Treatment of IBD: where we are and where we are going. *Am J Gastroenterol* (2015) 110:114–26. doi: 10.1038/ajg.2014.357

72. Naito Y, Takagi T, Handa O, Ishikawa T, Nakagawa S, Yamaguchi T, et al. Enhanced intestinal inflammation induced by dextran sulfate sodium in tumor necrosis

factor-alpha deficient mice. *J Gastroenterol Hepatol* (2003) 18:560–9. doi: 10.1046/j.1440-1746.2003.03034.x

73. Jones MK, Kawanaka H, Baatar D, Szabo IL, Tsugawa K, Pai R, et al. Gene therapy for gastric ulcers with single local injection of naked DNA encoding VEGF and angiopoietin-1. *Gastroenterology* (2001) 121:1040–7. doi: 10.1053/gast.2001.29308

74. Park JE, Keller GA, Ferrara N. The vascular endothelial growth factor (VEGF) isoforms: differential deposition into the subepithelial extracellular matrix and bioactivity of extracellular matrix-bound VEGF. *Mol Biol Cell* (1993) 4:1317–26. doi: 10.1091/mbc.4.12.1317

75. Carmeliet P, Ng YS, Nuyens D, Theilmeier G, Brusselmans K, Cornelissen I, et al. Impaired myocardial angiogenesis and ischemic cardiomyopathy in mice lacking the vascular endothelial growth factor isoforms VEGF164 and VEGF188. *Nat Med* (1999) 5:495–502. doi: 10.1038/8379

76. Lauer G, Sollberg S, Cole M, Krieg T, Eming SA. Generation of a novel proteolysis resistant vascular endothelial growth factor165 variant by a site-directed mutation at the plasmin sensitive cleavage site. *FEBS Lett* (2002) 531:309–13. doi: 10.1016/S0014-5793(02)03545-7

77. Massena S, Christoffersson G, Vagesjo E, Seignez C, Gustafsson K, Binet F, et al. Identification and characterization of VEGF-a-responsive neutrophils expressing CD49d, VEGFR1, and CXCR4 in mice and humans. *Blood* (2015) 126:2016–26. doi: 10.1182/blood-2015-03-631572

78. Shibuya M. Structure and function of VEGF/VEGF-receptor system involved in angiogenesis. *Cell Struct Funct* (2001) 26:25–35. doi: 10.1247/csf.26.25

79. Ferrara N. Vascular endothelial growth factor and the regulation of angiogenesis. *Recent Prog Horm Res* (2000) 55:15–35; discussion 35-16.

80. Senger DR, Ledbetter SR, Claffey KP, Papadopoulos-Sergiou A, Peruzzi CA, Detmar M. Stimulation of endothelial cell migration by vascular permeability factor/vascular endothelial growth factor through cooperative mechanisms involving the alphavbeta3 integrin, osteopontin, and thrombin. *Am J Pathol* (1996) 149:293–305.

frontiers | Frontiers in Immunology

TYPE Original Research
PUBLISHED 28 April 2023
DOI 10.3389/fimmu.2023.1134178

OPEN ACCESS

EDITED BY
Teresa Bellon,
University Hospital La Paz Research Institute (IdiPAZ), Spain

REVIEWED BY
Lukas Jörg,
Insel Gruppe AG, Switzerland
Philippe Guilpain,
Université de Montpellier, France

*CORRESPONDENCE
Oded Shamriz
oded.shamriz@mail.huji.ac.il
Yuval Tal
yuvalt@hadassah.org.il

†These authors have contributed equally to this work and share first authorship

RECEIVED 30 December 2022
ACCEPTED 10 April 2023
PUBLISHED 28 April 2023

CITATION
Rubin L, Talmon A, Ribak Y, Kessler A, Martin Y, Haran TK, Shamriz O, Adini I and Tal Y (2023) Novel targeted inhibition of the IL-5 axis for drug reaction with eosinophilia and systemic symptoms syndrome.
Front. Immunol. 14:1134178.
doi: 10.3389/fimmu.2023.1134178

Novel targeted inhibition of the IL-5 axis for drug reaction with eosinophilia and systemic symptoms syndrome

Limor Rubin[1†], Aviv Talmon[1†], Yaarit Ribak[1], Asa Kessler[2], Yossi Martin[3], Tal Keidar Haran[4], Oded Shamriz[1,5*], Irit Adini[6] and Yuval Tal[1*]

[1]Allergy and Clinical Immunology Unit, Department of Medicine, Hadassah Medical Organization, Faculty of Medicine, Hebrew University of Jerusalem, Jerusalem, Israel, [2]Department of Medicine, Hadassah Medical Organization, Faculty of Medicine, Hebrew University of Jerusalem, Jerusalem, Israel, [3]Psychiatric Department, Hadassah Medical Organization, Faculty of Medicine, Hebrew University of Jerusalem, Jerusalem, Israel, [4]Department of Pathology, Hadassah Medical Organization, Faculty of Medicine, Hebrew University of Jerusalem, Jerusalem, Israel, [5]The Lautenberg Center for Immunology and Cancer Research, Institute of Medical Research Israel-Canada, Faculty of Medicine, Hebrew University of Jerusalem, Jerusalem, Israel, [6]Department of Surgery, Center for Engineering in Medicine and Surgery, Massachusetts General Hospital, Harvard Medical School, Boston, MA, United States

Background: The drug reaction with eosinophilia and systemic symptoms (DRESS) syndrome represents a severe hypersensitivity reaction. Up-to-date treatment is based on withdrawal of medication, supportive care, and immunosuppression using high-dose corticosteroid (CS) therapy. However, evidence-based data are lacking regarding second-line therapy for steroid-resistant or steroid-dependent patients.

Objectives: We hypothesize that the interleukin (IL)-5 axis plays a critical role in the pathophysiology of DRESS; hence, inhibition of this signaling pathway could offer a potential therapy for steroid-dependent and/or steroid-resistant cases, and it may offer an alternative to CS therapy in certain patients more prone to CS toxicity.

Methods: Herein, we collected worldwide data on DRESS cases treated with biological agents targeting the IL-5 axis. We reviewed all cases indexed in PubMed up to October 2022 and performed a total analysis including our center experience with two additional novel cases.

Results: A review of the literature yielded 14 patients with DRESS who were treated with biological agents targeting the IL-5 axis as well as our two new cases. Reported patients are characterized by a female-to-male ratio of 1:1 and a mean age of 51.8 (17–87) years. The DRESS-inducing drugs, as expected from the prospective RegiSCAR study, were mostly antibiotics (7/16), as follows: vancomycin, trimethoprim-sulfamethoxazole, ciprofloxacin, piperacillin-tazobactam, and cefepime. DRESS patients were treated with anti-IL-5 agents (mepolizumab and reslizumab) or anti-IL-5 receptor (IL-5R) biologics (benralizumab). All patients have clinically improved under anti-IL-5/IL-5R

biologics. Multiple doses of mepolizumab were needed to achieve clinical resolution, whereas a single dose of benralizumab was often sufficient. Relapse was noted in one patient receiving benralizumab treatment. One patient receiving benralizumab had a fatal outcome, although mortality was probably related to massive bleeding and cardiac arrest due to coronavirus disease 2019 (COVID-19) infection.

Conclusion: Current treatment guidelines for DRESS are based on case reports and expert opinion. Understanding the central role of eosinophils in DRESS pathogenicity emphasizes the need for future implementation of IL-5 axis blockade as steroid-sparing agents, potential therapy to steroid-resistant cases, and perhaps an alternative to CS treatment in certain DRESS patients more prone to CS toxicity.

KEYWORDS

drug reaction with eosinophilia and systemic symptoms (DRESS), interleukin (IL), monoclonal antibodies (mAbs), IL-5 antibody, biotherapeutic agent

1 Introduction

Drug reaction with eosinophilia and systemic symptoms (DRESS), also known as drug-induced hypersensitivity syndrome, is a severe type of intravenous cutaneous drug-induced eruption accompanied by visceral organ involvement, most commonly the liver. The prognosis of patients with DRESS is linked to the severity of visceral involvement, with an approximate mortality rate of 2%–10% mainly due to liver failure (1).

The pathophysiology is multifactorial and associated with drug metabolism, specific human leukocyte antigen (HLA), and viral reactivation especially of the human Herpesviridae (HHV) family. The immunological response directed against viral reactivation and/or culprit drug precipitating the disease includes $CD4^+$ and $CD8^+$ T-cell activation and hence the development of a cytokine cascade with the production of interleukin (IL)-5, IL-4, IL-13, IL-17, IL-25, and eotaxin-1 (2). In addition, dermal dendritic cells, endothelial cells, and monomyelocytes secrete thymus activation-regulated chemokine (TARC/CCL17), IL-33, transforming growth factor β, and thymic stromal lymphopoietin. These chemokines, in synergy with IL-5, promote eosinophil chemoattraction, activation, proliferation, and infiltration and hence result in eosinophilic inflammation and tissue damage (3) (Figure 1).

Consequently, patients with DRESS present with increased eosinophil levels in the blood, skin, and involved organs. The diagnosis of DRESS is based on clinical and biological criteria as calculated by the RegiSCAR score, such as fever >38°C, acute rash, lymphadenopathy, internal organ involvement, and blood count abnormalities including atypical lymphocytes and eosinophilia, found in 80% of patients (4). There are no randomized trials evaluating treatments for DRESS following the withdrawal of the culprit drug. The current mainstay of treatment is topical and systemic corticosteroids (CSs) (5).

During the last 5 years, limited reports of DRESS patients who were treated with immunotherapy inhibiting the IL-5 axis were presented. Maverakis et al. (6) were the first to describe the potential advantages of anti-IL-5/anti-IL-5 receptor (IL-5R) monoclonal antibodies (mAbs) over current therapies to DRESS patients, emphasizing the rapid onset, once-monthly dosing, and safety, with avoidance of the immunosuppressive and metabolic adverse events of prolonged high-dose systemic CSs. Recently, Gschwend et al. (7) reviewed 14 patients with DRESS who were treated with mAbs inhibiting the IL-5 axis. Patients were reported to have been successfully treated with the anti-IL-5 agents mepolizumab (7–11) and reslizumab (12), as well as the anti-IL-5R agent benralizumab (7, 13–15).

Herein, we aimed to present our experience with two new cases and conduct a literature review as a proof of concept to the hypothesis that IL-5 inhibition offers an efficient and safe therapeutic strategy for specific cases of DRESS.

2 Methods

2.1 Study design and patients

This is a retrospective analysis of computerized medical records of patients who were diagnosed with DRESS and treated with IL-5 modulation in the period of February to September 2022. Patients were diagnosed and treated at the Division of Medicine, Hadassah Medical Center, Jerusalem, Israel. Data regarding clinical manifestations, treatments, and outcomes were retrieved from the files and analyzed.

Abbreviations: CS, corticosteroid; DRESS, drug reaction with eosinophilia and systemic symptoms; ECT, electroconvulsive therapy; ER, emergency room; IL, interleukin; i.v., intravenous; IVIG, intravenous immunoglobulin; LFT, liver function test; mAbs, monoclonal antibodies; SC, subcutaneous; CT, computerized tomography.

10.3389/fimmu.2023.1134178

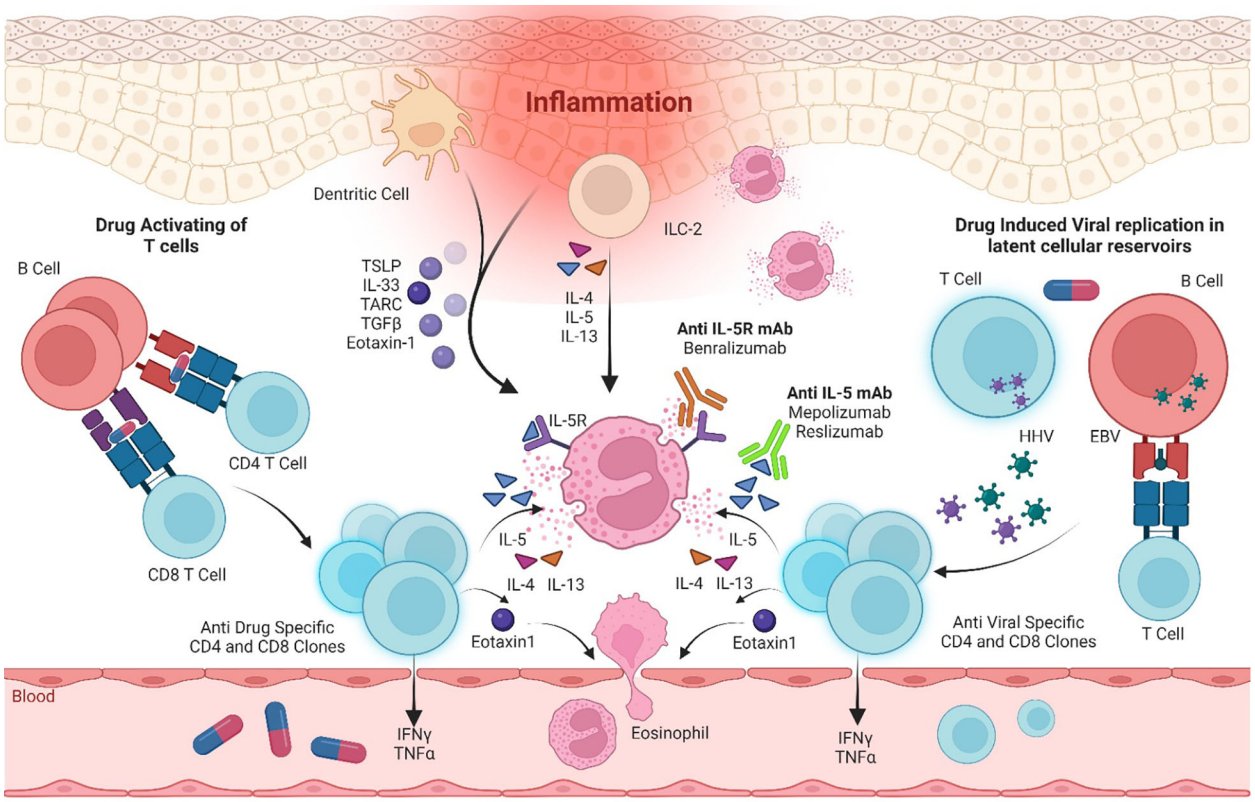

FIGURE 1
Immunological pathways in DRESS pathogenesis and immunotherapy targeted inhibition of the IL-5 axis. IL, interleukin; IL-5R, interleukin-5 receptor; mAb, monoclonal antibody; EBV, Epstein–Barr virus; HHV, Herpesviridae virus; ILC-2, Type 2 innate lymphoid cells; TSLP, thymic stromal lymphopoietin; TARC, thymus- and activation-regulated chemokine; TGFβ, transforming growth factor β; IFN-γ, interferon γ; TNFα, tumor necrosis factor α.

2.2 Systematic review of the literature

In addition, we conducted a systematic review of the literature concerning patients with DRESS who were treated with IL-5-inhibiting mAbs. We used PubMed for data search. Keywords included "DRESS" and ("IL-5" or "benralizumab" or "mepolizumab" or "reslizumab"). Inclusion criteria consisted of English-language reports of DRESS patients who were treated with mAbs targeting the IL-5 axis and published in the period of May 2018 to October 2022. Only studies in which the DRESS diagnosis was based on the RegiSCAR score were included (Supplementary Table S1) (4). This score is available in Supplementary Table S1. Studies with a misdiagnosis of DRESS or a limited availability of full text were excluded. Data were analyzed for the clinical presentation, course, and outcome.

2.3 Ethical considerations

The reported patients from our medical center have signed a written informed consent for the publication of their clinical data.

3 Results

3.1 Patient description

Our search yielded two female patients (17 and 59 years old) who were admitted to our medical center within the study period. A summary of their clinical characteristics is presented in Table 1. Patient (P)1 presented with rash, hepatitis, fever, eosinophilia, and lymphadenopathy induced by olanzapine. She was CS-resistant, and subcutaneous (s.c.) mepolizumab was initiated as a single dose of 300 mg. P2 developed rash, eosinophilia, fever, hepatitis, and acute kidney injury following treatment with vancomycin. She was treated with s.c. benralizumab 30 mg. Both patients have demonstrated clinical resolution of their symptoms following IL-5 inhibitory treatment without recurrence in a follow-up of 10–12 months. The trend of hepatocellular liver enzyme levels and absolute eosinophil counts of P1 following treatments with CSs and mepolizumab is presented in Figure 2. The clinical presentation and skin histopathology of P1 and P2 are presented in Figure 3. The full clinical and laboratory description of the two patients is presented in the Supplementary Material.

10.3389/fimmu.2023.1134178

TABLE 1 Clinical characteristics of DRESS patients treated with IL-5-inhibiting biologics.

Patient	Age (years)	Sex	Ethnicity	Medical history	Offending drug	Clinical manifestations of DRESS	RegiSCAR DRESS score	Maximal eosinophil count (cells/ml)	Histopathology	Treatment	IL-5-modulating treatment	Indications for anti-IL-5/IL-5R biologics	Outcome	Follow-up (months)
P1	17	F	J	Psychosis	Olanzapine	Rash, hepatitis, fever, eosinophilia, lymphadenopathy	6	1,620	Skin biopsy suggestive of DRESS	CS	Mepolizumab 300 mg, s.c. single dose	CS-resistant, avoid steroid toxicity	Complete resolution of relapsing DRESS syndrome and complete weaning from CSs	12
P2	59	F	J	HTN	Vancomycin	Rash, eosinophilia, fever, hepatitis, acute kidney injury	7	1,600	Skin biopsy suggestive of DRESS	CS	Benralizumab 30 mg s.c. single dose	First-line treatment to avoid steroid toxicity	Complete resolution of relapsing DRESS syndrome and complete weaning from CSs	10

F, female; J, Jew; HTN, hypertension; anti-IL-5R, anti-interleukin-5 receptor; CSs, corticosteroids; s.c., subcutaneous.

3.2 Literature review

A review of the literature yielded 14 patients with DRESS who were treated with biological agents targeting the IL-5 axis (Table 2). The first case was reported on May 2018. Nine studies that met the inclusion criteria (7–15) and our two clinical cases were included in the analysis. The reported patients are characterized by a female-to-male ratio of 1:1 and a mean age of 51.8 (17–87) years. The DRESS-inducing drugs, as expected from the prospective RegiSCAR study, were mostly antibiotics (7/16), as follows: vancomycin, trimethoprim-sulfamethoxazole, ciprofloxacin, piperacillin-tazobactam, and cefepime. The DRESS patients were treated with anti-IL-5 agents (mepolizumab and reslizumab) or anti-IL-5R biologics (benralizumab).

3.2.1 Reslizumab

Reslizumab was administered in one 62-year-old woman with imatinib-induced DRESS (12). Her RegiSCAR DRESS score was 3, and histopathology was not available when confirming the DRESS diagnosis. Reslizumab treatment has enabled complete resolution of the patient's symptoms, facilitated desensitization, and succeeded in safely maintaining the drug imatinib treatment for 2 years.

3.2.2 Mepolizumab

Six DRESS patients were treated with mepolizumab (7–11). The mean (range) age of the patients was 50.8 (17–70) years. The RegiSCAR score calculated ranged between 5 and 7. Four out of seven patients had histopathologic evidence supporting eosinophilic inflammation. Five out of seven DRESS patients treated with mepolizumab need two or more doses, and only two have clinically improved following a single dose. All patients received concurrent CS therapy, one received additional therapy with intravenous immunoglobulin (IVIG), and two received concurrent immunosuppressant therapy with cyclosporine and one with cyclophosphamide. The clinical indication for the initiation of anti-IL-5-targeted therapy was due to steroid resistance and dependence in three and two patients, respectively. In one patient, IL-5-blocking agents were initiated to avoid CS toxicity.

All patients responded with complete resolution of DRESS symptoms, laboratory recovery, and complete weaning off from steroid therapy. Relapse was noted in one patient.

3.2.3 Benralizumab

Seven DRESS patients were treated with benralizumab (7,13–15). The mean patient age was 68.7 (34–87) years. The RegiSCAR score ranged from 5 to 8. All patients receiving benralizumab had histopathology supporting tissue eosinophilic infiltration. The indication for benralizumab initiation was CS resistance in all patients. Two patients required two or more doses. Relapse was noted in one patient receiving benralizumab treatment (15). Moreover, one patient had a fatal outcome, although mortality was probably related to massive bleeding and cardiac arrest due to coronavirus disease 2019 (COVID-19) infection (13).

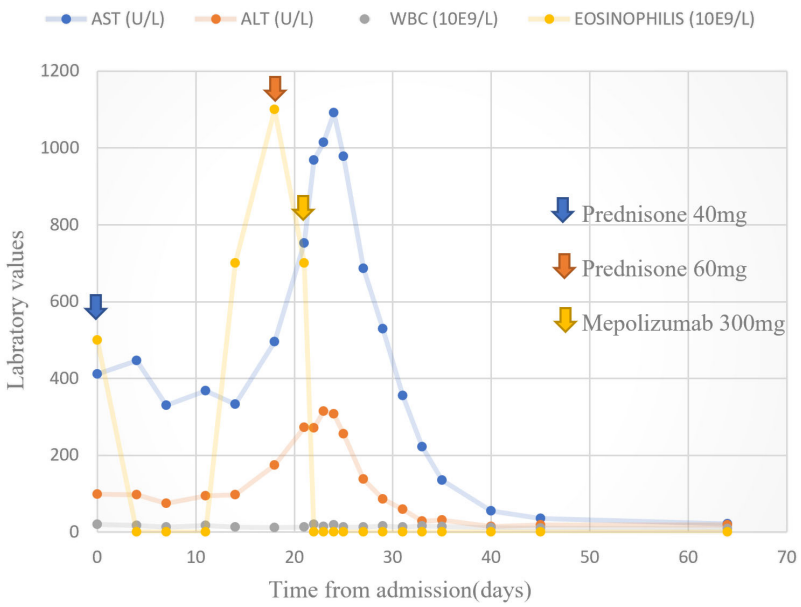

FIGURE 2
Hepatocellular liver enzymes and absolute eosinophil count. Trend of hepatocellular liver enzymes and absolute eosinophil counts following treatments with prednisone and mepolizumab in patient 1.

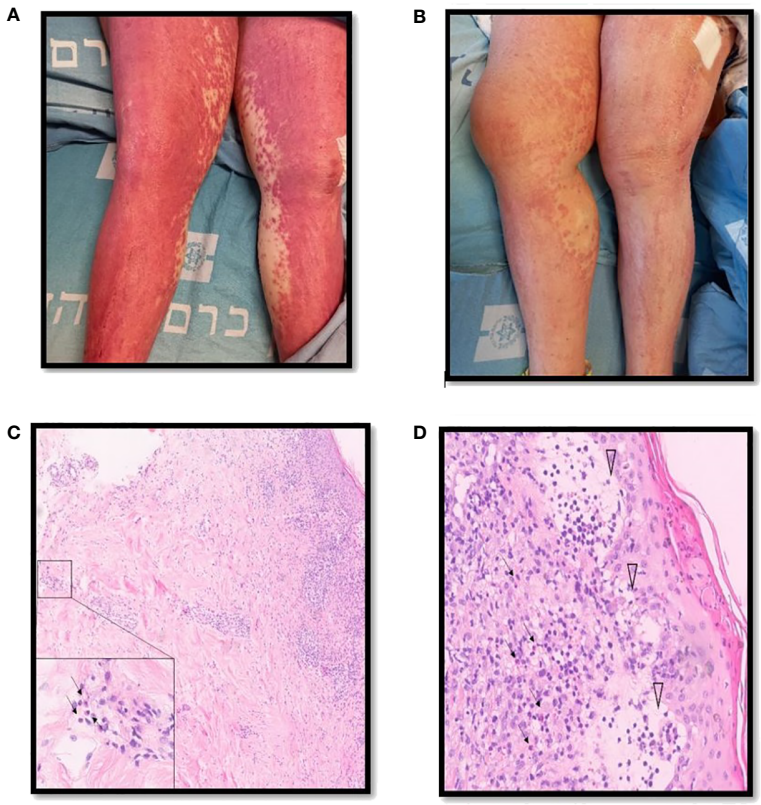

FIGURE 3
Clinical description and skin histopathology of the patients. **(A)** Clinical presentation of DRESS in patient 2 consisting of diffuse erythematous rash involving the lower limbs. **(B)** One week following benralizumab therapy, partial resolution of the skin rash. **(C)** Punch biopsy of skin consisting of hematoxylin and eosin stain demonstrating changes compatible with the clinical diagnosis of DRESS, most notably an inflammatory infiltrate composed of lymphocytes and numerous eosinophils stretching from the epidermis to the deep dermis in ×10 magnification. The inset demonstrates eosinophils present in the deep dermis in ×100 magnification (arrows). **(D)** Secondary changes including parakeratosis and interstitial edema with blister formation in the papillary dermis (arrowheads) in ×40 magnification.

TABLE 2 Clinical characterizations of the DRESS patients treated off-label with monoclonal antibodies of the IL-5 axis.

Biological therapy/ mechanism	No. of patients	Gender	Age (years)	RegiSCAR DRESS score [a]	Histopathology	Drug inducing DRESS	IL-5 axis treatment regimen (Indication)	Additional combined, adjunct treatment	Outcome	Ref.
Reslizumab/ /anti-IL-5 IgG4κ monoclonal antibody	1	F	62	3	NA	Imatinib	Initial dose 100 mg i.v. 2 weeks later, a second dose of 200 mg i.v. (CS-dependent, desensitization)	Prednisolone, antihistamine Dexamethasone [g]	Complete resolution of symptoms. Reslizumab enabled desensitization to safely maintain imatinib treatment for 2 years.	(12)
Mepolizumab /anti- IL-5 IgG1κ monoclonal antibody	1	F	17	6	**Skin Biopsy**- Suggestive of DRESS	Olanzapine	Single loading dose 300 mg s.c. (CS-dependent)	Hydrocortisone followed by prednisone	Complete resolution of relapsing DRESS syndrome and complete weaning from CSs; **f/o**- 6 months symptom-free	Current report
	1	F	56	6	**Skin biopsy**- a spongiotic reaction pattern, spongiotic vesicles, small pustules with lymphocyte, and eosinophil predominance; **Bone marrow biopsy**- reactive, hypercellular marrow with marked eosinophilia	Trimethoprim-sulfamethoxazole	100 mg s.c., monthly, for 3 months (CS-dependent)	Dexamethasone and IVIG, followed by a reduced dose of prednisone [c]	Complete resolution of relapsing DRESS syndrome and complete weaning from CSs; 6-month follow-up – no recurrence	(8)
	1	M	56	6	NA	Pregabalin	**Initial dose**- 600 mg, s.c. split to 300 mg on consecutive days; **Maintenance dose**-300 mg, s.c. every 4 weeks (CS-resistant)	Methylprednisolone followed by prednisolone [d]	Rapid effect on eosinophil count and resolution of pulmonary symptoms in a patient with acute pneumonitis secondary to DRESS **f/o**- readmission due to fibrotic sequelae.	(9)
		M	50s	5	**Skin biopsy**- urticarial pustular reaction pattern, minor interface change, the presence of eosinophils **Myocardium biopsy**- lymphohistiocytic and eosinophilic infiltrate with no necrosis	Ciprofloxacin	2 doses of 300 mg s.c. with a 3-week interval (CS-resistant myocarditis)	Oral prednisolone, methylprednisolone 3 pulses, followed by cyclophosphamide and cyclosporine [e]	The patient completed a 6-month course of cyclophosphamide without complications and his prednisolone and cyclosporine have both been entirely weaned with complete clinical and laboratory recovery and no features of cardiac dysfunction	(10)
		F	45	NA	**Myocardium biopsy**- dense eosinophilic infiltrates and myocardial necrosis with few giant cell	Lamotrigine	300 mg i.v. monthly for 3 months followed by 500 mg monthly up to 1 year (CS-dependent myocarditis)	Methylprednisolone, mycophenolate mofetil, colchicine, cyclosporine, followed by a reduced dose of prednisone [f]	Patient has remained asymptomatic and discontinued her mycophenolate, taper slowly prednisone. **f/o** - 1 year symptom-free	(11)

(Continued)

10.3389/fimmu.2023.1134178

TABLE 2 Continued

Biological therapy/ mechanism	No. of patients	Gender	Age (years)	RegiSCAR DRESS score [a]	Histopathology	Drug inducing DRESS	IL-5 axis treatment regimen (Indication)	Additional combined, adjunct treatment	Outcome	Ref.
		M	62	7	NA	Amoxicillin	Three doses of 100 mg s.c. (CS-resistant)	Systemic high-dose CSs*	Rapid improvement, complete remission of DRESS and weaning from CSs	(7)
		M	70	6	NA	Piperacillin/ vancomycin/ meropenem	Single dose of 100 mg s.c. (To avoid CS toxicity-during sepsis)	Systemic CSs*	Minor improvement, possibly because TEN/DRESS overlap	(7)
Benralizumab /anti-IL-5 receptor IgG1κ monoclonal antibody		F	59	7	**Skin Biopsy**- Suggestive of DRESS	Vancomycin	Single loading dose 30 mg s.c. (First-line treatment to avoid CS toxicity)	Hydrocortisone 100 mg followed with prednisone 40 mg	Complete resolution of relapsing DRESS syndrome and complete weaning from CSs; **f/o** – 4 m symptom-free	Current report
		F	54	7	**Skin Biopsy**- Perivascular, lymphohistiocytic infiltrate, and eosinophils.	Esomeprazole, piperacillin-tazobactam	Single dose 30 mg s.c. (First-line treatment, CS-resistant)	Methylprednisolone [h]	Clinical and laboratory improvement over the following 18 days	(13)
		M	58	8	**Skin Biopsy**- Perivascular, lymphohistiocytic infiltrate, and eosinophils.	Midazolam	Single dose 30 mg s.c. (First-line treatment, CS-resistant)	Methylprednisolone [i]	Cutaneous improvement, decline in liver function tests and eosinophil levels; developed disseminated intravascular coagulation secondary to COVID-19 and died from cardiac arrest after massive bleeding 17 days later.	
		F	87	5	**Skin Biopsy**-Suggestive of DRESS	Allopurinol-pregabalin	Single dose 30 mg s.c. (CS-resistant)	Methylprednisolone followed by prednisone [j]	Rapid and complete clinical recovery (defined as regression of cutaneous-systemic symptoms and eosinophilia) with concurrent tapering of low-dose GC	(15)
		M	74	6	**Skin Biopsy**-Suggestive of DRESS	Allopurinol	Single dose 30 mg s.c. (CS-resistant)	Methylprednisolone followed by prednisone [j]		
		F	67	7	**Skin Biopsy**-Suggestive of DRESS	Ibuprofen-paracetamol	Single dose 30 mg s.c. followed by two doses of mepolizumab 100 mg s.c. (4-week interval) (CS-resistant)	Methylprednisolone followed by prednisone [j]	Long relapsing course of DRESS before starting benralizumab, clinical relapse and eosinophilia 4 months after the injection and mepolizumab was initiated. **f/o**- symptom-free under treatment	
		M	43	8	**Skin biopsy**- eczematiform toxidermia; **Blood smear**- severe	Cefepime	2 doses of 30 mg s.c.	Topical CSs, methylprednisolone and	Decreased eosinophilia within 2 days, resolution of hemophagocytic	(14)

(Continued)

10.3389/fimmu.2023.1134178

TABLE 2 Continued

Biological therapy/ mechanism	No. of patients	Gender	Age (years)	RegiSCAR DRESS score [a]	Histopathology	Drug inducing DRESS	IL-5 axis treatment regimen (Indication)	Additional combined, adjunct treatment	Outcome	Ref.
					hemophagocytic lymphohistiocytosis with profound thrombocytopenia		with a 4-week interval (CS-resistant)	IVIG followed by prednisone [k]	lymphohistiocytosis, and improvement in both organ dysfunction and skin lesions	
		M	39	6	**Liver biopsy** - eosinophilic hepatitis	Metamizole	3 doses of 30 mg s.c. at 4-week intervals (CS-resistant)	Prednisone*	Rapid suppression of eosinophils and hepatitis improved. CS could be reduced to under 10 mg prednisolone after 7 months.	(7)

M, male; F, female; CSs, corticosteroids; ANEM, acute necrotizing eosinophilic myocarditis; IVIG, intravenous immunoglobulin; s.c., subcutaneous injection; i.v., intravenous injection; NA, data are not available.

[a]According to RegiSCAR DRESS validation scoring system criteria; cutoff points include the following: suspected cases as definite (scores 6–8), probable (scores 4–5), possible (scores 2–3), and no DRESS (score <2).

[b]One patient in addition to benralizumab received two doses of mepolizumab 100 mg (4-week interval).

[c]Dexamethasone 10 mg four times a day and i.v. IgG 70 g (1 g/kg) for 2 days; after clinical improvement, she was started on prednisone 70 mg daily and then was weaned by 10 mg fortnightly; two and a half weeks later, prednisone was reduced to 60 mg daily; after DRESS syndrome diagnosis, prednisone dose was increased to 110 mg per day for 2 days with good response; within 3 days of the first dose given together with mepolizumab, prednisone dose was reduced to 10 mg weekly, until 20 mg over the next 6 weeks, and thereafter it was tapered at a slower rate until it was ceased completely in 3 months.

[d]Upon DRESS diagnosis i.v. methylprednisolone (1 g daily for 6 days), followed by prednisolone 60 mg daily due to progression of DRESS symptoms Mepolizumab was administered.

[e]Initially, 75 mg oral prednisolone 5 days and tapering down, following diagnosis of myocarditis a 3-day course of i.v. 250 mg methylprednisolone was administered, with transition to oral prednisolone 1 mg/kg. However, due to troponin elevation, another 3-day course of 500 mg methylprednisolone followed by a 3-day course of methylprednisolone 1 g combined treatment of mepolizumab with 6-month course of monthly intravenous 1,500 mg cyclophosphamide; 3 weeks following mepolizumab injection troponinemia–another dose of mepolizumab and CS pulse.

[f]Methylprednisolone 500 mg two times per day and mycophenolate mofetil 1,000 mg two times per day in addition to colchicine 0.6 mg two times per day, followed by prednisone 60 mg daily, and cyclosporine 100 mg two times per day, upon tapering to 30 mg prednisone relapse-with mepolizumab and slow taper of prednisone at 2.5 mg.

[g]Oral prednisolone 15 mg was imitated prior to DRESS diagnosis, antihistamines were administered during desensitization and intravenous dexamethasone was given before, but not after reslizumab.

[h]Methylprednisolone 125 mg for 3 days, 70 mg for 4 days followed by benralizumab due to clinical deterioration.

*CS dose or type of agent not reported.

[i]Methylprednisolone 125 mg for 3 days followed by benralizumab due to clinical deterioration.

[j]Methylprednisolone 125 mg for 3–4 days followed by 40–60 mg prednisolone, a single administration of benralizumab and concurrent tapering of CS.

[k]Methylprednisolone i.v. 2 mg/kg/day, then 1 g/day for 3 days and IVIG 1 g/day for 2 days.

10.3389/fimmu.2023.1134178

4 Discussion

DRESS syndrome is a rare life-threatening hypersensitivity reaction; hence, scarce data exist regarding treatment protocols. Data presented in our study, including two unreported patients from our medical center, support treatment of DRESS with mAbs directed toward IL-5 or IL-5R, which are already Food and Drug Administration (FDA)-approved for other eosinophilic disorders.

IL-5 plays a crucial role in eosinophilic pathophysiology and is proposed as a novel therapeutic target for hypereosinophilic syndrome and rare eosinophilic conditions (16, 17). This cytokine is the major differentiation factor for eosinophils, playing a pivotal role in innate and acquired immune responses and eosinophilia (18). The IL-5R is a heterodimer comprising one alpha subunit (IL-5Rα) and one beta subunit (IL-5Rβ) that, upon activation by IL-5 signals, stimulate the Janus kinase (JAK)–signal transducer and activator of transcription proteins (STATs) pathway (19). Therefore, the reduction of blood eosinophil levels by antagonizing IL-5 and its receptor using mAbs recently becomes an important immunotherapeutic strategy (Figure 1).

Second-line therapy for patients with DRESS and severe organ involvement who do not respond to systemic CSs or for patients in whom CSs are contraindicated includes cyclosporine, IVIG, cyclophosphamide, and the JAK inhibitor tofacitinib, despite evidence of high failure rates, relapse, and excess of adverse events including serious infections (20–23).

With novel targeted biological agents and a better understanding of the key role of the IL-5 axis in DRESS, there are case reports of treatment with anti-IL-5 or anti-IL-5R mAbs, such as mepolizumab, reslizumab, or benralizumab. Mepolizumab is an anti-IL-5 humanized IgG1κ antibody that is FDA-approved for the treatment of severe eosinophilic asthma, hypereosinophilic syndrome, and eosinophilic granulomatosis with polyangiitis (EGPA) (24). Reslizumab is an anti-IL-5 humanized IgG4κ antibody with FDA approval for severe eosinophilic asthma (25), and benralizumab is a humanized fucosylated IgG1κ anti-IL-5Rα antibody approved by the FDA for the treatment of severe eosinophilic asthma (26).

Two previously published studies involving large cohorts reported treatment with anti-IL-5 agents in DRESS patients. In a European international multicenter cohort, Kridin et al. (27) identified four DRESS patients who were treated with anti-IL-5 biologics. DRESS patients treated with anti-IL-5/IL-5R agents were mostly CS-refractory cases who had longer hospitalizations, increased rates of intensive care unit admissions, and a higher risk of relapses (27). Gschwend et al. (7) summarized 14 DRESS patients treated with anti-IL-5 agents. While treatment with reslizumab or mepolizumab appeared to require repeated doses to achieve clinical resolution in most patients, a single dose of benralizumab was shown to be sufficient, thus indicating that treatment with benralizumab is more efficient than that with mepolizumab or reslizumab (7).

P1 in our report emphasizes the complexity in the initiation and prolonged administration of CS therapy in the psychiatric patient due to its adverse effects (28). This also stresses the role of therapy with an IL-5-/IL-5R-targeting mAbs as a CS-sparing agent. Gschwend et al. (7) recommended using anti-IL-5/IL-5R biologics in specific DRESS patients including those with a severe course, CS-resistant disease, severe disease with concomitant infection, or severe end-organ damage at presentation. P1 further expands these criteria, as her psychiatric disorder indicated the need for a CS-sparing treatment. This can be further implemented on DRESS patients with underlying disorders that constitute relative or absolute contraindications for prolonged CS treatment, such as uncontrolled diabetes. On the other hand, P2 emphasizes the role of early initiation of therapy with an IL-5-/IL-5R-targeting mAb to avoid CS toxicity, as the CS effect on bone reabsorption is a secondary insult to a patient presenting with a pathologic bone fracture from osteomyelitis (29).

Systemic CSs are still considered to be the mainstay of treatment for DRESS. Early initiation of a steroid-sparing agent is vital to reduce CS side effects. Cumulatively, as evident from our patients and all others reviewed (Table 2) (7, 30), it is evident that therapy with mAbs directed toward the IL-5/IL-5R axis combined with adjunct treatments could offer an alternative to CS therapy in some patients. DRESS patients eligible to receive anti-IL-5/IL-5R mAbs include those recommended by Gschwend et al. (7) and other patients with a high risk for CS toxicity including patients with psychiatric disorders or comorbidities such as metabolic disorders, immunocompromised patients, and the elderly.

This study presents several limitations, mainly its retrospective design and small number of patients. Furthermore, the characteristics of patients such as age and sex and drug treatments differed among the different studies. A multicenter study with a larger sample size is required for prolonged follow-up and investigation of the proper dose regimen of anti-IL-5/IL-5R treatment for DRESS. DRESS often shows severe symptoms in the acute phase with serious disease sequelae in the chronic phase. Therefore, careful follow-up is required. Since there is no definite view on how to treat and which regimen to follow, the use of mAbs directed toward the IL-5/IL-5R axis is an important emerging issue in DRESS therapy deserving further clinical investigations.

In conclusion, future implementation of mAbs directed toward the IL-5/IL-5R axis in DRESS cases presents a promising therapeutic strategy in DRESS patients. Selected DRESS patients eligible to receive anti-IL-5-/IL-R-blocking agents as first-line treatment consist of patients with contraindications to CS therapy, while the risk of relapse may still exist. IL-5-modulating agents can also be used in DRESS patients with a CS-dependent or -resistant clinical course. Thus, anti-IL-5/IL-5R biologics may offer a novel therapeutic modality in these patients.

Data availability statement

The raw data supporting the conclusions of this article will be made available by the authors, without undue reservation.

Ethics statement

Written informed consent was obtained from the individual(s) for the publication of any potentially identifiable images or data included in this article.

Author contributions

LR: treatment of patients and writing of the manuscript; AT: mansucruipt revisions and figure design, YR, AK, and YM: manuscript revisions and treatment of patients; TH: pathology workup; IA: manuscript revisions; OS and YT: correspocnding authors and manuscript design and revisions. All authors contributed to the article and approved the submitted version.

Conflict of interest

The authors declare that the research was conducted in the absence of any commercial or financial relationships that could be construed as a potential conflict of interest.

Publisher's note

Supplementary material

The Supplementary Material for this article can be found online at: https://www.frontiersin.org/articles/10.3389/fimmu.2023.1134178/full#supplementary-material

References

1. Ichai P, Laurent-Bellue A, Saliba F, Moreau D, Besch C, Francoz C, et al. Acute liver Failure/Injury related to drug reaction with eosinophilia and systemic symptoms: outcomes and prognostic factors. *Transplantation* (2017) 101(8):1830–7. doi: 10.1097/TP.0000000000001655

2. Musette P, Janela B. New insights into drug reaction with eosinophilia and systemic symptoms pathophysiology. *Front Med (Lausanne)* (2017) 4:179. doi: 10.3389/fmed.2017.00179

3. Ganeshanandan L, Lucas M. Drug reaction with eosinophilia and systemic symptoms: a complex interplay between drug, T cells, and herpesviridae. *Int J Mol Sci* (2021) 22(3):1127. doi: 10.3390/ijms220311271127

4. Kardaun SH, Sekula P, Valeyrie-Allanore L, Liss Y, Chu CY, Creamer D, et al. Drug reaction with eosinophilia and systemic symptoms (DRESS): an original multisystem adverse drug reaction. results from the prospective RegiSCAR study. *Br J Dermatol* (2013) 169(5):1071–80. doi: 10.1111/bjd.12501

5. Martinez-Cabriales SA, Rodriguez-Bolanos F, Shear NH. Drug reaction with eosinophilia and systemic symptoms (DReSS): how far have we come? *Am J Clin Dermatol* (2019) 20(2):217–36. doi: 10.1007/s40257-018-00416-4

6. Maverakis E, Ji-Xu A, Bruggen MC. Targeting interleukin-5 with benralizumab: a novel treatment for drug rash with eosinophilia and systemic symptoms. *Allergy* (2022) 77(8):2287–9. doi: 10.1111/all.15283

7. Gschwend A, Helbling A, Feldmeyer L, Mani-Weber U, Meincke C, Heidemeyer K, et al. Treatment with IL5-/IL-5 receptor antagonists in drug reaction with eosinophilia and systemic symptoms (DRESS). *Allergo J Int* (2022), 1–8. doi: 10.1007/s40629-022-00224-7

8. Ange N, Alley S, Fernando SL, Coyle L, Yun J. Drug reaction with eosinophilia and systemic symptoms (DRESS) syndrome successfully treated with mepolizumab. *J Allergy Clin Immunol Pract* (2018) 6(3):1059–60. doi: 10.1016/j.jaip.2017.10.020

9. Thein OS, Sutton B, Thickett DR, Parekh D. Mepolizumab rescue therapy for acute pneumonitis secondary to DRESS. *BMJ Case Rep* (2019) 12(10). doi: 10.1136/bcr-2019-231355

10. Truong K, Kelly S, Bayly A, Smith A. Successful mepolizumab treatment for DRESS-induced refractory eosinophilic myocarditis and concurrent thyroiditis. *BMJ Case Rep* (2021) 14(7). doi: 10.1136/bcr-2021-242240e24224014/7/e242240

11. Kowtoniuk R, Pinninti M, Tyler W, Doddamani S. DRESS syndrome-associated acute necrotizing eosinophilic myocarditis with giant cells. *BMJ Case Rep* (2018), 2018. doi: 10.1136/bcr-2018-22646bcr2018226461

12. Park H, Choi GS, Lee EM. Successful treatment of imatinib-induced DRESS syndrome using reslizumab without cessation of imatinib: a case report. *Case Rep Oncol* (2021) 14(3):1548–54. doi: 10.1159/000519471cro-0014-1548

13. Schmid-Grendelmeier P, Steiger P, Naegeli MC, Kolm I, Claudia Cecile Valerie L, Maverakis E, et al. Benralizumab for severe DRESS in two COVID-19 patients. *J Allergy Clin Immunol Pract* (2021) 9(1):481–483.e2. doi: 10.1016/j.jaip.2020.09.039

14. Mesli F, Dumont M, Soria A, Groh M, Turpin M, Voiriot G, et al. Benralizumab: a potential tailored treatment for life-threatening DRESS in the COVID-19 era. *J Allergy Clin Immunol Pract* (2021) 9(9):3529–3531.e1. doi: 10.1016/j.jaip.2021.06.047

15. Lang CCV, Schmid-Grendelmeier P, Maverakis E, Bruggen MC. Reply to "Benralizumab: a potential tailored treatment for life-threatening DRESS in the COVID-19 era". *J Allergy Clin Immunol Pract* (2021) 9(9):3531–2. doi: 10.1016/j.jaip.2021.06.048

16. Harish A, Schwartz SA. Targeted anti-IL-5 therapies and future therapeutics for hypereosinophilic syndrome and rare eosinophilic conditions. *Clin Rev Allergy Immunol* (2020) 59(2):231–47. doi: 10.1007/s12016-019-08775-4

17. Shamriz O, Hershko AY, Talmon A, Ribak Y, Elazary AS, Horev L, et al. The efficacy of off-label IL-5-modulating treatment in rare eosinophil-mediated diseases. *Allergol Int* (2021) 70(2):266–8. doi: 10.1016/j.alit.2020.10.001

18. Kouro T, Takatsu K. IL-5- and eosinophil-mediated inflammation: from discovery to therapy. *Int Immunol* (2009) 21(12):1303–9. doi: 10.1093/intimm/dxp102dxp102

19. Broughton SE, Nero TL, Dhagat U, Kan WL, Hercus TR, Tvorogov D, et al. The betac receptor family - structural insights and their functional implications. *Cytokine* (2015) 74(2):247–58. doi: 10.1016/j.cyto.2015.02.005

20. Joly P, Janela B, Tetart F, Rogez S, Picard D, D'Incan M, et al. Poor benefit/risk balance of intravenous immunoglobulins in DRESS. *Arch Dermatol* (2012) 148(4):543–4. doi: 10.1001/archderm.148.4.dlt120002-c

21. Kim D, Kobayashi T, Voisin B, Jo JH, Sakamoto K, Jin SP, et al. Targeted therapy guided by single-cell transcriptomic analysis in drug-induced hypersensitivity syndrome: a case report. *Nat Med* (2020) 26(2):236–43. doi: 10.1038/s41591-019-0733-7

22. Laban E, Hainaut-Wierzbicka E, Pourreau F, Yacoub M, Sztermer E, Guillet G, et al. Cyclophosphamide therapy for corticoresistant drug reaction with eosinophilia and systemic symptoms (DRESS) syndrome in a patient with severe kidney and eye involvement and Epstein-Barr virus reactivation. *Am J Kidney Dis* (2010) 55(3):e11–4. doi: 10.1053/j.ajkd.2009.10.054

23. Nguyen E, Yanes D, Imadojemu S, Kroshinsky D. Evaluation of cyclosporine for the treatment of DRESS syndrome. *JAMA Dermatol* (2020) 156(6):704–6. doi: 10.1001/jamadermatol.2020.0048

24. Pavord ID, Bel EH, Bourdin A, Chan R, Han JK, Keene ON, et al. From DREAM to REALITI-a and beyond: mepolizumab for the treatment of eosinophil-driven diseases. *Allergy* (2022) 77(3):778–97. doi: 10.1111/all.15056

25. Hashimoto S, Kroes JA, Eger KA, Mau Asam PF, Hofstee HB, Bendien SA, et al. Real-world effectiveness of reslizumab in patients with severe eosinophilic asthma - first initiators and switchers. *J Allergy Clin Immunol Pract* (2022) 10(8):2099–2108.e6. doi: 10.1016/j.jaip.2022.04.014

26. Zhu M, Yang J, Chen Y. Efficacy and safety of treatment with benralizumab for eosinophilic asthma. *Int Immunopharmacol* (2022) 111:109131. doi: 10.1016/j.intimp.2022.109131

27. Kridin K, Bruggen MC, Walsh S, Bensaid B, Ranki A, Oppel E, et al. Management and treatment outcome of DRESS patients in Europe: an international multicentre retrospective study of 141 cases. *J Eur Acad Dermatol Venereol* (2023) 37(4):753–62. doi: 10.1111/jdv.18808

28. Dubovsky AN, Arvikar S, Stern TA, Axelrod L. The neuropsychiatric complications of glucocorticoid use: steroid psychosis revisited. *Psychosomatics* (2012) 53(2):103–15. doi: 10.1016/j.psym.2011.12.007

29. Lane NE. Glucocorticoid-induced osteoporosis: new insights into the pathophysiology and treatments. *Curr Osteoporos Rep* (2019) 17(1):1–7. doi: 10.1007/s11914-019-00498-x

30. Pitlick MM, Li JT, Pongdee T. Current and emerging biologic therapies targeting eosinophilic disorders. *World Allergy Organ J* (2022) 15(8):100676. doi: 10.1016/j.waojou.2022.100676100676

frontiers | Frontiers in Immunology

TYPE Original Research
PUBLISHED 09 May 2023
DOI 10.3389/fimmu.2023.1169057

OPEN ACCESS

EDITED BY
Oded Shamriz,
Hadassah Medical Center, Israel

REVIEWED BY
Masaru Kato,
Hokkaido University, Japan
Frédéric Coutant,
Université de Lyon, France

*CORRESPONDENCE
Panpan Zhang
panpanzhang2016@163.com
Shengyun Liu
fccliusy2@zzu.edu.cn

RECEIVED 18 February 2023
ACCEPTED 21 April 2023
PUBLISHED 09 May 2023

CITATION
Li M, Zhang Y, Zhang W, Sun J, Liu R, Pan Z, Zhang P and Liu S (2023) Type 1 interferon signature in peripheral blood mononuclear cells and monocytes of idiopathic inflammatory myopathy patients with different myositis-specific autoantibodies. *Front. Immunol.* 14:1169057. doi: 10.3389/fimmu.2023.1169057

Type 1 interferon signature in peripheral blood mononuclear cells and monocytes of idiopathic inflammatory myopathy patients with different myositis-specific autoantibodies

Mengdi Li[1], Yusheng Zhang[1], Wenzhe Zhang[2], Jinlei Sun[1], Rui Liu[1], Zhou Pan[1], Panpan Zhang[1*] and Shengyun Liu[1*]

[1]Department of Rheumatology and Clinical Immunology, The First Affiliated Hospital of Zhengzhou University, Zhengzhou, China, [2]Department of Radiology, The Third Affiliated Hospital of Zhengzhou University, Zhengzhou, China

Background: Myositis-specific autoantibodies (MSAs) are clinically used to diagnose and define idiopathic inflammatory myopathy (IIM) subsets. However, the underlying pathogenic mechanisms of patients with different MSAs remain unclear.

Methods: A total of 158 Chinese patients with IIM and 167 gender- and age-matched healthy controls (HCs) were enrolled. Transcriptome sequencing (RNA-Seq) was performed with peripheral blood mononuclear cells (PBMCs), followed by the identification of differentially expressed genes (DEGs) and analysis of gene set enrichment analysis, immune cell infiltration, and WGCNA. Monocyte subsets and related cytokines/chemokines were quantified. The expressions of interferon (IFN)-related genes were validated using qRT-PCR and Western blot in both PBMCs and monocytes. We also performed correlation analysis and ROC analysis to explore the potential clinical significance of the IFN-related genes.

Results: There were 1,364 genes altered in patients with IIM, including 952 upregulated and 412 downregulated genes. The type I interferon (IFN-I) pathway was remarkably activated in patients with IIM. Compared with patients with other MSAs, IFN-I signatures were significantly activated in patients with anti-melanoma differentiation-associated gene 5 (MDA5) antibodies. In total, 1,288 hub genes associated with IIM onset were identified using WGCNA, including 29 key DEGs associated with IFN signaling. The patients had more CD14brightCD16- classical, CD14brightCD16+ intermediate, and fewer CD14dimCD16+ non-classical monocyte subsets. Plasma cytokines like IL-6 and TNF and chemokines including CCL3 and MCPs increased. The validation of IFN-I-related gene expressions was consistent with the findings from RNA-Seq. The IFN-related genes were correlated with laboratory parameters and helpful for IIM diagnosis.

Conclusion: Gene expressions were remarkably altered in the PBMCs of IIM patients. Anti-MDA5+ IIM patients had a more pronounced activated IFN signature than others. Monocytes exhibited a proinflammatory feature and contributed to the IFN signature of IIM patients.

KEYWORDS

idiopathic inflammatory myopathy, anti-MDA5+ dermatomyositis, interferon, monocytes, RNA-sequencing

1 Introduction

Idiopathic inflammatory myopathies (IIM) are a group of rare autoimmune diseases mainly affecting the skeletal muscles and other organs (1). Myositis-specific antibodies (MSAs), defined as autoantibodies found specifically in IIM patients, have been found to be strongly correlated with clinical manifestations and prognosis (2). Autoantibody specificities correlate with clinical features, such as the associations between anti-TIF1γ antibodies and high malignancy risk, and anti-melanoma differentiation-associated gene 5 (MDA5) antibodies and rapidly progressive interstitial lung disease (ILD) (3, 4). Muscle gene expression profiles, metabolic signatures, and pathways in plasma and urine samples were found different in MSA-typed IIM patients (5, 6). Compared with conventional subgrouping based on clinical phenotypes, autoantibody profiles perform better in knowing the immune mechanisms in IIM (7). Nowadays, the pathogenesis of IIM is not fully understood, so studies that are focused on different MSA-typed patients may provide valuable clues.

Hypotheses on the pathogenesis of IIM have been proposed as endoplasmic reticulum stress, vasculopathy, acquired interferonopathy, and so on (8–10). In the blood, skin, and muscles of IIM, upregulation of the IFN pathway has been verified and can reflect disease activity (11–13). Previous studies have highlighted the role of the adaptive immune system, especially T cells and B cells, in the immunopathogenesis of IIM (7, 14, 15). There is also a few evidence suggesting the involvement of monocyte/macrophage in IIM. Macrophage infiltration has been found in the muscles of all types of IIM, which is responsible for antigen presenting, necrotic muscle fiber invasion and elimination, and cytokine and chemokine production of IFN, IL-6, TNF-α, and so on (15–17). The activation and distribution pattern of monocytes/macrophages differs in the muscles of dermatomyositis (DM) and polymyositis (PM), and the macrophage infiltration mode relates to the serological subtypes (15, 18, 19). Activated monocytes/macrophages might be responsible for the cytokine storm in anti-MDA5-associated ILD (20). Aberrant mitochondrial biology in juvenile dermatomyositis (JDM) monocytes stimulates the expression of IFN-stimulated genes (ISGs) (21). Taken together, monocyte/macrophage may play a role in IIM pathogenesis.

The transcriptomic profile of peripheral blood mononuclear cells (PBMCs) of IIM patients needs to be further explored, especially for patients with distinct serological features. Therefore, we performed RNA-seq, bioinformatic analysis, and experimental validations in PBMCs to investigate immune cell and gene expression alterations in patients with different MSAs.

2 Materials and methods

2.1 Patient enrollment

A total of 158 IIM patients were recruited between October 2021 and October 2022 in the First Affiliated Hospital of Zhengzhou University (China). All patients were over 18 years old at the disease onset and met the Bohan and Peter criteria (22). Patients with other concurrent autoimmune diseases were excluded. This study was authorized by the Ethics Committee of Zhengzhou University's First Affiliated Hospital (KY-2021-00805), and all participants provided written informed consent.

Anti-MDA5 and anti-TIF1γ antibodies were assayed using enzyme-linked immunosorbent assay (MBL, Japan). Anti-Jo-1, anti-EJ, anti-PL-7, anti-PL-12, anti-SRP, anti-Ro52, anti-PM-Scl 75, anti-PM-Scl 100, anti-Ku, and anti-Mi-2 antibodies were detected using line immunoassays (EUROIMMUN, Germany). For RNA-seq, 23 IIM patients who were newly diagnosed or in active disease status as well as eight gender- and age-matched healthy controls (HCs) were enrolled. Among these 23 patients, nine were anti-MDA5+, four were anti-Jo-1+, five were anti-TIF1γ+, and five were MSAs-. For flow cytometry, PBMCs were obtained from 40 IIM patients [anti-MDA5+ (n = 12), MSAs- (n = 10), anti-Jo-1+ (n = 7), anti-TIF1γ+ (n = 5), anti-EJ+ (n = 3), anti-PL-12+ (n = 2), and anti-PL-7+ (n = 1)] and 39 HCs. Plasma from 25 patients [anti-MDA5+ (n = 16), anti-TIF1γ+ (n = 5), anti-Jo-1+ (n = 3), and MSAs- (n = 1)] and 29 HCs were used for cytokine/chemokine quantification. For real-time quantitative polymerase chain reaction (qRT-PCR), the PBMC cDNA was obtained from 93 IIM patients [anti-MDA5+ (n = 29) and anti-MDA5- (n = 64)] and 57 matched HCs. The monocyte cDNA was obtained from 14 IIM patients [anti-Jo-1+ (n = 3), anti-Mi-2+ (n = 3), MSAs- (n = 3), anti-MDA5+ (n = 2), anti-TIF1γ+ (n = 2), and anti-PL-7+ (n = 1)] and 18 matched HCs. For Western blot analysis, PBMCs were obtained from five patients [anti-Jo-1+ (n = 2), MSAs- (n = 2), and anti-MDA5+ (n = 1)] and eight HCs. Monocytes were obtained from eight patients [anti-MDA5+ (n = 2), anti-Jo-1+ (n = 2), anti-TIF1γ+ (n = 1), and MSAs- (n = 3)] and eight HCs. The patients'

clinical characteristics, laboratory parameters, and MSAs detected are shown in Table 1.

2.2 PBMC and monocyte isolation

Peripheral blood (5–10 ml) was collected into EDTA-containing tubes (BD, UK). PBMCs were separated by density gradient centrifugation using Human Lymphocyte Separation Medium (Dakewe, China). The monocytes were isolated from PBMCs using CD14 MicroBeads (Miltenyi Biotec, Germany) according to the manufacturer's instructions.

2.3 RNA-seq analysis

Following the manufacturer's instructions, total RNA was extracted using mirVana miRNA Isolation Kit (Ambion, USA).

TABLE 1 Baseline clinical characteristics of idiopathic inflammatory myopathy (IIM) patients in this study.

	RNA sequencing	Validation experiments	
	IIM (*n* = 23)	MDA5 (*n* = 36)	Non-MDA5 (*n* = 99)
Age at baseline, years, mean ± SD	54.91 ± 13.99	51.06 ± 9.43	53.35 ± 12.48
Female, *n* (%)	19 (82.61)	21 (58.33)	78 (78.79)
Disease duration, months, median (interquartile range, IQR)	3 (3–12)	3 (1.17–9)	12 (3–24)
Clinical features, *n* (%)			
Fever	7 (30.43)	15 (41.67)	26 (26.26)
Gottron papules	7 (30.43)	10 (27.78)	13 (13.13)
Gottron sign	2 (8.7)	10 (27.78)	11 (11.11)
Heliotrope rash	13 (56.52)	20 (55.56)	29 (29.29)
Shawl-sign rash	8 (34.78)	10 (27.78)	23 (23.23)
V-sign rash	6 (26.09)	9 (25)	24 (24.24)
Mechanic's hands	2 (8.7)	4 (11.11)	15 (15.15)
Myalgia	7 (30.43)	14 (38.89)	33 (33.33)
Muscle weakness	8 (34.78)	20 (55.56)	55 (55.56)
Dysphagia	3 (13.04)	4 (11.11)	20 (20.2)
Arthralgia	8 (34.78)	17 (47.22)	33 (33.33)
Raynaud's phenomenon	2 (8.7)	1 (2.78)	8 (8.08)
Weight loss	1 (4.35)	8 (22.22)	10 (10.1)
Interstitial lung disease	6 (26.09)	22 (61.11)	55 (55.56)
Malignancy	1 (4.35)	0	1 (1.01)
Laboratory features			
WBC count ($\times10^9$/L), median (IQR)	5.4 (4.4–6.2)	5.41 (4.44–7.7)	6.6 (5.4–8.66) (*n* = 95)
PLT count ($\times10^9$/L), mean ± SD	212.87 ± 72.12	219.64 ± 78.45	232.91 ± 77.99 (*n* = 94)
Lymphocyte count ($\times10^9$/L), median (IQR)	1.15 (0.65–1.78)	0.89 (0.51–1.36)	1.33 (0.78–1.84) (*n* = 95)
Hgb (g/L), mean ± SD	118.83 ± 12.7	124.48 ± 13.42	125.33 ± 15.11 (*n* = 95)
ALT (U/L), median (IQR)	61 (13–119) (*n* = 21)	34.5 (17.5–50.5)	22 (12–45) (*n* = 91)
AST (U/L), median (IQR)	59 (19.5–136.5) (*n* = 21)	32.5 (20.25–49)	25.5 (15–52.25) (*n* = 90)
CK (U/L), median (IQR)	115 (27.5–914.25) (*n* = 22)	43 (28.25–98.25)	85 (41–599.5) (*n* = 93)
LDH (U/L), median (IQR)	271 (225.75–479.5) (*n* = 22)	312.5 (219.25–362)	302.5 (223.75–419) (*n* = 94)
ESR (mm/h), median (IQR)	17 (13.5–32) (*n* = 21)	19 (10.25–32.75)	12 (6–22.75) (*n* = 88)
CRP (mg/L), median (IQR)	2.09 (1.25–13.43) (*n* = 21)	1.5 (1.5–9.84)	2.46 (1–11.86) (*n* = 87)

(Continued)

TABLE 1 Continued

	RNA sequencing	Validation experiments	
	IIM (*n* = 23)	MDA5 (*n* = 36)	Non-MDA5 (*n* = 99)
C3 (g/L), mean ± SD	1.02 (0.91–1.17) (*n* = 19)	1.07 ± 0.16 (*n* = 31)	1.02 ± 0.21 (*n* = 85)
C4 (g/L), mean ± SD	0.28 ± 0.11 (*n* = 19)	0.3 (0.24-0.34) (*n* = 32)	0.26 ± 0.08 (*n* = 84)
IgA (g/L), mean ± SD	3.03 ± 1.12 (*n* = 18)	2.87 ± 0.97 (*n* = 29)	2.16 ± 0.96 (*n* = 80)
IgG (g/L), median (IQR)	10.4 (8.65–14.1) (*n* = 18)	11.90 (10.05–13.35) (*n* = 29)	10.9 (8.83–13.5) (*n* = 80)
IgM (g/L), mean ± SD	1 (0.68–1.65) (*n* = 18)	1.07 ± 0.38 (*n* = 29)	1.1 (0.8–2) (*n* = 79)
Ferritin (ng/ml), median (IQR)	462.05 (212.33–734.5) (*n* = 18)	519.25 (305.93–1183.95) (*n* = 34)	228.5 (103.4–355) (*n* = 80)
KL-6 (U/ml), median (IQR)	566 (277–1314.5) (*n* = 21)	747.5 (559.75–1316.75) (*n* = 32)	563 (262–1367) (*n* = 71)
Anti-MDA5 Abs (U/ml), mean ± SD	141.8 ± 57.74 (*n* = 9)	140.7 ± 62.21	0
Myositis autoantibodies, *n* (%)			
MDA5	9 (39.13)	36 (100)	0
Jo-1	4 (17.39)	2 (5.56)	22 (22.22)
TIF1γ	5 (21.74)	1 (2.78)	15 (15.15)
EJ	0	0	10 (10.1)
PL-7	0	1 (2.78)	9 (9.09)
PL-12	0	0	4 (4.04)
Mi-2	0	1 (2.78)	6 (6.06)
NXP-2	0	0	2 (2.02)
SRP	0	1 (2.78)	2 (2.02)
MSAs Neg	5 (21.74)	0	34 (34.34)
Ro52	2 (8.7)	10 (27.78)	42 (42.42)
PM-Scl	0	0	6 (6.06)
Ku	0	0	4 (4.04)
Treatment, *n* (%)			
Prednisone	11 (47.83)	23 (63.89)	67 (67.68)
Immunosuppressive agents	10 (43.48)	16 (44.44)	40 (40.4)
IVIG	3 (13.04)	2 (5.56)	4 (4.04)
Without treatment	7 (30.43)	10 (27.78)	19 (19.19)

qRT-PCR, real-time quantitative polymerase chain reaction; WB, Western blotting; MDA5, anti-melanoma differentiation-associated gene 5 antibody; WBC, white blood cell count; PLT, platelet count; Hgb, hemoglobin; ALT, alanine aminotransferase; AST, aspartate aminotransferase; CK, creatine kinase; LDH, lactate dehydrogenase; ESR, erythrocyte sedimentation rate; CRP, C-reactive protein; C3, complement 3; C4, complement 4; IgA, immunoglobulin A; IgG, immunoglobulin G; IgM, immunoglobulin M; KL-6, Krebs von den Lungen-6; MSAs, myositis-specific antibodies; Jo-1, anti-histidyl-tRNA synthetase antibody; TIF1-γ, anti-transcription intermediary factor-1γ antibody; PL-7, anti-threonyl-tRNA synthetase antibody; PL-12, anti-alanyl-tRNA synthetase antibody; Ku, anti-Ku antibody; EJ, anti-glycyl-tRNA synthetase antibody; PM-Scl, anti-polymyositis scleroderma antibody; Mi-2, anti-Mi-2 antibody; NXP-2, anti-nuclear matrix protein 2 antibody; SRP, anti-signal recognition particle antibody; Ro52, anti-Ro52 antibody; immunosuppressive agents, immunomodulatory drugs include CYC, MTX, AZA, and ciclosporin A; IVIG, intravenous immunoglobulin.

Agilent 2100 Bioanalyzer (Agilent Technologies, USA) was utilized to evaluate the RNA integrity. Samples with an RNA integrity number greater than 7 were analyzed further. The libraries were constructed, following the manufacturer's protocol, with TruSeq Stranded mRNA LTSample Prep Kit (Illumina, USA). These libraries were then sequenced on the Illumina sequencing platform (HiSeqTM 2500 or Illumina HiSeq X Ten), yielding 125/150 bp paired-end reads. Trimmomatic was used to remove ploy N-containing and low-quality reads (23). The clean reads were then mapped to the reference genome with hisat2 (24).

2.4 Identification of differentially expressed genes

The "DESeq2" package (version 1.36.0) was used to identify the DEGs between 23 IIM patients and HCs, with the cutoff criteria of |

$\log_2$ fold change| >1 and p_{adj} <0.05. After rlog transformation, principal component analysis (PCA) was performed using "plotPCA" in "DESeq2" package to identify the clustering of samples. The "ggplot2" and "ComplexHeatmap" packages were used to show the DEGs compared between groups. The top 15 DEGs selected by |$\log_2$ fold change| were visualized using Cytoscape software (version 3.9.1).

2.5 Immune infiltration analysis

To quantify the relative abundance of 22 types of immune cells, we run the CIBERSORT R script (version 1.03) with 1,000 permutations and no quantile normalization. The correlations of immune cells in patients were calculated using Spearman correlation analysis and were visualized with the "corrplot" package (version 0.92). The Wilcoxon test was performed to compare the fraction of immune cells.

2.6 Flow cytometry and plasma protein detection

PBMCs were incubated with Human TruStain FcX (BioLegend, USA) and stained with the following antibodies: FITC anti-human CD14 and Alexa Fluor 647 anti-human CD16 (BioLegend, USA). The stained cells were assessed using the FACSCelesta (BD Biosciences, USA). Data were analyzed using FlowJo software (V10.6.2., Tree Star). Nine plasma proteins, including IL-6, IL-8, CSF-1, CCL3, TNF, MCP-1, MCP-2, MCP-3, and MCP-4, were targeted and quantified by Olink multiplex proximity extension assay following the manufacturer's instructions. The protein abundance levels were reported as normalized protein expression values on a $\log_2$ scale.

2.7 Gene set enrichment analysis

To perform gene set enrichment analysis (GSEA), all genes ranked by $\log_2$ fold change were analyzed using the "clusterProfiler" package (version 4.4.4), with the reference gene set C2-CP sub-collection (c2.cp.v2022.1.Hs.entrez.gmt) from the Molecular Signatures Database (MSigDB). All or core enriched genes in selected pathways were extracted to calculate the mean value of fragments per kilobase of transcript per million mapped reads (FPKM) for each group and were visualized using the "ComplexHeatmap" package (version 2.12.1) in the form of $\log_2$ (FPKM + 1).

2.8 Weighted gene co-expression network analysis

To construct the co-expression network of weighted gene co-expression network analysis (WGCNA), the genes whose counts were less than 10 in more than 90% of the samples were removed. After being standardized by $\log_2$(FPKM + 1), the top 5,000 genes ordered by median absolute deviation were chosen as input. All 31 samples were analyzed with the "WGCNA" package (version 1.71) in R. The optimal soft-thresholding power was automatically picked as 12 (scale-free R^2 = 0.8560). The adjacency matrix was used to construct the topological overlap matrix (TOM) and the topological difference matrix (dissTOM) by the dynamic cutting technique. The minimum cluster size = 30, and deepSplit = 2 was set to construct the primary modules. Then, cutHeight was set as 0.25 to merge the modules. In total, 14 merged modules were finally found. The relationships between module eigengenes and traits were assessed by Pearson's correlation. The traits included the presence or absence of IIM, patient MSA types, clinical features of the disease, and immune cell infiltration results. The top seven modules correlated to the "IIM" trait were selected. After calculating the gene significance (GS) and module membership (MM), the WGCNA hub genes were identified with the criteria of MM >0.8 and GS >0.2. The key IFN genes were identified as the intersection of WGNCA hub genes, DEGs (IIM/HCs), and genes from the Reactome IFN signaling. The protein–protein interaction (PPI) network of the 29 key IFN genes, constructed using the STRING database, was visualized using Cytoscape software (version 3.9.1).

2.9 Quantitative real-time polymerase chain reaction

Total RNA was extracted using TRIzol Reagent (Ambion, USA) according to the manufacturer's instructions. Then, cDNA was obtained using PrimeScript RT Master Mix (Takara, Japan). RNA concentration and quality were determined as measured by NanoDrop One (Thermo Scientific, USA). Quantitative real-time PCR proceeded using TB Green Premix Ex Taq II (Takara, Japan) on Applied Biosystems QuantStudio 3 and 5 (Thermo Fisher Scientific, USA). The *GAPDH* gene was used as an endogenous control. The primer sequences used are listed in Supplementary Table S1. The relative expression levels were determined by the $2^{-\Delta\Delta CT}$ method.

2.10 Western blot analysis

Total protein from PBMCs or monocytes was extracted using Total Protein Extraction Kit for Animal Cultured Cells and Tissues (Invent, USA). The protein concentration of each sample was measured with Pierce BCA Protein Assay Kit (Thermo Fisher Scientific, USA). Approximately 10–20 μg of proteins from each sample was separated on FuturePAGE 4-12% 11 Wells (ACE, China) and transferred to 0.45-μm polyvinylidine fluoride (PVDF) membranes (Merck Millipore, Ireland). After being blocked using Quick Block Western blocking solution (Beyotime, China) for 20 min, the PVDF membranes were incubated with primary antibodies (1:1,000 dilution) overnight at 4°C. Then, the membranes were incubated with Goat Anti-Rabbit IgG (H&L)-HRP Conjugated (EASYBIO, BE0101, 1:10,000) for 1 h at room temperature. The membranes were then visualized with Pierce ECL

Western Blotting Substrate (Thermo Scientific, USA). Densitometry analysis was performed using Image-J software (NIH). β-Actin was used as an internal control. In the need for stripping and re-probing, the Restore Western Blot Stripping Buffer was used (Thermo Scientific, USA).

The primary antibodies used were Phospho-Stat1 (#9167), Phospho-Stat2 (#88410), Phospho-IRF-7 (#12390), Phospho-SHP-1 (#8849), β-actin (#4970), Stat1(#14995), Stat2 (#72604), IRF-7 (#13014), and SHP-1 (#3759). All primary antibodies used in this study were purchased from Cell Signaling Technology (USA) and used at 1:1,000 dilution.

2.11 Statistical analysis and ROC analysis

Statistical analysis and graphing were performed using GraphPad Prism 9 (GraphPad Software, USA) or R (version 4.2.1; https://www.R-project.org/). The data were presented as the average ± standard deviation (SD), and test results are summarized as "ns" for not significant, *$p < 0.05$, **$p < 0.01$, ***$p < 0.001$, and ****$p < 0.0001$. Statistical significance was considered as $p < 0.05$.

The Wilcoxon test was used to compare the immune cell fractions between groups. The Spearman correlation analysis was performed to investigate the relationship between immune cells and to calculate the correlations between gene expressions and clinical laboratory indicators, including the level of anti-MDA5 Abs. Comparisons between two groups were made using the Welch's *t*-test, unpaired *t*-test, or Mann Whitney test as appropriate. Kruskal–Wallis test, followed by Dunn's multiple-comparisons test, was used to compare the three groups.

To assess the performance of distinguishing IIM from HCs, anti-MDA5+ IIM from HCs, or anti-MDA5+ IIMs from anti-MDA5- IIMs, receiver operating characteristic (ROC) curve analyses were performed for each validated gene. The area under the curve (AUC) was calculated with a 95% confidence interval (CI). The ROC analysis results were interpreted as: AUC <0.70, low diagnostic accuracy; 0.70–0.90, moderate diagnostic accuracy; and ≥0.90, high diagnostic accuracy. The ROC curves are shown with *p*-value <0.05.

3 Results

3.1 Identification of DEGs between IIM and HC

To characterize the gene expressions of IIM patients with different MSA types, we identified the DEGs between HC and IIM or MSA-typed samples (Figure 1). From the PCA plot (Figure 1A), the transcriptomic profiling of patients with IIM was significantly altered compared with HCs. However, the expression of transcriptomic profiling was narrowed for patients with IIM of different MSAs. A total of 1,364 DEGs were identified in patients with IIM compared with HCs, including 952 upregulated and 412 downregulated genes (Figure 1B). The heat map shows the expressions of these DEGs in each sample characterized by MSAs (Figure 1C). The Venn diagram shows the overlap of DEGs identified between the HC group and IIM or MSA-typed patients (Figure 1D), from which there were some DEGs expressed uniquely in MSA-typed groups, and most of the DEGs were shared in common. The top 15 DEGs identified in different MSA-typed IIM patients are shown in Figure 1E.

3.2 Landscape of immune cells in the PBMCs of patients with IIM

In order to evaluate the fractions of immune cells in the PBMCs of patients with IIM, CIBERSORTx analysis was performed. By using the CIBERSORT algorithm, the percentages of 22 types of immune cells were quantified in all samples (Figure 2A). Compared with HCs, elevated proportions of monocytes, macrophage M0, and neutrophils, as well as decreased proportions of memory B cells, CD8+ T cells, resting memory CD4+ T cells, and resting NK cells, were shown in IIMs (Figure 2B). The correlation heat map showed that the monocytes were negatively correlated with CD8+ T cells ($r = -0.7$, $p < 0.001$), resting NK cells ($r = -0.66$, $p < 0.001$), and M1 macrophages ($r = -0.49$, $p < 0.05$) (Figure 2C). Immune cell infiltration analysis was also performed in IIM patients with different MSAs (Supplementary Figures S1A–D). From the above-mentioned results, the monocyte fractions were significantly increased in the PBMCs of patients with IIM as well as in anti-MDA5+ DM patients, anti-Jo-1+ IIM patients, and MSA- IIM patients.

To further investigate the potential role of monocytes, we quantified the subsets and related plasma cytokines of monocytes in IIM patients. Three monocyte subpopulations—CD14brightCD16- (classical), CD14brightCD16+ (intermediate), and CD14dimCD16+ (non-classical) monocytes—were quantified within the broad monocyte gate defined by forward and side scatter (Figure 3A). The proportion of broad monocytes also increased in patients (25.92% ± 10.78% *vs.* 15.82% ± 4.43%, $p < 0.0001$) identified by flow cytometry, which supported our results in the immune infiltration analysis (Figure 3B). At the same time, elevated proportions of classical (69.87% ± 17.58% *vs.* 62.61% ± 9.41%, $p = 0.0012$) and intermediate (9.56% ± 7.90% *vs.* 5.67% ± 3.30%, $p = 0.0108$) populations and decreased non-classical (6.84% ± 7.08% *vs.* 9.41% ± 5.12%, $p = 0.0018$) monocyte subpopulations were identified in IIM patients (Figure 3C). Consistent with the monocyte fraction changes analyzed according to MSA types (Supplementary Figure S2), the fraction of broad monocytes increased in the PBMCs of anti-MDA5+ (23.36% ± 13.11% *vs.* 15.82% ± 4.43%, $p = 0.0009$), anti-Jo-1+ (29.79% ± 9.82% *vs.* 15.82% ± 4.43%, $p = 0.0089$), and MSA- (21.17% ± 5.08% *vs.* 15.82% ± 4.43%, $p = 0.0018$) IIM patients (Supplementary Figures S2A–D). From the monocyte subpopulations quantified in MSA-typed patients (Supplementary Figures S2E–H), the percentages of classical (70.21% ± 11.24% *vs.* 62.61% ± 9.41%, $p = 0.0382$) and intermediate (10.32% ± 6.02% *vs.* 5.67% ± 3.30%, $p = 0.0040$) monocyte subpopulations were also elevated in anti-MDA5+ patients; a decreased non-classical (5.12% ± 4.67% *vs.* 9.41% ± 5.12%, $p = 0.0004$) monocyte subpopulation (Supplementary Figure S2E) was observed as well. As in Figure 3D,

10.3389/fimmu.2023.1169057

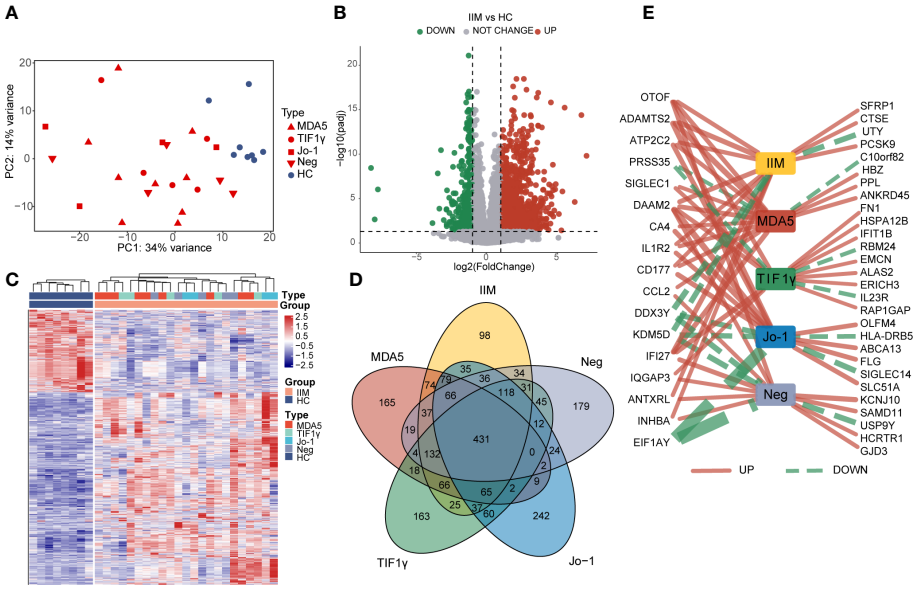

FIGURE 1
Identification of differentially expressed genes (DEGs) in patients with idiopathic inflammatory myopathies (IIM). **(A)** Principal component analysis (PCA) of transcriptomic profiling in IIM patients with different myositis-specific autoantibodies (n = 23) and healthy controls (HCs; n = 8). **(B)** Volcano plot showing DEGs between the IIM and HC groups (p_{adj} < 0.05, |$\log_2$ fold change| >1). **(C)** Heat map of DEGs between the IIM and HC groups. **(D)** Venn diagram showing the overlap of DEGs identified by comparing the HC group and patient groups (p_{adj} < 0.05, |$\log_2$ fold change| >1). **(E)** Top15 DEGs identified by comparing the patient groups with HCs. The solid red and dashed green lines represent the up- and downregulated DEGs separately. The increase of the line width means an increase of |$\log_2$ fold change| from 4.35 to 22.54.

the expression levels of monocyte-related cytokines or chemokines also increased in the plasma of patients with IIM, including IL-8 (5.72 ± 2.15 *vs.* 4.28 ± 0.96, $p < 0.0001$), CSF-1 (9.30 ± 0.38 *vs.* 8.93 ± 0.23, $p = 0.0001$), IL-6 (3.78 ± 1.53 *vs.* 2.31 ± 0.43, $p < 0.0001$), CCL3 (6.73 ± 0.88 *vs.* 5.49 ± 0.57, $p < 0.0001$), TNF (3.86 ± 0.45 *vs.* 3.09 ± 0.28, $p < 0.0001$), MCP-1 (13.06 ± 0.84 *vs.* 11.45 ± 0.48, $p < 0.0001$), MCP-2 (11.43 ± 1.10 *vs.* 9.67 ± 1.06, $p < 0.0001$), and MCP-3 (4.27 ± 1.59 *vs.* 1.04 ± 0.64, $p < 0.0001$).

3.3 Gene set enrichment analysis identified interferon-related signaling pathways in IIM

To reveal the potential pathogenic pathways involved in IIM, we performed GSEA with all genes and visualized pathway gene expression profiles according to MSAs. The top 15 pathways enriched in patients with IIM are shown in Figure 4A. The IFN-I and IFN-II signaling pathways were enriched in the top 15 pathways (Figure 4B). Remarkably, three IFN-related pathways were enriched in anti-MDA5+ DM patients (Figure 4C), and these three signaling pathways were significantly activated in anti-MDA5+ patients (Figure 4D). A pathway enrichment analysis was also performed in patients with IIM of different MSAs (Supplementary Figures S3A–C). The results demonstrated that the IFN-I and IFN-II signaling pathways were activated in patients with anti-TIF1-γ antibodies (Supplementary Figure S3D) and MSA-negative patients (Supplementary Figure S3E). However, differently from patients with other MSAs, only the IFN-I signaling pathway was activated in patients with anti-Jo-1 antibody (Supplementary Figure S3F).

The genes in interferon-related pathways were extracted and visualized in heat maps (Figures 4E, F). For all genes in these two interferon-related pathways, the patients with different MSAs had distinct expression profiles (Figure 4E). The reactome interferon signaling was only enriched in the MDA5 group, and based on the core enriched genes, certain genes like *ISG20*, *IFNA2*, and *IFNB1* were specifically highly expressed in anti-MDA5+ patients (Figure 4F). Above all, in contrast with HCs, the activation of interferon-related pathways and the upregulation of IFN-related genes were demonstrated in PBMCs of patients with IIM. The expression of IFN-I and IFN-II related genes was much more prominent in anti-MDA5+ DM patients compared with patients with other MSAs.

3.4 Weighted gene co-expression network analysis identified key IFN genes

To investigate the potential key genes in IIM, we performed WGCNA analysis to construct gene co-expression networks, identified gene modules related to clinical features, and found out the key DEGs involved in IIM interferon signaling. The optimal soft threshold value was selected as 12 (scale-free $R^2 = 0.8560$) to establish a scale-free network (Figure 5A). A total of 14 merged gene modules were obtained (Figure 5B). Traits including the presence or absence of IIM, autoantibody type of patients, clinical features of the disease, and immune infiltration of samples were

10.3389/fimmu.2023.1169057

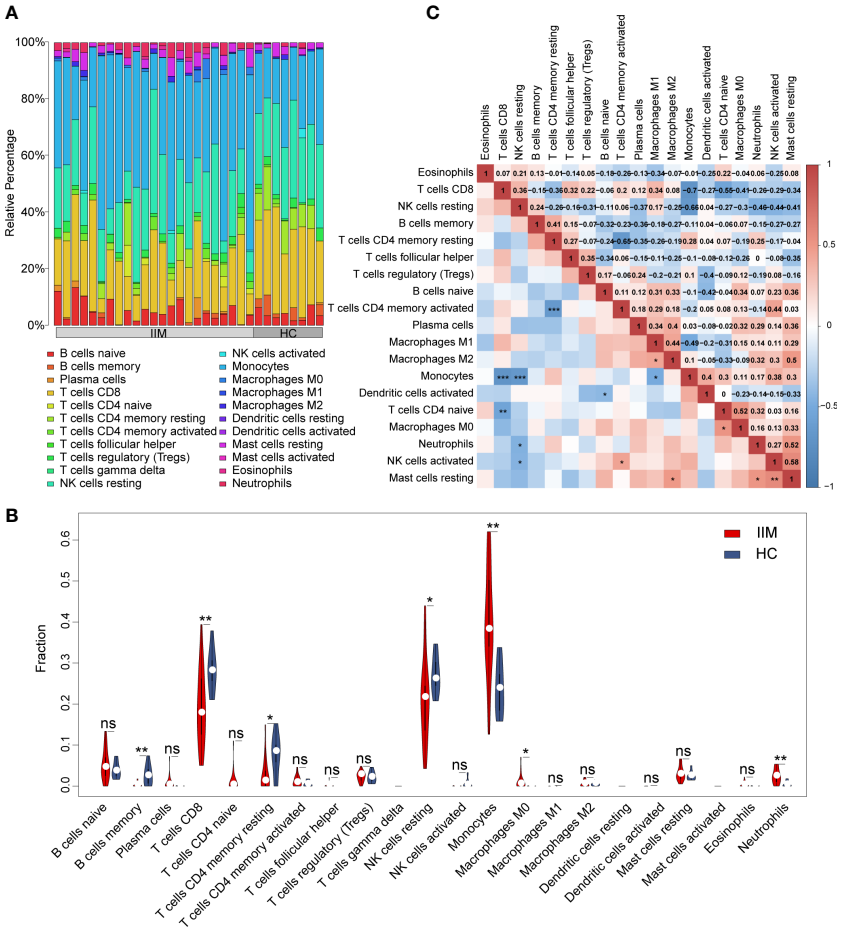

FIGURE 2
Landscape of immune infiltration in patients with idiopathic inflammatory myopathies (IIM). **(A)** Relative percentage of immune cells identified in patients with IIM (n = 23) and healthy controls (HCs; n = 8). **(B)** Violin plot showing the comparisons of immune cell fractions between patients with IIM and HCs. ***P < 0.001; **P < 0.01; *P < 0.05; ns, no significance. **(C)** Correlation analyses of immune cells in all patients. ***P < 0.001; **P < 0.01; *P < 0.05.

used to identify key gene modules. Based on the heat map, the overall IIM trait had closer relationships with the modules than each autoantibody-typed IIM trait (Figure 5C).

Thus, we selected seven modules based on their eigengene correlations with the IIM trait for further analysis: magenta (r = 0.79, p = 1e-07), yellow-green (r = 0.78, p = 2e-07), dark orange (r = -0.63, p = 1e-04), yellow (r = 0.61, p = 3e-04), dark red (r = 0.47, p = 0.007), light cyan (r = 0.43, p = 0.01), and dark green (r = -0.41, p = 0.02) modules. At the same time, these modules also showed close relationships with other traits (Figure 5C). For the IIM trait, a total of 1,288 hub genes were identified in the seven modules with the following criteria: |GS| >0.2 and |MM| >0.8 (Figure 5D).

To further identify significant genes involved in interferon signaling pathways, a conjoint analysis was performed with the DEGs of IIM, hub genes identified in WCGNA, and 204 genes from the reactome IFN signaling. A total of 29 genes were recognized as overlapped genes (Figure 5E), and a PPI network of these genes was constructed to demonstrate their relationships, which contained *TRIM25*, *DDX58*, *IRF7*, *STAT1*, *STAT2*, and so on (Figure 5F). Moreover, *IFIH1*, *ADAR*, and, *TBX21* were identified as hub genes, which were also related to IFN pathways.

3.5 Validation of IFN-related genes in the PBMCs of patients with IIM

To validate our findings, we further evaluated the interested IFN-related genes in IIM patients. *TRIM25*, *DDX58*, *IRF7*, *STAT1*, and *STAT2* genes were chosen from among the 29 common genes. *IFIH1*, *ADAR*, and *TBX21* were selected from WGCNA hub genes, in which *IFIH1* was also from IIM DEGs and *ADAR* belonged to the reactome interferon signaling. We also validated *MNDA* from the DEGs of patients with IIM.

As shown in Figure 6A, the upregulation of *IRF7* (1.51 ± 0.99 *vs.* 1.06 ± 0.36, p = 0.0044), *STAT1* (1.27 ± 0.58 *vs.* 1.06 ± 0.39, p = 0.0126), and *MNDA* (1.27 ± 0.44 *vs.* 1.02 ± 0.17, p = 0.0008) and the downregulation of *ADAR* (0.95 ± 0.41 *vs.* 1.01 ± 0.16, p = 0.0480) and *TBX21* (0.49 ± 0.38 *vs.* 1.07 ± 0.44, p < 0.0001) were detected in patients with IIM compared with HCs. We also detected the levels of IRF7, STAT1, STAT2, and SHP-1 proteins. As shown in Figure 6B, the increased protein expression of IRF7 (1.13 ± 0.32 *vs.* 0.79 ± 0.18, p = 0.0336), STAT1 (1.14 ± 0.30 *vs.* 0.66 ± 0.20, p = 0.0055), STAT2 (1.12 ± 0.36 *vs.* 0.56 ± 0.10, p = 0.0234), p-STAT1 (1.00 ± 0.27 *vs.* 0.57 ± 0.19, p = 0.0063), and p-STAT2 (1.03 ± 1.16

10.3389/fimmu.2023.1169057

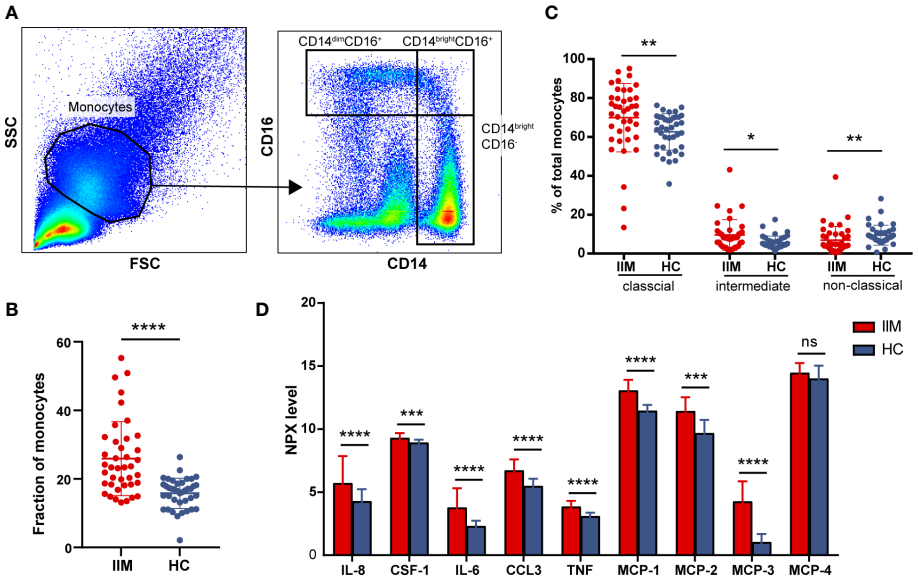

FIGURE 3
Monocyte subpopulations and plasma protein expressions quantified in idiopathic inflammatory myopathies (IIM). **(A)** Representative flow cytometry gating scheme to identify CD14dimCD16+, CD14brightCD16+, and CD14brightCD16- monocyte subpopulations in peripheral blood mononuclear cells (PBMCs) of IIM patients (n = 40) and healthy controls (HCs; n = 39). **(B)** Elevated monocyte fractions in PBMCs of IIM patients. **(C)** Changed frequencies of monocyte subpopulations in patients with IIM. **(D)** Expression levels of macrophage–monocyte-related proteins in the plasma of IIM patients (n = 25) and HCs (n = 29). ****P < 0.0001; ***P < 0.001; **P < 0.01; *P < 0.05; ns, no significance.

vs. 0.64 ± 0.09, p = 0.0001) was shown in the PBMCs of patients with IIM, and this altered protein expression mode represents the activation of IFN-I signaling and downstream JAK–STAT pathways. To further investigate the clinical meaning of these nine validated genes, we performed ROC analyses and calculated correlations between their mRNA expression and clinical laboratory data. As in Figure 6C, *TBX21* (AUC = 0.8848, 95%CI = 0.8206–0.9490) had a moderate value in IIM diagnosing, and *ADAR* (AUC = 0.6180, 95%CI = 0.5135–0.7224), *STAT1* (AUC = 0.6394, 95%CI = 0.5346–0.7442), *MNDA* (AUC = 0.6880, 95%CI = 0.5889–0.7872), and *IRF7* (AUC = 0.6287, 95%CI = 0.5251–0.7323) had a low diagnostic value. Their expressions were also related to some clinical indicators, such as WBC, ESR, AST, and so on (Figure 6D).

To know the expressions of the validated genes in anti-MDA5+ patients, comparisons were also made within IIM patients. Increased levels of *IFIH1* (1.55 ± 0.59 *vs.* 1.01 ± 0.21, p = 0.0011), *IRF7* (1.99 ± 1.02 *vs.* 1.06 ± 0.36, p < 0.0001), *STAT1* (1.56 ± 0.58 *vs.* 1.06 ± 0.39, p = 0.0001), and *MNDA* (1.43 ± 0.53 *vs.* 1.02 ± 0.17, p = 0.0003) as well as decreased levels of *TBX21* (0.52 ± 0.54 *vs.* 1.07 ± 0.44, p < 0.0001) were shown in anti-MDA5+ IIM patients in contrast with HCs (Figure 7A). Compared with patients without anti-MDA5 antibodies, elevated expressions of *DDX58* (1.19 ± 0.49 *vs.* 0.81 ± 0.44, p = 0.0056), *IFIH1* (1.55 ± 0.59 *vs.* 0.84 ± 0.41, p < 0.0001), *IRF7* (1.99 ± 1.02 *vs.* 1.11 ± 0.79, p = 0.0001), *STAT1* (1.56 ± 0.58 *vs.* 1.05 ± 0.48, p = 0.0008), *STAT2* (1.18 ± 0.45 *vs.* 0.85 ± 0.46, p = 0.0008), *ADAR* (1.16 ± 0.43 *vs.* 0.86 ± 0.38, p = 0.0072), and *TRIM25* (1.28 ± 0.48 *vs.* 0.99 ± 0.67, p = 0.0005) were found in anti-MDA5+ IIM patients (Figure 7A). Moreover, for anti-MDA5+ IIM patients, correlation analyses of the levels of anti-MDA5 Abs with IFN-I genes were performed. The levels of anti-MDA5 Abs correlated positively with *IRF7* (r = 0.4837, 95%CI = 0.1314–0.7276, p = 0.0078), *IFIH1* (r = 0.4739, 95%CI = 0.1188–0.7215, p = 0.0094), and *STAT1* (r = 0.3754, 95%CI = -0.0011–0.6586, p = 0.0448) (Figure 7B), while there was no correlation between the levels of anti-MDA5 Abs with *DDX58*, *STAT2*, *ADAR*, *MNDA*, *TBX21*, and *TRIM25*. For anti-MDA5+ IIM diagnosis, *IFIH1* (AUC = 0.8028, 95%CI = 0.6944–0.9113), *IRF7* (AUC = 0.8100, 95%CI = 0.7053–0.9146), *MNDA* (AUC = 0.7586, 95%CI = 0.6317–0.8855), *STAT1* (AUC = 0.7923, 95%CI = 0.6860–0.8987), and *TBX21* (AUC = 0.8333, 95%CI = 0.6870–0.9796) had a moderate potential, and *TRIM25* (AUC = 0.6627, 95%CI = 0.5220–0.8033) had a low potential (Figure 7C). Eight of the nine validated genes could distinguish anti-MDA5+ IIM patients from anti-MDA5- patients, and most of them showed a moderately distinguished value (Figure 7C).

From the discussion above, genes related to IFN pathway were highly expressed in patients with IIM, at both mRNA and protein levels. These IFN-related genes also had the potential in disease diagnosis and were correlated with multiple laboratory parameters, indicating their clinical significance for IIM. Moreover, compared with anti-MDA5- patients with IIM, a more predominant IFN gene signature was shown in anti-MDA5+ IIM patients, indicating the pathogenetic difference of patients with different MSAs.

3.6 Expression of IFN-related genes in monocytes of patients with IIM

As we have demonstrated above, monocytes and monocyte subpopulations were remarkably altered in the PBMCs of patients

10.3389/fimmu.2023.1169057

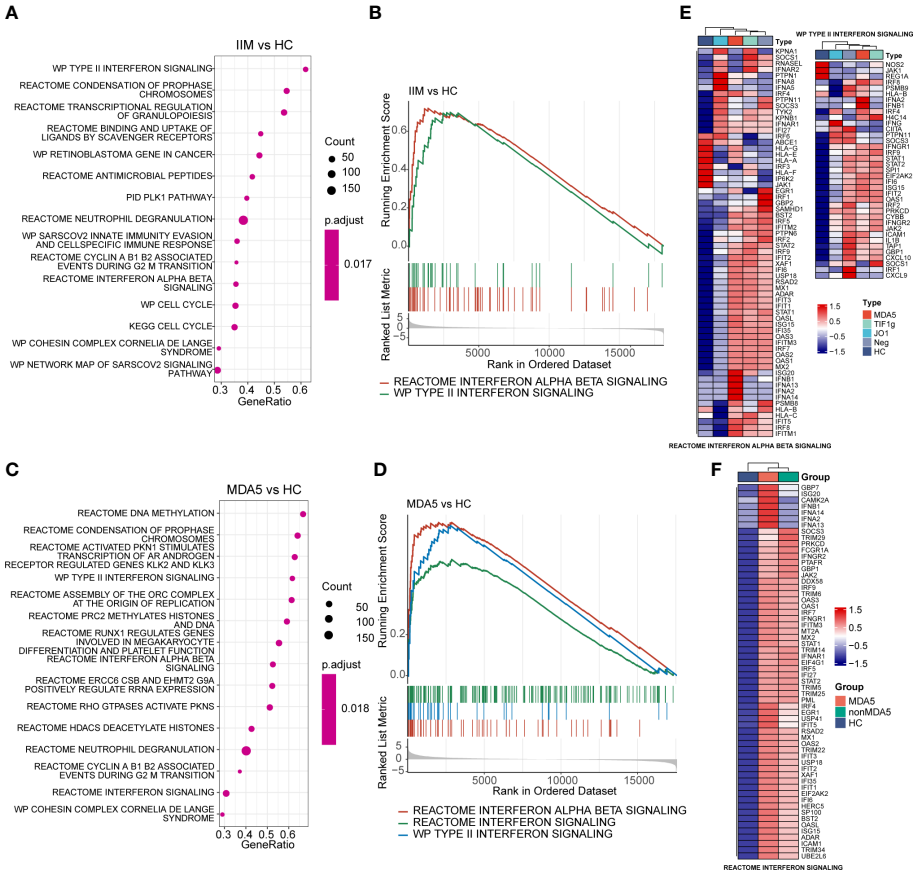

FIGURE 4
Gene set enrichment analysis of patients with idiopathic inflammatory myopathies (IIM) and anti-MDA5+ dermatomyositis (DM) patients. **(A)** Top 15 significantly enriched pathways in patients with IIM (n = 23) compared with healthy controls (HCs; n = 8). **(B)** Two interferon (IFN)-related pathways enriched in patients with IIM: reactome interferon alpha beta signaling pathway and WP type II interferon signaling pathway. **(C)** Top 15 significantly enriched pathways in anti-MDA5+ DM patients (n = 9) compared with HCs. **(D)** Three IFN-related pathways enriched in the MDA5 group: reactome interferon alpha beta signaling pathway, reactome interferon signaling pathway, and WP type II interferon signaling pathway. **(E)** Gene expression heat map of IFN-related pathways in IIM patients with different myositis-specific autoantibodies. **(F)** Expression pattern of the core enrichment gene in the reactome interferon signaling enriched in anti-MDA5+ DM patients.

with IIM. The levels of monocyte related cytokines were increased as well (Figure 3). Next, IFN-related gene expression was then quantified in monocytes. The results revealed that *DDX58* (1.66 ± 0.80 *vs.* 1.09 ± 0.48, p = 0.0294), *IFIH1* (1.56 ± 0.63 *vs.* 1.06 ± 0.41, p = 0.0304), *IRF7* (2.78 ± 1.25 *vs.* 1.05 ± 0.37, $p < 0.0001$), *STAT1* (1.67 ± 0.70 *vs.* 1.06 ± 0.39, p = 0.0116), *STAT2* (1.91 ± 0.80 *vs.* 1.03 ± 0.26, p = 0.0013), *ADAR* (1.44 ± 0.47 *vs.* 1.03 ± 0.25, p = 0.0027), and *TRIM25* (1.53 ± 0.41 *vs.* 1.02 ± 0.20, p = 0.0005) were elevated in the monocytes of patients with IIM (Figure 8A). Increased protein levels of IRF7 (0.87 ± 0.30 *vs.* 0.48 ± 0.15, p = 0.0058) and p-STAT2 (0.82 ± 0.30 *vs.* 0.49 ± 0.20, p = 0.0198) and decreased SHP1 (0.28 ± 0.10 *vs.* 0.54 ± 0.18, p = 0.0029) levels were also shown (Figure 8B). The ROC analysis indicated that *IRF7* (AUC = 0.9145, 95%CI = 0.8001–1.0000) expressed by monocytes had a high accuracy in the diagnosis of IIM (Figure 8C), and monocyte-expressed *STAT1* (AUC = 0.7650, 95%CI = 0.5672–0.9627), *STAT2* (AUC = 0.8611, 95%CI = 0.7115–1.0000), *IFIH1* (AUC = 0.7262, 95%CI = 0.5314–0.9209), *DDX58* (AUC = 0.7183, 95%CI = 0.5348–0.9017), *ADAR* (AUC = 0.8056, 95%CI = 0.6510–0.9601), and *TRIM25* (AUC = 0.8968, 95%CI = 0.7895–1.0000) demonstrated a moderate value in the diagnosis of patients with IIM (Figure 8C).

From these results, IFN-related genes were highly expressed by monocytes of IIM patients. Combined with its elevated subpopulations and related cytokine levels, monocytes may play an important role in IIM disease.

4 Discussion

Our study shows that gene expression profiles are significantly altered in patients with IIM, including the activation of IFN signaling. IFN-related genes were more prominently expressed in anti-MDA5+ IIM patients compared with patients with other MSAs. Monocytes rose in patients, exhibited a proinflammatory feature, and contributed to IFN signature.

Interferons are cytokines that can be widely produced by cells to induce antiviral states and regulate immune responses when the human body is invaded by pathogens (25). Type I interferon (IFN-I), type II interferon (IFN-II), and type III interferon (IFN-III) share

10.3389/fimmu.2023.1169057

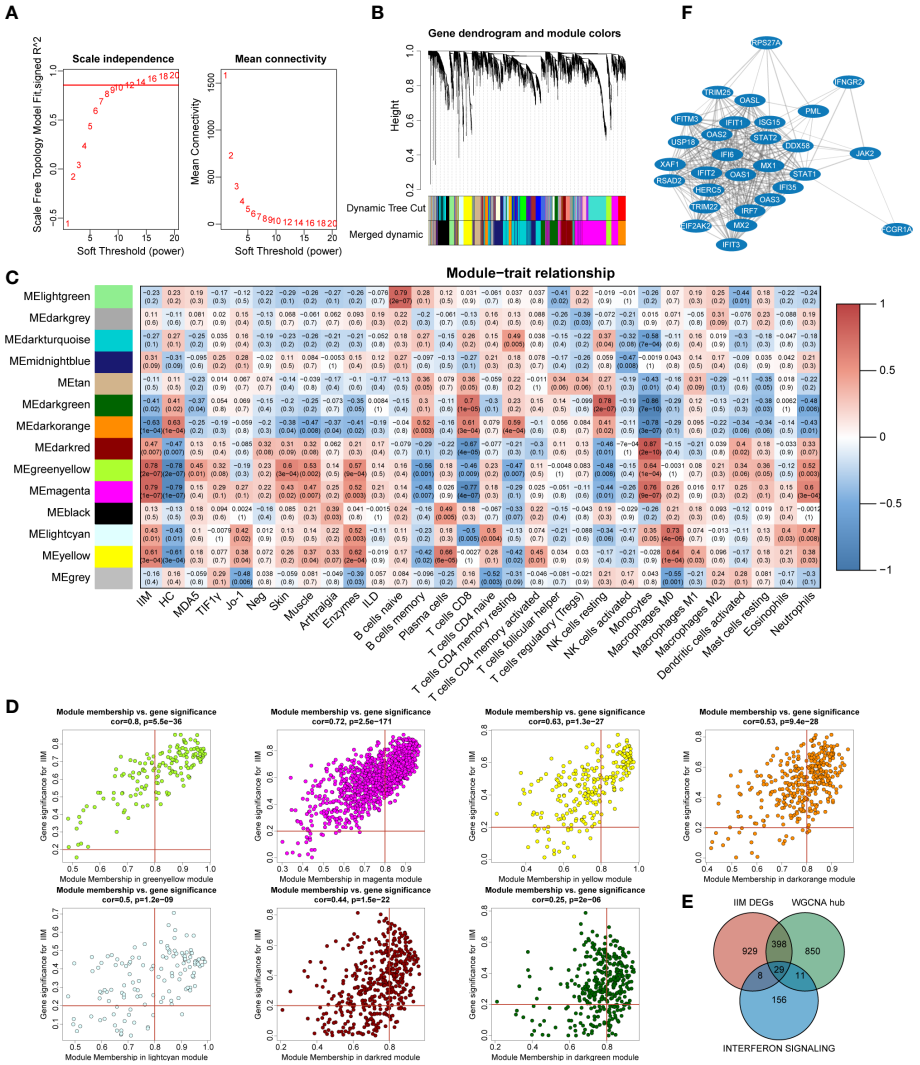

FIGURE 5
Identification of key interferon-related differentially expressed genes (DEGs) in idiopathic inflammatory myopathies (IIM). **(A)** Analysis of the network topology for selecting the optimal soft threshold power. **(B)** Gene clustering dendrogram and modules merged. **(C)** Correlation between modules and sample traits. **(D)** Scatter plots of gene significance for IIM *vs.* module membership (MM) in yellow-green, magenta, yellow, dark green, dark orange, light cyan, and dark red modules. **(E)** Venn diagram identifying 29 key interferon-related DEGs of IIM. **(F)** Protein–protein interaction network of the 29 key interferon-related DEGs.

overlapping downstream pathways like the JAK–STAT signaling pathway (26). Aberrant IFN signatures, especially IFN-I, have been reported in IIM. As described before, an activated IFN signature has been verified in diverse tissue types (11–13). The IFN signature also differs in clinical phenotypic IIM subsets, such as activated IFN pathways in the muscles of adult DM patients, instead of in others like PM (10, 27). Moreover, distinct expressions of IFN1-inducible and IFN2-inducible genes were also observed in the muscles of patients (27). In DEG identification of this study, MSA-typed IIM patients shared most of the overlapped DEGs, with some being uniquely expressed, where *IFI27* (*ISG12*), identified as a commonly upregulated topmost DEG in patients, was reported to be transcriptionally upregulated in response to IFN-I (28). Pathway enrichment analysis revealed the consistent activation of IFN-related pathways. More topmost IFN-related genes were enriched in anti-MDA5+ patients, while anti-Jo-1+ patients had fewer enriched IFN-related pathways. Just as in a study by Iago Pinal-Fernandez et al., IFN-I inducible genes were highly expressed in DM and moderately expressed in anti-synthetase syndrome (27).

We verified nine IFN-related genes in an expanded patient cohort. At both mRNA and protein levels, our validation confirms the IFN signaling activation in IIM PBMCs, and the genes involved are helpful in disease diagnosis. Anti-MDA5+ patients had a more pronounced degree of IFN-related gene deregulation than anti-MDA5- patients. Previous studies have pointed out the key role of IFN pathways in IIM pathophysiology (10)—for instance, IFN-I disrupts myoblast differentiation and induces myotube atrophy *in vitro* as well as undermines vascular network organization (29). Mitochondrial dysfunctions mediated by IFN-β-induced ROS lead to muscle inflammation and thus can cause a disease to be self-sustaining (28). Accumulating evidence indicates the possible correlation of MSAs and IFN in IIM. In an experimental myositis

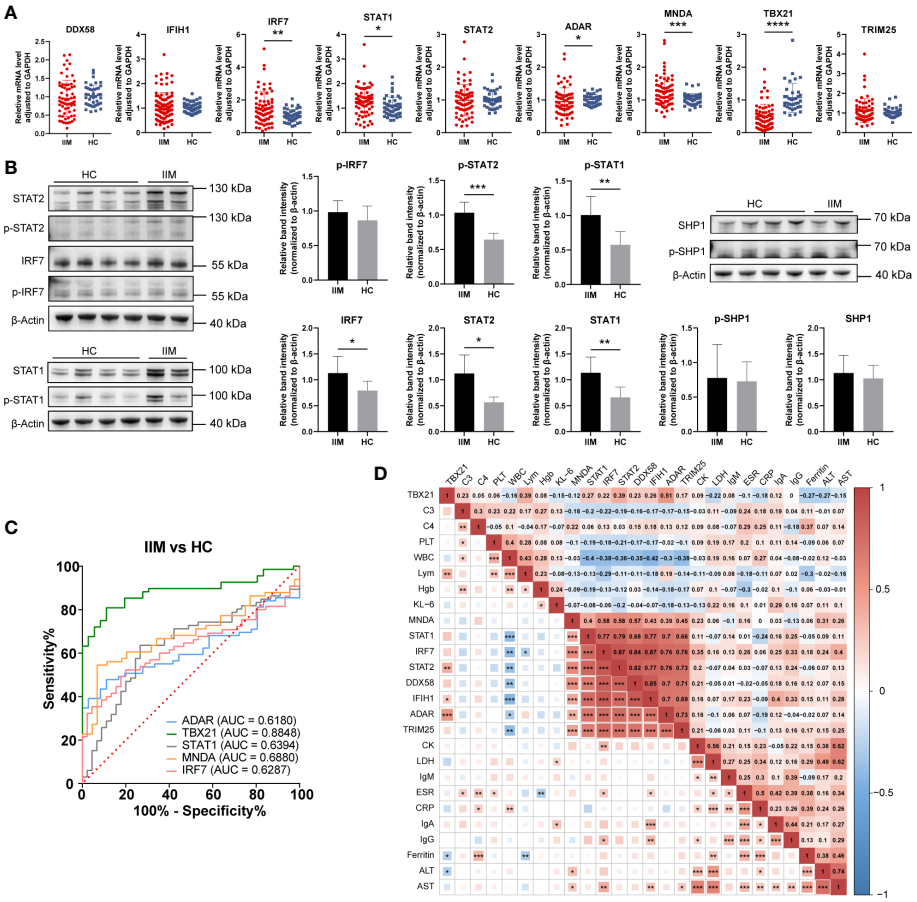

FIGURE 6
Validation of interferon-related genes in the peripheral blood mononuclear cells of patients with idiopathic inflammatory myopathies (IIM). **(A)** Expression levels of *DDX58*, *IFIH1*, *IRF7*, *STAT1*, *STAT2*, *ADAR*, *MNDA*, *TBX21*, and *TRIM25* detected in patients with IIM (n = 93) and heathy controls (HCs; n = 57) by qRT-PCR. **(B)** Expression of IRF7, p-IRF7, STAT1, p-STAT1, STAT2, p- STAT2, SHP1, and p-SHP1 detected in patients with IIM (n = 5) and HCs (n = 8) by Western blotting. **(C)** Receiver operating characteristic analyses of the validated genes in the diagnosis of IIM. **(D)** Heat map of the correlation between laboratory parameters and gene expressions in patients with IIM. *p < 0.05, **p < 0.01, ***p < 0.001, and ****p < 0.0001.

model induced with TIF1γ, IFN-I is essential (30). The TRIM33/TIF1γ deficiency results in a high and sustained expression of interferon-β gene in macrophages (31). Immune complexes (ICs) containing anti-Jo-1 and RNA may act as endogenous inducers to activate IFN-α production (32). In muscle tissues from anti-Jo-1+ IIM patients, the B-cell-activating factor of the tumor necrosis factor family (BAFF) is involved in autoantibody production, of which the levels may be influenced by IFN-I (33). Our work complements the previous studies by characterizing the gene expression profiles of PBMCs in IIM patients with different MSAs. Our finding supports the clinical treatment consideration targeted by the IFN pathway, including the use of anti-IFN-α antibody sifalimumab and the use of JAK inhibitors like ruxolitinib and tofacitinib (29, 34, 35).

Upregulated IFN signatures in anti-MDA5+ IIM patients have been reported, especially when compared with anti-MDA5- patients. The serum IFN-α of anti-MDA5+ patients can be used as a biomarker and may reflect the existence of a rapidly progressive interstitial lung disease (36). A stronger IFN-I signature was found in the skin tissue of anti-MDA5+ than anti-MDA5- DM, and IFN-κ, mainly secreted by keratinocytes, possibly participates in skin pathophysiology (37). The expressions of ISGs were also upregulated in a muscle biopsy of anti-MDA5+ DM; however, the IFN score was lower than in classic DM patients (38). Our research shows that the PBMCs of anti-MDA5+ IIM patients have a more pronounced IFN signature, which is correlated positively with the level of anti-MDA5 Abs. This observation may be explained by many findings that highlighted the correlations of anti-MDA5 antibodies (Abs) and IFN. The MDA5 protein is a viral dsRNA sensor which can induce antiviral gene transcription like IFN-I genes and promote proinflammatory cytokine production (39). Abs may bind to MDA5+ cells to induce the aberrant activation of IFN pathway (39). ICs formed by MDA5 and Abs induce IFN-α production *in vitro*, and other monoclonal autoantibodies that existed in anti-MDA5+ DM patients could trigger IFN-γ production directly (40, 41). Combined with previous evidence, our findings strongly support the anti-IFN treatment choice for IIM patients with anti-MDA5 antibody. Additionally, pathways like neutrophil granulation and DNA methylation were also highly activated in anti-MDA5+ patients. Methylation alterations have been found out in affected muscles of JDM, which relate to a self-renewal capacity (42). The aberrant DNA methylation in CD4+ T

10.3389/fimmu.2023.1169057

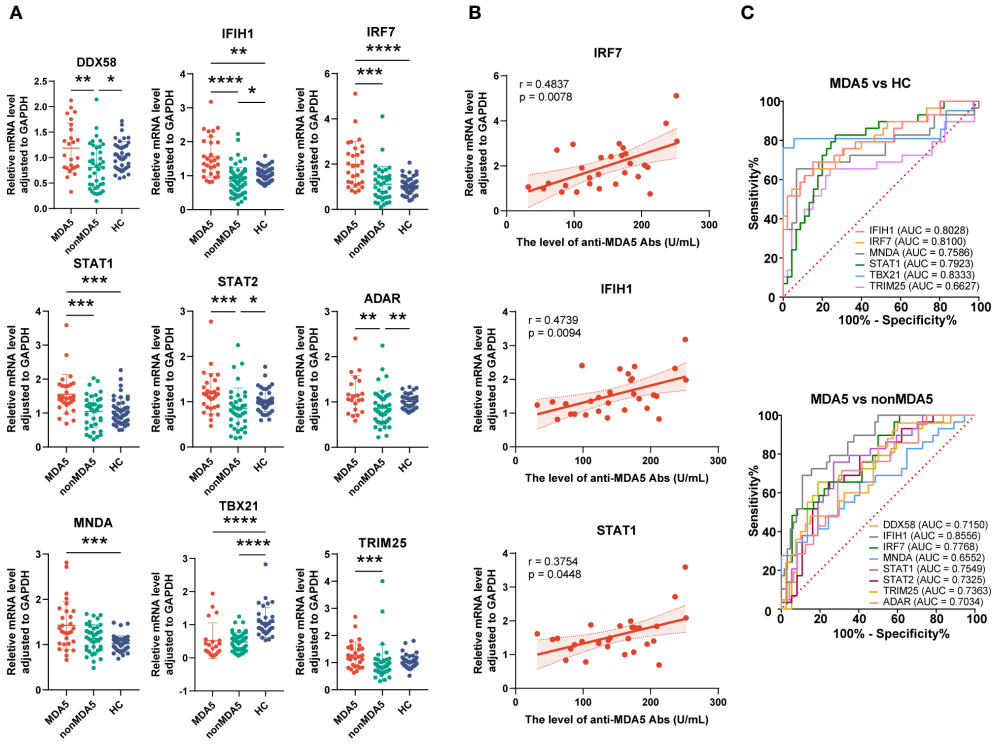

FIGURE 7
Expression of interferon-related genes in the peripheral blood mononuclear cells of anti-MDA5+ idiopathic inflammatory myopathy (IIM) patients. **(A)** The expression levels of the nine validated genes were compared among anti-MDA5+ IIM patients (*n* = 29), anti-MDA5- IIM patients (*n* = 64), and healthy controls (*n* = 57). **(B)** Correlation analyses of anti-MDA5 antibody levels with the expressions of *IFIH1*, *IRF7*, and *STAT1* genes in anti-MDA5+ IIM patients, with the correlation coefficient *r* values, *p* values, and 95% confidence intervals indicated. **(C)** Receiver operating characteristic analyses of the validated genes in distinguishing anti-MDA5+ patients. **p* < 0.05, ***p* < 0.01, ****p* < 0.001, and *****p* < 0.0001.

cells was also found to be associated with systemic lupus erythematosus (SLE) and systemic sclerosis (43).

The monocytes in our study fill a gap of previous studies showing the proinflammatory role of monocytes in IIM. Both from immune cell infiltration and flow cytometry results, the monocytes increased. Patients with IIM had more classical and intermediate monocyte subpopulations and also fewer non-classical subpopulations. This change was also manifested by anti-MDA5+ patients. The plasma levels of monocyte-related proinflammatory cytokines and chemokines increased, and the monocytes in patients had upregulated IFN-related gene expressions. Consistent with a previous research, patients with IIM had increased monocytes (44). Active IIM patients were found with decreased classical and increased intermediate monocyte subsets, and intermediate monocytes increased in treatment-responsive patients, while it decreased in non-responders (45, 46). Our data showed elevated classical and intermediate as well as reduced non-classical subset fractions of monocytes, representing more proinflammatory and fewer anti-inflammatory phenotypic monocytes in IIM. Monocytes/macrophages have been verified as the major producer of inflammatory cytokines in the arthritic lesions of rheumatoid arthritis (47). We also found the plasma level of proinflammatory cytokines like IL-6 and TNF as well as chemokines like CCL3 and MCPs to have been increased, suggesting the possibly promoted proinflammatory cytokine secretion by monocytes and enhanced chemotaxis to damaged sites. The monocytes in patients also expressed upregulated IFN-related genes, which, with its increased amount, may be a potentially significant cell source of IFN signatures. The monocytes/macrophages have been found to be associated with the IFN signature of PBMCs of SLE, in which the classical subset is the primary IFN-I responder (48). Here in this research, we find that the monocytes of IIM patients exhibited a proinflammatory characteristic, including increase to a broad population and altered subset fractions, and possibly promoted cytokine/chemokine production, which also contribute to the IFN signature. In the study of Ye et al., the immune signatures of peripheral B and T cells were demonstrated, revealing the IFN-I signature in anti-MDA5+ DM patients (14). We investigated the transcriptomic profiling of IIM patients with different MSAs in our study. The IFN-I and IFN-II signatures were prominent in anti-MDA5+ IIM patients compared with patients with other MSAs. In addition, we emphasized the pivotal role of monocytes in patients with IIM. Monocytes exhibited a proinflammatory feature and contributed to the IFN signature of IIM patients in our study.

5 Limitations

This study had several limitations. Firstly, patients with IIM of all kinds of MSAs were not enrolled. Secondly, this was a single-center study. Thirdly, absolute count beads were not added in

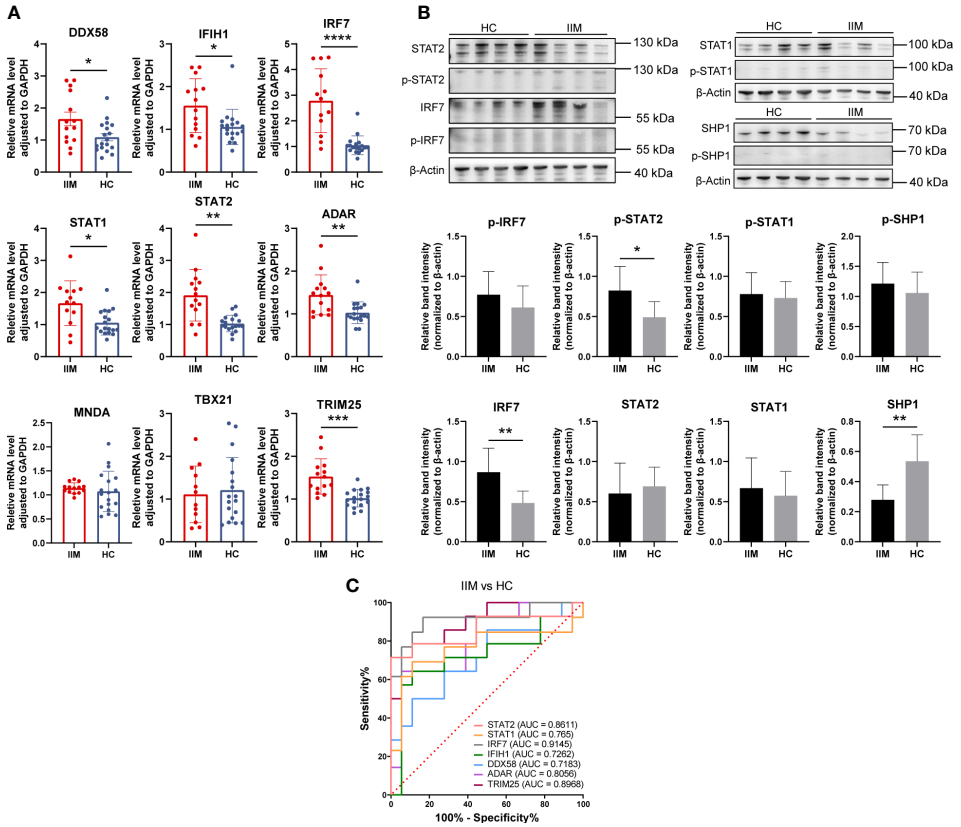

FIGURE 8
Validation of interferon-related genes in the monocytes of patients with idiopathic inflammatory myopathies (IIM). **(A)** Expression levels of *DDX58*, *IFIH1*, *IRF7*, *STAT1*, *STAT2*, *ADAR*, *MNDA*, *TBX21*, and *TRIM25* detected in the monocytes of patients with IIM (n = 14) and healthy controls (HCs; n = 18) by qRT-PCR. **(B)** Expression of IRF7, p-IRF7, STAT1, p-STAT1, STAT2, p-STAT2, SHP1, and p-SHP1 detected in the monocytes of patients with IIM (n = 8) and HCs (n = 8) by Western blotting. **(C)** Receiver operating characteristic analyses of the genes expressed by monocytes in the diagnosis of IIM. *p < 0.05, **p < 0.01, ***p < 0.001, and ****p < 0.0001.

performing the flow cytometry experiment, so it was not able to calculate the absolute counts of monocytes in our study. Fourthly, the mechanisms and factors influencing the activation of the IFN pathway in patients with anti-MDA5+ IIM need to be further explored. Furthermore, the proinflammatory role of monocytes with IFN-I activation in the pathogenesis of anti-MDA5+ IIM patients is worth exploring.

6 Conclusions

In conclusion, our study demonstrated that the genes in patients with IIM were remarkably altered compared with HCs. IFN signatures were found in IIM patients with different MSAs. IFN expression profiling was more prominent in anti-MDA5+ DM patients. The monocytes showed a proinflammatory characteristic and contributed to the IFN signature of PBMCs of IIM patients.

Data availability statement

The data presented in the study are deposited in the NCBI's Sequence Read Archive (SRA) repository, accession number PRJNA960687.

Ethics statement

The studies involving human participants were reviewed and approved by the Ethics Committee of the First Affiliated Hospital of Zhengzhou University. The patients/participants provided their written informed consent to participate in this study.

Author contributions

Study design: PZ, SL, and ML. Sample collection: PZ, ML, YZ, JS, ZP, and SL. Sample processing, experimental validation, and data analysis: ML, PZ, and YS. Drafting of the article: ML. Review and editing: PZ, YZ, WZ, RL, and SL. All authors contributed to the article and approved the submitted version.

Funding

This study was supported by the National Natural Science Foundation of China (82101889) and Joint Project of Medical

Science and Technology Key Program of Henan Province (LHGJ20210278).

Acknowledgments

We thank all the patients who participated in this study. We preferentially thank the healthy volunteers for their blood donation.

Conflict of interest

The authors declare that the research was conducted in the absence of any commercial or financial relationships that could be construed as a potential conflict of interest.

Publisher's note

Supplementary material

The Supplementary Material for this article can be found online at: https://www.frontiersin.org/articles/10.3389/fimmu.2023.1169057/full#supplementary-material

References

1. Lundberg IE, Fujimoto M, Vencovsky J, Aggarwal R, Holmqvist M, Christopher-Stine L, et al. Idiopathic inflammatory myopathies. *Nat Rev Dis Primers* (2021) 7(1):86. doi: 10.1038/s41572-021-00321-x

2. Preusse C, Eede P, Heinzeling L, Freitag K, Koll R, Froehlich W, et al. NanoString technology distinguishes anti-TIF-1γ(+) from anti-Mi-2(+) dermatomyositis patients. *Brain Pathol* (2021) 31(3):e12957. doi: 10.1111/bpa.12957

3. Fiorentino DF, Chung LS, Christopher-Stine L, Zaba L, Li S, Mammen AL, et al. Most patients with cancer-associated dermatomyositis have antibodies to nuclear matrix protein NXP-2 or transcription intermediary factor 1γ: antibodies to NXP-2 and TIF-1γ in cancer-associated dermatomyositis. *Arthritis Rheumatism* (2013) 65 (11):2954–62. doi: 10.1002/art.38093

4. Sato S, Hoshino K, Satoh T, Fujita T, Kawakami Y, Fujita T, et al. RNA Helicase encoded by melanoma differentiation-associated gene 5 is a major autoantigen in patients with clinically amyopathic dermatomyositis: association with rapidly progressive interstitial lung disease. *Arthritis Rheumatol* (2009) 60(7):2193–200. doi: 10.1002/art.24621

5. Pinal-Fernandez I, Casal-Dominguez M, Derfoul A, Pak K, Miller FW, Milisenda JC, et al. Machine learning algorithms reveal unique gene expression profiles in muscle biopsies from patients with different types of myositis. *Ann Rheum Dis* (2020) 79 (9):1234–42. doi: 10.1136/annrheumdis-2019-216599

6. Liu D, Zhao L, Jiang Y, Li L, Guo M, Mu Y, et al. Integrated analysis of plasma and urine reveals unique metabolomic profiles in idiopathic inflammatory myopathies subtypes. *J Cachexia Sarcopenia Muscle* (2022) 13(5):2456–72. doi: 10.1002/jcsm.13045

7. Venalis P, Lundberg IE. Immune mechanisms in polymyositis and dermatomyositis and potential targets for therapy. *Rheumatology* (2014) 53(3):397–405. doi: 10.1093/rheumatology/ket279

8. Corona-Sanchez EG, Martínez-García EA, Lujano-Benítez AV, Pizano-Martinez O, Guerra-Durán IA, Chavarria-Avila E, et al. Autoantibodies in the pathogenesis of idiopathic inflammatory myopathies: does the endoplasmic reticulum stress response have a role? *Front Immunol* (2022) 13:940122. doi: 10.3389/fimmu.2022.940122

9. McLellan K, Papadopoulou C. Update on biomarkers of vasculopathy in juvenile and adult myositis. *Curr Rheumatol Rep* (2022) 24(7):227–37. doi: 10.1007/s11926-022-01076-4

10. Bolko L, Jiang W, Tawara N, Landon-Cardinal O, Anquetil C, Benveniste O, et al. The role of interferons type I, II and III in myositis: a review. *Brain Pathol* (2021) 31(3):e12955. doi: 10.1111/bpa.12955

11. Walsh RJ, Kong SW, Yao Y, Jallal B, Kiener PA, Pinkus JL, et al. Type I interferon–inducible gene expression in blood is present and reflects disease activity in dermatomyositis and polymyositis. *Arthritis Rheumatol* (2007) 56(11):3784–92. doi: 10.1002/art.22928

12. Wong D, Kea B, Pesich R, Higgs BW, Zhu W, Brown P, et al. Interferon and biologic signatures in dermatomyositis skin: specificity and heterogeneity across diseases. *Nataf S editor. PloS One* (2012) 7(1):e29161. doi: 10.1371/journal.pone.0029161

13. Soponkanaporn S, Deakin CT, Schutz PW, Marshall LR, Yasin SA, Johnson CM, et al. Expression of myxovirus-resistance protein a: a possible marker of muscle disease activity and autoantibody specificities in juvenile dermatomyositis. *Neuropathol Appl Neurobiol* (2019) 45(4):410–20. doi: 10.1111/nan.12498

14. Ye Y, Chen Z, Jiang S, Jia F, Li T, Lu X, et al. Single-cell profiling reveals distinct adaptive immune hallmarks in MDA5+ dermatomyositis with therapeutic implications. *Nat Commun* (2022) 13(1):6458. doi: 10.1038/s41467-022-34145-4

15. Zhao L, Wang Q, Zhou B, Zhang L, Zhu H. The role of immune cells in the pathogenesis of idiopathic inflammatory myopathies. *Aging Dis* (2021) 12(1):247. doi: 10.14336/AD.2020.0410

16. Mainetti C, Terziroli Beretta-Piccoli B, Selmi C. Cutaneous manifestations of dermatomyositis: a comprehensive review. *Clinic Rev Allerg Immunol* (2017) 53 (3):337–56. doi: 10.1007/s12016-017-8652-1

17. Zong M, Lundberg IE. Pathogenesis, classification and treatment of inflammatory myopathies. *Nat Rev Rheumatol* (2011) 7(5):297–306. doi: 10.1038/nrrheum.2011.39

18. Rostasy KM, Piepkorn M, Goebel HH, Menck S, Hanefeld F, Schulz-Schaeffer WJ. Monocyte/macrophage differentiation in dermatomyositis and polymyositis. *Muscle Nerve* (2004) 30(2):225–30. doi: 10.1002/mus.20088

19. Yasin SA, Schutz PW, Deakin CT, Sag E, Varsani H, Simou S, et al. Histological heterogeneity in a large clinical cohort of juvenile idiopathic inflammatory myopathy: analysis by myositis autoantibody and pathological features. *Neuropathol Appl Neurobiol* (2019) 45(5):495–512. doi: 10.1111/nan.12528

20. Gono T, Okazaki Y, Kuwana M. Antiviral proinflammatory phenotype of monocytes in anti-MDA5 antibody-associated interstitial lung disease. *Rheumatology* (2022) 61(2):806–14. doi: 10.1093/rheumatology/keab371

21. Wilkinson MGL, Moulding D, McDonnell TCR, Orford M, Wincup C, Ting JYJ, et al. Role of CD14+ monocyte-derived oxidised mitochondrial DNA in the inflammatory interferon type 1 signature in juvenile dermatomyositis. *Ann Rheum Dis* (2023) 82(5):658–69. doi: 10.1136/ard-2022-223469

22. Bohan A, Peter JB. Polymyositis and dermatomyositis (first of two parts). *N Engl J Med* (1975) 292(7):344–7. doi: 10.1056/NEJM197502132920706

23. Bolger AM, Lohse M, Usadel B. Trimmomatic: a flexible trimmer for illumina sequence data. *Bioinformatics* (2014) 30(15):2114–20. doi: 10.1093/bioinformatics/btu170

24. Kim D, Langmead B, Salzberg SL. HISAT: a fast spliced aligner with low memory requirements. *Nat Methods* (2015) 12(4):357–60. doi: 10.1038/nmeth.3317

25. McNab F, Mayer-Barber K, Sher A, Wack A, O'Garra A. Type I interferons in infectious disease. *Nat Rev Immunol* (2015) 15(2):87–103. doi: 10.1038/nri3787

26. Gallay L, Mouchiroud G, Chazaud B. Interferon-signature in idiopathic inflammatory myopathies. *Curr Opin Rheumatol* (2019) 31(6):634–42. doi: 10.1097/BOR.0000000000000653

27. Pinal-Fernandez I, Casal-Dominguez M, Derfoul A, Pak K, Plotz P, Miller FW, et al. Identification of distinctive interferon gene signatures in different types of myositis. *Neurology* (2019) 93(12):e1193–204. doi: 10.1212/WNL.0000000000008128

28. Meyer A, Laverny G, Allenbach Y, Grelet E, Ueberschlag V, Echaniz-Laguna A, et al. IFN-β-induced reactive oxygen species and mitochondrial damage contribute to muscle impairment and inflammation maintenance in dermatomyositis. *Acta Neuropathol* (2017) 134(4):655–66. doi: 10.1007/s00401-017-1731-9

29. Ladislau L, Suárez-Calvet X, Toquet S, Landon-Cardinal O, Amelin D, Depp M, et al. JAK inhibitor improves type I interferon induced damage: proof of concept in dermatomyositis. *Brain* (2018) 141(6):1609–21. doi: 10.1093/brain/awy105

30. Okiyama N, Ichimura Y, Shobo M, Tanaka R, Kubota N, Saito A, et al. Immune response to dermatomyositis-specific autoantigen, transcriptional intermediary factor 1γ can result in experimental myositis. *Ann Rheum Dis* (2021) 80(9):1201–8. doi: 10.1136/annrheumdis-2020-218661

31. Ferri F, Parcelier A, Petit V, Gallouet AS, Lewandowski D, Dalloz M, et al. TRIM33 switches off Ifnb1 gene transcription during the late phase of macrophage activation. *Nat Commun* (2015) 6:8900. doi: 10.1038/ncomms9900

32. Eloranta ML, Barbasso Helmers S, Ulfgren AK, Rönnblom L, Alm GV, Lundberg IE. A possible mechanism for endogenous activation of the type I interferon system in myositis patients with anti-Jo-1 or anti-ro 52/anti-ro 60 autoantibodies. *Arthritis Rheumatol* (2007) 56(9):3112–24. doi: 10.1002/art.22860

33. Kryštůfková O, Barbasso Helmers S, Venalis P, Malmström V, Lindroos E, Vencovský J, et al. Expression of BAFF receptors in muscle tissue of myositis patients with anti-Jo-1 or anti-Ro52/anti-Ro60 autoantibodies. *Arthritis Res Ther* (2014) 16 (5):454. doi: 10.1186/s13075-014-0454-8

34. Higgs BW, Zhu W, Morehouse C, White WI, Brohawn P, Guo X, et al. A phase 1b clinical trial evaluating sifalimumab, an anti-IFN-α monoclonal antibody, shows target neutralisation of a type I IFN signature in blood of dermatomyositis and polymyositis patients. *Ann Rheum Dis* (2014) 73(1):256–62. doi: 10.1136/annrheumdis-2012-202794

35. Paik JJ, Casciola-Rosen L, Shin JY, Albayda J, Tiniakou E, Leung DG, et al. Study of tofacitinib in refractory dermatomyositis: an open-label pilot study of ten patients. *Arthritis Rheumatol* (2021) 73(5):858–65. doi: 10.1002/art.41602

36. Horai Y, Koga T, Fujikawa K, Takatani A, Nishino A, Nakashima Y, et al. Serum interferon-α is a useful biomarker in patients with anti-melanoma differentiation-associated gene 5 (MDA5) antibody-positive dermatomyositis. *Mod Rheumatol* (2015) 25(1):85–9. doi: 10.3109/14397595.2014.900843

37. Cassius C, Amode R, Delord M, Battistella M, Poirot J, How-Kit A, et al. MDA5+ dermatomyositis is associated with stronger skin type I interferon transcriptomic signature with upregulation of IFN-κ transcript. *J Invest Dermatol* (2020) 140 (6):1276–9. doi: 10.1016/j.jid.2019.10.020

38. Allenbach Y, Leroux G, Suárez-Calvet X, Preusse C, Gallardo E, Hervier B, et al. Dermatomyositis with or without anti-melanoma differentiation-associated gene 5 antibodies. *Am J Pathol* (2016) 186(3):691–700. doi: 10.1016/j.ajpath.2015.11.010

39. Nombel A, Fabien N, Coutant F. Dermatomyositis with anti-MDA5 antibodies: bioclinical features, pathogenesis and emerging therapies. *Front Immunol* (2021) 12:773352. doi: 10.3389/fimmu.2021.773352

40. Wang K, Zhao J, Wu W, Xu W, Sun S, Chen Z, et al. RNA-Containing immune complexes formed by anti-melanoma differentiation associated gene 5 autoantibody are potent inducers of IFN-α. *Front Immunol* (2021) 12:743704. doi: 10.3389/fimmu.2021.743704

41. Coutant F, Bachet R, Pin JJ, Alonzo M, Miossec P. Monoclonal antibodies from b cells of patients with anti-MDA5 antibody-positive dermatomyositis directly stimulate interferon gamma production. *J Autoimmun* (2022) 130:102831. doi: 10.1016/j.jaut.2022.102831

42. Wang M, Xie H, Shrestha S, Sredni S, Morgan GA, Pachman LM. Methylation alterations of WT1 and homeobox genes in inflamed muscle biopsy samples from patients with untreated juvenile dermatomyositis suggest self-renewal capacity. *Arthritis Rheumatol* (2012) 64(10):3478–85. doi: 10.1002/art.34573

43. Lei W, Luo Y, Lei W, Luo Y, Yan K, Zhao S, et al. Abnormal DNA methylation in CD4+ T cells from patients with systemic lupus erythematosus, systemic sclerosis, and dermatomyositis. *Scand J Rheumatol* (2009) 38(5):369–74. doi: 10.1080/03009740902758875

44. Wilfong EM, Bartkowiak T, Vowell KN, Westlake CS, Irish JM, Kendall PL, et al. High-dimensional analysis reveals distinct endotypes in patients with idiopathic inflammatory myopathies. *Front Immunol* (2022) 13:756018. doi: 10.3389/fimmu.2022.756018

45. Torres-Ruiz J, Carrillo-Vazquez DA, Padilla-Ortiz DM, Vazquez-Rodriguez R, Nuñez-Alvarez C, Juarez-Vega G, et al. TLR expression in peripheral monocyte subsets of patients with idiopathic inflammatory myopathies: association with clinical and immunological features. *J Transl Med* (2020) 18(1):125. doi: 10.1186/s12967-020-02290-3

46. Tang Q, Gheorghe KR, Bruton M, Fernandes-Cerqueira C, Harris RA, Nennesmo I, et al. Features of repeated muscle biopsies and phenotypes of monocytes in paired blood samples and clinical long-term response to treatment in patients with idiopathic inflammatory myopathy: a pilot study. *Clin Exp Rheumatol* (2020) 38(1):42–9.

47. Roberts CA, Dickinson AK, Taams LS. The interplay between Monocytes/Macrophages and CD4(+) T cell subsets in rheumatoid arthritis. *Front Immunol* (2015) 6:571. doi: 10.3389/fimmu.2015.00571

48. Han S, Zhuang H, Lee PY, Li M, Yang L, Nigrovic PA, et al. Differential responsiveness of monocyte and macrophage subsets to interferon. *Arthritis Rheumatol* (2020) 72(1):100–13. doi: 10.1002/art.41072

frontiers | Frontiers in Immunology

TYPE Review
PUBLISHED 12 May 2023
DOI 10.3389/fimmu.2023.1125257

OPEN ACCESS

EDITED BY
Oded Shamriz,
Hadassah Medical Center, Israel

REVIEWED BY
Yaoxiang Sun,
The Affiliated Yixing Hospital of Jiangsu University, China
Edoardo Rosato,
Sapienza University of Rome, Italy
Philippe Guilpain,
Université de Montpellier, France
Nicolò Costantino Brembilla,
University of Geneva, Switzerland

*CORRESPONDENCE
Jinlan Jiang
jiangjinlan@jlu.edu.cn
Ping Li
l i_ping@jlu.edu.cn

†These authors have contributed equally to this work and share first authorship

RECEIVED 16 December 2022
ACCEPTED 24 April 2023
PUBLISHED 12 May 2023

CITATION
Zhao K, Kong C, Shi N, Jiang J and Li P (2023) Potential angiogenic, immunomodulatory, and antifibrotic effects of mesenchymal stem cell-derived extracellular vesicles in systemic sclerosis. *Front. Immunol.* 14:1125257. doi: 10.3389/fimmu.2023.1125257

Potential angiogenic, immunomodulatory, and antifibrotic effects of mesenchymal stem cell-derived extracellular vesicles in systemic sclerosis

Kelin Zhao[1†], Chenfei Kong[2†], Naixu Shi[3], Jinlan Jiang[2*] and Ping Li[1*]

[1]Department of Rheumatology and Immunology, China-Japan Union Hospital, Jilin University, Changchun, China, [2]Scientific Research Center, China-Japan Union Hospital, Jilin University, Changchun, China, [3]Department of Stomatology, China-Japan Union Hospital, Jilin University, Changchun, China

Systemic sclerosis (SSc) is an intricate systemic autoimmune disease with pathological features such as vascular injury, immune dysregulation, and extensive fibrosis of the skin and multiple organs. Treatment options are limited; however, recently, mesenchymal stem cell-derived extracellular vesicles (MSC-EVs) have been acknowledged in preclinical and clinical trials as being useful in treating autoimmune diseases and are likely superior to MSCs alone. Recent research has also shown that MSC-EVs can ameliorate SSc and the pathological changes in vasculopathy, immune dysfunction, and fibrosis. This review summarizes the therapeutic effects of MSC-EVs on SSc and the mechanisms that have been discovered to provide a theoretical basis for future studies on the role of MSC-EVs in treating SSc.

KEYWORDS

systemic sclerosis, fibrosis, mesenchymal stem cell, extracellular vesicle, vascular injury

1 Introduction

Systemic sclerosis (SSc) is a complex and chronic connective tissue disorder with an incidence of 17.6 per 10,000 (1). The pathogenesis of SSc is dominated by disorders in three major areas of pathophysiology: vasculopathy, immune dysfunction, and fibrosis. The disease progression is cumulative with amplified effects that primarily involve endothelial cell (EC) activation and the recruitment of inflammatory cells, followed by the release of various factors. This results in fibroblast activation and the deposition of extracellular matrix (ECM) proteins (2).

However, the etiology of SSc is complex and unclear since epigenetics, environmental factors, and a history of infection and drugs may all contribute to SSc. Genetics is the primary factor, and a survey has shown the percentage of relatives of patients with SSc suffering from the disease is higher than that of the general population (3). In addition, genetic factor studies at different levels of genetic information have advanced considerably with the development of technology and lower costs. There is a close relationship between human leukocyte antigen (HLA) locus genes and SSc, and 32 non-HLA loci have been identified (4). This opens up promising possibilities for the use of precision medicine for SSc patients. It has been shown that viruses could trigger SSc, in particular parvovirus B19 (5), cytomegalovirus, Epstein–Barr virus, and retroviruses (6). Intriguingly, recent findings that SARS-CoV-2 may be involved in the occurrence of SSc have been disputed. Although COVID-19 in patients only affects the incidence of SSc minimally (7), both diseases have manifestations of endothelial damage, making it possible for them to correlate (8).

Clinically, SSc is primarily characterized by skin fibrosis and the accelerated progression of organ-associated complications, which include the early appearance of arthropathy, gastrointestinal dysmotility, myositis, and Raynaud's phenomenon (9), and late stages of severe pulmonary or cardiac complications with significant morbidity and mortality rates (10). Further characteristics of SSc include a prevalence rate that is approximately four times higher in women than that in men, an age of onset between 30 and 60 years (1), an incidence rate higher in North America than that in northern Europe (11), and a more rapid and severe disease progression in African-American patients (12).

Faced with cumulative and persistent multi-organ symptoms, no single approach to the treatment of SSc has proven uniformly effective. Current clinical treatments are mainly palliative, and current management strategies focus on treating the symptoms, accompanied by systemic immunotherapy (13). Early intervention with drugs for vascular modulation, especially during the early symptoms of vascular injury, substantially mitigates sclerosis associated with pulmonary hypertension and reduces the risk of mortality associated with scleroderma renal crisis (14, 15). Immunosuppressive drugs are typically used during the active and diffuse phases of the disease and may result in a poor prognosis for patients with SSc (13). In addition, hematopoietic stem cell transplantation and several agents targeting potential drivers of disease pathogenesis, such as T cells, B cells, transforming germinal factor (TGF) β, and interleukin (IL)-6, are under evaluation as possible therapeutic agents in clinical trials (16–18).

Mesenchymal stem cells (MSCs) have the capacity to not only modulate immune cell activity but also stimulate tissue regeneration, mainly by secreting extracellular vesicles (EVs), which in turn play a role in the functional treatment of diseases (19). EVs secreted by MSCs contain a variety of bioactive substances such as DNA, mRNA, long non-coding RNA (lncRNA), proteins, and lipids and may be classified into three subtypes based on their size: exosomes (Exos; 30–100 nm), microvesicles (50–2,000 nm), and apoptotic bodies (50–5,000 nm) (20). Exos have the highest degree of homogeneity and are the most complex and versatile of the three types. Therefore, due to the highest value of theory and application, Exos receive the most attention in academic papers on EV. MSC-EVs can be classified as adipose tissue-derived MSCs (ASCs), bone marrow MSCs (BM-MSCs), umbilical cord MSCs (UC-MSCs), menstrual fluid MSCs (MenSCs), human-induced pluripotent stem cell MSCs, and human amniotic fluid MSCs (AF-MSCs) (21). EVs from ASCs, UC-MSCs, and BM-MSCs exhibit a capacity for wound healing; however, BM-MSC-EVs have stronger induction effects on fibroblasts, and the greatest induction of keratinocytes belongs to UC-MSC-EVs (22). Thus, when considering their use, it should be noted that EVs from different sources of MSCs can differ in efficacy.

There are still some challenges in the clinical application of MSC-EVs, for instance, high and sustained production, prolonged *in vivo* action, and avoidance of macrophage clearance (23, 24). However, compared to MSC transplantation, MSC-EVs possess a number of advantageous characteristics, including smaller size, singularity, long circulatory half-life, low immunogenicity, easy coating of therapeutic substances, easy crossing of the blood–brain barrier, easy production and storage, and no tumorigenicity (25). Therefore, various clinical studies are currently underway regarding the therapeutic applications of MSC-derived EVs (MSC-EVs) in autoimmune diseases (ADs) (26), including SSc. This review summarizes the possible pathogenesis of SSc and explores the potential use of MSC-EVs in SSc treatment. MSC-EVs may contribute to the treatment of SSc by improving vascular lesions, regulating immune dysfunction, and inhibiting fibrosis.

2 Pathophysiology of systemic sclerosis

Despite the fact that the exact causes of SSc are not well understood, numerous studies have shown that endogenous and exogenous environmental factors or risk factors trigger gene activation. The subsequent onset of SSc is associated with endothelial damage, microvascular injury, inflammation, and autoimmune activation (27, 28). These factors inevitably cause abnormal differentiation of fibroblasts and the accumulation of collagen and ECM proteins in tissues. SSc progression is discussed below in three parts: vascular injury, the immune response, and fibrosis.

2.1 Vascular injury and microangiopathy

EC activation is the main event at the beginning of SSc (29), wherein the enhanced expression of adhesion molecules, such as vascular cell adhesion protein 1, intercellular adhesion molecule, and E-selectin, lead to activation of the abnormal secretion of vasoactive factors (30). The adhesion molecules with adhesion mainly recruit inflammatory cells, while the disturbed vasoactive factors lead to frequent and constant fluctuations in microvascular tone (31). Platelet activation, which is caused by vascular changes, increases microvessel permeability; therefore, microvascular leaks

can develop (32). Moreover, platelet activation enhances the proliferation of vascular smooth muscle cells (VSMCs) and pericytes, leading to a thickening of the vessel wall and luminal narrowing (31). These events then cause microvascular damage, tissue hypoxia, and oxidative stress (33).

2.2 Inflammation and the immune response

In the early inflammatory phase of SSc, Toll-like receptor (TLR) signaling, which acts as a significant indicator of inflammation, can be provoked by non-specific or pathogenic injury, which may result in inflammation induction and the activation of innate immune cells (monocytes/macrophages, plasmacytoid dendritic cells (pDCs), and others). The upregulated production of CXCL4 in plasmacytoid DCs can lead to the differentiation of monocytes into pro-inflammatory DCs that enhance TLR-mediated cytokine expression and impact T cells (34, 35). In addition, monocytes participate in fibrosis through the inflammatory response and differentiate into macrophages or fibroblast-like cells. Macrophages are also engaged in the inflammatory and fibrotic aspects of SSc. Macrophages can generate classically activated (M1) and/or alternatively activated (M2) macrophages that are distinguishable based on their different surface markers. M1 macrophages are effector phagocytes that increase significantly in the early stage of SSc inflammation and generate pro-inflammatory cytokines, such as tumor necrosis factor-alpha (TNF-α), IL-6, and IL-1 (36). M2 macrophages restrain M1 responses by releasing anti-inflammatory cytokines, including IL-4, IL-13, and IL-10 when the repair mechanism is initiated after sustained damage. In addition, they facilitate the production of ECM proteins and pro-fibrotic cytokines and reinforce the anti-inflammatory response by triggering Th2 effector activity (36). Thus, M2 macrophages are considered to be important pathogenic factors in SSc.

Among the various adaptive immune responses, T cells participate significantly in the pathophysiology of SSC and markedly affect the synthesis of autoantibodies (37). CD4+ and CD8+ T cells have been confirmed in the skin (38, 39) and lungs (40, 41) of patients with SSc. Initial CD4+ T cells (Th0) can differentiate into Th1, Th2, and Th17, as well as Treg (T-regulatory) and Tfh (T-follicular helper) cells (42–44). Th2 cells, characterized by the secretion of anti-inflammatory cytokines IL-4 and IL-13, predominate over Th1 cells (45). Moreover, both Th17 cells and IL-17 production have been recognized as being elevated in patients with SSc, and they aggravate early inflammatory responses (46, 47). Treg cells could result in the advancement of SSc by transforming into pathogenic effector T cells, and their number can be reduced (48, 49) to inhibit immune activation (50). Therefore, an imbalance of Th1/Th2/Th17/Treg cytokines is a crucial causal factor for SSc. B cells also play a role in SSc, and their efficacy is linked to antigen presentation, DC maturation, and autoantibody production, varying across phenotypes (51). Different phenotypes exhibit different CD antigens on the cell surface, such as memory B cells with increased expression of CD95, CD80, and CD86, and peripheral blood B cells with a higher expression of CD19 (52–55).

2.3 Fibrosis

Due to persistent tissue damage, inflammation, and immune cell activation, SSc comprises a gradual fibrotic condition affecting tissues and organs (56). Clinical and pathological SSc is characterized by fibrosis accompanied by massive α-SMA-positive myofibroblasts, accumulation of ECM proteins (collagens, elastin, glycosaminoglycans, tenascin, and fibronectin) in tissue, and regulation of growth factor (TGF)-β and other profibrotic mediators (57). Circulating CD14 monocyte precursor pericytes and ECs have been suggested as potential sources of myofibroblast overproduction through epithelial–mesenchymal transition and endothelial–mesenchymal transition (58). The subsequent steady accumulation of ECM proteins stiffens the skin and organs while decreasing elasticity, thereby leading to mechanical stress. Mechanical stress further maintains fibroblast activation and intensifies the progression of the fibrotic process in tissues (59). This may be due to fibroblasts in patients with SSc exhibiting structural focal adhesion kinase activation, which integrates TGF-β signaling and integrin-mediated mechanical transduction so as to promote continuous myofibroblast differentiation and reactive oxygen species production (59).

The soluble mediators related to fibrosis in SSc are TGF-β, connective tissue growth factor (CTGF), and platelet-derived growth factor (PDGF). TGF-β, a pleiotropic factor secreted by macrophages and other cells or stored in the ECM, is believed to be the master regulator of fibrosis. As an inactive precursor, TGF-β-associated signaling cascades are consistently activated in fibrotic tissues (60). CTGF, a cysteine-rich matricellular protein, has a synergistic effect together with TGF-β, endothelin-1, and angiotensin II in inducing fibrosis (61). CTGF levels are significantly higher in the sera of SSc patients than those in the sera of healthy individuals and are positively correlated with the degree of fibrosis (62). PDGFs, which are heterodimeric peptides produced by platelets, macrophages, ECs, and fibroblasts, play an important role in fibrosis as well. PDGFs act as powerful mitogens and chemoattractants and convert mesenchymal cells into profibrotic cell types (63).

3 Potential therapeutic effects of MSC-EVs in SSc

MSC-EV transplantation, which is an emerging and novel therapy, has been confirmed to be beneficial for SSc in bleomycin or hypochlorous acid (HOCl)-induced, or chronic graft-versus-host disease (cGVHD) mouse models, and TGF-β1-induced model of human myofibroblast (Table 1). These preclinical studies are mainly focused on the antifibrotic effect of MSC-EVs in SSc and the mechanisms involved (64, 65). The discovery of effective improvements of MSC-EVs in SSc *in vitro* and *in vivo* is a

TABLE 1 Effect of MSC-EVs on SSc.

	Source of MSCs	Experiment models	Properties of MSC-EVs	Mechanisms	References
1	Human umbilical cord	Bleomycin-induced mouse model	Antifibrosis	Reduction of deposition of extracellular matrix and inhibition of the epithelial–mesenchymal transition process	(64)
			Immunomodulation	Facilitating M1 macrophage polarization and suppressing M2 macrophage polarization, leading to the restoration of the balance of M1/M2 macrophages	
2	Adipose tissue	TGF-β1-induced model of human myofibroblasts	Antifibrosis	ASC-EVs can better improve anti-fibrotic and pro-remodeling functions than ASCs *in vitro*	(65)
3	Bone marrow	HOCl-induced murine model	Antifibrosis	IFN-γ-pre-activation improved the therapeutic effects of MSC-EV in the SSc model. Low doses of IFN-γ decreased the expression of fibrotic markers, while high doses improved remodeling markers *in vivo*	(66)
			Immunomodulation	High dose of IFN-γ-pre-activation upregulated anti-inflammatory markers in MSC-EV, including iNos, IL1ra, and IL-6 *in vivo*	
4	Bone marrow	Bleomycin-induced dermal fibrosis in mice	Antifibrosis	Inhibition of collagen type I expression by miR-196b-5p in exosomes might be one of the mechanisms by which MSCs suppress skin fibrosis *in vivo*	(67)
5	Bone marrow	Bleomycin-induced dermal fibrosis in mice	Antifibrosis	The intervention of fibrosis of the SSC model by miRNAs they carry and regulate the WNT and TGF-β signaling pathways	(68)
			Immunomodulation	Reduction of the numbers of mast cells and infiltrating macrophages and lymphocytes, and the levels of the inflammatory cytokines IL-6, IL-10, and Tnf-α in BLM-treated mice	
6	Human umbilical cord	Bleomycin-induced dermal fibrosis in mice	Antifibrosis	Attenuating myofibroblast activation and collagen deposition in dermal fibrosis by downregulating the TGF-β/Smad signaling pathway *in vivo*	(64)
7	Human adipose tissue	HOCl-induced SSc model	Antifibrosis	Alleviating SSc and regulating methylation and apoptosis *via* miR-29a-3p	(69)
8	Human umbilical cord	cGVHD mouse model	Immunomodulation	Suppressing the activation of macrophages and B-cell immune response	(70)

MSC-EVs, mesenchymal stem cell-derived extracellular vesicles; SSc, systemic sclerosis; MSCs, mesenchymal stem cells; ASCs, adipose tissue-derived mesenchymal stem cells; HOCl, hypochlorous acid; BLM, bleomycin; cGVHD, chronic graft-versus-host disease.

breakthrough in the field of SSc therapeutic approaches. Recent advances have been made in the exploration of the biogenesis, cargo, and biological potential of MSC-EVs and in understanding their molecular mechanisms in angiogenesis and immunomodulation, which is the key to SSc treatment. These advances have led to promising improvements being observed in other diseases through MSC-EV treatment (71, 72). In view of the heterogeneity of pathways involved in SSc pathogenesis and progression, as well as the existence of crosstalk among vascular injury, the immune response, and fibrosis in SSc, long-term single-target treatment could lead to adverse reactions (73, 74). Thus, for SSc, MSC-EVs enriched with multiple efficacious biokines perhaps improve through various pathways, which may include angiogenesis and the modulation of inflammation and fibrosis (Figure 1). This evidence points out that MSC-EVs may become a potential tool for SSc. The effects of MSC-EVs on vascular injury, immune imbalance, and fibrosis in different disease models are described below.

3.1 Pro-angiogenic effects

Vascular injury and the thickening of the vessel wall are key components of SSc. In the early stage of SSc, if the extent of the vascular injury can be reduced, subsequent fibrosis can be considerably inhibited (75). Recent studies have demonstrated the MSC-EV-mediated delivery of cytokines, proteins, microRNA (miRNA), mRNA, and lncRNA as a significant component of the angiogenic process (72, 76). MSC-EVs have been shown to have pro-angiogenic properties in wound-healing models and ischemic conditions such as diabetic foot ulcers (DFUs), full-thickness wounds, myocardial infarction (MI), and acute kidney injury.

3.1.1 Angiogenic function of MSC-EVs

ECs boost angiogenesis (the formation of fresh blood vessels from existing ones) and the secretion of several factors, including nitric oxide, endothelin, and prostacyclin (77). Therefore, they are

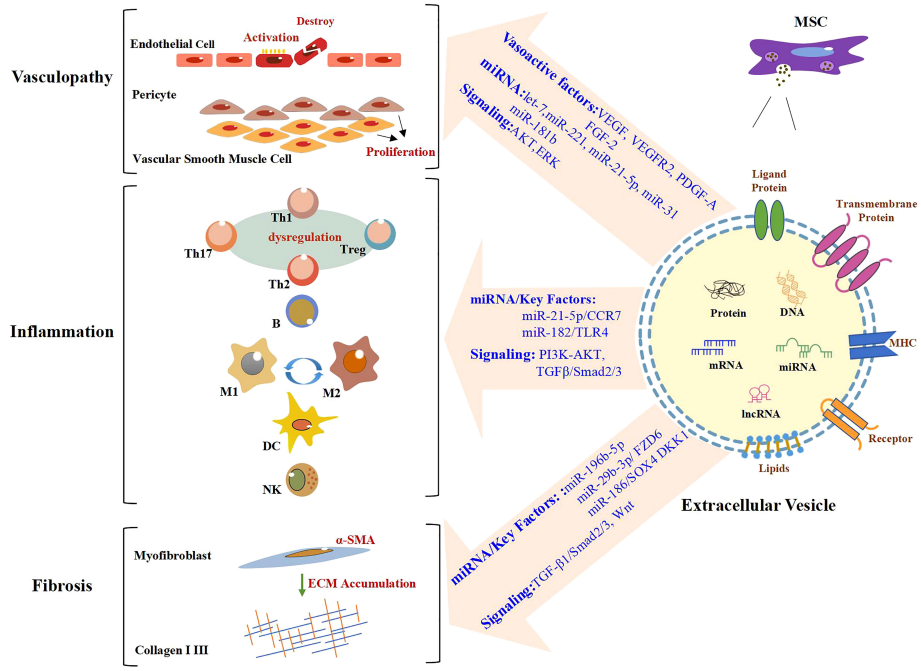

FIGURE 1
Role of MSC-EVs in the modulation of SSc. In the stage of vasculopathy in SSc, endothelial cells are activated and even destroyed. Vascular smooth muscle cells and pericytes proliferate abnormally. A large number of immune cells also participate in the process of SSc. Likewise, there are large numbers of α-SMA-positive myofibroblasts, which produce excessive amounts of extracellular matrix (ECM), in particular Collagen I and III, resulting in fibrosis. MSC-EVs promote angiogenesis by regulating vasoactive factors and signaling pathways and carrying miRNA. MiRNA/key factors and signaling pathways are involved in the modulation of inflammation and fibrosis by MSC-EVs. Text in blue indicates mechanisms involved in SSc. MSC-EVs, mesenchymal stem cell-derived extracellular vesicles; SSc, systemic sclerosis.

valuable targets under ischemic conditions and require vascular regeneration. Studies have indicated that MSC-EVs enhance the migration of human umbilical vein endothelial cells (HUVECs) and promote proliferation and vessel-like structure formation in a dose-dependent manner in human microvascular endothelial cells (HMECs) *in vivo* and *in vitro* (78, 79). Another research has shown that MSC-Exos are internalized by HUVECs and accumulate around the nucleus (80). The characteristics of MSC-EVs can influence pathological changes in vascular-rich tissue, similar to Raynaud's phenomenon, which affects over 95% of SSc patients and comprises occasional color changes in the extremities in cold environments (81). SSc-associated interstitial lung disease (SSc-ILD), one of the causes of death, is chiefly caused by damage to the alveolar epithelium and blood vessels in the lung region (82). Similarly, MSC-EVs are effective against other structural cells that are associated with blood vessels. Studies on abnormal proliferation and the migration of smooth muscle cells have demonstrated that MSC-EVs can alleviate asthma or pulmonary arterial hypertension *in vivo* and/or *in vitro* (83, 84). On this basis, MSC-EVs are promising as prospective therapeutic targets for SSc-related vasculopathy.

3.1.2 Angiogenic molecular mechanisms of MSC-EVs

MSC-EVs most likely promote angiogenesis by upregulating vasoactive factors such as vascular endothelial-derived growth factor (VEGF), VEGF receptor (R)2, PDGF-A, and fibroblast growth factor (FGF)-2 in HUVECs *in vitro* and *in vivo* skin injury models (85). Studies conducted on primary MSCs originating from BM, ASCs, and UCs have revealed that all of the aforementioned cell-derived Exos promote angiogenesis by secreting angiogenesis-mediated factors such as VEGF-A, FGF-2, hepatocyte growth factor, and PDGF-BB during wound healing (22). In addition, exposure to vasoactive factors can strengthen the therapeutic effect of MSC-EVs and encourage better angiogenesis. Lopatina et al. previously showed that PDGF pretreatment of human ASC-EVs reinforces pro-angiogenic capacity by elevating the levels of secreted pro-angiogenic proteins. Conditioned media derived from AF-MSCs incorporating VEGF and TGF-β1 have been found to improve proliferation, the migration of human skin fibroblasts *in vitro*, and wound healing *in vivo* (86). As for the angiogenic effects of MSC-EVs, vasoactive factors may be targeted by MSC-EVs, which would influence the properties of MSC-EVs.

Other angiogenic mechanisms that warrant further study are the signaling pathways that involve MSC-derived proteins. A comprehensive analysis previously showed that ASC-EVs contain proteins that are linked to signal transduction pathways. A total of 277 proteins associated with the ECM, glycoproteins, angiogenesis, TGF-β signaling, the inflammatory response, and blood coagulation have been found to be enriched in EVs. It has been found that ASC-EVs facilitate angiogenesis through increased expression of Ang-1 and Flk-1 in HUVECs, involving the let-7/argonaut 1/VEGF signaling pathway in a fat grafting nude mouse model (87). Additionally, ASC-MVs have been found to be readily

internalized by HUVECs. ASC-MV proliferation, migration, and angiogenesis are promoted through the AKT and ERK signaling pathways *in vitro* and in an *in vivo* skin injury model (85). The activation of these signaling pathways often involves not only proteins but also genetic materials such as miRNA, mRNA, and lncRNA.

It has been found that although MSC-EVs carry different genes than their parent cells, they can still regulate angiogenesis. Eirin et al. found that 386 miRNAs were enriched in ASC-EVs compared to parental cells. MicroRNA-148, one of these detected miRNAs, regulates angiogenesis aimed at transcription factors, inhibits tumor angiogenesis, and suppresses the sprouting of ECs from vessels *in vivo* and/or *in vitro* (88–90). Other miRNAs and even genes in their families also act independently from the key factors related to regulatory angiogenesis (91–94). Additionally, miR-221 was found to impact vasoactivity by exerting effects on VSMCs and ECs (95). Meanwhile, EVs obtained from MSCs have been known to exhibit a high level of pro-angiogenic miRNA-21-5p. The pro-angiogenic function of miRNA-21-5p in MSC-EVs was verified in DFU models by knockdown and overexpression of the gene, and it was also further determined that miRNA-21-5p may promote angiogenesis and improve ischemic tissue by stimulating VEGFR and by activating serine/threonine kinase AKT and mitogen-activated protein kinase in receptor cells such as ECs (96). Furthermore, for ischemic diseases, studies revealed that miR-31 was rich in ASC-MVs, especially in endothelial differentiation medium-pretreated ASC-MVs, and that miR-31 has been strongly implicated in angiogenesis in HUVECs and endothelial progenitor cells (97) in promoting migration and tube formation *in vitro* and *in vivo*. Moreover, both the miR-31-miR-720 and the VEGF-miR-31 pathways may be involved (98, 99). In addition, factor-inhibiting HIF-1, an anti-angiogenic gene, has been identified as a target of miR-31 in HUVECs, and together they may mediate angiogenesis (79). Additional studies have shown that MSC-Exos and its Exo-transmitted miR-125a can promote endothelial tip cell generation for EC, resulting in vascular sprouting by inhibiting the expression of DLL4, an angiogenesis inhibitor *in vivo* and *in vitro* (100). ASC-Exos promote the mobility and angiogenesis of brain microvascular endothelial cells after oxygen-glucose deprivation *via* the microRNA-181b/TRPM7 axis *in vitro* (101). Significant progress has been made in the study of miRNA in MSC-EVs. These miRNAs are not only involved in MSC-EVs promoting angiogenesis but also have immunomodulatory and antifibrosis effects (Table 2). MSC-EV delivery can protect miRNAs from degradation by ribonucleases, thereby ensuring that the miRNAs are able to perform their crucial roles in recipient cells. Interestingly, another study showed that proteins in EVs do not originate from the transcription of miRNAs.

3.2 Immunomodulatory effects

Abnormal immune cells were exhibited in SSc focusing on the dysregulation of the Th1/Th2/Th17/Treg and M1/M2 cytokine (2). MSC-EVs have an auto-immunosuppressive property that attenuates inflammation and immune responses in inflammatory and autoimmune diseases (119). MSCs act as immunomodulators by delivering EVs that modulate the generation, differentiation, efficacy, and interactions of adaptive and innate immune cells, such as T cells, B cells, macrophages, natural killer (NK) cells, and DCs in

TABLE 2 The miRNA of MSC-EVs is involved in angiogenesis, immunomodulation, and antifibrosis.

	Properties of MSC-EVs	Classification of MSC-EVs	MiRNA	References
1	Angiogenesis	Porcine ASC-EVs	MicroRNA-148	(88, 90)
		Human MSC-Exos	MiRNA-21-5p	(96)
		ASC-MVs	MiRNA-31	(79)
		MSC-Exos	MiRNA-125a	(100)
		ASC-Exos	MicroRNA-181b	(101)
2	Immunomodulation	MSC-Exos	MiRNA-23a-3p	(102)
		BM-MSC-Exos	MiRNA-146a-5p	(103)
		MSC-Exos	MiRNA-125a and miRNA-125b	(104)
		ASC-Exos	MiRNA-10a	(105)
		MSC-Exos	MiRNA-182	(106)
		BM-MSC-Exos	MiRNA-34c-5p	(107)
3	Antifibrosis	MSC-EVs	MiRNA-29a-3p	(69)
		MSC-EVs	MicroRNA-29b-3p	(108)
		BM-MSC-EVs	MicroRNA-186	(109)
		MSC-Exos	MiRNA-196b-5p	(67)

TABLE 3 The fibrotic target tissues of MSC-EVs.

	Target tissues	Target cells	Results	Key mechanisms	References
1	Skin	Fibroblasts	Promotion of proliferation and migration in SSc	MiR-29b-3p/PI3K-Akt, Erk1-2, and Smad3-TGF-β1	(110)
		Myofibroblasts	Suppressing myofibroblasts differentiation	MicroRNAs (miR-21, miR-23a, miR-125b, and miR-145)/TGF-β-SMAD2	(111)
2	Lung	Lung epithelial cells	Better proliferative capacity of alveolar epithelial cell line	Activation of FGF2 signaling	(112)
		Pulmonary vascular endothelial cells	Reduction of tissue fibrosis and vascular endothelial remodeling	Umbilical cord MSC-exosomal TNF-stimulated gene 6	(113)
		Alveolar macrophages	Alleviating lung inflammation and fibrosis	Polarization of macrophages to m2 anti-inflammatory phenotype	(114)
3	Heart	Cardiomyocytes	Improving cardiac function and alleviating fibrosis	MiR-22/methyl CpG binding protein 2	(115)
4	Kidney	Tubular epithelial cells	Attenuating tubular epithelial-myofibroblast transdifferentiation of renal tubular epithelial cells	MiR-335-5p/ADAM19	(116)
5	Colon	Intestinal epithelial cells	Inhibition of EMT	MiR-200b/ZEB1, ZEB2	(117)
		Macrophage	Reduction of inflammatory cytokines	MiR-146a/TRAF6, IRAK1	(118)

MSC-EVs, mesenchymal stem cell-derived extracellular vesicles; MSC, mesenchymal stem cell; EMT, epithelial-to-mesenchymal transition.

inflammatory diseases (120). Likewise, the anti-inflammatory and immunomodulatory properties of MSC-EVs are probably of great significance in the treatment of SSc.

3.2.1 T cells

In the early stages of SSc, the inhibition of inflammation is an important goal of therapy. At this stage, M1 macrophages and Th1 cells are the main cells involved in the upregulation of type I interferon (IFN) (121). In tissues, M1 macrophages with IFNs are transformed into M2 macrophages to promote fibrosis, after synergistic involvement with the responses of Th2 to exposure to IL-6 and IL-13 (122). Increased numbers of Treg cells facilitate the inhibition of immune activation and prevent themselves from transferring to Th2- and Th17-like cells for antifibrotic progress in skin tissues (123). As MSC-EVs activate different effector substances depending on different biological environments, the disorder in SSc could be regulated by them.

3.2.1.1 Th cells

MSC-EVs modulate the functions and activities of Th cells. It has been demonstrated that MSC-EVs regulate CD4 T cells in the conversion between Th1 and Th2 and decrease the Th17 differentiation of peripheral blood mononuclear cells in asthmatic mice (124). In dextran sulfate sodium-induced colitis models, olfactory ecto-derived MSC-EVs have been found to remarkably reduce Th1/Th17 subpopulations, accompanied by reduced serum levels of IL-17, IL-6, and IFN-γ and elevated levels of TGF-β and IL-10 secreted by T cells (125). Interestingly, pro-inflammatory cytokines, such as IL-10 (126) and IFN preconditioned MSC, could enhance CD4 T-cell inhibition while inducing Treg cells and Th17. In addition, the molecular mechanisms of the MSC-EV-mediated regulation of Th cells focus on cargoes in EV, for example, by transferring miR-23a-3p to regulate the Treg/Th17 balance in aplastic anemia (102), miR-146a-5p/IRAK1 axis to regulate the Th17/Treg imbalance in immune thrombocytopenia (103), miR-125a and miR-125b to inhibit Th17 cell differentiation in colitis (104), and miR-10a loading to promote Th17 and Treg responses while decreasing Th1 responses (105).

3.2.1.2 Treg cells

MSC-EVs substantially promote the conversion of monocytes to Treg cells and the immune-suppression capacity of Treg cells (127, 128), which is possibly triggered by TGF-β from MSC-EVs exposed to IFN-γ (129). Meanwhile, MSC-EVs could lead to the differentiation of Treg cells to reverse the imbalance between T-effector and Treg cells, which has been confirmed regarding the imbalance of Th1/Th4/Th17/Treg cells (105). It has been noted that Treg regulation occurs mainly through antigen-presenting cells (APCs) and is not dependent on CD4+ T cells in asthmatic mice (124). Subsequent studies have also confirmed that the differentiation of Treg cells is mediated by activated APCs, which are induced by MSC-EVs in a myeloid differentiation primary response-dependent manner (128). Treg differentiation can also suppress the proliferation of T cells indirectly, which is a property of MSC-Exos, but not of MSCs (130). The ability of MSC-EVs to regulate the function, homing, and phenotype of immune cells may result in the development of novel therapies for inflammatory diseases and ADs (26, 120). Nevertheless, further research is needed to elucidate the molecular mechanisms of the MSC-EV-mediated regulation of immune cell activities.

3.2.2 B lymphocytes

B lymphocytes play a major role in the adaptive immune response and MSC-EVs have been shown to regulate the proliferation and function of B cells. Khare et al. (131) sequenced MSC-EV co-cultured with B cells and identified upregulated genes

related to B-cell proliferation and Ca^{2+} mobilization *via* B-cell receptors *in vitro*. Guo et al. earlier revealed that MSC-EVs suppressed fibrosis in a mouse model of sclerodermatous chronic graft-versus-host disease by inhibiting Tfh/germinal center B-cell interactions and reducing the frequency of B cell-activating factor (BAFF)-expressing B cells (70). Furthermore, MSC-EVs have been found to regulate Breg cells through the PI3K-AKT signaling pathway *in vitro*, but the role of MSCs in regulating Breg cells still needs to be explored (132).

3.2.3 Macrophages

Macrophages orchestrate both the initiation and resolution of inflammation. An imbalance in the phenotypes and activation of macrophages has been considered critical in the development of inflammatory, autoimmune, and fibrotic diseases. Accumulating evidence has suggested that MSC-EVs promote macrophage polarization and phagocytic capacity (133). The regulation of EVs in the conversion between M1 and M2 macrophages has also been found in some cases of SSc (134). Meanwhile, MSC-EVs reduce macrophage infiltration in tissues by carrying miRNAs in SSc (68). Interestingly, in renal interstitial fibrosis, Hu et al. (107) showed that MSC-Exos may inhibit macrophage activation by delivering miR-34c-5p in Exos to macrophages *via* CD81-epidermal growth factor receptor (EGFR) complex aids. In another context, it was noted that MSC-EVs could reverse the polarization of M1 to M2 macrophages; further, it was found that miR-182 from MSC-EVs can suppress TLR4, as part of its underlying mechanism of action in myocardial ischemia–reperfusion injury (106).

3.2.4 DCs and NK cells

DCs and NK cells are essential for the innate immune response, and the effect of MSC-EVs on both cells has been explored in some studies *in vitro*. Several reports have shown that MSC-EVs could suppress the proliferation and maturation of DCs, thus regulating the immune response. The coincubation of DCs derived from BM with MSC-EVs has been found to reduce IL-6 release, increase IL-10 and TGF-β levels, and downregulate lymphocyte proliferation (135). MSC-EVs loaded with miR-21-5p are able to depress the target gene C–C chemokine receptor type 7 (CCR7) and reduce the migratory capacity of the CCR7-ligand CCL21, thereby suppressing the secretion of inflammatory cytokines (136). Previous studies have demonstrated that MSC-EVs could suppress the proliferation of NK cells in a manner similar to DCs (130). In recent research, an analogous study showed that human fetal liver-derived MSC-Exos not only inhibited NK-cell proliferation but also suppressed NK-cell activation and cytotoxicity *via* latency-associated peptides and TGF-β and thrombospondin 1 and induced downstream TGF-β/Smad2/3 signaling. Nevertheless, research on the topic remains limited. Despite the growing research on MSC-EVs and immune cells, the precise molecular mechanisms underlying their interactions needs additional study (137). Innate immune responses also occur in the course of SSc. Regulation of DCs and NK cells by MSC-EVs should play a role in SSc.

3.3 Antifibrotic effects

MSC-EV treatment can ameliorate fibrosis of the skin and lungs, which is a clear sign of SSc. Furthermore, the clinical fibrotic manifestations of SSc involve alterations in the heart, kidney, and colon, and several experimental studies have examined the antifibrotic effect of MSC-EVs in other diseases (Table 3). Presently, investigations of fibrosis are restricted to the preclinical phase. Many preclinical trials have been conducted to set up various SSc models. There are many methods to induce SSc given the various underlying causes of fibrosis (Supplementary Table 1); however, no experimental models have been able to perfectly reproduce the pathophysiological spectrum of SSc.

3.3.1 Antifibrotic function of MSC-EVs

MSC-EVs have been confirmed to be beneficial for SSc due to their antifibrotic effects. Rozier et al. evaluated the antifibrotic function of ASCs and their EVs by co-culturing them with TGF-β1-induced myofibroblasts (65). However, the underlying therapeutic mechanisms remain unclear. Several studies have investigated the potential antifibrotic properties of MSC-EVs in bleomycin-induced mouse models of scleroderma (64, 134). These effects were exhibited in the amelioration of the following aspects. MSC-EVs can suppress myofibroblast differentiation and inhibit the expression of collagen types I and III in a skin-defect mouse model (111). Studies on the molecular markers of fibrosis and remodeling have shown that MSC-EVs might diminish scar formation by decreasing the ratios between collagen types I and III in a diabetic mouse model (138). In addition, ASC-EVs decrease scar formation *via* modulating the ratios of type I and III collagen, TGF-β1 and TGF-β3, matrix metalloproteinase-3 and tissue inhibitor of metalloproteinases 1, and abnormal activation of fibroblasts *in vivo* (139). These effects have been noted in many fibrotic diseases (140).

3.3.2 Antifibrotic molecular mechanisms of MSC-EVs

Many studies have confirmed that MSC-EVs, typified by Exos, can act as antifibrotic agents through various mechanisms of action in the treatment of fibrotic diseases. Among the signaling pathways involved, TGF-β and Wnt signaling are regarded as the core pathways involved in fibrosis in SSc (141, 142). In addition, the effects of Exos on reducing fibrotic markers through the TGF pathway have also been confirmed in SSc (64). The phosphorylation levels of α-SMA, Smad2/3, and collagen I and III in fibroblasts treated with Exos have been found to be markedly decreased. Furthermore, MSC-derived Exos have been found to suppress the transition of dermal fibroblasts to myofibroblasts by inhibiting the NF-κB, Hedgehog, Wnt/β-catenin, PI3K/Akt, Erk1/2, and TGF-β1/Smad2/3 signaling pathways (140). Moreover, it has been shown that EV alleviates fibrosis by carrying cargo, such as RNA, through activation of the aforementioned signaling pathways. Results of high-throughput RNA sequencing and functional analysis of MSC-EVs suggest that a group of specific microRNAs

can prevent excessive myofibroblast revitalization by blocking the TGF-β/Smad2 signaling pathways *in vivo* (111). MiR-29b-3p, carried by BM-MSC-EVs in bilayered thiolated alginate/PEG diacrylate hydrogels, inhibits the proliferation and migration of ECs and fibroblasts by curbing the PI3K/Akt, Erk1/2, and TGF-β1/Smad3 signaling pathways in a full-thickness skin defect model of rats and rabbit ears, thereby allowing for scar-free wound healing (110). In a study on BMSC-EV-based treatment, the gene activity in the Wnt signaling pathway that was hyperactivated by bleomycin stimulation was significantly lowered or related to ECM–receptor interactions and the cell cycle (68).

Several investigations have explored the role of MSC-EV-carried miRNAs in fibrosis. In SSc, miR-29a-3p from MSCs and ASCs has been confirmed to be beneficial for fibrosis in HOCl-induced mice (69). In other fibrotic diseases, a group of uMSC-EVs composed of miR-21, miR-23a, miR-imno125b, and miR-145, whose expression is changed, was thought to be related to the modulation of pro-fibrotic genes (110, 111). Among the various features of fibrosis, MSC-EVs also display efficacy in the inhibition of fibroblast proliferation. MiR-29b-3p and miR-186, both secreted by BMMSC-EVs, have been reported to downregulate FZD6, SOX4, and DKK1 expression to inhibit fibroblast activation and proliferation in idiopathic pulmonary fibrosis, respectively (108, 109). Likewise, elevated collagen levels are one of the main factors contributing to ECM deposition in fibrosis. MiR-212-5p, miR-133b (143), miR-192-5p (144), miR-196b-5p (67), and let-7a (145) have been found to reduce the levels of type I and/or type III collagens, and miR-212-5p downstream may inhibit the NLRC5/VEGF/TGF-β1/SMAD axis, while miR-192-5p targets IL-17RA. Similarly, fibrosis and remodeling factors are targets of miRNAs from MSC-EVs. EVs from MSCs and ASCs exhibit a mechanism of action that comprises the secretion of miR-29a-3p, which could diminish the levels of several profibrotic, remodeling, and anti-apoptotic factors and methylases in HOCl-induced mice (69). In the aforementioned studies, MSC-EVs further exerted a positive effect on fibrosis. Despite the progress that has been made in recent studies, ameliorating fibrosis with MSC-EVs remains in the preclinical stage.

4 Conclusions and prospects

It is possible that MSC-EVs could ameliorate SSc and the pathological changes in vasculopathy, immune dysfunction, and fibrosis by regulating key factors and signaling pathways. Despite the positive effects of MSC-EVs in SSc, further extensive clinical studies are required to establish the applicability of EVs in treating SSc. A focus area is modification and engineering, which could enhance the therapeutic effects of MSCs-EVs. Future exploration of strategies, including chemical stimulation from MSCs, MSC genetic modification, and physical variables of MSCs, could generate more effective MSCs-EVs for supporting the desired outcomes. Undoubtedly, enhancing the effectiveness of MSC-EV treatment will be an important trend in future clinical applications.

Author contributions

NS participated in the investigation. JJ and PL reviewed and supervised the manuscript. All authors contributed to the paper and approved the submitted draft. All authors contributed to the article and approved the submitted version.

Funding

Jilin Provincial Development and Reform Commission (2022C044-8), Jilin Provincial Department of Education (JJKH20211146), Natural Science Foundation of Jilin Provincial Department of Science and Technology (YDZJ202201ZYTS104).

Conflict of interest

The authors declare that the research was conducted in the absence of any commercial or financial relationships that could be construed as a potential conflict of interest.

Publisher's note

Supplementary material

The Supplementary Material for this article can be found online at: https://www.frontiersin.org/articles/10.3389/fimmu.2023.1125257/full#supplementary-material

References

1. Bairkdar M, Rossides M, Westerlind H, Hesselstrand R, Arkema EV, Holmqvist M. Incidence and prevalence of systemic sclerosis globally: a comprehensive systematic review and meta-analysis. *Rheumatol (Oxford)* (2021) 60(7):3121–33. doi: 10.1093/rheumatology/keab190

2. Cutolo M, Soldano S, Smith V. Pathophysiology of systemic sclerosis: current understanding and new insights. *Expert Rev Clin Immunol* (2019) 15(7):753–64. doi: 10.1080/1744666X.2019.1614915

3. Kuo CF, Luo SF, Yu KH, See LC, Zhang W, Doherty M. Familial risk of systemic sclerosis and Co-aggregation of autoimmune diseases in affected families. *Arthritis Res Ther* (2016) 18(1):231. doi: 10.1186/s13075-016-1127-6

4. Villanueva-Martin G, Martin J, Bossini-Castillo L. Recent advances in elucidating the genetic basis of systemic sclerosis. *Curr Opin Rheumatol* (2022) 34(6):295–301. doi: 10.1097/BOR.0000000000000897

5. Arvia R, Zakrzewska K, Giovannelli L, Ristori S, Frediani E, Del Rosso M, et al. Parvovirus B19 induces cellular senescence in human dermal fibroblasts: putative role in systemic sclerosis-associated fibrosis. *Rheumatol (Oxford)* (2022) 61(9):3864–74. doi: 10.1093/rheumatology/keab904

6. Randone SB, Guiducci S, Cerinic MM. Systemic sclerosis and infections. *Autoimmun Rev* (2008) 8(1):36–40. doi: 10.1016/j.autrev.2008.07.022

7. Chang R, Yen-Ting Chen T, Wang SI, Hung YM, Chen HY, Wei CJ. Risk of autoimmune diseases in patients with covid-19: a retrospective cohort study. *EClinicalMedicine* (2023) 56:101783. doi: 10.1016/j.eclinm.2022.101783

8. Matucci-Cerinic M, Hughes M, Taliani G, Kahaleh B. Similarities between covid-19 and systemic sclerosis early vasculopathy: a "Viral" challenge for future research in scleroderma. *Autoimmun Rev* (2021) 20(10):102899. doi: 10.1016/j.autrev.2021.102899

9. Varga J, Abraham D. Systemic sclerosis: a prototypic multisystem fibrotic disorder. *J Clin Invest* (2007) 117(3):557–67. doi: 10.1172/JCI31139

10. Condliffe R, Kiely DG, Peacock AJ, Corris PA, Gibbs JS, Vrapi F, et al. Connective tissue disease-associated pulmonary arterial hypertension in the modern treatment era. *Am J Respir Crit Care Med* (2009) 179(2):151–7. doi: 10.1164/rccm.200806-953OC

11. Bergamasco A, Hartmann N, Wallace L, Verpillat P. Epidemiology of systemic sclerosis and systemic sclerosis-associated interstitial lung disease. *Clin Epidemiol* (2019) 11:257–73. doi: 10.2147/CLEP.S191418

12. Gelber AC, Manno RL, Shah AA, Woods A, Le EN, Boin F, et al. Race and association with disease manifestations and mortality in scleroderma: a 20-year experience at the johns Hopkins scleroderma center and review of the literature. *Med (Baltimore)* (2013) 92(4):191–205. doi: 10.1097/MD.0b013e31829be125

13. Volkmann ER, Andreasson K, Smith V. Systemic sclerosis. *Lancet* (2023) 401 (10373):304–18. doi: 10.1016/S0140-6736(22)01692-0

14. Zanatta E, Polito P, Favaro M, Larosa M, Marson P, Cozzi F, et al. Therapy of scleroderma renal crisis: state of the art. *Autoimmun Rev* (2018) 17(9):882–9. doi: 10.1016/j.autrev.2018.03.012

15. Humbert M, Coghlan JG, Ghofrani HA, Grimminger F, He JG, Riemekasten G, et al. Riociguat for the treatment of pulmonary arterial hypertension associated with connective tissue disease: results from patent-1 and patent-2. *Ann Rheum Dis* (2017) 76 (2):422–6. doi: 10.1136/annrheumdis-2015-209087

16. Ebata S, Oba K, Kashiwabara K, Ueda K, Uemura Y, Watadani T, et al. Predictors of rituximab effect on modified rodnan skin score in systemic sclerosis: a machine-learning analysis of the desires trial. *Rheumatol (Oxford)* (2022) 61(11):4364–73. doi: 10.1093/rheumatology/keac023

17. van Laar JM, Farge D, Sont JK, Naraghi K, Marjanovic Z, Larghero J, et al. Autologous hematopoietic stem cell transplantation vs intravenous pulse cyclophosphamide in diffuse cutaneous systemic sclerosis: a randomized clinical trial. *JAMA* (2014) 311(24):2490–8. doi: 10.1001/jama.2014.6368

18. Khanna D, Lin CJF, Furst DE, Goldin J, Kim G, Kuwana M, et al. Tocilizumab in systemic sclerosis: a randomised, double-blind, placebo-controlled, phase 3 trial. *Lancet Respir Med* (2020) 8(10):963–74. doi: 10.1016/S2213-2600(20)30318-0

19. Jeppesen DK, Fenix AM, Franklin JL, Higginbotham JN, Zhang Q, Zimmerman LJ, et al. Reassessment of exosome composition. *Cell* (2019) 177(2):428–45.e18. doi: 10.1016/j.cell.2019.02.029

20. van Niel G, D'Angelo G, Raposo G. Shedding light on the cell biology of extracellular vesicles. *Nat Rev Mol Cell Biol* (2018) 19(4):213–28. doi: 10.1038/nrm.2017.125

21. Mushahary D, Spittler A, Kasper C, Weber V, Charwat V. Isolation, cultivation, and characterization of human mesenchymal stem cells. *Cytometry A* (2018) 93(1):19–31. doi: 10.1002/cyto.a.23242

22. Hoang DH, Nguyen TD, Nguyen HP, Nguyen XH, Do PTX, Dang VD, et al. Differential wound healing capacity of mesenchymal stem cell-derived exosomes originated from bone marrow, adipose tissue and umbilical cord under serum- and xeno-free condition. *Front Mol Biosci* (2020) 7:119. doi: 10.3389/fmolb.2020.00119

23. Imai T, Takahashi Y, Nishikawa M, Kato K, Morishita M, Yamashita T, et al. Macrophage-dependent clearance of systemically administered B16bl6-derived exosomes from the blood circulation in mice. *J Extracell Vesicles* (2015) 4:26238. doi: 10.3402/jev.v4.26238

24. Wen S, Dooner M, Papa E, Del Tatto M, Pereira M, Borgovan T, et al. Biodistribution of mesenchymal stem cell-derived extracellular vesicles in a radiation injury bone marrow murine model. *Int J Mol Sci* (2019) 20(21):5468. doi: 10.3390/ijms20215468

25. Barreca MM, Cancemi P, Geraci F. Mesenchymal and induced pluripotent stem cells-derived extracellular vesicles: the new frontier for regenerative medicine? *Cells* (2020) 9(5):1163. doi: 10.3390/cells9051163

26. Liu H, Chen Y, Yin G, Xie Q. Therapeutic prospects of micrornas carried by mesenchymal stem cells-derived extracellular vesicles in autoimmune diseases. *Life Sci* (2021) 277:119458. doi: 10.1016/j.lfs.2021.119458

27. Gabrielli A, Avvedimento EV, Krieg T. Scleroderma. *N Engl J Med* (2009) 360 (19):1989–2003. doi: 10.1056/NEJMra0806188

28. Fuschiotti P. Current perspectives on the immunopathogenesis of systemic sclerosis. *Immunotargets Ther* (2016) 5:21–35. doi: 10.2147/ITT.S82037

29. Geyer M, Muller-Ladner U. The pathogenesis of systemic sclerosis revisited. *Clin Rev Allergy Immunol* (2011) 40(2):92–103. doi: 10.1007/s12016-009-8193-3

30. Mostmans Y, Cutolo M, Giddelo C, Decuman S, Melsens K, Declercq H, et al. The role of endothelial cells in the vasculopathy of systemic sclerosis: a systematic review. *Autoimmun Rev* (2017) 16(8):774–86. doi: 10.1016/j.autrev.2017.05.024

31. Kahaleh B. The microvascular endothelium in scleroderma. *Rheumatol (Oxford)* (2008) 47 Suppl 5:v14–5. doi: 10.1093/rheumatology/ken279

32. Bruni C, Frech T, Manetti M, Rossi FW, Furst DE, De Paulis A, et al. Vascular leaking, a pivotal and early pathogenetic event in systemic sclerosis: should the door be closed? *Front Immunol* (2018) 9:2045. doi: 10.3389/fimmu.2018.02045

33. Trojanowska M. Cellular and molecular aspects of vascular dysfunction in systemic sclerosis. *Nat Rev Rheumatol* (2010) 6(8):453–60. doi: 10.1038/nrrheum.2010.102

34. Carvalheiro T, Zimmermann M, Radstake T, Marut W. Novel insights into dendritic cells in the pathogenesis of systemic sclerosis. *Clin Exp Immunol* (2020) 201 (1):25–33. doi: 10.1111/cei.13417

35. Lu TT. Dendritic cells: novel players in fibrosis and scleroderma. *Curr Rheumatol Rep* (2012) 14(1):30–8. doi: 10.1007/s11926-011-0215-5

36. Funes SC, Rios M, Escobar-Vera J, Kalergis AM. Implications of macrophage polarization in autoimmunity. *Immunology* (2018) 154(2):186–95. doi: 10.1111/imm.12910

37. Fuschiotti P. T Cells and cytokines in systemic sclerosis. *Curr Opin Rheumatol* (2018) 30(6):594–9. doi: 10.1097/BOR.0000000000000553

38. Sakkas LI, Xu B, Artlett CM, Lu S, Jimenez SA, Platsoucas CD. Oligoclonal T cell expansion in the skin of patients with systemic sclerosis. *J Immunol* (2002) 168 (7):3649–59. doi: 10.4049/jimmunol.168.7.3649

39. Kalogerou A, Gelou E, Mountantonakis S, Settas L, Zafiriou E, Sakkas L. Early T cell activation in the skin from patients with systemic sclerosis. *Ann Rheum Dis* (2005) 64(8):1233–5. doi: 10.1136/ard.2004.027094

40. Luzina IG, Atamas SP, Wise R, Wigley FM, Choi J, Xiao HQ, et al. Occurrence of an activated, profibrotic pattern of gene expression in lung Cd8+ T cells from scleroderma patients. *Arthritis Rheum* (2003) 48(8):2262–74. doi: 10.1002/art.11080

41. Kowal-Bielecka O, Kowal K, Highland KB, Silver RM. Bronchoalveolar lavage fluid in scleroderma interstitial lung disease: technical aspects and clinical correlations: review of the literature. *Semin Arthritis Rheum* (2010) 40(1):73–88. doi: 10.1016/j.semarthrit.2008.10.009

42. Zhang M, Zhang S. T Cells in fibrosis and fibrotic diseases. *Front Immunol* (2020) 11:1142. doi: 10.3389/fimmu.2020.01142

43. Ricard L, Jachiet V, Malard F, Ye Y, Stocker N, Riviere S, et al. Circulating follicular helper T cells are increased in systemic sclerosis and promote plasmablast differentiation through the il-21 pathway which can be inhibited by ruxolitinib. *Ann Rheum Dis* (2019) 78(4):539–50. doi: 10.1136/annrheumdis-2018-214382

44. Baraut J, Michel L, Verrecchia F, Farge D. Relationship between cytokine profiles and clinical outcomes in patients with systemic sclerosis. *Autoimmun Rev* (2010) 10(2):65–73. doi: 10.1016/j.autrev.2010.08.003

45. Chizzolini C, Parel Y, Scheja A, Dayer JM. Polarized subsets of human T-helper cells induce distinct patterns of chemokine production by normal and systemic sclerosis dermal fibroblasts. *Arthritis Res Ther* (2006) 8(1):R10. doi: 10.1186/ar1860

46. Dufour AM, Borowczyk-Michalowska J, Alvarez M, Truchetet ME, Modarressi A, Brembilla NC, et al. Il-17a dissociates inflammation from fibrogenesis in systemic sclerosis. *J Invest Dermatol* (2020) 140(1):103–12.e8. doi: 10.1016/j.jid.2019.05.026

47. Chizzolini C, Dufour AM, Brembilla NC. Is there a role for il-17 in the pathogenesis of systemic sclerosis? *Immunol Lett* (2018) 195:61–7. doi: 10.1016/j.imlet.2017.09.007

48. Mathian A, Parizot C, Dorgham K, Trad S, Arnaud L, Larsen M, et al. Activated and resting regulatory T cell exhaustion concurs with high levels of interleukin-22 expression in systemic sclerosis lesions. *Ann Rheum Dis* (2012) 71(7):1227–34. doi: 10.1136/annrheumdis-2011-200709

49. Klein S, Kretz CC, Ruland V, Stumpf C, Haust M, Hartschuh W, et al. Reduction of regulatory T cells in skin lesions but not in peripheral blood of patients with systemic scleroderma. *Ann Rheum Dis* (2011) 70(8):1475–81. doi: 10.1136/ard.2009.116525

50. Slobodin G, Rimar D. Regulatory T cells in systemic sclerosis: a comprehensive review. *Clin Rev Allergy Immunol* (2017) 52(2):194–201. doi: 10.1007/s12016-016-8563-6

51. Thoreau B, Chaigne B, Mouthon L. Role of b-cell in the pathogenesis of systemic sclerosis. *Front Immunol* (2022) 13:933468. doi: 10.3389/fimmu.2022.933468

52. Sato S, Fujimoto M, Hasegawa M, Takehara K. Altered blood b lymphocyte homeostasis in systemic sclerosis: expanded naive b cells and diminished but activated memory b cells. *Arthritis Rheum* (2004) 50(6):1918–27. doi: 10.1002/art.20274

53. Whitfield ML, Finlay DR, Murray JI, Troyanskaya OG, Chi JT, Pergamenschikov A, et al. Systemic and cell type-specific gene expression patterns in scleroderma skin. *Proc Natl Acad Sci U.S.A.* (2003) 100(21):12319–24. doi: 10.1073/pnas.1635114100

54. Lafyatis R, O'Hara C, Feghali-Bostwick CA, Matteson E. B cell infiltration in systemic sclerosis-associated interstitial lung disease. *Arthritis Rheum* (2007) 56 (9):3167–8. doi: 10.1002/art.22847

55. Mavropoulos A, Simopoulou T, Varna A, Liaskos C, Katsiari CG, Bogdanos DP, et al. Breg cells are numerically decreased and functionally impaired in patients with systemic sclerosis. *Arthritis Rheumatol* (2016) 68(2):494–504. doi: 10.1002/art.39437

56. Khan K, Xu S, Nihtyanova S, Derrett-Smith E, Abraham D, Denton CP, et al. Clinical and pathological significance of interleukin 6 overexpression in systemic sclerosis. *Ann Rheum Dis* (2012) 71(7):1235–42. doi: 10.1136/annrheumdis-2011-200955

57. van Caam A, Vonk M, van den Hoogen F, van Lent P, van der Kraan P. Unraveling ssc pathophysiology; the myofibroblast. *Front Immunol* (2018) 9:2452. doi: 10.3389/fimmu.2018.02452

58. Piera-Velazquez S, Li Z, Jimenez SA. Role of endothelial-mesenchymal transition (Endomt) in the pathogenesis of fibrotic disorders. *Am J Pathol* (2011) 179 (3):1074–80. doi: 10.1016/j.ajpath.2011.06.001

59. Ho YY, Lagares D, Tager AM, Kapoor M. Fibrosis–a lethal component of systemic sclerosis. *Nat Rev Rheumatol* (2014) 10(7):390–402. doi: 10.1038/nrrheum.2014.53

60. Varga J, Pasche B. Transforming growth factor beta as a therapeutic target in systemic sclerosis. *Nat Rev Rheumatol* (2009) 5(4):200–6. doi: 10.1038/nrrheum.2009.26

61. Leask A, Denton CP, Abraham DJ. Insights into the molecular mechanism of chronic fibrosis: the role of connective tissue growth factor in scleroderma. *J Invest Dermatol* (2004) 122(1):1–6. doi: 10.1046/j.0022-202X.2003.22133.x

62. Abraham D. Connective tissue growth factor: growth factor, matricellular organizer, fibrotic biomarker or molecular target for anti-fibrotic therapy in ssc? *Rheumatol (Oxford)* (2008) 47 Suppl 5:v8–9. doi: 10.1093/rheumatology/ken278

63. Trojanowska M. Role of pdgf in fibrotic diseases and systemic sclerosis. *Rheumatol (Oxford)* (2008) 47 Suppl 5:v2–4. doi: 10.1093/rheumatology/ken265

64. Li M, Zhang HP, Wang XY, Chen ZG, Lin XF, Zhu W. Mesenchymal stem cell-derived exosomes ameliorate dermal fibrosis in a murine model of bleomycin-induced scleroderma. *Stem Cells Dev* (2021) 30(19):981–90. doi: 10.1089/scd.2021.0112

65. Rozier P, Maumus M, Bony C, Maria ATJ, Sabatier F, Jorgensen C, et al. Extracellular vesicles are more potent than adipose mesenchymal stromal cells to exert an anti-fibrotic effect in an in vitro model of systemic sclerosis. *Int J Mol Sci* (2021) 22 (13):6837. doi: 10.3390/ijms22136837

66. Rozier P, Maumus M, Maria ATJ, Toupet K, Jorgensen C, Guilpain P, et al. Lung fibrosis is improved by extracellular vesicles from ifngamma-primed mesenchymal stromal cells in murine systemic sclerosis. *Cells* (2021) 10(10):2727. doi: 10.3390/cells10102727

67. Baral H, Uchiyama A, Yokoyama Y, Sekiguchi A, Yamazaki S, Amalia SN, et al. Antifibrotic effects and mechanisms of mesenchymal stem cell-derived exosomes in a systemic sclerosis mouse model: possible contribution of mir-196b-5p. *J Dermatol Sci* (2021) 104(1):39–47. doi: 10.1016/j.jdermsci.2021.08.006

68. Jin J, Ou Q, Wang Z, Tian H, Xu JY, Gao F, et al. Bmsc-derived extracellular vesicles intervened the pathogenic changes of scleroderma in mice through mirnas. *Stem Cell Res Ther* (2021) 12(1):327. doi: 10.1186/s13287-021-02400-y

69. Rozier P, Maumus M, Maria ATJ, Toupet K, Lai-Kee-Him J, Jorgensen C, et al. Mesenchymal stromal cells-derived extracellular vesicles alleviate systemic sclerosis *Via* mir-29a-3p. *J Autoimmun* (2021) 121:102660. doi: 10.1016/j.jaut.2021.102660

70. Guo L, Lai P, Wang Y, Huang T, Chen X, Geng S, et al. Extracellular vesicles derived from mesenchymal stem cells prevent skin fibrosis in the cgvhd mouse model by suppressing the activation of macrophages and b cells immune response. *Int Immunopharmacol* (2020) 84:106541. doi: 10.1016/j.intimp.2020.106541

71. Ha DH, Kim HK, Lee J, Kwon HH, Park GH, Yang SH, et al. Mesenchymal stem/stromal cell-derived exosomes for immunomodulatory therapeutics and skin regeneration. *Cells* (2020) 9(5). doi: 10.3390/cells9051157

72. Rautiainen S, Laaksonen T, Koivuniemi R. Angiogenic effects and crosstalk of adipose-derived mesenchymal Stem/Stromal cells and their extracellular vesicles with endothelial cells. *Int J Mol Sci* (2021) 22(19):10890. doi: 10.3390/ijms221910890

73. Gyorfi AH, Matei AE, Distler JHW. Targeting tgf-beta signaling for the treatment of fibrosis. *Matrix Biol* (2018) 68-69:8–27. doi: 10.1016/j.matbio.2017.12.016

74. Bergmann C, Distler JH. Canonical wnt signaling in systemic sclerosis. *Lab Invest* (2016) 96(2):151–5. doi: 10.1038/labinvest.2015.154

75. Guiducci S, Giacomelli R, Cerinic MM. Vascular complications of scleroderma. *Autoimmun Rev* (2007) 6(8):520–3. doi: 10.1016/j.autrev.2006.12.006

76. Bian D, Wu Y, Song G, Azizi R, Zamani A. The application of mesenchymal stromal cells (Mscs) and their derivative exosome in skin wound healing: a comprehensive review. *Stem Cell Res Ther* (2022) 13(1):24. doi: 10.1186/s13287-021-02697-9

77. Kruger-Genge A, Blocki A, Franke RP, Jung F. Vascular endothelial cell biology: an update. *Int J Mol Sci* (2019) 20(18):4411. doi: 10.3390/ijms20184411

78. Mou S, Zhou M, Li Y, Wang J, Yuan Q, Xiao P, et al. Extracellular vesicles from human adipose-derived stem cells for the improvement of angiogenesis and fat-grafting application. *Plast Reconstr Surg* (2019) 144(4):869–80. doi: 10.1097/PRS.0000000000006046

79. Kang T, Jones TM, Naddell C, Bacanamwo M, Calvert JW, Thompson WE, et al. Adipose-derived stem cells induce angiogenesis *Via* microvesicle transport of mirna-31. *Stem Cells Transl Med* (2016) 5(4):440–50. doi: 10.5966/sctm.2015-0177

80. Lopatina T, Bruno S, Tetta C, Kalinina N, Porta M, Camussi G. Platelet-derived growth factor regulates the secretion of extracellular vesicles by adipose mesenchymal stem cells and enhances their angiogenic potential. *Cell Commun Signal* (2014) 12:26. doi: 10.1186/1478-811X-12-26

81. Wigley FM, Flavahan NA. Raynaud's phenomenon. *N Engl J Med* (2016) 375 (6):556–65. doi: 10.1056/NEJMra1507638

82. Bruni C, Occhipinti M, Pienn M, Camiciottoli G, Bartolucci M, Bosello SL, et al. Lung vascular changes as biomarkers of severity in systemic sclerosis-associated interstitial lung disease. *Rheumatol (Oxford)* (2023) 62(2):696–706. doi: 10.1093/rheumatology/keac311

83. Shan L, Liu S, Zhang Q, Zhou Q, Shang Y. Human bone marrow-mesenchymal stem cell-derived exosomal microrna-188 reduces bronchial smooth muscle cell proliferation in asthma through suppressing the Jarid2/Wnt/Beta-catenin axis. *Cell Cycle* (2022) 21(4):352–67. doi: 10.1080/15384101.2021.2020432

84. Zhang Z, Ge L, Zhang S, Wang J, Jiang W, Xin Q, et al. The protective effects of msc-exo against pulmonary hypertension through regulating Wnt5a/Bmp signalling pathway. *J Cell Mol Med* (2020) 24(23):13938–48. doi: 10.1111/jcmm.16002

85. Ren S, Chen J, Duscher D, Liu Y, Guo G, Kang Y, et al. Microvesicles from human adipose stem cells promote wound healing by optimizing cellular functions *Via* akt and erk signaling pathways. *Stem Cell Res Ther* (2019) 10(1):47. doi: 10.1186/s13287-019-1152-x

86. Jun EK, Zhang Q, Yoon BS, Moon JH, Lee G, Park G, et al. Hypoxic conditioned medium from human amniotic fluid-derived mesenchymal stem cells accelerates skin wound healing through tgf-Beta/Smad2 and Pi3k/Akt pathways. *Int J Mol Sci* (2014) 15 (1):605–28. doi: 10.3390/ijms15010605

87. Li X, Xie X, Lian W, Shi R, Han S, Zhang H, et al. Exosomes from adipose-derived stem cells overexpressing Nrf2 accelerate cutaneous wound healing by promoting vascularization in a diabetic foot ulcer rat model. *Exp Mol Med* (2018) 50 (4):1–14. doi: 10.1038/s12276-018-0058-5

88. Eirin A, Riester SM, Zhu XY, Tang H, Evans JM, O'Brien D, et al. Microrna and mrna cargo of extracellular vesicles from porcine adipose tissue-derived mesenchymal stem cells. *Gene* (2014) 551(1):55–64. doi: 10.1016/j.gene.2014.08.041

89. Yu J, Li Q, Xu Q, Liu L, Jiang B. Mir-148a inhibits angiogenesis by targeting Erbb3. *J BioMed Res* (2011) 25(3):170–7. doi: 10.1016/S1674-8301(11)60022-5

90. Kim H, Ko Y, Park H, Zhang H, Jeong Y, Kim Y, et al. Microrna-148a/B-3p regulates angiogenesis by targeting neuropilin-1 in endothelial cells. *Exp Mol Med* (2019) 51(11):1–11. doi: 10.1038/s12276-019-0344-x

91. Lee DY, Deng Z, Wang CH, Yang BB. Microrna-378 promotes cell survival, tumor growth, and angiogenesis by targeting sufu and fus-1 expression. *Proc Natl Acad Sci U S A* (2007) 104(51):20350–5. doi: 10.1073/pnas.0706901104

92. Kuehbacher A, Urbich C, Zeiher AM, Dimmeler S. Role of dicer and drosha for endothelial microrna expression and angiogenesis. *Circ Res* (2007) 101(1):59–68. doi: 10.1161/CIRCRESAHA.107.153916

93. Ma J, Zhang J, Wang Y, Long K, Wang X, Jin L, et al. Mir-532-5p alleviates hypoxia-induced cardiomyocyte apoptosis by targeting Pdcd4. *Gene* (2018) 675:36–43. doi: 10.1016/j.gene.2018.06.087

94. Huang B, Huang LF, Zhao L, Zeng Z, Wang X, Cao D, et al. Microvesicles (Mivs) secreted from adipose-derived stem cells (Adscs) contain multiple micrornas and promote the migration and invasion of endothelial cells. *Genes Dis* (2020) 7(2):225–34. doi: 10.1016/j.gendis.2019.04.005

95. Chistiakov DA, Sobenin IA, Orekhov AN, Bobryshev YV. Human mir-221/222 in physiological and atherosclerotic vascular remodeling. *BioMed Res Int* (2015) 2015:354517. doi: 10.1155/2015/354517

96. Huang C, Luo W, Wang Q, Ye Y, Fan J, Lin L, et al. Human mesenchymal stem cells promote ischemic repairment and angiogenesis of diabetic foot through exosome mirna-21-5p. *Stem Cell Res* (2021) 52:102235. doi: 10.1016/j.scr.2021.102235

97. Wang HW, Huang TS, Lo HH, Huang PH, Lin CC, Chang SJ, et al. Deficiency of the microrna-31-Microrna-720 pathway in the plasma and endothelial progenitor cells from patients with coronary artery disease. *Arterioscler Thromb Vasc Biol* (2014) 34 (4):857–69. doi: 10.1161/ATVBAHA.113.303001

98. Suarez Y, Fernandez-Hernando C, Yu J, Gerber SA, Harrison KD, Pober JS, et al. Dicer-dependent endothelial microrna are necessary for postnatal angiogenesis. *Proc Natl Acad Sci U S A* (2008) 105(37):14082–7. doi: 10.1073/pnas.0804597105

99. Greco S, De Simone M, Colussi C, Zaccagnini G, Fasanaro P, Pescatori M, et al. Common micro-rna signature in skeletal muscle damage and regeneration induced by duchenne muscular dystrophy and acute ischemia. *FASEB J* (2009) 23(10):3335–46. doi: 10.1096/fj.08-128579

100. Liang X, Zhang L, Wang S, Han Q, Zhao RC. Exosomes secreted by mesenchymal stem cells promote endothelial cell angiogenesis by transferring mir-125a. *J Cell Sci* (2016) 129(11):2182–9. doi: 10.1242/jcs.170373

101. Yang Y, Cai Y, Zhang Y, Liu J, Xu Z. Exosomes secreted by adipose-derived stem cells contribute to angiogenesis of brain microvascular endothelial cells following oxygen-glucose deprivation in vitro through microrna-181b/Trpm7 axis. *J Mol Neurosci* (2018) 65(1):74–83. doi: 10.1007/s12031-018-1071-9

102. Shi QZ, Yu HM, Chen HM, Liu M, Cheng X. Exosomes derived from mesenchymal stem cells regulate Treg/Th17 balance in aplastic anemia by transferring mir-23a-3p. *Clin Exp Med* (2021) 21(3):429–37. doi: 10.1007/s10238-021-00701-3

103. He Y, Ji D, Lu W, Li F, Huang X, Huang R, et al. Bone marrow mesenchymal stem cell-derived exosomes induce the Th17/Treg imbalance in immune thrombocytopenia through mir-146a-5p/Irak1 axis. *Hum Cell* (2021) 34(5):1360–74. doi: 10.1007/s13577-021-00547-7

104. Yang R, Huang H, Cui S, Zhou Y, Zhang T, Zhou Y. Ifn-gamma promoted exosomes from mesenchymal stem cells to attenuate colitis *Via* mir-125a and mir-125b. *Cell Death Dis* (2020) 11(7):603. doi: 10.1038/s41419-020-02788-0

105. Bolandi Z, Mokhberian N, Eftekhary M, Sharifi K, Soudi S, Ghanbarian H, et al. Adipose derived mesenchymal stem cell exosomes loaded with mir-10a promote the differentiation of Th17 and treg from naive Cd4(+) T cell. *Life Sci* (2020) 259:118218. doi: 10.1016/j.lfs.2020.118218

106. Zhao J, Li X, Hu J, Chen F, Qiao S, Sun X, et al. Mesenchymal stromal cell-derived exosomes attenuate myocardial ischaemia-reperfusion injury through mir-182-Regulated macrophage polarization. *Cardiovasc Res* (2019) 115(7):1205–16. doi: 10.1093/cvr/cvz040

107. Hu X, Shen N, Liu A, Wang W, Zhang L, Sui Z, et al. Bone marrow mesenchymal stem cell-derived exosomal mir-34c-5p ameliorates rif by inhibiting the core fucosylation of multiple proteins. *Mol Ther* (2022) 30(2):763–81. doi: 10.1016/j.ymthe.2021.10.012

108. Wan X, Chen S, Fang Y, Zuo W, Cui J, Xie S. Mesenchymal stem cell-derived extracellular vesicles suppress the fibroblast proliferation by downregulating Fzd6 expression in fibroblasts *Via* micrrna-29b-3p in idiopathic pulmonary fibrosis. *J Cell Physiol* (2020) 235(11):8613–25. doi: 10.1002/jcp.29706

109. Zhou J, Lin Y, Kang X, Liu Z, Zhang W, Xu F. Microrna-186 in extracellular vesicles from bone marrow mesenchymal stem cells alleviates idiopathic pulmonary fibrosis *Via* interaction with Sox4 and Dkk1. *Stem Cell Res Ther* (2021) 12(1):96. doi: 10.1186/s13287-020-02083-x

110. Shen Y, Xu G, Huang H, Wang K, Wang H, Lang M, et al. Sequential release of small extracellular vesicles from bilayered thiolated Alginate/Polyethylene glycol diacrylate hydrogels for scarless wound healing. *ACS Nano* (2021) 15(4):6352–68. doi: 10.1021/acsnano.0c07714

111. Fang S, Xu C, Zhang Y, Xue C, Yang C, Bi H, et al. Umbilical cord-derived mesenchymal stem cell-derived exosomal micrornas suppress myofibroblast differentiation by inhibiting the transforming growth factor-Beta/Smad2 pathway during wound healing. *Stem Cells Transl Med* (2016) 5(10):1425–39. doi: 10.5966/sctm.2015-0367

112. Kim YS, Kim JY, Cho R, Shin DM, Lee SW, Oh YM. Adipose stem cell-derived nanovesicles inhibit emphysema primarily *Via* an Fgf2-dependent pathway. *Exp Mol Med* (2017) 49(1):e284. doi: 10.1038/emm.2016.127

113. Chaubey S, Thueson S, Ponnalagu D, Alam MA, Gheorghe CP, Aghai Z, et al. Early gestational mesenchymal stem cell secretome attenuates experimental bronchopulmonary dysplasia in part *Via* exosome-associated factor tsg-6. *Stem Cell Res Ther* (2018) 9(1):173. doi: 10.1186/s13287-018-0903-4

114. Mansouri N, Willis GR, Fernandez-Gonzalez A, Reis M, Nassiri S, Mitsialis SA, et al. Mesenchymal stromal cell exosomes prevent and revert experimental pulmonary fibrosis through modulation of monocyte phenotypes. *JCI Insight* (2019) 4(21): e128060. doi: 10.1172/jci.insight.128060

115. Feng Y, Huang W, Wani M, Yu X, Ashraf M. Ischemic preconditioning potentiates the protective effect of stem cells through secretion of exosomes by targeting Mecp2 *Via* mir-22. *PLoS One* (2014) 9(2):e88685. doi: 10.1371/journal.pone.0088685

116. Qiu Z, Zhong Z, Zhang Y, Tan H, Deng B, Meng G. Human umbilical cord mesenchymal stem cell-derived exosomal mir-335-5p attenuates the inflammation and tubular epithelial-myofibroblast transdifferentiation of renal tubular epithelial cells by reducing Adam19 protein levels. *Stem Cell Res Ther* (2022) 13(1):373. doi: 10.1186/s13287-022-03071-z

117. Yang J, Zhou CZ, Zhu R, Fan H, Liu XX, Duan XY, et al. Mir-200b-Containing microvesicles attenuate experimental colitis associated intestinal fibrosis by inhibiting epithelial-mesenchymal transition. *J Gastroenterol Hepatol* (2017) 32(12):1966–74. doi: 10.1111/jgh.13797

118. Wu H, Fan H, Shou Z, Xu M, Chen Q, Ai C, et al. Extracellular vesicles containing mir-146a attenuate experimental colitis by targeting Traf6 and Irak1. *Int Immunopharmacol* (2019) 68:204–12. doi: 10.1016/j.intimp.2018.12.043

119. Shen Z, Huang W, Liu J, Tian J, Wang S, Rui K, et al. Effects of Mesenchymal Stem Cell-Derived Exosomes on Autoimmune Diseases. *Am Front Immunol* (2021) 12: 749192. doi: 10.3389/fimmu.2021.749192

120. Harrell CR, Jovicic N, Djonov V, Arsenijevic N, Volarevic V. Mesenchymal stem cell-derived exosomes and other extracellular vesicles as new remedies in the therapy of inflammatory diseases. *Cells* (2019) 8(12):1605. doi: 10.3390/cells8121605

121. Jaguin M, Houlbert N, Fardel O, Lecureur V. Polarization profiles of human m-Csf-Generated macrophages and comparison of M1-markers in classically activated macrophages from gm-csf and m-csf origin. *Cell Immunol* (2013) 281(1):51–61. doi: 10.1016/j.cellimm.2013.01.010

122. Lescoat A, Lecureur V, Varga J. Contribution of monocytes and macrophages to the pathogenesis of systemic sclerosis: recent insights and therapeutic implications. *Curr Opin Rheumatol* (2021) 33(6):463–70. doi: 10.1097/BOR.0000000000000835

123. MacDonald KG, Dawson NAJ, Huang Q, Dunne JV, Levings MK, Broady R. Regulatory T cells produce profibrotic cytokines in the skin of patients with systemic sclerosis. *J Allergy Clin Immunol* (2015) 135(4):946–55.e9. doi: 10.1016/j.jaci.2014.12.1932

124. Du YM, Zhuansun YX, Chen R, Lin L, Lin Y, Li JG. Mesenchymal stem cell exosomes promote immunosuppression of regulatory T cells in asthma. *Exp Cell Res* (2018) 363(1):114–20. doi: 10.1016/j.yexcr.2017.12.021

125. Tian J, Zhu Q, Zhang Y, Bian Q, Hong Y, Shen Z, et al. Olfactory ecto-mesenchymal stem cell-derived exosomes ameliorate experimental colitis *Via* modulating Th1/Th17 and treg cell responses. *Front Immunol* (2020) 11:598322. doi: 10.3389/fimmu.2020.598322

126. Li Y, Ren X, Zhang Z, Duan Y, Li H, Chen S, et al. Effect of small extracellular vesicles derived from il-10-Overexpressing mesenchymal stem cells on experimental autoimmune uveitis. *Stem Cell Res Ther* (2022) 13(1):100. doi: 10.1186/s13287-022-02780-9

127. Riazifar M, Mohammadi MR, Pone EJ, Yeri A, Lasser C, Segaliny AI, et al. Stem cell-derived exosomes as nanotherapeutics for autoimmune and neurodegenerative disorders. *ACS Nano* (2019) 13(6):6670–88. doi: 10.1021/acsnano.9b01004

128. Nojehdehi S, Soudi S, Hesampour A, Rasouli S, Soleimani M, Hashemi SM. Immunomodulatory effects of mesenchymal stem cell-derived exosomes on experimental type-1 autoimmune diabetes. *J Cell Biochem* (2018) 119(11):9433–43. doi: 10.1002/jcb.27260

129. Zhang Q, Fu L, Liang Y, Guo Z, Wang L, Ma C, et al. Exosomes originating from mscs stimulated with tgf-beta and ifn-gamma promote treg differentiation. *J Cell Physiol* (2018) 233(9):6832–40. doi: 10.1002/jcp.26436

130. Di Trapani M, Bassi G, Midolo M, Gatti A, Kamga PT, Cassaro A, et al. Differential and transferable modulatory effects of mesenchymal stromal cell-derived extracellular vesicles on T, b and nk cell functions. *Sci Rep* (2016) 6:24120. doi: 10.1038/srep24120

131. Khare D, Or R, Resnick I, Barkatz C, Almogi-Hazan O, Avni B. Mesenchymal stromal cell-derived exosomes affect mrna expression and function of b-lymphocytes. *Front Immunol* (2018) 9:3053. doi: 10.3389/fimmu.2018.03053

132. Adamo A, Brandi J, Caligola S, Delfino P, Bazzoni R, Carusone R, et al. Extracellular vesicles mediate mesenchymal stromal cell-dependent regulation of b cell Pi3k-akt signaling pathway and actin cytoskeleton. *Front Immunol* (2019) 10:446. doi: 10.3389/fimmu.2019.00446

133. Phinney DG, Di Giuseppe M, Njah J, Sala E, Shiva S, St Croix CM, et al. Mesenchymal stem cells use extracellular vesicles to outsource mitophagy and shuttle micrornas. *Nat Commun* (2015) 6:8472. doi: 10.1038/ncomms9472

134. Yu Y, Shen L, Xie X, Zhao J, Jiang M. The therapeutic effects of exosomes derived from human umbilical cord mesenchymal stem cells on scleroderma. *Tissue Eng Regener Med* (2022) 19(1):141–50. doi: 10.1007/s13770-021-00405-5

135. Shahir M, Mahmoud Hashemi S, Asadirad A, Varahram M, Kazempour-Dizaji M, Folkerts G, et al. Effect of mesenchymal stem cell-derived exosomes on the induction of mouse tolerogenic dendritic cells. *J Cell Physiol* (2020) 235(10):7043–55. doi: 10.1002/jcp.29601

136. Reis M, Mavin E, Nicholson L, Green K, Dickinson AM, Wang XN. Mesenchymal stromal cell-derived extracellular vesicles attenuate dendritic cell maturation and function. *Front Immunol* (2018) 9:2538. doi: 10.3389/fimmu.2018.02538

137. Fan Y, Herr F, Vernochet A, Mennesson B, Oberlin E, Durrbach A. Human fetal liver mesenchymal stem cell-derived exosomes impair natural killer cell function. *Stem Cells Dev* (2019) 28(1):44–55. doi: 10.1089/scd.2018.0015

138. Dalirfardouei R, Jamialahmadi K, Jafarian AH, Mahdipour E. Promising effects of exosomes isolated from menstrual blood-derived mesenchymal stem cell on wound-healing process in diabetic mouse model. *J Tissue Eng Regener Med* (2019) 13(4):555–68. doi: 10.1002/term.2799

139. Wang L, Hu L, Zhou X, Xiong Z, Zhang C, Shehada HMA, et al. Exosomes secreted by human adipose mesenchymal stem cells promote scarless cutaneous repair by regulating extracellular matrix remodelling. *Sci Rep* (2017) 7(1):13321. doi: 10.1038/s41598-017-12919-x

140. Huang Y, Yang L. Mesenchymal stem cell-derived extracellular vesicles in therapy against fibrotic diseases. *Stem Cell Res Ther* (2021) 12(1):435. doi: 10.1186/s13287-021-02524-1

141. Wei J, Fang F, Lam AP, Sargent JL, Hamburg E, Hinchcliff ME, et al. Wnt/Beta-catenin signaling is hyperactivated in systemic sclerosis and induces smad-dependent fibrotic responses in mesenchymal cells. *Arthritis Rheum* (2012) 64(8):2734–45. doi: 10.1002/art.34424

142. Gillespie J, Ross RL, Corinaldesi C, Esteves F, Derrett-Smith E, McDermott MF, et al. Transforming growth factor beta activation primes canonical wnt signaling through down-regulation of axin-2. *Arthritis Rheumatol* (2018) 70(6):932–42. doi: 10.1002/art.40437

143. Cao D, Wang Y, Zhang Y, Zhang Y, Huang Q, Yin Z, et al. Regulation of connective tissue growth factor expression by mir-133b for the treatment of renal interstitial fibrosis in aged mice with unilateral ureteral obstruction. *Stem Cell Res Ther* (2021) 12(1):171. doi: 10.1186/s13287-021-02210-2

144. Li Y, Wang F, Guo R, Zhang Y, Chen D, Li X, et al. Exosomal sphingosine 1-phosphate secreted by mesenchymal stem cells regulated Treg/Th17 balance in aplastic anemia. *IUBMB Life* (2019) 71(9):1284–92. doi: 10.1002/iub.2035

145. Wang B, Yao K, Huuskes BM, Shen HH, Zhuang J, Godson C, et al. Mesenchymal stem cells deliver exogenous microrna-Let7c *Via* exosomes to attenuate renal fibrosis. *Mol Ther* (2016) 24(7):1290–301. doi: 10.1038/mt.2016.90

10.3389/fimmu.2023.1125257

Glossary

AD	autoimmune disease
AF-MSC	amniotic fluid-derived mesenchymal stem cell
APC	antigen-presenting cell
ASC	adipose tissue-derived mesenchymal stem cell
BAFF	B-cell activating factor
BM-MSC	bone marrow-derived mesenchymal stem cell
Breg	B-regulatory cell
CTGF	connective tissue growth factor
CCR7	C–C chemokine receptor type 7
DFU	diabetic foot ulcer
EC	endothelial cell
ECM	extracellular matrix
EMT	epithelial-to-mesenchymal transition
EV	extracellular vesicle
Exos	Exosomes
FGF	fibroblast growth factor
HLA	human leukocyte antigen
HMEC	human microvascular endothelial cell
HOCl	hypochlorous acid
HUVEC	human umbilical vein endothelial cell
IFN	interferon
IL	interleukin
lncRNA	long non-coding RNA
IPF	idiopathic pulmonary fibrosis
MAPK	mitogen-activated protein kinase
MenSC	menstrual fluid-derived mesenchymal stem cell
MI	myocardial infarction
miRNA	microRNA
MSC	mesenchymal stem cell
MSC-EV	mesenchymal stem cell-derived extracellular vesicle
NK	natural killer
pDC	plasmacytoid dendritic cell
PDGF	platelet-derived growth factor
SSc	systemic sclerosis
SSc-Fb	fibroblasts from patients with systemic sclerosis
SSc-ILD	SSc-associated interstitial lung disease
Tfh	T-follicular helper cell
TGF	transforming germinal factor
Tβ-Fb	TGF-β1-induced myofibroblasts
TLR	Toll-like receptor
TNF	tumor necrosis factor
Treg	T-regulatory
UC-MSC	umbilical cord-derived mesenchymal stem cell
VEGF	vascular endothelial-derived growth factor
VSMC	vascular smooth muscle cell

frontiers | Frontiers in Immunology

TYPE Brief Research Report
PUBLISHED 15 August 2023
DOI 10.3389/fimmu.2023.1172896

OPEN ACCESS

EDITED BY
Roberto Paganelli,
YDA, Institute for Advanced Biologic Therapies, Italy

REVIEWED BY
Ariel Munitz,
Tel Aviv University, Israel
Raffaele D'Amelio,
Sapienza University of Rome, Italy

*CORRESPONDENCE
Alon Y. Hershko
alonh@hadassah.org.il

†These authors have contributed equally to this work and share first authorship

‡These authors have contributed equally to this work and share last authorship

RECEIVED 23 February 2023
ACCEPTED 31 July 2023
PUBLISHED 15 August 2023

CITATION
Ribak Y, Rubin L, Talmon A, Dranitzki Z, Shamriz O, Hershkowitz I, Tal Y and Hershko AY (2023) Administration of BNT162b2 mRNA COVID-19 vaccine to subjects with various allergic backgrounds. *Front. Immunol.* 14:1172896. doi: 10.3389/fimmu.2023.1172896

Administration of BNT162b2 mRNA COVID-19 vaccine to subjects with various allergic backgrounds

Yaarit Ribak†, Limor Rubin†, Aviv Talmon†, Zvi Dranitzki, Oded Shamriz, Isca Hershkowitz, Yuval Tal‡ and Alon Y. Hershko*‡

Allergy and Clinical Immunology Unit, Department of Medicine, Hadassah Medical Organization, Faculty of Medicine, Hebrew University of Jerusalem, Jerusalem, Israel

Background: The mRNA-based COVID-19 vaccine was introduced to the general public in December 2020. Shortly thereafter, safety concerns were raised due to the reporting of allergic reactions. Allergy-related disorders were suspected to be significant risk factors and the excipient polyethylene glycol was suggested to be a robust allergen.

Methods: This is a retrospective study analysis. Subjects with putative risk factors for severe allergic reactions to the Pfizer-BioNTech BNT162b2 vaccine were referred for vaccination under observation at the Unit of Allergy and Clinical Immunology. Data was collected for each subject, including demographic details, medical history and previous reactions to any allergen. When appropriate, skin tests were done prior to vaccination.

Results: A total of 346 subjects received 623 vaccine doses under observation. The study included patients with various allergy-related disorders (n=290) and those with allergy to a previous COVID-19 vaccine dose (n=56). Both groups showed female predominance (78% and 88%, p=NS). Patients without reactions to previous doses reported more drug allergy (80% vs. 39%, p<0.001) and previous anaphylaxis (64% vs. 14%, p<0.001). There was no difference in sensitivity to other allergens, including polyethylene glycol. Under observation, mild allergic reactions were noted in 13 individuals characterized by female gender (100%), a history of anaphylaxis (69%) and drug allergy (62%). In 7 subjects, allergy was treated with antihistamines while others recovered spontaneously.

Conclusion: Our study demonstrates that vaccination under specialist-supervision is a powerful tool for reducing over-diagnosis of systemic reactions and for rapid and reliable collection of vaccine safety data.

KEYWORDS

COVID- 19, vaccination, drug allergy, anaphylaxis, polyethylene glycol

Introduction

The rollout of COVID-19 vaccination in December 2020 was accompanied by concerns that the vaccine may be highly allergenic. This fear was prompted by several reports in the public media of individuals with a history of allergy who developed anaphylaxis immediately following injection. A high rate of allergic reactions to the mRNA-based vaccine was also suggested by clinical data (1) and polyethylene glycol (PEG) was suspected as a major culprit allergen (2, 3). PEG is present in a large variety of medications, cosmetic products and detergents and induces allergic reactions. A previous case series presented subjects who developed anaphylaxis to medications with excipients containing this compound (4). Therefore, it was suggested that, following vaccine injection, preexisting PEG-specific IgE activates mast cells and stimulates anaphylactic responses (5).

The uncertainty that accompanied the vaccination campaign rollout prompted the UK authorities to issue a statement that any individual with a medical history of anaphylactic responses to food, medications, or vaccines should not be vaccinated (6, 7). It was estimated that this decision would exclude 3-5% of the general population from the campaign due to self-reported severe allergic reactions to any allergen (7). This directive was revised three weeks later leaving only allergic reactions to vaccine components as the major contraindication (7). Concomitantly, experts suggested the existence of several risk factors including allergic sensitization to other vaccines, mastocytosis and severe asthma (8).

Consequently, frequent recommendation changes led to uncertainty regarding vaccine safety and to excessive reporting of allergic reactions (9) accompanied by both patient and physician hesitancy. The need for rapid collection of data regarding the risk for allergic reactions to the COVID-19 vaccine prompted the assembly of an intervention team at our hospital. This team constituted a framework for individuals whose putative risk factors would otherwise not allow them to be vaccinated.

Methods

Protocol for vaccination under observation

This retrospective study presents the outcomes of a program for the vaccination of individuals with a history of allergy or related conditions that were considered as risk factors for anaphylaxis (Figure 1). These patients were referred from various regions of the country by their primary-care physicians to the Unit of Allergy and Clinical Immunology (UACI) from January to December 2021. Subjects were interviewed by the medical team for demographic data, medical history and details related to previous reactions to any allergen. Skin tests for the Pfizer-BioNTech BNTT162B2 and polyethylene glycol (PEG) were done for patients who had reported the following: immediate allergy to a previous COVID-19 vaccine dose; reactions to PEG-based laxatives; multi-drug allergies; sensitivity to relevant substances (e.g., detergents). Testing was also done in response to specific requests from the treating-clinician. Selected subjects received anti-histamines prior to vaccine injection and could receive injections in a graded manner. Premedication was administered to patients who reported an immediate reaction to a previous vaccine dose, subjects carrying an epinephrine autoinjector, and those with chronic spontaneous urticaria and angioedema or mastocytosis. Premedication was occasionally withheld despite these indications based on clinical judgement. All patients received Pfizer-BioNTech BNTT162B2, were observed for 1 hr and treated for reactions as needed.

Statistical analysis

Continuous variables were compared by using student's t-test. The comparison of proportions was performed by using Fisher's exact test. Categorical variables with less than 5 observations in both groups were excluded from the analysis. The Bonferroni method was used for calculating adjusted p-value. Adjusted p-values<0.05 were considered significant.

The statistical analysis was performed with R (v. 4.0.2).

Ethical considerations

Access to medical records for the purpose of this study was approved by the local Institutional Ethics Committee of Hadassah Medical Center in keeping with the principles of the Declaration of Helsinki (application number 0279-21-HMO). Due to the retrospective design of this study, no consent procedures were required.

Results

Characterization of study population

The study includes 346 subjects who were given 623 doses of COVID-19 vaccine under supervision (Table 1). Of these, 290 reported various allergy-related disorders while 56 had a history of allergy to a previous COVID-19 vaccine dose. The two categories showed a different mean age (57 ± 18 vs. 47 ± 17 years, respectively, p=0.005). Interestingly, both groups presented a robust female predominance (78% and 88%, respectively, p=NS). Each category was administered different proportions of vaccine doses 1, 2 and 3. Patients who did not have a history of reactions to previous doses had a higher rate of allergy to other drugs (80% vs. 39%, p<0.001) and previous episodes of anaphylaxis (64% vs. 14%, p<0.001). No difference was noted between the two groups with regards to previous allergic reactions to other specific allergens, including polyethylene glycol as well as other associated disorders, such as chronic urticaria or mastocytosis. However, patients with a putative COVID-19 vaccine allergy patients were more likely to receive anti-

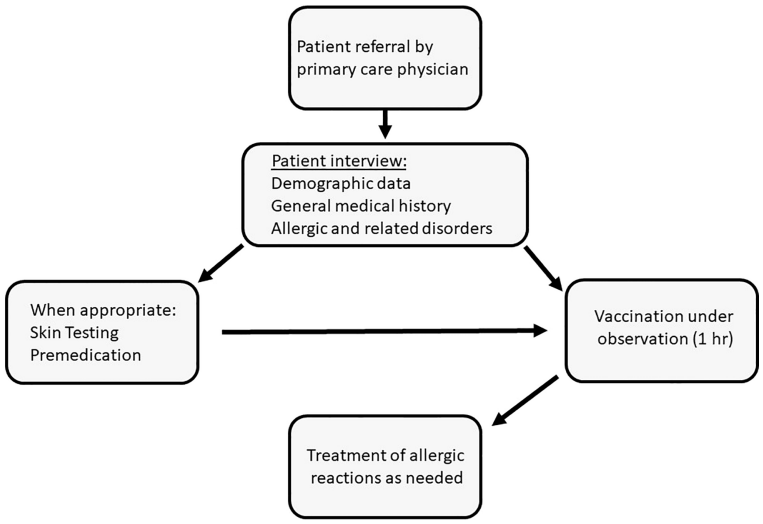

FIGURE 1
Vaccination under observation of subjects deemed to be at high risk for allergic reactions to the mRNA-based COVID-19 vaccine: algorithm of patient management.

TABLE 1 Characterization of study population.

Characteristic				History of allergy to COVID-19 vaccine		
				No (n=290)	Yes (n=56)	Adjusted p-value (Bonferroni)
Age, yrs; mean ± S.D., range				57 ± 18, 14-89	47 ± 17, 7-84	0.005
Female gender; n (%)				226 (78)	49 (88)	NS
Vaccine dose administered during study; n (%)						
		1st		282 (98)	2* (5)	<0.001
		2nd		232 (80)	46 (80)	NS
		3rd		38 (13)	22 (39)	<0.001
History of allergy and related disorders; n (%)						
	Allergic reactions					
		Drug hypersensitivity		230 (80)	22 (39)	<0.001
		Food allergy		42 (15)	2 (4)	NS
		Insect venom allergy		18 (6)	2 (4)	NS
		Contrast media				
			gadolinium	5 (2)	0 (0)	NS
			Iodinated	12 (4)	1 (2)	NS
		Suspected PEG hypersensitivity**		10 (3)	4 (7)	NS
		Latex		8 (3)	1 (2)	NS
		Blood transfusion		2 (1)	0 (0)	NS

(Continued)

TABLE 1 Continued

Characteristic			History of allergy to COVID-19 vaccine		
			No (n=290)	Yes (n=56)	Adjusted p-value (Bonferroni)
	Related conditions				
		Previous anaphylaxis	184 (64)	8 (14)	<0.001
		Epipen carrier	37 (13)	1 (2)	NS
		Chronic spontaneous urticaria or angioedema	29 (10)	4 (7)	NS
		Mastocytosis	6 (2)	0 (0)	NS
Antihistamine pre- medication, n (%)			46 (16)	41 (73)	<0.001

histamine premedication when vaccinated under observation (16% vs. 73%, p<0.001).

Evaluation of reactions to prior COVID vaccine doses

In most cases, reactions to a previous vaccine dose occurred within 1 hour (59%) and were treated with antihistamines (n=14, 25%) followed by corticosteroids (n=10, 18%) and epinephrine (n=7, 13%) (Table 2). We evaluated the validity of these events as allergic reactions. Consequently, 1% of the events (n=2) was ruled out due to an onset time that exceeded 1 hour after injection. Conversely, 18% of the cases (n=10) were judged to be likely based on an immediate onset, involvement of more than 1 organ-system and at least one supporting objective finding. The remaining 80% (n=45) were immediate responses that were classified as unlikely since they did not meet the criteria for probable allergy.

TABLE 2 Characteristics of previously reported allergic reactions to COVID-19 vaccine.

Parameter		
Time of onset		
	< 30 min	24 (43)
	30 min - 1 hr	9 (16)
	N/A	23 (41)
Treatment; n (%)		
	Epinephrin	7 (13)
	Antihistamines	14 (25)
	Corticosteroids	10 (18)
Validation of allergic reactions; n (%)		
	Ruled-out	1 (2)
	Unlikely	45 (80)
	Likely	10 (18)

N/A, not available.

Allergic reactions to vaccination under observation at the Allergy Unit

Thirteen individuals reported an immediate response following the administration of COVID-19 vaccine under supervision during the study period (Table 3). Their mean age was 48 ± 13.6 (range 27-69) and, strikingly, they were all females. Most of these patients reported hypersensitivity to one or more drug (8/13, 62%) and a previous episode of anaphylaxis (9/13, 69%). The majority of this group had been administered anti-histamine premedication prior to vaccination (10/13, 77%). All allergic reactions were mild and 7 were treated with antihistamines. Objective findings were found in only 5 individuals (rash, local reaction, cough, rhinitis). The 3 patients who were suspected of having PEG allergy had mild rash and subjective sensations of tingling and swelling (patients 2, 4 and 8, respectively).

Discussion

This communication summarizes our experience in administering the Pfizer-BioNTech BNT162b2 to patients who were deemed to be at high risk for anaphylaxis. Several insights can be drawn from this study, which may be useful in clinical practice and in the understanding of challenges associated with future vaccination campaigns.

In line with previous studies, our work supports the conclusion that the Pfizer-BioNTech BNT162b2 is safe, and that PEG does not appear to be a significant allergen (9). It should be stressed that proven allergic sensitization to a specific component of a vaccine does not necessarily constitute a contra indication for vaccine administration. For example, it has been shown that children with egg allergy who receive egg-based influenza vaccine do not experience an increased rate of anaphylaxis (10). The Pfizer-BioNTech vaccine contains the putative allergen PEG whose capacity to induce sensitization corresponds to its molecular

TABLE 3 Patients who reported allergic reactions under observation.

		History of allergy and related disorders						Vaccination under observation	
Patient	Age/ Gender	Drug	Previous COVID-19 vaccine	PEG	Other	Anaphylaxis	Autoinjector	Antihistamine premedication	Reaction under observation
1	27/F	none	–	–	–	Yes	Yes	Yes	Throat tingling §
2	30/F	none	Yes	Yes	–	–	–	Yes	Redness and pruritus on chest
3	34/F	none	–	–	Chronic urticaria	–	–	Yes	Arm pruritus
4	39/F	>1	–	Yes	Chronic urticaria	Yes	–	Yes	Lip tingling
5	41/F	none	Yes	–	–	–	–	Yes	General tingling §
6	45/F	>1	–	–	Chronic urticaria	Yes	–	Yes	Local reaction §
7	49/F	>1	–	–	–	–	–	–	Multiple symptoms* §
8	49/F	>1	Yes	Yes	–	Yes	–	Yes	Swelling of face**
9	56/F	1	Yes	–	Insect	Yes	Yes	Yes	Cough
10	56/F	1	Yes	–	Insect	Yes	–	Yes	Pruritus, tongue swelling** §
11	62/F	>1	–	–	–	Yes	–	–	Rhinitis
12	67/F	none	–	–	–	Yes	Yes	Yes	Lip angioedema (late)
13	69/F	>1	–	–	–	Yes	–	–	Mouth tingling

*, Rash, dyspnea, shivering, elevated blood pressure and tachycardia, clear lungs; clinical impression of anxiety; **, no objective finding; §, treated with antihistamines.

weight. Therefore, a reaction to a specific formulation of PEG does not necessarily predict sensitization to others (2). In our study, patients with a history of PEG allergy did not experience significant adverse events to the vaccine, and this may be attributed to its low molecular weight as an excipient, low injection volume and route of administration. Additionally, we have recently conducted a study on blood samples from 79 volunteers demonstrating an increase in PEG-specific IgG but not IgE, which was undetectable both before or after vaccine administration (11).

Furthermore, it has previously been shown that in subjects who report a reaction to the vaccine, subsequent doses are well-tolerated (12). Accordingly, we have previously demonstrated that the vast majority of reactions to the COVID-19 vaccine could not be validated as allergic, even when reporting had been done by healthcare workers (4). It has also been shown that reporting of allergy events was characterized by female gender and a self-reported history of allergy to other drugs (4). Interestingly, these two features were predominant in the present study as well, in which most subjects were referred due to anticipation of an allergic reaction while only a minority had already experienced a response to the vaccine. Intriguingly, subjects who were referred to our Unit following a previous response to the vaccine had a considerably low rate of reported allergy to other drugs, compared to the rest of the study population. Although this finding is not entirely understood, it could be at least partially explained by their younger age.

Analysis of immediate reactions that were observed during this study under our supervision may shed light on possible precipitating factors. All reactions were reported by female subjects and most of them had a history of allergy to other drugs and previous anaphylaxis. Although this may be partially explained by subjective complaints, it also raises the possibility of gender variances in response to drugs. These findings may be useful in predicting patients who are likely to develop immediate symptoms following vaccination.

This study has several limitations. First, the work was conducted in single center. However, this limitation is alleviated by the fact that patients were referred from various parts of the country and therefore the data was collected on a national level. Second, the retrospective design may entail an inherent bias. Nevertheless, data was collected by structured forms and we propose that this method of acquisition reduces the potential bias. Third, the number of patients who were recruited and the rate of allergic events compromise its statistical power. However, to the best of our knowledge, we present here the largest series of subjects thus far who were vaccinated safely despite guideline warnings. A related publication that was previously published (12) assessed the safety of vaccine administration to 18 subjects who had reacted to the first dose. In comparison, we report safety in 346 patients with a variety of putative risk factors and we show complete absence of significant systemic reactions. Consequently, we provide here

comprehensive evidence to refute contraindications that were issued by leading health organizations.

In conclusion, our study highlights vaccination under specialist-observation as a powerful tool for allowing the administration of vaccine despite official contra-indications. This method can provide rapid support to hesitant individuals and their treating physicians as well as reliable data to policy leaders in crises such as an outbreak of a pandemic.

Data availability statement

The raw data supporting the conclusions of this article will be made available by the authors, without undue reservation.

Ethics statement

Access to medical records for the purpose of this study was approved by the local Institutional Ethics Committee of Hadassah Medical Center in keeping with the principles of the Declaration of Helsinki (application number In review 0279-21-HMO).

Author contributions

YL, LR, and AT—contributed to study design, data collection, and wrote the first draft. ZD and OS—contributed to data collection. IH—organized and analyzed the data. YT and AH—contributed to conception, design and manuscript preparation. All authors contributed to manuscript revision, read, and approved the submitted version

Acknowledgments

The authors wish to thank Yehuda Shovman for his assistance in the statistical data analysis.

Conflict of interest

The authors declare that the research was conducted in the absence of any commercial or financial relationships that could be construed as a potential conflict of interest.

Publisher's note

All claims expressed in this article are solely those of the authors and do not necessarily represent those of their affiliated organizations, or those of the publisher, the editors and the reviewers. Any product that may be evaluated in this article, or claim that may be made by its manufacturer, is not guaranteed or endorsed by the publisher.

References

1. Blumenthal KG, Robinson LB, Camargo CAJr, Shenoy ES, Banerji A, Landman AB, et al. Acute allergic reactions to mRNA COVID-19 Vaccines. *JAMA* (2021) 325 (15):1562–5. doi: 10.1001/jama.2021.3976

2. Banerji A, Wickner PG, Saff R, Stone CA, Robinson LB, Long AA, et al. mRNA Vaccines to prevent COVID-19 disease and reported allergic reactions: Current evidence and suggested approach. *J Allergy Clin Immunol Pract* (2021) 9(4):1423–37. doi: 10.1016/j.jaip.2020.12.047

3. De Vrieze J. Pfizer's vaccine raises allergy concerns. *Science* (2021) 371(6524):10–1. doi: 10.1126/science.371.6524.10

4. Sellaturay P, Nasser S, Ewan P. Polyethylene glycol-induced systemic allergic reactions (anaphylaxis). *J Allergy Clin Immunol Pract* (2021) 9(2):670–5. doi: 10.1016/j.jaip.2020.09.029

5. Cabanillas B, Akdis CA, Novak N. Allergic reactions to the first COVID-19 vaccine: A potential role of polyethylene glycol? *Allergy* (2021) 76(6):1617–8. doi: 10.1111/all.14711

6. Turner PJ, Ansotegui IJ, Campbell DE, Cardona V, Ebisawa M, El-Gamal Y, et al. COVID-19 vaccine-associated anaphylaxis: A statement of the World Allergy Organization Anaphylaxis Committee. *World Allergy Organ J* (2021) 14(2):100517. doi: 10.1016/j.waojou.2021.100517

7. Rutkowski K, Mirakian R, Till S, Rutkowski R, Wagner A. Adverse reactions to COVID-19 vaccines: A practical approach. *Clin Exp Allergy* (2021) 51(6):770–7. doi: 10.1111/cea.13880

8. Caminati M, Guarnieri G, Senna G. Who is really at risk for anaphylaxis due to covid-19 vaccine? *Vaccines* (2021) 9(1):1–3. doi: 10.3390/vaccines9010038

9. Anis E, Alroy Preis S, Cedar N, Tal Y, Hershkowitz I, Hershko AY. Reporting of allergic reactions during Pfizer-BioNTech BNTT162B2 vaccination in Israel. *J Allergy Clin Immunol Pract* (2022) 10(11):2969–76. doi: 10.1016/j.jaip.2022.07.012

10. McNeil M, DeStefano F. Vaccine-associated hypersensitivity. *J Allergy Clin Immunol* (2018) 141(2):463–72. doi: 10.1016/j.jaci.2017.12.971

11. Bavli Y, Chen B-M, Gross G, Hershko A, Yurjeman K, Roffler S, et al. Anti-PEG antibodies before and after a first dose of Comirnaty® (mRNA-LNP-based SARS-CoV-2 vaccine). *J Control Release* (2023) 354:316–22. doi: 10.1016/j.jconrel.2022.12.039

12. Kessel A, Bamberger E, Nachshon L, Rosman Y, Confino-Cohen R, Elizur A. Safe administration of the Pfizer-BioNtTech COVID-19 vaccine following an immediate reaction to the first dose. *Allergy* (2021) 76(11):3538–40. doi: 10.1111/all.15038

Frontiers in Immunology

Explores novel approaches and diagnoses to treat immune disorders.

The official journal of the International Union of Immunological Societies (IUIS) and the most cited in its field, leading the way for research across basic, translational and clinical immunology.

Discover the latest Research Topics

See more →

Frontiers

Avenue du Tribunal-Fédéral 34
1005 Lausanne, Switzerland
frontiersin.org

Contact us

+41 (0)21 510 17 00
frontiersin.org/about/contact